

This work is protected by copyright and other intellectual property rights and duplication or sale of all or part is not permitted, except that material may be duplicated by you for research, private study, criticism/review or educational purposes. Electronic or print copies are for your own personal, non-commercial use and shall not be passed to any other individual. No quotation may be published without proper acknowledgement. For any other use, or to quote extensively from the work, permission must be obtained from the copyright holder/s.



**Antiproliferative, proapoptotic and DNA methylation  
activity of sesqui- and diterpenoids in ovarian cancer  
cells**

**Idowu Eniafe Fadayomi**

**Thesis submitted to Keele University for the degree of  
Doctor of Philosophy**

**October 2021**

**Antiproliferative, proapoptotic and DNA methylation  
activity of sesqui- and diterpenoids in ovarian cancer  
cells**

**Idowu Eniafe Fadayomi**

**School of Pharmacy and Bioengineering, Faculty of  
Medicine and Health Sciences, Keele University**

**Thesis submitted to Keele University for the degree of  
Doctor of Philosophy**

**October 2021**

**Abstract**

Ovarian cancer is a gynaecological malignancy associated with the highest level of death. Its resistance against anti-cancer drugs in recent time has exacerbated the problem. Hence, the search for novel drugs from plants used in traditional medicine is imperative. This study investigated the *in vitro* anti-ovarian cancer activities of *Justicia insularis* T. Anderson and mechanisms of action of its bioactive constituents, two plant-derived diterpenoids (andrographolide and triptolide) and four sesquiterpene lactones (dehydroleucodine, alantolactone, parthenolide and costunolide). The bioactive compounds from *J. insularis* were isolated and characterised using bioassay-guided fractionation, mass spectrometry and nuclear magnetic resonance spectroscopy. The antiproliferative activity of the sesqui- and diterpenoids was evaluated against human ovarian cancer cell lines (CIS-A2780, OVCAR-8 and OVCAR-4) using Sulforhodamine B and trypan blue exclusion assays. Pro-apoptotic activity was evaluated using enzymatic assays and flow cytometry. Global DNA methylation and DNA methyltransferases (DNMTs) activity were measured using ELISA assay. Gene-specific CpG methylation and mRNA expression of panel of tumour suppressor genes were quantified using pyrosequencing and RT-qPCR respectively. The two major bioactive compounds in *J. insularis* were identified as diterpenoids, 16 $\alpha$ / $\beta$ -hydroxy-cleroda-3,13(14) dien-15,16-olide and 16-oxocleroda-3,13(14) dien-15-oic acid. Sesqui- and diterpenoids showed strong growth inhibitory activity, decreased cell viability and induced apoptosis via intrinsic and extrinsic pathways. They possessed DNMT inhibitory activity, upregulated the expression of notable tumour suppressor genes. Furthermore, sesquiterpene lactones showed significant global and gene specific CpG methylation activity. In conclusion, sesqui- and diterpenoids possess strong anti-ovarian cancer activity and bear the potential to be developed as drug candidates for cancer treatment. Therefore, *in vivo* studies of their anti-ovarian cancer activity would be essential in the future.

### **Declaration**

This is to certify that this original research was carried out by Idowu Eniafe Fadayomi. All experiments such as: isolation and characterization of the natural compounds from *J. insularis*, *in vitro* biological assays and the molecular mechanisms of all compounds investigated were performed by the researcher. However, the initial extraction of the plant materials was done by Dr Okiemute Rosa Johnson-Ajinwo, and the nuclear magnetic resonance (NMR) spectrometry and liquid chromatography mass spectrometry (LC MS) part of this study were done by Prof Tim Claridge and Dr James McCullagh / Elisabete Pires respectively.

## **Table of Contents**

Abstract .....	i
Declaration .....	ii
List of Figures .....	xi
List of Tables .....	xxi
Abbreviations .....	xxii
Acknowledgements .....	xxvi
<b>Chapter One: Introduction .....</b>	<b>1</b>
1.1 Cancer .....	2
1.1.1 Worldwide incidence of cancer and severity .....	3
1.2 Ovarian cancer .....	4
1.2.1 Ovarian cancer incidence and severity .....	5
1.2.2 Aetiological and risk factors of ovarian cancer .....	6
1.2.3 Ovarian cancer types, therapy and associated genetic mechanism.....	7
1.3 Epigenetics and cancer formation.....	8
1.3.1 DNA methylation.....	9
1.3.1.1 Methylation patterns in ovarian cancer.....	12
1.3.1.2 Quantification of DNA methylation .....	13
1.3.1.3 DNA 5-Hydroxymethylcytosine (5-hmC).....	14
1.3.2 Histone modification (acetylation and methylation) .....	16
1.3.3 MicroRNAs in epigenetic modulation.....	18
1.4 Apoptosis and cancer formation and treatment .....	19
1.5 Therapeutic agents based on epigenetics .....	22
1.5.1 5-Azacytidine (Aza): A known nucleoside DNMT1 inhibitor .....	22
1.5.2 5-Aza-2'-Deoxycytidine (5-aza-CdR) and zebularine (Zeb).....	23

---

1.5.3	Non-nucleoside synthetic compounds that are known DNMT inhibitors .....	25
1.5.3.1	SGI-1027.....	25
1.5.3.2	Procainamide derivatives.....	26
1.6	Plant-derived natural products: A promising agent in cancer treatment .....	27
1.6.1	Sesquiterpene lactones (SLs).....	29
1.6.1.1	Parthenolide .....	31
1.6.1.2	Costunolide.....	33
1.6.1.3	Alantolactone (Ala): The major bioactive compound in plants with many pharmacological activities .....	35
1.6.1.4	Dehydroleucodine.....	37
1.6.2	Diterpenoids.....	39
1.6.2.1	Andrographolide .....	40
1.6.2.2	Triptolide .....	42
1.6.3	Other plant phytochemicals with epigenetic activities .....	44
1.7	The Genus <i>Justicia</i> : A genus with wide application in traditional medicine across the world .....	46
1.7.1	<i>Justicia insularis</i> T. Anderson: African edible plant with wide application in traditional medicine .....	47
1.8	Aims, objectives and research questions .....	49
1.8.1	Research Questions.....	49
1.8.2	Aims of this study.....	49
1.8.3	Objectives of this study .....	50
<b>Chapter Two: General Materials and Methods.....</b>		<b>52</b>
2.1	Materials .....	53
2.1.1	Natural compounds and control drugs.....	53

---

2.1.2	Plant materials .....	53
2.1.3	Reagents.....	53
2.1.4	Cancer cell culture and assays materials .....	54
2.1.5	Materials used in biochemical and molecular assays .....	54
2.1.6	The human ovarian epithelial cancer cell lines and Immortalized normal human ovarian epithelial cell line .....	55
2.2	Methods .....	60
2.2.1	Extraction procedure for <i>Justicia insularis</i> .....	60
2.2.2	Solvent partition of plant extracts.....	62
2.2.3	Purification of bioactive compounds of <i>Justicia insularis</i> .....	62
2.2.4	Gas chromatography mass spectrometry analysis .....	63
2.2.5	Liquid chromatography mass spectrometry (LC-MS) analysis.....	64
2.2.6	Nuclear magnetic resonance (NMR) spectroscopy .....	65
2.2.7	Preparation of cell culture growth medium and 1X trypsin .....	65
2.2.8	Trypsinization and cell counting .....	66
2.2.9	Cell lines resuscitation from cryopreserved state .....	67
2.2.10	Cryopreservation of cells for future use .....	67
2.2.11	Cell growth inhibitory assay.....	68
2.2.12	Trypan blue assay .....	70
2.2.13	Apoptosis assays.....	70
2.2.13.1	Apoptosis detection using caspase 3/7 marker .....	71
2.2.13.2	Evaluation of extrinsic pathway of apoptosis using caspase 8 marker.....	71
2.2.13.3	Evaluation of intrinsic pathway of apoptosis using caspase 9 marker .....	72
2.2.13.4	Evaluation of mitochondria membrane potential activities.....	72
2.2.13.5	Light microscopy .....	74

---

2.2.13.6 Nuclear and actin staining fluorescence microscopy.....	74
2.2.13.7 Flow cytometry analysis of apoptosis using annexin V .....	75
2.2.14 Cell cycle analysis .....	76
2.2.15 Quantification of global and gene specific DNA methylation .....	77
2.2.15.1 Cell pellet preparation.....	77
2.2.15.2 DNA extraction.....	78
2.2.15.3 Quantification of global 5- methylcytosine DNA methylation.....	79
2.2.15.4 Pyrosequencing assay for quantification of gene specific DNA methylation .....	80
2.2.15.4.1 Bisulfite conversion of DNA .....	81
2.2.15.4.2 Polymerase chain reaction (PCR) .....	82
2.2.15.4.3 Agarose gel electrophoresis .....	82
2.2.15.4.4 Pyrosequencing procedure .....	83
2.2.16. Quantitative reverse transcription polymerase chain reaction (RT-qPCR) .....	86
2.2.16.1 Cell sample preparation and RNA extraction .....	86
2.2.16.2 Quantitative reverse transcription polymerase chain reaction (RT-qPCR) procedure.....	87
2.2.17. Evaluation of inhibitory activity of natural compounds against DNMT .....	90
2.2.17.1 Cell pellet preparation for DNMT assay .....	90
2.2.17.2 Nuclear extraction procedure and protein quantification .....	90
2.2.17.3 DNMT inhibitory assay .....	91
2.3 Statistical analysis.....	92
2.4 Graphical Summary of methods used in this study .....	93
<b>Chapter Three: Characterisation of Anti-Ovarian Cancer Diterpenoids in <i>Justicia</i> <i>Insularis</i> T. Anderson and their Roles in Apoptosis, DNA Methylation and Gene Expression.....</b>	<b>94</b>

---

3.1	Introduction.....	95
3.2	Results.....	96
3.2.1	Yield of plant extracts and partitioned fractions of <i>J. insularis</i> .....	96
3.2.2	Growth inhibitory activity of <i>J. insularis</i> extracts and fractions .....	97
3.2.3	Column purification results of the ethyl acetate fraction of <i>J. insularis</i> .....	100
3.2.4	Purification of pure compounds from active fractions of JI EA 4-4 and EA4-6 .....	102
3.2.5	Structural identification of compound 1 and 2 .....	105
3.2.6	Antiproliferative activities of purified compounds 1 and 2 from <i>Justicia insularis</i> .....	113
3.2.7	Cytotoxicity of compound 1 using trypan blue exclusion cell viability assay ...	116
3.2.8.	Apoptosis induction by compound 1 .....	118
3.2.8.1	Morphological effects of compound 1 on ovarian cancer cell lines .....	118
3.2.8.2	Nuclear and actin staining of ovarian cancer cell lines for apoptosis evaluation using fluorescence microscopy .....	121
3.2.8.3	Apoptosis study by caspase 3/7 activity .....	124
3.2.8.4	Effect of compound 1 on caspase 8 activity .....	126
3.2.8.5	Effect of Compound 1 on caspase 9 activity in ovarian cancer cells .....	128
3.2.8.6	Flow cytometry analysis of apoptosis using annexin V and propidium iodide ..	129
3.2.8.7	Results of mitochondrial membrane potential activities of compound 1 .....	134
3.2.8.8	Cell cycle analysis of compound 1 .....	136
3.2.9	Evaluation of the effect of compound 1 on global DNA methylation.....	140
3.2.10	Quantification of the effect of compound 1 on gene specific promoter methylation using pyrosequencing assay .....	141
3.2.11	DNMT inhibitory activities of compound 1 .....	148

---

---

3.2.12	Gene expression modulatory effects of compound 1 using quantitative reverse transcription polymerase chain reaction (RT-qPCR).....	149
3.3	Discussion.....	152
3.3.1	Phytochemical identification of the bioactive compounds in <i>Justicia insularis</i>	152
3.3.2	Biological activities <i>Justicia insularis</i> and its bioactive compounds .....	153
3.3.2.1	Antiproliferative activity of <i>Justicia insularis</i> - isolated bioactive compounds..	153
3.3.2.2	Pro-apoptotic activity of Compound 1 .....	155
3.3.2.3	DNA methylation and gene expression modulatory activities of compound 1 ..	157
3.4	Conclusion .....	158
<b>Chapter Four: Anti-Ovarian Cancer Activity of Andrographolide and Triptolide, and their Roles in DNA Methylation and Modulation of Gene Expression .....</b>		<b>160</b>
4.1	Introduction.....	161
4.2	Results.....	162
4.2.1	Growth inhibitory activity of andrographolide and triptolide against ovarian cancer cells.....	162
4.2.2	Evaluation of the cytotoxic effect of Andr and Tpl using trypan blue assay .....	165
4.2.3	Andr and Tpl induced morphological changes in ovarian cancer cells .....	167
4.2.4	Staining of the nuclear and actin structure of ovarian cancer cell line for apoptosis evaluation using fluorescence microscopy .....	170
4.2.5	Change in caspase 3/7 activity in response to Andr and Tpl treatment.....	173
4.2.6	Caspase 8 Activity effect of Andr and Tpl as marker of extrinsic pathway.....	174
4.2.7	Effect of Andr and Tpl on caspase 9 activity as marker of intrinsic pathway of apoptosis .....	176
4.2.8	Analysis of apoptosis using annexin V and propidium iodide .....	178
4.2.9	Effect of Andr and Tpl on mitochondrial membrane potential activity .....	182

4.2.10	Effect of Andr and Tpl on cell cycle .....	184
4.2.11	Effect of Andr and Tpl on Global 5-methylcytosine DNA methylation .....	188
4.2.12	Gene specific promoter methylation analysis using pyrosequencing.....	189
4.2.13	Inhibition of DNMT enzymatic activities by Andr and Tpl .....	192
4.2.14	Gene expression modulatory effects of Andr and Tpl using RT-qPCR .....	194
4.3	Discussion.....	197
4.3.1	Antiproliferative activity of andrographolide and triptolide .....	197
4.3.2	Pro-apoptotic activity of andrographolide and triptolide.....	199
4.3.3	DNA methylation and gene expression modulatory activities of Andr and Tpl	202
4.4	Conclusion .....	203
<b>Chapter Five: Antiproliferative, Apoptotic and DNMT Inhibitory Activities of Sesquiterpene Lactones (SLs) in Ovarian Cancer Treatment.....</b>		<b>205</b>
5.1	Introduction.....	206
5.2	Results.....	207
5.2.1	Antiproliferative activity of sesquiterpene lactones (SLs) and 5'azacytidine ...	207
5.2.2	Cytotoxic activities of SLs and Aza using trypan blue exclusion assay.....	211
5.2.3	Morphological effects of SLs and Aza on ovarian cancer cell lines .....	215
5.2.4	Evaluation of change in nuclear and actin structure of ovarian cancer cells.....	218
5.2.5	Evaluation of apoptotic activities of SLs and Aza using caspase 3/7 assay .....	221
5.2.6	Effect of SLs and Aza on caspase 8 activity.....	223
5.2.7	Evaluation of caspase 9 activity by SLs and Aza .....	226
5.2.8	Flow cytometry analysis of apoptosis using annexin V and propidium iodide ..	228
5.2.10	Cell cycle analysis of ovarian cancer cell lines in response to SLs treatment....	234
5.2.11	Quantification of Global 5-methylcytosine DNA Methylation .....	239

5.2.12	Quantitative assessment of change in gene specific promoter methylation in response to treatment with SLs using pyrosequencing assay .....	240
5.2.13	DNMT inhibitory activities of SLs and Aza.....	245
5.2.14	Quantitative evaluation of change in gene expression using quantitative reverse transcription polymerase chain reaction ((RT-qPCR) .....	246
5.3	Discussion.....	250
5.3.1	Effect of SLs on cell proliferation .....	250
5.3.2	Induction of apoptosis.....	252
5.3.3	Effects on global and gene specific DNA methylation, DNMTs and tumour suppressor gene expression and DNMT enzymatic activity.....	255
5.4	Conclusion .....	257
	<b>Chapter Six: General Discussion, Conclusions and Future Study .....</b>	<b>259</b>
6.1	General discussion .....	260
6.2	Limitations of study .....	265
6.3	Conclusions.....	265
6.4	Future study .....	267
	References.....	269
	Appendices.....	295

---

**List of Figures**

Figure 1. 1: Multistep processes of cancer formation featuring genetic instability and inflammation by innate immune cells as underlying mechanisms. ....	3
Figure 1. 2: Structure of 5-azacytidine .....	23
Figure 1. 3: Structure of 5-Aza-2-deoxycytidine and zebularine .....	25
Figure 1. 4: Structure of SGI-1027 .....	26
Figure 1. 5: Structure of procainamide .....	26
Figure 1. 6: Chemical structures of the different subtypes of sesquiterpene lactones. ....	30
Figure 1. 7: Structure of parthenolide .....	33
Figure 1. 8: Structure of Costunolide.....	35
Figure 1. 9: Structure of alantolactone.....	37
Figure 1. 10: Structure of Dehydroleucodine .....	39
Figure 1. 11: Structures of andrographolide .....	42
Figure 1. 12: Structures of triptolide.....	44
Figure 1. 13: A picture of <i>Justicia insularis</i> T.Anderson taking at the collection venue in Nigeria.....	48
Figure 2. 1: A flow chart for the extraction procedure of <i>J. insularis</i> . Partitioning was done based on the different polarity of the organic solvents.....	61
Figure 3. 1: Mean concentration-response curve of the organic (DCM/MeOH) extract (A) and fractions of <i>J. insularis</i> : n-hexane (B) and ethyl acetate (C) on CIS-A2780, OVCAR-8 and OVCAR-4 ovarian cancer cell lines and HOE cells.. ....	98
Figure 3. 2: Analytical HPLC chromatogram of fractions of <i>Justicia insularis</i> showing several peaks with the main compounds indicated by retention time.....	103

---

Figure 3. 3: Analytical and Semi preparative HPLC chromatogram of JI ethyl acetate (EA) sub-fractions.....	104
Figure 3. 4: Analytical HPLC chromatogram of purified active compounds in EA of <i>Justicia insularis</i> .....	105
Figure 3. 5: GC-MS chromatograms and electron ionization mass spectra of purified active compound 1 (top) and 2 (bottom) from ethyl acetate sub-fraction 4-6 (EA4-6-12 and EA4-6-13) of <i>J. insularis</i> . .....	106
Figure 3. 6: LC-MS chromatogram (A) and negative ESI-MS spectrum (B) of isolated compound 1 showing the MS of the major peak at retention time of 12.87 min.....	107
Figure 3. 7: LC-MS chromatogram (A) and negative ESI-MS spectrum (B) of isolated compound 2 at retention time of 13.45 min.....	108
Figure 3. 8: NMR data analysis of <i>Justicia insularis</i> of purified compound 1 in CDCl <sub>3</sub> : (A) <sup>1</sup> H NMR and (B) <sup>13</sup> C NMR.....	109
Figure 3. 9: NMR data analysis of <i>Justicia insularis</i> purified compound 2 in CDCl <sub>3</sub> : (A) <sup>1</sup> H NMR and (B) <sup>13</sup> C NMR.....	110
Figure 3. 10: Chemical structure of 16 $\alpha$ / $\beta$ -hydroxy-cleroda-3,13 (14) dien-15,16-olide (compound 1) (A) and 16-oxocleroda-3,13(14) dien-15-oic-acid (Compound 2) (B) .....	113
Figure 3. 11: Mean concentration-response curve of the growth inhibitory activity of isolated compound 1 and 2 from <i>Justicia insularis</i> on CIS-A2780, OVCAR-8 and OVCAR-4 cell lines.....	114
Figure 3. 12: Trypan blue exclusion viability test for compound 1 on ovarian cancer cell lines: CIS-A2780 (A) and OVCAR-8 (B).. .....	117
Figure 3. 13: Morphological effects of compound 1 on CIS-A2780 ovarian cancer cell line at different concentrations (10 and 20 $\mu$ M) and time points (48 and 72 h) using light microscopy.....	119

Figure 3. 14: Morphological effects of compound 1 on OVCAR-4 ovarian cancer cell line at different times (48 and 72 h) and concentrations (10 and 20  $\mu$ M) using light microscopy..... 120

Figure 3. 15: Fluorescence microscopy images of CIS-A2780 cells showing morphological changes in the nucleus and actin filament in response to drug treatment..... 122

Figure 3. 16: Fluorescence microscopy images of OVCAR-8 cell line taking with 40x objective lens, showing morphological changes in the nucleus and actin filament in response to drug treatment..... 123

Figure 3. 17: Caspase 3/7/ apoptosis activities by compound 1 on ovarian cancer cell lines (CIS-A2780, OVCAR-8 and OVCAR-4)..... 125

Figure 3. 18: Effect of compound 1 on caspase 8 activity (initiator caspase) in ovarian cancer cell lines (CIS-A2780, OVCAR-8 and OVCAR-4).. ..... 127

Figure 3. 19: Caspase 9 activity (initiator caspase) effect of compound 1 on ovarian cancer cell lines (CIS-A2780 and OVCAR-8).. ..... 129

Figure 3. 20: Representative samples of the flow cytometry graph of CIS-A2780 cell line treated with compound 1 and the positive control (Cbp) at different concentrations..... 131

Figure 3. 21: Representative samples of the flow cytometry graph of OVCAR-8 cell line treated with compound 1 and the positive control (Cbp) at different concentrations..... 132

Figure 3. 22: Evaluation of apoptotic activities of compound 1 on CIS-A2780 (A) and OVCAR-8 (B) cells using annexin V and propidium iodide staining analysed with flow cytometry.. ..... 133

Figure 3. 23: Activeness of mitochondrial membrane potential of CIS-A2780 ovarian cancer cell line in response to treatment with compound 1..... 135

---

Figure 3. 24: Flow cytometry representative sample graphs of CIS-A2780 cell line showing number of cells in each cell cycle phase in response to treatment with compound 1 and the positive control (Cbp) for 48hrs.....	137
Figure 3. 25: Representative samples of the flow cytometry graph of OVCAR-8 cell line showing number of cells in each cell cycle phase in response to treatment with compound 1 for 48hrs.....	138
Figure 3. 26: Effects of compound 1 on the cell cycle of ovarian cancer cells..	139
Figure 3. 27: Optimal standard curve generated with 5-mC standard positive control ....	140
Figure 3. 28: Percentage of 5-methylcytosine DNA methylation in CIS-A2780 treated with compound 1 and 5-azacytidine..	141
Figure 3. 29: Percentage of gene specific promoter methylation of <i>MLH1</i> (A), <i>HOXA9</i> (B), <i>PTEN</i> (C) <i>APC</i> (D), <i>TP53</i> (E), <i>KLF6</i> (F) and <i>RASSF1</i> (G) genes in ovarian cancer cell line (CIS-A2780) in response to treatment with compound 1 using 5'azacytidine as positive control..	143
Figure 3. 30: Representative samples of pyrosequencing CpG pyrogram reports of <i>MLH1</i> gene on CIS-A2780 cells..	144
Figure 3. 31: Representative samples of pyrosequencing CpG pyrogram reports for <i>HOXA9</i> and <i>PTEN</i> genes on CIS-A2780 cells..	145
Figure 3. 32: Representative samples of pyrosequencing CpG pyrogram reports of <i>APC</i> and <i>PP53</i> genes on CIS-A2780 cell line.....	146
Figure 3. 33: Representative samples of pyrosequencing CpG pyrogram reports of <i>KLF6</i> and <i>RASSF1</i> genes on CIS-A2780 cell line..	147
Figure 3. 34: DNMT inhibitory activities of compound 1 using the nuclear extracts of CIS-A2780 and OVCAR-4 cell lines..	149

Figure 3. 35: Modulation of DNMTs expression in response to treatment with compound 1 and 5'azacytidine using RT-qPCR..... 150

Figure 3. 36: Modulation of the expression of different tumour suppressor genes in response to treatment with compound 1 and 5'azacytidine using RT-qPCR.. ..... 151

Figure 4. 1: Mean concentration response curve of the growth inhibitory activity of Andr (A), Tpl (B) and Ptx (C) against ovarian cancer cell lines (CIS-A2780, OVCAR-8, and OVCAR-4) and HOE..... 163

Figure 4. 2: Trypan blue exclusion test for Andr and Tpl cytotoxicity on CIS-A2780 (A) and OVCAR-8 (B) cell line at different concentrations for 48 hours..... 166

Figure 4. 3: Effects of Andr and Tpl on the morphology of CIS-A2780 ovarian cancer cell line at time (48 and 72 h) and concentration dependent manner using light microscopy.. ..... 168

Figure 4. 4: Morphological effects of Andr and Tpl on OVCAR-4 ovarian cancer cell line at time (48 and 72 hours) and concentration dependent manner using light microscopy..... 169

Figure 4. 5: Morphological changes in the nuclear and actin filament of CIS-A2780 cells in response to treatment with Andr, Tpl and Ptx using fluorescence microscopy..... 171

Figure 4. 6: Morphological effects of Andr, Tpl and Ptx on the nuclear and actin filament of OVCAR-8 using fluorescence microscopy.. ..... 172

Figure 4. 7: Change in caspase 3/7 activity in response to Andr and Tpl on ovarian cancer cell lines: CIS-A2780 (A) and OVCAR-8 (B) for 48 hours.. ..... 174

Figure 4. 8: Caspase 8 activity effect of Andr and Tpl on CIS-A2780 (A) and OVCAR-8 (B) ovarian cancer cell lines.. ..... 175

Figure 4. 9: Effects of Andr and Tpl on caspase 9 activity on ovarian cancer cell lines: CIS-A2780 (A) and OVCAR-8 (B) for 48 hours using Ptx as positive control.. ..... 177

Figure 4. 10: Representative samples of the flow cytometry graph of CIS-A2780 cell line treated with diterpenoids (Andr and Tpl) and the positive control (Ptx) at two different concentrations..	179
Figure 4. 11: Representative samples of the flow cytometry graph of OVCAR-8 cell line treated with diterpenoids (Andr and Tpl) and the positive control (Ptx) at two different concentrations..	180
Figure 4. 12: Flow cytometry analysis of the apoptotic activity of diterpenoids (Andr and Tpl) and positive control (Ptx) in CIS-A2780 cells (A) and OVCAR-8 using annexin V and propidium iodide staining..	181
Figure 4. 13: Effect of Andr and Tpl on the mitochondrial membrane potential activity in CIS-A2780 ovarian cancer cell line..	183
Figure 4. 14: Representative samples of the flow cytometry graph of CIS-A2780 (A) and OVCAR-8 (B) cell lines showing number of cells in each cell cycle phase in response to treatment with diterpenoids (Andr and Tpl) and the positive control (Ptx).....	186
Figure 4. 15: Cell cycle analysis of CIS-A2780 (A) and OVCAR-8 (B) cell lines in response to treatment with diterpenoids (Andr and Tpl) and positive control (Ptx) using propidium iodide staining..	187
Figure 4. 16: Percentage of 5-methylcytosine DNA methylation in CIS-A2780 treated with Andr and Tpl, and Aza (positive control)..	189
Figure 4. 17: CpG methylation pyrograms of <i>MLH1</i> gene in CIS-A2780 cells. Control (A), and Andr (B), Tpl (C) and Aza (D) treated representative samples. ....	190
Figure 4. 18: CpG methylation pyrograms of <i>HOXA9</i> gene in CIS-A2780 cells. Control (A), and Andr (B), Tpl (C) and Aza (D) treated representative samples.....	191
Figure 4. 19: CpG methylation analysis of <i>MLH1</i> (A) and <i>HOXA9</i> (B) genes in CIS-A2780 cell line after treatment with Andr and Tpl.....	192

---

Figure 4. 20: DNMT inhibitory activities of Andr and Tpl on the nuclear extracts of CIS-A2780 (A) and OVCAR-4 (B) cell lines..	193
Figure 4. 21: Modulation of <i>DNMTs</i> expression in response to treatment with Andr and Tpl using RT-qPCR..	195
Figure 4. 22: Modulation of the expression of different tumour suppressor genes in response to drug treatment..	196
Figure 5. 1: Mean concentration-response curve of antiproliferative activities of SLs and Aza on CIS-A2780, OVCAR-8 and OVCAR-4 cell lines.....	209
Figure 5. 2: Trypan blue exclusion cytotoxic test for four SLs (Deh, Pat Cos and Ala) against CIS-A2780 ovarian cancer cell line at different concentrations (5, 10 and 20 $\mu$ M) and time point 24 h (A), 48 h (B) and 72 hr (C)..	212
Figure 5. 3: Trypan blue exclusion test for four SLs (Deh, Pat Cos and Ala) against OVCAR-8 ovarian cancer cell line at different concentrations (5, 10 and 20 $\mu$ M) and time point 24 h (A), 48 h (B) and 72 hr (C)..	213
Figure 5. 4: Trypan blue exclusion test for SLs (Deh, Pat Cos and Ala) against OVCAR-4 ovarian cancer cell line at different concentrations (5, 10 and 20 $\mu$ M) and time point 24 h (A), 48 h (B) and 72 hr (C)..	214
Figure 5. 5: Morphological effects of SLs (Deh, Pat, Cos and Ala) and Aza on CIS-A2780 cells at time (48 and 72h) and concentration dependent manner using light microscopy..	216
Figure 5. 6: Morphological effects of SLs (Deh, Pat, Cos and Ala) and Aza on OVCAR-4 cells at time (48 and 72h) and concentration dependent manner using light microscopy..	217

Figure 5. 7: Fluorescence microscopy images of CIS-A2780 cell line taking with 40x objective lens, showing morphological changes in the nucleus and actin filament in response to drug treatment..... 219

Figure 5. 8: Fluorescence microscopy images of OVCAR-8 cell line showing morphological changes in the nucleus and actin filament in response to drug treatment. Images were taking with 40x objective lens..... 220

Figure 5. 9: Effect of SLs (Deh, Pat, Cos and Ala) on caspase 3/7 activity in ovarian cancer cell lines; CIS-A2780 (A), OVCAR-8 (B) and OVCAR-4 (C)..... 222

Figure 5. 10: Caspase 8 activity caused by four SLs (Deh, Pat, Cos and Ala) on ovarian cancer cell lines CIS-A2780 (A), OVCAR-8 (B) and OVCAR-4 (C)..... 225

Figure 5. 11: Effect of four SLs (Deh, Pat, Cos and Ala) on caspase 9 activity in ovarian cancer cell: CIS-A2780 (A), OVCAR-8 (B) and OVCAR-4 (C).. ..... 227

Figure 5. 12: Representative samples of flow cytometry graph of CIS-A2780 cell line treated with four SLs (Deh, Pat, Cos and Ala) and Aza, and stained with annexin V and propidium iodide..... 229

Figure 5. 13: Representative samples of flow cytometry graph of OVCAR-8 cell line treated with SLs (Deh, Pat, Cos and Ala) and the positive control (Aza) using annexin V and propidium iodide staining.. ..... 230

Figure 5. 14: Flow cytometry analysis of the apoptotic activities of SLs (Deh, Pat, Cos and Ala) and Aza using annexin V and propidium iodide staining..... 231

Figure 5. 15: Flow cytometry graph of representative samples of CIS-A2780 cell line treated with SLs (Deh, Pat, Cos and Ala) and Aza using DiIC1(5) staining..... 233

Figure 5. 16: Flow cytometry analysis of the mitochondrial membrane potential activity of the four SLs (Deh, Pat, Cos and Ala) and Aza in CIS-A2780 ovarian cancer cell line using DiIC1 (5) stain.. ..... 234

Figure 5. 17: Representative samples of flow cytometry graph of the cell cycle effects of SLs (Deh, Pat, Cos and Ala) and Aza on CIS-A2780 cells using propidium iodide staining. .... 236

Figure 5. 18: Representative samples of flow cytometry graph of the cell cycle effects of SLs (Deh, Pat, Cos and Ala) and the positive control (Aza) on OVCAR-8 cells using propidium iodide staining. .... 237

Figure 5. 19: Flow cytometry analysis of the cell cycle activity of SLs (Deh, Pat, Cos and Ala) and Aza on CIS-A2780 cell line (A) and OVCAR-8 cell line (B) using propidium iodide staining..... 238

Figure 5. 20: Quantification of 5-methylcytosine DNA methylation in ovarian cancer cells, CIS-A2780 (A) and OVCAR-4 (B) treated with the SLs (Deh, Pat, Cos and Ala). Aza was used as positive control and media was used as negative control (without drug).. ..... 240

Figure 5. 21: Percentage of gene specific promoter methylation of ovarian cancer cell line (Cis-A2780) in response to drug treatment, using 5'azacytidine as positive control.. ..... 241

Figure 5. 22: Representative samples of pyrosequencing CpG pyrogram report for *MLH1* gene on CIS-A2780 cell line. Control (A), Deh (B), Ala (C), Pat (D), Cos (E) and Aza (F). .... 242

Figure 5. 23: Representative samples of pyrosequencing CpG pyrogram report for *HOXA9* gene on CIS-A2780 cell line. Control (A), Deh (B), Ala (C), Pat (D), Cos (E) and Aza (F). .... 243

Figure 5. 24: Representative samples of CpG pyrogram report for *TP53* gene on CIS-A2780 cell line. Control (A), Deh (B), Ala (C), Pat (D), Cos (E) and Aza (F). .... 244

Figure 5. 25: Bradford protein standard curve generated with bovine serum albumin (BSA). .... 245

Figure 5. 26: DNMT inhibitory activities of the SLs (Deh, Pat, Cos and Ala) on CIS-A2780 (A) and OVCAR-4 (B) cell lines.. ..... 246

Figure 5. 27: Modulation of *DNMTs* expression in response to treatment with SLs and Aza using RT-qPCR..... 248

Figure 5. 28: Down and up-regulatory activities of SLs and Aza on the expression of tumour genes using RT-qPCR.. ..... 249

---

**List of Tables**

Table 2. 1: Summary list of reagents used, showing their catalogue numbers and supplying companies .....	57
Table 2. 2: Forward, reversed and sequencing primers used for pyrosequencing assay and their annealing temperatures .....	84
Table 2. 3: Primers used for RT-qPCR and their annealing temperatures.....	88
Table 3. 1: The <i>in vitro</i> half maximal growth inhibitory concentration (IC <sub>50</sub> ) values of <i>J. insularis</i> extracts and fractions against ovarian cancer (CIS-A2780, OVCAR-8 and OVCAR-4) cell lines using SRB assay.....	99
Table 3. 2: The results of the growth inhibitory activities of EA fractions and EA4 sub-fractions of <i>J. insularis</i> on OVCAR-4 ovarian cancer cell line.....	101
Table 3. 3: Side by side comparison of <sup>13</sup> CNMR spectra of isolated compound 1 and 2 from this study with <sup>13</sup> CNMR literature data.....	111
Table 3. 4: Side by side comparison of <sup>1</sup> HNMR spectra of isolated compound 1 and 2 from this study with <sup>1</sup> HNMR literature data.....	112
Table 3. 5: Results of the antiproliferative activities of <i>J. insularis</i> isolated compound 1 and 2 through inhibition of growth in ovarian cancer (CIS-A2780, OVCAR-8 and OVCAR-4) cell lines.....	115
Table 4. 1: The growth inhibitory activities (IC <sub>50</sub> ) of Andr and Tpl against ovarian cancer (CIS-A2780, OVCAR-8, and OVCAR-4) cell lines and HOE using SRB assay.....	164
Table 5. 1 Results of the antiproliferative activities of SLs and Aza on ovarian cancer cell lines (CIS-A2780, OVCAR-8 and OVCAR-4) and HOE cell line using cell growth inhibitory assay.....	210

---

**Abbreviations**

5-hmC	5-hydroxymethylcytosine
5-mC	5-methylcytosine
AFLP	Amplified fragment length polymorphism
Ala	Alantolactone
Andr	Andrographolide
Apaf-1	Apoptosis activating factor 1
APC	APC regulator of WNT signalling pathway
Aza	5-azacytidine
Bax	Bcl-2 associated X protein
Bcl-2	B-cell lymphoma protein 2
BLAST	Basic local alignment search tool
<i>BRAF</i>	B-Raf proto-oncogene, serine/threonine kinase
<i>BRCA1</i>	Breast cancer type 1 susceptibility gene
BSTFA	N,O-bis(trimethylsilyl) trifluoroacetamide)
Caspase	Cysteine aspartic protease
Cbp	Carboplatin
Cos	Costunolide
CTNNB1	Catenin beta 1
DAPI	4', 6-diamidino-2-phenylindole
Deh	Dehydroleucodine
DISC	Death inducing signalling complex
DMSO	Dimethyl sulfoxide
DNA	Deoxyribonucleic acid
DNMT	DNA methyltransferase

---

dNTP	Deoxyribonucleotide triphosphate
EGCG	Epigallocatechin-3-gallate
ELISA	Enzyme linked immunosorbent assay
Fas	Fas cell surface death receptor
FasL	Fas Ligand
FBS	Fetal bovine serum
FDA	Food and drug administration
FITC	Fluorescein isothiocyanate
<i>FOLR1</i>	Folate receptor 1
GATA4	GATA binding protein 4
GC MS	Gas chromatography mass spectrometry
HAT	Histone acetyltransferase
HDAC	Histone deacetylase
HDM	Histone demethylase
HLMT	Histone lysine methyltransferase
HMT	Histone methyltransferase
HOE	Human ovarian surface epithelial
<i>HOXA9</i>	Homeobox A9
HPLC	High performance liquid chromatography
IC <sub>50</sub>	50% inhibitory concentration
JI-EA4	<i>Justicia insularis</i> ethyl acetate fraction 4
JI-EA4-6	<i>Justicia insularis</i> sub-fraction 6 of ethyl acetate fraction 4
<i>KIF14</i>	Kinesin family member 14
<i>KLF6</i>	Kruppel like factor 6
<i>KRAS</i>	KRAS proto-oncogene, GTPase

LC MS	Liquid chromatography mass spectrometry
LINE	Long interspersed nuclear element
LUMA	Luminometric methylation assay
MDS	Myelodysplastic syndrome
miRNA	micro ribonucleic acid
<i>MLH1</i>	MutL homolog 1
mRNA	Messenger ribonucleic acid
NF- $\kappa$ B	Nuclear factor kappa B
NMR	Nuclear magnetic resonance
PI3K	Phosphatidylinositol 3-kinase
PARP	Poly ADP(Adenosine-diphosphate)- ribose polymerase
Pat	Parthenolide
PCR	polymerase chain reaction
PENSTREP	Penicillin streptomycin
PI	Propidium iodide
PKB/AKT	Protein kinase B
PS	Phosphatidylserine
<i>PTEN</i>	Phosphatase and tensin homolog
Ptx	Paclitaxel
<i>RASSF1</i>	Ras associated domain family member 1
RFLP	Restriction fragment length polymorphism
RNA	Ribonucleic acid
RPMI	Roswell Park Memorial Institute
RT-qPCR	Quantitative reverse transcription polymerase chain reaction
SI	Selectivity index

SLs	Sesquiterpene lactones
SRB	Sulforhodamine B
TAE	Tris-acetate-EDTA
TCA	Trichloroacetic acid
TET	Ten-eleven translocation
TFA	Trifluoroacetic acid
TNF	Tumour necrosis factor
tNGBS	Targeted next generation bisulfite sequencing
<i>TP53</i>	Tumour protein p53
Tpl	Triptolide
<i>TUSC3</i>	Tumour suppressor candidate 3
VEGFA	Vascular endothelial growth factor A
WIF1	WNT inhibitory factor 1

## **Acknowledgements**

I thank God for the privilege and grace to complete this study, because the past four years of this study has been a challenging period. I would like to acknowledge the Nigerian Government for the sponsorship through Tertiary Education Trust Fund (TETFUND) and my Institution (Adeyemi College of Education, Nigeria) to undertake my PhD programme at Keele University, UK.

I would like to tender my special appreciation to my lead supervisor; Dr. Wen-Wu Li for his relentless effort towards the supervision of this study. His mentorship role culminated in my outstanding research work and dissemination of results at various conferences/symposia. I would also want to acknowledge his immense effort in providing me with necessary trainings on the use of GC-MS and HPLC and also for helping with NMR and LC-MS data analysis. Likewise, I am most grateful to my co-supervisor; Prof. Nicholas Forsyth, for his wealth of knowledge, expertise and guidance throughout the period of this study. Much thanks to my advisor; Prof. Paul Horrocks for his immense support when I needed him most, and for his relentless effort towards ensuring that I complete my study at Keele University, even at the time of extreme financial challenges.

Furthermore, I would like to appreciate the effort of other contributors for the trainings and expertise guidance without which this research would have been an illusory and my research experience and expertise wouldn't have been complete. Therefore, I am grateful to Dr. Mark Kitchen for his immense contributions and trainings on designing of gene specific primers for pyrosequencing, bisulfite conversion assay and pyrosequencing technique. His expertise and wealth of experience on the use of pyrosequencing was really helpful. I really appreciate Prof. Tim Claridge and Dr. James McCullagh / Elisabete Pires (Oxford University) who helped with NMR and LC-MS measurements of my isolated compounds respectively. I am

really grateful to Dr. Vinoj George for his guidance on primer design for RT-qPCR. I really appreciate Dr. Okiemute Rosa Johnson-Ajinwo and Sara Maarfia (visiting PhD student from Algeria) for the training given to me on cancer cell culture assay. Also the plant material investigated in this study was provided by Dr. Okiemute Rosa Johnson-Ajinwo. I really appreciate Katy Cressy for training on flow cytometry and qPCR, and her immense help and support with John Misra on ordering of reagents and materials used in this study. I also appreciate Prof. Nicholas Forsyth's research group members for support especially Rakad Mohammed Al-Jumaily who provided the DNMT primers used in this study and for his guidance on DNA extraction and DNA methylation study. I am also grateful for the support I received from Dr. Alan Richardson's research group especially the support of Mohammed Jawad, Dr. Emily Crowley and Suad Ibrahim in the area of cell cytotoxicity, apoptosis assays and protein quantification. I acknowledge the support I also received from my colleague namely; Vibin Alageswaran for his help with fluorescence imaging.

I really appreciate the supports I received from the staff of Biology Department, Adeyemi College of Education, Nigeria, most especially Mr Sanni Rafiu and my Head of Department; Dr. Omolara Awe for their immense support and guidance. I would also like to appreciate my pastors: Pastor Olorunfemi Samson and Pastor Marcus Chilaka for their encouragement.

Finally, I am grateful to my family most especially my wife; Sola Victoria Fadayomi and children; Emmanuella and Davina for their sacrifice and moral support during my study. I also appreciate the love and support shown by my mother and siblings. I would not take for granted the love and support shown by my family friends. Thanks to the families of Jacob Oluwafemi and Adekolurejo Oloyede for their love and support.

# **Chapter One**

## **Introduction**

## **1.1 Cancer**

Cancer is a group of diseases that have the characteristics of uncontrolled cell growth and spread of abnormal cells which leads to mass of cells generally referred to as tumour, and this condition could subsequently lead to death if not controlled (American Cancer Society, 2016). Uncontrolled cell growth usually leads to a progressive increase in the number of cells undergoing mitotic division that eventually develop into tumour. The process of transformation of normal cells into neoplastic state is known to be a multistep phenomenon, and this has been initially categorized into six hallmarks including their ability to: sustain proliferative signalling, escape growth suppressors, escape programmed cell death, induce limitless replicative potential, induce angiogenesis and activate cell invasion and metastasis (Hanahan and Weinberg, 2000). However, progress in cancer research over a decade has identified reprogramming of metabolic energy and escaping of immune destruction as part of the hallmarks of cancer formation, and the underlying mechanism of all these multi-steps are genomic instability and inflammation by innate immune cells (Figure 1.1) (Hanahan and Weinberg, 2011). Normal human cells except stem cells have limited replicative potential which is usually between 60-70 divisions before becoming senescent due to loss of telomere function. However, cancer cells have limitless replicative potential acquired through their self-sufficient growth signals, insensitivity to antigrowth signals and resistance to apoptosis (Hanahan and Weinberg, 2000). This abnormal growth in cells could affect different body organs or tissues such as lung, colon, breast, prostate, colon, liver, blood, brain, thyroid and ovaries etc. These tumours could be classified into: carcinoma, sarcoma, lymphomas and leukaemia based on the tissue type of origin.



**Figure 1. 1: Multistep processes of cancer formation featuring genetic instability and inflammation by innate immune cells as underlying mechanisms** (Hanahan and Weinberg, 2011).

### 1.1.1 Worldwide incidence of cancer and severity

Cancer is one of the most feared diseases of the 20th century with fast increasing incidence in the 21st century (Balachandran and Govindarajan, 2005). It is a serious deadly disease among the population all over the world, affecting both developing and developed countries (Sharmila and Padma, 2013; Pop *et al.*, 2019). It is the second leading cause of death globally and its mortality is projected to be more than double in the next 20-40 years (Amin *et al.*, 2009; Thun *et al.*, 2010; Busch *et al.*, 2015). Millions of diagnoses are made every year with increasing death all over the world (Sharmila and Padma, 2013). In 2018, the estimated incidence of cancer worldwide was 17 million with about 9.6 million death (Bray *et al.*, 2018; Ferlay *et al.*, 2019). In the United States, cancer is the second leading cause of death and accounts for 25% of the death in humans (Balachandran and Govindarajan, 2005; Subramaniam *et al.*, 2014). The estimated incidence of new cancer cases in the United States

was about 1.8 million with 606, 520 deaths (Siegel, Miller and Jemal, 2020). In the UK, the yearly incidence of cancer between 2015-2017 was about 367,000, the yearly incidence has been projected to increase to 513,951 by 3035 (Cancer Research UK, 2018). The burden of cancer is gradually increasing in Africa, about 715,000 cases and 542,000 deaths were recorded in 2008, the number of new cancer cases and deaths have increased to 1,055,172 and 693,487 respectively in 2018 (IARC, 2020). In 2018, 115,950 new cases and 70,327 cancer deaths were recorded in Nigeria (IARC, 2019). Cancer still remains a disease with an increasing incidence worldwide.

## **1.2 Ovarian cancer**

Ovarian cancer begins when the cells of the ovaries grow uncontrollably thereby leading to mass of cells called neoplasm. The ovaries are the female reproductive organ that produces the eggs and also serve as the main source of oestrogen and progesterone hormones in female (American Cancer Society, 2016). The ovary is made up of three different kinds of cells that develop into different ovarian cancer. These include; epithelia ovarian tumour that develops from the cells that cover outer surface of the ovary, the germ cell tumours develop from egg producing cells and the stromal tumour arise from the tissues that hold the ovaries together (Gyparaki and Papavassiliou, 2015; American Cancer Society, 2016). These tumours are either benign or malignant. The malignant epithelial ovarian cancer known as the ovarian carcinomas accounts for 85% to 90% of ovarian cancers (SIGN, 2013). Furthermore, there are different treatment options for ovarian cancer, which include: surgery, chemotherapy, radiotherapy and targeted therapy. But the choice of treatment depends mainly on the type and stage of the cancer (American Cancer Society, 2016). However, a combination of chemotherapy with surgery or radiotherapy is often used when it has metastasised beyond the ovaries (Cancer Research UK, 2020). Drugs resistant and

ovarian cancer relapses after initial sensitivity have been a great challenge in the treatment of ovarian cancer (Gyparaki and Papavassiliou, 2015).

### **1.2.1 Ovarian cancer incidence and severity**

In all over the world, ovarian cancer is the most severe of the gynaecological malignancy associated with the highest level of lethality due to lack of efficient screening method and also lack of early symptoms (Odukogbe *et al.*, 2004; Banerjee and Kaye, 2011; Colombo *et al.*, 2014; Haaften *et al.*, 2015; Dong, Lu and Lu, 2016). Each year, ovarian cancer is diagnosed in about quarter of a million women worldwide, and stands as the seventh commonest and seventh leading cause of cancer mortality among women with around 156,600 mortality estimate figure on yearly basis (Zuberi *et al.*, 2015; Reid, Permeth and Sellers, 2017; Torre *et al.*, 2018; Momenimovahed *et al.*, 2019). In 2018, worldwide incidence of ovarian cancer was 295,414 new cases (Bray *et al.*, 2018). Torre *et al.* (2018) further established that ovarian cancer incidence and death in the less developed worlds were higher than in the developed world.

Ovarian cancer is the fifth leading cause of cancer lethality in the United States with about 14,070 deaths and 22,240 new cases estimated in 2018 (American Cancer Society, 2018; Torre *et al.*, 2018). In the United Kingdom, it is the 6<sup>th</sup> most frequent cancer among females with about 20 diagnoses every day between 2014-2017, given a yearly diagnosis of around 7,400 new cases. It is known to be the 6<sup>th</sup> cause of cancer death among females with about 4,116 deaths record in 2017 (Cancer Research UK, 2020). In 2014, 7378 new cases were reported which shows there were 23 new cases among 100,000 women, this has been projected to increase by 15% by 2035, resulting in 32 new cases among 100,000 females and the death rate was also projected to reduce by 37% by 2035 (Cancer Research UK, 2020). It is rare among women under the age of 30 years, but with occurrence increasing

with age (SIGN, 2013). Increased risk factors of ovarian cancer include the following: increase in age, obesity after menopause, family of ovarian and breast cancer and women with breast cancer. Also, pregnant women, breastfeeding mothers and women that use control pills and contraceptive injections have lower risk of ovarian cancer (American Cancer Society, 2016).

### **1.2.2 Aetiological and risk factors of ovarian cancer**

Ovarian cancer is associated with several risk factors known to influence its incidence worldwide. Factors that could increase the risk of ovarian cancer include asbestos, tobacco smoking, age at menopause, hormone replacement therapy (HRT), talcum powder, infertility, medical conditions such as overweight and obesity, endometriosis, diabetes type 1 and 2. However, the use of oral contraceptives have been reported to lower the risk to ovarian cancer by 25-28%, longer breastfeeding reduces the risk of epithelial ovarian cancer by about 24%, multiparity also have synergistic relationship with breastfeeding in the reduction of individual risk to ovarian cancer (Burghaus *et al.*, 2017; Reid, Permeth and Sellers, 2017; Cancer Research UK, 2020). Sung *et al.* (2016) reported that the synergy between first birth and breastfeeding for less than six month reduced the risk to epithelia ovarian cancer by 40%. Zhang, Binns and Lee (2002) have also reported that frequent and long-time consumption of tea especially green tea could reduce the risk of ovarian cancer. Other factors that have been known to reduce the risk of ovarian cancer include; pregnancy, hysterectomy, tubal ligation (Soegaard *et al.*, 2007; Salehi *et al.*, 2008). Even though the aetiological cause of ovarian cancer remains unclear, the risk of women with family history of breast cancer and ovarian cancer remains very high, which suggest that genetic predisposing genes such as oncogenes and tumour suppressor genes play a major role in the aetiology of ovarian cancer (Salehi *et al.*, 2008; Wentzensen *et al.*, 2016).

### 1.2.3 Ovarian cancer types, therapy and associated genetic mechanism

Ovarian cancers are generally classified into epithelia, germ cell, sex cord stromal and borderline ovarian tumours, and epithelial and germ cell ovarian tumours are the most and rarely common types respectively. Furthermore, ovarian cancer can be categorized into two basic groups, type I and type II (Dong, Lu and Lu, 2016). Type I are the slow growing tumours with mutation in *KRAS*, *PTEN* *BRAF* *AND* *CTNNB1* etc. The type II ovarian cancer progress to high grade serous carcinomas at a faster rate and they are the common subtype of ovarian cancer with 70% to 80% of all the epithelial ovarian cancer cases (Gyparaki and Papavassilious, 2015; Dong, Lu and Lu, 2016; Tomar *et al.*, 2016). From the molecular point of view, the type I low grade tumours are stable genetically, while the high-grade cancers are characterized with high genomic instability usually with *P53* mutation in over 90% or even 100% diagnosis (Colombo *et al.*, 2014; Gyparaki and Papavassilious, 2015). The various subtypes of ovarian cancer with different molecular aetiology are currently been grouped together as a single entity and are treated the same way; however, treatment still depends on the cancer stage of progression. If it is still confined to the ovary (Stage 1), it can be removed surgically, but if it has metastasized beyond the ovaries but limited to the pelvis (Stage 2), metastasized beyond the pelvis to the abdominal cavity (Stage 3) and when it has moved to other body organ like liver, lung (Stage 4), chemotherapy and surgery are basically employed in the three later stages (Colombo *et al.*, 2014; Gyparaki and Papavassilious, 2015; Cancer Research UK, 2019). The two most common drugs that are currently been used in chemotherapy for ovarian cancer treatment are carboplatin and paclitaxel, however, cancer cells have started showing some resistance to chemotherapeutic drugs in recent times, as the drugs efficiency in treating cancer has reduced, this has posted a threat to the treatment of ovarian cancer, hence the need to explore alternative treatment methods for ovarian cancer (Banjerjee and Kaye; Colombo *et al.*, 2014; Johnson *et al.*, 2014;

Earp and Cunningham, 2015; Gyparaki and Papavassiliou, 2015). Recent research on ovarian cancer has shown that it is not a single entity but heterogeneous disease. The understanding of the biology and molecular changes in ovarian cancer has offered a new way to ovarian cancer treatment, which promises to be more effective. The most effective of this development is the strategy that is targeted towards inhibition of angiogenesis using bevacizumab and polyadenosine diphosphate-ribose polymerase (PARP) inhibitors such as Olaparib, Niraparib and rucaparib (Robison *et al.*, 2013; Colombo *et al.*, 2014; Schmid and Oehler, 2014; Cancer Research UK, 2020). Furthermore, research is also focused on the use of inhibitors of growth factor signalling or folate receptor inhibitors and immunotherapeutic approaches in ovarian cancer treatment (Cortez *et al.*, 2017).

### **1.3 Epigenetics and cancer formation**

Epigenetics deals with the study of heritable changes in gene expression that does not affect the sequence of the genetic material (Gyparaki and Papavassiliou, 2015). Epigenetic changes encompass methylation of DNA, microRNAs, nucleosome remodelling and histone modifications (Dawson and Kouzarides, 2012; Pop *et al.*, 2019). The epigenetic mechanisms are regulated by distinct proteins that are capable of modifying the arrangement and add or remove some functional groups from the genetic material without changing in the gene sequence, thereby subsequently modulating gene expression (Pop *et al.*, 2019). Recent research has focused on the relationship between epigenetics and cancer formation. Tumour initiation and progression have been known to be aided by the DNA methylation of the CpG islands of the promoter region of tumour suppressor gene which is the best studied epigenetic modification in cancer, and this is present in about 70% of all mammalian promoters (Dawson and Kouzarides, 2012). However, hypomethylation of the promoter region of genes are believed to induce proto-oncogenes activation and hypermethylation of

the promoter region of notable tumour suppressor genes such as *RASSF1A*, and *PTEN* etc is strongly associated with silencing of specific gene expression (Zuberi *et al.*, 2015; Notaro *et al.*, 2016). Although, global DNA hypomethylation is frequently noticed in most malignant cells, likewise, DNA hypermethylation is frequently observed in the CpG islands of specific promoter regions of tumour suppressor and apoptotic genes thereby silencing their expression (Amin *et al.*, 2009; Busch *et al.*, 2015). CpG islands are commonly altered during tumour formation and play a prominent role in transcriptional regulation (Baylin and Jones, 2012; Dawson and Kouzarides, 2012).

The molecular understanding of these epigenetic changes is the hallmark of research in recent years, so that its potential in cancer treatment can be fully elucidated (Stresemann *et al.*, 2006; Gyparaki and Papavassiliou, 2015). Since epigenetic modification of the DNA such as DNA methylation, histone modifications are generally reversible in nature unlike gene mutation, epigenetic modifications have therefore become target approach as alternative method for cancer treatment including ovarian (Erdmann *et al.*, 2015; Tomar *et al.*, 2016; Montgomery and Srinivasan, 2019). The different epigenetic mechanisms could be targeted with the use of plant derived natural products with pharmacological relevance for cancer treatment (Jasek *et al.*, 2019; Pop *et al.*, 2019).

### **1.3.1 DNA methylation**

The first described covalent modification of the DNA and the most extensively characterized chromatin modification is DNA methylation (Dawson and Kouzarides, 2012). It is an epigenetic alteration that changes gene expression without subsequent changes in the sequence of the genetic material that is the DNA (Fahy *et al.*, 2012; Erdmann *et al.*, 2015). In this phenomenon, a methyl group is added to the 5-carbon on cytosine nucleotide of the DNA thereby silencing the expression of tumour suppressor genes, and this process

is catalysed by an enzyme called DNA methyl-transferases (DNMTs) (Earp and Cunningham, 2015; Kurdyukov and Bullock, 2016; Jasek *et al.*, 2019; Tomasetti *et al.*, 2019). The human genome is made up of about five types of *DNMT* genes, which are *DNMT1*, *DNMT2*, *DNMT3A*, *DNMT3B* and *DNMT3L* which codes for proteins with specific functions (Cui and Xu, 2018). The *DNMT3A*, *DNMT3B* have been grouped together and usually known as de novo DNMTs and they are responsible for producing new DNA methylation, In contrast, *DNMT1* which is located at the replication fork, is known to be responsible for the maintenance of DNA methylation by ensuring that the newly synthesised DNAs from the parent strands are methylated after replication, the *DNMT2* which is known to be the smallest DNMT in mammals, is believed to play an active role in recognition of DNA damage, recombination and repair of mutated DNA (Stresemann *et al.*, 2006; Fahy *et al.*, 2012; Subramaniam *et al.*, 2014; Zhang and Xu, 2017). DNMTs have two regions, the C-terminal and the N-terminal regulatory domains through with these proteins interact with the DNA. However, *DNMT2* does not have the regulatory N-terminal region but composed mainly of the C-terminal domain (Kadayifci, Zheng and Pan, 2018). In cancer tissues and cell, the level of DNMTs, most especially *DNMT3B*, *DNMT3A* and *DNMT3L*, are known to be high, this may be associated with the hypermethylation of the CpG rich region of the promoter of various tumour suppressor genes in malignant cancer (Subramaniam *et al.*, 2014). CpG dinucleotides are located in the CpG islands occurring at about 60% of all gene promoter regions in repeated sequences, and if there is methylation in the promoter CpG islands, the genes will not be expressed as a result of failure of transcription factors to recognise the promoter site (Fahy *et al.*, 2012; Monticelli, 2019). DNA methylation is known to be important in embryonic development, inactivation of X-chromosome, genetic imprinting etc. However, the inability to maintain DNA methylation, thereby causing aberrant methylation patterns that do cause under-expression and

overexpression of certain proteins is the hallmark mechanism that ultimately results in diverse diseases including cancer (Esteller, 2008; Tellez-plaza *et al.*, 2014; Hervouet *et al.*, 2018). In research, inhibition of DNMT enzymatic activities has led to decrease in tumour formation through the re-expression of suppressed tumour suppressor genes (Subramaniam *et al.*, 2014). Milutinovic *et al.* (2004) confirmed that the knock down of DNMT1 leads to the expression of quite a number of genes that function in stress response and cell cycle arrest. He further confirmed the expression of silenced genes in human lung carcinoma cell line and in early developing kidney cells lines through the antisense knock down of *DNMT1*. The stability of DNA methylation and its ability to be reversed, in such a way that DNA hypermethylation can be reversed by inhibition of *DNMTs*, thereby leading to the expression of tumour suppressor genes, made it to be of high therapeutic target. Up till date, only few DNMT inhibitors have been discovered with only two available drugs in the circulation, these drugs are: azacytidine and decitabine (Fahy *et al.*, 2012; Zhou *et al.*, 2016). Hence, there is need for the discovery of other novel DNMT inhibitors for cancer treatment.

The role of epigenetics in cancer is unquestionable. Change in the unmethylated CpG islands to methylated CpG islands of the 5' promoter region of genes causes inactivation of gene transcription in several human cancers (Chmelarova *et al.*, 2013). For instance, the *P53* gene which is an important tumour suppressor gene; its methylation has been reported in several malignancies such as breast carcinomas, human gliomas, acute lymphoblastic leukaemia and hepatocellular carcinoma (Kang *et al.*, 2001; Pogribny and James, 2002; Agirre *et al.*, 2003; Amatya *et al.*, 2005). The *P53* gene has 11 exons and the first exon (213bp) is within 8-10kb away from the second exon. The promoter activity is localized to 85bp region (nucleotide 760-844) for full promoter activity and the *P53* gene functions in cell cycle arrest, senescence and apoptosis (Chmelarova *et al.*, 2013). Since, much data has not been revealed on the methylation status of this *P53* gene in ovarian cancer, there is need to

investigate the methylation of the promoter region of this gene and evaluate changes in the CpG methylation of the promoter due to drug treatment, as a novel strategy for ovarian cancer treatment.

### 1.3.1.1 Methylation patterns in ovarian cancer

There are two major DNA methylation patterns in ovarian cancer and in all other cancer types generally, the hypermethylation of the site specific promoter regions which do result in the silencing of tumour suppressor genes such as *BRCA1*, *P53*, thereby leading to cancer formation, these genes are involved in various cellular processes such as DNA repair, cell cycle, cell adhesion, apoptosis and angiogenesis which are all important in cancer development, and the hypomethylation of repeated DNA sequences leading to over expression of tumour causing genes known as oncogene, thereby causing genetic instability by promoting chromosomal rearrangement (Liu *et al.*, 2009; Sharma, Kelly and Jones, 2010; Earp and Cunningham, 2015). Many tumour suppressor genes silenced by DNA hypermethylation have been well characterized, these include: *BRCA1*, *RASSF1A*, *CCBE1*, *OPCML*, *MGMT*, *HOXA9*, and *hMLH1* ( Maldonado and Hoque, 2010; Lonning *et al.*, 2011; Gloss and Samimi, 2014; Dong, Lu and Lu, 2016). Chmelarova *et al.* (2013) reported *P53* promoter methylation in 51.5% of ovarian cancer. Theriault *et al.* (2014) suggested that the overexpression of *KF14* in ovarian cancer, which is a significant oncogenic gene that codes for mitotic kinase, could be explained by the hypomethylation of the promoter region of this gene. The upregulation of this gene could be an important therapeutic target (Gyparaki and Papavassiliou, 2015). Also, hypermethylation of the promoter region of the tumour suppressor candidate 3 (*TUSC3*) silenced the expression of this gene and this is suggested to be a good prognostic factor for ovarian cancer (Pils *et al.*, 2013). Therefore, epigenetic modulation of DNA methylation of these genes could be targeted as an

alternative treatment method for ovarian cancer by silencing the overexpressed oncogene and reactivating the expression of repressed tumour suppressor gene in ovarian cancer.

### **1.3.1.2 Quantification of DNA methylation**

DNA methylation occurs in both the global genome and at gene specific promoter region. Hence, the techniques to be used depend on the region where DNA methylation is to be assessed. Wide range of technique are available for profiling the methylation status of a whole genome when the candidate gene is unknown, these methods include: enzyme-linked immunosorbent assay (ELISA), luminometric methylation assay (LUMA), long interspersed nuclear elements (LINE-1), restriction fragment length polymorphism (RFLP), amplified fragment length polymorphism (AFLP), mass spectrometry, and high performance liquid chromatography-ultraviolet (HPLC-UV) etc. When DNA methylation is to be assessed at the promoter region of a known gene, digestion based assay followed by PCR and qPCR, and bisulfite conversion followed by methylation specific PCR, bead array, pyrosequencing and sequencing are often frequently been employed (Liu, *et al.*, 2009; Kurdyukov and Bullock, 2016). Each of the above stated methods or techniques have their set back and good quality in terms of the quantity and quality of the starting material (DNA) required, specificity, sensitivity and reliability, expertise and equipment required, and cost effectiveness. Comparison of the sensitivity of some of the techniques has been conducted (Lisanti *et al.*, 2013). However, Kurdyukov and Bullock (2016) recommended LINE-1 followed by pyrosequencing, LC-MS/MS and LUMA for profiling the whole genome methylation. Also, ELISA is often being used by researchers because there are several ELISA based commercial kits for the quantification of DNA methylation status; this method is quick, cheap, and easy to perform.

In assessing the methylation status of specific promoter region, bisulfite sequencing such as whole genome bisulfite sequencing and targeted next generation bisulfite sequencing (tNGBS) are often known as the gold standard. However, the use of bisulfite sequencing can prove to be challenging, but pyrosequencing and methylation-specific PCR are good method to be used and in each method DNA bisulfite conversion is usually the starting point. Several researchers use the methylation specific PCR for the detection of methylation at specific gene promoter region (Chmelarova *et al.*, 2013).

Pyrosequencing is a technique that quantitatively monitors the real-time integration of nucleotides by the enzymatic conversion of released pyrophosphate into a proportional light signal (Tost and Gut, 2007). It is accurate, reproducible and quantitatively measures the level of DNA methylation for each CpG sites in the sequenced region, and can detect very small differences down to 5% in methylation; it is also a good technique for heterogeneous samples where cells have differentially-methylated gene of concern (Kurdyukov and Bullock, 2016). In this method, the level of methylation at each CpG site in a sequence is determined from the ratio of thymine and cytosine after bisulfite treatment and PCR. Apart from the identification of methylated CpG site that apparently leads to silenced gene expression in cancer, pyrosequencing is a reference method for the validation of newly developed DNA methylation analysis methods, monitors demethylation induced by chemicals in cancer and also offers wide range of use in detecting methylation other diseases such as neurological disorders, as well as monitoring methylation patterns in specific allele (Schatz *et al.*, 2004; White *et al.*, 2006; Yang, 2006; Tost and Gut, 2007).

### **1.3.1.3 DNA 5-Hydroxymethylcytosine (5-hmC)**

DNA 5-hydroxymethylcytosine have been identified as an intermediate between DNA methylation and demethylation. This process involves the addition of hydroxyl group to the

5-methylcytosines to form 5-hydroxymethylcytosine, and this process is catalysed by the ten-eleven translocation (TETs) family proteins include TET1, TET2 and TET3 (Dawson and Kouzarides, 2012; Tan and Shi, 2012; Morales, Monzo and Navarro, 2017; Monticelli, 2019). The presence of 5-hydroxymethylcytosines in the human genome or cancer cells are usually lower when compared with 5-methylcytosine. Even though DNA methylation is usually considered to be the most stable epigenetic modification, studies on the global distribution of DNA methylation during embryonic formation and development had identified loss of DNA methylation in the zygote at the early formation stage, and the dynamic nature of DNA methylation was shown in pluripotent and differentiated cells (Dawson and Kouzarides, 2012). 5-hmC is suggested to be likely having both transcriptional and silencing function. Thus, the TET proteins capable of performing both gene activating and repressive functions (Wu and Zhang, 2011). The TET1 have preference for region enriched with CpG on the DNA in relation to its catalytic function which has been localized to 5mC and 5hmC enriched regions (Dawson and Kouzarides, 2012). The detection of 5-hydroxymethylcytosine is seen as a novel achievement in the field of epigenetic research (Kriaucionis and Heintz, 2009; Tahiliani *et al.*, 2009). 5-hmC has been linked with tumour formation and seen as an intermediate between further oxidation and final DNA demethylation of 5-methylcytosine (Münzel, Globisch and Carell, 2011; Kraus *et al.*, 2012; Hahn *et al.*, 2013; Tomasetti *et al.*, 2019). The formation of 5-hmC from 5-mC automatically leads to decrease in the levels of 5-mC at any given nucleotide position or in the whole global genome. Hence, the conversion of 5-mC into 5-hmC might be a fundamental step in the demethylation of DNA (Hahn *et al.*, 2013; Rasmussen and Helin, 2020). However, studies have showed a reduced expression of TET genes and 5-hmC in ovarian cancer compared to normal ovarian tissues which depicts the fact that decreased expression of TET may be involved in the cell transformation (Zhang *et al.*, 2015). 5-hmC

may be a useful biomarker for cancers diagnosis. Hence, understanding the relationship between TET genes, DNMTs, 5-hmC and 5-mC would be a great target for cancer treatment.

### **1.3.2 Histone modification (acetylation and methylation)**

In addition to the role played by DNA methylation in the regulation of gene expression, the post-translational modification of histone protein plays a major role in the epigenetic regulation of gene expression. The histone protein which contains the nucleosome core is made up of the globular C-terminal domain and N-terminal tail. Post-translational modifications that usually occur at the N-terminal tails of the histone include methylation, acetylation, ubiquitylation, sumoylation, phosphorylation and ADP ribosylation which therefore, alter the structure of chromatin and affect DNA accessibility to transcriptional factors; however, histone acetylation and methylation are the two most studied mechanisms of histone modification that regulate epigenetic modification (Shankar *et al.*, 2016; Pradhan *et al.*, 2019). Depending on the residues modified and the type of modification, histone modifications can either cause gene activation or repression unlike DNA methylation (Sharma, Kelly and Jones, 2010).

The steady state of histone acetylation and methylation are dynamically regulated by series of enzymes that either add or remove covalent modulations to histone proteins. These enzymes include: histone methyltransferases (HMTs) and Histone acetyltransferases (HATs) that add methyl and acetyl respectively; as well as histone demethylases (HDMs) that remove methyl group and histone deacetylases (HDACs) that remove acetyl group (Sharma, Kelly and Jones, 2010; Thakur *et al.*, 2014; Montgomery and Srinivasan, 2019). Acetylation of histone enables binding of transcription factors to DNA by opening chromatin structure, on the contrary deacetylation leads to transcriptional repression by

condensing the chromatin (Huang, Plass and Gerhäuser, 2011; Pradhan *et al.*, 2019; Tomasetti *et al.*, 2019).

Histone methylation can occur at the lysine and arginine residues; the methylation of histone lysine may activate or repress the expression of gene depending on where the lysine residue methylated is located; for instance, methylation at H3K9, H3K27 and H4K20 lead to transcriptional inactivation whereas H3K4, H3K36 and H3K79 leads to activation of transcription; Histone lysine methylation is achieved by histone lysine methyltransferases (HLMs) (Thakur *et al.*, 2014).

In addition to the specific roles played by histone modifications and DNA methylation in gene expression, they both interact to determine gene expression. To illustrate, HMTs such as G9a, SUV39H1 and PRMT5 directly recruit DNMTs, thereby directing DNA methylation to specific target within the genome, leading to gene silencing; furthermore to the direct recruitment of DNMTs, HMTs and HDMs also influence DNA methylation by regulating DNMT protein stability; in the same way, DNMTs can achieve gene silencing and condensation of chromatin by recruiting HDACs and methyl-binding proteins (Sharma, Kelly and Jones, 2010).

Aberrant modification of histone such as acetylation and deacetylation, and methylation and demethylation are key factors in tumour transformation. This has been linked with many human cancers (Huang, Plass and Gerhäuser, 2011). High expression level of HDACs is usually observed in cancer cells whereas higher histone acetylation level is being described in normal cells in comparison with cancer cells. In ovarian cancer, histone modification contribute to progression by down-regulating genes, such as silencing of *GATA4* and 6 gene as a result of hypoacetylation of histones H3 and H4 ( Maldonado and Hoque, 2010).

### **1.3.3 MicroRNAs in epigenetic modulation**

Another epigenetic mechanism that modify gene expression is microRNAs (miRNA), these are small non-coding RNAs of about 20-22 nucleotides capable of inhibiting the expression of genes after transcription of DNA into mRNA (Thakur *et al.*, 2014; Acunzo *et al.*, 2015; Tomasetti *et al.*, 2019). Up till date, thousands of miRNA have been identified in the human genome and are known to be involved in the regulation of major biological processes such as, development, differentiation, proliferation and apoptosis (Sharma, Kelly and Jones, 2010; Di Leva *et al.*, 2014; Montgomery and Srinivasan, 2019). They are involved in the regulation of the process through which mRNA formed from transcription has been translated into proteins by imperfect base-pairing to the mRNA or by affecting the stability of mRNA. However, this mechanism may be altered in many diseases including cancer (Thakur *et al.*, 2014; Acunzo *et al.*, 2015). Research has revealed that miRNA expression is down-regulated during tumour formation and this has been implicated in tumour initiation and progression. However, many miRNAs can function as either as tumour suppressors or oncogenes depending on tumour type (Di Leva *et al.*, 2014). Genetic and epigenetic mechanisms are both involved in the regulation of miRNAs expression. Epigenetic changes such as histone modifications, DNA hypo and hypermethylation can influence the expression of miRNA through its promoter region (Tomasetti *et al.*, 2019; Yao, Chen and Zhou, 2019). Also, miRNAs themselves can modulate epigenetic pathway inside cell by modulating the expression of DNA methylation and histone modification enzymes (Montgomery and Srinivasan, 2019). miRNA have been suggested to be involved in the resistance of cancer cells to chemotherapy by modulating the expression of the drug target proteins or its downstream effectors and also other miRNAs (Acunzo *et al.*, 2015). However, miRNA could also increase the sensitivity of cancer cells to chemotherapy, such as the increased sensitivity of non-small lung cancer cells to chemotherapy. The drug

sensitivity was achieved through the down-regulation of the vascular endothelial growth factor A (VEGFA) and inactivation of PI3K/AKT pathway by miR-126 (Zhu *et al.*, 2012). The pharmacological relevance of miRNA involves its use in targeted therapy for cancer treatment is been explored by researchers. However, the major problem is the activation of other pathways by miRNA that are capable of causing cancer recurrence, and also the delivery problem in an in vivo model, as research is still ongoing on the use of specific tumour delivery nanoparticles (Acunzo *et al.*, 2015). Additionally, miRNAs could be targeted for cancer treatment with the use of phytochemicals present in food or traditional medicinal plants that are able to regulate the expression of miRNAs (Duru *et al.*, 2015).

#### **1.4 Apoptosis and cancer formation and treatment**

One of the major underlining mechanisms of cancer formation is the ability of cells to escape programmed cell death (Hanahan and Weinberg, 2011). This is a mechanism within multicellular organisms to control the rate of cell proliferation and division of damaged cells. Apoptosis brings about many biochemical changes in human cells, such changes include: membrane blebbing, cell shrinkage, nuclear and DNA fragmentation, chromosomal condensation within cells, that consequently caused cell death, through series of programmed events (Wong, 2011). However, when cells escape the programmed cell death mechanisms, it consequently leads to uncontrolled proliferation of cells that ultimately develop into tumour, cancer metastasis and resistance to cytotoxic drugs (Fulda and Debatin, 2006; Wong, 2011). Apoptosis pathway is one of the most studied mechanisms of cancer formation and treatment by researchers. The activation of the pathways of apoptosis is essential for cancer treatment and this is the major pathway that is being employed for cancer treatment by various cytotoxic agents (Wong, 2011). However, cells could escape the apoptosis mechanisms due to defects in the signalling pathways that could be caused by

DNA mutation, epigenetic alteration in genes controlling apoptosis. The apoptosis signalling pathways (intrinsic or extrinsic) could be re-activated with cytotoxic compounds. These anticancer drugs usually trigger the release of phosphatidylserine protein in the outer layer of cellular membrane as a marker of early apoptosis, and activate the cysteine proteases family called caspases and these caspases are capable of activating each other and usually lead to morphological changes in the cell and ultimately cell death (Fulda and Debatin, 2006; Wong, 2011).

The caspases activity could be initiated through extrinsic and intrinsic pathways. In extrinsic pathway, the pro-caspase 8 is activated by the death inducing signalling complex (DISC) which is formed by the binding of the death ligands such as TNF and FasL, to the death receptors (Fas) that creates binding sites for adaptor protein. The activated initiator caspase 8 then triggers the cleaving of the executioner caspase 3, 6 and 7 that causes cell death (Wong, 2011). However, in the intrinsic pathway, the cascade of caspase 9 is activated through the mitochondrial release of cytochrome *c* into the cytoplasm that is mediated by cell internal factors such as genetic damage, oxidative stress and hypoxia, and binds to the apoptosis activating factor 1 (Apaf-1) (Ghobrial, Witzig and Adjei, 2005; Gopisetty, Ramachandran and Singal, 2006; Wong, 2011). The activated caspase 9 triggers the activation of executioner caspase 3, 6 or 7 that causes cell death. The intrinsic pathway is regulated by the Bcl-2 family of protein including Bax and Bcl-2. The Bax promotes the release of the cytochrome *c* by the mitochondria into the cytoplasm while the Bcl-2 blocked the release of cytochrome *c* (Ghobrial, Witzig and Adjei, 2005; Wong, 2011). The balanced regulation of Bax (pro-apoptotic protein) and Bcl-2 (anti-apoptotic protein) is essential for apoptosis. However, overexpression of anti-apoptotic proteins (Bcl-2) and under-expression of pro-apoptotic proteins and alteration in other apoptotic mechanisms which could be

caused by genetic instability such as DNA mutation, epigenetic changes that include histone modification and DNA methylation is one of the hallmarks of cancer formation.

The relationship between epigenetics and apoptosis have been established through various researches. Epigenetics is known to modulate the expression of major genes that function in the different apoptotic pathways. Murai *et al.* (2005) evaluated the DNA methylation level and expression of *BNIP3* which is a member of the pro-apoptotic member of the Bcl-2 protein that function in apoptosis. It was further observed that the *BNIP3* gene was inactivated by DNA methylation and deacetylation of the histone H3. However, the apoptotic activities of the *BNIP3* gene was restored when treated with 5-aza<sup>2'</sup>-deoxycytidine (5-aza-dC). This study suggested that DNA methylation of the 5' position of the cytosine base of the DNA at the CpG Island and deacetylation of the histone play a key role in the silencing of *BNIP3* expression. Furthermore, in the review of Gopisetty, Ramachandran and Singal (2006), several genes such as *BNip3*, *P73*, *XAF1*, *Apaf1*, *P14ARF*, *Fas*, *DR4*, *Dr5*, *DcR1*, *DcR2*, *TMS1* and *DAPK* that function either directly or indirectly in apoptosis were known to be down-regulated by DNA methylation in several cancer types. Furthermore, DNA methylation of the CpG island of the promoter region of *TP53* have been reported to be associated with the down-regulation of the expression of this gene (Agirre, *et al.*, 2003). The *TP53* gene is a tumour suppressor gene that controls cell proliferation. It further function in the repair of damaged DNA by activating other DNA repair genes, and if damaged DNA is not repaired it subsequently inhibits its division and triggers apoptotic signals. Also, DNA methylation of the promoter of *TUSC3* which is a tumour suppressor gene, have led to the silencing of its expression. Lopez-Serra and Esteller (2012) identified that different miRNA plays major role in the regulation of genes that function in cell cycle, apoptosis, growth inhibition and cell proliferation. However, it was further identified that DNA methylation of the CpG island of the promoter region of tumour

suppressor miRNA such as miR-124a and miR-34b/c lead to silencing of their expression that consequently lead to alteration in the miRNA functions in regulating tumour associated genes.

### **1.5. Therapeutic agents based on epigenetics**

Up till date, only two drugs have been approved for the treatment of myeloid dysplastic syndrome and myeloid leukaemia. These drugs are azacytidine and decitabine with chemical names 5-azacytidine and 5-aza-2'-deoxycytidine respectively. Azacytidine was approved in 2004, while decitabine was approved in 2006. These two compounds are known to be inhibitors of DNMTs (Fahy *et al.*, 2012; Busch *et al.*, 2015). They are nucleoside analogues which are mainly cytidine derivatives.

#### **1.5.1. 5-Azacytidine (Aza): A known nucleoside DNMT1 inhibitor**

The synthesis of 5-azacytidine (Aza) was first carried out over decades ago, and this compound has been shown to possess a wide range of anticancer activities against cancer cells and specifically as acute myelogenous leukaemia therapeutic agent (Christman, 2002). It has been well studied in clinical trials and shown to completely normalise blood counts and bone marrow and eliminate transfusion dependence in responding patients and was approved on 19<sup>th</sup> of May, 2004 by the U.S. Food and Drug Administration (FDA) for the treatment of myelodysplastic syndrome (MDS) and its subtypes (Kaminskas *et al.*, 2005). Aza is a cytidine analogue compound which is the mostly used as DNA methyltransferase inhibitor that function through mechanism-dependent inhibition of the enzyme that catalyse the formation of DNA methylation when incorporated into the DNA (Akone *et al.*, 2020). After incorporation, Aza is phosphorylated into 5-azacytidine monophosphate, diphosphate and triphosphate by uridine-cytidine kinase, pyrimidine monophosphate and diphosphate

kinases respectively, and the phosphorylated Aza is further reduced into 5-azadeoxycytidine triphosphate by nucleoside diphosphate kinases, thereby binding with DNMT1 and inhibit methylation in DNA undergoing replication resulting in DNA hypomethylation (Lubert *et al.*, 2001; Kaminskas *et al.*, 2005; Stresemann *et al.*, 2006; Braiteh *et al.*, 2008). Aza has also been shown to lead to re-activation of silenced gene (Christman, 2002). It is generally known to have high toxicity level, however, no death was observed in patients treated with Aza in clinical studies but showed adverse effects such as nausea, vomiting, constipation, diarrhoea, anorexia, neutropenia, fevers, injection site events, headache, dizziness and liver function abnormalities in 16% of patients with inter-current hepatobiliary disorders and in two of the patients with cirrhosis history (Kaminskas *et al.*, 2005). Therefore, there is need for the discovery of more other DNA demethylating agents with less toxicity profile for cancer treatment and prevention

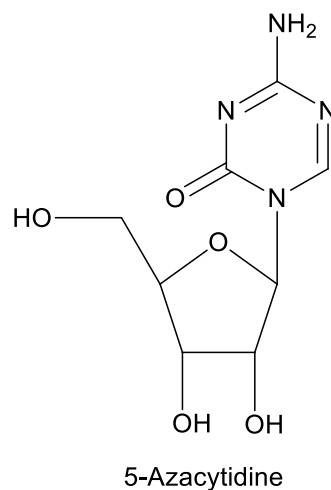


**Figure 1. 2: Structure of 5-azacytidine**

### 1.5.2 5-Aza-2'-Deoxycytidine (5-aza-CdR) and zebularine (Zeb)

5-Aza-2'- deoxycytidine is a known nucleoside DNMT inhibitor that is used for the treatment of cancers (Akone *et al.*, 2020). 5-aza-CdR is a deoxyribose analogue of 5-

azacytidine that is incorporated into the DNA during DNA replication in the S phase of cell cycle by DNA polymerase; this cytosine analogue is recognised as cytosine by enzyme in the DNMT sites and form a covalent complex with the cysteine of the enzyme at the 6-position of the cytosine analogues, thereby resulting in DNA repair and DNMT degradation and DNA becomes hypomethylated (Huang, Plass and Gerhäuser, 2011). 5-aza-CdR is shown to be more active than 5-azacytidine as it shows greater anti-tumour activities and DNA methylation inhibition as reported by Momparler *et al.* (1984). It has been demonstrated to inhibit DNMT, increased TET2 and decrease DNA methylation (Rocha *et al.*, 2019). It is more specific as it is being incorporated into the DNA directly and less toxic than azacytidine; however, still known to be a toxic compound (Lyko and Brown, 2005).

Zebularine is another nucleoside analogue that is known to inhibit DNMT expression; it is a derivative of 5-azacytidine and has similar structure with 5-aza-CdR and used in addition to azacytidine and decitabine but no clinical trial report has been revealed on this compound (Fahy *et al.*, 2012). It is integrated into the DNA and known to be more stable than decitabine and azacytidine, it is also suggested to be less toxic (Huang, Plass and Gerhäuser, 2011). Cheng *et al.* (2003) reported that zebularine reactivated the silenced *P16* gene by demethylating its promoter region in mice using both in-vitro and in-vivo assays. Another nucleoside analogue known to be an inhibitor of DNMT is 5-fluoro-2'-deoxycytidine (FdCyd), however, must be used with cytidine deaminase inhibitor tetrahydrouridine (Thu) to prevent rapid metabolism of the compound. This compound is presently in phase I and II clinical trials for cancer treatment (Beumer *et al.*, 2008). The DNA demethylating role of nucleoside DNMT inhibitors is suggested to be associated with their toxicity which makes them not suitable as therapeutic agents in human cancer treatment (Huang, Plass and Gerhäuser, 2011).

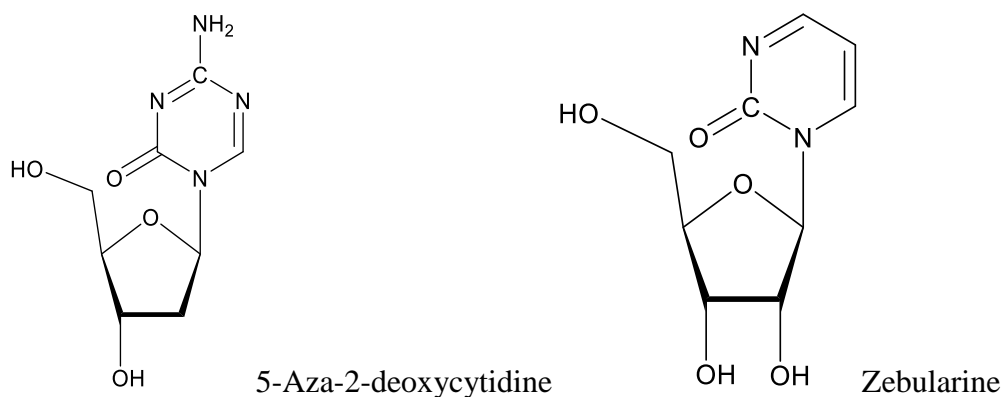


**Figure 1. 3: Structure of 5-Aza-2-deoxycytidine and zebularine**

### 1.5.3 Non-nucleoside synthetic compounds that are known DNMT inhibitors

Non-nucleoside compounds are also known to inhibit DNMT expression by directly blocking the activities of DNMTs; they therefore appear not to be too toxic like nucleoside compounds. There are various kinds of non-nucleoside compounds that have been reported to inhibit DNMT expression. Notable among them are: SGI-1027, procaine and procainamide.

#### 1.5.3.1 SGI-1027

SGI-1027 is a 4-anilinoquinoline derivative from quinolone, which is substituted with aromatic and heterocyclic rings that cause DNMT depletion; it has been developed by SuperGen and shown to inhibit DNMT1 expression and lead to DNA demethylation (Fahy *et al.*, 2012). Datta *et al.* (2009) reported that SGI-1027 inhibits the expression of DNMT1, DNMT3A and DNMT3B and also M.Sssl with closely ranged IC<sub>50</sub> of 6 to 13 $\mu$ M. He further reported a total degradation of DNMT1 protein in cancer cell lines treated with this compound through a proteasomal pathway. Demethylation of DNA and re-expression of silenced tumour suppressor genes such as *P16*, *MLH1* and *TIMP3* was also observed. However, the underlying mechanism of action remains unclear (Fahy *et al.*, 2012).

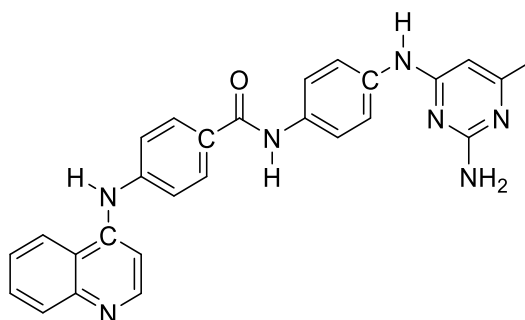


**Figure 1. 4: Structure of SGI-1027**

### 1.5.3.2 Procainamide derivatives

Several years ago, procaine and procainamide have been known to be active anaesthetic and antiarrhythmic agents respectively. They both have affinity for the CpG-rich sequences, thereby preventing the binding of DNA methyltransferases to DNA (Lyko and Brown, 2005). The role of procainamide in DNA demethylation was first reported in 1988 (Fahy *et al.*, 2012). Villar-Garea *et al.* (2003) have shown that procaine is an effective demethylating agent. In his study, the level of 5-methylcytosine methylation was reduced by 40% when breast cancer cell lines were treated with procaine. Silenced tumour suppressor gene was also found to be re-expressed. This made procaine to be of good epigenetic therapeutic target for cancer treatment.

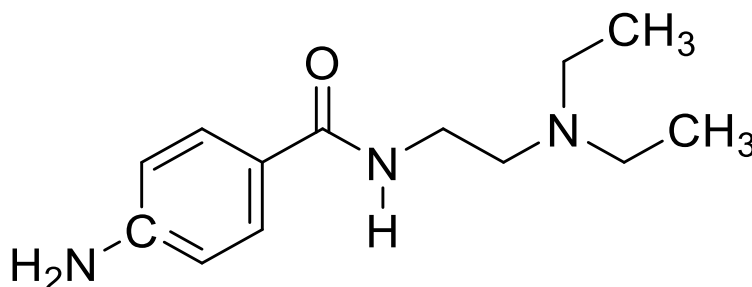


**Figure 1. 5: Structure of procainamide**

## 1.6 Plant-derived natural products: A promising agent in cancer treatment

Historically, the use of plants in the treatment of diseases including cancer has found its way into medicine long time ago (Cragg and Newman, 2005, 2013; Newman and Cragg, 2016). Many continents such as Asia and Africa, and countries such as India, China and Nigeria etc. are bestowed with wide varieties of plants with medicinal values, some of which have been shown to be important medicinal plants (Moundipa *et al.*, 1999; Mittal, Sharma and Batra, 2014). Plants have found its usefulness in medicine in various different ways which include the direct usage of crude extract of plants in the treatment of different diseases as a result of the present of the natural constituents, or the use of the natural compounds from plants in the production of drugs for disease treatment. Natural products or compounds are chemical compounds that have pharmacological activities which are produced from living organisms found in the physical world. They are mainly extracted from plant and many other sources such as marine organisms and micro-organisms (Cragg and Newman, 2005). Most of the active ingredient of medicines had their source from natural products; its wide application in drug discovery with about 80% of drug substances from natural products showed that is widely acceptable (Harvey, 2008). Natural products derived from plant source have received attention for drug discovery in the treatment of many diseases for the past few decades (Krifa *et al.*, 2013; Harvey, Edrada-Ebel and Quinn, 2015). Generally, natural products have been extensively utilized in the synthesis of various drugs such as tubocurarine, colchicine, nicotine, quinine and majority of the cancer drugs such as vinblastine, vincristine, topotecan and irinotecan, taxol, camptothecin, etoposide and paclitaxel are derived from plants (Cragg and Newman, 2005; Mittal, Sharma and Batra, 2014). Numerous plant species are being used for drug discovery in medicine. In Hartwell's review of plants used in cancer treatment, more than 3000 species of plants were listed for the treatment of cancer (Cragg and Newman, 2005). However, the vast usage of plant in

medicine for the treatment of various diseases including cancer is due to the presence of various active substances such as flavonoids, alkaloids, vitamins tannins, and coumarins and these compounds interact with the biological host and the pathogens thereby interrupting the growth of the pathogens and setting the host body free of disease (Mittal, Sharma and Batra, 2014).

The quest for plant anti-cancer agents had commenced in the 1950s with the early discovery and development of vinca alkaloids, vincristine and vinblastine, this made the United States National Cancer Institute (NCI) to start plant collection programme in 1960 in the temperate regions (Cragg and Newman, 2005). This resulted in the discovery of many therapeutic agents like taxanes and caamptothecins which have wide range of cytotoxic properties. Their development and acceptability into medicine took a wide range of 30 years which is between 1960s and 1990s. This program was abruptly stopped in 1982, which was later commenced in 1986 due to the development of new screening technologies. The programme now targeted the tropical and sub-tropical regions of the world and none of the discovered agents is yet to reach the stage of general use in medicine (Cragg and Newman, 2005).

Many plant-derived anticancer agents have been developed over the ages. These plant-derived compounds are known to perform their various anti-cancer activities through various mechanisms of action which include induction of DNA repair, suppression of cell cycle progression and induction of apoptosis in the cell (Krifa *et al.*, 2013). As at present, there are very few natural products that have been known to inhibit DNMT activity and demethylating DNA, such as curcumin, epigallocatechin-3-gallate (EGCG), Genistein etc (Busch *et al.*, 2015). Therefore, there is need to discover more natural products that could function as DNA demethylating and DNMT inhibiting agents. Also, the discovery of natural products from medicinal plant is an inexhaustible field of research, as many plants that are

readily available in the environments worldwide have received little or no scientific attention. Hence, there is need to explore the medicinal value of many other plant-derived natural compound in ovarian cancer treatment and elucidate their roles in epigenetic regulation.

### **1.6.1 Sesquiterpene lactones (SLs)**

Sesquiterpene lactones are natural compounds which are derived from plants that are frequently used in traditional medicine for the treatment of inflammation and neoplasm; these natural compounds are known to be colourless, bitter and are stable members of the terpenoids, which are secondary metabolites of plants that have chemical affinity for lipids (Bocca *et al.*, 2004; Ghantous *et al.*, 2010; Haaften *et al.*, 2015; Schefer *et al.*, 2017). Research on the sesquiterpene lactone natural compounds started shortly after the large scale plant screening programme carried out by the National Cancer Institute in USA in the 1960s (Ghantous *et al.*, 2010). They formed the large group of plant secondary metabolites that are mainly gotten from the family Asteraceae and Magnoliaceae and they are 15-carbon compound comprising of three isoprene units and a lactone group with different sub types (Figure 1.6) (Yang *et al.*, 2011; Abood *et al.*, 2017; Gao *et al.*, 2017; Li *et al.*, 2020). SLs are the active constituents of many plants used in traditional medicine for the treatment of inflammatory diseases (Gao *et al.*, 2017). They have formed a significant group of natural products with pharmacological relevance (Kim and Choi, 2019). They have gained relevance in drug discovery for cancer treatment because of their ability to target specific signalling pathways; their chemical properties are alkylation, affinity for lipid and molecular geometry; many SLs are in clinical trials, and these include artemisinin, parthenolide and thapsigargin etc. (Bocca *et al.*, 2004; Ghantous *et al.*, 2010). It has been suggested that the  $\alpha$ -methylene- $\gamma$ -lactones and the  $\alpha,\beta$ -unsaturated cyclopentenones are responsible for the

biological activity of the sesquiterpenes (Abood *et al.*, 2017). However, despite the fact that SLs are known to be the active compounds of most plants used in traditional medicine for the treatment of inflammation and cancer, not all sesquiterpene lactones compounds have been studied, there is still a wide gap in knowledge as the roles of majority of them in DNA methylation have not been studied. Hence, the need to explore the roles of some of the sesquiterpene lactone compounds in DNA methylation for the treatment of ovarian cancer.

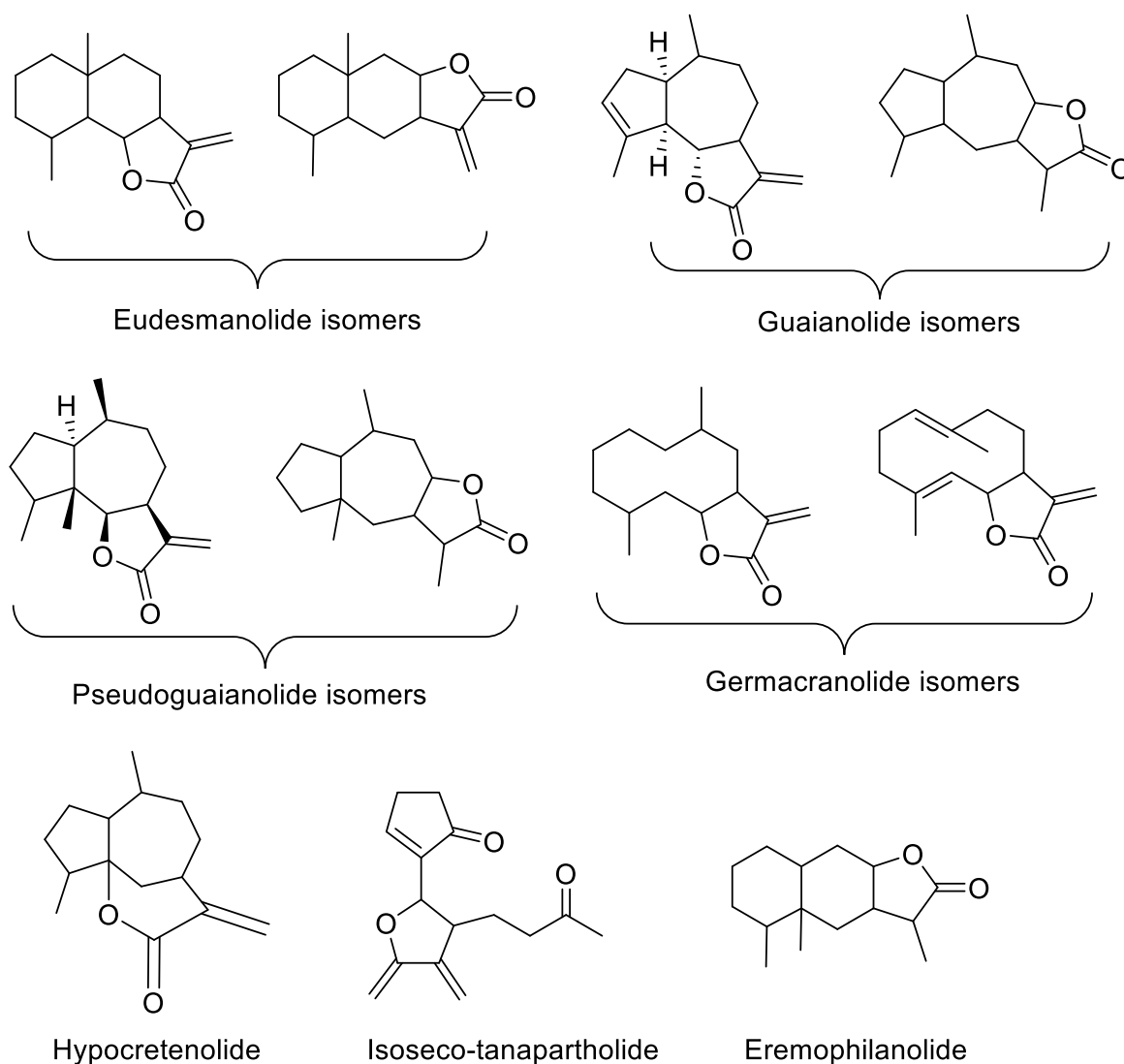


**Figure 1. 6: Chemical structures of the different subtypes of sesquiterpene lactones (Ghantous *et al.*, 2010).**

### **1.6.1.1 Parthenolide**

Parthenolide is a natural compound that is derived from feverfew plant (*Tanaecetum parthenium*) (Pajak, Gajkowska and Orzechowski, 2008; Lin *et al.*, 2017; Talib and Al Kury, 2018). This feverfew had its origin from the Bakan states; it has been cultivated for over centuries among the European people and was been used for ornamental and medicinal importance by the Greeks and the Europeans in the early years and the plant name was derived from the latin word '*febrifugia*' (Ghantous *et al.*, 2013). Feverfew is a perennial plant that is majorly found in garden and at road sides and belongs to the Asteraceae family (Pareek *et al.*, 2011). This medicinal plant is widely used in folk medicine for the treatment of diverse kinds of diseases; among the medicinal use of this plant in the early centuries include: usage in the treatment of arthritis pain, aids digestion, used as insect repellent, infertility treatment, aids uterine contraction at childbirth and menstrual irregularities, skin wound, as anticoagulant additive and dizzy sensation, stomach and toothache, migraines, all these functions are due to the anti-inflammatory properties possessed by this plant (Pajak, Gajkowska and Orzechowski, 2008; Ghantous *et al.*, 2013). The plants possess quite a number of natural compounds but sesquiterpene lactone is known as the major active component, other constituents found in this plant include flavonoid, glycoside etc. (Pareek *et al.*, 2011). However, this plant did not gain popularity in phytomedicine until its chronic effect was reported in 1978 (Pareek *et al.*, 2011).

Parthenolide is the most important bioactive compound of sesquiterpene lactone present in this medicinal plant, and it is usually found in the shoots usually the leaves and flowers and in the root but with minimal presence of parthenolide (Smolinski and Pestka, 2005; Liu *et al.*, 2009). This compound has anti-tumour and anti-inflammatory effects. This compound has been shown to have the ability to promote cell differentiation and induce apoptosis; the

biological properties of parthenolide as an effective anticancer agent is widely due to its ability to inhibit nuclear factor kappa B (NF- $\kappa$ B) and antiapoptotic gene transcription that is mediated STATs (Pajak, Gajkowska and Orzechowski, 2008). The inhibition of NF- $\kappa$ B activation by parthenolide is achieved by preventing the activation of I $\kappa$ B kinase (IKK) and IKK $\beta$  induced by TNF- $\alpha$  without altering p38 activation (Hehner *et al.*, 2017). The NF- $\kappa$ B activation is common to the various cancer types in human, which include leukaemia, lymphoma and other solid tumours (Oka *et al.*, 2007). The therapeutic potential of parthenolide in multiple myeloma has been reported by Suvannasankha *et al.* (2008) that this compound inhibited the growth of multiple myeloma cell lines by overcoming the effects of rapid increase in cell number by cytokines interleukin-6 and the insulin-like growth factor 1. Guzman *et al.* (2017) had also reported the apoptotic effect of parthenolide in human acute myelogenous leukaemia (AML). Furthermore, Liu *et al.* (2017) reported that parthenolide inhibited the proliferation of colorectal cancer through induction of apoptosis, and further inhibited the migration and invasion of the cancer cells. The pharmacological relevance of parthenolide against various cancer types such as lung cancer (Lin *et al.*, 2017; Talib and Al Kury, 2018), breast cancer (Jafari, Nazeri and Enferadi, 2018), gastric cancer (Li *et al.*, 2018), epithelial ovarian cancer (Lee *et al.*, 2012). Liu *et al.* (2009) observed the inhibition of the expression of DNA methyltransferase 1 enzyme (DNMT1) by parthenolide at IC<sub>50</sub> of about 3.5 $\mu$ M. The roles of this compound in the inhibition of NF- $\kappa$ B activation have been well studied by several researchers (Pajak, Gajkowska and Orzechowski, 2008; Guzman *et al.*, 2017; Hehner *et al.*, 2017). However, there are few data on its roles as DNMT 1 inhibitor, there is need for more studies to confirm its roles in the inhibition of DNMT 1 and other DNMTs. Also, there is need to investigate the re-expression of silenced specific tumour suppressor gene in ovarian cancer as a result of DNA methylation caused by over expression of DNMT enzymes.

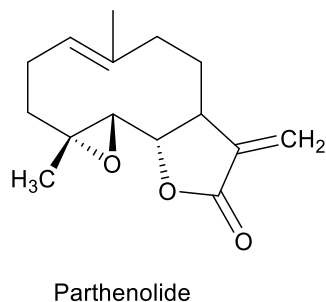


**Figure 1. 7: Structure of parthenolide**

### 1.6.1.2 Costunolide

Costunolide is a natural active sesquiterpene lactone compound that is isolated from medicinal plants that possess anti-inflammatory and anti-cancer activities; such plants include *Saussurea lappa*, *Saussurea radix*, *Magnolia sieboldii* and *Laurus nobilis* (Bocca *et al.*, 2004; Choi *et al.*, 2012). *Saussurea species* and *Magnolia sieboldii* are both Chinese medicinal plants that are been used for the treatment of various cancer types; they belong to the family Compositae and Magnoliaceae respectively; the dried root of *Saussurea lappa* is also used in folk medicine for the treatment of abdominal pain, indigestion and dysentery and nausea diseases (Park *et al.*, 1996; Lee *et al.*, 2001; Jeong *et al.*, 2002). *Laurus nobilis* is an ornamental plant that is mainly cultivated in the USA and Europe such as in Turkey, Portugal, Spain Italy and France for its aromatic leave; it belongs to the family Lauraceae and the plants' seeds oils serve as source of food, cosmetic and also used for medicinal purposes (Barla *et al.*, 2007). Barla *et al.* (2007) confirmed the presence of costunolide in the fruits of *L nobilis* through a bioactivity guided isolation. Saosathan *et al.* (2019) had also found that that costunolide is the most active compound with anti-cancer activities present in *Magnolia sirindhorniae*. This compound has also been found to be one of the most active constituent of *Vladimiria souliei*, which belong to the family Compositae and usually found in China (Mao *et al.*, 2019)

Costunolide is a crystalline colourless powder with the molecular formula  $C_{15}H_{20}O_2$ , which is known to be effective for cancer treatment through inhibition of cell proliferation, metastasis, angiogenesis, and programmed cell death (Rasul, Parveen and Ma, 2012; Kim and Choi, 2019). This compound is also known to be effective in treating other diseases such as anti-inflammatory, and it is a known apoptotic inducer. The biological activities of costunolide is achieved through its  $\alpha$ -methylene- $\gamma$ -lactone functional group, this functional region of costunolide is capable of reacting with the proteins that perform specific functions in different pathways for cancer formation and progression (Kim and Choi, 2019). Several researchers have reported the apoptotic activities of this compound (Choi *et al.*, 2012; Lee *et al.*, 2012). Yang *et al.* (2011) reported that costunolide induced apoptosis in platinum-resistant ovarian cancer cell lines MPSC1<sup>PT</sup>, A2780<sup>PT</sup>, and SKOV3<sup>PT</sup> and confirmed that this compound is more potent than cisplatin in cell growth inhibition. Furthermore, costunolide has been shown to inhibit the growth of drug resistant ovarian cancer cell line (OAW42-A) and induced apoptosis by upregulating the expression of pro-apoptotic gene (Bax) and downregulating the expression of anti-apoptotic gene (Bcl-2) (Fang *et al.*, 2019). Furthermore, the apoptotic activity of costunolide is also mediated through mitochondrial dependent pathway (Yan *et al.*, 2019). Bocca *et al.* (2004) also showed that costunolide does not only inhibit proliferation of the human breast cancer MCF-7 cells but also interacts with the microtubule proteins to inhibit cell growth. Barla *et al.* (2007) asserted that the costunolide from the hexane and dichloromethane fractions of *L. nobilis* was cytotoxic to ovarian cancer cell line A2780 at IC<sub>50</sub> 4.9  $\mu$ g/mL and 6.4  $\mu$ g/mL respectively. Jeong *et al.* (2002) observed the anti-angiogenesis effect of costunolide and claimed that the process of inhibition of angiogenesis by costunolide may be by blocking the angiogenesis factor signalling pathway. The antioxidant activities of this compound have been investigated (Eliza *et al.*, 2010). Several researches have been carried out on the roles of costunolide in

different cancer types such as: myeloid leukaemia (Cai *et al.*, 2018), colon cancer (Zhuge *et al.*, 2018), liver cancer (Mao *et al.*, 2019) and gastric cancer (Yan *et al.*, 2019). Hu, Liu and Yao (2018) demonstrated that costunolide inhibited the proliferation of colorectal cancer cells through activation of *P53*. This suggested that costunolide is capable of modulating the expression of important genes that function in cancer pathways. However, no major study has been carried out on its role in DNA methylation. Therefore, its roles in DNA demethylation will be explored in this study.

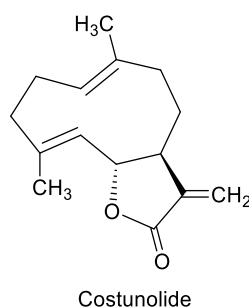


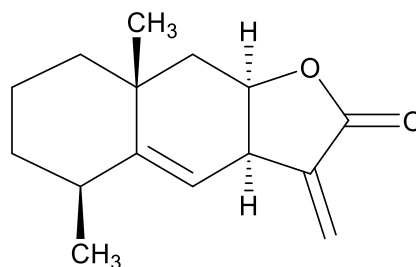
**Figure 1. 8: Structure of Costunolide**

### **1.6.1.3 Alantolactone (Ala): The major bioactive compound in plants with many pharmacological activities**

Alantolactone is a plant derived natural compound that is usually isolated from the root of *Inula helenium* and some other medicinal plants such as *Saussurea lappa*, *Inula japonica*, *Aucklandia lappa*, *Inula racemosa* and *Radix inulae* (Gokbulut and Sarer, 2013; Rasul *et al.*, 2013; Kumar *et al.*, 2014; Cui *et al.*, 2018). *Inula helenium* is a perennial herbaceous medicinal plant that is usually found in Asia (China), Europe and Africa, belong to the family Compositae and often used as insect repellent, antidiuretic agent and in treating cough (Jiang, Xu and Wang, 2016). Alantolactone is one of the major active sesquiterpene lactone compounds that is most abundant in the root of *Inula helenium* plant, and has been confirmed to have diverse pharmacological activities such as anti-bacteria, antifungal, anti-

inflammatory and anti-proliferative (Cantrell *et al.*, 1999; Shi *et al.*, 2011; Chen *et al.*, 2012; Cui *et al.*, 2018). Several researchers have reported the anticancer activities of this compound against various human malignancies. For instance, Khan *et al.* (2012) discovered effective inhibition of growth and induction of apoptosis in glioblastoma cells when treated with Ala. Lei *et al.* (2012) has also reported that Ala inhibited the proliferation of liver cancer cell lines through activation of apoptotic pathways and cell cycle arrest in G2-M phase. He further reported a decrease in NF-kP/P65 protein which he claimed may be responsible for Ala induced apoptosis in cancer. Zhao *et al.* (2015) has also observed that Ala inhibited proliferation of lung squamous cancer cells, induced apoptosis and cell cycle G1/G0 phase arrest. He further noticed down regulation of cyclin-dependent kinases expression, upregulation of caspases-8, -9, -3, PARP and Bax expression and inhibition of apoptotic factor Bcl-2 by alantolactone. Furthermore, Cui *et al.* (2018) demonstrated that Ala induced apoptosis in breast cancer through the loss of mitochondrial mediated caspase activation pathway. Several other researchers have also reported the apoptotic and cell cycle arrest action of alantolactone on several other cancer types such as multiple myeloma cells, human cervical cancer cells, breast cancer cells, colorectal cancer cells and human hepatoma cells (Chun *et al.*, 2015; Yao *et al.*, 2015; Ding *et al.*, 2016; Jiang, Xu and Wang, 2016; Zhang *et al.*, 2016; Yin *et al.*, 2019). Ala have been reported to inhibit the growth and migration of osteosarcoma through the inhibition of PI3/AKT pathway (Zhang *et al.*, 2020). The inhibition of cancer cell growth by Ala has been well reported in other types of cancer including gastric cancer (He *et al.*, 2019; Zhang and Zhang, 2019), hepatocellular carcinoma (Kang *et al.*, 2019), lung cancer (Liu *et al.*, 2019) and pancreatic cancer (He *et al.*, 2018; Zheng *et al.*, 2019), but its mechanism of action has not been fully established (Kang *et al.*, 2019). Up till date, its anticancer activities on ovarian cancer have not been reported. Also,

the role of Ala in DNA methylation has not been studied. There is need to for more research on the mechanism of action of this sesquiterpene lactone compound.



Alantolactone

**Figure 1. 9: Structure of alantolactone**

#### 1.6.1.4 Dehydroleucodine

Dehydroleucodine is a natural compound that is usually present in *Artemisia douglasiana*, a medicinal plant that is mostly used in traditional medicine for the treatment of peptic ulcer and stomach and intestinal disorders in Cuyo region of Argentina; species of *Artemisia* are also often used in Korea for the treatment of diarrhoea (Maria *et al.*, 2000; Wendel *et al.*, 2008). The main active compound in this plant is dehydroleucodine, which is a sesquiterpene lactone compound of the guianolide group; this compound is an isolate of the aerial part of this medicinal plant (Suhaiman *et al.*, 2011; Abood *et al.*, 2018). This compound has also been isolated and purified from *Gynoxys verrucosa*, a member of the Asteraceae family, which is a medicinal plant used in Equador for the treatment of skin infection and healing of wounds (Bailon-Moscoco *et al.*, 2015; Ordóñez *et al.*, 2016). Reports from various researchers showed that dehydroleucodine possess anti-inflammatory, antimicrobial and antiparasitic properties: Guardia *et al.* (2003) reported the anti-inflammatory activities of dehydroleucodine and suggested that its inhibition of inflammation may be due to its interference with transcription factors such as NF- $\kappa$ B and

cytokines; Jimenez *et al.* (2014) confirmed dehydroleucodine's apoptotic activities in *Trypanosomma cruzi* which is a protozoan parasite responsible for chagas disease; and Mustafi *et al.* (2015) showed that dehydroleucodine increased the sensitivity of *Pseudomonas aeruginosa* to antibiotics, this pathogenic organism is well known to be highly resistant to antibiotics. He further suggested that the activities of dehydroleucodine in increasing sensitivity to antibiotic agents may be at the bacterial transcription level. The antimicrobial activities of dehydroleucodine have also been reported by Vega *et al.* (2009). Dehydroleucodine compound has also been shown to have anti-oxidant and antidiarrheal activities (Maria *et al.*, 2000; Wendel *et al.*, 2008). Furthermore, this compound has been shown to inhibit the proliferation of adipocytes and downregulated histone demethylase and histone methyltransferases expression (Abood *et al.*, 2018). Several researchers have also reported the cytotoxicity activities of dehydroleucodine against various cancer types including; human leukaemia (Vera *et al.*, 2012), human cervical carcinoma, breast adenocarcinoma and human embryonic lung fibroblast (Costantino *et al.*, 2013), brain tumour (Bailon-Moscoso *et al.*, 2015), human leukaemia cells (Ordóñez *et al.*, 2016), and malignant melanoma (Costantino *et al.*, 2016). They have also shown that dehydroleucodine induces cell cycle arrest and triggers senescence and apoptosis (Costantino *et al.*, 2013). However, up till date, the cytotoxicity activities of dehydroleucodine on ovarian cancer type have not been revealed. Also, little is known about the mechanism of action of this compound in eliciting apoptosis and cell cycle arrest. Therefore, this study will focus on the cytotoxic activities of this compound in ovarian cancer and also reveal the mechanism of action.

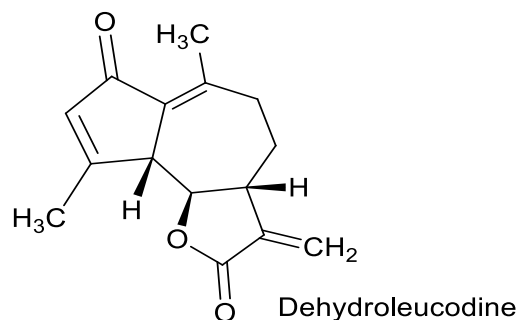


**Figure 1. 10: Structure of Dehydroleucodine**

### 1.6.2 Diterpenoids

Diterpenoids are chemical compounds with four isoprene subunits (two terpenes) which are mostly isolated from different parts (root bark, leaves and bud) of numerous plant species such as *Euphorbia ebracteolata*, *Euphorbia fischeriana*, *Isodon flavidus*, *Daphne genkwa*, *Jatropha curcas*, *Scutellaria barbata*, which are mostly Chinese traditional medicines (Zhao *et al.*, 1991; Zhan *et al.*, 2005; Zhang *et al.*, 2012; Yuan *et al.*, 2016). They are of biological and pharmacological relevance as they are known to have anti-inflammatory and antimicrobial activities. Examples of diterpenoids are epi-jatrophol, jatrophaldehyde, epi-jatrophaldehyde, flavidusin A and B, langduin A, 12-deoxyphorbo-13hexadecanoate, prostratin, andrographolide, cembrene A, labdane, taxadiene, stemodene and triptolide (Zhao *et al.*, 1991, 2015; Zhang *et al.*, 2012). Diterpenoids have been shown to have moderate to high cytotoxic activities on different cancer cell types (Zhan *et al.*, 2005; Zhang *et al.*, 2012; Yuan *et al.*, 2016). The anti-cancer activities of different diterpenoids have been reported against different cancer cells such as: human lung cancer (Ha *et al.*, 2017), melanoma cancer (Fallahian *et al.*, 2017), cervical, breast and lung cancers (Campos-Xolalpa *et al.*, 2017) and colon cancer (Zhang *et al.*, 2018). Activation of apoptosis pathways and cell cycle arrest have been known to be the major underlying mechanism for diterpenoids anti-cancer activities (Fallahian *et al.*, 2017; Jian *et al.*, 2018; Zhang *et al.*,

2018). These groups of bioactive natural compounds have been suggested to have epigenetic regulation on important genes that function in the regulation of apoptosis and cell cycle in different cancer types (Nardi *et al.*, 2018). However, there are just few or no data available on the epigenetic activities of notable diterpenes with anticancer activities, especially their roles in the inhibition of DNA methyltransferase enzymes that catalyse both global DNA methylation and gene specific methylation at the CpG islands of genes that function in the regulation of apoptosis, cell cycle and cell proliferation. Hence, this study tends to investigate the anti-ovarian cancer activities of few notable diterpenoids and their mechanisms of action especially in apoptosis and epigenetic regulation.

#### **1.6.2.1 Andrographolide**

Andrographolide is a natural compound that is isolated from *Andrographis paniculata* which belong to the family Acanthaceae. This is a bitter plant that is commonly used in Chinese traditional medicine for the treatment of various diseases such as diarrhoea, fever, dysentery ( Zhu *et al.*, 2013; Khan *et al.*, 2018). *A. paniculata* is an indigenous medicinal plant in the Southern Asia, and different part of this plant, importantly the leaves, stem and the roots are traditionally used in herbal medicine (Dai *et al.*, 2019).. Andrographolide is the main compound in this plant with bioactive activities (Jarukamjorn and Nemoto, 2008). The pharmacological relevance of andrographolide include its use as anti-inflammatory agent, anti-cancer agent and immune suppressor in different diseases such as liver injury, obesity, chronic inflammatory joint disease, skin disease and diabetics (Dai *et al.*, 2019). Several studies have reported the anticancer activities of andrographolide against different cancer cells such as: prostate cancer cells (Forestier-Román *et al.*, 2019), colon cancer cells ( Zhang *et al.*, 2017; Khan *et al.*, 2018), breast cancer cells (Peng *et al.*, 2018), gastric cancer (Lim *et al.*, 2017) and liver cancer cells (Shi *et al.*, 2017). Andrographolide have been shown

to have anti-inflammatory activities through the inactivation of NF- $\kappa$ B (Abu-Ghefreh *et al.*, 2009; Zhu *et al.*, 2013). This compound has shown moderate cytotoxic activity against colon cancer but does not show any significant cytotoxic activity against hepatocellular carcinoma, leukaemia and prostate cancer, even at higher concentration of about 200 $\mu$ M (Geethangili *et al.*, 2008). Andrographolide further showed growth inhibitory activities on melanoma cell line by regulating angiogenic factors (Sheeja, Guruvayoorappan and Kuttan, 2007). Nateewattana *et al.* (2014) further reported the anticancer activities of andrographolide and its analogue against malignant tumour of the bile duct epithelial (cholangiocarcinoma). Andrographolide had low cytotoxic activities against the cancer cells while its analogue showed very high cytotoxicity at growth inhibitory concentration of 8.0  $\mu$ M when cancer cell was exposed to drug treatment over 24 h. it was further revealed that the anti-cancer activities of andrographolide analogue was due to its effective suppression of the expression of DNA topoisomerase II  $\alpha$ , even though andrographolide parent compound showed weak inhibition of topoisomerase II  $\alpha$ . The andrographolide analogue further caused cell arrest at G0-G1 phase, induced PARP cleavage and caspase 3 activities, increased expression of P53 and Bax protein. Andrographolide induced apoptosis and caused cell arrest at G0-G1 phase in jurkat cell line and pancreatic cell lines at higher concentration ( Geethangili *et al.*, 2008; Bao *et al.*, 2013). The apoptotic inducing activities of andrographolide was revealed to be through activation of Bax and inhibition of Bcl-2 proteins that regulate apoptosis. Additionally, its apoptotic activity was due to release of cytochrome *c* from the mitochondria, activation of caspase 3 and cleavage of the PARP while its cell cycle activity was through reduced expression of proteins that regulate cell cycle such as; cyclin D1, E, and increased expression of *p21* (Bao *et al.*, 2013). Furthermore, this compound also inhibited invasion, migration and proliferation of gastric cancer cells by blocking the cell cycle and promoting apoptosis (Dai *et al.*, 2017). However, to the best

of my knowledge, little or no data is available on the roles of andrographolide in DNA methylation and DNMT inhibition. Therefore, this study will explore these novel mechanisms of andrographolide activities and its anti-ovarian cancer activities.

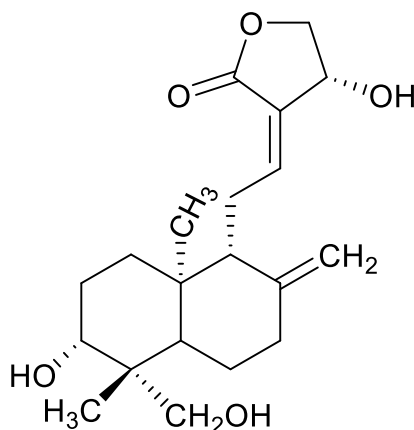


**Figure 1. 11: Structures of andrographolide**

### 1.6.2.2 Triptolide

Triptolide is a bioactive chemical compound that is isolated from *Tripterygium wilfordii* Hook F which belong to the Celastraceae family. *Tripterygium wilfordii* is a Chinese traditional herb with various health benefits (Zhao *et al.*, 2010; Zhang *et al.*, 2017). Triptolide is a diterpenoid that have strong anti-inflammatory and anti-cancer activities, and capable of causing immune suppression (Zheng *et al.*, 2011). Triptolide is known to have growth inhibitory and cytotoxic activities against different cancer types, and these have been shown to be through cell cycle arrest activity and modulation of the expression of various proteins involved in apoptotic pathways (Sun *et al.*, 2017; Gao *et al.*, 2018; Varghese *et al.*, 2018). Triptolide is known to induce apoptosis through the upregulation of the expression of Bax, release of cytochrome *c* into the cytoplasm, cleavage of poly (ADP-ribose) polymerase-1 (PARP-1) protein inhibition of specificity protein 1 (Sp1) that further

downregulated NF- $\kappa$ B (Zhang *et al.*, 2017). Triptolide was shown to be cytotoxic against Jurkat cell (human T lymphocyte), HT29 (human colorectal adenocarcinoma), RPM18226 (multiple myeloma), SMMC-7721 (human hepatocellular carcinoma) cell lines even at very low concentration at time dependent manner, and it was further shown that it causes apoptosis through activation of caspase 3/7 and caused cell cycle arrest at G0-G1 in these cancer types (Chan, Cheng and Sin, 2001; Zhao *et al.*, 2010; Zheng *et al.*, 2011). Triptolide was further shown to cause cell cycle arrest in multiple myeloma at G2-M phase, inhibited growth and caused apoptosis by caspase activation (Zhao *et al.*, 2010). This compound further inhibited the proliferation of acute myeloid leukaemia, bile duct cancer (cholangiocarcinoma) and lung cancer, induced apoptosis and caused cell cycle arrest in the G0-G1 phase in lung cancer (Tengchaisri *et al.*, 1998; Zhou *et al.*, 2011; Nardi *et al.*, 2018).

Several researches have also shown the roles of triptolide in epigenetic regulation. Zhao *et al.* (2010) have demonstrated that triptolide decreased the methylation of histone H3K4, H3K9, H3K27, H3K36 and H3K79 by down-regulation of histone methyltransferase proteins. Furthermore, this compound also up-regulated the expression of five major proteins (WIF1, FRZB, ENY2, DKK1 and SFRP1) that function as inhibitors of Wnt signalling. However, triptolide does not caused any significant changes to DNA methylation at the CpG islands of the promoter region of the Wnt signalling inhibitors (Nardi *et al.*, 2018). Contrastingly, Mao *et al.* (2018) reported a significant DNA demethylation at the CpG island of *WIF1* gene in lung cancer cell when exposed to triptolide at concentration dependent manner. Triptolide have also been reported to downregulate the expression of miR-144 in nasopharyngeal carcinoma cells, the over expression of this microRNA is known to down regulate the expression of PTEN, and this is one of the mechanisms involved in cell migration and invasion, however, the downregulation of miR-144 by triptolide further lead to upregulation of PTEN protein and inhibition of angiogenesis (Wu *et al.*, 2019). Even

though, several studies have revealed the cytotoxic activities of triptolide on several cancer types, there is still little data on its activities on ovarian cancer. Also, the DNA demethylating activities of triptolide is yet to be established as the few available data does not suggest the same view. Therefore, this study will further the study on the anti-ovarian cancer activities of triptolide and its role in DNA methylation and inhibition of DNA methyltransferase enzymes.

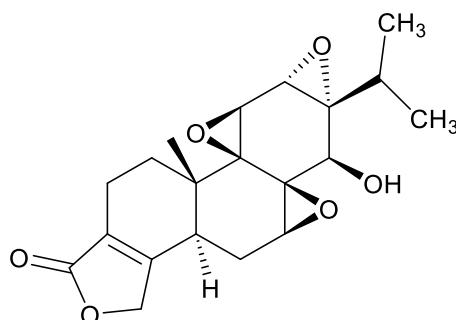


**Figure 1. 12: Structures of triptolide**

### 1.6.3 Other plant phytochemicals with epigenetic activities

Several other compounds have been reported to inhibit DNMT1, caused gene specific demethylation and subsequently upregulated gene expression (Florea *et al.*, 2016). Valproic acid which is a fatty acid had been reported to cause DNA demethylation (Rocha *et al.*, 2019). Furthermore, flavonoids are large groups of plant secondary metabolites that have epigenetic activities (Busch *et al.*, 2015). These phytochemicals are widely distributed in plant, including plants that serve as source of food, vegetables and medicinal herb, and they function in pigmentation and also provide protection against pests and plant diseases (War *et al.*, 2012). The biological activities of these naturally occurring polyphenol (flavonoids) such as curcumin, quercetin, resveratrol and catechins have been reported by various researchers to include: antibacterial, analgesic function, hepatocellular properties,

induction of apoptosis, anti-inflammatory, anti-allergic and so on (Hodek, Trefil and Stiborova, 2002; Chung *et al.*, 2010). These compounds have been suggested to be able to bring about epigenetic changes in the two well-studied epigenetic mechanisms which are DNA methylation and histone acetylation; specifically, epigallocatechin-3-gallate (EGCG) which is a member of the flavan-3-ol subclass that is found in apples, grapes, and the most commonly found flavonoid in green tea has been reported to induce apoptosis, cell cycle arrest and also act as inhibitor of DNMT by direct enzyme action thereby decreasing the level of 5-methylcytosine (Busch *et al.*, 2015). Rajavelu *et al.* (2011) have reported the inhibitory activities of several polyphenols such as: EGCG, theaflavin, theaflavin-3-gallate, thearubigins present in green tea and coffee on DNMT3A. Pandey, Shukla and Gupta (2010) observed a drastic demethylation of *GSTP1* promoter in human prostate cancer cells, leading to re-expression of this gene as a result of inhibitory activities of polyphenols present in green tea on DNMT enzymes. Luo *et al.* (2008) has also demonstrated that flavonoids inhibited proliferation of cells in ovarian cancer cell lines. He further observed inhibition in the expression of vascular endothelial growth factor (VEGF), which is an important factor in angiogenesis that is necessary for the growth of tumour cells. Quercetin, fisetin and myricetin that belong to the subclass flavonols have also been shown to inhibit DNMT with an  $IC_{50}$  1.6 $\mu$ mol/L, 3.5 $\mu$ mol/L and 1.2 $\mu$ mol/L respectively, thereby reducing DNA methylation (Lee, Shim and Zhou, 2005). He further reported that EGCG was found to be more potent with lower  $IC_{50}$  ranging from 0.21 to 0.47 $\mu$ M. Studies on various other classes of flavonoids such as flavones (luteolin and apigenin), flavanones (hesperetin and naringenin), and isoflavones (genistein and daidzein) have also confirmed their inhibitory activities on DNMT enzyme, apoptotic activities and cell cycle arrest in cancer cells such as prostate and oesophageal carcinoma (Busch *et al.*, 2015). In particular, genistein which is an isoflavone has been shown to reduce genomic DNA hypermethylation and this lead to

increased expression of retinoic acid receptor  $\beta$  (RAR $\beta$ ) protein and p16<sup>INK4a</sup>. It was further asserted that genistein inhibits DNMT1, DNMT3A and DNMT3B, which results in the re-expression of tumour suppressor genes that have been silenced (Fang, Chen and Yang, 2007; Zhang and Chen, 2011).

### **1.7 The Genus *Justicia*: A genus with wide application in traditional medicine across the world**

The genus *Justicia* with about 600 species worldwide is the largest genus in the Acanthaceae family, which has about 250 genera with approximately 2500 species. *Justicia* species are both found in the pantropical and tropical regions of the world. The species of this genus are either perennial herb or subshrub and are known to be erect or scandent. About 31 species of this genus have been studied; the chemical properties of only 23 have been reported and 18 of the species have only been studied chemically and biologically in the last decades (Corrêa and de Alcântara, 2011).

The most commonly studied species include: *Justicia pectoralis*, *Justicia procumbens*, *Justicia gendarussa* and *Justicia anselliana*, majority of the other species have not been studied at all. Several species of this genus are widely used in traditional medicine across regions for the treatment of various disorders including: rheumatism and arthritis, respiratory disorder, inflammation, epilepsy, headache, fever, mental disorders etc. (Corrêa and de Alcântara, 2011). Studies have also revealed the anticancer activities of some of the members of this genus against several cancer types such as, lymphocytic leukaemia, nasopharyngeal carcinoma, cervical carcinoma etc.; phytochemical analysis of specific species of *Justicia* has also revealed the presence of flavonoids, alkaloids, lignans, terpenoids, vitamins, fatty acid and oils (Corrêa and Alcântara, 2012; Joseph *et al.*, 2017). However, the anticancer activities of some of the species of *Justicia* namely: *insularis* and

*adhatoda* have not been pharmacologically confirmed. This study will look in detail into the pharmacological relevance of an African edible species *Justicia insularis* in ovarian cancer treatment, characterise the bioactive compounds and evaluate their roles in epigenetic regulation.

### **1.7.1 *Justicia insularis* T. Anderson: African edible plant with wide application in traditional medicine**

*Justicia insularis* T. Anderson is an herbaceous plant that is highly present in the tropical part of Africa (Telefo, Moundipa and Tchouanguép, 2004). It is a perennial plant that grows in a wide variety of habitat ranging from moist forest to dry savannah; the plant is about 2m tall with angular stem and belongs to the family Acanthaceae (Ajiboye, Yakubu and Oladiji, 2013; Adeyemi and Babatunde, 2014). This plant is locally known as Mmeme among the Ibibio ethnic group of Nigeria (Ajibesin *et al.*, 2007). The plant has simple leaves type which has opposite arrangement and the flowers have different colours such as white, pink and purple (Telefo *et al.*, 2012). *Justicia insularis* is an edible herbaceous plant. In some part of Africa such as Nigeria and Cameroon, the leaves are being used in making vegetable and groundnut soup and are even eaten as spinach when cooked and have a lot of nutritional values according to Adeyemi and Babatunde (2014). They also reported that this plant is rich in mineral elements such as calcium, iron, manganese, zinc and sodium but low in magnesium, phosphorus and potassium, also the protein and fat present in this plant is reported to be low.

The phytochemical analysis of *Justicia insularis* revealed the presence of alkaloids, glycosides, flavonoids, saponin, anthocyanins, leucoanthocyanins, tanins, steroids and terpens (Tona *et al.*, 1998; Telefo, Moundipa and Tchouanguép, 2004; Mpiana *et al.*, 2012). *J insularis* is a medicinal plant that is being widely used for the treatment of various diseases

and ailments across Africa. In Nigeria, it is used in treating digestive disease, as weaning agent and laxative (Ajibesin *et al.*, 2007). In the Western part of Cameroon, extract of *J insularis* is used with three other plants with medicinal importance, namely; *Aloe buettneri*, *Hibiscus macranthus* and *Dicliptera verticillat*, for the treatment of infertility among female, dysmenorrhea, and regulation of the menstrual cycle, and in Senegal, the extract from the boiled plant is used to reduce pain among women during delivery (Telefo *et al.*, 2012). In Togo and Some part of Ghana, the decoction of this plant is used to open the bowel of little children and the leaves are also used in healing wound (Adeyemi and Babatunde, 2014). The anti-sickling activities of this plant have also been reported by Mpiana *et al.* (2011). It could be seen that the medicinal use of this plant have been well studied, however, its anticancer activities and mechanism of action have not been reported. Therefore, this study will look at the anticancer activities of this plant, identify the active natural compounds present in this plant that can inhibit DNMTs expression thereby acting as demethylating agent.



**Figure 1. 13: A picture of *Justicia insularis* T. Anderson taking at the collection venue in Nigeria**

## 1.8 Aims, objectives and research questions

### 1.8.1 Research Questions

In order to direct the focus of this study, and to achieve the aims and objectives of this study, the researcher generated some specific questions to be answered in this study. These research questions are:

- i. Do *Justicia insularis* T. Anderson and its bioactive compounds have antiproliferative activities?
- ii. Do sesquiterpene lactones and diterpenoids have anti-ovarian cancer activities?
- iii. Are the anti-proliferative/growth inhibitory activities of sesquiterpene lactones, diterpenoids and the bioactive compounds of *J. insularis* due to apoptosis?
- iv. Do sesquiterpene lactones, diterpenoids and the bioactive compounds of *J. insularis* cause global DNA demethylation and gene specific DNA demethylation in ovarian cancer cells?
- v. Are sesquiterpene lactones, diterpenoids and *J. insularis* isolated compounds capable of causing tumour suppressor gene re-expression in ovarian cancer?
- vi. Do sesquiterpene lactones, diterpenoids and *J. insularis* isolated compounds have DNMT inhibitory activities?
- vii. Does the investigated sesquiterpene lactones, diterpenoids and *J. insularis* identified bioactive compounds have the potential to be developed into drugs?

### 1.8.2 Aims of this study

The overall aim of this study is to evaluate plant-derived compounds for the potential treatment of ovarian cancer. Specific aims of this research are to:

- i. Characterize and identify the bioactive natural compounds with anti-ovarian cancer activities in *Justicia insularis* T. Anderson.
- ii. Evaluate the anti-ovarian cancer activities of sesquiterpene lactones and diterpenoids.
- iii. Investigate the roles of the studied natural compounds in the inhibition of DNA methyltransferase enzymes (DNMTs) in ovarian cancer.
- iv. Investigate the roles of the studied natural compounds in the modulation of DNA methylation and gene expression in ovarian cancer.
- v. Evaluate the mechanisms of apoptosis induction of each of the studied compounds.

### 1.8.3 Objectives of this study

In this research, several objectives were identified to achieve the main aims of the research itemised above. These objectives include:

- i. To carry out extraction of bioactive compounds of *Justicia insularis* and partition the bioactive extract based on solvent polarity.
- ii. To investigate the *in vitro* anti-proliferative activities of *Justicia insularis* extracts, four sesquiterpene lactones and two diterpenoids.
- iii. To purify, isolate, identify and characterize the structure of the bioactive compounds of *Justicia insularis* with anti-cancer activities using HPLC, GC MS, LC MS and NMR.
- iv. To evaluate the cytotoxic activities of the natural compounds using trypan blue assay.
- v. To determine the selectivity index (SI) of the studied bioactive compounds.
- vi. To evaluate changes in apoptotic markers such as caspase 3/7, 8 and 9 due to drug treatment.

- vii. To evaluate the effects of the natural compounds on the mitochondrial membrane potential of ovarian cancer cells as a marker of apoptosis using cytoflex flow cytometry.
- viii. To evaluate the cell cycle arrest activities of the natural compounds studied on ovarian cancer cells.
- ix. To evaluate morphological effects of the natural compounds on ovarian cancer cells using light and fluorescence microscopies.
- x. To evaluate the effects of the natural compounds investigated on global and gene specific DNA methylation in ovarian cancer using ELISA and pyrosequencing assays respectively.
- xi. To evaluate the direct DNMTs enzymatic inhibitory activities of the natural compounds using ELISA based technique.
- xii. To evaluate the roles of the compounds investigated in the modulation of gene expression using RT-qPCR.

## **Chapter Two**

### **General Materials and Methods**

## **2.1 Materials**

### **2.1.1 Natural compounds and control drugs**

The sesquiterpene lactones and the diterpenoids investigated in this study including the positive control drugs (dehydroleucodine, alantolactone, andrographolide and paclitaxel) were purchased from Sigma Aldrich, while parthenolide, costunolide, triptolide, carboplatin and 5-azacytidine were purchased from Abcam Plc, UK (Table 2.1).

### **2.1.2 Plant materials**

*Justicia insularis* (T. Anders) (leaves) plant sample was sourced from Nigeria. The plant was identified by Mr Ozioko O. Alfred, who is a botanist, and sample deposited at the International Centre for Ethno medicine and Drug Development (INTERCEDD) Nigeria, with specimen voucher number as INTERCEDD/1590. The plant was pulverized after drying under shade for 7-10 days at 25°C. The pulverized sample was stored at room temperature for further study. The pulverized plant sample was provided for this study by Rosa Okiemute Johnson-Ajinwo.

### **2.1.3 Reagents**

Several analytical chemicals were purchased and used in this study. These chemicals include: Mecaptoethanol, glacial acetic acid, pyridine and N, O-bis(trimethylsilyl) trifluoroacetamide (BSTFA) which were procured from Sigma Aldrich, while tris-acetate-EDTA, dichloromethane, methanol, ethyl acetate, n-hexane and n-butanol were products of Fischer Scientific, UK. (Table 2.1).

#### **2.1.4 Cancer cell culture and assays materials**

In the culturing of ovarian cancer cell lines used in this study for biological assays, several materials and necessary equipment were used. These include: Panasonic Incu Safe CO<sub>2</sub> incubator, haemocytometer, water bath, Megafuge 8 Centrifuge, micro centrifuge, Olympus light microscope, BioTek Synergy 2 multi-mode microplate reader, multi-channel pipette, biological safety cabinet, vortex mixer, Fisherbrand sonicator, Nuaire -86°C Ultralow freezer, pipette gun, pipettes, industrial methylated Spirit (IMS), Test-tubes, T-25 and T-75 cell culture flasks, 15 and 50 mL polypropylene tubes. Several plates of different well number such as 6, 12, 24, 48 and 96 were used in this study. 2mL cryovials, 1.5 and 2 mL eppendorf tubes, Mr Frosty freezing container (Nalgene), liquid nitrogen cell storage dewars and 15 and 50 mL tubes were also used. Fetal bovine serum (FBS), Roswell Park Memorial Institute (RPMI) 1640 media, PenStrep (penicillin/streptomycin), L-glutamine, and phosphate buffered saline (PBS) 1X which were products of Lonza and Corning UK, were also used, while dimethyl sulfoxide (DMSO), trypsin-EDTA solution were purchased from Sigma Aldrich. Several other reagents were purchased for biological assays, including: sulforhodamine B (acid red 52), trizma base and trypan blue purchased from Sigma Aldrich. Caspase-Glo 3/7, caspase-Glo 8 and caspase-Glo 9 assay kits were procured from Promega, UK, and trichloroacetic acid (TCA), mitoprobe DiIC1 assay kit and actinRed™ 555 ReadyProbes™ reagents were purchased from Fischer Scientific, UK.

#### **2.1.5 Materials used in biochemical and molecular assays**

Several reagents and kits were used in the biochemical and molecular assays. These include; RNase A, RNeasy Mini Kit, DNeasy Blood and Tissue Kit and QuantiFast SYBR® Green RT-PCR Kit from Qiagen, UK. MethylFlash Global DNA Methylation (5-mC) ELISA Easy Kit (Colorimetric), EpiQuik DNMT Activity/Inhibition Assay Ultra Kit

(Colorimetric), EpiQuik Nuclear Extraction Kit, EZ DNA Methylation Kit Gold. Supplied with capped columns were purchased from Epigentek. Annexin V-FITC, annexin V buffer and propidium iodide solution were purchased from Miltenyi Biotec Ltd. ActinRed™ 555 ReadyProbes™ Reagent was purchased from Fisher Scientific, DAPI for nucleic acid staining, Copper (II) sulfate solution, propidium iodide, Ribonuclease A from bovine pancreas were purchased from Sigma Aldrich. TAE buffer (Tris-acetate-EDTA) (50x), agarose, streptavidin sepharose™ high performance, gene ruler 100 bp plus DNA ladder and dNTP mix were products of Fisher scientific, high-performance GoTaq® G2 DNA polymerase with Mg-free buffer system and ethidium bromide were from Promega, PyroMark PCR kit, PyroMark gold Q24 reagents, PyroMark wash buffer, PyroMark binding buffer, PyroMark annealing buffer and primers were purchased from Qiagen.

Other materials and equipment used include: Fisherbrand™ Pasteur pipets, polypropylene blue pipet tip, 0.2 mL microAmp™ optical 8-tube strip and caps, Bio-Rad electrophoresis and tank, blood tube rotator SBI, mini spin-ependorf, nanodrop 2000 spectrophotometer (Thermo Scientific), applied biosystem verity 96 well thermocycler, galaxy mini centrifuge, agilent technologies stratagene MX3000P, Gel Doc-it®2 310 imager with UVP software, weighting balance, centrifuge 5424 R-ependorf, Nikon eclipse Ti-S fluorescence microscopy, pyromark Q 24 (Qiagen), cytoflex (Beckman Coulter), rocker, Agilent technologies 5975C gas chromatography mass spectrometry, Agilent technologies 1220 infinity LC and rotatory evaporator RE 100.

#### **2.1.6 The human ovarian epithelial cancer cell lines and Immortalized normal human ovarian epithelial cell line**

In this study, the anti-cancer activities of the compounds investigated were tested against three different types of human ovarian cancer cell lines (CIS-A2780, OVCAR-8 and

OVCAR-4) and normal human ovarian surface epithelial (HOE) cells. The HOE was a normal ovarian epithelium cells that have been immortalized using the simian virus 40 (SV40) T antigen to overcome cell senescence, and was purchased from Applied Biological Materials (ABM) (Uche, 2017). The ovarian cancer cell lines (CIS-A2780, OVCAR-8 and OVCAR-4) were purchased from American tissue culture collection. OVCAR-4 cell line originated from ovarian cancer patient that showed resistance to cisplatin treatment while OVCAR-8 cell line was from patient with ovarian cancer that showed resistance to carboplatin (Rogan *et al.*, 1984; Uche, 2017). CIS-A2780 cell line was derived from A2780 cells exposed to cisplatin which makes the cells resistant to cisplatin (Godwin *et al.*, 1992). The HOE cell line was used to determine the selectivity index of all the compounds investigated in this study.

**Table 2. 1: Summary list of reagents used, showing their catalogue numbers and supplying companies**

Reagents/compounds/kits	Catalogue number	Supplier
5-Azacytidine	Ab142744	Abcam Plc.
Carboplatin	ab120828	
Costunolide	ab142981	
Parthenolide	ab120849	
Triptolide	ab120720	
Cytoflex daily QC fluorospheres	B53230	Beckman Coulter life Science
Primers (Pyrosequencing primers)	KU128545	Biomers
EpiQuik DNMT Activity/Inhibition Assay Ultra Kit (Colorimetric)	P-3009-48	Epigentek group (Insight Biotechnology Limited, Cambridge Bioscience)
EpiQuik Nuclear Extraction Kit	OP-0002-1	
EZ DNA Methylation Kit Gold	D5005	
MethylFlash Global DNA Methylation (5- mC) ELISA Easy Kit (Colorimetric)	P-1030-48	
L-glutamine	BE17-605E	Lonza / Corning
PENSTREP (penicillin/streptomycin)	BE17-603E	
1X Phosphate buffered saline (PBS)	21-040-CVR	
RPMI 1640	15-040-CVR	
Trypsin-EDTA solution	BE02-007E	
Annexin V Binding buffer	130-092-820	Miltenyi Biotec Ltd
Annexin V-FITC	130-093-060	
Annexin V-FITC Kit	130-092-052	
Propidium Iodide solution	130-093-233	
Caspase-Glo 3/7	G8091	Promega
Caspase-Glo 8	G8201	
Caspase-Glo 9 assay kits	G8211	
	H5041 M7805	

Ethidium bromide solution, molecular grade High-Performance GoTaq® G2 DNA Polymerase with Mg-Free Buffer System		
DNeasy Blood and Tissue Kit	69504	Qiagen
PyroMark binding buffer	979006	
PyroMark denaturation solution	979007	
PyroMark PCR Kit	978793	
PyroMark annealing buffer	979009	
PyroMark Gold Q24 reagents	970802	
PyroMark wash buffer, 10x	979008	
QuantiFast SYBR® Green RT-PCR Kit	204154	
RNase A	19101	
RNeasy Mini Kit	74104	
Alantolactone	SML0415	Sigma Aldrich
Andrographolide	365645	
Copper (II) sulfate solution	C2284	
Chloroform-d <sub>3</sub>	151823	
DAPI for nucleic acid staining	D9542	
Dehydroleucodine	365645	
Dimethyl sulfoxide (DMSO)	D2438	
Glacial acetic acid (GAA)	A/0360/PB17	
Mecaptoethanol	M6250	
N,O-bis(trimethylsilyl) trifluoroacetamide (BSTFA)	D4196	
Paclitaxel	62734	
RT-qPCR primers	KU119247	
Propidium iodide	P4170	
Pyridine	D2438	
Ribonuclease A from bovine pancreas	R4875	
Trizma base	T6791	
Trypan blue	T8154	

Reagents/compounds/kits	Catalogue number	Supplier
ActinRed™ 555 ReadyProbes™ Reagent	R37112	ThermoFisher
Agarose	BP1356-500	Scientific
Dichloromethane	10396410	
dNTP mix	R0193	
Ethyl acetate	10756351	
Fetal bovine serum	10500064	
GeneRuler 100 bp Plus DNA Ladder	SM0322	
Methanol	M/4056/17	
Mitoprobe DiIC1 Assay Kit	M34151	
N-butanol	B/4800/17	
N-hexane	10401631	
Streptavidin Sepharose ® High performance	GE17-5113-01	
Trichloroacetic acid (TCA)	BP555-250	
TAE Buffer (Tris-acetate-EDTA) (50X)	B49	
Acid red 52 / Sulforhodamine B dye	A0600	Tokyo Chemical Industry (TCI) UK Ltd.

## 2.2 Methods

### 2.2.1 Extraction procedure for *Justicia insularis*

The extraction of *Justicia insularis* crude powder was carried out using solvent extraction method (organic and aqueous solvent) (Figure 2.1) already established by NCI for thorough screening of bioactive compounds from plants (Mccloud, 2010; Johnson-Ajinwo, Richardson and Li, 2015; Johnson-Ajinwo, 2017). In brief, 1000g of the plant sample was macerated in 2000mL of dichloromethane (DCM) and 2000mL of methanol (MeOH) (1:1 mixture of DCM/MeOH) for 72hours. The ratio of solvent used to plant sample was 4:1 (4000mL/1000g). After 72hours, the mixture was prepared for filtration to yield the DCM/MeOH *J. insularis* extract. the residue from the filtration was further macerated with 2000mL of methanol for 72hours before further filtration and repeated two more times within 24hours maceration period. The residue was there after soaked in 2000mL of deionized water and filtered after 72hours. This was also repeated two more times within 24hours each to increase the yield. The DCM/MeOH extract was combined with methanol extract (organic extract) (21.0g, 2.1% yield) after drying using rotary evaporator at less than 40°C and the little remaining solvent in the extract was further removed using desiccator under vacuum. The aqueous extract was frozen at -80°C for 24hours before being lyophilized to dryness. The weight of each extract (organic and aqueous extracts) were used in the determination of the percentage yield from the plant sample using the formula below.

$$\% \text{ yield} = \frac{\text{Weight of extract obtained (g)}}{\text{Sample weight (g)}} \times 100\%$$

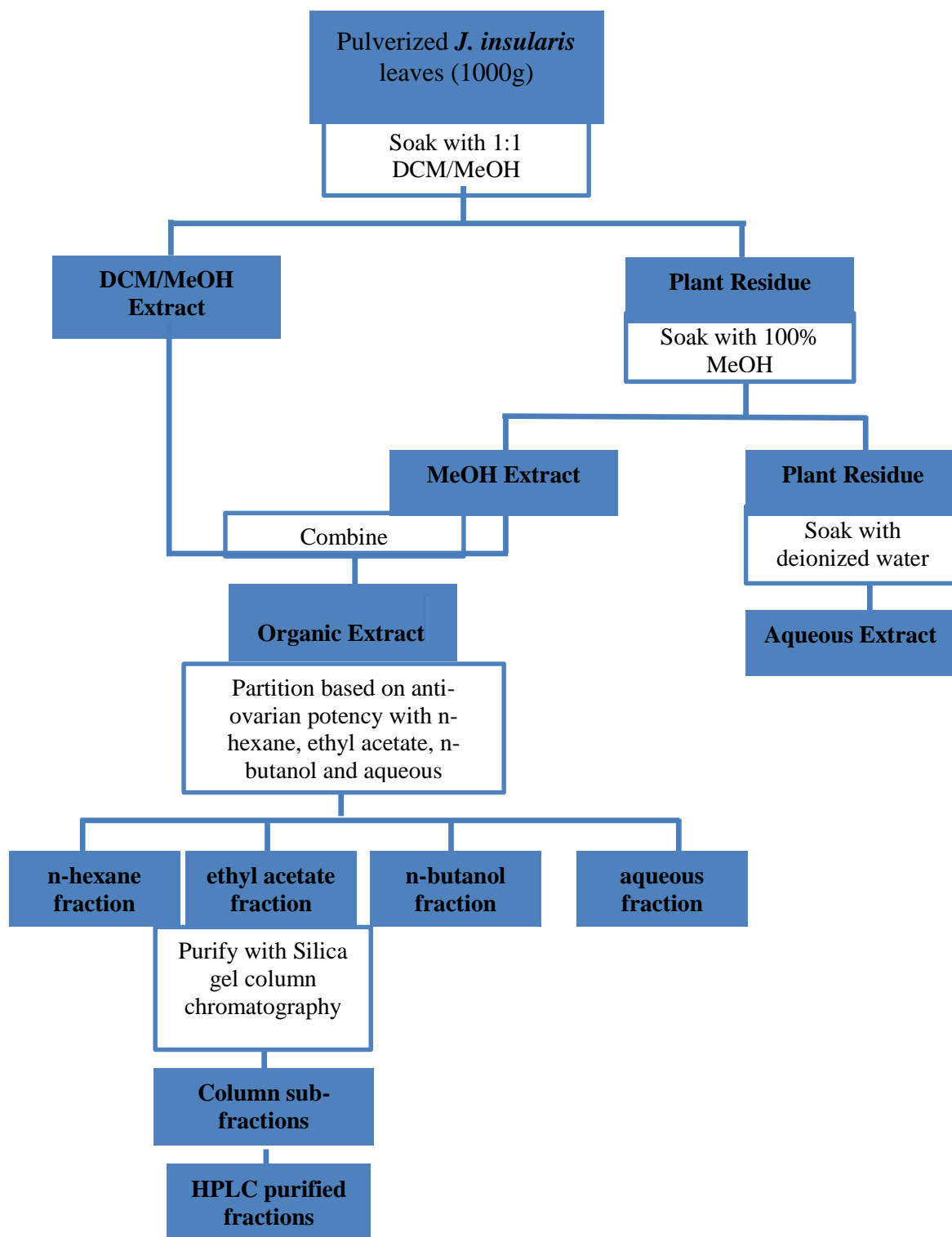


**Figure 2. 1:** A flow chart for the extraction procedure of *J. insularis*. Partitioning was done based on the different polarity of the organic solvents. Further fractionation and purification of active compound was done using column chromatography and HPLC.

### 2.2.2 Solvent partition of plant extracts

Because the organic extract of *Justicia insularis* was more potent against ovarian cancer cell lines than the aqueous extract (Chapter 3), its constituents were further separated using three organic solvents (n-hexane, ethyl acetate, and n-butanol) and water based on their polarity increase (Figure 2.1) (Johnson-Ajinwo, 2017). In brief, 5g of the organic extract was prepared in 300 mL of 90% methanol and firstly partitioned with 150 mL n-hexane. This was repeated for three times. The hexane fractions were combined and evaporated to produce the n-hexane fraction. Furthermore, methanol was evaporated from the residue before it was prepared in 300mL water and the components further separated with 150 mL of ethyl acetate three times and n-butanol similarly. The fractions were evaporated using rotary evaporator and complete removal was achieved using desiccator under vacuum. The three organic fractions and aqueous fraction were obtained and percentage yield was calculated as previously described under section 2.2.1.

The four fractions were assayed for their antiproliferative activities against ovarian cancer cell lines (Section 2.2.13) and the most significantly active fraction was further purified to obtain the active compounds with anti-cancer activities using column chromatography and reverse phase high performance liquid chromatography (HPLC).

### 2.2.3 Purification of bioactive compounds of *Justicia insularis*

The glass column was firstly prepared by suspending 50-80g of silica gel in hexane. The suspended silica gel was poured into the column and allowed to settle with little solvent above the gel. The bioactive ethyl acetate fraction of *Justicia insularis* was dissolved in hexane and gently transferred to the surface of the gel in the column using Pasteur pipette. The fractions were eluted with 200mL of n-hexane/ethyl acetate in the following ratios (4:1,

3:1, 2:1, 1:1, 1:2, 1:3, and 1:4) consecutively as optimised with thin layer chromatography using different ratios of hexane and ethyl acetate combination as mobile phase. The column was finally washed using 100% methanol to obtain the more polar fractions. The sub-fractions were dried as previously described using rotary evaporator and desiccator.

The various sub-fractions from column purification were further assayed for anti-cancer activities and the most significantly active sub-fractions were further purified with semi-preparative HPLC. Briefly, the components of each sub-fraction were separated with Agilent 1220 LC, USA. Two solvents were used as mobile phase. Solvent A consisted of 100% water and solvent B was 100% methanol. The mobile phase calibration started with an initial 50% of solvent B, which rose by 50% within 25 minutes to reach 100% of solvent B, and solvent B was kept at 100% for 10 minutes at a flow rate of 4 mL/min at 215nm absorbance on HPLC column particle size of 5 µm, 9.4 mm diameter and 250 mm length (Phenomenex, UK). The several purified sub-fractions eluted at the varying retention time obtained were been dried using rotary evaporator and purified HPLC fractions were further analysed for purity using analytical HPLC column with particle size of 5 µm, 4.6 mm diameter and 250 mm length (Phenomenex, UK) at 1mL/min flow rate. Solvent systems and mobile phase gradient remained the same as used for semi-preparative HPLC. Further identification of compound was carried out using gas chromatography-mass spectrometry (GC-MS), liquid chromatography mass spectrometry (LC MS) and nuclear magnetic resonance (NMR) spectroscopy.

#### **2.2.4 Gas chromatography mass spectrometry analysis**

1.0 mg of the n-hexane bioactive fraction of *J insularis* plant extracts was dissolved in 10 µL of pyridine and 50 µL of *N,O*-bis (trimethylsilyl)-trifluoroacetamide (BSTFA) (Johnson-Ajinwo, Richardson and Li, 2019). The solution was thereafter incubated in the oven for up

to 2h at 40°C - 50°C to produce the trimethylsilyl (TMSi) derivatives. 1-2 µL of the derivatized n-hexane fraction analysis was done using GC-MS (de Andrade *et al.*, 2012). Alternatively, 1.0-2.0 mg of the ethyl acetate bioactive fractions of *Justicia insularis* were dissolved in 200 µL of ethyl acetate and sonicated at < 40°C for 5mins. 1-2 µL of the prepared fraction was subsequently injected into the GC-MS. The GC-MS is made up of an Agilent 7890, that is coupled to model (5975C MSD) Agilent MS (Agilent Technologies, US) with an instrument column of HP5-MS.

The gas chromatography started at 60°C oven temperature and maintained for 2min, before further increase to 300°C by gaining 10°C increment every 1 min. The temperature was maintained at 300°C for 4 min at constant helium pressure (10psi). The mass spectra for the samples were obtained at a range of 40-1000 in the scan mode in *m/z*. The spectrum obtained for each peak was compared with spectra in the NIST library for possible spectra similarities and suggested compound name for the chromatograms obtained for the ethyl acetate samples.

### **2.2.5 Liquid chromatography mass spectrometry (LC-MS) analysis**

In order to determine the high resolution molecular mass of the isolated compounds, the purified sub-fractions and isolated compounds from *J. insularis* were analysed by LC-MS. Briefly, sample containing 0.1 mg/mL was injected onto the liquid chromatography system of the LC MS. Two mobile phases were used, consisting of mobile phase A containing Milli-Q water with 0.1% formic acid, and mobile phase B consisting of solution of acetonitrile and 0.1% formic acid. A flow rate of 0.4 mL/min was maintained throughout the running time. The mass spectra of the compounds were created from the liquid chromatography eluent ions that was generated with the mass spectrometer coupled to the chromatography

system using HESI II electrospray ion source (Uche *et al.*, 2017). A full-MS method was used in positive or negative ion mode and a scan range of 60-900.

### **2.2.6 Nuclear magnetic resonance (NMR) spectroscopy**

The identification and structural elucidation of the HPLC isolated pure compounds were done using NMR spectroscopy. Briefly, 2-4 mg of each of the isolated compound was prepared in 600  $\mu$ L of deuterated chloroform ( $\text{CDCl}_3$ ).  $^1\text{H}$  and  $^{13}\text{C}$  NMR spectra were recorded with a Bruker (DPX-500) at a frequency of 500 and 125 MHz respectively. Heteronuclear single quantum coherence (HSQC) spectroscopy was also done to show carbon and proton atom correlation. The chemical shifts ( $\delta$ ) and the coupling constants are in parts per million (ppm) and hertz (Hz) respectively. Furthermore, the  $^1\text{H}$  and  $^{13}\text{C}$  NMR spectra were analysed using ACD/Labs Freeware (Advanced Chemistry Development Incorporated, Ontario, Canada) and the NMR data of each compound were compared with reported literature data.

### **2.2.7 Preparation of cell culture growth medium and 1X trypsin**

The Rosewell Park Memorial Institute (RPMI 1640) medium bought from Lonza and Corning was used in the culturing of human ovarian cancer cell lines (CIS-A2780, OVCAR-8 and OVCAR-4) and normal human epithelial ovarian cell line (HOE). The medium was prepared according to the method of Johnson-Ajinwo (2017) by supplementing 500 mL of the RPMI growth medium with 10% fetal bovine serum (FBS) (50 mL), 50  $\mu\text{g}/\text{mL}$  penicillin-streptomycin (Pen strep) (5 mL from 5000  $\mu\text{g}/\text{mL}$  stock) and 2 mM glutamine (5 mL from 200mM stock) (Johnson-Ajinwo, Richardson and Li, 2015). A working stock solution of 1X trypsin was prepared by pipetting 5 mL from 10X trypsin into 45 mL PBS. The prepared medium and trypsin were stored at 4°C, and warmed to 37°C when required

for cell culture. Cells were grown and maintained in a standard humidified panasonic incubator with 37°C, 5% carbon dioxide (CO<sub>2</sub>) conditions throughout this study.

### **2.2.8 Trypsinisation and cell counting**

Cells were repeatedly trypsinised when they were above 80% confluent level. The cell confluence is assessed through direct observation using an Olympus CKX41 light microscope. To detach the adherent cells from T25 cell culture flask for routine passage or for experiment. The method of Johnson-Ajinwo (2017) was used. Briefly, the growth media was aspirated and the cells were washed with 2 mL of phosphate buffered saline (PBS) and subsequently exposed to 1-1.5 mL of 0.01% trypsin (1x trypsin). While cells grown in T75 cell culture flask were washed with 4 mL of PBS and trypsinised with 4 mL of 1x trypsin solution. The cells were shaken and incubated at 37°C for 5-7 min to enhance cell detachment. After complete cells detachment, 1.5-2mL and 4 mL of growth media wer used to neutralise the trypsin activity in T25 and T75 flasks respectively. This was transferred into a sterile 15 mL polypropylene tube and centrifuged at room temperature using a Thermo Scientific centrifuge at 150 g for 3min. The neutralised trypsin was decanted from the cells and fresh media was added to the cells, the cells were gently mixed and 0.2-0.4 mL and 0.5-0.8 mL were added to T25 and T75 cell culture flasks containing 8 and 16 mL of fresh media respectively. The cells in the flasks were incubated until confluence required for experiment or passaging is reached. However, for the purpose of experiment, minimum number of cells (100 cells) was counted using the glass haemocytometer with coverslip. Briefly, 50 µL cells were mixed with an equal volume of 0.4% trypan blue in 1.5 mL eppendorf tube, 10 µL of trypan blue treated cells were pipette to the haemocytometer chambers and covered with coverslip. The grid lines of the haemocytometer were focused with the Olympus CKX41 light microscope using 10X objective lens. Unstained cells (Live cells) in the four sets of

the 16 corner squares were counted with hand tally counter. Only the cells within the squares and on the right-hand bottom boundary lines were counted. The average cells in the four sets of the 16 squares was calculated and multiplied by  $10^4$  and further multiplied by 2 due to 1:1 dilution with trypan blue to determine the cell number per mL. Stained cells (dead cells) were also counted when required to determine cell viability. This method of cell counting was used to determine the required volume of media and the density of cell required for each experimental assays.

### **2.2.9 Cell lines resuscitation from cryopreserved state**

Cells in cryopreserved state were collected from the liquid nitrogen dewars and placed in a 50 mL tube to defrost at 37°C in water bath. The cells were transferred to 15 mL polypropylene tube containing 5 mL of pre-warmed media. Cells were centrifuged at 150g for 3min at room temperature. The media was aspirated and the cells were re-suspended in T25 culture flask containing 8 mL of growth media. The cells were grown for 24h at 37°C and 5% carbon dioxide (CO<sub>2</sub>) in the incubator before the media was changed to remove death cells and residual DMSO. The adherent cells were routinely passaged three to four times before being used for further experiments (Johnson-Ajinwo, 2017).

### **2.2.10 Cryopreservation of cells for future use**

Cells were cryopreserved when they are not used for an immediate experiment but planned for future use as the study progresses, this process helps to keep the cells within limited passage number and maintains the cell morphology to ensure consistency in experimental results. Basically, cells with less than 20 passage number were grown for 4 to 6 days to obtain 50% confluence in T75 culture flask. The cells were trypsinised as described above, centrifuged and re-suspended in 2 mL medium containing 10% DMSO (Johnson-Ajinwo,

2017). Cells were aliquot and transferred into four 2 mL sterile cryovials, each containing 0.5 mL and kept in a Mr Frosty freezing container (Nalgene), containing 200 mL isopropanol and stored at -80°C in a freezer for 24hours before transfer into a dewar containing liquid nitrogen where the cells are stored for future use.

### **2.2.11 Cell growth inhibitory assay**

Sulforhodamine B (SRB) assay (Vichai and Kirtikara, 2006) was used to determine the cell proliferation inhibitory activity of the natural products and the plant extracts investigated in this study. The SRB assay is a standard *in vitro* cytotoxicity assay for the evaluation of the anti-cancer activities of plant extracts and pure compounds. This method has been used in several studies, including the American National Cancer Institute (NCI) studies on the screening of the anti-cancer activity of plant extracts (Rubinstein *et al.*, 1990; Skehan *et al.*, 1990; Vichai and Kirtikara, 2006; Witham *et al.*, 2007; Robinson *et al.*, 2013; Johnson-ajinwo, Richardson and Li, 2015; Orellana and Kasinski, 2016). This assay is based on the stoichiometric binding property of SRB to the cellular protein of cells under a slight acidic conditions and then extracted in basic condition.

In this study, the drugs preparation and the assay were prepared according to the method of Johnson-Ajinwo (2017). Briefly, the stock total concentration of 100 mg/mL and 20mM for plant extract and pure compounds were prepared respectively. Most pure compounds and plant extracted with organic solvents were prepared in DMSO while plants extracted with deionised water were prepared in deionised water and stored at -20°C until when required for experiment. The ovarian cancer (CIS-A2780, OVCAR-8 and OVCAR-4) and HOE cell lines grown in RPMI were seeded in 96 well plates, each well containing cells in 80µL growth medium. 5000 cells of each of OVCAR-4 and HOE cells were seeded per well while CIS-A2780 and OVCAR-8 cells were seeded at 2000 cells per well due to their rapid

growth. The seeded plates were incubated for 24 hours, after which 20  $\mu\text{L}$  of plant extracts and pure compounds containing highest concentrations of 1000  $\mu\text{g}/\text{mL}$  and 200  $\mu\text{M}$  respectively, prepared from 2-fold serial dilution obtained from an initial 100 times dilution of the prepared stock concentrations were added to each well. The addition of 20  $\mu\text{L}$  of prepared drug to growing cells in 80  $\mu\text{l}$  growth media resulted in further 5 times dilution of the drug concentration to yield the drug final concentration. The treated cell cultures were incubated at 37°C under 5%  $\text{CO}_2$  for 72h in a humidified atmosphere.

After 72 hours, cell medium was drained and the cells were fixed for 30-45 minutes with 100  $\mu\text{L}$  of 10% TCA on ice before drying. Cells staining was done with 0.4% SRB for 30 min before washing with 100  $\mu\text{L}$  of 1% acetic acid three to four times. The plates were allowed to dry before 100  $\mu\text{l}$  of Tris-base (10mM) were added, and the plates shaken for 10 min to disband the proteins that are bound to the SRB dye. The spectroscopic plate reader (Multi-mode microplate reader BioTEK Synergy 2, USA) was used to measure the absorbance at 570 nm. 0.2% DMSO contained in the highest concentration of each drug prepared in DMSO was used as negative control while carboplatin, paclitaxel and 5-azacytidine were used as positive control throughout this study. Non-linear regression on Graph pad PRISM 6.0 software was used in data analysis for the determination of  $\text{IC}_{50}$  values. The selectivity index (SI) of the growth inhibitory activities of the compounds on ovarian cancer cell lines were determined against immortalized normal human ovarian epithelia cells using the formula below. The SI value suggests the selectivity of the cytotoxic activity of the compounds for cancer cells rather than the normal cells. A higher SI value suggests theoretically that the natural compounds are more cytotoxic to cancer cells and with high safety level on the normal cells.

$$\text{SI} = \frac{\text{IC}_{50} \text{ of normal cell line}}{\text{IC}_{50} \text{ of cancer cell line}}$$

### 2.2.12 Trypan blue assay

The cytotoxicity of the plant natural compounds or cell viability was studied using trypan blue assay (TBA). This assay determines whether the effect in the cell growth assays was through induction of cell death (Menyhárt *et al.*, 2016; Uche *et al.*, 2016). Briefly described, the cells (CIS-A2780, OVCAR-8, OVCAR-4) were seeded in 12 well plates at a density of  $1 \times 10^5$  cells per well in 1mL of growth media. Three different concentrations of the studied compounds (5, 10 and 20  $\mu\text{M}$ ) were administered to the cells after 24h incubation. Medium containing 0.1% DMSO was used as negative control while 5-azacytidine, carboplatin and paclitaxel were used as positive control. The cell viability was determined using haemocytometer and trypan blue exclusion at different time point (24, 48 and 72hrs) after treatment. The supernatant was removed, followed by trypsinisation of adherent cells, the cells trypsinised and the cells in the supernatant were combined, centrifuged for 3 minutes at 150 g and re-suspended into 200  $\mu\text{L}$  fresh growth media. 50  $\mu\text{L}$  cells were mixed with an equal volume of 0.4% trypan blue thoroughly. Then, numbers of live and dead cells in 20  $\mu\text{L}$  of the suspension mixture were counted using the haemocytometer with the aid of the microscope. The percentage (%) of cell death was there after determined and data presented in graph.

### 2.2.13 Apoptosis assays

Several techniques were employed in this study for the evaluation of the apoptotic activities of the various natural products studied. The methods used include evaluation of caspase 3/7 activities, caspase 8 activities, caspase 9 activities, morphological evaluation for biochemical changes in the cell structure, flow cytometry analysis of stained cells with Annexin V and propidium iodide, cell cycle analysis and mitochondria membrane potential activity.

### **2.2.13.1 Apoptosis detection using caspase 3/7 marker**

The caspase 3/7 activity effect of the investigated compounds was carried out using caspase 3/7 assay kit from Promega Corporation, on a 96-well microplate following the manufacturer's assay guide. Briefly, the cells (CIS-A2780, OVCAR-8 and OVCAR-4) were seeded in 96 well plates containing cell density of 5000 cells/well in 80  $\mu$ L growth media, and exposed to two different doses (10 and 20  $\mu$ M) of each compound after 24 h incubation. After 48 h exposure to compounds treatment, the cells were incubated with 25  $\mu$ L of Caspase 3/7 Glo-reagent on a rocker at room temperature in the dark 40 min. The luminescence was estimated with a BioTEK Synergy 2 microplate reader (USA). SRB assay was performed for each treatment at the same condition on different well plates, this helps to quantify the actual caspase 3/7 activation with response to compound treatment and cell number.

### **2.2.13.2 Evaluation of extrinsic pathway of apoptosis using caspase 8 marker**

Caspase-Glo 8 kit (Promega Corporation, Madison, WI, USA) was used to evaluate extrinsic pathway of apoptosis signalling by the various compounds under investigation. Similar to the caspase 3/7 activity procedure, this assay was performed in 96-well microplate according to the manufacturer's instruction. Briefly,  $5 \times 10^3$  ovarian cancer cells (CIS-A2780, OVCAR-8 and OVCAR-4) were seeded in 80  $\mu$ L growth media per well. After 24 h incubation, the cells were treated with each compound at two different concentrations (10 and 20  $\mu$ M). 25  $\mu$ L of Caspase 8 Glo-reagent was added after 48 h post-treatment period, and the cells incubated in the dark at room temperature for 40 min on a gentle rocker. The luminescence was measured by a BioTEK Synergy 2 microplate reader (USA). In like manner, SRB assay was performed and this helps to quantify the actual caspase 8 marker activity of each compound.

### **2.2.13.3 Evaluation of intrinsic pathway of apoptosis using caspase 9 marker**

Caspase-Glo 9 assay kit from Promega Corporation was used to evaluate initiation of apoptosis through intrinsic. In a similar manner to the caspase 3/7 and 8 activities procedures, this assay was also performed in 96-well microplate following the manufacturer's protocol. The cancer cell lines (CIS-A2780, OVCAR-8 and OVCAR-4) were used in this assay.  $5 \times 10^3$  cells in 80  $\mu$ L growth media were seeded in 96 well plates. The cells were exposed two different concentrations (10 and 20  $\mu$ M) of each compound after 24 h incubation. After 48 hours post treatment with the natural compounds, 25  $\mu$ L of Caspase 9 Glo-reagent was added and the cells incubated for 40 min at room temperature in the dark on a rocker. BioTEK Synergy 2 multi-mode microplate reader (USA) was used to measurement the luminescence. SRB assay was also performed, and this aid the quantification of the actual effect of each drug on caspase 9 marker activities.

### **2.2.13.4 Evaluation of mitochondria membrane potential activities**

The mitochondrial membrane potential functions in the generation of ATP within the cell. However, when the mitochondrial permeability transition pore is opened, the mitochondrial membrane loses its intactness and leads to the release of cytochrome in the mitochondria into the cytosol of the cytoplasm that further activates the downstream of intrinsic apoptotic pathway. The activeness of the mitochondrial membrane potential could be evaluated using cationic cyanine dye which is capable of accumulating in an active mitochondrial membrane. However, the intensity of the accumulation of the cationic cyanine dyes could reduce significantly when cells are treated with drugs capable of disrupting the mitochondrial membrane potential and causing apoptosis, and this could be qualitatively measured using flow cytometry. Therefore, the effect of the natural compounds on the mitochondria membrane potential was evaluated as a maker of apoptosis using mitoprobe

<sup>TM</sup> DiIC1(5). Briefly, CIS-A2780 cell line was seeded in 12 well plates at a density of  $2 \times 10^5$  cells per well in 1 mL of growth media and incubated for 24 hours. Cells were treated with the studied compounds after 24 hours' incubation. 0.1% medium was used as negative control. Cell pellets were collected after 48 hours post treatment. The supernatant was removed into 15mL tube followed by trypsinisation of adherent cells, the cells trypsinised and the cells in the supernatant were combined, centrifuged for 3 minutes at 150 g and re-suspended into 1mL growth media which was transferred into sterile 2 mL Eppendorf tube and centrifuged at 300 g for 5 minutes at 4°C and the supernatant was aspirated. Prior to experiment DiIC1 and CCCP were equilibrated to room temperature, and the assay was performed according to the protocol for the <sup>TM</sup> DiIC1(5) assay provided by the manufacturer. In brief, 1 mL PBS was added to the pellet, 1  $\mu$ L of 50 mM carbonyl cyanide 3- chlorophenylhydrazone (CCCP) (final concentration of 50 nM) was added to the control tube (i.e untreated cells now treated with CCCP thereby serving as positive control) and incubated at 37°C for 5 minutes. 5  $\mu$ L of 10  $\mu$ M of DiIC1 at final concentration of 50 nM was added to each sample tube including the positive control tubes (cells treated with CCCP) and negative control tubes (untreated cells) and incubated at 37°C, 5% CO<sub>2</sub> for 30 minutes. After incubation, cells were centrifuged for 7 minutes at 200 g. supernatant discarded and cells were re-suspended in 400  $\mu$ L PBS and analysed on a cytoflex flow cytometer with 633 nm excitation using emission filters appropriate for Alexa fluor® 633 dye. Prior to cell analysis on flow cytometry, daily QC was performed to verify the alignment of the cytoflex flow cytometer. After cell analysis on the cytoflex, cells were gated to exclude debris. The percentage accumulation of cationic cyanine and level of decrease in the mitochondrial membrane potential of the cells were calculated. The data were subjected to statistical analysis to determine significant changes in the mitochondrial membrane potential activities of the cells.

### **2.2.13.5 Light microscopy**

Ovarian cancer cell lines (CIS-A2780 and OVCAR-4) were seeded in 24 well plates at a cell density of 10,000 cells/ well in 500  $\mu$ L growth media. After 24 hour of incubation, cells were exposed to different concentrations (5, 10 and 20  $\mu$ M) of the natural compounds, while the control was exposed to 0.1% of the vehicle (DMSO). Images were taken after 48 and 72 hours of drug exposure with 10X objective lens using Olympus CKX41 light microscope.

### **2.2.13.6 Nuclear and actin staining fluorescence microscopy**

4', 6-diamidino-2-phenylindole (DAPI) and actinRed<sup>TM</sup> 555 ready probes reagents were used to stain the nucleus and the actin filament of the cell respectively, and images taking using fluorescence microscope. Briefly, Ovarian cancer cell lines (CIS-A2780 and OVCAR-8) were seeded in 24 well plates at a cell density of 20,000 cells/ well in 500  $\mu$ l growth media, and exposed to 10 and 20  $\mu$ M of the natural compounds after 24 hours of incubation. After 48hours exposure to drug treatment, the media was aspirated from the cells and rinsed three times with PBS. The cells were not allowed to dry out and were immediately fixed for 10 min in 3.7% formaldehyde. The fixative was aspirated and cells rinsed three times with PBS. The cells were permeabilised in 500  $\mu$ L of 0.2% triton X-100 for 5 min. The triton was aspirated and cells rinsed three times with PBS. One drop of actinRed<sup>TM</sup> 555 ready probes reagents was added per 500  $\mu$ L of PBS and incubated for 30 minutes away from light, the stain was removed and cells washed 2-3 times in PBS. The cells were further incubated with 300 nM DAPI staining solution for 5 min at room temperature. The DAPI labelling solution was aspirated and cells were rinsed three times in PBS. The cells were imaged with X40 objective lens on the fluorescence microscopy.

### **2.2.13.7 Flow cytometry analysis of apoptosis using annexin V**

Annexin V is a cellular protein that is frequently used by several researchers in the evaluation of apoptosis due to its preferential binding affinity to phosphatidylserine (PS) at the outer leaflet of the plasma membrane. Phosphatidylserine is located in the inner leaflet of the plasma membrane under normal condition. However, upon initiation of apoptosis, PS is translocated to the outer leaflet of the membrane. The flow cytometry is a technique that uses laser beam to analyse cells that are fluorescently labelled. In this experiment, OVCAR-8 and CIS-A2780 cell lines were seeded in 12 well plates at a density of  $2 \times 10^5$  cells per well in 1 mL of growth media and incubated for 24 hours. Two different concentrations of the studied compounds ( $IC_{50}$  value and  $\times 2$  of  $IC_{50}$  values of each compound) were administered to the cells after 24 hours of incubation. 0.1% medium was used as negative control and cell pellets were collected at 48 hours. Briefly, the supernatant was removed into 15mL tube followed by trypsinisation of adherent cells, the cells trypsinised and the cells in the supernatant were combined, centrifuged for 3 minutes at 150 g and re-suspended into 1 mL growth media which was transferred into sterile 2 mL Eppendorf tube and centrifuged at 300 g for 5 minutes at 4°C. Supernatant was aspirated and the pellet was washed in 1 mL cold PBS. Centrifugation was repeated at the same condition and supernatant aspirated. Cells were then washed in 500  $\mu$ L annexin-V binding buffer and centrifuged at 300 g for 10 minutes, supernatant aspirated and cell pellet re-suspended in 100  $\mu$ L of binding buffer before 10  $\mu$ L of annexin V-FITC purchased from Miltenyi Biotec Ltd. was added using the reagent protocol from the manufacturer. Cells thoroughly mixed with annexin V-FITC and incubated for 15 minutes in the dark at room temperature. After incubation, cells were washed in binding buffer and centrifuged at 300 g for 10 minutes. Supernatant aspirated and cells re-suspended in 500  $\mu$ L binding buffer before 5  $\mu$ L of propidium iodide was added to distinguish cells in early apoptosis from cells in late

apoptosis prior to flow cytometry analysis on Beckman Coulter Cytoflex equipped with CytExpert software for data acquisition and analysis. Prior to cell analysis on flow cytometry, daily QC was performed to verify the alignment of the cytoflex flow cytometer. The population of the cell was gated on the side scatter area (SSC) and forward scatter area (FSC) to exclude the debris and doublet. The data was distributed in the FITC and PE channels. The data was analysed using the CytExpert software.

#### **2.2.14 Cell cycle analysis**

Similar to apoptosis assay setup, OVCAR-8 and CIS-A2780 cell lines were seeded in 12 well plates at a density of  $2 \times 10^5$  cells per well in 1 mL of growth media and incubated for 24 hours. Two different concentrations of the studied compounds at approximate ( $IC_{50}$  value and  $\times 2$  of  $IC_{50}$  value of each compound) were administered to the cells after incubation for 24 hours, while 0.1% of DMSO in medium was used as negative control. In all cell cycle assays, cell pellets were collected after 48 hours of treatment with each compound to evaluate their early effects on cell homeostasis. The supernatant was removed into 15 mL tube followed by trypsinisation of adherent cells, the cells trypsinised and the cells in the supernatant were combined, centrifuged for 3 minutes at 150 g and re-suspended into 1 mL growth media which was transferred into sterile 2 mL Eppendorf tube and centrifuged at 150 g for 5 minutes at 4°C. Supernatant was aspirated and the pellet was washed in 1 mL cold PBS. Centrifugation was repeated at the same condition and supernatant aspirated. Cells were fixed in 70% ethanol by slowly adding the ethanol to the sample with vortexing. The samples were either used after 45-1hr fixation or stored at -20°C till needed. Before use, cells were centrifuged at 500  $\times g$  for 5 min, ethanol removed and cells washed with 1 mL PBS. This was repeated twice. After centrifugation, cells were re-suspended in 300  $\mu L$  solution of propidium iodide with 50  $\mu L$  of ribonuclease solution, incubated in the dark for

30-45 minutes before being analysed with flow cytometry. The cell population was gated as explained earlier. However, the cell cycle phase was presented as histogram on the PE channel with count on the vertical channel.

### **2.2.15 Quantification of global and gene specific DNA methylation**

DNA methylation was quantified at the genome level and at gene specific promoter region using enzyme-linked immunosorbent assay (ELISA) technique and pyrosequencing respectively. Prior to DNA methylation quantification, ovarian cancer cells were treated with the compounds under investigation, cell pellet prepared and DNA extracted. Detailed procedures were described under each section below.

#### **2.2.15.1 Cell pellet preparation**

CIS-A2780 and OVCAR-4 cell lines were seeded in 6 well plates at a density of  $4 \times 10^5$  and  $6 \times 10^5$  cells per well in 2 mL of growth media respectively. The cells were incubated for 24 hours. Two different concentrations of the studied compounds at approximately  $IC_{50}$  value and  $x2$  of  $IC_{50}$  value of each compound were administered to the cells after 24 hours of incubation. 0.1% medium was used as negative control. Each of the treatment was in three repeats. Cell pellets were collected at 72hours. Briefly, the supernatant was removed into 15mL tube, followed by trypsinisation of adherent cells, the cells trypsinised and the cells in the supernatant were combined, centrifuged for 3 minutes at 150 g and re-suspended into 1mL growth media which was transferred into sterile 2 mL Eppendorf tube and centrifuged at 2000 g for 3 minutes at 4°C. The supernatant was aspirated and the pellet was washed with 1 mL cold PBS. Centrifugation was repeated at the same condition and supernatant aspirated. The cell pellets were stored at -20°C/-80 °C for DNA extraction.

### **2.2.15.2 DNA extraction**

DNA was extracted using QIAamp DNA mini kit (Qiagen) according to the manufacturer's instructions. The prepared cell pellets were thawed at room temperature and subsequently re-suspended in 200  $\mu$ L PBS. 20  $\mu$ L of proteinase K was added and for the purpose of obtaining genomic DNA that is RNA free, 4  $\mu$ L of an RNase A (100 mg/mL) (Qiagen) was added to the sample. Furthermore, 200  $\mu$ L AL buffer was added and sample was briefly vortexed for 15 seconds and incubation was done for 10 minutes at 56°C in water bath. After incubation, ethanol (96-100%) was added at volume of 200  $\mu$ L, and samples mixed by vortexing for 15 s, followed by centrifugation of the samples, which was performed briefly to remove the drops from the inside of the lid and the solution was transferred to the 2 mL QIAamp mini spin column collection tube. The column was centrifuged for 1 min at 6,000 g, and the tube containing the filtrate was discarded and the mini spin column was placed in a new 2 mL collection tube, AW1 buffer at a volume of 500  $\mu$ L was added to the samples without wetting the rim and centrifuged at 6,000 g for 1 minute, and the tube containing the filtrate was discarded and the mini spin column was placed in a clean collection tube, followed by washing with 500  $\mu$ L AW2 buffer and further centrifuged at 20,000 g for 3 minutes before discarding the filtrate. The centrifugation was repeated at the same speed for 1 minute. The mini spin column was then positioned on a new 1.5 microcentrifuge tube, 40  $\mu$ L distilled water was added and incubated at room temperature for 5 minutes before centrifugation at 6,000 g for 1 minute to elute the DNA. The DNA elution step was repeated to increase the yield of the DNA. DNA quality and concentration was determined by spectrophotometric analysis at 260 nm with a NanoDrop 2000/2000c (Thermo Scientific). DNA extracted was stored at -20°C for further study.

### **2.2.15.3 Quantification of global 5- methylcytosine DNA methylation**

The total 5-methylcytosine in DNA content was detected using MethylFlash™ Global DNA methylation (5-mC) ELISA easy kit (Colorimetric) (Epigentek NY, USA) according to the manufacturer's instructions. Genomic DNA isolated as described above was concentrated with distilled water to 25 ng/μL in a final volume of 40 μL. 100 ng of genomic DNA for each sample was used as starting material. Briefly, diluted wash buffer (1x wash buffer) was prepared by adding 13 mL of wash buffer (10x wash buffer) with 117 mL of distilled water, which was used for later washing of samples in the 96-well plate. Diluted positive control (PC) was prepared by diluting 1 μL of PC with 9 μL of Negative control (NC). In order to generate a standard curve, 6 concentrations points for the positive control was prepared by combining PC, diluted PC, and NC to generate 0.1%, 0.2%, 0.5%, 1.0%, 2.0% and 5.0% PC/well. For the assay, 100 μL of binding solution (BS) was added to all the wells, 2 μL of NC was added to the negative control well and 2 μL of PC at different concentrations (0.1%-5%) were added to the positive control wells respectively. 4 μL (100 ng) of the concentrated DNA (25 ng/μL) prepared from the stock DNA extracted from the cancer cells treated with different compounds were added to each sample well. Three repeats were done for each of the samples for the purpose of analysis and result reliability. Furthermore, each of the samples including NC and PC were performed in duplicate, and sample replicates were loaded in vertical arrangement to reduce cross variation between replicates. The solution the wells was mixed by gently tilting the plates side by side several times to ensure the solution coated the bottom of the well evenly. The plate was covered with plate seal and incubated at 37°C for 1 hour. After 1 h incubation, the BS was removed from each well and washed with 150 μL of the diluted WB each time for three times. The 5-mC detection complex solution was prepared adding 1 μL of 5-mC antibody (mcAb), 1 μL of signal indicator (SI) and 0.5 μL of enhancer solution (ES) to 1 mL of diluted wash buffer (WB). Thereafter, 50

$\mu\text{L}$  of the 5-mC detection complex solution was added to each well. The plate was covered and incubated at room temperature for 50 minutes. After that, the 5-mC detection complex solution was removed from each well and each well was washed with 150  $\mu\text{L}$  of diluted WB each time for five times. 100  $\mu\text{L}$  of developer solution (DS) was added to each well in a column with a multi-channel pipette and the plate was tilted gently and incubated at room temperature for 3-4 minutes. The colour change was monitored in the samples wells and positive control wells. The DS turned blue in the presence of sufficient methylated DNA after a few minutes while the NC control colour remained generally unchanged. The enzyme reaction was halted when the colour in the 5% PC wells turned deep blue by adding stop solution (SS) to each well in a column using a multi-channel pipette to ensure that replicates of the same sample are stopped at the same time. The solution was mixed gently by shaking against a flat surface where the assay was performed for 1-2 minutes which allowed the colour reaction to be completely stopped as the colour turned yellow and the absorbance was measured on a micro-plate reader (BioTek, Synergy 2) at 450nm. Standard curve was determined, and the percentage of 5-mC was calculated with the formula below using the logarithmic second order regression.

$$5\text{-mC}\% = e^{[(Y-b)/a]} \div S \times 100\%$$

Where S is the amount of DNA (ng) used as starting material, Y is OD value of each of the assayed samples, while a and b represent slope and intercept of Y respectively.

#### **2.2.15.4 Pyrosequencing assay for quantification of gene specific DNA methylation**

Pyrosequencing technique was used in the quantification of DNA methylation at the CpG sites of the promoter region. The PyroMark Q24 system with the PyroMark Q24 application software 2.0 was used in this study. PyroMark assay design 2.0 software was used to design

primers (forward, reverse and sequencing primers with either the forward or reverse primer biotin labelled) (Table 2.2 and Appendix 2) for all the genes (*MLH1*, *TUSC3*, *BRCA1*, *TP53*, *APC*, *KLF6*, *RASSF1*, *PTEN*, *FOLR1*, and *HOXA9*) evaluated in this study. Several molecular procedures were carried out in this assay. At first, DNA extracted from ovarian cancer cell line (CIS-A2780) was bisulfite converted. The bisulfite converted DNA was used as starting material for PCR. The primers were optimized, PCR products were checked with gel electrophoresis before used for pyrosequencing. Each of the procedures is described in detail below.

#### **2.2.15.4.1 Bisulfite conversion of DNA**

Bisulfite conversion of the DNA samples was done using EZ DNA methylation-Gold™ kit from Zymo research (Epigenetics Company) according to the manufacturer's instruction. Briefly, CT conversion reagent was prepared by adding 900 µL water, 300 µL M-dilution buffer, and 50 µL M-dissolving buffer to each of the CT conversion reagent tube. The prepared CT conversion reagent was mixed by vortexing and shaking for 15 minutes. 130 µL of the CT conversion solution was added to 20 µL of DNA samples containing 500-600 ng in PCR tubes. The PCR tubes were placed in the thermal cycler and run with an initial condition at 98°C for 10 min followed by 64°C for 2 hr 30 min. The product was stored for up to 20 hours at 4°C. 600 µL of M-binding buffer was added to zymo-spin™ IC column and placed on the collection tubes. The samples were transferred to the column and mixed by inverting the column several times and centrifuged at full speed for 30 seconds. The flow-through was discarded and 100 µL of M-wash buffer was added to the column and centrifuged at full speed for 30 seconds. This was followed by 200 µL of M-desulphonation buffer addition to the column and incubated at room temperature for 15-20 minutes before further centrifugation was done at full speed for 30 seconds. Washing was done with 200 µL of M-wash buffer and centrifuged at full speed for 30 seconds, and this was done twice. The column was placed in 1.5 mL micro centrifuge tube, and 21 µL of M-elution buffer was

added to the column matrix and was centrifuged at full speed for 30 seconds. Elute was taken back into the column and re-centrifuged at full speed for 30 seconds to increase the yield of the bisulfite converted DNA. The bisulfite converted DNA was either used immediately for further experiment or stored at -20°C before used.

#### **2.2.15.4.2 Polymerase chain reaction (PCR)**

PCR was performed using PyroMark® PCR kit from Qiagen. Bisulfite converted DNA of CIS-A2780 ovarian cancer cell line was used as starting material. The PyroMark® PCR kit reagents (PyroMark PCR master mix, coral load concentrate, MgCl<sub>2</sub>, Q-solution, RNase-free water) and the forward and reverse primers were thawed (Figure 2.2). The individual solutions were mixed and placed on ice. The PCR was performed in a total reaction volume of 25 µL. The reaction mix contains 12.5 µL PyroMark PCR master mix, 2.5 µL Coral load concentrate, 5.5 µL of RNase-free water, 1.25 µL forward primer and 1.25 µL reverse primer. The reaction mix was mixed thoroughly and dispensed appropriately into the PCR plates. 2 µL of bisulfite converted DNA was used as template and added to the individual PCR wells containing the reaction mix. The thermo cycler was programmed with an initial PCR activation step for 15 min at 95°C, followed by three step cycling involving 30 s denaturation at 94°C, annealing at 52-54°C for 30 s and extension at 72°C for 30 s in 45 cycles with another final extension of 10 min at 72°C. The PCR plates were placed in the thermo cycler and the cycling programme was run. The PCR product was checked by agarose gel analysis prior to pyrosequencing.

#### **2.2.15.4.3 Agarose gel electrophoresis**

2.0% agarose gel was prepared by dissolving 4.0 g agarose in 200 mL 1X TAE (Tris acetate EDTA) electrophoresis buffer in 800 mL beaker. The bottle was shaking to suspend the agarose and was immediately microwaved for 4 mins and shaking was done after 2 min to ensure that agarose dissolve completely. 5 µL of 10 mg/mL ethidium bromide was added and thoroughly mixed by shaking. The gel was casted with the combs well-arranged and

allowed to wait for 40 min at room temperature before removing the comb and placed into the electrophoresis tank. 1  $\mu\text{L}$  of loading dye was mixed with 1  $\mu\text{L}$  of DNA ladder and 4  $\mu\text{L}$  of deionized water. 5  $\mu\text{L}$  of the PCR product of each sample and DNA ladder were loaded on the gel in the tank and 1X TAE buffer was allowed to flow over the gel. The voltage was set 100V and the gel was run for 1 hr 20 minutes. The gel was visualized on the Gel Doc-it®2 imager and images captured using UVP software.

#### **2.2.15.4.4 Pyrosequencing procedure**

PyroMark Q24 reagents were used for analyzing pyrosequencing reactions. The PyroMark Q24 system was switched on and the template for the plate was prepared on the PyroMark Q24 software. The pyroMark Q24 machine protocol for pyrosequencing and Qiagen protocol were used in this study. Briefly, the volumes of enzyme mix, substrate mix and each of the nucleotide to be added to the cartridge was checked on the PyroMark Q24 software pre run information. The metal tray for the PyroMark Q24 plate was placed on the heating plate set at 80 °C. The binding mixture was prepared by adding 40  $\mu\text{L}$  of binding buffer, 29  $\mu\text{L}$  of Molecular Biology Grade Water and 1  $\mu\text{L}$  of beads per reaction. Each volume was multiplied by number of samples. The annealing mixture was prepared by adding 1.8  $\mu\text{L}$  of sequencing primer to 600  $\mu\text{L}$  of annealing buffer. 70  $\mu\text{L}$  of the binding mixture was added to 24-well PCR tubes and 10  $\mu\text{L}$  of PCR product was added into each of the PCR tube, the tubes were closed with a strip cap and mixed at 1400 rpm for at least 15 min. 25  $\mu\text{L}$  of the annealing mixture was added to the wells of the PyroMark Q24 plate. The cartridge was prepared accordingly and placed in the appropriate position on the PyroMark Q24 instrument. The trays of the workstation were filled with water, 70% ethanol, 1x washing buffer and denaturation solution respectively. The vacuum was switched on in the suction probe, and placed on the prime tray with distilled water to aspirate approximately

70 mL. The PCR tubes were removed from the shaker, the lids were taken off, and the solution in the PCR tube was carefully suctioned with the vacuum switched on. The suction probe having the sample/bead was washed with 70% ethanol for 10 s. It was further placed in the tray with denaturing solution, and flushed for 10 s, followed by aspiration 1x washing buffer for up to 20s and the suction probe was tilted for a few s. The vacuum suction probe was placed on top of the PyroMark Q24. The vacuum was switched off and the handle lowered on the PyroMark Q24 plate. The suction probe was gently tilted for about 15-30 sec to release the bead into the plate containing the sequencing primer. The vacuum suction probe was rinsed with distilled water. The plate was placed on the metal tray and heat at 80 °C for 5 min until little bubbles appear. This was allowed to cool for 5 min and subsequently placed on the PyroMark Q24 system instrument and started running. After the run, plate was discarded, cartridge rinsed and data was analysed. The percentage methylation at each variable CpG sites was arranged on the Excel spreadsheet for further analysis.

**Table 2. 2: Forward, reversed and sequencing primers used for pyrosequencing assay and their annealing temperatures**

Gene	Primer	Primer sequence 5' to 3'	Annealing Temp. (°C) used for PCR
<i>TP53</i>	F	GGGTTTGTGATTTGGTAGGTATT	53
	R	TCTCCCCCTACCCCATCTCTTAACT	
	S	TCTTCCCATACACCT	
<i>BRCA1</i>	F	AGTTTGGGGTAAGTAGTTTTGTAAG	53
	R	TCCCTCAAACCACCACCCCATTA	
	S	GGTAAGTAGTTTTGTAAGGT	

<i>RASSF1</i>	F	AGTTTTTGTTTTATTGGGGTAGGAA	53
	R	CCTCCCACCAAAAACCACTCTTATAC	
	S	TTATAGATTTTATTTATTATAGGGA	
<i>TUSC3</i>	F	GGATAGAAGAAAAAGGAGGTAGAA	53
	R	CCCCTTTTAATAACACCATTACTC	
	S	GTGTTGTTAGGTAGTTTG	
<i>MLH1</i>	F	TAAGGGGAGAGGAGGAGT	53
	R	AATACCAATCAAATTTCTCAACTCTAT	
	S	TTGTTTTTATTGGTTGGATAT	
<i>HOXA9</i>	F	AGTAGTTGTTTAGTGG	52
	R	TTCCCCCCCCTATTAC	
	S	AGGGTTTTAGGTGGTG	
<i>KLF6</i>	F	GGAGTTTTTGGGAAGATGTTGTATAT	52
	R	CTCTACCAACCTAAAATTTACATAAACT	
	S	AGATGTTGTATATGGGG	
<i>PTEN</i>	F	GGTGTTTTTTGGGTTTTTGAAAT	54
	R	TCCCCCAAATCTATATCCTCATAATATC	
	S	GAGAGTTTTTATTTTAGGGTAA	
<i>APC</i>	F	AGAGAAGGTTAGTAAGTGTGTAAT	53
	R	CCCCCCCCCTTACTACTTACCCT	
	S	GTTGTTTAGGTAGTAATGGTTTA	

### **2.2.16. Quantitative reverse transcription polymerase chain reaction (RT-qPCR)**

Change in gene expression due to the activities of the studied compounds on ovarian cancer cells was evaluated using RT-qPCR. RNA was used as starting materials. The procedures for cell pellet preparation, RNA extraction are RT-qPCR are described below.

#### **2.2.16.1 Cell sample preparation and RNA extraction**

CIS A2780 cell line was seeded in 6 well plates at a density of  $3 \times 10^5$  cells per well in 2 mL of growth media and incubated for 24 hours. Two different concentrations of the studied compounds at approximately  $IC_{50}$  value and  $x2$  of  $IC_{50}$  value of each compound were administered to the cells after 24 hours of incubation. 0.1% DMSO in medium was used as negative control. Each of the treatment was done in three repeats. Cell pellets were collected after 72hours incubation. Briefly, the supernatant was removed into 15mL tube followed by trypsinisation of adherent cells, the cells trypsinised and the cells in the supernatant were combined, centrifuged for 3 minutes at 150 g and re-suspended into 1mL growth media which was transferred into sterile 1.5 mL Eppendorf tube and centrifuged at 2000 g for 3 minutes at 4°C. Supernatant was aspirated and the pellet was washed with 1 mL cold PBS. Centrifugation was repeated at the same condition and supernatant aspirated. The pellet was stored at -20°C/-80°C for RNA extraction. RNeasy® Mini kit was used in RNA extraction. The kit extraction protocol according to the manufacturer was used. Briefly, the cell pellets were equilibrated to room temperature and 350 µL of buffer RLT containing 10 µL mercaptoethanol was added. 350 µL of 70% ethanol was added and mixed well by pipetting. Up to 700 µL of the sample was transferred to an RNeasy mini spin column and the columns were placed in a 2 mL collection tube. The samples in the columns were centrifuged at 8,000 g for 15 s and the flow through was discarded. 700 µL buffer RW1 was added to the RNeasy spin column and centrifuged at 8000 g for 15 s and the flow through was discarded.

Furthermore, 500  $\mu\text{L}$  buffer RPE was added to the samples and centrifuged at 8000 g for 15 s and the flow through was discarded. 500  $\mu\text{L}$  buffer RPE was further added and centrifuged at 8000 g for 2 min. The RNeasy spin column was placed in a new 2 mL collection tube and centrifuged at full speed for 1 min to dry the membrane. The spin column was placed in a new 1.5 mL collection tube, and 30  $\mu\text{L}$  of RNase-free water was added directly to the spin column membrane and was centrifuged at 8000 g for 1 min to elute the RNA. The RNA eluate was further pipetted into the RNeasy spin column and centrifuged at the same speed and time to increase RNA concentration. RNA quality and concentration was determined by spectrophotometric analysis at 260 nm with a NanoDrop 2000/2000c. RNA isolated was stored at  $-80^{\circ}\text{C}$  for further study.

#### **2.2.16.2 Quantitative reverse transcription polymerase chain reaction (RT-qPCR) procedure**

RT-qPCR was performed using QuantiFast<sup>®</sup> SYBR green RT-PCR kit and the manufacturer's protocol was used in the assay set up. The RNA samples were concentrated into 100 ng/ $\mu\text{L}$ . The QuantiFast RT mix was taken from  $-20^{\circ}\text{C}$  immediately before use for the experiment. The QuantiFast SYBR green RT-PCR master mix, RNA template, primers and RNase-free water were thawed. The individual solutions were mixed and placed on ice. RT-qPCR was performed in a 12.5  $\mu\text{L}$  total reaction volume. The reaction mix containing 6.25  $\mu\text{L}$  2x QuantiFast SYBR green RT-PCR master mix, 1.25  $\mu\text{L}$  forward primer, 1.25  $\mu\text{L}$  reverse primer, 0.25  $\mu\text{L}$  quantifast RT mix. The 2x QuantiFast SYBR green RT-PCR master mix contains HotStar Taq Plus DNA, QuantiFast SYBR Green RT-PCR-Buffer, dNTP mix and fluorescent dyes. The reaction mix was mixed thoroughly and dispensed appropriately into the PCR plates. 2.5  $\mu\text{L}$  of RNase free water was added to 1  $\mu\text{L}$  template RNA (100 ng/ $\mu\text{L}$ ) and added to the individual PCR wells containing the reaction mix. The real time

cycler was programmed with an initial 1 cycle of reverse transcription for 10 min at 50°C and PCR initial activation step for 5 min at 95°C followed by two step cycling involving 10 s denaturation at 95°C and combined annealing/extension at 60°C for 30 s in 40 cycles. However, the annealing temperature varies with the different primers used (Table 2.3). Primers were designed using the Integrated DNA technologies PrimerQuest® Tool, the gene transcripts were determined and obtained from Ensembl/National Center for Biotechnology Information (NCBI) (Appendix 1). Primer-BLAST was done to check for primer specificity, and primer self-complementarity check was also done and melting temperatures ( $T_m$ ) determined. All the primers used were desalted and optimised to determine their annealing temperatures. The PCR plates were placed in the real-time cycler and the cycling programme was run. The CT values were arranged in excel worksheet and the mRNA expression was determined with the CT values, the relative gene expression changes were calculated based on  $2^{-\Delta\Delta CT}$  method (Livak and Schmittgen, 2001). *GAPDH* was used as an internal control gene to normalize the variations in gene expression.

**Table 2. 3: Primers used for RT-qPCR and their annealing temperatures**

Gene	Primer	Primer sequence 5' to 3'	Annealing Temp. (°C) used for RT-qPCR
<i>TP53</i>	F	GTTCCGTCTGGGCTTCTT	56
	R	GTTGTAGTGGATGGTGGTACAG	
<i>BRACA1</i>	F	CTCAGTGTCCAACCTCTCTAACC	56
	R	GCTTCTCAGTGGTGTTCAAATC	
<i>RASSF1</i>	F	GGAGTACAATGCCAGATCAA	50
	R	GTCATCCACCACCAAGAACT	

<i>TUSC3</i>	F	AACTCCTGGCGCTATTCATC	54
	R	TGTCCATTGTGTGGGTTCTT	
<i>MLH1</i>	F	GCCATTGTCACAGAGGATAAGA	54
	R	CCCACGAAGGAGTGGTTATG	
<i>KLF6</i>	F	CTTAGAGACCAACAGCCTGAAC	56
	R	CTTCCCATGAGCATCTGTAAGG	
<i>PTEN</i>	F	CCCACCACAGCTAGAACTTATC	50
	R	ATCACCACACACAGGTAACG	
<i>APC</i>	F	AGCCTCGATGAGCCATTTATAC	58
	R	TAGGTGTCCCTTCAACACAATAC	
<i>FOLR1</i>	F	GGAAGAATGCCTGCTGTTCTA	60
	R	CTTGTAGGAGTGAGTCCAGATTTC	
<i>DNMT1</i>	F	GCCTCTCCATCGGACTTGC	60
	R	CACTGCTACTTAAATTATCCTTTCCT GCT	
<i>DNMT3A</i>	F	AGAGCAGAGGACGAGC	60
	R	ATTATCGTGGTCTTTGGAGG	
<i>DNMT3B</i>	F	TAATAAGTCGAAGGTGCGTC	60
	R	TCTGAAGCCATTTGTTCTCG	
<i>DNMT3L</i>	F	<u>TGCTAGACAGACCCCATTTCCT</u>	60
	R	ATTGACCACTCAGGGCCCATTG	

## **2.2.17. Evaluation of inhibitory activity of natural compounds against DNMT**

### **2.2.17.1 Cell pellet preparation for DNMT assay**

CIS-A2780 and OVCAR-4 cell lines grown to 70-80% confluence in a culture flask were collected into 15 mL tube by aspirating the media, washed cells in flask with PBS, trypsinised the cells and added fresh medium. The collected cells were centrifuged at 300 g for 5 min. The cell number was determined with the haemocytometer. The media were aspirated and cells washed twice with PBS, and the PBS was then removed after centrifugation at 300 g for 5 min. Samples were stored at -20°C for nuclear extraction.

### **2.2.17.2 Nuclear extraction procedure and protein quantification**

Nuclear extraction was done using Epiquick™ nuclear extraction kit and manufacture's protocol. Briefly,  $3 \times 10^6$  CIS-A2780 and OVCAR-4 cell lines pellets prepared were thawed and re-suspended in 300 µL of diluted pre-extraction buffer (NE1) buffer and transferred into a 1.5 mL microcentrifuge vial, incubated on ice for 10 min and was vortexed for 10 seconds before centrifuging the cells at 14,000 g for 1 min. The cytoplasmic extract was removed from the nuclear pellet. 30 µL of extraction buffer (NE2) containing DTT solution and protease inhibitor cocktail (PIC) at 1:1000 ratio was added and incubated on ice for 15 min. The suspension was centrifuged at 21,000 g at 4°C for 10 minutes and the supernatant collected into 1.5 mL tubes. The protein concentration was measured using standard Bradford protein assay. Briefly, eight concentrations of bovine serum albumin (BSA) standard were prepared starting from 2000 µg/mL. 300 µL of the working reagent was added to 10 µL of the standard and sample wells. The wells were thoroughly mixed and incubated for at least 5 min. the absorbance was measured at 595nm using the plate reader and the protein concentration calculated. The nuclear extract was stored at -80°C until further use.

### **2.2.17.3 DNMT inhibitory assay**

The DNMT inhibitory activities of the natural compounds were evaluated using Epiquick™ DNMT activity/inhibition assay ultra-kit (colorimetric) and protocol. Briefly, 50 µL of diluted adomet (MU3) were added to the blank and positive control wells, 1 µL of the DNMT enzyme control (MU4) was added to the positive control well. 45 µL of diluted MU3 and 5 µL of nuclear extracts were added to the sample wells without inhibitor. 40 µL of diluted MU3 was added to the sample wells with inhibitors. 5 µL of nuclear extracts and 5 µL of inhibitor solution were added to the sample wells with inhibitor to make a total volume of 50 µL per well. The strip-well microplate was tightly covered with adhesive covering film to avoid evaporation during incubation. The plate was incubated at 37°C for about 120 min. The reaction solution was removed from each well and washed three times with 150 µL of diluted wash buffer (MU1) each time. The diluted capture antibody (MU5) was added to each well at volume of 50 µL and covered with aluminium foil before incubating at room temperature for 60 min. Thereafter, the solution was removed and wells washed with 150 µL of diluted MU1 for three times. The diluted detection antibody (MU6) was added and the plate was incubated at room temperature for 30 min. The solution was removed after incubation and plate washed with 150 µL of diluted MU1 four times. 50 µL of diluted enhancer solution (MU7) solution was added to each well, then carefully covered with aluminium foil and incubated at room temperature for 30 min. The solution was removed and wells washed with 150 µL of the diluted MU1 for five times. Signal was detected by adding 100 µL of developer solution (MU8) to each well and incubated at room temperature for 10 min away from direct light. The colour changes in the sample and control wells were monitored. The MU8 solution turned blue in the presence of methylated DNA. The enzyme reaction was stopped using 100 µL of stop solution (MU9) when the colour in the positive control wells turned blue. The solutions were mixed well and incubated for 1-2

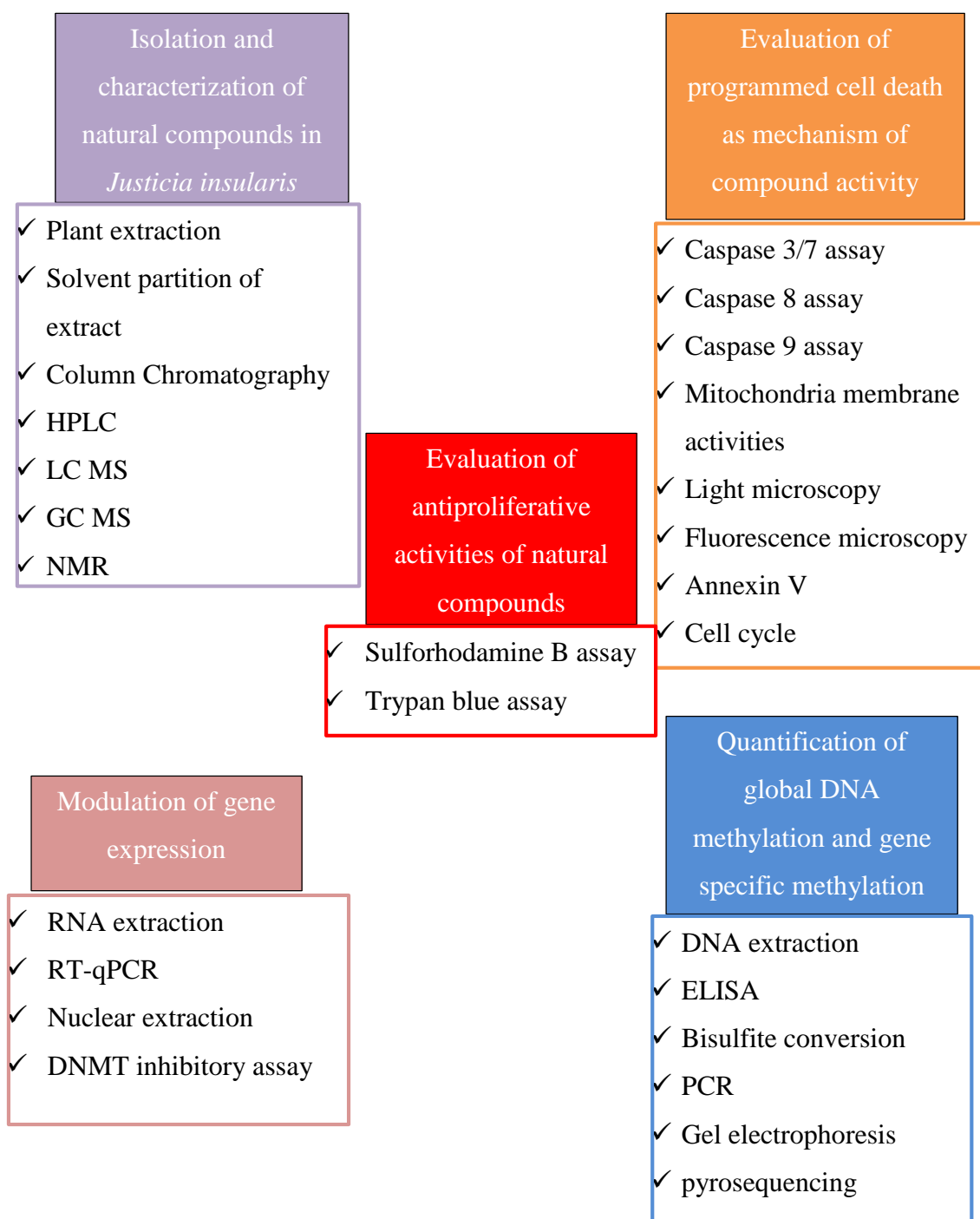
min to allow the colour reaction to be completely stopped. The absorbance was read on the microplate reader within 2-10 min at 450 nm. The data was then analysed according to the manufactures' guide using the formula below.

$$\text{DNMT inhibition \%} = \left( 1 - \frac{\text{Inhibitor Sample OD} - \text{Blank OD}}{\text{No inhibitor sample OD} - \text{Blank OD}} \right) \times 100\%$$

### **2.3 Statistical analysis**

All data generated from this study were organized in Microsoft Excel and were independently subjected to statistical analysis for better interpretation and presentation using GraphPad prism 6 software (GraphPhad Software Inc.). Briefly, the data obtained from SRB assay as measured using plate reader at 570nm absorbance was analysed by non-linear regression using the GraphPad prism 6 software to fit a four-parameter sigmoidal dose-response curve to determine the concentration that inhibited 50% cell growth (IC<sub>50</sub>). The IC<sub>50</sub> values were obtained from at least three repeated experiments each in triplicate. The mean IC<sub>50</sub> was calculated, the standard error of the mean (SEM) was determined and the mean concentration growth response curve was generated. The data from trypan blue assay, apoptosis assays and DNA methylation studies were analysed using percentages and fold increase, and the results were presented in bar charts. Furthermore, one-way analysis of variance (ANOVA) and student t test were used to test if the difference between the mean of control and treatments and mean of treatment at different concentrations were significant. Post hoc Dunnetts' test was used to determine which of the concentration of the treatment was significant to the control, while Tukey test was used to determine which of the concentration of a particular treatment was significant when compared.

## 2.4 Graphical Summary of methods used in this study



## **Chapter Three**

### **Characterisation of Anti-Ovarian Cancer Diterpenoids in *Justicia Insularis* T. Anderson and their Roles in Apoptosis, DNA Methylation and Gene Expression**

### 3.1 Introduction

This chapter focused on the anti-ovarian cancer activities of *Justicia insularis* T. Anderson, characterization of its bioactive compounds and their roles in epigenetic regulation (DNA methylation) and apoptosis. *Justicia insularis* T. Anderson is a typical member of the Acanthaceae family which is an edible plant that is present in the tropical part of Africa (Telefo, Moundipa and Tchouanguep, 2004; Adeyemi and Babatunde, 2014). This plant is traditionally used in Africa for the treatment of diverse diseases such as digestive disease, infertility, menstrual cycle irregularities, dysmenorrhea, pains during delivery, wounds, bowel problem and as weaning and laxative agent (Ajibesin *et al.*, 2007; Telefo *et al.*, 2012; Adeyemi and Babatunde, 2014). However, despite the medicinal relevance of this plant, the plant had received less scientific attention over the ages. Additionally, the anti-cancer activities of this plant have not been investigated and the bioactive compounds in this plant are yet to be elucidated. Therefore, this study will be a novel research revealing the anti-ovarian cancer activities of this plant, identifying the bioactive natural compounds and evaluating their roles in DNA methylation and apoptosis.

Several scientific techniques and methods were used in this chapter. Briefly, the pulverized plant sample was extracted with organic solvent and deionized water. The bioactive compounds were isolated through bioassay-guided fractionation using solvent partition, silica gel column chromatography and high performance liquid chromatography (HPLC). The isolated bioactive compounds were characterized using gas chromatography mass spectroscopy (GC-MS), liquid chromatography mass spectroscopy (LC-MS) and nuclear magnetic resonance (NMR) spectroscopy techniques. The growth inhibitory and cytotoxic activities of the extracts and the isolated bioactive compounds were evaluated on ovarian cancer cell lines (CIS-A2780, OVCAR-8 and OVCAR-4) and immortalised human ovarian

epithelia (HOE) cell line using Sulforhodamine (SRB) assay and trypan blue exclusion cell viability assay. The IC<sub>50</sub> which is the concentration that caused 50% inhibition in the cancer growth was determined and the selectivity index (SI) of the bioactive compounds was determined with the HOE. The possible route of cell death by the isolated compounds was proposed to be through apoptosis. This was investigated by evaluating changes in various apoptotic markers such as: caspase 3/7, 8, and 9, phosphatidylserine, mitochondrial membrane potential and change in cell morphology using light and fluorescence microscopy. The epigenetic activity of the isolated compound was also evaluated using enzyme linked immunosorbent assay (ELISA) based techniques, pyrosequencing and RT-qPCR. The results of these assays are presented under different sub-headings below.

## **3.2 Results**

### **3.2.1 Yield of plant extracts and partitioned fractions of *J. insularis***

The extracts of *J. insularis* are presented as organic and aqueous extracts. The percentage yield of the total extract (organic and aqueous) is 28.5g (2.9%). The organic extract has the higher yield of 21.0g (2.1%) than the aqueous extract that yielded 7.5g (0.75%). The high yield observed in the organic extract may possibly be due to the extraction method or an indication that there are more non-polar compounds than polar compounds in *J. insularis*. Furthermore, the *in vitro* growth inhibitory activity of the extracts was evaluated on the ovarian cancer cells (CIS-A2780, OVCAR-8 and OVCAR-4) (Figure 3.1 and Table 3.1). Based on the higher growth inhibitory activity of the organic extract, the organic extract partitioned based on solvent polarity using three organic solvents (n-hexane, ethyl acetate (EA) and butanol) and deionized water. The weight and yield of the solid fractions recovered are 4.6g (25%), 6.0g (33.3%), 2.5g (13.9%) and 3.0g (16.7%) for n-hexane, ethyl acetate,

n-butanol and aqueous fractions respectively. The yield of ethyl acetate was significantly higher than the yields of n-butanol and aqueous, and slightly higher than the n-hexane yield.

### 3.2.2 Growth inhibitory activity of *J. insularis* extracts and fractions

The growth inhibitory activities of the different extracts (organic and aqueous extracts) and fractions of *J. insularis* were tested against ovarian cancer (CIS-A2780, OVCAR-8 and OVCAR-4) cell lines and HOE cells. The results of the preliminary evaluation of the growth inhibitory activity of the plant extracts and fractions showing the growth response curve of the organic extract and fractions on the ovarian cancer cell lines are presented in Figure 3.1. The concentrations that inhibited 50% growth ( $IC_{50}$  values) in the cancer cell lines and HOE cells are also presented in Table 3.1. The organic extract of *J. insularis* significantly inhibited ovarian cancer growth with  $IC_{50}$  values of  $9.1 \pm 0.55$   $\mu\text{g/mL}$ ,  $10.7 \pm 0.6$   $\mu\text{g/mL}$  and  $19.2 \pm 0.5$   $\mu\text{g/mL}$ , on CIS-A2780, OVCAR-8 and OVCAR-4 respectively. The selectivity index of the organic extract was 1.2, which suggests that the organic extract shows high cytotoxicity to the HOE cell line. However, the aqueous extract of *J. insularis* had  $IC_{50}$  values above the 50  $\mu\text{g/mL}$  threshold on CIS-A2780, OVCAR-8 and OVCAR-4.

The results for the partitioned fractions of the organic extract showed the  $IC_{50}$  values of n-hexane, EA, butanol and aqueous fractions are  $7.3 \pm 0.3$ ,  $5.2 \pm 0.2$ ,  $115.0 \pm 16.4$  and  $49.0 \pm 4.0$   $\mu\text{g/mL}$  respectively in CIS-A2780 cell line. In OVCAR-8, the  $IC_{50}$  values are  $6.1 \pm 1.8$ ,  $7.5 \pm 1.7$ ,  $101.7 \pm 2.2$  and  $71.5 \pm 14.9$   $\mu\text{g/mL}$  for n-hexane, EA, butanol and aqueous fractions are respectively, while n-hexane, EA, butanol and aqueous fractions showed  $IC_{50}$  values of  $19.5 \pm 1.0$ ,  $25.7 \pm 1.5$ ,  $118.4 \pm 4.6$  and  $80.0 \pm 0.8$   $\mu\text{g/mL}$  respectively in OVCAR-4 (Table 3.1). The results suggest that n-hexane and EA fractions are the most active fractions of the organic extract of *J. insularis*. This further shows that lesser growth inhibitory activities were observed in the fractions partitioned with more polar solvents (butanol and aqueous).

Thus, further purification of the bioactive ethyl acetate fractions was carried out to characterize the bioactive compounds.

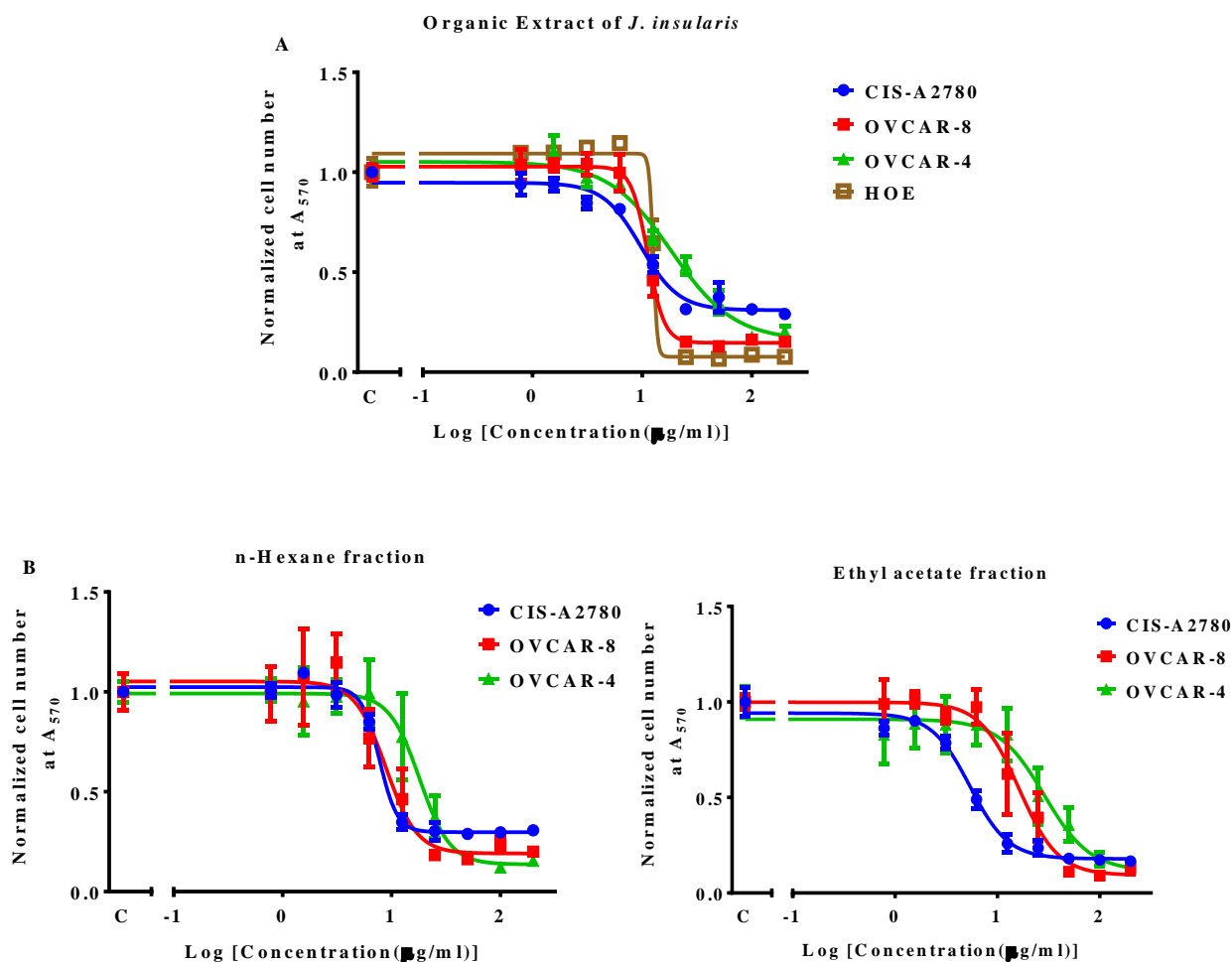


**Figure 3. 1: Mean concentration-response curve of the organic (DCM/MeOH) extract (A) and fractions of *J. insularis*: n-hexane (B) and ethyl acetate (C) on CIS-A2780, OVCAR-8 and OVCAR-4 ovarian cancer cell lines and HOE cells. The cancer cell lines were treated with (0.78 – 200 µg/mL) concentrations of the extracts for 72h. The data generated were analysed as mean ± SEM of three repeated experiments each in triplicate. 0.2% DMSO in vehicle (media) was used as negative control and is denoted with C.**

**Table 3. 1: The *in vitro* half maximal growth inhibitory concentration (IC<sub>50</sub>) values of *J. insularis* extracts and fractions against ovarian cancer (CIS-A2780, OVCAR-8 and OVCAR-4) cell lines using SRB assay. Cell number was estimated by SRB staining after post-treatment period of 72h. The IC<sub>50</sub> results were expressed as mean  $\pm$ SEM from three independently repeated experiments and the selectivity index (SI) for the organic extract was determined as the ratio of the IC<sub>50</sub> value for HOE to the IC<sub>50</sub> of cancer cell lines and the mean SI was calculated based on the three individual SIs. However, the actual SI for the aqueous extract could not be determined because no definite IC<sub>50</sub> value was determined for CIS-A2780, OVCAR-4 and HOE cell lines.**

Extracts tested	CIS-A2780	OVCAR-8	OVCAR-4	HOE IC <sub>50</sub>	SI with	SI with	SI with	Mean
	IC <sub>50</sub> (μg/mL)	IC <sub>50</sub> (μg/mL)	IC <sub>50</sub> (μg/mL)	( μg/mL)	CIS-A2780	OVCAR-8	OVCAR-4	SI (n=3)
Organic Extract	9.1±0.5	10.7±0.6	19.2±0.5	14.1±4.2	1.5	1.3	0.7	1.2±0.3
Aqueous Extract	>200	99.8±0.3	> 150.0	>200	1	2	1.3	1.4±0.4
n-Hexane fraction	7.3±0.3	6.1±1.8	19.5±1.0	-	-	-	-	-
Ethyl acetate fraction	5.2±0.2	7.5±1.7	25.7±1.5	-	-	-	-	-
Butanol fraction	115.0±16.4	101.7±2.2	188.4±4.6	-	-	-	-	-
Aqueous fraction	49.0±4.0	71.5±14.9	80.0±0.8	-	-	-	-	-

### 3.2.3 Column purification results of the ethyl acetate fraction of *J. insularis*

The ethyl acetate fraction of *J. insularis* was subjected to silica gel column chromatography fractionation based on solvents polarity using combinations of n-hexane and ethyl acetate (4:1, 3:1, 2:1, 1:1, 1:2, 1:3 and 1:4) based on thin layer chromatography (TLC) profile obtained, and the final elution was done with methanol. Ten sub-fractions were obtained and their ovarian cancer cell growth inhibitory activities were evaluated using cell growth assay on OVCAR-4 cell line (Table 3.2). Each of the sub-fractions from the ethyl acetate fraction showed significant anti-cancer activity. However, EA4 was the most active fraction of JI-EA while the least activities were observed in EA9 and EA10 which were eluted with ethyl acetate/methanol and methanol respectively. EA4 which was the most active fraction was further purified using column chromatography to yield sub-fractions of EA4. The growth inhibitory activity of the sub-fractions of EA4 from column chromatography was evaluated (Table 3.2). Sub-fractions EA4-4 and EA4-6 were further purified using semi-preparative high performance liquid chromatography.

**Table 3. 2: The results of the growth inhibitory activities of EA fractions and EA4 sub-fractions of *J. insularis* on OVCAR-4 ovarian cancer cell line.**

Ethyl acetate fractions of <i>J.insularis</i>	IC <sub>50</sub> Value (µg/mL) on OVCAR-4 cell line	EA4 Sub-fractions of <i>J.insularis</i>	IC <sub>50</sub> Value (µg/mL) on OVCAR-4 Cell line
EA1	7.2±0.8	EA4-1	6.8±1.0
EA2	5.9±0.1	EA4-2	9.1±2.6
EA3	6.7±0.1	EA4-3	5.3±1.1
➔ EA4	4.1±0.4	➔ EA4-4	3.0±0.4
EA5	6.2±0.4	EA4-5	9.4±0.5
EA6	5.7±0.8	➔ EA4-6	2.6±0.2
EA7	12.0±0.3	EA4-7	10.3±2.4
EA8	11.5±0.3	EA4-8	4.8±0.9
EA9	43.7±1.4	EA4-9	5.8±0.9
EA10	68.4±3.3	EA4-10	7.2±0.8
		EA4-11	14.2±2.3

### 3.2.4 Purification of pure compounds from active fractions of JI EA 4-4 and EA4-6

Isolation of active compounds from the most active sub-fraction EA4-4 and EA4-6 was carried out using semi-preparative reversed-phase HPLC to yield different chromatogram peaks and pure compounds. Before doing semi-preparative HPLC, analytical HPLC of EA4 and EA4 sub-fractions (EA4-4 and EA4-6) along with the n-hexane, ethyl acetate, butanol and aqueous fractions, was carried out, to show the chemical profiles of phytochemicals in *J. insularis* and their retention times.

The analytical chromatograph of ethyl acetate and n-hexane fraction showed that they both have a major peak at Rt 22.4-22.6 min which is absent or not prominent in aqueous and n-butanol fractions (Figure 3.2). This could suggest this major peak is likely the bioactive compound and why the two fractions showed higher and similar anticancer activities. However, since the major peak in EA and n-hexane had similar retention time, ethyl acetate fraction was purified because of available milligram that was further purified using column chromatography to yield reasonable quantity of product. The analytical chromatograph of the yielded sub-fraction JI-EA4 showed similar chromatogram with the EA fraction (Figure 3.3).

The JI ethyl acetate sub-fraction 4-4 and 4-6 (JI-EA4-4 and JI-EA4-6) were further purified using semi-preparative HPLC (Figure 3.3) and the bioactive compounds were isolated. The purified compounds were further analysed for purity using analytical HPLC column at a flow rate of 1mL/min (Figure 3.4).

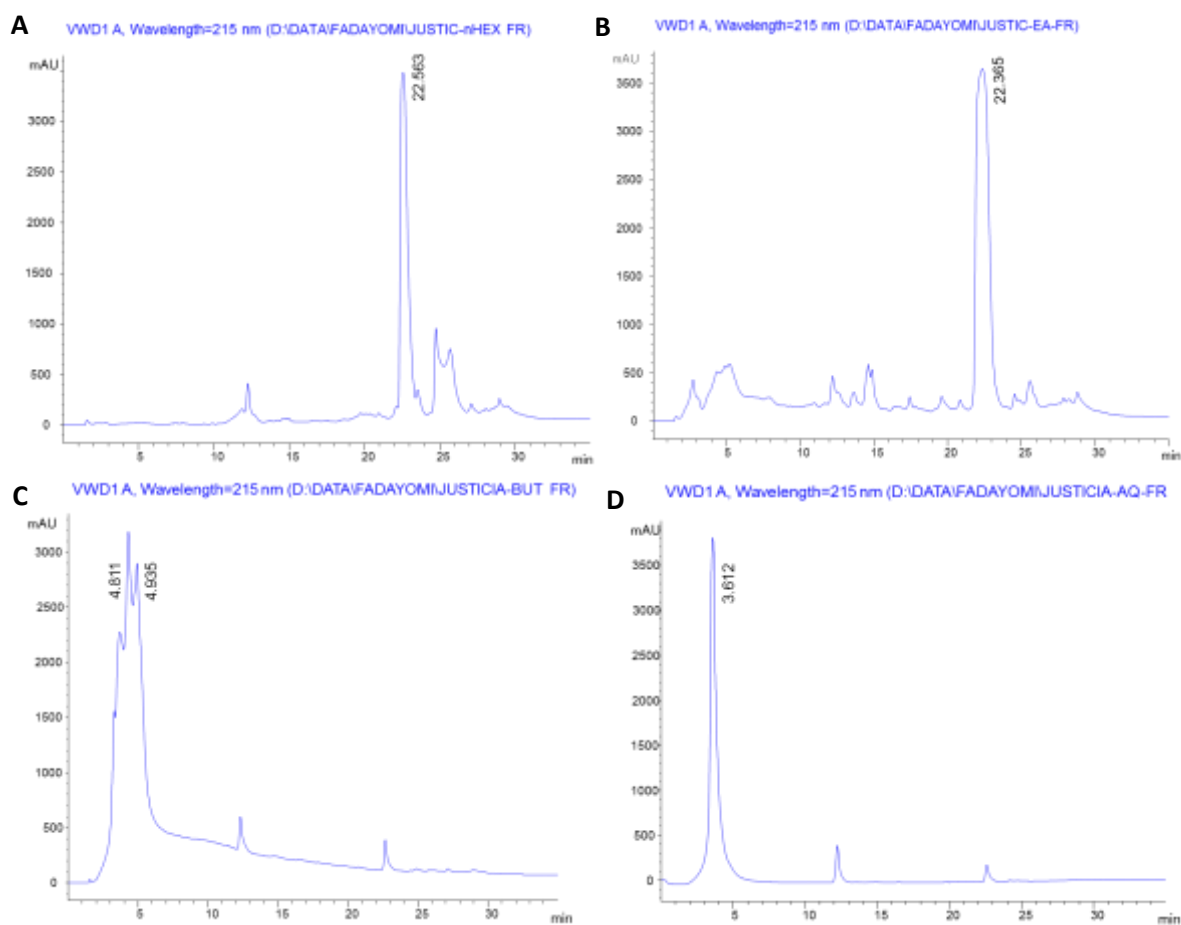


**Figure 3. 2:** Analytical HPLC chromatogram of fractions of *Justicia insularis* showing several peaks with the main compounds indicated by retention time; (A) n-hexane fraction, (B) Ethyl acetate fraction (C) n-butanol fraction and (D) aqueous fraction.

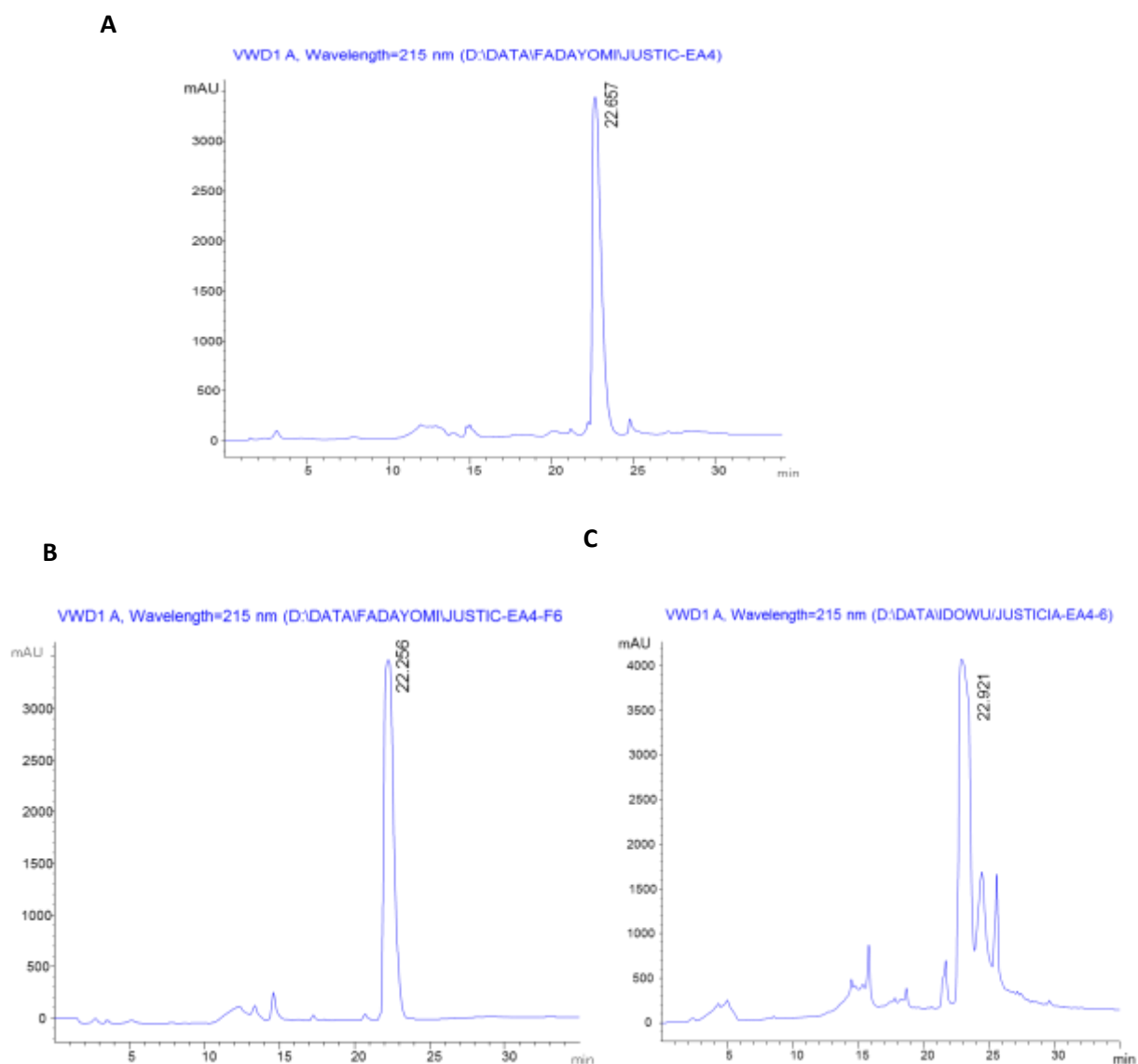


**Figure 3. 3: Analytical and Semi preparative HPLC chromatogram of JI ethyl acetate (EA) sub-fractions:** Analytical JI-EA4 (A), Analytical JI-EA4-6 (B) and Semi preparative JI-EA4-6, (C). Both the JI-EA4 and JI-EA4-6 showing the major peak (1) indicated by retention time similar to the chromatogram of ethyl acetate fraction.

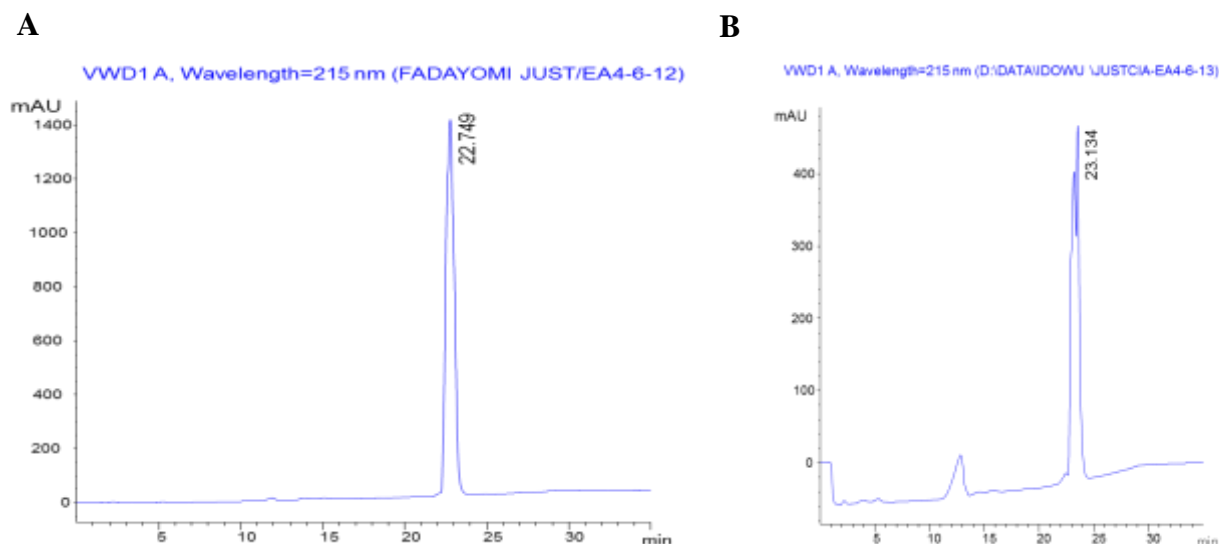


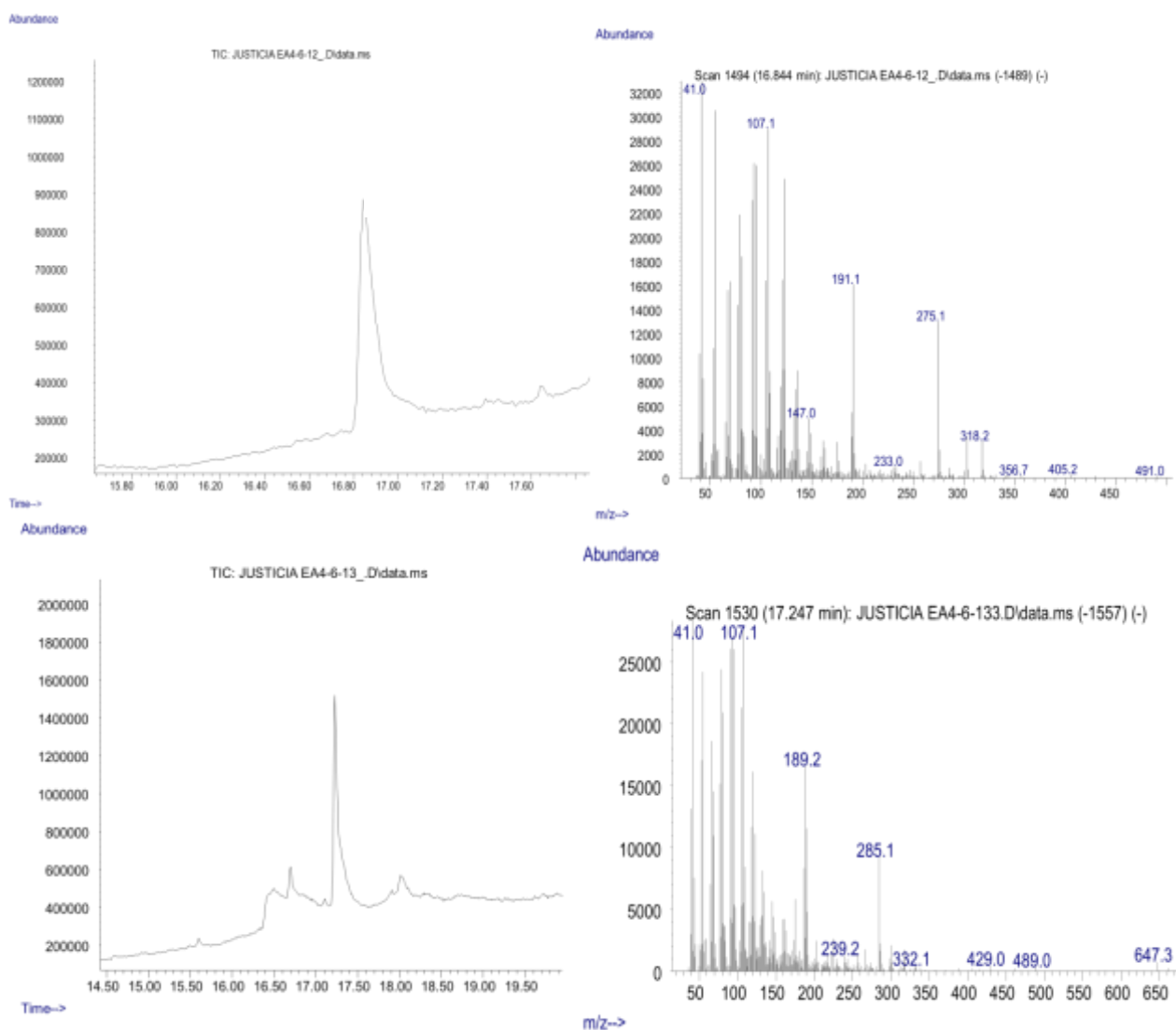
**Figure 3. 4: Analytical HPLC chromatogram of purified active compounds in EA of *Justicia insularis*. (A) EA4-6-12 at 22.749 retention time (Compound 1) and (B) EA4-6-13 at retention time 23.134 (compound 2)**

### 3.2.5 Structural identification of compound 1 and 2

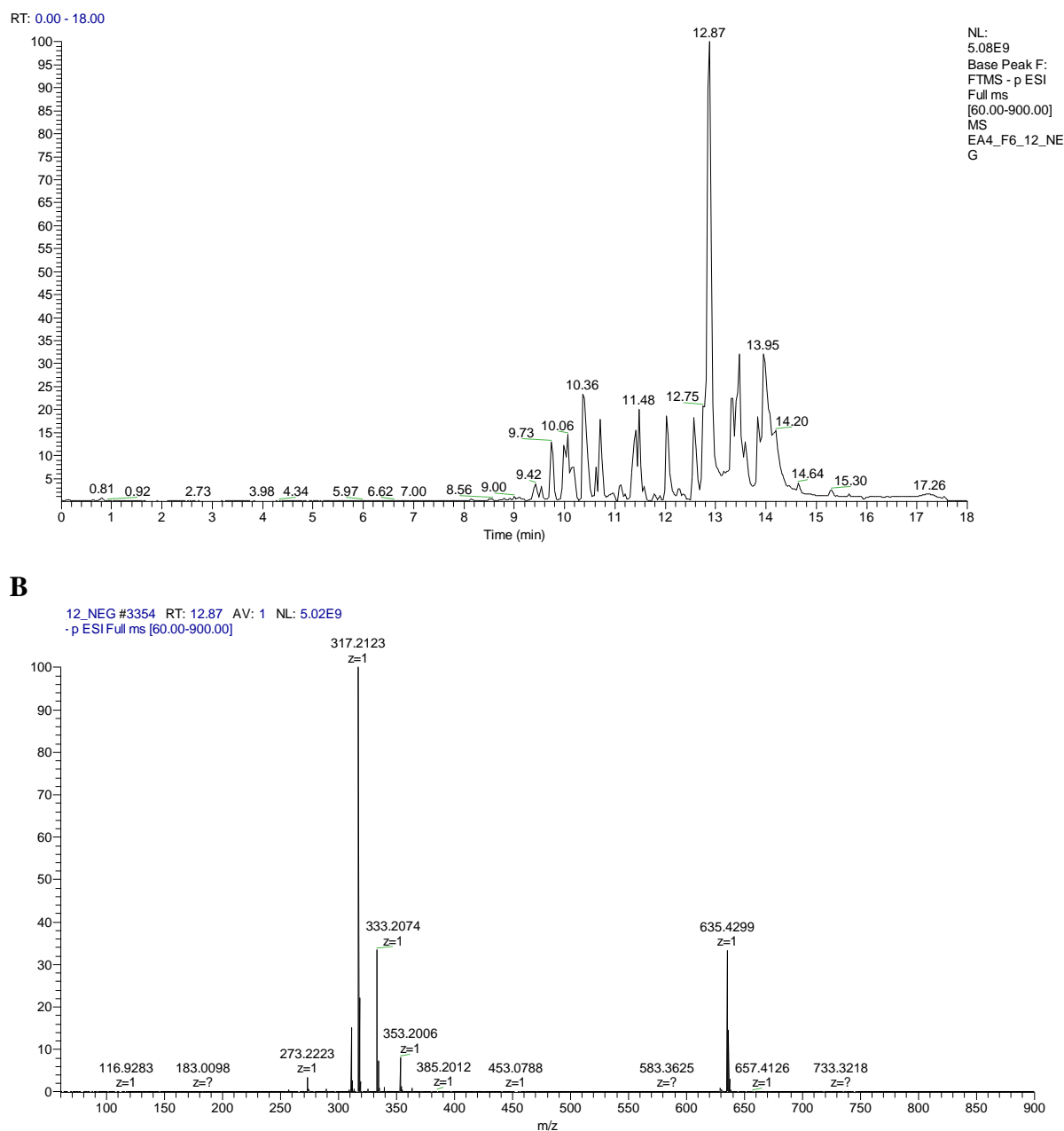
The GC-MS chromatogram analysis of compound 1 and 2 was carried out. The GC-MS of compound 1 showed a mass of 318.2 (Figure 3.5) which was further confirmed by high resolution of LC-MS with a molecular formula  $C_{20}H_{30}O_3$  (Figure 3.6). Further  $^1H$ NMR and  $^{13}C$  NMR analysis (Figure 3.8) and (Table 3.3 and 3.4) indicated that compound 1 was a diterpenoid (16 $\alpha/\beta$ -hydroxy-cleroda-3,13(14) dien-15,16-olide). The  $^{13}C$  NMR of compound 1 indicated as a 1:1 mixture of 16-hydroxy epimers were similar to the  $^{13}C$ NMR data of Hara *et al.* (1995) and Müller *et al.* (2015) which were also reported as 1:1 mixture of 16-hydroxy epimers (Table 3.3 and 3.4) (Figure:3.10).

GC-MS of compound 2 also showed a mass of 318.2 (Figure 3.5). High resolution of LC-MS further confirmed the exact mass and the molecular formula as  $C_{20}H_{30}O_3$  (Figure 3.7). The analysis of the  $^1H$ NMR and  $^{13}C$ NMR data (Figure 3.9) and (Table 3.3 and 3.4) showed that compound 2 was a diterpenoid, 16-oxocleroda-3,13(14) dien-15-oic acid (Figure 3.10).

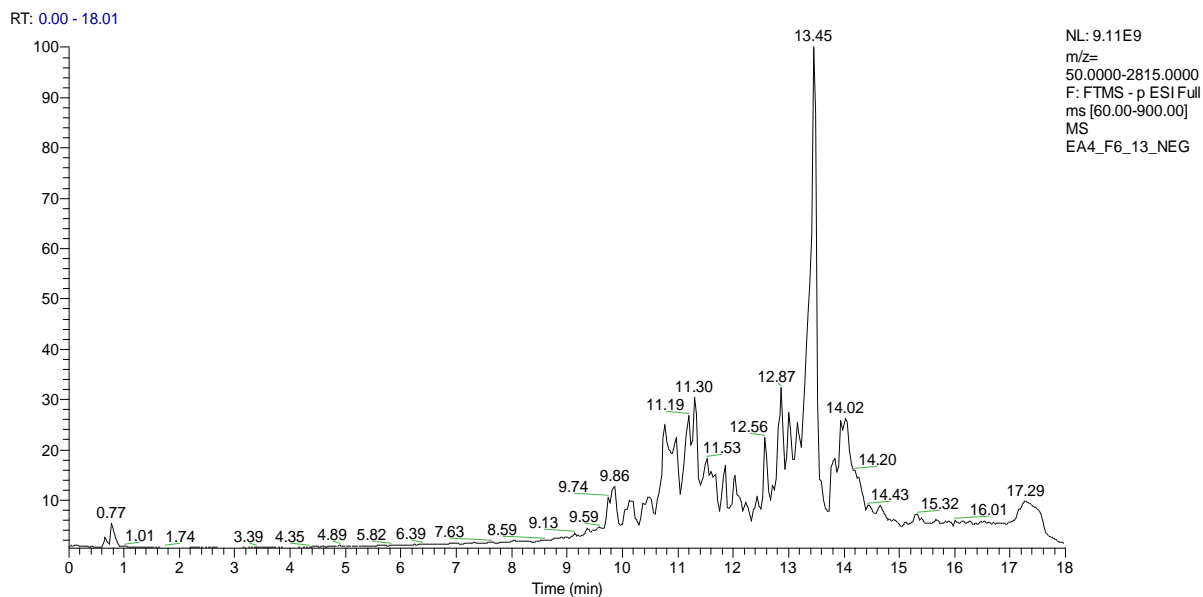
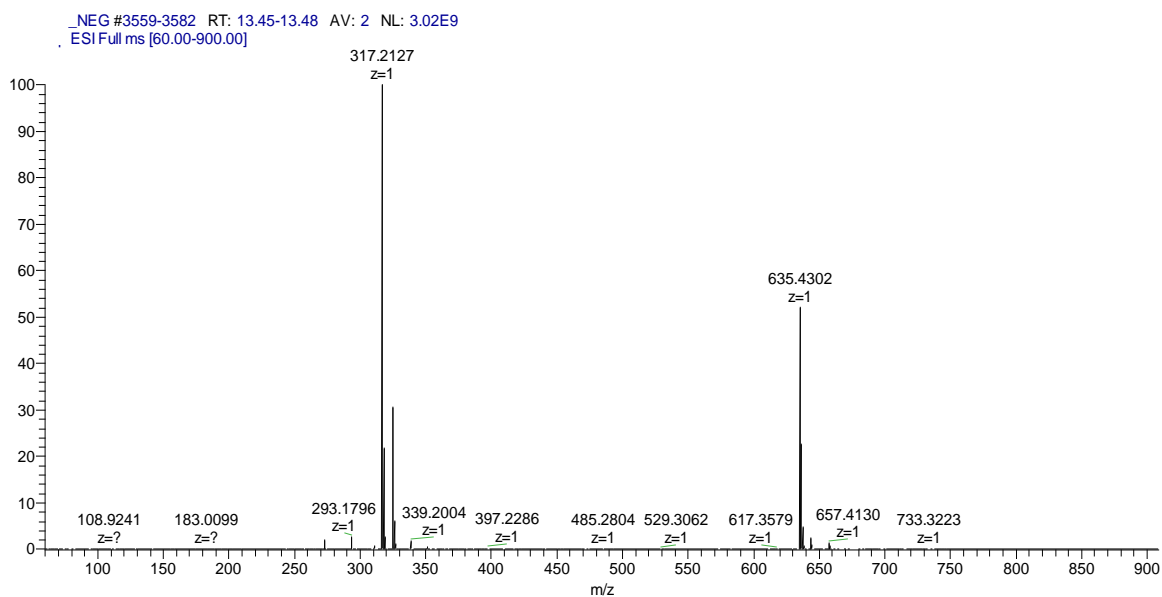
The NMR data were consistent with those reported by Phadnis *et al.*, (1988), Hara *et al.*, (1995). The chemical structure of these compounds from other plant species have been characterised and reported by several researchers (Phadnis *et al.*, 1988; Kijjoa *et al.*, 1993; Sashidhara *et al.*, 2010).



**Figure 3. 5: GC-MS chromatograms and electron ionization mass spectra of purified active compound 1 (top) and 2 (bottom) from ethyl acetate sub-fraction 4-6 (EA4-6-12 and EA4-6-13) of *J. insularis*.**



**Figure 3. 6:** LC-MS chromatogram (A) and negative ESI-MS spectrum (B) of isolated compound 1 showing the MS of the major peak at retention time of 12.87 min. The found masses of  $m/z$  at 317.2123[M-H]<sup>-</sup> and 635.4299 [2M-H]<sup>-</sup> were consistent with their theoretical masses of 317.2117 and 635.4312 respectively.

**A****B**

**Figure 3. 7: LC-MS chromatogram (A) and negative ESI-MS spectrum (B) of isolated compound 2 at retention time of 13.45 min. The found masses of  $m/z$  at 317.2127[M-H]<sup>-</sup> and 635.4302 [2M-H]<sup>-</sup> were consistent with their theoretical masses of 317.2117 and 635.4312 respectively.**

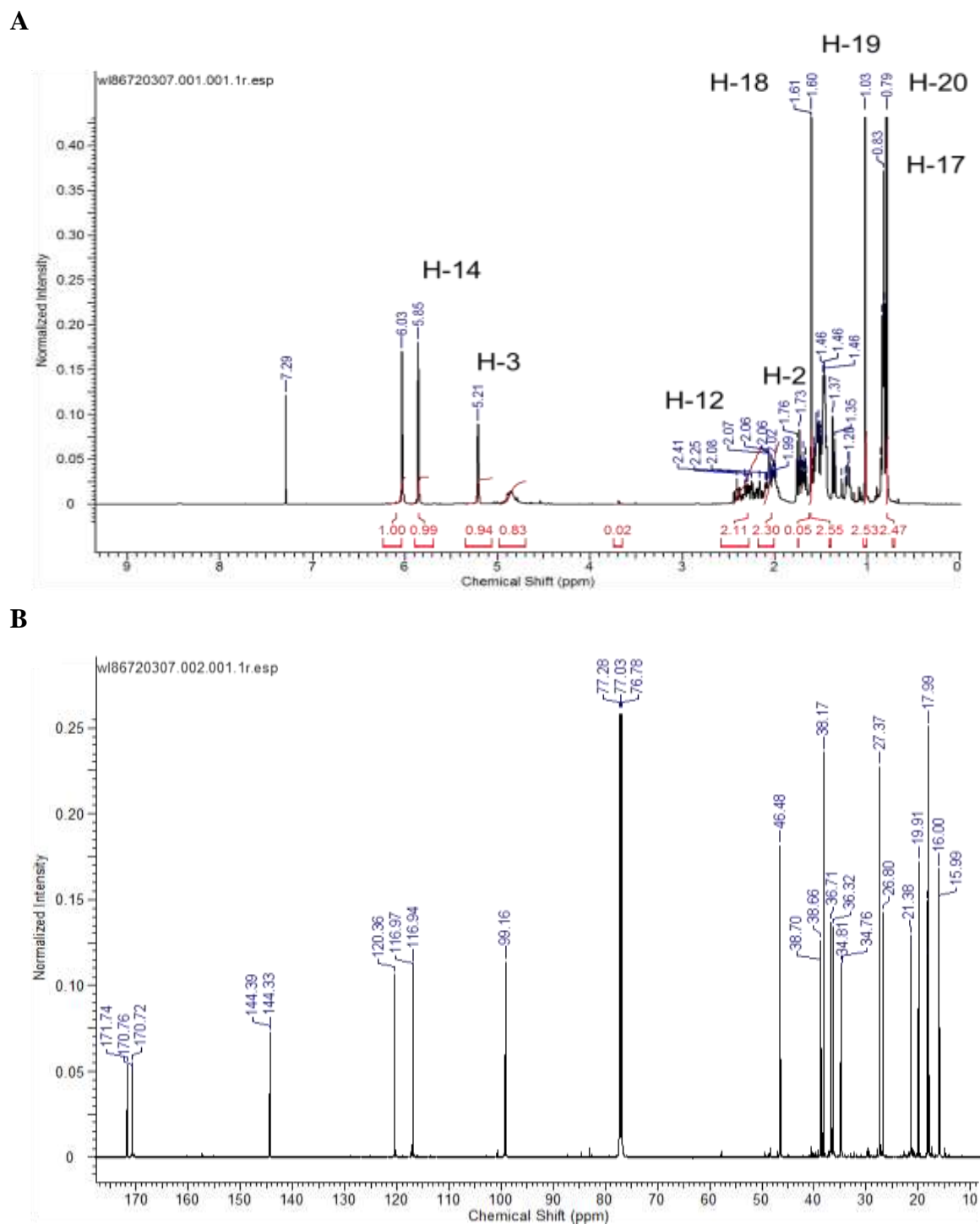
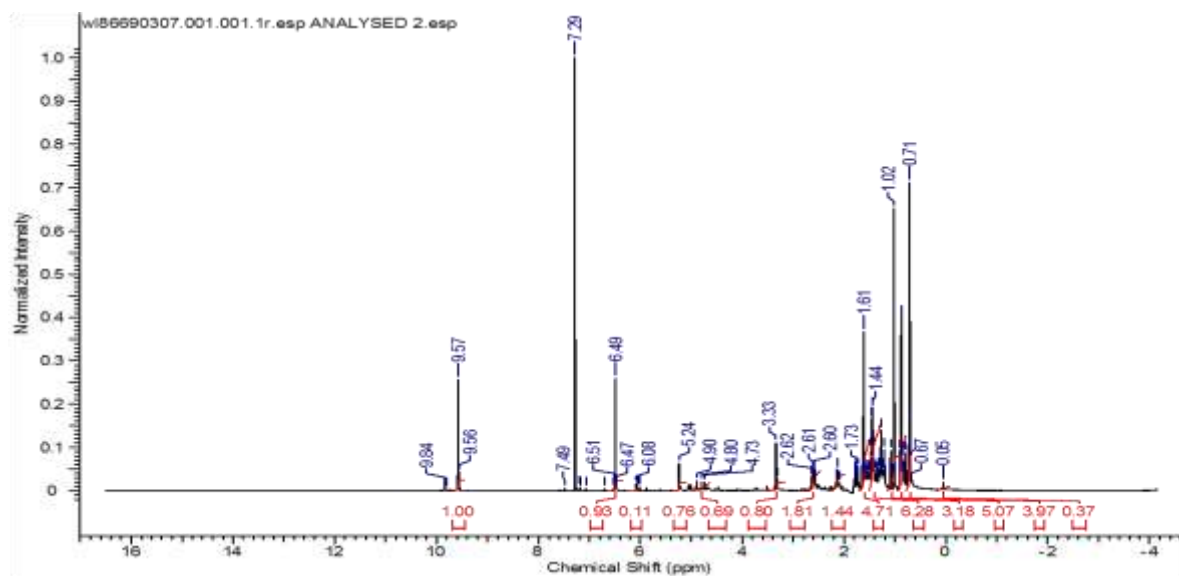


**Figure 3. 8:** NMR data analysis of *Justicia insularis* of purified compound 1 in  $\text{CDCl}_3$ :

(A)  $^1\text{H}$  NMR and (B)  $^{13}\text{C}$  NMR.

A



B

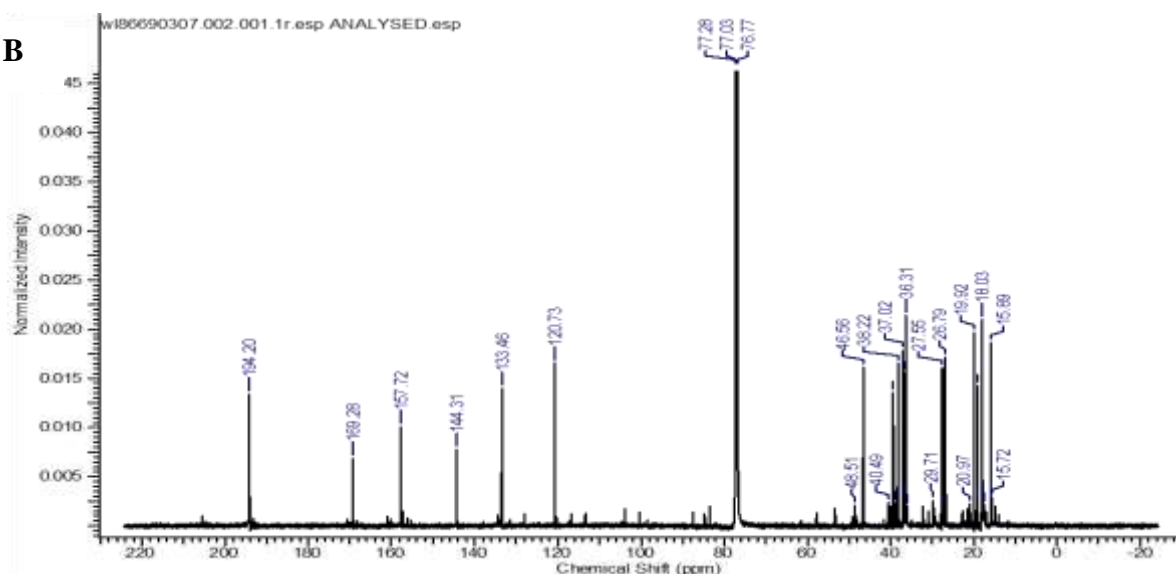


Figure 3. 9: NMR data analysis of *Justicia insularis* purified compound 2 in  $\text{CDCl}_3$ :

(A)  $^1\text{H}$  NMR and (B)  $^{13}\text{C}$  NMR.

**Table 3. 3: Side by side comparison of <sup>13</sup>CNMR spectra of isolated compound 1 and 2 from this study with <sup>13</sup>CNMR literature data.**

Position C	<sup>13</sup> CNMR spectral data of isolated compound 1 compared with literature				<sup>13</sup> CNMR spectral data of isolated compound 2 compared with literature	
	Phadnis <i>et al.</i> (1988)	Hara <i>et al.</i> (1995)	Müller <i>et al.</i> , (2015)	Isolated compound 1	Hara <i>et al.</i> (1995)	Isolated compound 2
1.	18.06	18.3	18.4	18.0	18.1	18.1
2.	21.57	26.8	26.9	26.79, 26.80	26.8	26.8
3.	120.68	120.3, 120.4	120.55, 120.48	120.36, 120.43	120.7	120.7
4.	114.53	144.3, 144.3	144.52, 144.46	144.33, 144.39	144.2	144.3
5.	38.40 <sup>a</sup>	38.1	38.3	38.2	38.2	38.2
6.	26.97 <sup>b</sup>	36.7	36.8	36.7	36.8	36.8
7.	36.58	27.4	27.5	27.37	27.6	27.6
8.	36.97	36.3, 36.3	36.48, 36.44	36.36, 36.32	36.3	36.3
9.	38.92 <sup>a</sup>	38.6, 38.7	38.82, 38.79	38.66, 38.70	39.3	39.4
10.	46.79	46.5	46.60	46.5	46.6	46.6
11.	27.62 <sup>b</sup>	34.8, 34.8	34.93, 34.88	34.8	37.0	37.0
12.	35.09	21.3, 21.4	21.50, 21.47	21.35, 21.38	19.2	19.2
13.	171	171.0	170.71, 170.66	170.72, 170.76	157.7	157.7
14.	117.04	116.8	117.18, 117.15	116.94, 116.97	133.8	133.5
15.	172	172.0	171.7	171.7	170.9	169.3
16.	99.69	99.3	99.16, 99.14	99.14, 99.16	194.2	194.3
17.	16.11	15.9	16.1	16.00	15.9	15.9
18.	18.52	17.9	18.1	18.23	18.0	18.0
19.	18.20	19.9	20.0	19.9	19.9	19.9
20.	20.08	18.1	18.3	18.2	18.0	18.1

<sup>a</sup> and <sup>b</sup> Values that could be interchanged in any vertical column.

**Table 3. 4: Side by side comparison of <sup>1</sup>HNMR spectra of isolated compound 1 and 2 from this study with <sup>1</sup>HNMR literature data.**

Position <sup>1</sup> H	<sup>1</sup> HNMR spectral data of isolated compound 1 compared with literature				<sup>1</sup> HNMR spectral data of isolated compound 2 compared with literature		
	Phadnis <i>et al.</i> (1988)	Hara <i>et al.</i> (1995)	Müller <i>et al.</i> (2015)	Isolated compound 1	Phadnis <i>et al.</i> (1988)	Hara <i>et al.</i> (1995)	Isolated compound 2
<b>1</b>	—	—	1.56-1.49 (m, 2H)	1.48-1.55 (overlapped, m, 2H)	—	—	1.79 (dt, 12.8, 3.3Hz 1H); 1.46 (overlapped, 1H)
<b>2</b>	2.01 (br)	—	2.10-1.91 (m, 2H)	2.03 (overlapped, 2H)	2.06 (br)	—	2.10 (m, 2H)
<b>3</b>	5.2 (br)	5.18 (br s)	5.19 (s, 1H)	5.21 (br, s, 1H)	5.15 (br)	5.20 (br, s)	5.24 (br, 1H)
<b>7</b>				1.46 (overlapped, 2H)			1.5 (overlapped, 2H)
<b>8</b>				1.47 (m, 1H)			1.62 (overlapped, 1H)
<b>10</b>				1.35 (dd, 12, 2.0 Hz, 1H)			1.43 (overlapped, 1H)
<b>11</b>				1.73 (dd, 16.4, 3.3 Hz, 1H); 1.68 (ddd, 14.2, 9.1, 4.9 Hz, 1H)			1.26 (overlapped, 2H)
<b>12</b>	2.24 (m)		2.44-2.10 (m, 2H)	2.40 (ddd, 14.2, 5.0, 1.4 Hz, H <sub>α</sub> ); 2.32 (ddd, 14.2, 5.0, 1.3 Hz, 1H <sub>β</sub> ); 2.25 (ddd, 12.5, 4.3, 1.4 Hz, 1H <sub>α</sub> ); 2.15 (ddd, 14.1, 4.7, 1.7 Hz, 1H <sub>β</sub> )			2.57 (ddd, 10.9, 5.2, 1.6 Hz, 1H); 2.30 (ddd, 11.2, 4.4, 3.7 Hz, 1H)
<b>14</b>	5.83 (s)	5.83 (s)	5.84 (s, 1H)	5.85 (s, 1H)	6.37 (s)	6.48 (s)	6.49 (s, 1H)
<b>16</b>	6.04 (s)	6.03 (s)	6.00 (d, 6.0 Hz, 1H)	6.03 (br s, 1H)	9.46 (s)	9.53 (s)	9.57 (s, 1H)
<b>17</b>	0.83 (d)	0.82 (d, 6.0); 0.81 (d, 6.0)	0.81 (br s, 3H)	0.83 (d, 5.5 Hz, 3H <sub>α</sub> ); 0.82 (d, 5.8 Hz, 3H <sub>β</sub> )	0.73 (d)	0.84 (d, 6.4)	0.87 (d, 3H)
<b>18</b>	1.61 (d)	1.60 (s)	1.58 (s, 3H)	1.61 (d, 3H <sub>α</sub> ); 1.60 (1s, 3H <sub>β</sub> )	1.5 (d)	1.59 (s)	1.61 (s, 3H)
<b>19</b>	1.0	1.01 (s)	1.00 (s, 3H)	1.03 (s, 3H)	0.93 (s)	0.99 (s)	1.02 (s, 3H)
<b>20</b>	0.75 (s)	0.78 (s)	0.77 (s, 3H)	0.79 (s, 3H)	0.62 (s)	0.68 (s)	0.71 (s, 3H)

Singlet (s), doublet (d), triplet (t), multiplet (m) doublet of triplet (dt) and broad (br)

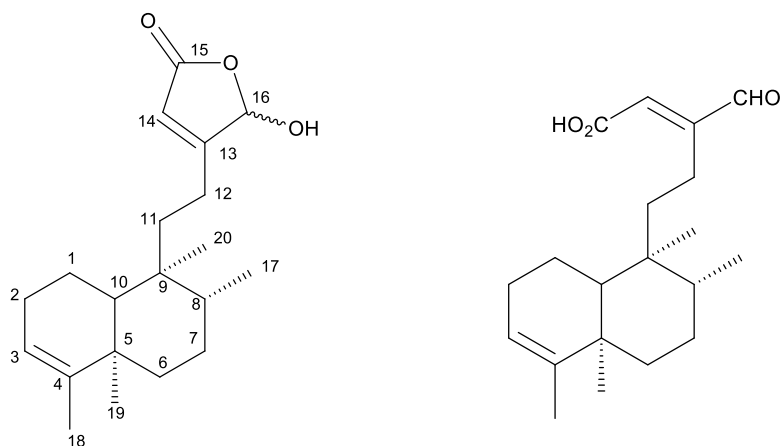


**Figure 3. 10: Chemical structure of 16 $\alpha$ / $\beta$ -hydroxy-cleroda-3,13 (14) dien-15,16-olide (compound 1) (A) and 16-oxocleroda-3,13(14) dien-15-oic-acid (Compound 2) (B)**

### 3.2.6 Antiproliferative activities of purified compounds 1 and 2 from *Justicia insularis*

The *in vitro* antiproliferative activities of compound **1** and **2** were tested on ovarian cancer cell lines (CIS-A2780, OVCAR-8, and OVCAR-4) and immortalised normal human ovarian epithelia (HOE) cell line using cell growth assay SRB assay. The mean growth response curve of the growth inhibitory activity of compound **1** and **2** is presented in Figure 3.11, and the concentration inhibiting 50% growth ( $IC_{50}$ ) in the cells lines is represented in Table 3.5. Compound **1** significantly inhibited growth in ovarian cancer cell lines CIS-A2780, OVCAR-8 and OVCAR-4 with  $IC_{50}$  values of  $8.1 \pm 0.8$ ,  $4.4 \pm 0.2$  and  $5.7 \pm 0.3$   $\mu$ M respectively. Furthermore, the result suggested that OVCAR-8 and OVCAR-4 cell were more sensitive to compound **1** treatment than CIS-A2780 cell. Also, compound **2** inhibited growths in OVCAR-8 and OVCAR-4 ovarian cancer cell lines with  $IC_{50}$   $11.8 \pm 0.5$  and  $16.6 \pm 2.8$   $\mu$ M respectively (Table 3.5). Compound **1** showed higher inhibitory activity than compound **2** in the cancer cell lines (Table 3.5). The selectivity index of compound **1** was higher than that of compound **2** and positive control (carboplatin). This suggested that

compound 1 is less toxic to immortalised human ovarian epithelial cells but more cytotoxic to ovarian cancer cells.

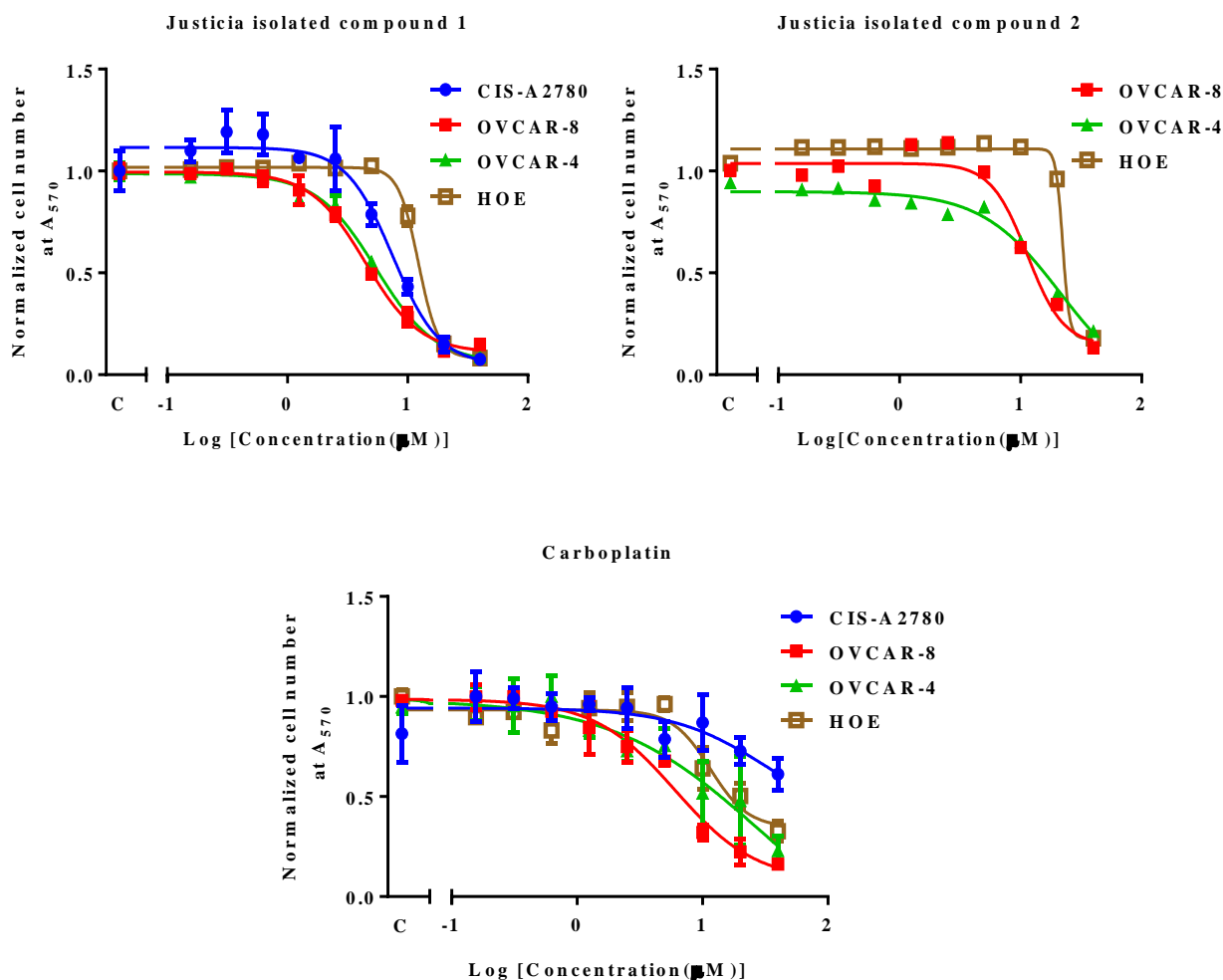


**Figure 3. 11: Mean concentration-response curve of the growth inhibitory activity of isolated compound 1 and 2 from *Justicia insularis* on CIS-A2780, OVCAR-8 and OVCAR-4 cell lines.** The cancer cell lines were treated with different concentrations of each compound (0.16-40 $\mu$ M) for 72h. The data generated were presented as mean  $\pm$  SEM of three repeated experiments in triplicate. The negative control contains 0.2% DMSO in vehicle (media) and is denoted with C.

**Table 3. 5: Results of the antiproliferative activities of *J. insularis* isolated compound 1 and 2 through inhibition of growth in ovarian cancer (CIS-A2780, OVCAR-8 and OVCAR-4) cell lines. The number of cells was estimated by SRB staining after post-treatment period of 72hours. Carboplatin was used as a positive control and the results are expressed as mean  $\pm$ SEM, n=3 experiments. The selectivity index (SI) was determined as the ratio of the IC<sub>50</sub> of HOE with each ovarian cancer cell line, and the mean SI for compound 1 was calculated based on the three individual SIs, while the mean SI values for compound 2 and carboplatin were calculated with two individual SIs because the SI values with CIS-A2780 could not be determined.**

Isolated Compounds	CIS-A2780 IC <sub>50</sub> (μM)	OVCAR-8 IC <sub>50</sub> (μM)	OVCAR-4 IC <sub>50</sub> (μM)	HOE IC <sub>50</sub> (μM)	SI with CIS-A2780	SI with OVCAR-8	SI with OVCAR-4	Average SI
Compound 1	8.1 $\pm$ 0.8 (2.5 μg/mL)	4.4 $\pm$ 0.2 (1.4 μg/mL)	5.7 $\pm$ 0.3 (1.8 μg/mL)	12.1 $\pm$ 0.1 (3.9 μg/mL)	1.5	2.8	2.1	2.1 $\pm$ 0.5
Compound 2	Not determined	11.8 $\pm$ 0.5 (3.8 μg/mL)	16.6 $\pm$ 2.8 (5.3 μg/mL)	22.8 $\pm$ 0.7 (7.3 μg/mL)	-	1.9	1.4	1.7 $\pm$ 0.3
Carboplatin	>40	8.2 $\pm$ 2.2	17.6 $\pm$ 4.6	13.0 $\pm$ 3.7	-	1.6	0.7	1.2 $\pm$ 0.5

### 3.2.7 Cytotoxicity of compound 1 using trypan blue exclusion cell viability assay

Compound 1 showed high growth inhibitory activities with IC<sub>50</sub> less than 10µM on the ovarian cancer cell lines using SRB assay. However, the route of activity could either be through inhibition of cell division (cytostatic) or through cell death (cytotoxic). Therefore, trypan blue exclusion assay was used to investigate whether the growth inhibitory activities of compound 1 was by induction of cell death. However, due to limited mass availability of compound 2, no further studies on its mechanism of action was carried out. In this assay, CIS-A2780 and OVCAR-8 cell lines were treated with three different concentrations of compound 1 for 48 hours. The results were analysed by calculating the percentage of cell death. One-way ANOVA and post hoc Dunnett's multiple comparison test were used to compare if the percentage cell death induced by the treatments at different concentrations compared to the control were significant. Additionally, one-way ANOVA was also used to test if the percentage cell death induced by compound 1 at different concentrations was significant and Tukey multiple comparison test showed which concentration was significant.

In CIS-A2780 cell line, compound 1 reduced the cell viability by inducing significant cell death at each of the concentration (5, 10 and 20 µM). The cell death induced by compound 1 was also concentration dependent (Figure 3.12). The percentage of cell death induced by compound 1 (16, 30 and 74%) at the different concentration (5, 10 and 20 µM) was significantly higher than percentage of cell death induced by the positive control (Carboplatin) (8, 11 and 14%). Furthermore, Compound 1 also induced significant cell death in OVCAR-8 cell line when compared with the control. Dunnett's multiple comparison test showed that each of the different concentration (5, 10 and 20 µM) of compound 1 showed significant different to the control. In addition, the percentage of cell death induced by

compound **1** was concentration dependent. The positive control (Carboplatin) also induced significant cell death when compared with the untreated cell (Control) and they are significantly different at the different concentrations (5, 10 and 20  $\mu$ M). However, the percentage of cell death induced by carboplatin was not concentration dependent. Furthermore, compound **1** induced higher cell death (44, 57 and 73%) than carboplatin (39, 49 and 56%) (Figure 3.12) in OVCAR-8. The results suggest that the cell growth inhibitory activities of compound **1** earlier reported using SRB assay was majorly by induction of cell death.

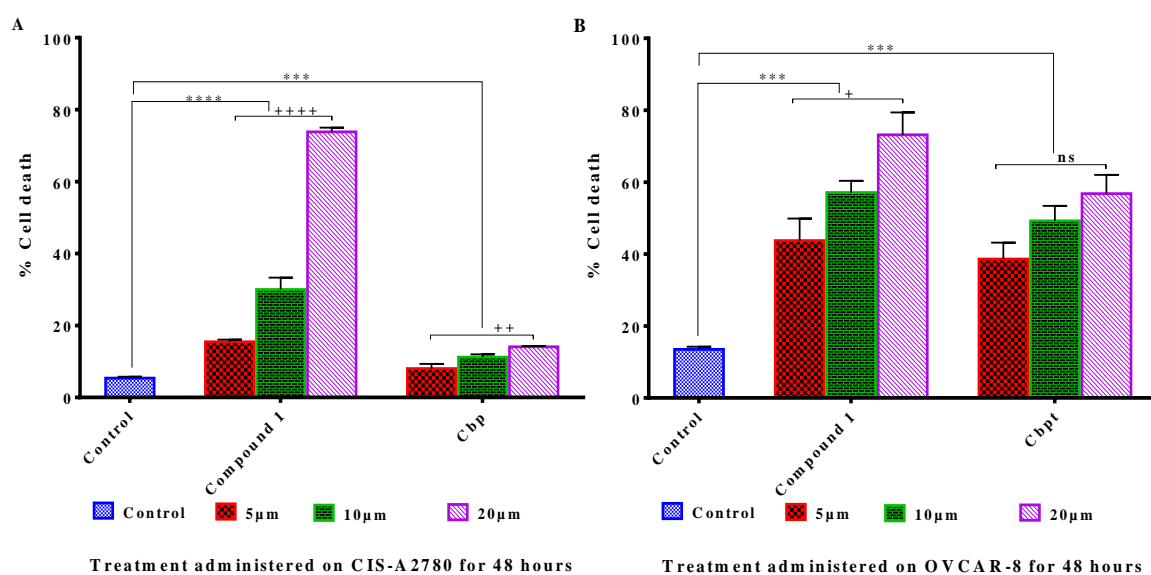


**Figure 3. 12: Trypan blue exclusion viability test for compound 1 on ovarian cancer cell lines: CIS-A2780 (A) and OVCAR-8 (B).** Carboplatin (Cbp) was used as positive control and negative control group contains 0.1% DMSO in growth media. The percentages of cell deaths were estimated and recorded as means  $\pm$  SEM from three independently repeated experiments. Levels of significant different between negative control and treatment were denoted with asterisk (\*\*\*,  $p < 0.001$  and \*\*\*\*,  $p < 0.0001$ ), while significant difference within concentrations of the same treatment was denoted with plus sign (+,  $p < 0.05$  and ++,  $p < 0.01$ ).

### **3.2.8. Apoptosis induction by compound 1**

Based on the significant growth inhibitory and cytotoxic activities of compound **1** on ovarian cancer cell lines, there was need to investigate the possible mechanism of induction of cell death by compound **1**. Several apoptosis biomarkers were evaluated and the results presented below.

#### **3.2.8.1 Morphological effects of compound 1 on ovarian cancer cell lines**

The morphological effects of compound **1** was studied on ovarian cancer CIS-A2780 and OVCAR-4 cell lines treated with different concentrations at different time points. Morphological effect was evaluated by direct observation under the light microscope. Compound **1** caused cell shrinkage, detachment and membrane blebbing in both CIS-A2780 and OVCAR-4 cells (Figure 3.13 and 3.14). In CIS-A2780 cells, the morphological changes induced by compound **1** increased with concentration but no major differences were observed at different time points. The morphological changes caused by compound **1** was higher than the slight morphological effects of the positive control (Carboplatin) at higher dose on CIS-A2780 cells. Compound **1** and carboplatin further caused similar morphological changes such as cell detachment, shrinkage and blebbing in OVCAR-4. These changes induced by compound **1** and carboplatin in OVCAR-4 were not time dependent.

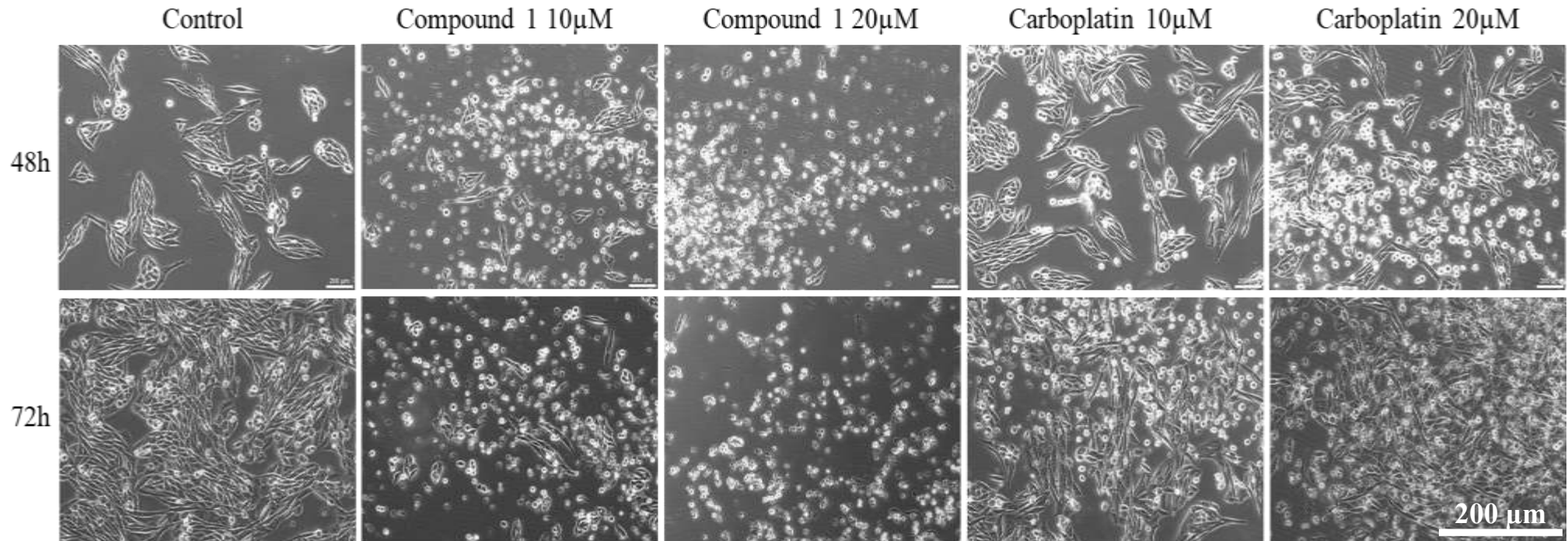


**Figure 3. 13: Morphological effects of compound 1 on CIS-A2780 ovarian cancer cell line at different concentrations (10 and 20 $\mu$ M) and time points (48 and 72 h) using light microscopy.** Carboplatin (Cbp) was used as positive control and negative control contains 0.1% DMSO in growth media. Images were taken with X10 objective lens on 200 $\mu$ m scale.

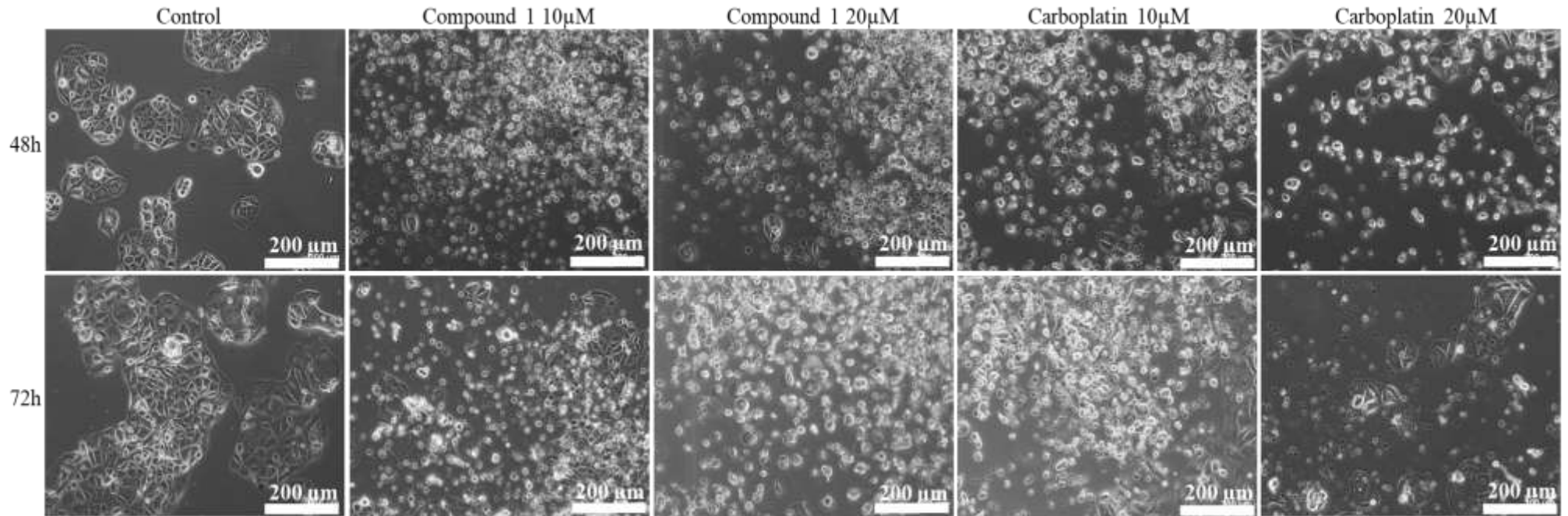


**Figure 3. 14: Morphological effects of compound 1 on OVCAR-4 ovarian cancer cell line at different times (48 and 72 h) and concentrations (10 and 20  $\mu\text{M}$ ) using light microscopy.** Carboplatin (Cbp) was used as positive control and negative control was treated with media containing 0.1% DMSO. Images were taken with X10 objective lens on 200 $\mu\text{m}$  scale.

### **3.2.8.2 Nuclear and actin staining of ovarian cancer cell lines for apoptosis evaluation using fluorescence microscopy**

Apoptosis is known to be associated with morphological changes in cellular structure and causing disruption to the actin filament network. The cleavage of the actin filament network is further capable of initiating or mediating apoptosis thereby bringing about the appearance of apoptosis features such as rounded cells and condensed chromatin (White *et al.*, 2001; Desouza, Gunning and Stehn, 2012). Therefore, the effect of compound **1** on the actin arrangement and the nucleus was investigated to evaluate apoptosis using fluorescence microscopy. Briefly, CIS-A2780 and OVCAR-8 cell lines were treated with compound **1** (10 and 20 $\mu$ M) for 48 h and 72 h before staining with DAPI and actinRed<sup>TM</sup> 555 and imaged with fluorescence microscopy. Cells that show clear smaller nuclei, fragmented nuclei, condensed chromatin and high fluorescence intensity were identified as being apoptotic. Compound **1** caused morphological changes in the nuclei and actin structure of CIS-A2780 and OVCAR-8 cells (Figure 3.15 and 3.16). The apoptotic features caused by compound **1** increased with concentration but the difference was not significant with time. Furthermore, compound **1** reduced the capacity of the actin filament to form a network, this was more prominent at 72h and this effect increased with concentration in CIS-A2780 and OVCAR-8. The actin filament aggregated rather than forming a network at 72 h in response to drug treatment. Similar results were also obtained for the positive control (carboplatin) in OVCAR-8, while no major morphological changes were observed in CIS-A2780 cells treated with carboplatin (Figure 3.15).

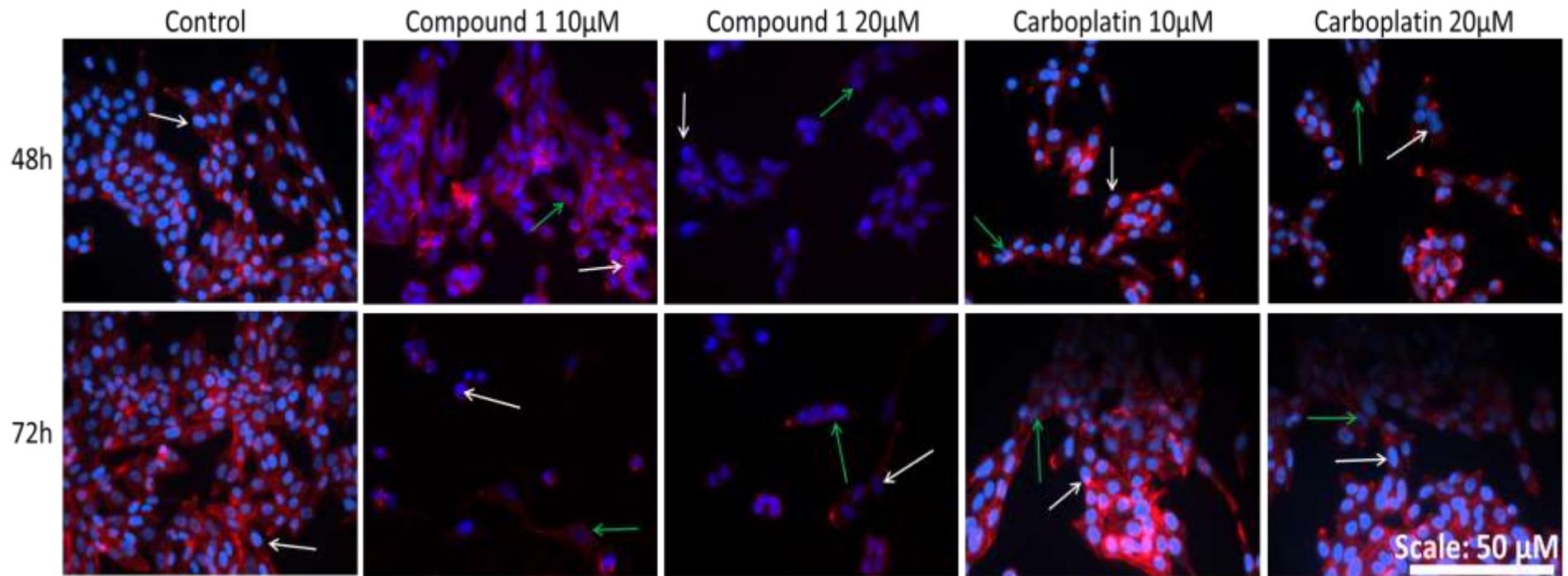


**Figure 3. 15: Fluorescence microscopy images of CIS-A2780 cells showing morphological changes in the nucleus and actin filament in response to drug treatment.** CIS-A2780 was co-stained with DAPI (blue) and Actin (red) for nuclear and actin filament changes respectively. White and green arrows are pointing to viable cell nuclei and apoptotic cell nuclei respectively.

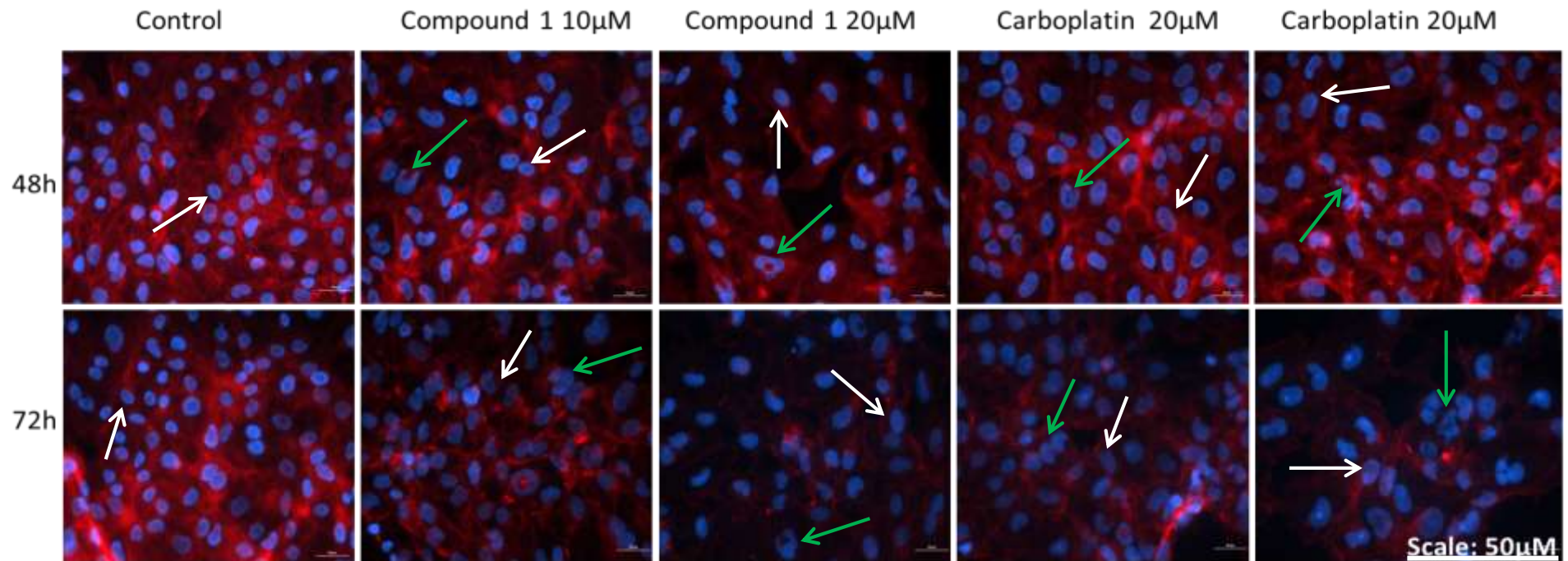


**Figure 3. 16: Fluorescence microscopy images of OVCAR-8 cell line taking with 40x objective lens, showing morphological changes in the nucleus and actin filament in response to drug treatment.** OVCAR-8 was co-stained with DAPI (blue) and Actin (red) for nuclear and actin filament changes respectively. White and green arrows are pointing to viable cell nuclei and apoptotic cell nuclei respectively.

### 3.2.8.3 Apoptosis study by caspase 3/7 activity

To investigate whether the significant induction of cell death by compound **1** was due to induction of apoptosis, the level of caspase 3/7 activation by compound **1** was measured on  $5 \times 10^3$  cells treated with two different concentrations of compound **1** for 48 hours. The results show that compound **1** increased caspase 3/7 activity in CIS-A2780 cells at higher dose by 4-fold when compared with the control. Its caspase 3/7 activity was significant at higher dose (20  $\mu$ M) when compared with the control. Furthermore, its caspase 3/7 activity was concentration dependent. The positive control (Cbp) also caused a significant increase in caspase 3/7 activity at higher dose when compared with the control. Cbp increased caspase activity by 2-fold. The caspase 3/7 activity effect of compound **1** was higher than the effect of Cbp used as positive control (Figure 3.17). In OVCAR-8 cells, compound **1** caused 7-fold increase in caspase 3/7 activity at higher dose. Its caspase 3/7 activity was significant when compared with the control at both doses (10 and 20  $\mu$ M). Its caspase 3/7 effect was concentration dependent. In the same manner, the positive control (Cbp) caused a 6-fold increase in caspase 3/7 activity. The caspase activity by Cbp was significant when compared with the control at higher concentration (20  $\mu$ M). The caspase 3/7 activity effect of Cbp was also concentration dependent (Figure 3.17). There was no significant difference observed in the caspase 3/7 activity induced by compound **1** and the positive control. Furthermore, in OVCAR-4, compound **1** increased caspase 3/7 activity by 11-fold. The caspase activity was increased significantly by compound **1** when compared with the control. Also, multiple comparison of the caspase 3/7 effect of compound **1** with the control showed that its activity was significantly different from the control at both 10 and 20  $\mu$ M. Compound **1** further showed dose dependent caspase 3/7 effect in OVCAR-4. In similar manner, increase in caspase 3/7 activity was also observed in cells treated with the positive control (Cbp) with 12-fold increase at higher dose and the activity was concentration

dependent (Figure 3.17). Compound 1 showed similar caspase 3/7 effect with the positive control. The results suggest that the high percentage of cell death induced by compound 1 was by activation of apoptosis pathway.

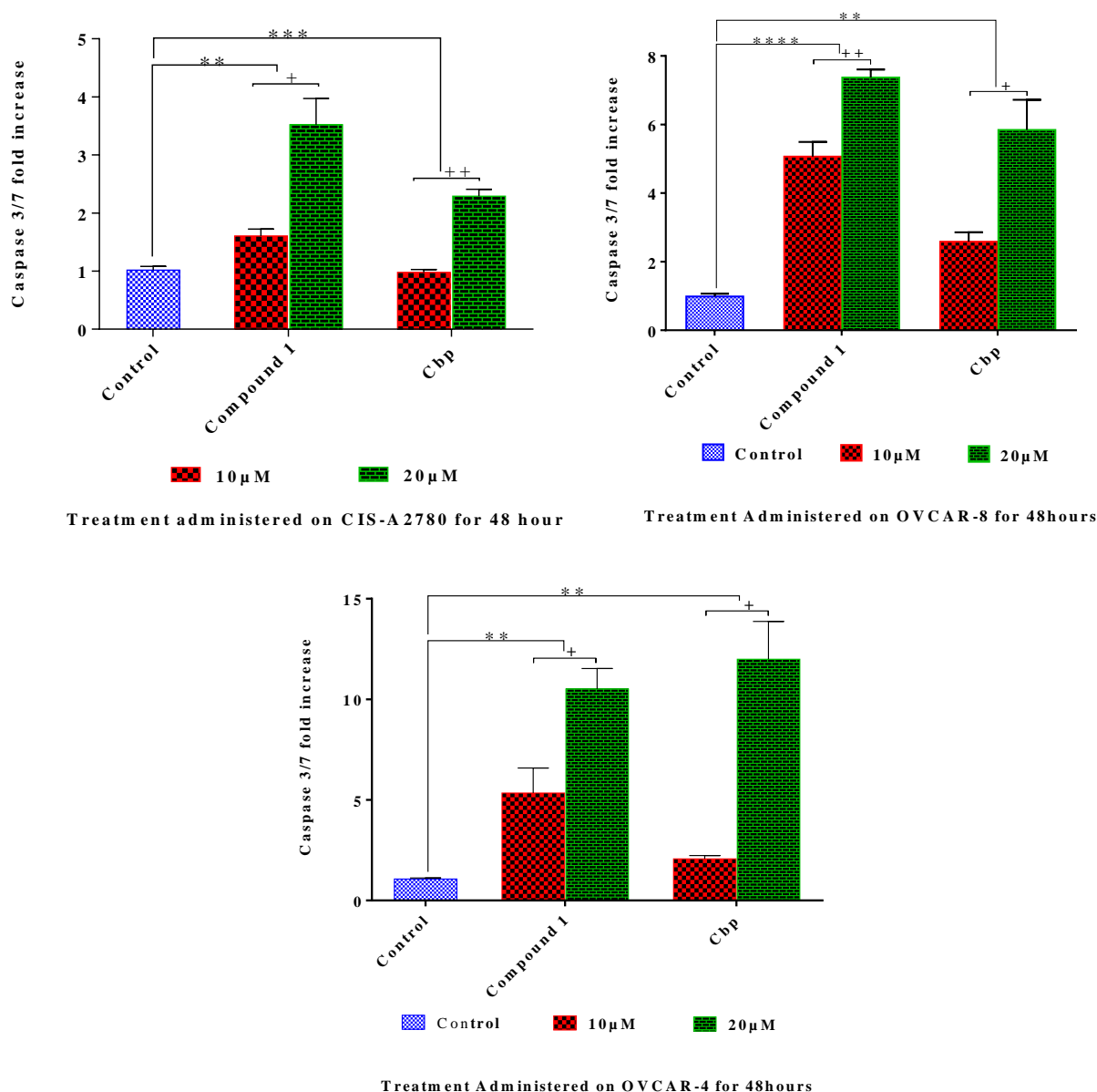


**Figure 3. 17: Caspase 3/7/ apoptosis activities by compound 1 on ovarian cancer cell lines (CIS-A2780, OVCAR-8 and OVCAR-4). Carboplatin (Cbp) was used as positive control at the same concentrations with the tested compound. The caspase activity was normalized with protein-based assay (SRB) performed under the same condition. The fold increase in caspase 3/7 activity were estimated and recorded as means of three repeated**

experiments. The fold increase in caspase 3/7 induced by compound 1 and positive control was compared with the negative control using one-way ANOVA with Dunnett's multiple comparison test. Significant difference between treatment and control is denoted with asterisk (\*), (\*,  $p < 0.05$ , \*\*,  $p < 0.01$ , \*\*\*,  $p < 0.001$  and \*\*\*\*,  $p < 0.0001$ ). Student t test was used to test for concentration dependent activity and the significant difference is denoted with plus sign (+), (+,  $p < 0.05$  and ++,  $p < 0.01$ ).

#### **3.2.8.4 Effect of compound 1 on caspase 8 activity**

The significant induction of caspase 3/7 activity (executioner caspase) by compound 1 in the results above suggested that the anticancer activity of compound 1 was through induction of apoptosis. However, this does not suggest the possible pathway of apoptosis induction. Therefore, the caspase 8 activity of compound 1 was evaluated to determine if the pathway of apoptosis induction was through extrinsic pathway. The results show that in CIS-A2780 cell line, compound 1 caused a 4-fold increase in caspase activity and this increase was significantly different when compared with the control. The caspase 8 activity effect of compound 1 was also concentration dependent. However, the positive control (Cbp) does not increase caspase 8 activity. The caspase 8 activity caused by compound 1 was higher than that of Cbp. Furthermore, in OVCAR-8, compound 1 increased caspase 8 activity significantly when compared with the control. It increased caspase 8 activity by 4-fold, and the increase in caspase activity was concentration dependent (Figure 3.18). Cbp also slightly increased caspase 8 activity in OVCAR-8 and its activity was significant when compared with the control. However, the caspase 8 activity effect of Cbp was not concentration dependent. The caspase 8 activity caused by compound 1 was higher than that of Cbp. Also, in OVCAR-4, compound 1 caused an approximate 2-fold increase in caspase 8 activity and this was significantly different from the control. The caspase 8 activity by

compound **1** was also concentration dependent. Cbp also increased caspase 8 activity by 2-fold in the same manner with compound **1**, but its caspase 8 effect was not concentration dependent. This suggests that the possible route of apoptosis induction by compound **1** was through the activation of caspase 8 that is capable of activating caspase 3/7 via extrinsic pathway.

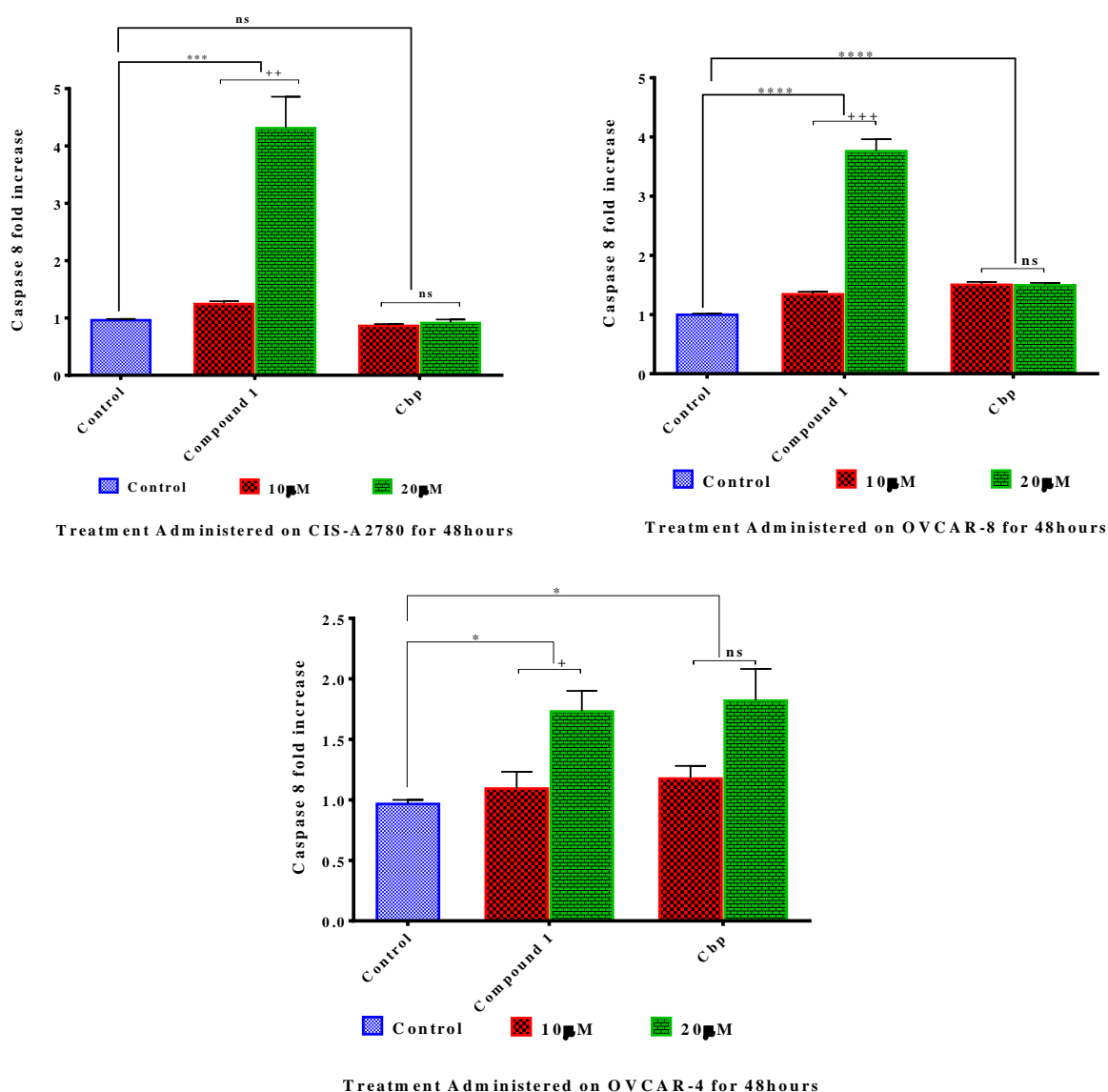


**Figure 3. 18: Effect of compound 1 on caspase 8 activity (initiator caspase) in ovarian cancer cell lines (CIS-A2780, OVCAR-8 and OVCAR-4).** Carboplatin (Cbp) was used as positive control at the same concentrations with the tested compound. The fold increase in caspase 8 activity induced by compound 1 and positive control was compared with the

negative control using one-way ANOVA with Dunnett multiple comparisons tests, while concentration dependence activity was tested with student t test. Significant difference between treatment and control is denoted with asterisk (\*). The significance level at  $p < 0.05$ ,  $p < 0.01$ ,  $p < 0.001$  and  $p < 0.0001$  are represented as (\*), (\*\*), (\*\*\*) and (\*\*\*\*) respectively while no significant different is denoted with (ns). Similar pattern was followed for significant difference within concentrations of the same compound for concentration dependent activity, and the significant level is represented with plus sign (+).

### **3.2.8.5 Effect of Compound 1 on caspase 9 activity in ovarian cancer cells**

Further evaluation of the pathway of apoptosis induction by compound **1** was investigated by assessing the level of caspase 9 marker in the cell lines. Caspase 9 marker is an initiator of apoptosis through intrinsic pathway. Change in the level of caspase 9 marker within the cells will suggest if compound **1** further induced apoptosis through intrinsic pathway. The results show that in CIS-A2780 cell line, the level of caspase 9 activity was increased by compound **1** by 6-fold. The caspase 9 activity caused by compound **1** was significant when compared with the control. The caspase 9 activity effect of compound **1** in CIS-A2780 cells was also dose dependent. In contrast, Cbp does not increase caspase 9 activity in CIS-A2780 cells. Likewise, in OVCAR-8, the caspase 9 activity effect of compound **1** when compared with the control was significant. It caused a 4-fold increase in caspase 9 activity. Furthermore, the caspase 9 activity effect of compound **1** was concentration dependent at (Figure 3.19). In similar manner, Cbp also increased caspase 9 activity by 2-fold and its activity was significant when compared with the control. It further caused a concentration dependent activity. The caspase 9 activity caused by compound **1** was significantly higher than that of Cbp (Figure 3.19).

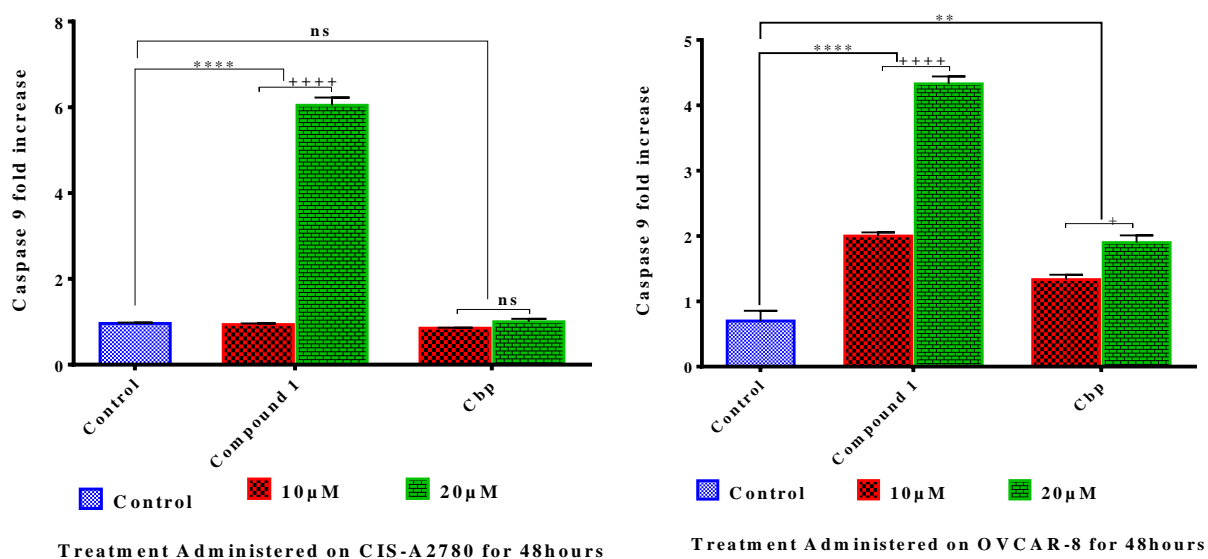


**Figure 3. 19: Caspase 9 activity (initiator caspase) effect of compound 1 on ovarian cancer cell lines (CIS-A2780 and OVCAR-8).** The results represent mean  $\pm$  SEM (n=3).

A standard drug (Carboplatin) was used as positive control (Cbp). Caspase 9 activity of compound 1 and Cbp was compared with the control using one-way ANOVA, while concentration dependent activity was tested with student t test. The significant different of compound comparison with the control is denoted with asterisk (\*), (\*,  $p < 0.05$ , \*\*,  $p < 0.01$ , \*\*\*,  $p < 0.001$  and \*\*\*\*,  $p < 0.0001$ ) while no significant different is denoted with (ns). Similar pattern was followed for concentration dependent activity using plus sign (+).

### 3.2.8.6 Flow cytometry analysis of apoptosis using annexin V and propidium iodide

To further evaluate the roles of compound 1 in the induction of apoptosis, CIS-A2780 and OVCAR-8 cell lines were treated with compound 1 at different concentrations. The cell pellets were treated with annexin V and propidium iodide (PI), followed by flow cytometry analysis (Figures 3.20 and 3.21). In CIS-A2780 cell line, the result demonstrated that compound 1 significantly induced apoptosis when compared with the control (Figure 3.22). In addition, multiple comparison of the apoptotic activity of each concentration of

compound **1** with the control showed that the apoptotic activity was only significant at higher concentrations (10 and 20  $\mu\text{M}$ ). The positive control (Cbp) induced significant percentage of apoptosis and this was significant at both concentrations (10 and 20  $\mu\text{M}$ ). Furthermore, the percentage of induced early and late apoptosis by compound **1** at 5  $\mu\text{M}$  (16.1% and 6.7%), 10  $\mu\text{M}$  (33.3% and 16.1%) and 20  $\mu\text{M}$  (34.8% and 25.3%) respectively were higher than that of the positive control (Cbp) at 10  $\mu\text{M}$  (17.8% and 10.0%) and 20  $\mu\text{M}$  (20.5% and 10.4%). The percentage of apoptosis induced by compound **1** was concentration dependent, while no concentration dependent activity was found in the positive control (Cbp). In OVCAR-8 cells, compound **1** caused a significant apoptotic activity, and the percentages of early and late apoptosis induced at each concentrations 5  $\mu\text{M}$  (40.8% and 25.8%), 10  $\mu\text{M}$  (42.9% and 35.6%) and 20  $\mu\text{M}$  (10.9% and 75.4%) respectively were significant when compared with the control using Dunnett's multiple comparison test. Furthermore, no significant concentration dependent activity was found in the apoptotic activity of compound **1** in OVCAR-8. The early and late apoptotic activity of the positive control (Cbp) at the different concentrations 10  $\mu\text{M}$  (44.5% and 23.7%) and 20  $\mu\text{M}$  (45.2% and 38.35%) were significant when compared with the control (4.8% and 11.8%) respectively (Figure 3.20). There was no major difference in the percentage of apoptosis induced by compound **1** at the different concentrations and the positive control (Figure 3.22). This result was in agreement with the caspase 3/7 results. The results further clearly indicated why compound **1** showed significant cytotoxic activities against ovarian cancer cell lines.

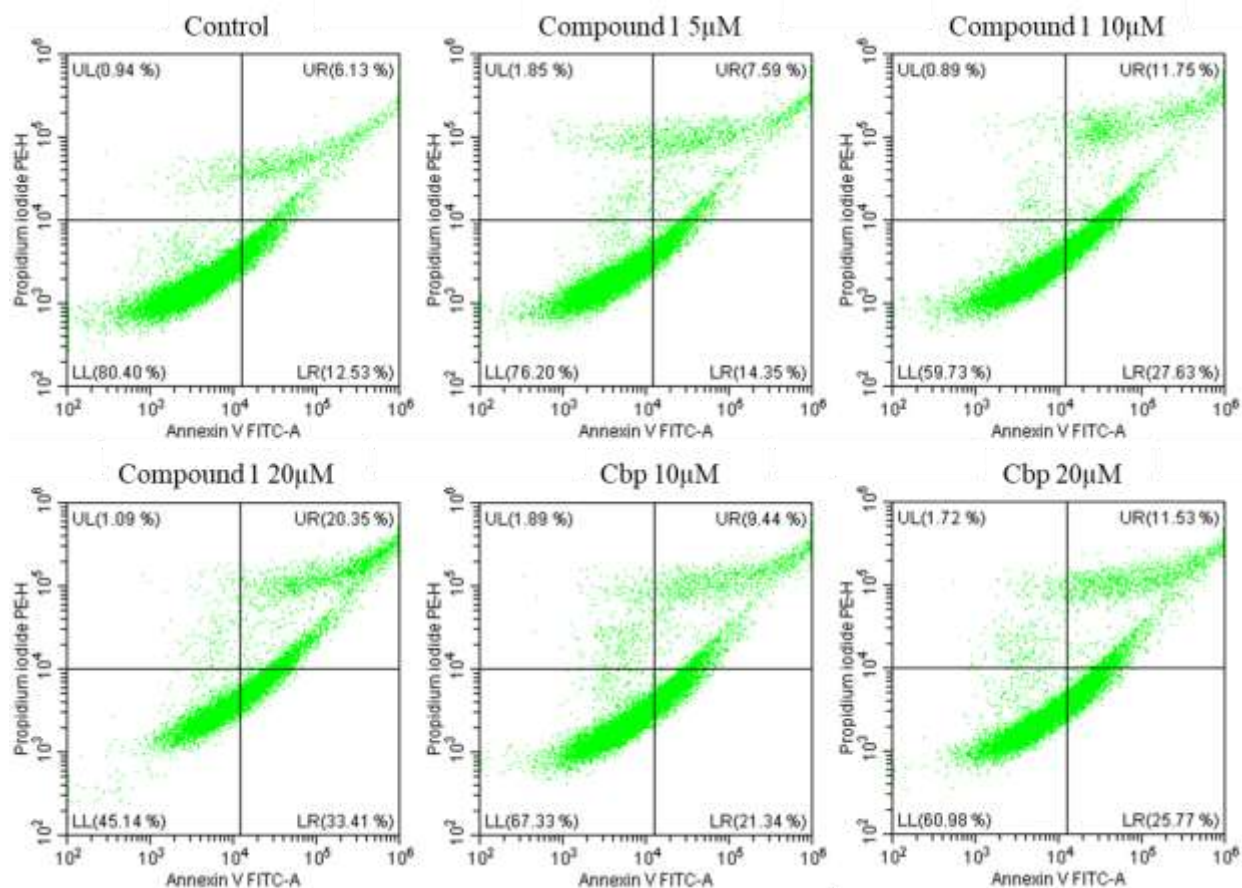


**Figure 3. 20: Representative samples of the flow cytometry graph of CIS-A2780 cell line treated with compound 1 and the positive control (Cbp) at different concentrations. Lower left (LL), upper left (UL), lower right (LR) and upper right (UR) represent live cells, necrotic cells, cells in early apoptosis and cells in late apoptosis respectively.**

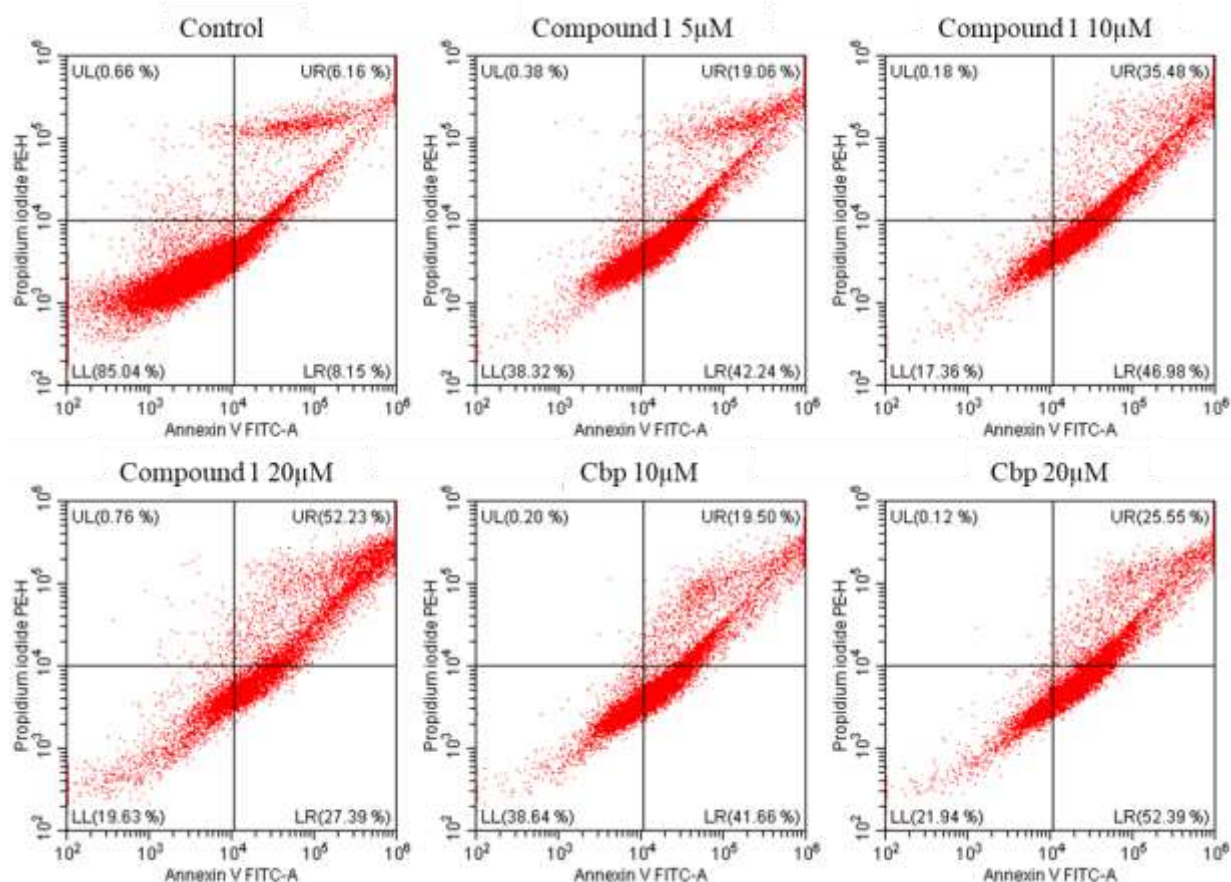


**Figure 3. 21: Representative samples of the flow cytometry graph of OVCAR-8 cell line treated with compound 1 and the positive control (Cbp) at different concentrations. Lower left (LL), upper left (UL), lower right (LR) and upper right (UR) represent live cells, necrotic cells, cells in early apoptosis and cells in late apoptosis respectively.**

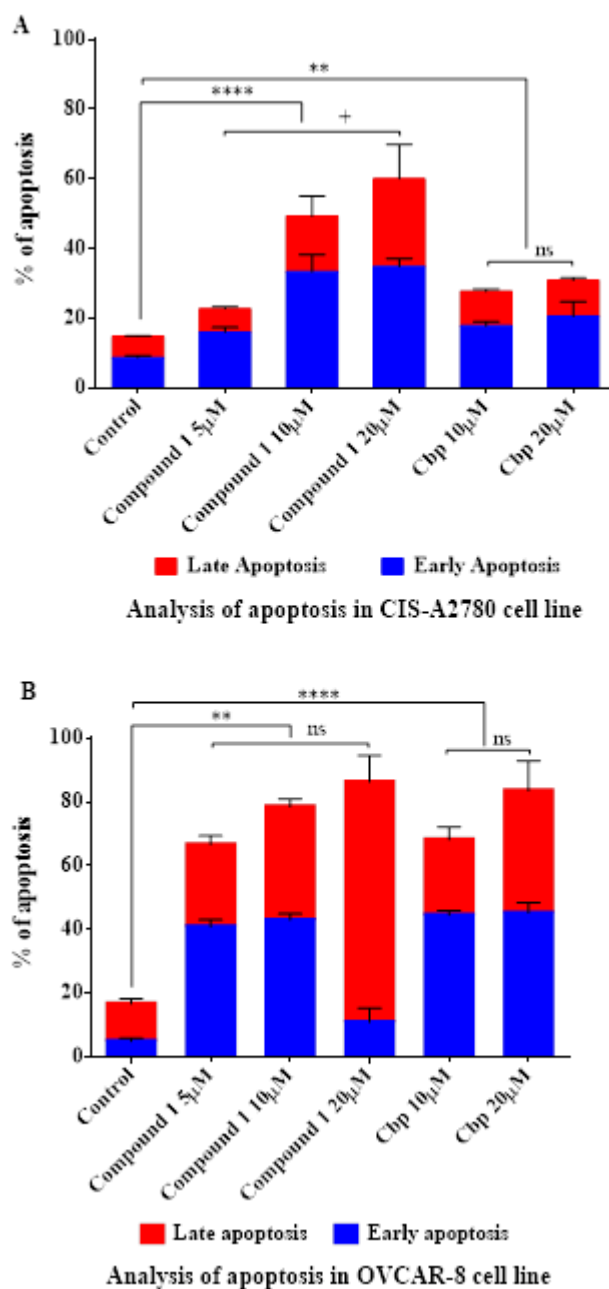


**Figure 3. 22: Evaluation of apoptotic activities of compound 1 on CIS-A2780 (A) and OVCAR-8 (B) cells using annexin V and propidium iodide staining analysed with flow cytometry.** The data represent the mean  $\pm$  SD of three repeats. The significant different between control and treatment is denoted with asterisk (\*), while concentration dependent activity is denoted with plus (+). The significance level at  $p < 0.05$ ,  $p < 0.01$ ,  $p < 0.001$  and  $p < 0.0001$  are represented as (\*), (\*\*), (\*\*\*) and (\*\*\*\*) respectively while no significant different is denoted with (ns).

### 3.2.8.7 Results of mitochondrial membrane potential activities of compound 1

The activeness of the mitochondrial potential of ovarian cancer cells was evaluated to further explore the pathway of apoptosis induction by compound 1 using mitoprobe™ DiIC1(5) assay. This was based on the ability of DiIC1(5) dye to accumulate in the mitochondrial of cells with active membrane potential. The level of decrease in the accumulation of the dye was quantitatively measured using flow cytometry (Figure 3.23). The result shows that compound 1 significantly reduced the intensity of accumulated DiIC1(5) stain in the cell when compared with the negative control. Compound 1 reduced the intensity of DiIC1(5) dye in the cell to 79, 67 and 44% at 5, 10 and 20  $\mu\text{M}$  respectively. However, the mitochondrial membrane potential activity of this compound was not concentration dependent (Figure 3.23). In addition, the multiple comparison of the mitochondrial membrane potential activity of compound 1 was only significant at higher concentrations (10 and 20  $\mu\text{M}$ ) when compared with the control. This result suggests that compound 1 disrupted the mitochondrial membrane potential of the cell that could aid the release of cytochrome *c* into the cytoplasm that is capable of activating apoptosis initiator (caspase 9) through the intrinsic pathway. However, the positive control drug (Carboplatin) seems not to affect the activeness of the mitochondrial membrane potential.

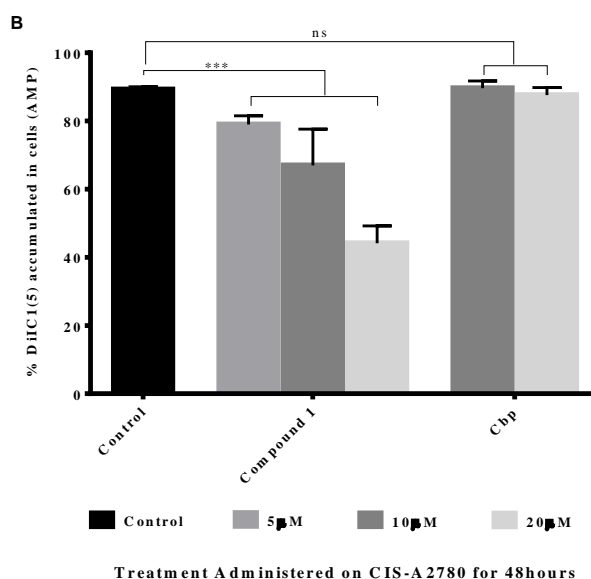
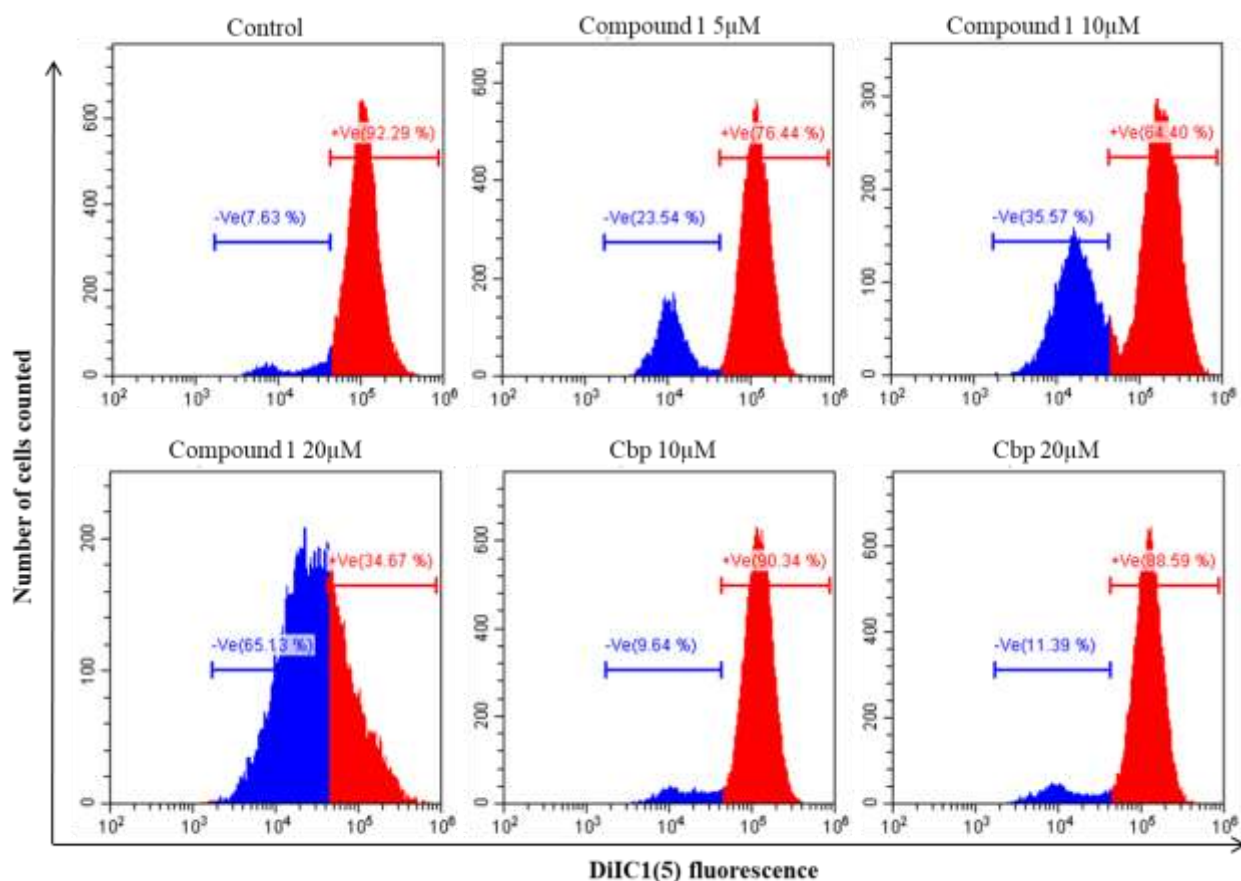


**Figure 3. 23: Activeness of mitochondrial membrane potential of CIS-A2780 ovarian cancer cell line in response to treatment with compound 1.** Representative samples of flow cytometry graph for each treatment condition and untreated cells (A) and the percentage of accumulated DiIC(5) intensity in histograms (B). Carboplatin (Cbp) was used as positive control and the negative control contain 0.1% DMSO in media. The data

represent the mean  $\pm$  SD of three repeated experiments. The red histogram represents intensity of accumulated DiIC(5) stain in cells (intact mitochondrial membrane potential) while the blue histogram represents reduction in the DiIC(5) accumulated within the cell (disrupted mitochondrial membrane potential) due to compound 1 treatment. The significance level at  $p < 0.001$  is represented as (\*\*\*), while no significant different is denoted with (ns).

### 3.2.8.8 Cell cycle analysis of compound 1

Apoptosis and cell cycle plays key roles in cell growth. Within the cell cycle, there are checkpoints that help to maintain genomic stability by protecting dividing cells during DNA damage, they either repair the damaged DNA or trigger cell death (apoptosis). Furthering our study on the mechanism of actions of compound 1, its effects on cell cycle was evaluated on ovarian cancer (CIS-A2780 and OVCAR-8) cell lines using propidium iodide followed by flow cytometry analysis (Figures 3.24 and 3.25). All data were collected from assay performed only 48 hrs after treatment with compound 1, to evaluate its early effects on cell homeostasis. The effect of compound 1 on the cell cycle of CIS-A2780 and OVCAR-8 cell lines is presented in Figure 3.26. In CIS-A2780, the result shows that Compound 1 significantly reduced the number of cells in the G<sub>0</sub>-G<sub>1</sub> phase when compared with the control, and induced S and G<sub>2</sub>-M phase cell arrest. Furthermore, compound 1 significantly increased the percentage of CIS-A2780 cells in the subG<sub>1</sub> phase at higher concentration (Figure 3.26). The percentage of cells arrested at S and G<sub>2</sub>-M phases by compound 1 was concentration dependent. In a similar manner, the positive control (Cbp) also reduced the number of cells in the G<sub>0</sub>-G<sub>1</sub> phase when compared with the control, and caused cell cycle arrest at both S and G<sub>2</sub>-M phases but no significant increase in cells in the subG<sub>1</sub> phase. In OVCAR-8, compound 1 increased the percentage of cells in the subG<sub>1</sub> phase, arrested cells

in the S and G<sub>2</sub>-M phases, and further reduced the number of cells in the G<sub>0</sub>-G<sub>1</sub> when compared with the control (Figure 3.26). The cell cycle arrest activities of compound **1** at S and G<sub>2</sub>-M were significant at each concentration (5, 10 and 20 μM) when compared with the control using Dunnett's multiple comparison test (Figure 3.26). The cell cycle arrest activity of compound **1** at the G<sub>2</sub>-M was concentration dependent. Likewise, the positive control (Cbp) also arrested cells in the S and G<sub>2</sub>-M, and subsequently reduced the number of cells in the G<sub>0</sub>-G<sub>1</sub> phase but no significant change in subG<sub>1</sub> phase when compared with the control. However, the cell cycle arrest activity of Cbp at S and G<sub>2</sub>-M phases were only significant at higher concentration (20 μM) when compared with the control using multiple comparison test.

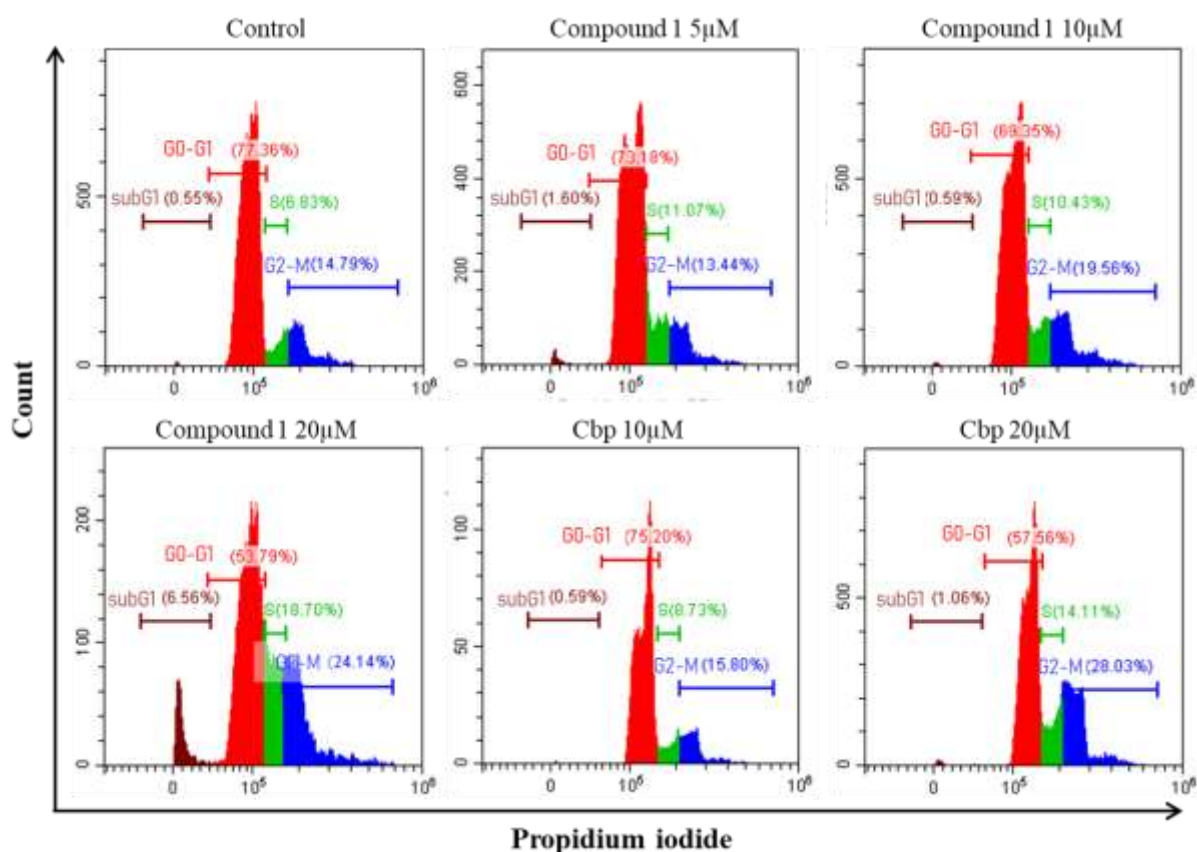


**Figure 3. 24:** Flow cytometry representative sample graphs of CIS-A2780 cell line showing number of cells in each cell cycle phase in response to treatment with compound **1** and the positive control (Cbp) for 48hrs. 0.1% DMSO was used as control.

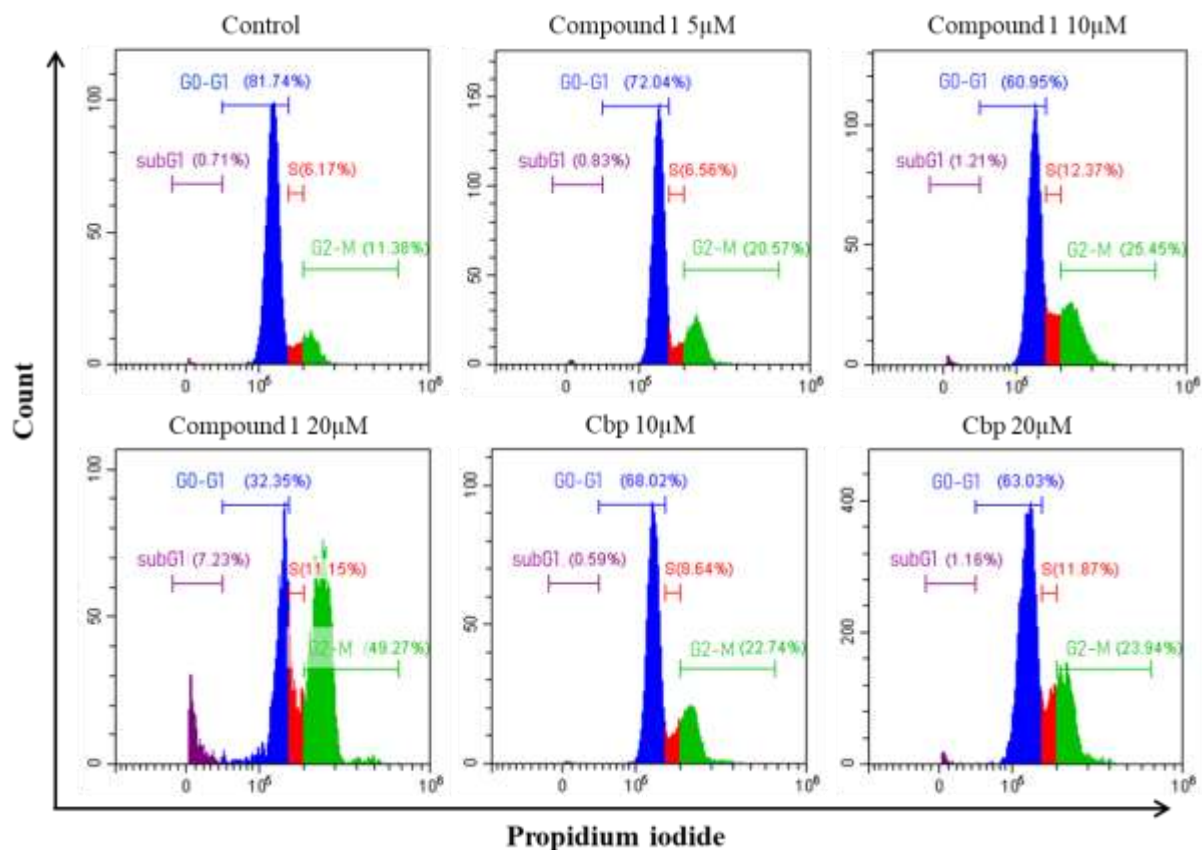


**Figure 3. 25: Representative samples of the flow cytometry graph of OVCAR-8 cell line showing number of cells in each cell cycle phase in response to treatment with compound 1 for 48hrs. Carboplatin (Cbp) was used as positive control and control contains 0.1% DMSO in growth media.**

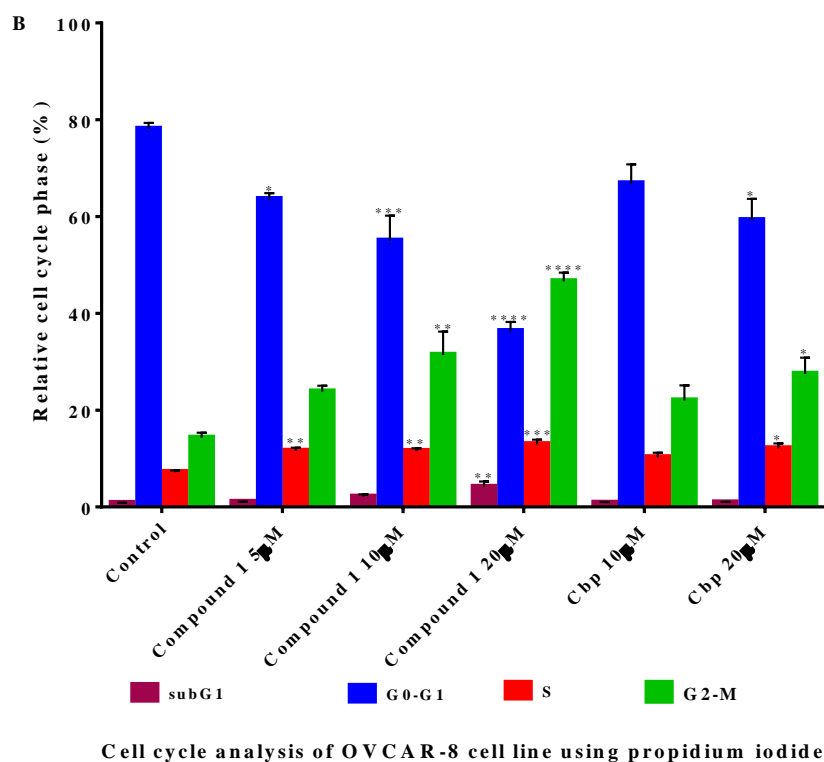
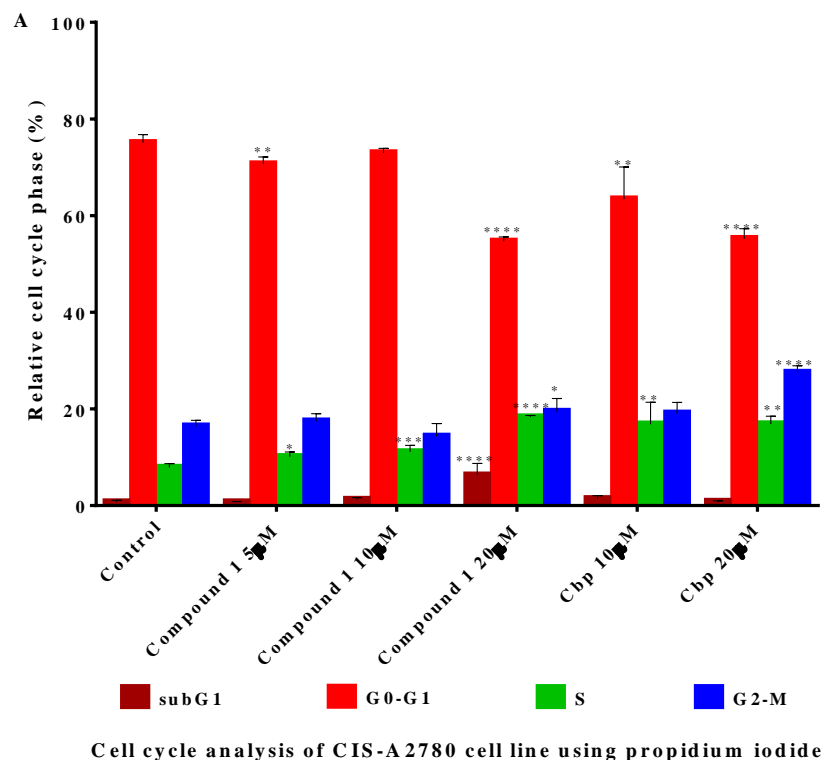


**Figure 3. 26: Effects of compound 1 on the cell cycle of ovarian cancer cells: CIS-A2780 (A) and OVCAR-8 (B) using propidium iodide staining, followed by flow cytometry analysis. Carboplatin (Cbp) was used as positive control and the percentage of cells in each**

phase of the cell cycle was presented in histogram as mean  $\pm$  SD of three repeated experiments. The number of cells in each cell cycle phase in response to compound **1** treatment was compared using one-way ANOVA and Dunnett's multiple comparisons test. The significance level of each concentration of the treated compound when compared with the control using Dunnett's multiple comparison test was denoted with asterisk (\*). While insignificant different is left without any symbol. The significance level at  $p < 0.05$ ,  $p < 0.01$ ,  $p < 0.001$  and  $p < 0.0001$  are represented as (\*), (\*\*), (\*\*\*) and (\*\*\*\*) respectively.

### 3.2.9 Evaluation of the effect of compound **1** on global DNA methylation

The effect of compound **1** on global 5'-methylcytosine DNA methylation was investigated. In brief, DNA isolated from CIS-A2780 cells treated with compound **1** was used as starting material for global DNA methylation quantification using ELISA. The optimal standard curve for 5-mC standard control was generated (Figure 3.27). The result indicated that compound **1** significantly reduced global 5-methylcytosine DNA methylation when compared with the control. Furthermore, the positive control also (5-azacytidine) significantly reduced 5' methylcytosine DNA methylation (Figure 3.28).

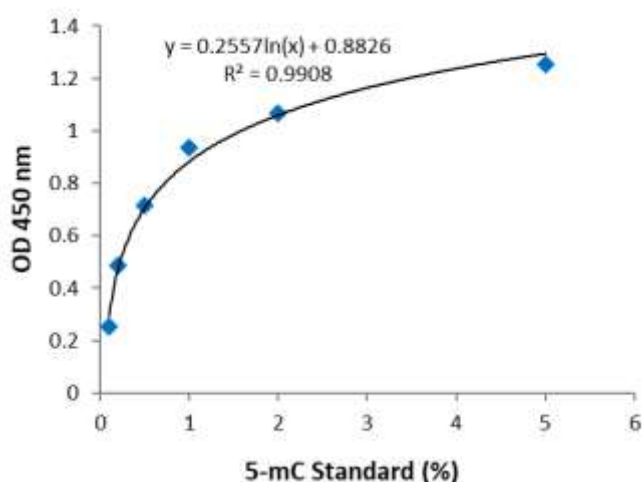


**Figure 3. 27: Optimal standard curve generated with 5-mC standard positive control**

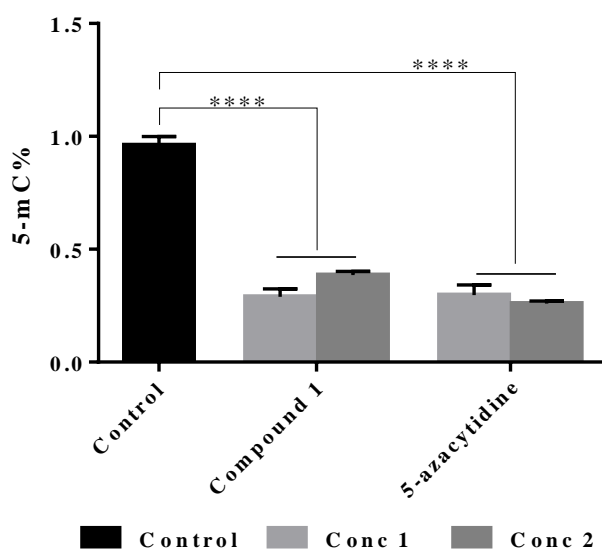


**Figure 3. 28: Percentage of 5-methylcytosine DNA methylation in CIS-A2780 treated with compound 1 and 5-azacytidine.** Data was presented as mean  $\pm$  SEM (n=3). Conc 1 and 2 are 10 and 20  $\mu$ M respectively for compound 1, and 5 and 10  $\mu$ M for 5-azacytidine. The 5-mC % was presented as  $5\text{-mC}/(5\text{-mC}+\text{C})$ . Significant different between each compound methylation activity compared with the control was analysed using one-way ANOVA and the significant different at  $p < 0.0001$  is denoted with asterisk (\*).

### 3.2.10 Quantification of the effect of compound 1 on gene specific promoter methylation using pyrosequencing assay

Pyrosequencing technique was used for the quantification of methylation at CpG site of specific genes that function in the regulation of cell growth. In this experiment, DNA samples extracted from Cis-A2780 were bisulfite converted and amplified using PCR (Appendix III). The PCR amplified bisulfite converted DNA samples were used as template for the pyrosequencing assay. The data collected in three repeats and in duplicate were arranged and the percentage of methylation at the CpG sites was calculated for tumour suppressor genes (*MLH1*, *PTEN*, *HOXA9*, *KLF6*, *TP53*, *APC* and *RASSF1*) (Figures 3.30-

3.33). Significance difference in the CpG methylation of treated and untreated samples was tested using one-way ANOVA. The results revealed that there is high CpG methylation (84.4%) at the promoter region of *MLH1* gene. The CpG methylation level of *HOXA9* and *PTEN* are 16% and 11.1% respectively, while *TP53*, *KLF6*, *APC* and *RASSF1* had less than 3% CpG methylation at their promoter region (Figure 3.29) The results show that compound 1 does not have significant effect on the CpG methylation level of *MLH1*, *HOXA9*, *KLF6*, *TP53*, *APC* and *RASSF1* tumour suppressor genes but caused a significant reduction in the CpG methylation of *PTEN* gene at higher concentration (Figure 3.29). Furthermore, the positive control (5-azacytidine) caused a significant decrease in the CpG methylation level of *HOXA9* gene but did not caused any significant reduction in the CpG methylation of *MLH1*, *PTEN*, *KLF6*, *TP53*, *APC* and *RASSF1* genes.

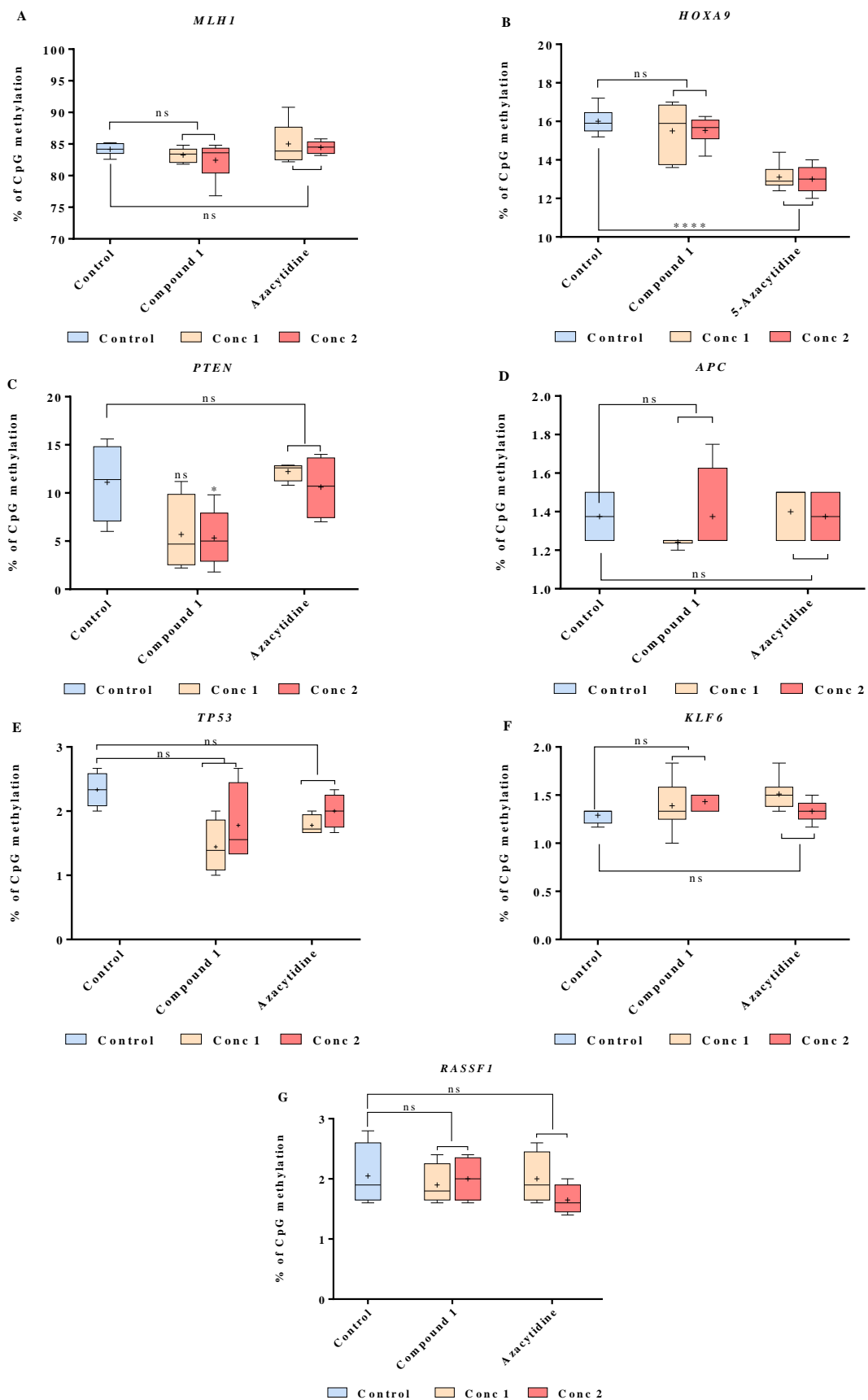


**Figure 3. 29: Percentage of gene specific promoter methylation of *MLH1* (A), *HOXA9* (B), *PTEN* (C) *APC* (D), *TP53* (E), *KLF6* (F) and *RASSF1* (G) genes in ovarian cancer**

cell line (CIS-A2780) in response to treatment with compound 1 using 5'azacytidine as positive control. Conc 1 and 2 are 10 and 20  $\mu$ M for compound 1, and 5 and 10  $\mu$ M for 5-Azacytidine respectively. The data represent the mean  $\pm$  SD of three repeated experiments. The percentage methylation activity of each compound was compared with the control and the significant level is denoted with asterisk (\*), (\*  $p < 0.05$  and \*\*\*\*  $p < 0.0001$ ), while no significant difference is denoted with ns.

### MLH1 gene

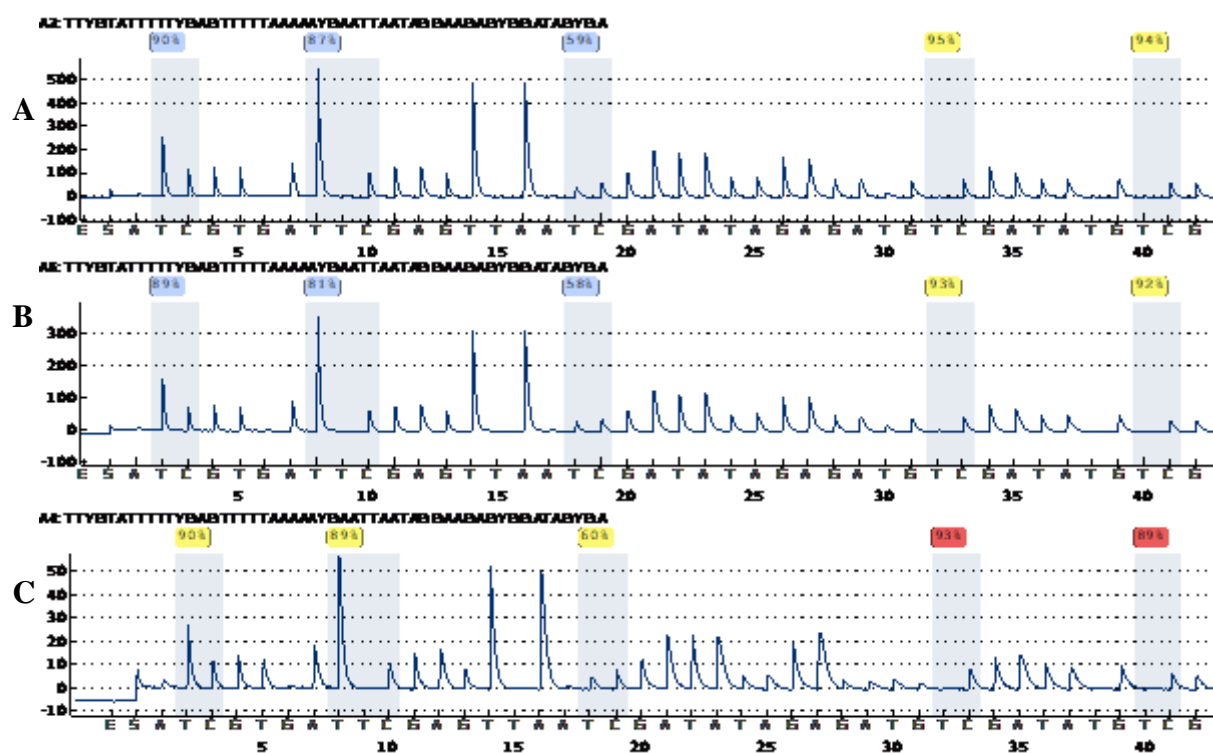
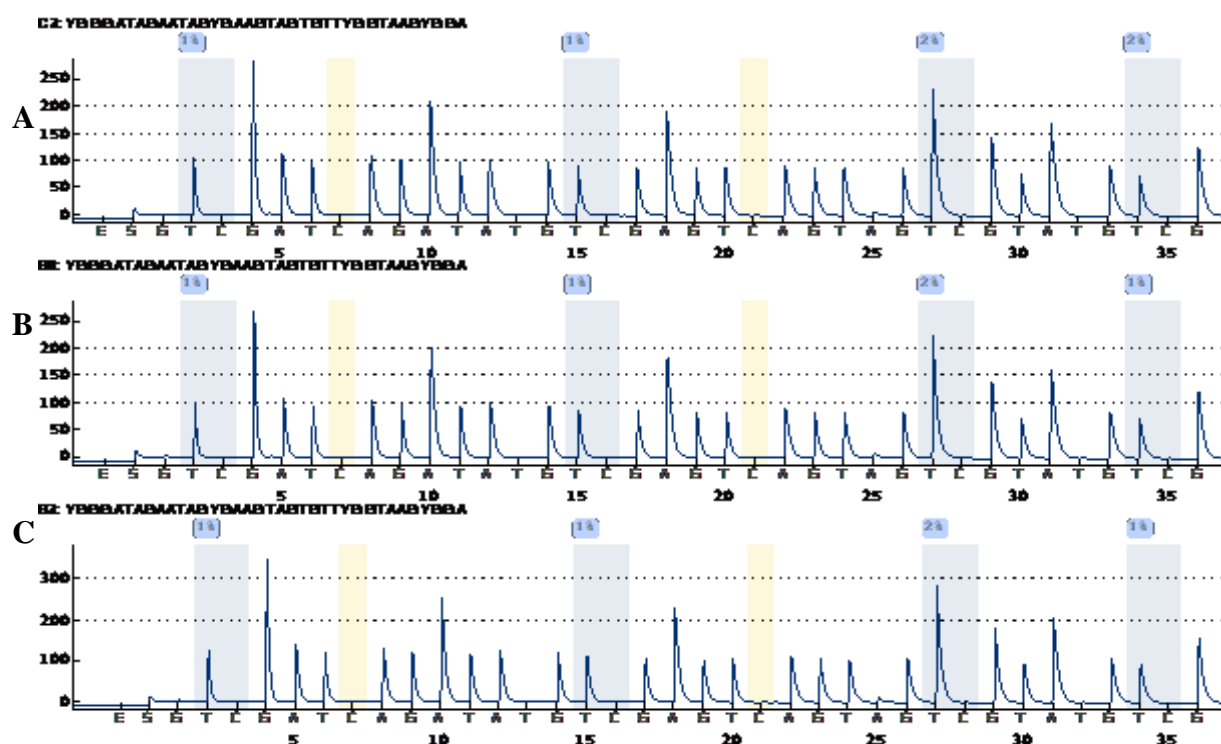


Figure 3. 30: Representative samples of pyrosequencing CpG pyrogram reports of *MLH1* gene on CIS-A2780 cells. Control (A), Compound 1 (B), 5'azacytidine (C).



**APC gene**



**TP53 gene**

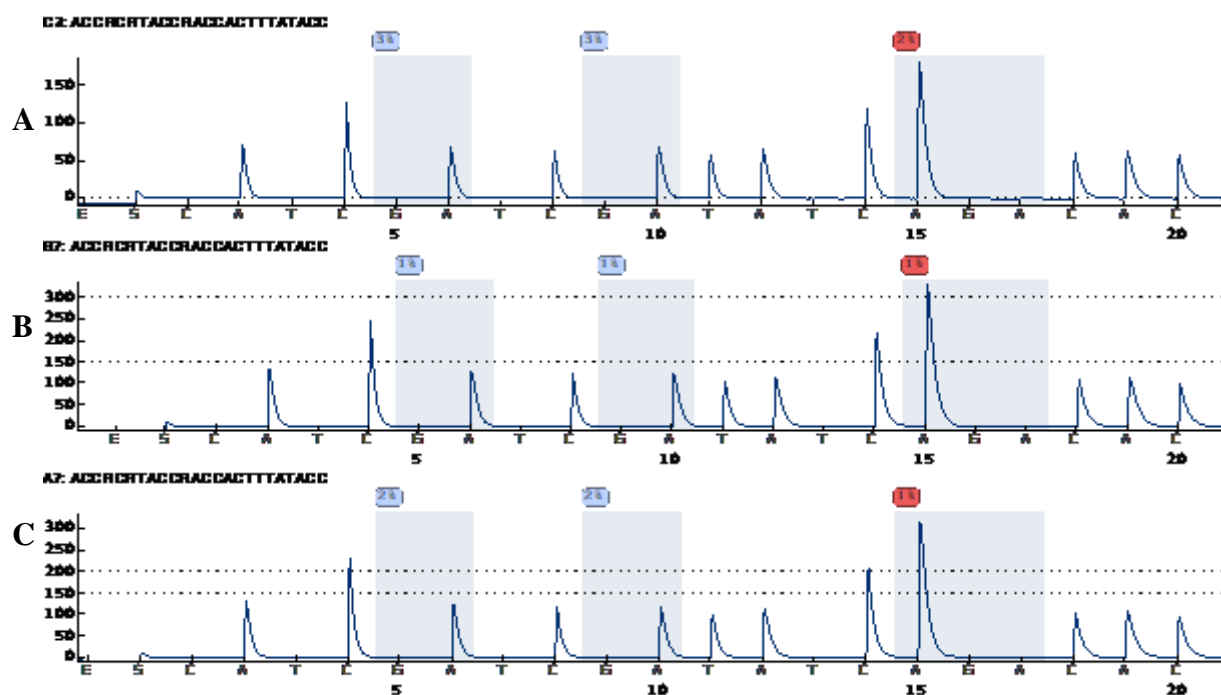
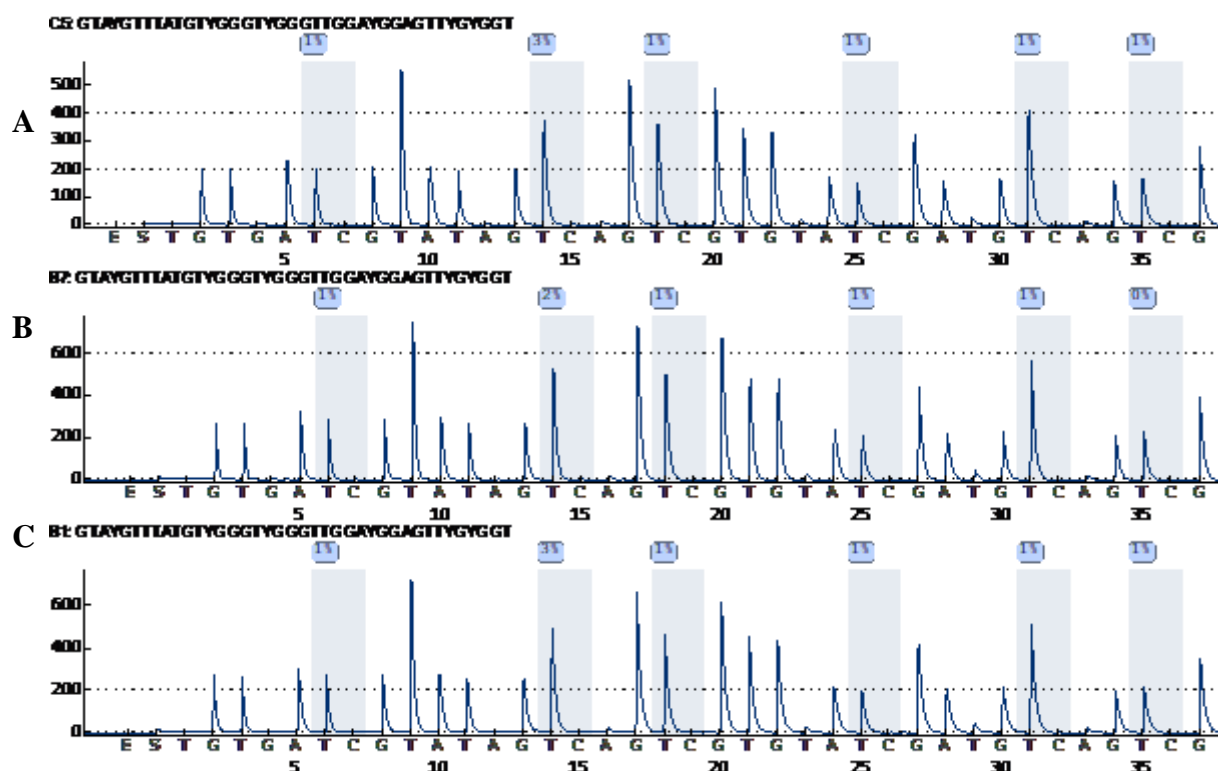


**Figure 3. 32: Representative samples of pyrosequencing CpG pyrogram reports of *APC* and *PP53* genes on CIS-A2780 cell line. Control (A), Compound 1 (B), 5’azacytidine (C).**

***KLF6* gene**



***RASSF1* gene**

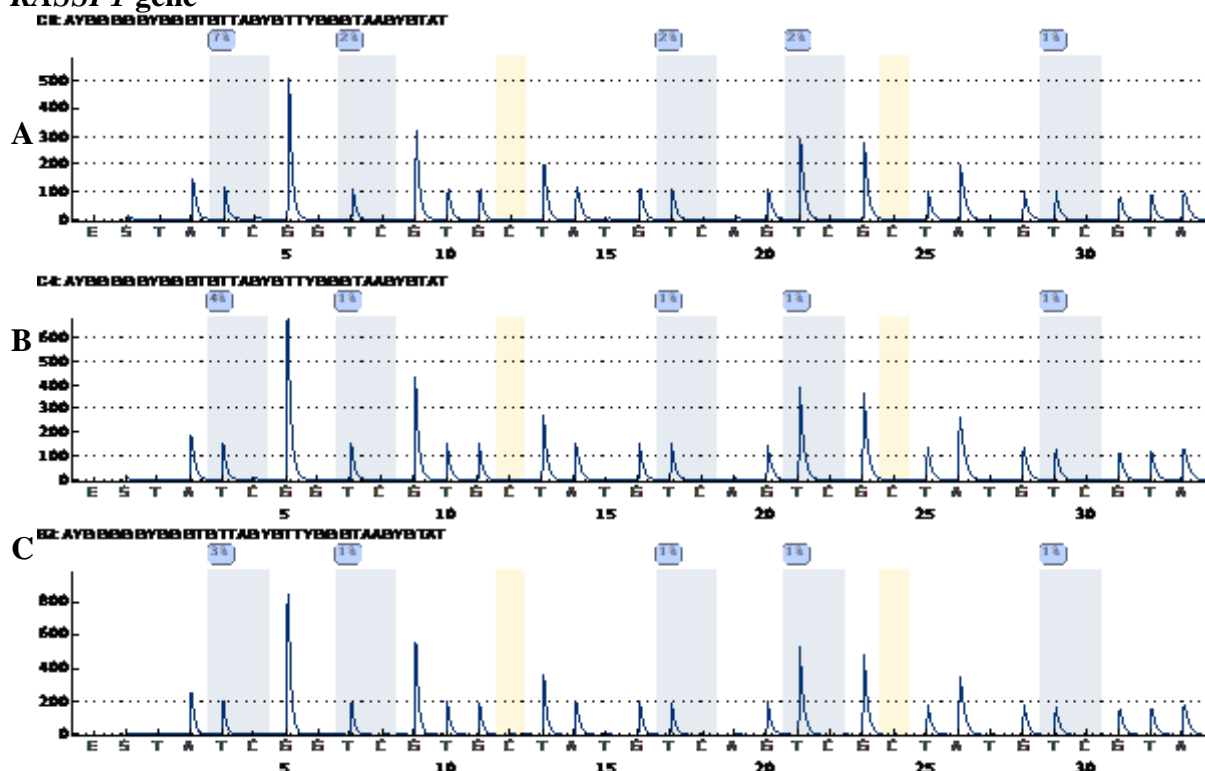
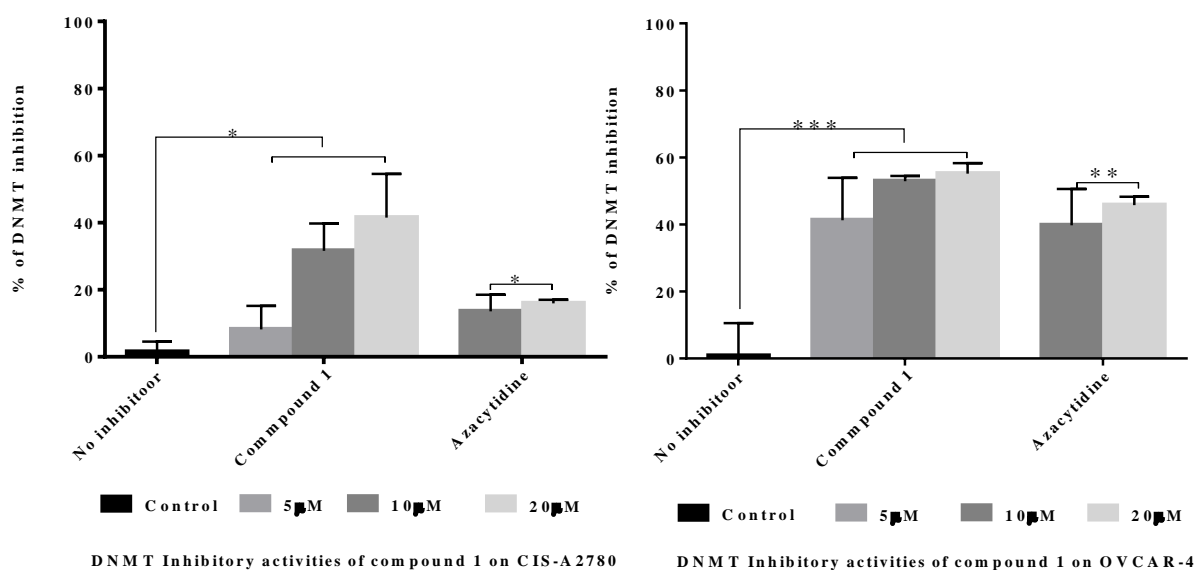


Figure 3. 33: Representative samples of pyrosequencing CpG pyrogram reports of *KLF6* and *RASSF1* genes on CIS-A2780 cell line. Control (A), Compound 1 (B), 5’azacytidine (C).

### 3.2.11 DNMT inhibitory activities of compound **1**

DNMTs are enzymes that catalyse the addition of methyl group to the fifth position region of cytosine backbone of the DNA. They also function in the maintenance and ensure successful replication of the methylated cytosine. The inhibitory activities of compound **1** was evaluated on the nuclear extracts (containing DNMT enzymes) of ovarian cancer cells (CIS-A2780 and OVCAR-4) using colorimetric assay. In CIS-A2780, the result shows that compound **1** significantly inhibited the enzymatic activity of DNMT when compared with the negative control using one-way ANOVA (Figure 3.34). However, the DNMT inhibitory activity of compound **1** was only significant at higher concentration (20  $\mu$ M). The positive control also significantly inhibited DNMT enzymatic activities. Compound **1** slightly caused higher DNMT inhibitory activity than the positive control. In OVCAR-4, compound **1** also caused significant inhibition of DNMT enzymatic activities when compared with the control. Dunnett's multiple comparison of the DNMT inhibitory activity of compound **1** with the control further showed that the DNMT inhibitory activity of compound **1** was significant at all the tested concentrations (5, 10 and 20  $\mu$ M). This result was similar to the DNMT inhibitory activities obtained for 5'azacytidine (positive control) in OVCAR-4.



**Figure 3. 34: DNMT inhibitory activities of compound 1 using the nuclear extracts of CIS-A2780 and OVCAR-4 cell lines.** 5'azacytidine which is a known DNMT inhibitor was used as positive control and the mean  $\pm$  SD values were presented in histogram. The significant different of each treatment with the control is denoted with (\*). The significance level at  $p < 0.05$ ,  $p < 0.01$  and  $p < 0.001$  are represented as (\*), (\*\*) and (\*\*\*) respectively.

### 3.2.12 Gene expression modulatory effects of compound 1 using quantitative reverse transcription polymerase chain reaction (RT-qPCR)

RT-qPCR was performed using quantifast<sup>®</sup> SYBR green RT-PCR kit to quantitatively measure the effects of compound 1 on the expression level of DNMTs and different tumour genes in ovarian cancer cell line (CIS-A2780). Every experiment was performed in triplicate, and the mRNA expression was calculated with the cycle threshold (Ct) values using *GAPDH* as an internal control gene for normalizing variations in gene expression. The mRNA fold expression was determined using  $2^{-\Delta\Delta Ct}$  method. The data collected were arranged and analysed using one-way ANOVA and graphically presented as mean  $\pm$  SD of three repeats. The results show that compound 1 significantly downregulated the expression of *DNMT1*, *DNMT3B* and *DNMT3L* while 5'azacytidine significantly downregulated the

expression of *DNMT1* (Figure 3.35) Compound 1 further significantly upregulated the expression of *PTEN* and *TP53* genes, while a slight upregulation of *BRCA1*, *KLF6*, *RASSF1* and *MLH1* genes was also observed (Figure 3.36) while 5'azacytidine caused a slight upregulation of *PTEN*, *TP53* and significantly upregulated the expression of *APC* and *FOLR1*.

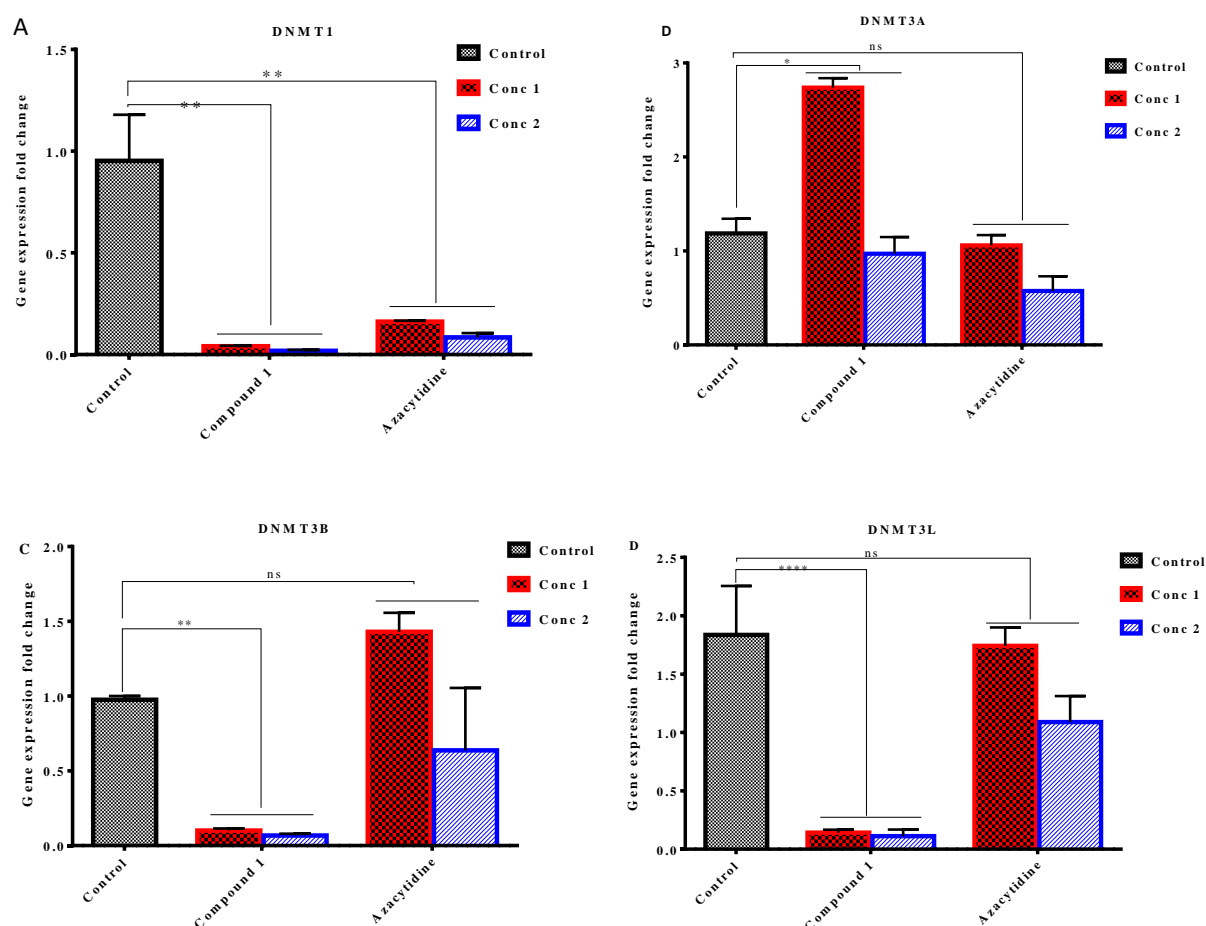


**Figure 3. 35: Modulation of DNMTs expression in response to treatment with compound 1 and 5'azacytidine using RT-qPCR. *DNMT1* (A), *DNMT3A* (B), *DNMT3B* (C) and *DNMT3L* (D).** The significant different of each treatment with the control is denoted with (\*). The significance level at  $p < 0.05$ ,  $p < 0.01$ ,  $p < 0.001$  and  $p < 0.0001$  are represented as (\*), (\*\*), (\*\*\*) and (\*\*\*\*) respectively.

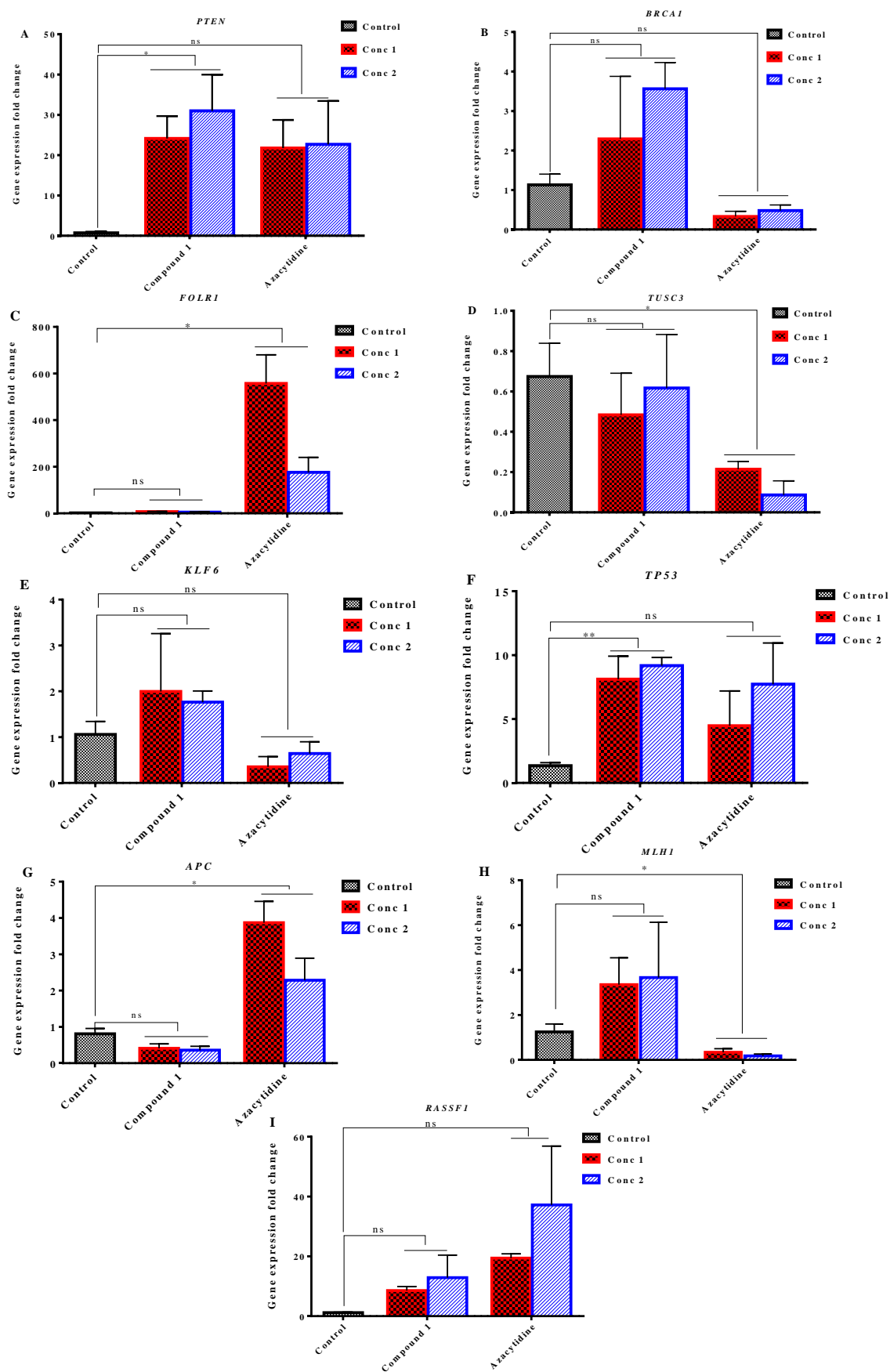


Figure 3.36: Modulation of the expression of different tumour suppressor genes in response to treatment with compound 1 and 5'azacytidine using RT-qPCR. Fold of

change of gene expression (PTEN (A), *BRCA1* (B), *FOLR1* (C), *TUSC3* (D), *KLF6* (E), *TP53* (F), *APC* (G), (H), *MLH1* and *RASSF1* genes (I) The significant different of each treatment with the control is denoted with (\*). The significance level at  $p < 0.05$ ,  $p < 0.01$ ,  $p < 0.001$  and  $p < 0.0001$  are represented as (\*), (\*\*), (\*\*\*) and (\*\*\*\*) respectively.

### 3.3 Discussion

#### 3.3.1 Phytochemical identification of the bioactive compounds in *Justicia insularis*

In this chapter, the *in vitro* anti-ovarian cancer activities of *J. insularis*, and identification of its bioactive compounds were investigated. The results of the initial extraction of the crude powder of *J. insularis* showed that the organic extract had higher yield (21g) than the aqueous yield (7.5g), this may be due to the sequence of extraction method or an indication that there are more non-polar than polar compounds in *J. insularis*. The organic extract was further partitioned based on solvent polarity to yield n-hexane, ethyl acetate, n-butanol and aqueous fractions. However, the n-hexane and the ethyl acetate fractions had higher yield than the n-butanol and aqueous fractions. Based on the biological activities of the partitioned fractions, the ethyl acetate fraction was purified using silica gel column chromatography to yield EA1-10. EA4 was further purified based on biological activity to yield EA4-1 to EA4-11. Final purification and isolation of the bioactive compounds from EA4-4 and EA4-6 was done using analytical and semi-preparative HPLC respectively. This lead to the isolation of several compounds from *J. insularis*. However, only isolated compound **1** and **2** had adequate yield required for further identification. The GC MS data suggested that compound **1** and **2** had the same molecular weight (318 g/mol). However, the compounds name and structure could not be identified with the GC MS data, because their mass spectra do not have a possible match with the GC-MS library mass spectrum for potential compounds. The molecular weight of compound **1** and **2** was further shown to be 318.2 g/mol. Furthermore,

compound **1** and **2** were identified as 16 $\alpha$ / $\beta$ -hydroxy-cleroda-3,13 (14) dien-15,16-olide and 16-oxocleroda-3,13(14) dien-15-oic acid respectively, based on their <sup>1</sup>HNMR and <sup>13</sup>C NMR chemical shifts that were similar to the reports of Phadnis *et al.* (1988), Müller *et al.* (2015) and Hara *et al.* (1995). These compounds were reported in *J. insularis* for the first time. However, there had been no report on their anti-ovarian cancer activities but little is known about their roles in other human cancers such as colon, prostate and breast cancers (Ma *et al.*, 1994).

### **3.3.2 Biological activities *Justicia insularis* and its bioactive compounds**

#### **3.3.2.1 Antiproliferative activity of *Justicia insularis*- isolated bioactive compounds**

The ability of cells to sustain proliferation and escape growth suppressor is one of the underlying mechanisms for cancer formation (Hanahan and Weinberg, 2011). However, in the search for plants and compounds with anti-cancer activities, their antiproliferative activity is usually a major mechanism to be evaluated. In this study, the growth inhibitory activity of the extracts and isolated compounds of *J. insularis* was evaluated with SRB assay. The results of the growth inhibitory activities of the extracts showed that the organic extract was more potent with IC<sub>50</sub> values less than 20 $\mu$ g/mL on all the ovarian cancer cell lines (CIS-A2780, OVCAR-8, and OVCAR-4) studied. These were significantly below the IC<sub>50</sub> value (50 $\mu$ g/mL) threshold stipulated by American National Cancer Institute as the prospective significant level of potent anti-cancer plant extract (Mccloud, 2010). The IC<sub>50</sub> values (9.1-19.2 $\mu$ g/mL) for the organic extract was quite lower compared with the report of Joseph *et al.* (2017), who reported IC<sub>50</sub> values of 42.8-171.13 $\mu$ g/mL for the anticancer activities of closely related species (*Justicia simplex*) on breast, brain and cervical cancer cell lines. The lower IC<sub>50</sub> value in this study could be due to either longer time treatment or that *J. insularis* is more potent than *J. simplex*. Furthermore, the growth inhibitory activity

of the organic extract was cancer cell line dependent with CIS-A2780 and OVCAR-8 showing lower IC<sub>50</sub> value of < 11 µg/mL than OVCAR-4 with higher IC<sub>50</sub> value of 19.2 µg/mL. The growth inhibitory activity of the partitioned fractions (n-hexane, ethyl acetate, n-butanol and aqueous) showed that the n-hexane and the ethyl acetate fractions had higher growth inhibitory activity. This suggested that the possible bioactive compounds in *J. insularis* are much of non-polar compounds. The results of the growth inhibitory activity of the isolated and identified bioactive compounds: 16α/β-hydroxy-cleroda-3,13 (14) dien-15,16-olide (compound **1**) and 16-oxocleroda-3,13(14) dien-15-oic acid (compound **2**) showed that compound **1** and **2** had high anti-ovarian cancer activity with IC<sub>50</sub> value < 10 µM, and IC<sub>50</sub> < 20 µM respectively in all the ovarian cancer cell lines studied. The growth inhibitory activity of compound **1** was similar to the reports of Ma *et al.* (1994) on different human cancers, such as: colon, prostate, breast cancer cell lines. Zhao *et al.* (1991) had also reported that compound **1** and **2** showed significant cytotoxic activities in breast, lung and colon tumour cell lines. The growth inhibitory activity of compound **1** reported in this study was also consistent with the report of Sari *et al.* (2013), who reported an IC<sub>50</sub> of 13.7 µM. These compounds were also known for their antifeedant activities (Phadnis *et al.*, 1988; Li, Morris-Natschke and Lee, 2016). Compound **1** showed higher growth inhibitory activity than the positive control (Cbp) which is a standard drug for ovarian cancer treatment, while compound **2** had similar growth inhibitory activity with Cbp. Furthermore, compound **1** showed more cancer specific activity than compound **2** and the positive control (Cbp). The positive control (carboplatin) showed cancer specific activity by showing higher growth inhibitory against OVCAR-8 than OVCAR-4. However, no growth inhibitory activity was demonstrated against CIS-A2780 cells. This showed that CIS-A2780 cell line was resistant to ovarian cancer treatment. Additionally, compound **1** had higher anti-ovarian cancer activity than compound **2** in all the ovarian cancer cell lines studied. These results agree

with the report of Zhao *et al.* (1991), who reported that compound **1** showed higher cytotoxic activities than compound **2** against lung, breast and colon cancer. Similarly, the higher anti-ovarian cancer activity reported for compound **1** in this study was consistent with to the report of Sashidhara *et al.* (2011), who reported higher lipid lowering activity for compound **1** with lesser and insignificant activity for compound **2**. The cytotoxic activities of compound **1** and **2** were suggested to be associated with their hydroxyl and carboxyl group on position 16 respectively, and this suggestion was made based on the lesser cytotoxic activities of the derivatives of these compounds when the hydroxyl group was substituted with acetyl and methyl groups Zhao *et al.* (1991). While Sashidhara *et al.* (2011) attributed the lipid lowering activity of compound **1** to the lactone group in its chemical structure. Compound **1** and **2** showed higher anti-ovarian cancer activities than the anti-cancer activities of other closely related diterpenes ((-)-3 $\alpha$ ,16 $\alpha$ -dihydroxycyclo-4(18),13(14)Z-dien-15,16-olide and (-)-3 $\beta$ ,16 $\alpha$ -dihydroxycyclo-4(18), 13(14)Z-dien-15,16-olide) (Sashidhara *et al.*, 2010). In addition, the trypan blue exclusion assay result showed that compound **1** reduced CIS-A2780 and OVCAR-8 cells viability by inducing significant cell death at different concentrations. Afolabi *et al.* (2017) had also reported that compound **1** reduced the viability of human leukemia HL-60 cell line. Similarly, Sari *et al.* (2013) had also reported that compound **1** reduced the viability of HL-60 cells. This result was also consistent with the growth inhibitory activity of compound **1**, and further suggested that the antiproliferative activity of compound **1** was mainly through induction of cell death.

### 3.3.2.2 Pro-apoptotic activity of Compound 1

Cancer cells are generally known for their characteristic features of escaping programmed cell death, which is a mechanism that maintains cell population and defence against damaged cells. However, apoptosis could be initiated in cancer cells through exposure to

external factors or stimuli. Furthermore, majority of the drugs used in cancer treatment usually alter the apoptosis pathways. Hence, this mechanism is often evaluated in the investigation of the anticancer activities of natural compounds. To further investigate the route of anticancer activity for compound **1**, its roles in the induction of apoptosis was evaluated. The initiation of apoptosis in the cells is often associated with morphological changes. In this study, the morphological changes in ovarian cancer cells in response to treatment with compound **1** was evaluated with light and fluorescent microscopy. The results demonstrated that compound **1** caused cell shrinkage and detachment, and reduced cell number which are features of apoptosis. The morphological changes induced by compound **1** was consistent with the report of Sari *et al.* (2013), who identified that compound **1** caused change in the shape such as smaller nuclei, chromatin condensation, fragmented nucleus and cell shrinkage in HL-60 cell compared with the control. The apoptotic activity of compound **1** was studied using flow cytometry analysis of cells stained with annexin V-FITC and PI. The results showed that compound **1** induced apoptosis in both CIS-A2780 and OVCAR-8 cells. Furthermore, the caspase 3/7 activity of compound **1** was evaluated, and the results showed that the cell death induced by compound **1** was via the activation of caspase 3/7 which is an apoptosis executioner. Additionally, the mechanism of apoptosis induction showed that compound **1** induced apoptosis through the extrinsic and intrinsic pathway by activation of caspase 8 and 9. Compound **1** further disrupted the mitochondrial membrane potential of the cell which would aid the release of cytochrome *c* into the cytoplasm that is capable of activating caspase 9 which is an apoptosis initiator through an intrinsic pathway. These results were consistent with the reviewed report of Lavanya, *et al.* (2018) on the anticancer activities of *Polyalthia longifolia*. Compound **1** has been isolated from this plant and is one of the major bioactive compound in this plant. Lavanya, *et al.* (2018) reviewed that this plant activated caspase 3 and caspase 9, and further

caused the loss of mitochondrial membrane potential of the cells. The ability of compound **1** to induce apoptosis through both intrinsic and extrinsic pathways explains why it showed very high anti-proliferative and cytotoxic activities on ovarian cancer cell lines. Compound **1** further increased the percentage of cells in the subG<sub>1</sub> phase of the cell cycle. Additionally, compound **1** caused cell cycle arrest at S and G<sub>2</sub>-M phases, this could possibly be part of the reason for its high anti-proliferative and apoptotic activities. The apoptotic and cell cycle arrest activities of compound **1** was consistent in both CIS-A2780 and OVCAR-8 cells, this suggested that that the apoptotic activity of compound **1** was not ovarian cancer cell line dependent. However, carboplatin which is a standard drug for ovarian cancer treatment induced apoptosis and caused cell cycle arrest at S and G<sub>2</sub>-M phases. This result was consistent with previous report that carboplatin caused cell cycle arrest at S and G<sub>2</sub>-M phases in human bladder carcinoma cell 5637 cell line (Wang *et al.*, 2010).

### **3.3.2.3 DNA methylation and gene expression modulatory activities of compound 1**

The DNA demethylating activity of compound **1** on the global DNA and gene specific CpG sites was evaluated. This is an underlining mechanism for most cancer formation. The fact that this process is reversible makes it a good target for cancer treatment. However, plant-derived natural products have been known to modulate epigenetic mechanisms (Thakur *et al.*, 2014). In our study, the results showed that compound **1** significantly reduced the global DNA methylation level of CIS-A2780 ovarian cancer cell line. However, gene specific DNA demethylation was only observed in *PTEN* gene at higher treatment dose, while no major gene specific demethylation activity was found at the CpG sites of the promoter region of *MLH1*, *HOXA9*, *APC*, *TP53*, *KLF6* and *RASSF1* genes. This is the first report on the DNA methylation activity of this compound. Compound **1** inhibited the enzymatic activities of DNMTs in ovarian cancer cell lines. Further evaluation of the specific DNMT

inhibited, showed that compound **1** significantly downregulated the expression of *DNMT1*, *DNMT3B* and *DNMT3L*. These are enzymes that catalyse the addition and maintenance of methyl group to the DNA. In addition, compound **1** upregulated the expression of *PTEN* and *TP53* genes which are tumour suppressor genes that help to control the rate of cell division, regulate cell growth and proliferation. This study seems to be the first to evaluated the roles of compound **1** in DNA methylation and inhibition of DNMT. The ability of compound **1** to down regulate the expression of DNMTs and upregulate the expression of tumour suppressor genes are suggested to be among the underlining mechanisms for its high anti-proliferative and apoptotic activities.

### 3.4 Conclusion

In conclusion, this study investigated the anti-ovarian cancer activities of *J. insularis* T. Anderson, characterized its bioactive compounds and evaluated their roles in DNA methylation and apoptosis. *J. insularis* plant and its constituent, compound **1** were found to be promising and potential anti-ovarian cancer agent. The major bioactive constituent of this plant with anticancer activities are 16 $\alpha$ / $\beta$ -hydroxy-cleroda-3,13 (14) dien-15,16-olide (compound **1**) and 16-oxocleroda-3,13(14) dien-15-oic acid (compound **2**) with compound **1** known to be the most promising anti-ovarian cancer agent. These compounds were identified in this plant for the first time. Furthermore, compound **1** was found to have high antiproliferative activity against ovarian cancer cells. It further caused cell cycle arrest at S and G<sub>2</sub>-M phases, and induced apoptosis through the activation of caspase executioner (Caspase 3/7) via both intrinsic and extrinsic pathways. Additionally, the ability of compound **1** to cause DNA demethylation, inhibit DNMTs enzymatic activities and upregulate the expression of tumour suppressor genes makes it a promising anti-cancer agent that could be studied further. Even though, *J. insularis* is an edible plant that is

ethnopharmacologically used for the treatment of different diseases. It is one of the least studied species in the genus *Justicia*. This study was the first to evaluate its anti-ovarian cancer activities, identified its bioactive compounds and elucidated their roles in apoptosis, DNA methylation and modulation of gene expression. Further study need to be carried out on the bioactive compounds identified, especially in the area of their epigenetic activities (histone modification and miRNA mediated post-transcriptional activity). Also, direct protein target identification for the mechanism of action of compound **1**, and *in vivo* study to validate its efficacy and toxicity would be essential. Additionally, all the bioactive compounds in this plant could not be identified in this study because of the available yield of the purified fractions. Therefore, future study should also focus on the identification of novel bioactive compounds from the other active fractions of *J. insularis*.

## **Chapter Four**

# **Anti-Ovarian Cancer Activity of Andrographolide and Triptolide, and their Roles in DNA Methylation and Modulation of Gene Expression**

## **4.1 Introduction**

Andrographolide (Andr) and triptolide (Tpl) are diterpenoids, which are group of compounds with four isoprene subunits that are mostly isolated from different parts of *Andrographis paniculata* and *Tripterygium wilfordii* respectively. These plants are Chinese traditional herbs with various health benefits (Zhao *et al.*, 2010; Zhu *et al.*, 2013). They are of biological and pharmacological relevance as they are known to have anti-inflammatory and anti-cancer activities (Mao *et al.*, 2018; Dai *et al.*, 2019). These diterpenoids have been shown to have moderate to high cytotoxic activities, induced apoptosis and caused cell cycle arrest in different cancer cell types (Zhao, *et al.*, 2010; Zheng *et al.*, 2011; Bao *et al.*, 2013; Gao *et al.*, 2018). Furthermore, triptolide have been suggested to have epigenetic regulation on important genes that function in the regulation of apoptosis and cell cycle (Nardi *et al.*, 2018). However, there is still need to explore it roles in DNMT inhibition, CpG demethylation and modulation of gene expression of tumour suppressor genes in ovarian cancer. Also, there is little or no data available on the roles of andrographolide in DNA methylation and DNMT expression. Therefore, the anti-ovarian cancer activities of andrographolide and triptolide was investigated in this study, and most importantly, their DNA methylation and DNMT inhibitory activities including modulation of gene expression were also evaluated. The anti-ovarian cancer activities of these compounds were investigated using several methods. In brief, the anti-proliferative and cytotoxic activities of these compounds were evaluated against ovarian cancer (CIS-A2780, OVCAR-8, and OVCAR-4) and immortalised human ovarian epithelia (HOE) cell lines using Sulforhodamine B (SRB) and trypan blue assays. The (IC<sub>50</sub>) and the selectivity index (SI) of these compounds were determined. Furthermore, the apoptotic activities of these compounds were evaluated using caspase 3/7, 8, and 9 assays, and other markers such as phosphatidylserine protein and mitochondrial membrane potential. The morphological

effects of these compounds were evaluated using light and fluorescence microscopy. ELISA based assay, pyrosequencing and RT-qPCR were used to evaluate their epigenetic activities.

## **4.2 Results**

### **4.2.1 Growth inhibitory activity of andrographolide and triptolide against ovarian cancer cells**

The effect of Andr and Tpl on the growth and proliferation of ovarian cancer cell lines (CIS-A2780, OVCAR-8 and OVCAR-4) and immortalised human ovarian epithelial cells (HOE) using SRB assay as described in chapter 2. The concentration that caused 50% inhibitory effect ( $IC_{50}$ ) was determined. The selectivity index (SI) of Andr and Tpl were also determine to show their safety level and if their activities were cancer specific. The mean concentration growth response curves for Andr and Tpl are presented in Figure 4.1, and the  $IC_{50}$  values for each compound is determined and presented in Table 4.1.

Tpl with  $IC_{50}$  at the nanomolar range was around 1000-fold more potent than Andr with  $IC_{50}$  at the micromolar range in all the three ovarian cancer cell lines. The  $IC_{50}$  values for the positive control (Ptx) in CIS-A2780, OVCAR-8 and OVCAR-4 were at the nanomolar range. Andr showed higher growth inhibitory activity in CIS-A2780 and OVCAR-8 than in OVCAR-4 cells. While Tpl showed higher selectivity towards CIS-A2780 and OVCAR-4 than in OVCAR-8. Tpl showed higher growth inhibitory activity against the ovarian cancer cells with lower  $IC_{50}$  values than Andr and the positive control (Ptx). Furthermore, the positive control (Ptx) showed higher cytotoxicity against HOE cells with an average selectivity index (SI) of 1.9 compared to Andr and Tpl that had average selectivity indexes of 2.7 and 5.2 respectively. This suggests that the growth inhibitory activity of Andr and Tpl was more cancer specific than the growth inhibitory activity of the positive control (Ptx).

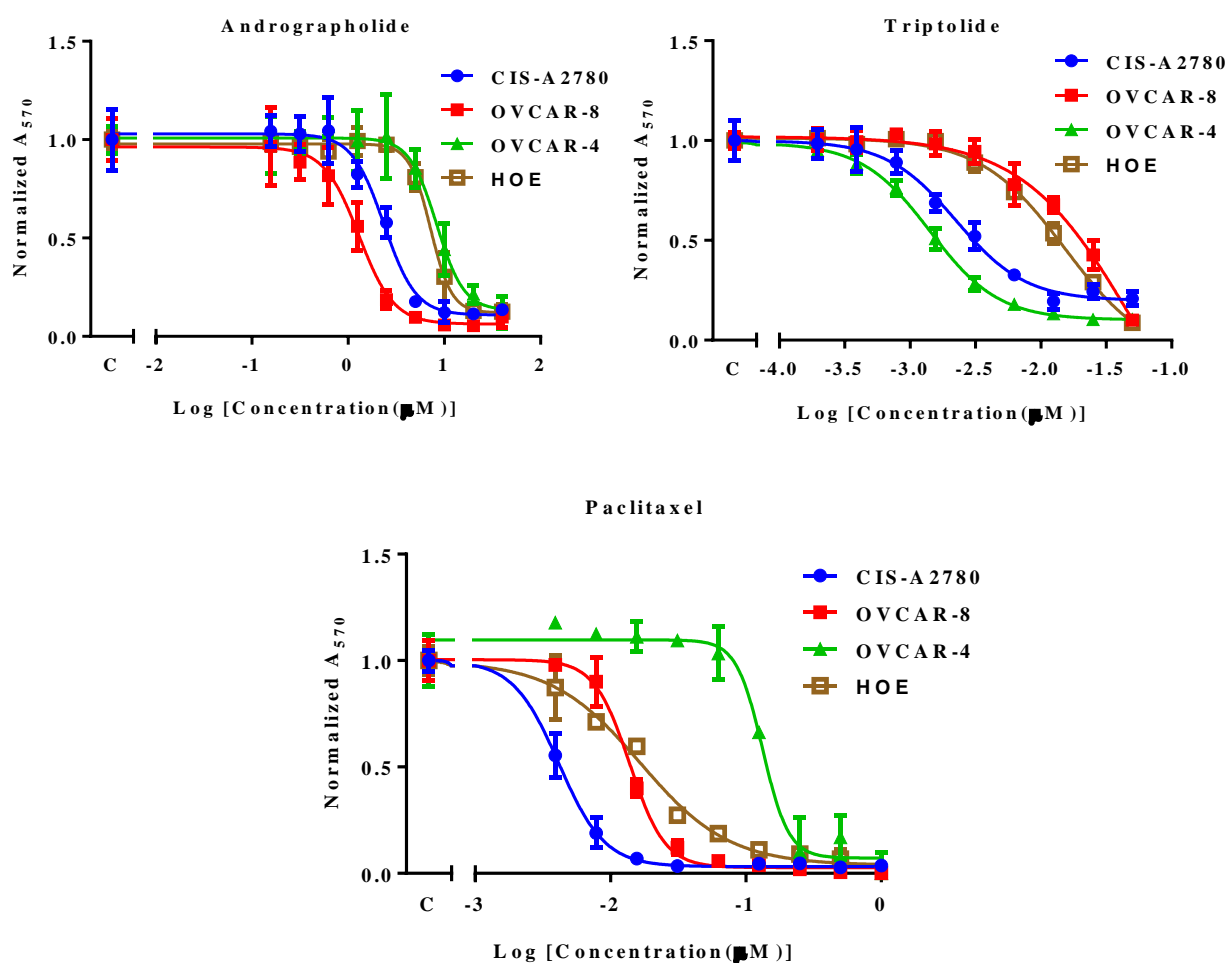


**Figure 4. 1:** Mean concentration response curve of the growth inhibitory activity of *Andr* (A), *Tpl* (B) and *Ptx* (C) against ovarian cancer cell lines (CIS-A2780, OVCAR-8, and OVCAR-4) and HOE. The cancer cell lines were treated with different concentrations of each compound for 72h. For *Andr* (0.16-40 µM), *Tpl* (0.2 – 50 nM) and for *Ptx* (4.0 – 1000 nM). The negative control is denoted with letter C.

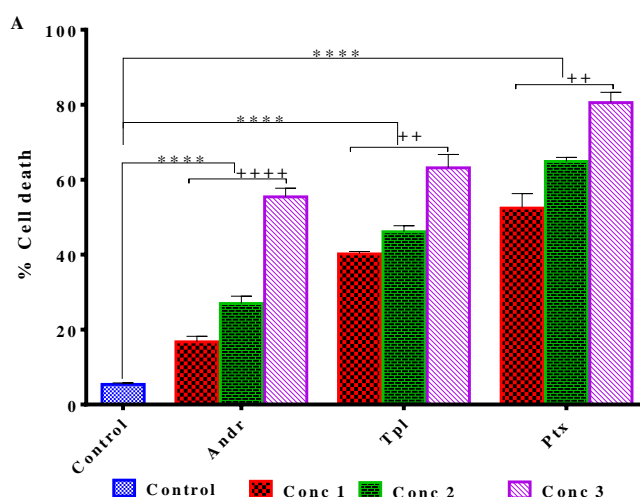
**Table 4. 1: The growth inhibitory activities (IC<sub>50</sub>) of Andr and Tpl against ovarian cancer (CIS-A2780, OVCAR-8, and OVCAR-4) cell lines and HOE using SRB assay. The IC<sub>50</sub> results represent the mean ± SEM of three repeated experiments performed in triplicate. SRB assay was used to estimate the cell number based on protein stained after 72h of post-treatment period. Paclitaxel (Ptx) was used as positive control. Nine different concentration of each drug was used, while control contains 0.2% vehicle (DMSO) for Andr, and 0.01% for Tpl and Ptx. The concentration for Andr ranges between (0.16 - 40 µM), for Tpl (0.2 - 50 nM) and Ptx (4.0 – 1000 nM). The selectivity index (SI) was determined as the ratio of IC<sub>50</sub> of HOE to IC<sub>50</sub> of each cancer cell line and the mean SI was determined (n=3).**

<b>Natural Compounds</b>	<b>CIS-A2780 IC<sub>50</sub> (µM)</b>	<b>OVCAR-8 IC<sub>50</sub> (µM)</b>	<b>OVCAR-4 IC<sub>50</sub> (µM)</b>	<b>HOE IC<sub>50</sub> (µM)</b>	<b>SI with CIS-A2780</b>	<b>SI with OVCAR-8</b>	<b>SI with OVCAR-4</b>	<b>Mean SI (n=3)</b>
Andrographolide	2.1±0.1	1.5±0.3	7.0±1.2	6.25±1.9	3.0	4.2	0.9	2.7±1.4 SD
Triptolide	0.002±0.0005	0.03±0.008	0.002±0.0007	0.015±0.006	7.5	0.5	7.5	5.2±3.3 SD
Paclitaxel	0.005±0.001	0.03±0.005	0.07±0.09	0.023±0.008	4.6	0.8	0.3	1.9±1.9 SD

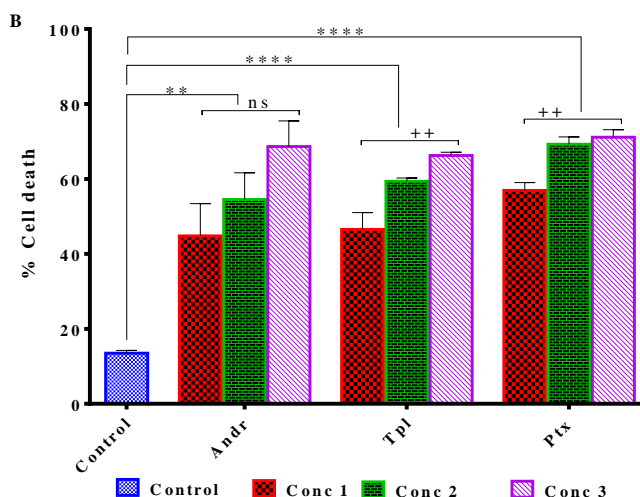
#### **4.2.2 Evaluation of the cytotoxic effect of Andr and Tpl using trypan blue assay**

The cytotoxic activity of Andr and Tpl was investigated to determine their effect on the viability of cells. This will further reveal if the effects of Andr and Tpl on the growth of ovarian cancer cells was through induction of cell death. Concisely, CIS-A2780 and OVCAR-8 cells were treated with Andr, Tpl and positive control (Ptx) at three different concentrations. After 48 h post-treatment period, cells stained with trypan blue dye were viewed with light microscope. The number of stained (cells with trypan blue uptake) and unstained (without trypan blue intake) cells were counted using the haemocytometer. The percentage of cell death was determined and subjected to one-way ANOVA to test for significant changes in cell death, in response to drug treatment. Post hoc Dunnett's multiple comparison test analysis was done to determine which concentration of the drug induced significant cell death compared with the control. Additionally, one-way ANOVA was also used to test if the percentage cell death induced by each drug at different concentrations was significant. In CIS-A2780 cells, Andr, Tpl and the positive control (Ptx) significantly reduced cell viability by inducing cell death (Figure 4.2). The cell death induced by Andr (16.7, 26.97 and 40.2%) at 5, 10 and 20 $\mu$ M respectively was comparably lower than the cell death induced by Tpl (40.2, 46.1 and 63.1%) at 0.01, 0.02 and 0.04 $\mu$ M. However, Ptx (positive control) caused higher cell death (52.4, 64.9 and 80.6%) at 0.25, 0.5 and 1  $\mu$ M than the cell death induced by Andr and Tpl. The cell death induced by Andr, Tpl and Ptx were concentration dependent. In OVCAR-8, Andr, Tpl and Ptx induced significant cell death when compared with the negative control. Furthermore, Dunnett's multiple comparison test shows that the cell death induced by Andr (44.8, 54.5 and 68.7%) at 5, 10 and 20 $\mu$ M respectively were all significant when compared with the control. While the cell death induced by Tpl (46.6, 59.4 and 66.2%) at 0.01, 0.02 and 0.04 $\mu$ M and Ptx (56.9, 69.3 and 71.1%) at 0.25, 0.5 and 1  $\mu$ M) respectively, were all significant when compared with the

cell death induced by the control (13.5%). Also, the percentage cell death induced by Tpl and Ptx was concentration dependent. There was no difference in the percentage of cell death induced by Andr, Tpl and the positive control (Ptx). The high percentage cell death induced by Andr and Tpl (Figure 4.2) suggest that their anti-growth inhibitory activity was mainly by cell death induction.



Treatment administered on CIS-A2780 for 48 hours



Treatment administered on CIS-A2780 for 48 hours

**Figure 4. 2: Trypan blue exclusion test for Andr and Tpl cytotoxicity on CIS-A2780 (A) and OVCAR-8 (B) cell line at different concentrations for 48 hours. Paclitaxel (Ptx)**

was used as positive control. The negative control was treated 0.1% vehicle (DMSO). Conc 1, 2 and 3 for Andr and Tpl are 5, 10 and 20  $\mu\text{M}$ , and 0.01, 0.02 and 0.04  $\mu\text{M}$  respectively. While they are 0.25, 0.5, and 1.0  $\mu\text{M}$  for Ptx. The results are presented as the mean  $\pm$  SEM of three repeated experiments. The level of significant different between negative control and treatment was denoted with asterisk (\*) while significant difference within concentrations of the same treatment for concentration dependent activity was denoted with plus sign (+). The significance level at  $p < 0.05$ ,  $p < 0.01$ ,  $p < 0.001$  and  $p < 0.0001$  are represented as (\*), (\*\*), (\*\*\*) and (\*\*\*\*) respectively while no significant different is denoted with (ns). Similar pattern was followed for significant difference within concentrations of the same compound.

#### **4.2.3 Andr and Tpl induced morphological changes in ovarian cancer cells**

The effects of diterpenoids (Andr and Tpl) were evaluated on the morphology of ovarian cancer cells to show if their cytotoxic activity was due to the induction of apoptosis. CIS-A2780 and OVCAR-4 cells ( $1 \times 10^4$  cell/well in 500  $\mu\text{L}$  growth media) were treated with different concentrations of Andr (5 and 10 $\mu\text{M}$ ) and Tpl (0.02 and 0.04  $\mu\text{M}$ ). While 0.5 and 1.0  $\mu\text{M}$  concentration was used for Ptx as the positive control. Changes in the morphology of the cells were observed directly under the microscope. Andr and Tpl induced significant morphological changes in both CIS-A2780 and OVCAR-8 ovarian cancer cells with apoptotic features such as: cell detachment, cell shrinkage, and membrane blebbing (Figures 4.3 and 4.4). Andr, Tpl and the positive control (Ptx) induced similar morphological changes in CIS-A2780 and OVCAR-8 cells. Furthermore, there was no noticeable difference in the morphological changes induced by Andr and Tpl at the different concentrations and time point. However, the morphological changes induced by Ptx increased with concentration in OVCAR-4.

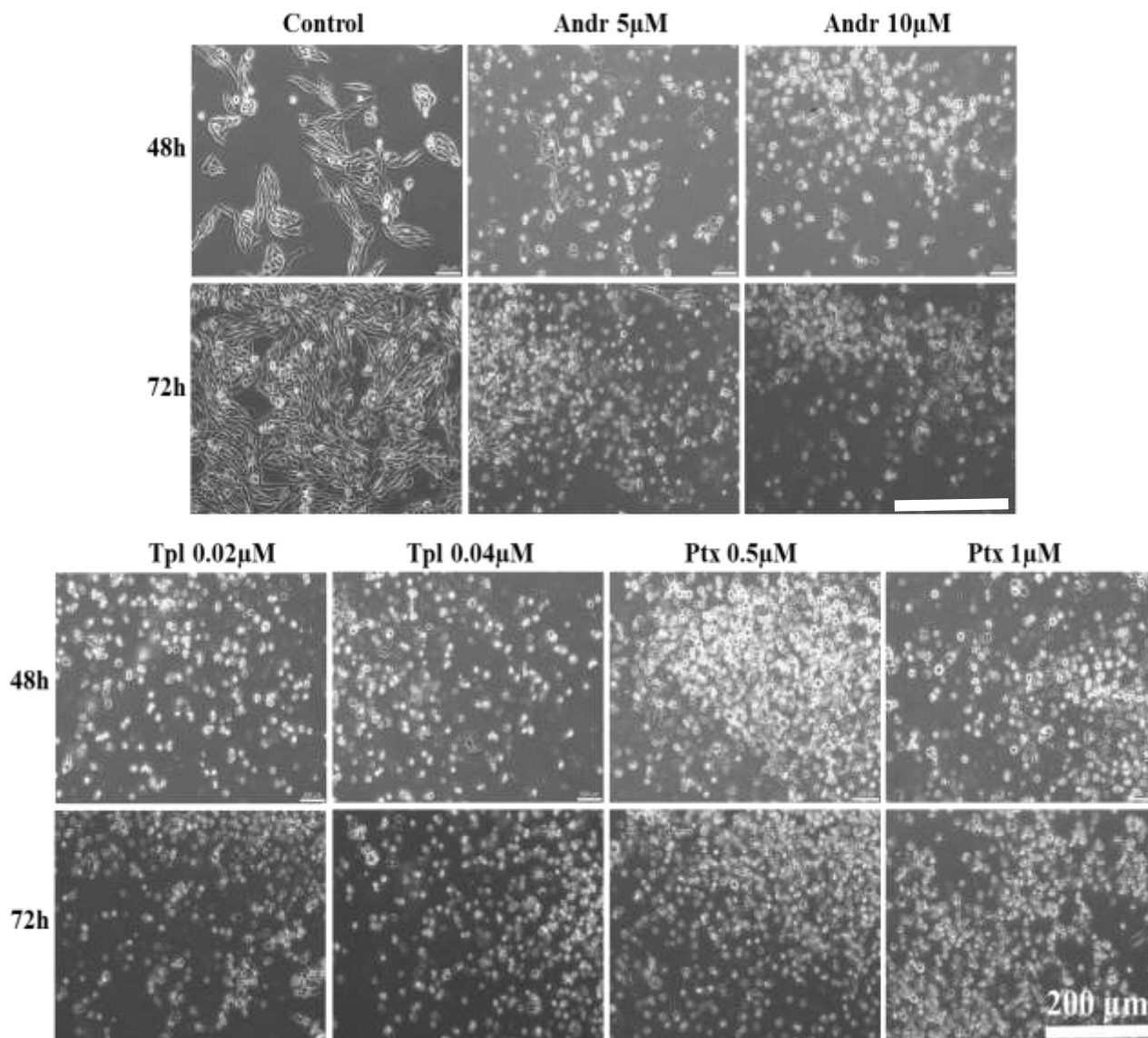


**Figure 4. 3: Effects of Andr and Tpl on the morphology of CIS-A2780 ovarian cancer cell line at time (48 and 72 h) and concentration dependent manner using light microscopy.** Ptx was used as positive control and negative control contains 0.1% DMSO in growth media. Images were taken with X10 objective lens on 200μm scale.

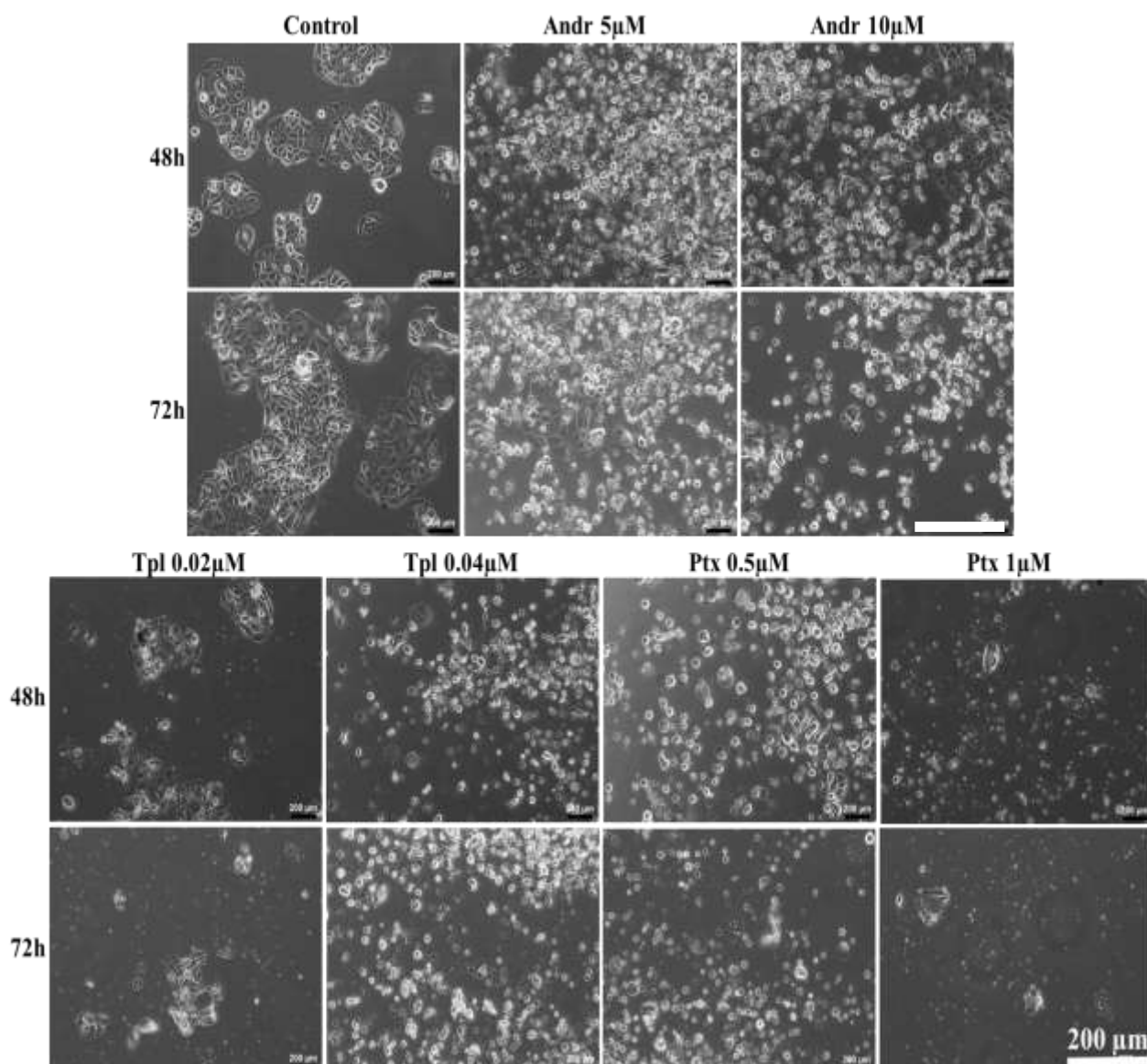


**Figure 4. 4: Morphological effects of Andr and Tpl on OVCAR-4 ovarian cancer cell line at time (48 and 72 hours) and concentration dependent manner using light microscopy. Ptx was used as positive control and negative control was treated with media containing 0.1% DMSO. Images were taken with X10 objective lens on 200µm scale.**

#### **4.2.4 Staining of the nuclear and actin structure of ovarian cancer cell line for apoptosis evaluation using fluorescence microscopy**

Morphological changes in the cell nuclear and actin filament structures are clear features of apoptosis. Evaluation of the morphological changes in these cellular structures could be used to investigate the apoptotic activities of tested drugs. Therefore, the effect of Andr and Tpl on the nuclear and actin arrangement of the cell was evaluated using fluorescence microscopy. In brief,  $2 \times 10^4$  CIS-A2780 and OVCAR-8 cells were exposed to different concentration of Andr (5 and 10  $\mu\text{M}$ ), and Tpl at 0.02 and 0.04  $\mu\text{M}$  for 48 and 72 h before staining with DAPI and actinRed<sup>TM</sup> 555 and imaged with fluorescence microscopy using 40x objective lens. Apoptotic features such as small and fragmented nuclei, condensed chromatin and high fluorescence intensity were observed in cells treated with Andr and Tpl in CIS-A2780 and OVCAR-8 cells (Figures 4.5 and 4.6). Tpl and Ptx induced more of these morphological changes than Andr in OVCAR-8 cells (Figure 4.6). The apoptotic features induced by Andr and Tpl slightly increased with concentration but no time dependent activity was observed. Andr, Tpl and Ptx affected the capacity of the actin filament to form a network at the different time points compared with the control in CIS-A2780 cells (Figure 4.5). Furthermore, Ptx reduced the capacity of the actin filament to form a network which was prominent at both 48 and 72 h in OVCAR-8. However, no major change was observed in the migration of the filament in cells treated with Andr and Tpl.

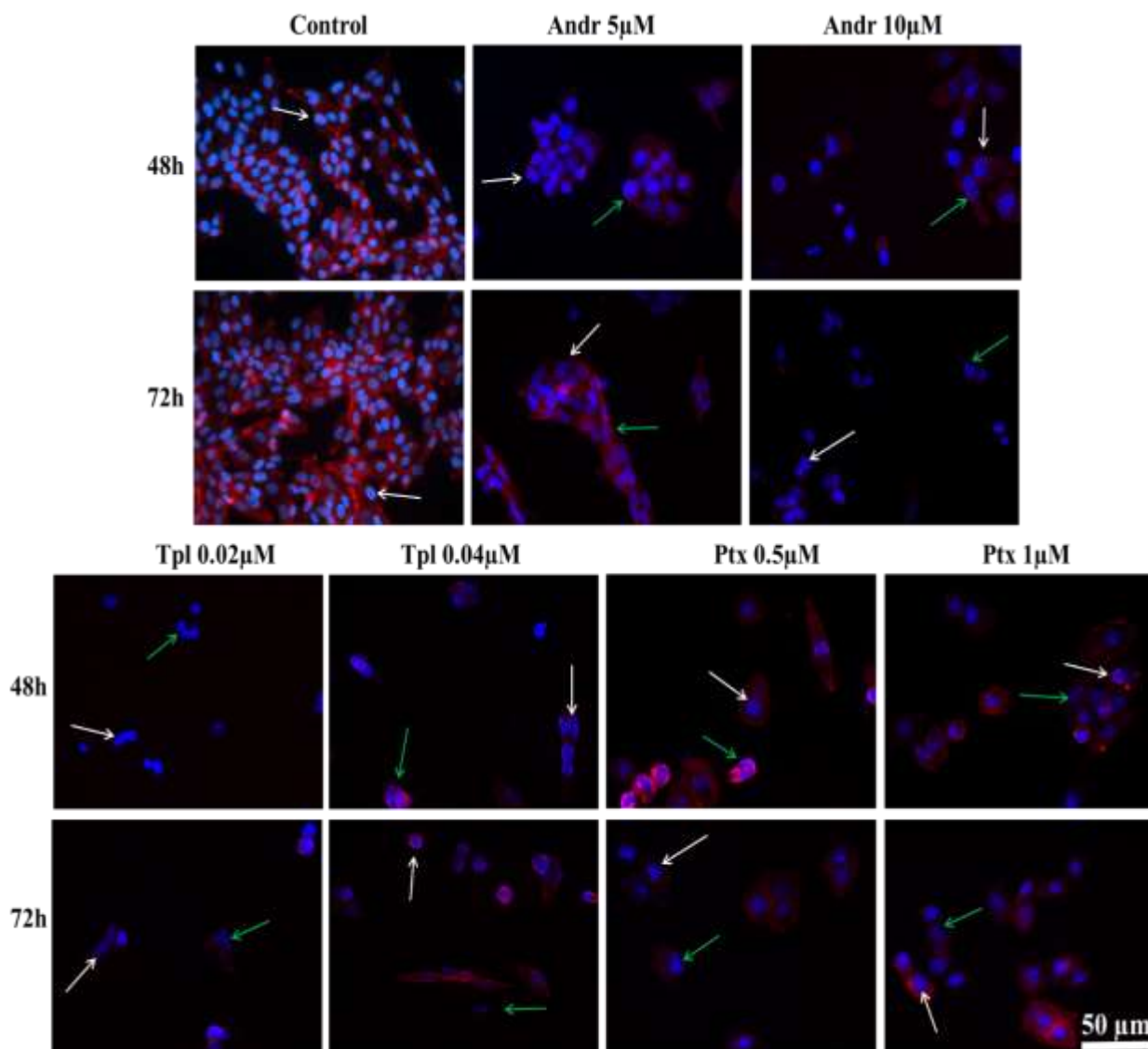


**Figure 4. 5: Morphological changes in the nuclear and actin filament of CIS-A2780 cells in response to treatment with Andr, Tpl and Ptx using fluorescence microscopy.** Images were taking with 40x objective lens. cells were co-stained with DAPI (blue) and actinRed™ 555 (red) for nuclear and actin filament changes respectively. Negative control contains 0.1% of the vehicle (DMSO). White arrows are pointing to viable cell nuclei while green arrows are pointing to apoptotic cell nuclei.

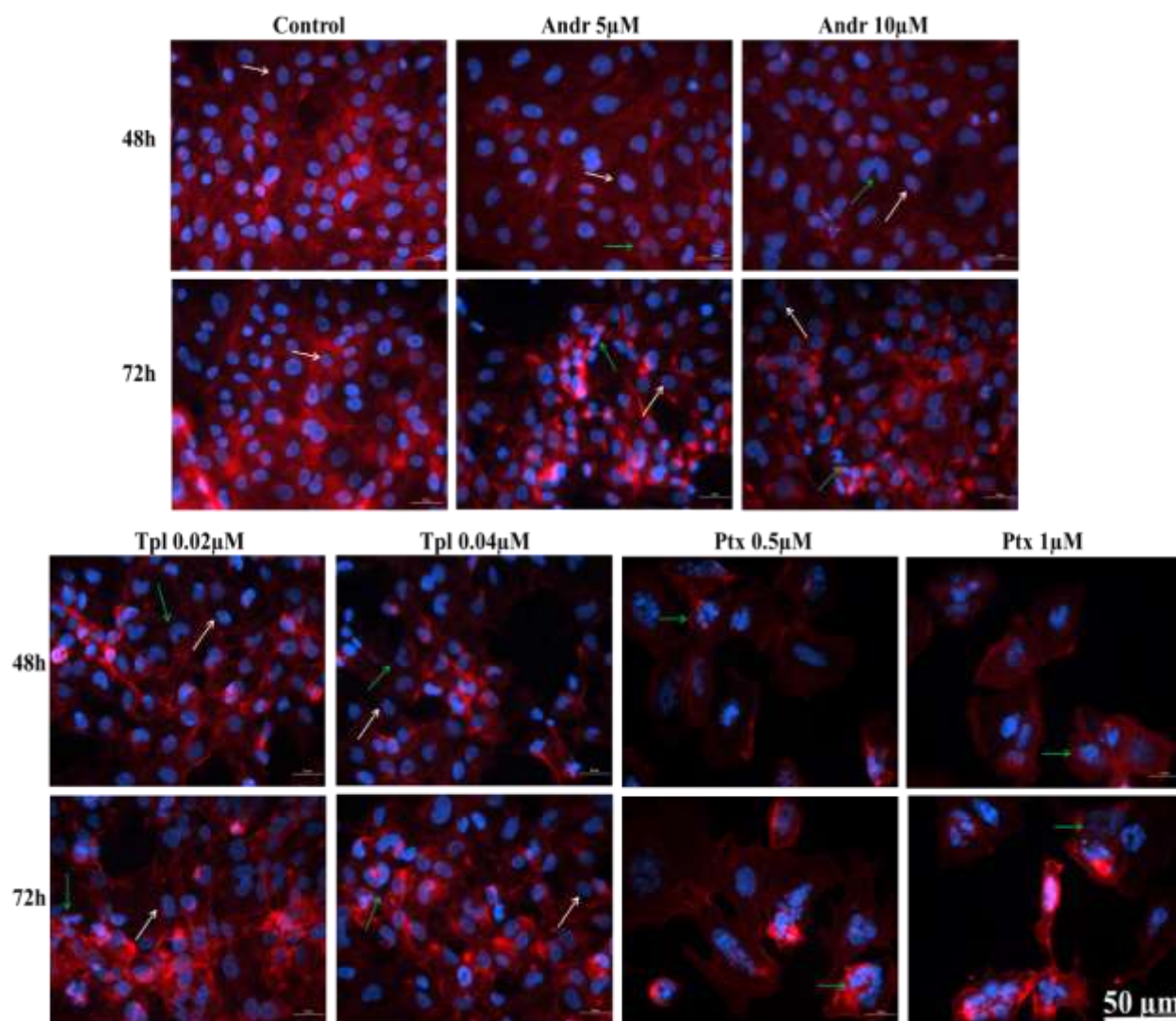


**Figure 4. 6: Morphological effects of Andr, Tpl and Ptx on the nuclear and actin filament of OVCAR-8 using fluorescence microscopy.** OVCAR-8 cells were co-stained with DAPI (blue) and actinRed<sup>TM</sup> 555 (red) for nuclear and actin filament changes respectively. 0.1% DMSO in growth media was used as negative control. White arrows are pointing to viable cell nuclei while green arrows are pointing to apoptotic cell nuclei.

#### **4.2.5 Change in caspase 3/7 activity in response to Andr and Tpl treatment**

Caspase 3/7 is an executioner caspase, the activation of this marker in cells is an indication of apoptosis. The effects of Andr and Tpl on this marker were evaluated on ovarian cancer cell lines (CIS-A2780 and OVCAR-8). The level of activation induced by Andr and Tpl will give an indication that the significant induction of cell death observed above was mainly due apoptosis induction. Concisely,  $5 \times 10^3$  cells treated with two different concentrations of each compound were treated with caspase 3/7 reagents after 48 h post drug treatment. The level of caspase 3/7 activation was quantitatively measured with the plate reader and data normalised with SRB data. The results show that in CIS-A2780 cells, 20  $\mu$ M of Andr caused 6-fold increase in caspase 3/7 activity when compared with the control. However, this was relatively lower than the caspase 3/7 effect of Tpl and Ptx that caused 41 and 67-fold increase respectively (Figure 4.7). The caspase 3/7 activity by Ptx was concentration dependent. But, no concentration dependent caspase 3/7 activity effect was found in CIS-A2780 cells treated with Andr and Tpl (Figure 4.7).

In OVCAR-8 cells, caspase 3/7 activity was increased significantly by Andr and Tpl. Andr and Tpl caused 10 and 12-fold increase respectively. Similarly, the positive control (Ptx) also increased caspase 3/7 activity in OVCAR-8 by 15-fold. The change in caspase 3/7 activity in response to Andr was concentration dependent, while no concentration dependent activity was observed in Tpl and Ptx treated cells (Figure 4.7). Furthermore, the caspase 3/7 activity effect of Ptx was slightly higher than the caspase 3/7 activity by Tpl. Andr had the least effect on caspase 3/7 activity in OVCAR-8 cells. The effects of Andr, tpl and Ptx on caspase 3/7 activity was consistent with their cytotoxic activity. The results suggest that the cytotoxic activity of Andr and Tpl was mainly through induction of apoptosis.

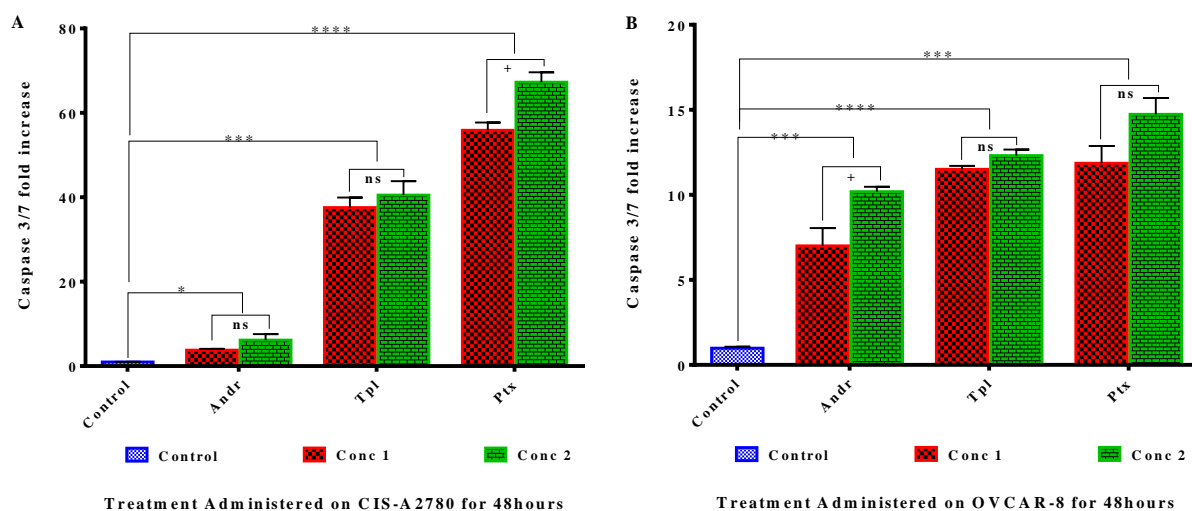


**Figure 4. 7: Change in caspase 3/7 activity in response to Andr and Tpl on ovarian cancer cell lines: CIS-A2780 (A) and OVCAR-8 (B) for 48 hours.** Paclitaxel (Ptx) was used as positive control at 0.5 and 1.0 $\mu$ M. While Conc 1 and 2 for Andr and Tpl are 10 and 20 $\mu$ M, and 0.02 and 0.04 $\mu$ M respectively. Caspase 3/7 activity of the control and the compounds were compared using one-way ANOVA, and the significant level denoted with asterisk (\*), (\* $p$  < 0.05, \*\* $p$  < 0.01, \*\*\* $p$  < 0.001 and \*\*\*\* $p$  < 0.0001) while concentration dependent activity was analysed with t-test, and significant level denoted with plus (+), (+ $p$  < 0.05).

#### 4.2.6 Caspase 8 Activity effect of Andr and Tpl as marker of extrinsic pathway

The caspase 8 activity of Andr and Tpl as an initiator caspase was evaluated to determine their possible pathway of apoptosis. Caspase 8 activity of Andr and Tpl was measured on ovarian cancer cell lines (CIS-A2780 and OVCAR-8) after 48 h post-treatment. The data collected were normalised with SRB data, generated from cells treated under the same condition. In CIS-A2780 cell line, the result shows that Andr and Tpl significantly increased caspase 8 activity by approximately 4 and 35-fold respectively. The positive control (Ptx) also increased caspase 8 activity by 7-fold. The caspase 8 activity effect of Andr and Tpl was concentration dependent (Figure 4.8). Furthermore, multiple comparisons test showed

that the caspase 8 activity by Andr and Tpl were significant at each concentration when compared with the control. However, the caspase 8 activity effect of Ptx was not concentration dependent. Tpl had more effect on caspase 8 activity than Andr and the positive control (Ptx).

Andr and Ptx increased caspase 8 activity in OVCAR-8 by 4-folds, while Tpl slightly increased caspase 8 activity. The caspase 8 activity by Andr was similar to that of Ptx but higher than the caspase 8 activity effect of Tpl. In addition, Tpl showed concentration dependent activity, while no concentration dependent activity was observed in Andr and Ptx treated cells (Figure 4.8). Also, the effect of Andr and Tpl on caspase 8 activity in OVCAR-8 cells was significant at each concentration when compared with the control using Dunnett's multiple comparisons test. These results demonstrated that Andr and Tpl are possibly inducing apoptosis through extrinsic pathway.

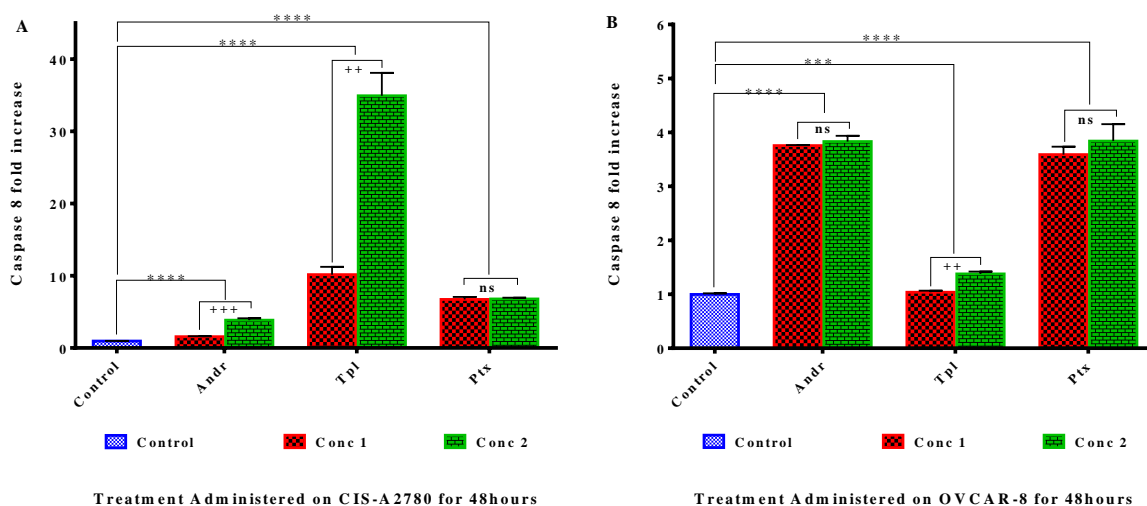


**Figure 4. 8: Caspase 8 activity effect of Andr and Tpl on CIS-A2780 (A) and OVCAR-8 (B) ovarian cancer cell lines.** Ptx was used as positive control. Conc 1 and 2 for Andr and Tpl are 10 and 20 $\mu$ M, and 0.02 and 0.04 $\mu$ M respectively. While they are 0.5 and 1.0 $\mu$ M for Ptx. One-way ANOVA was used to compare the caspase 8 activity of the control with

treated samples, and the significant level denoted with asterisk (\*), while student t-test was used to test for concentration dependent activity, and significant level denoted with plus (+). The significance level at  $p < 0.05$ ,  $p < 0.01$ ,  $p < 0.001$  and  $p < 0.0001$  are represented as (\*), (\*\*), (\*\*\*) and (\*\*\*\*) respectively while no significant different is denoted with (ns).

#### **4.2.7 Effect of Andr and Tpl on caspase 9 activity as marker of intrinsic pathway of apoptosis**

The effect of diterpenoids (Andr and Tpl) was evaluated on caspase 9 to demonstrate their possible apoptotic pathway of activity. The activation of the caspase 9 marker within the cells will suggest if the possible route of apoptosis activity of these compounds was through intrinsic pathway. In this assay, caspase 9 reagent was added to CIS-A2780 and OVCAR-8 cells treated with the tested compounds and the control, and the activation level was measured. In CIS-A2780 cell line Andr and Tpl increased the caspase 9 activity significantly, when each of the compound was compared with the control. Further comparison of each concentration of the tested compound with the control using Dunnett's multiple comparisons test, showed that the caspase 9 activity by Tpl was significant at both concentrations (0.02 and 0.04  $\mu\text{M}$ ), and the activity of Andr was significant at both 10 and 20  $\mu\text{M}$  concentrations. Andr and Tpl caused 5 and 49- fold increase in caspase 9 activity respectively, while Ptx caused 24-fold increase in caspase 9 activity. The caspase 9 activity by Tpl was higher than that of Ptx, while Andr had caused the least effect on caspase 9 activity. Furthermore, the effect of Andr and Tpl on caspase 9 activity was concentration dependent, but no concentration dependent activity was found in the positive control. Also, increase in caspase 9 activity was found in OVCAR-8 cells treated with Andr and Tpl and the increase was significant when compared with the control. Further multiple comparison showed that change in caspase 9 activity in response to Andr was only significant at higher

concentration (20  $\mu\text{M}$ ), while the caspase 9 activity by Tpl was significant at both concentrations (0.02 and 0.04 $\mu\text{M}$ ). Similarly, the positive control (Ptx) also increased caspase 9 activity and this was significant when compared with the control. Tpl and Ptx increased caspase 9 activity by 14 and 11-fold respectively, while Andr increased caspase 9 activity by 4-fold in OVCAR-8 cells. The caspase 9 activity effect of Tpl and Ptx was comparably similar and higher than the change in caspase 9 activity caused by Andr. The caspase 9 activity effect of both Andr and Tpl was concentration dependent, while no concentration dependent activity was found in Ptx (Figure 4.9). These results suggest that the apoptotic inducing activity of Andr and Tpl was mediated through the intrinsic pathway.

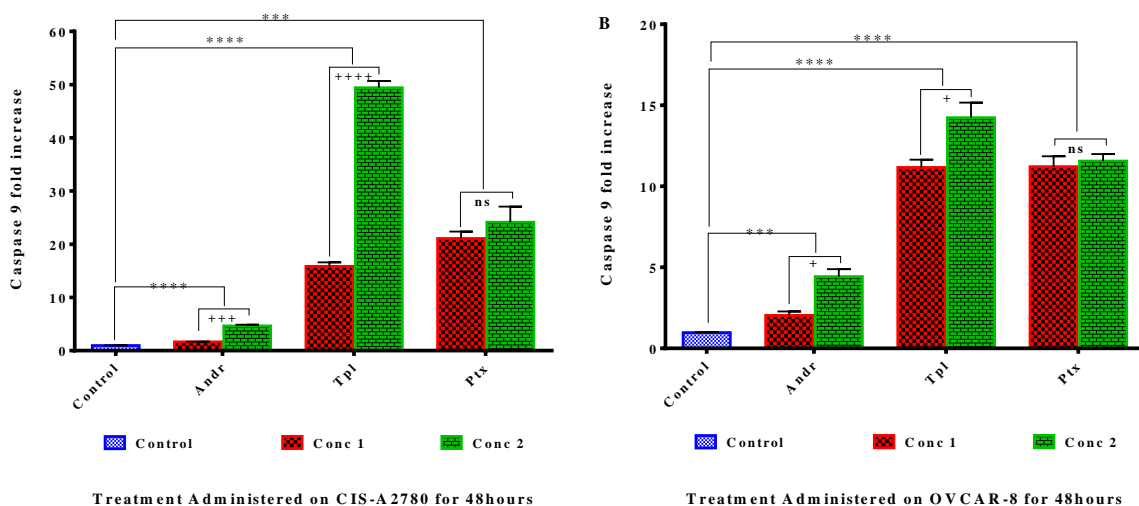


**Figure 4. 9: Effects of Andr and Tpl on caspase 9 activity on ovarian cancer cell lines: CIS-A2780 (A) and OVCAR-8 (B) for 48 hours using Ptx as positive control.** The results were presented as the mean  $\pm$  SD (n=3). Conc 1 and 2 for Andr and Tpl are 10 and 20 $\mu\text{M}$ , and 0.02 and 0.04 $\mu\text{M}$  respectively. While they are 0.5 and 1.0 $\mu\text{M}$  for Ptx. Caspase 9 activity of the control was compared with the activity of each compound using one-way ANOVA, and the significant level denoted with asterisk (\*), student t-test was used to test for concentration dependent activity, and the significant level was represented with plus (+). While insignificant activity was denoted with (ns).

#### **4.2.8 Analysis of apoptosis using annexin V and propidium iodide**

The proapoptotic activity of Andr and Tpl was further evaluated using annexin V and propidium followed by flow cytometry analysis. Ovarian cancer cells (CIS-A2780 and OVCAR-8) were treated with two concentrations of each compound for 48 h, after which the cell pellets were prepared and treated with annexin V and propidium iodide (PI), and further analysed with flow cytometry (Figures 4.10 and 4.11). In CIS-A2780 cell line, Andr significantly induced apoptosis when compared with the control. The apoptotic activity of Tpl was also significant (Figure 4.12). Additionally, multiple comparison of each concentration of the tested compounds with the control showed that the apoptotic activities of Andr was only significant at higher concentration (10  $\mu$ M), while the apoptotic activities of Tpl was significant at both concentrations (0.02 and 0.04  $\mu$ M). The percentage of early and late apoptosis induced by Tpl at both 0.02  $\mu$ M (23% and 23.1%) and 0.04  $\mu$ M (32.1% and 22.6%) respectively were higher than the early and late apoptosis induced by Andr at 5  $\mu$ M (9.5% and 7.9%) and 10  $\mu$ M (24.21 % and 16.3%). However, the positive control (Ptx) induced higher early and late apoptosis at both 0.5  $\mu$ M (16.98% and 59.7%) and 1.0  $\mu$ M (18.1% and 67.2%). The percentage of apoptosis induced by Ptx was further significant to the control. Furthermore, the percentage of apoptosis induced by Andr was concentration dependent, while no concentration dependent activity was found in Tpl and Ptx.

In OVCAR-8 cell line, the percentage of apoptosis induced by Andr and Tpl was significant at  $p < 0.0001$  when compared with the control. While the apoptotic activity of Ptx was significant (Figure 4.12). In addition, the percentage of apoptosis induced by Andr and Tpl at the different concentrations were all significant with the control using multiple comparison test. Also, the percentage of early and late apoptosis induced by Andr at 5  $\mu$ M (42.3% and 21.2%) and 10  $\mu$ M (40.3% and 36.0%) was slightly lower compared with Tpl

at both 0.02  $\mu\text{M}$  (44.4% and 34.0%) and 0.04  $\mu\text{M}$  (30.6% and 60.4%) and Ptx at both 0.5  $\mu\text{M}$  (9.7% and 84.5%) and 1.0  $\mu\text{M}$  (9.9% and 85.2%). However, the percentage of apoptosis induced by Andr, Tpl and Ptx were not concentration dependent.

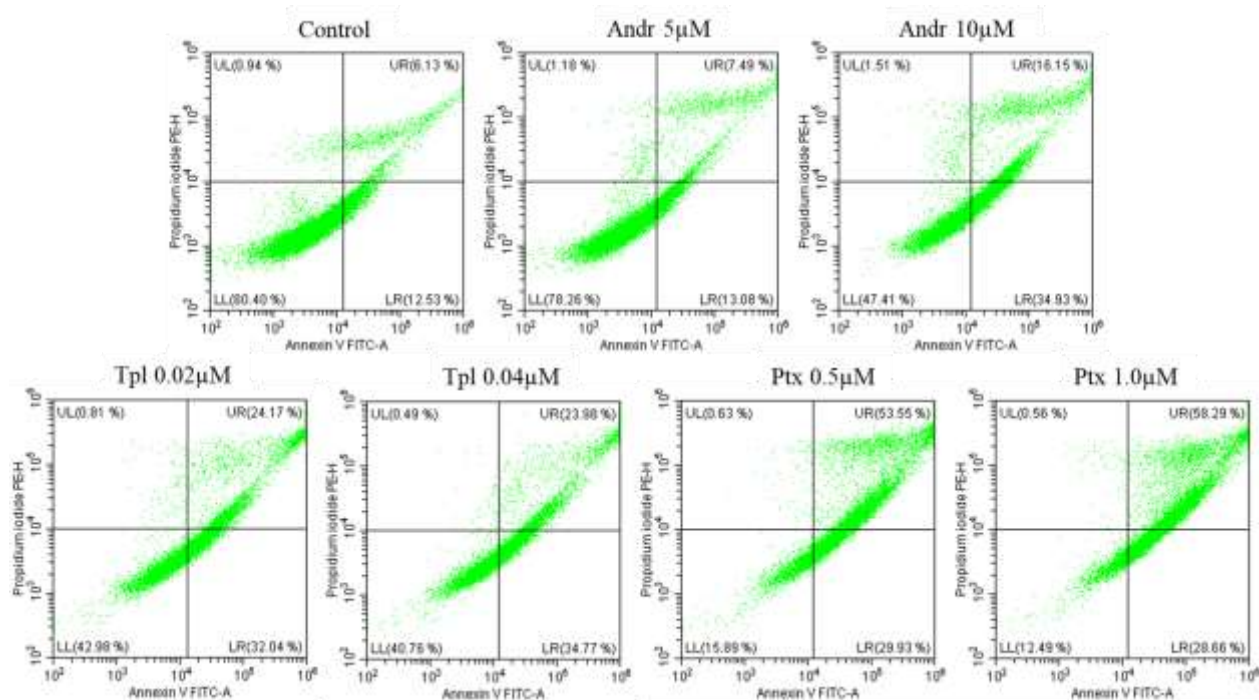


**Figure 4. 10: Representative samples of the flow cytometry graph of CIS-A2780 cell line treated with diterpenoids (Andr and Tpl) and the positive control (Ptx) at two different concentrations. LL, UL, LR and UR represent live cells, necrotic cells, cells in early apoptosis and cells in late apoptosis respectively.**

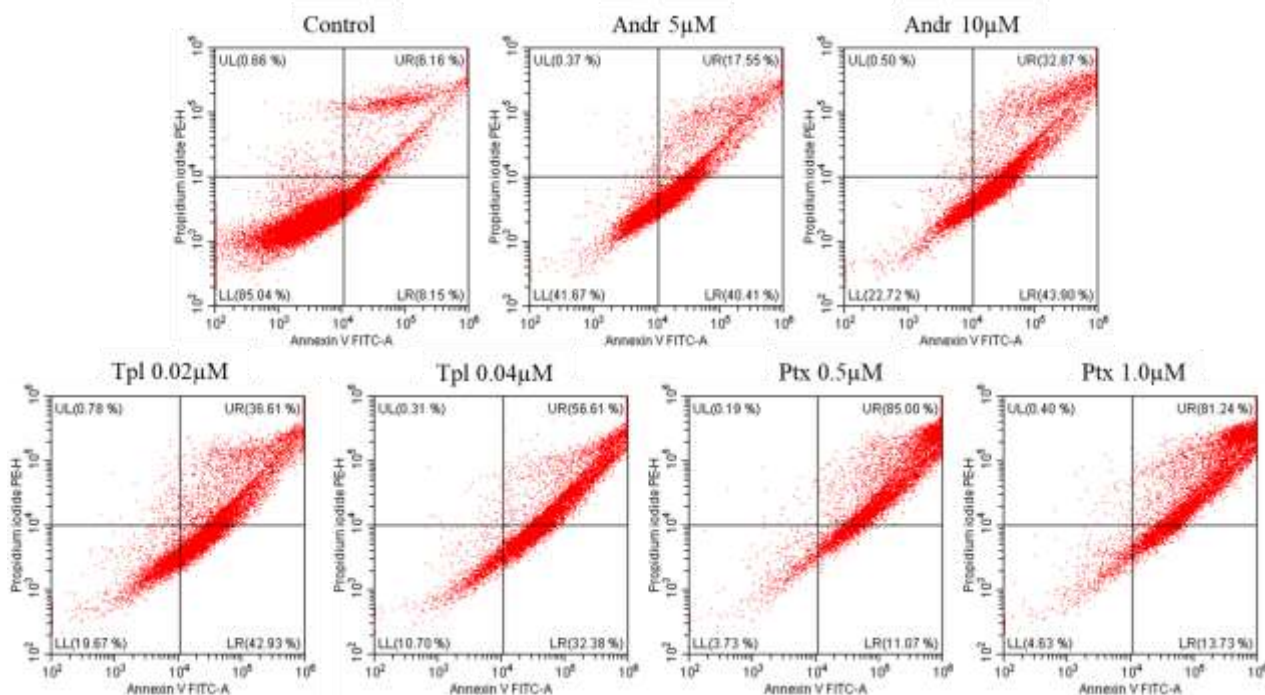


**Figure 4. 11: Representative samples of the flow cytometry graph of OVCAR-8 cell line treated with diterpenoids (Andr and Tpl) and the positive control (Ptx) at two different concentrations. LL, UL, LR and UR represent live cells, necrotic cells, cells in early apoptosis and cells in late apoptosis respectively.**

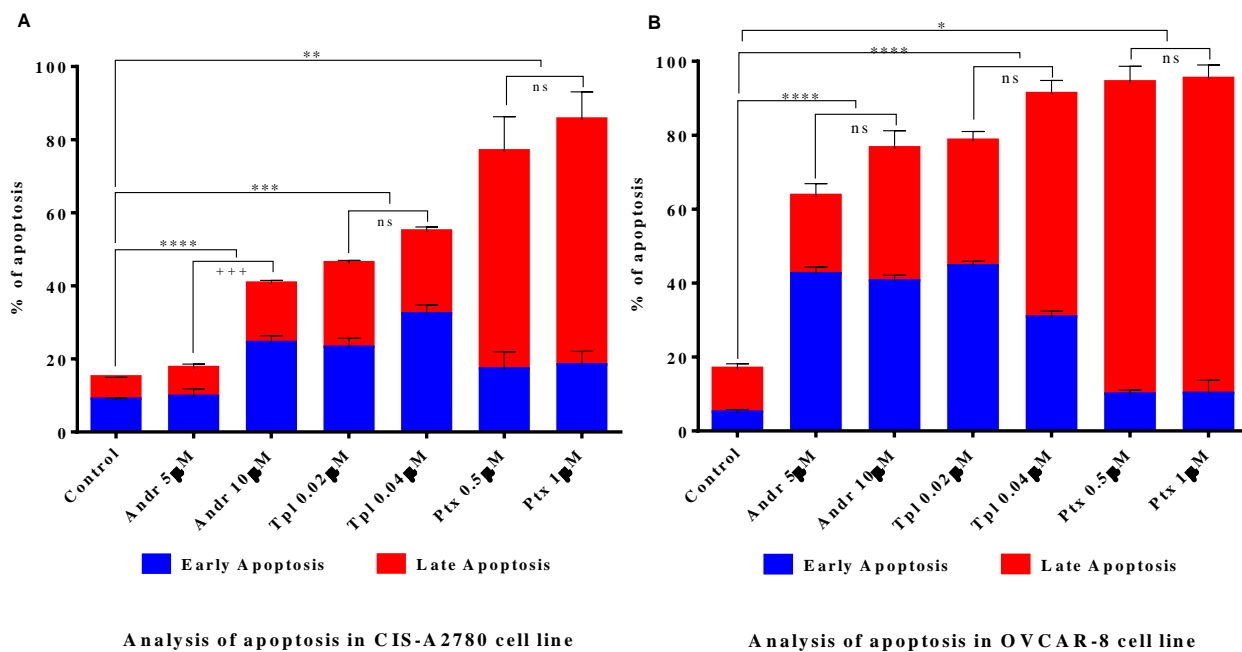


**Figure 4. 12: Flow cytometry analysis of the apoptotic activity of diterpenoids (Andr and Tpl) and positive control (Ptx) in CIS-A2780 cells (A) and OVCAR-8 using annexin V and propidium iodide staining.** The data represent the mean  $\pm$  SD (n=3). The apoptotic activity of each compounds was compared with the control using one-way ANOVA with Dunnett's multiple comparisons test. The ANOVA significant level is denoted with asterisk (\*). Student t-test was used to test for concentration dependent activity, and the significant level is denoted with plus (+). The significance level at  $p < 0.05$ ,  $p < 0.01$ ,  $p < 0.001$  and  $p < 0.0001$  are represented as (\*), (\*\*), (\*\*\*) and (\*\*\*\*) respectively while no significant different is denoted with (ns). Similar pattern was followed for significant difference within concentrations of the same compound.

#### **4.2.9 Effect of Andr and Tpl on mitochondrial membrane potential activity**

The mitochondrial potential activity of Andr and Tpl could further be used to investigate whether their apoptosis induction activity was initiated through the intrinsic pathway. This was evaluated using mitoprobe <sup>TM</sup> DiIC1(5) assay. To put it briefly, CIS-A2780 ovarian cancer cell line was treated at a density of  $2 \times 10^5$  with different concentrations of Andr and Tpl, while Ptx was used as positive. After 48 h post-treatment, the cell pellets were treated with mitoprobe <sup>TM</sup> DiIC1(5) reagents before flow cytometry analysis (Figure 4.13). The result reveals that Tpl disrupted the mitochondrial potential membrane of the cells when compared with the control, it significantly decrease the intactness and activeness of the cell mitochondrial membrane by decreasing the uptake of DiIC1(5) to 61.5 and 58.4% at 0.02 and 0.04  $\mu\text{M}$  respectively (Figure 4.13). In contrast, Andr does not caused significant changes to the mitochondrial membrane potential of the cell. However, there was slight decrease (86.6% (5  $\mu\text{M}$ ) and 81.9% (10  $\mu\text{M}$ )) in the intensity of DiIC1(5) accumulated in the cells compared with the control (89.2%). The positive control (Ptx) also significantly decreased the intensity of DiIC1(5) accumulation in the cell to 39.1% and 34.6% at 0.5 and 1  $\mu\text{M}$  respectively. The mitochondrial membrane potential activity of the positive control was significant when compared with the control. The mitochondrial potential activity of the positive control (Ptx) was higher than the activity of Tpl. Furthermore, no concentration dependent activity was found in the mitochondrial potential activity of Andr, Tpl and the positive control (Ptx). This result demonstrates that the apoptotic activity of Tpl through intrinsic pathway could be mediated through the release of cytochrome *c* into the cell cytoplasm that further activates down stream of apoptosis.

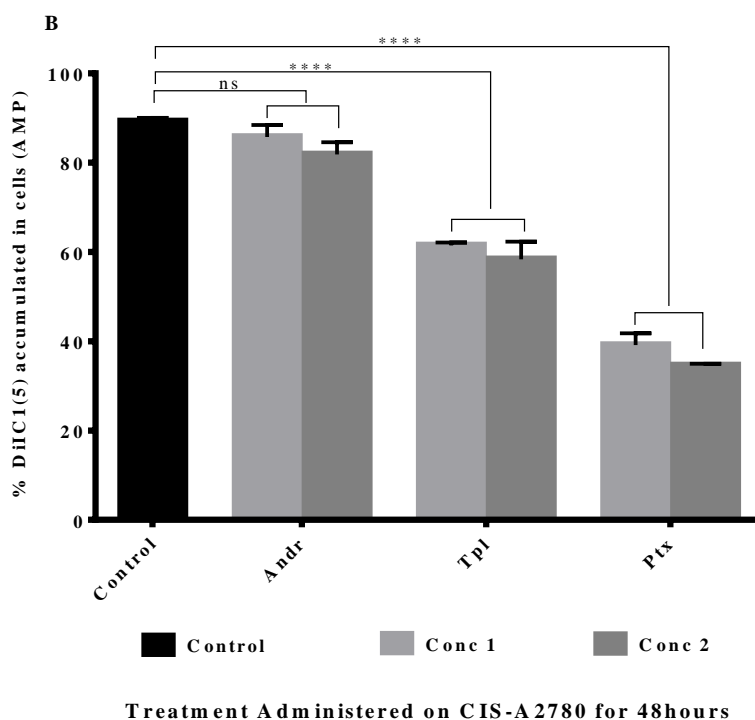
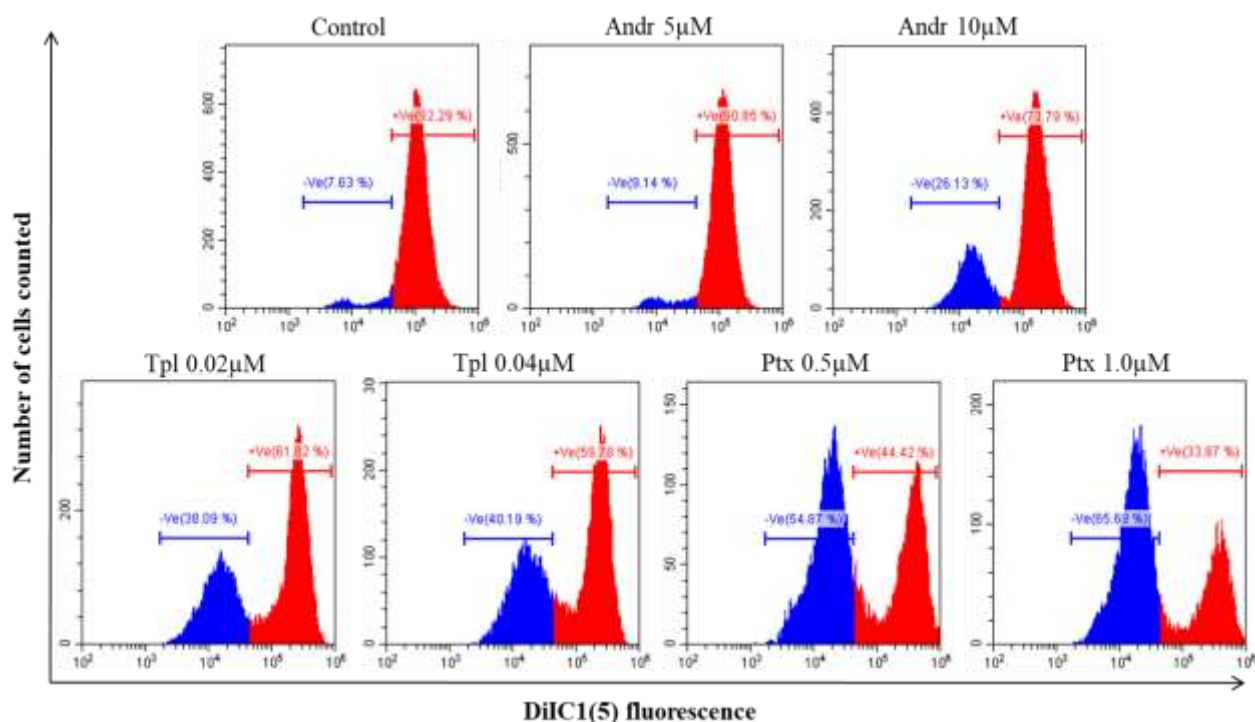


**Figure 4. 13: Effect of Andr and Tpl on the mitochondrial membrane potential activity in CIS-A2780 ovarian cancer cell line.** Representative samples of flow cytometry graph for each treatment condition and untreated cells (A) and the percentage of accumulated

DiIC1(5) intensity in histograms (B). Data were presented as the mean  $\pm$  SD (n=3). The intensity of accumulated DiIC1(5) stain (intact mitochondrial membrane potential) is represented with the red histogram, while the blue histogram represents reduction in the DiIC1(5) accumulated within the cell (disrupted mitochondrial membrane potential). 0.5 and 1  $\mu$ M Ptx was used as positive control, while the negative control contains 0.1% DMSO. For Andr, conc 1 and 2 are 5 and 10 $\mu$ M respectively, while conc 1 and 2 are (0.02 and 0.04  $\mu$ M) for Tpl. One-way ANOVA was used to compare the mitochondrial membrane potential activity of each compound with the control. The significance level at  $p < 0.0001$  is represented as (\*\*\*\*), while no significant different is denoted with (ns).

#### **4.2.10 Effect of Andr and Tpl on cell cycle**

The effect of diterpenoids (Andr and Tpl) on the cell cycle of ovarian cancer was evaluated using propidium iodide stain. CIS-A2780 and OVCAR-8 cells were treated with different concentrations of these compounds for 48hrs to evaluate the early effects on the compounds on cell cycle. After the 48hrs treatment, cell pellets collected were fixed and treated with propidium iodide before the cell cycle was analysed with flow cytometry (Figures 4.14). In CIS-A2780 cell line, the results indicate that 5 and 10  $\mu$ M of Andr significantly reduced the number of cells (68.6% and 67.8% respectively) in the G<sub>0</sub>-G<sub>1</sub> phase when compared with the control (75.1%), and significantly caused cell cycle arrest at S phase, the percentage of cells in the S phase increased to 11.1% and 12.1% compared with the control (7.9%). Furthermore, Andr significantly increased the percentage of cells in the subG<sub>1</sub> phase (Figure 4.15). Also, 0.02 and 0.04  $\mu$ M of Tpl significantly increased cells in the subG<sub>1</sub> phase (22.5% and 18.5%) respectively, reduced the number of cells in the G<sub>0</sub>-G<sub>1</sub> phase (47.0% and 46.7%) respectively, and subsequently caused increased and arrested cells at S (18.9 and 19.5%) and G<sub>2</sub>-M (12.2 and 15.9%) phases. Multiple comparison test further showed that the cell

cycle arrest activity of Andr and Tpl was significant at both concentrations (Figure 4.15). The positive control (Ptx) at 0.5 and 1  $\mu$ M also caused cell cycle arrest at S (26.0% and 23.5%), G<sub>2</sub>-M (45.5% and 39.3%) phases and increased cells in the subG<sub>1</sub> phase (15.1% and 15.0%).

Also, in OVCAR-8 cells, the percentage distribution of cells in the cell cycles phases of the negative control are: subG<sub>1</sub> (1.0%), G<sub>0</sub>-G<sub>1</sub> (78.1%), S (7.2%) and G<sub>2</sub>-M (14.3%). The number of cells in the G<sub>0</sub>-G<sub>1</sub> phase was significantly reduced by Andr (60.0% (5  $\mu$ M) and 51.5% (10  $\mu$ M). Andr further caused cell cycle arrest at S (14.7% and 15.3%) and G<sub>2</sub>-M (55.9% and 58.6%) phases. The cell cycle arrest activity of Andr was significant at both concentrations (5 and 10  $\mu$ M) (Figure 4.15). 0.02 and 0.04  $\mu$ M of Tpl caused significant reduction in the number of cells in the G<sub>0</sub>-G<sub>1</sub> phase (65.9% and 54.2%) respectively, while cell cycle arrest was observed at G<sub>2</sub>-M phase (19.4% and 31.5%). The positive control (Ptx) also caused cell cycle arrest at S (22.5% and 22.9%) and G<sub>2</sub>-M (55.9% and 58.6%) phases at 0.5 and 1  $\mu$ M respectively, and decreased cells in the G<sub>0</sub>-G<sub>1</sub> phase (19.0% and 16.5%). The positive control (Ptx) showed dominantly G<sub>2</sub>-M phase arrest compared with Andr and Tpl (Figure 4.15). Andr and Tpl increased the percentage of cells in the subG<sub>1</sub> phase (0.7% and 1.7%) and (1.7% and 15.9%) at lower and higher doses respectively. These results further supported why Andr and Tpl showed higher cytotoxic and apoptotic activities.

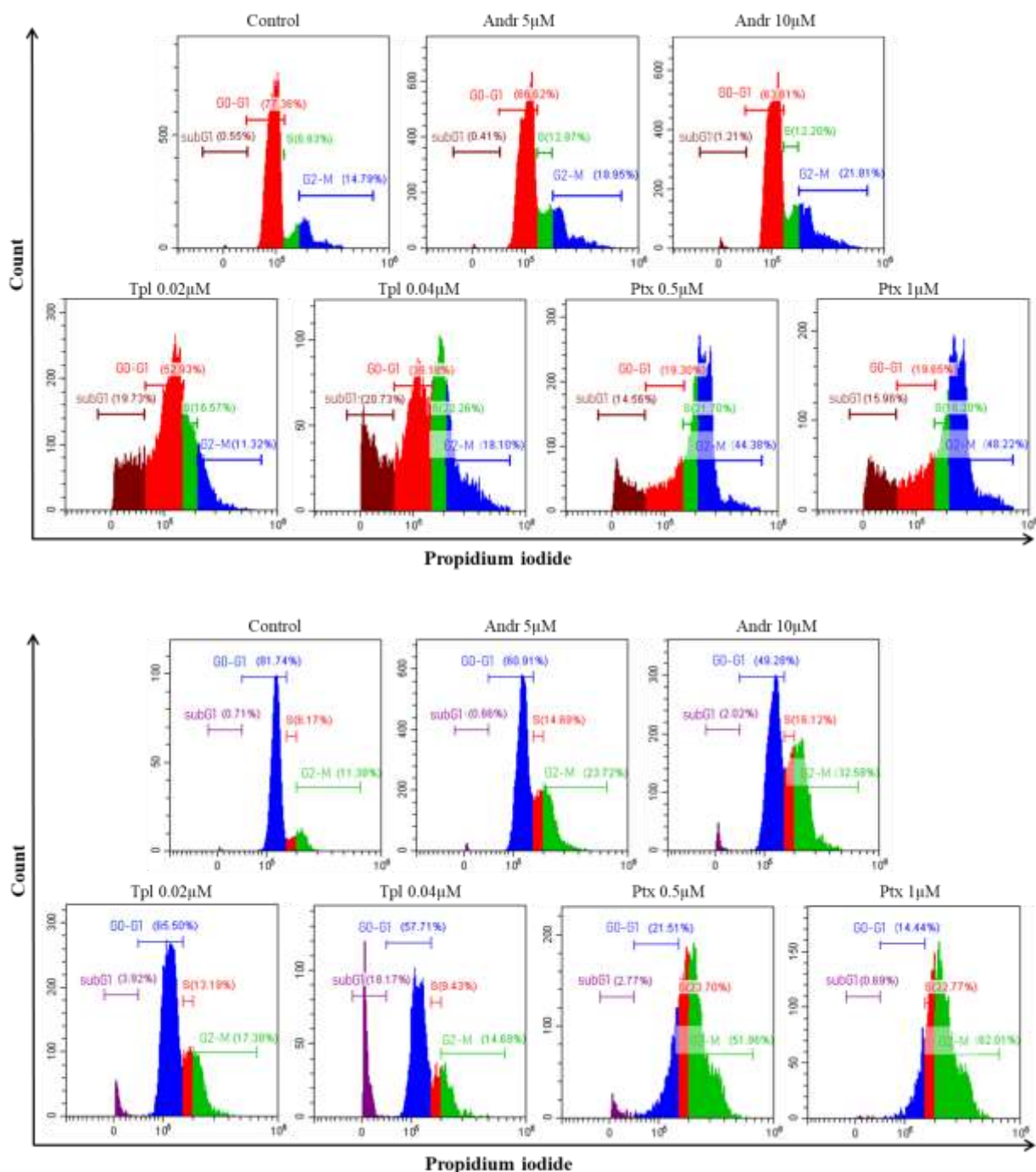
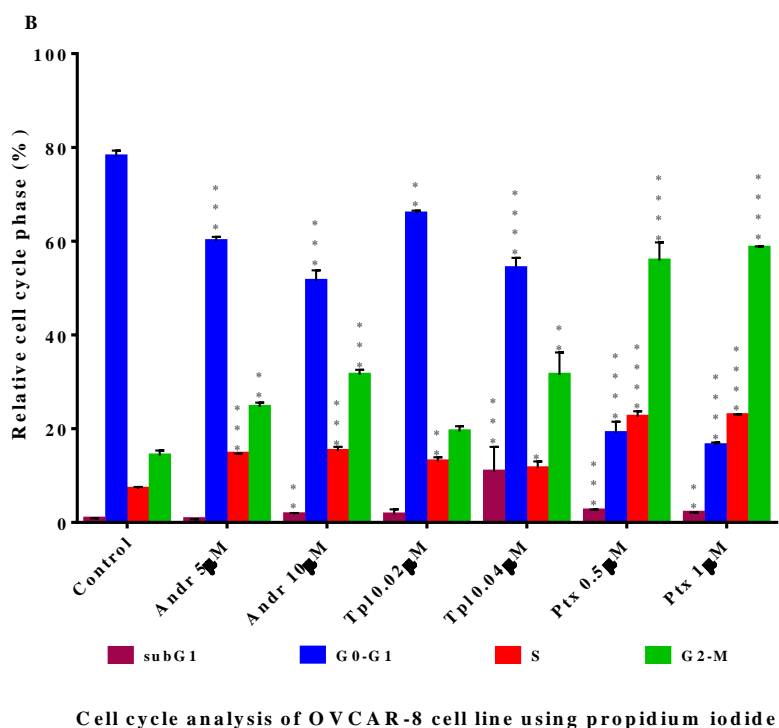
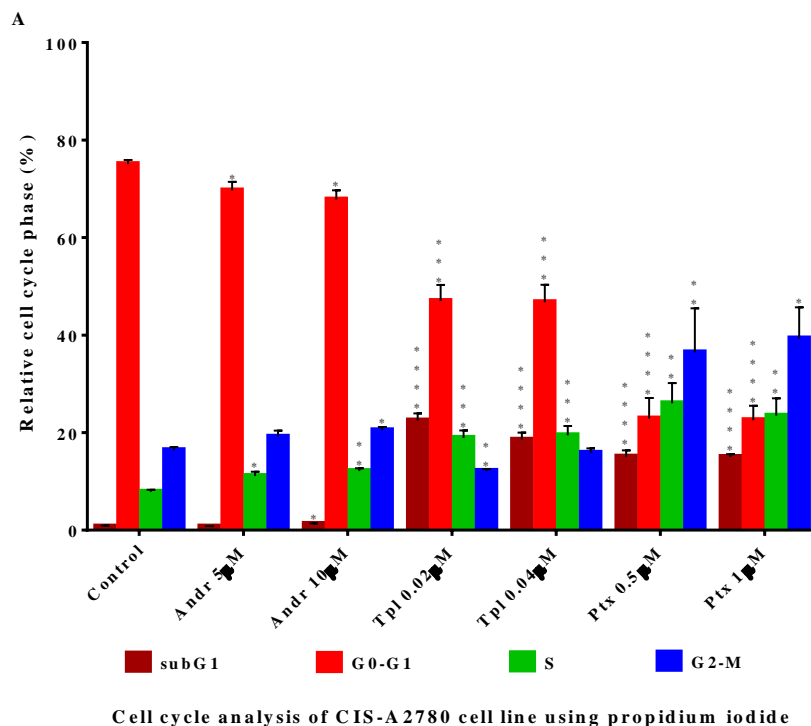


Figure 4. 14: Representative samples of the flow cytometry graph of CIS-A2780 (A) and OVCAR-8 (B) cell lines showing number of cells in each cell cycle phase in response to treatment with diterpenoids (Andr and Tpl) and the positive control (Ptx).



**Figure 4. 15: Cell cycle analysis of CIS-A2780 (A) and OVCAR-8 (B) cell lines in response to treatment with diterpenoids (Andr and Tpl) and positive control (Ptx) using propidium iodide staining.** The data represent the mean  $\pm$  SD of three repeated experiments. The number of cells in each cell cycle phase in compound treatment samples

and control samples were compared using one-way ANOVA and Dunnett's multiple comparisons test. The significance level was denoted with asterisk (\*). While insignificant different is left without any symbol. The significance level at  $p < 0.05$ ,  $p < 0.01$ ,  $p < 0.001$  and  $p < 0.0001$  are represented as (\*), (\*\*), (\*\*\*) and (\*\*\*\*) respectively.

#### **4.2.11 Effect of Andr and Tpl on Global 5-methylcytosine DNA methylation**

The global 5-methylcytosine (5-mC) DNA methylation activity of Andr and Tpl in ovarian cancer cell line (CIS-A2780) was evaluated. Concisely, DNA extracted from CIS-A2780 cells treated with two different concentrations of Andr, Tpl and Aza for 72h was used as template for the quantification of the total 5-methylcytosine DNA methylation using ELISA based kit. The positive control standard curve was generated (Figure 3.27 presented in Chapter 3), and the percentage of 5-methylcytosine was calculated in accordance with the manufactures' guide. The result shows that Andr significantly reduced the percentage of 5-methylcytosine in the CIS-A2780 cell when compared with the control treatment. Furthermore, no major 5-methylcytosine DNA methylation activity was found in cells treated with Tpl. The positive control (Aza) significantly reduced the 5' methylcytosine level in the cancer cell line when compared with the control group (Figure 4.16). The 5-methylcytosine activity of Andr was significantly higher than that of Tpl at  $p < 0.001$  when compared using one-way ANOVA. Furthermore, the 5-methylcytosine activity of Andr and Aza was not concentration dependent.

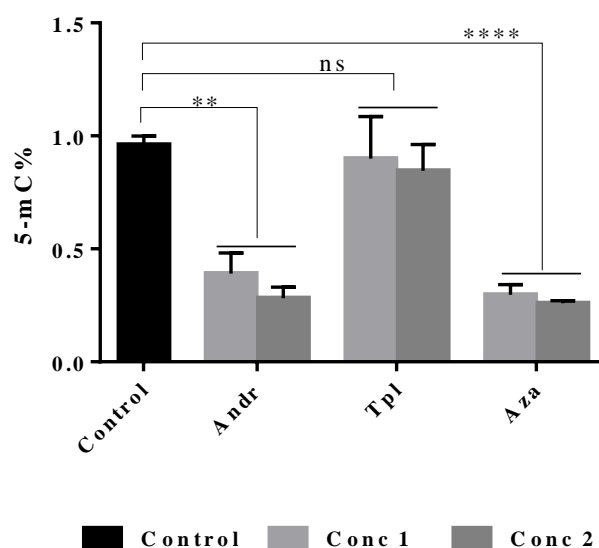


**Figure 4. 16: Percentage of 5-methylcytosine DNA methylation in CIS-A2780 treated with Andr and Tpl, and Aza (positive control).** Conc 1 and 2 are 5 and 10 $\mu$ M respectively for Andr and Aza, and 0.02 and 0.04 for Tpl. The 5-mC % was presented as 5-mC/(5-mC + C). Significant difference between each compound activity compared with the control was analysed using one-way ANOVA and the significant difference at  $p < 0.01$  and  $p < 0.0001$  are denoted with asterisk (\*\* and \*\*\*\*).

#### 4.2.12 Gene specific promoter methylation analysis using pyrosequencing

Methylation of the CpG sites of the promoter region of a gene is known to be a major process towards gene silencing. Therefore, the effects of Andr and Tpl in the demethylation of the CpG sites of specific genes was evaluated using pyrosequencing technique. In this assay, gene specific PCR products of bisulfite converted DNA samples extracted from CIS-A2780 cells treated with different concentration of Andr and Tpl were used as template for pyrosequencing reaction. The data generated were analysed and the percentage CpG methylation of the promoter region of each gene was presented graphically (Figures 4.17 and 4.18). The results demonstrate that Andr does not reduce the methylation level of the CpG site of *MLH1*. However, Tpl caused a slight decrease in the methylation level of *MLH1*

CpG sites but this was not significant ( $p \geq 0.88$ ) when compared with the control. Also, the positive control (Aza) does not induce any significant change in the methylation level of the CpG of *MLH1*. Andr caused demethylation at the CpG region of *HOXA9*, the result was significant when compared with the control. However, Tpl does not decrease the methylation level of the CpG at the promoter region of *HOXA9*. 5-azacytidine significantly caused demethylation to the CpG promoter region of *HOXA9* (Figure 4.19).

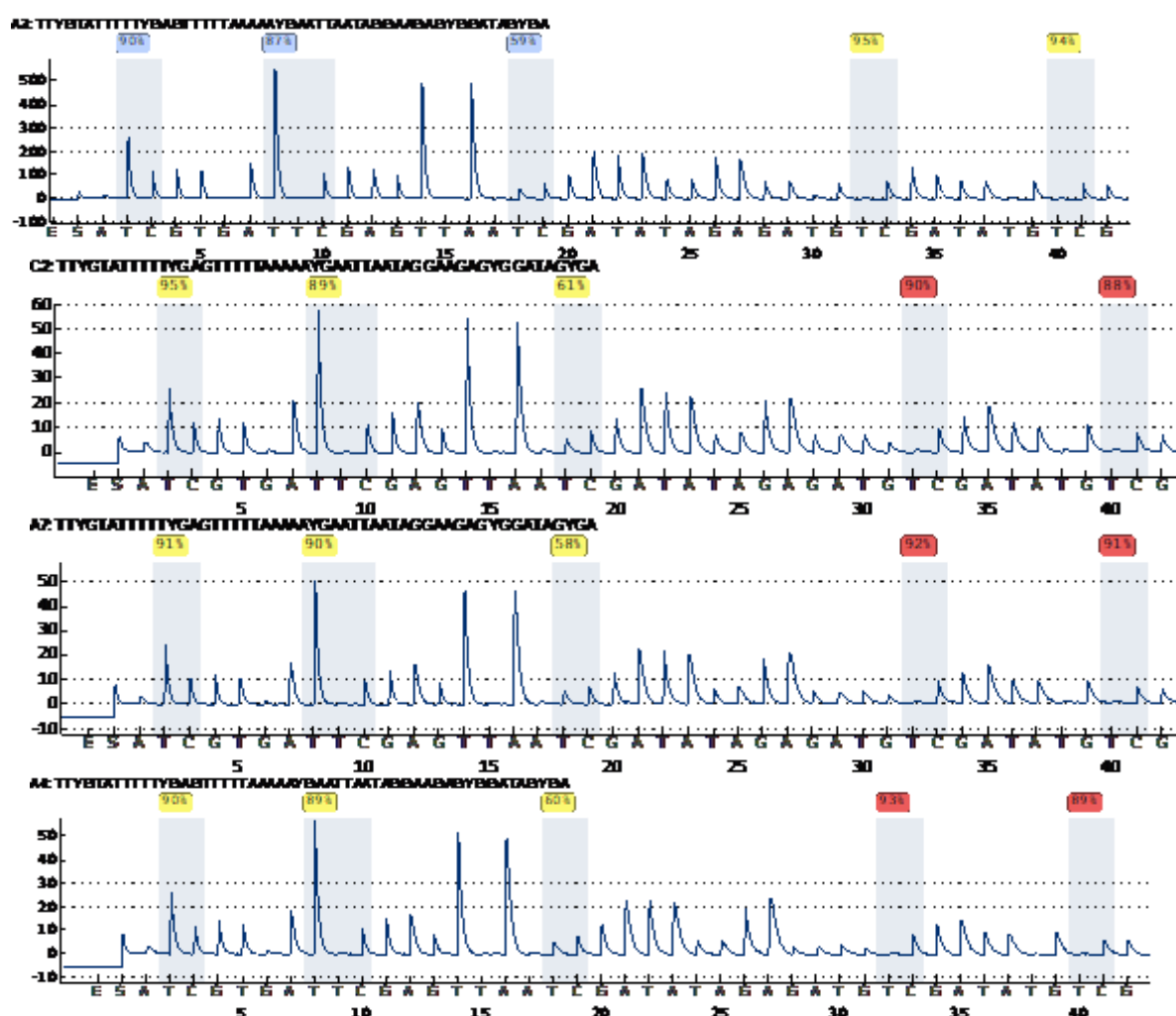


Figure 4. 17: CpG methylation pyrograms of *MLH1* gene in CIS-A2780 cells. Control (A), and Andr (B), Tpl (C) and Aza (D) treated representative samples.

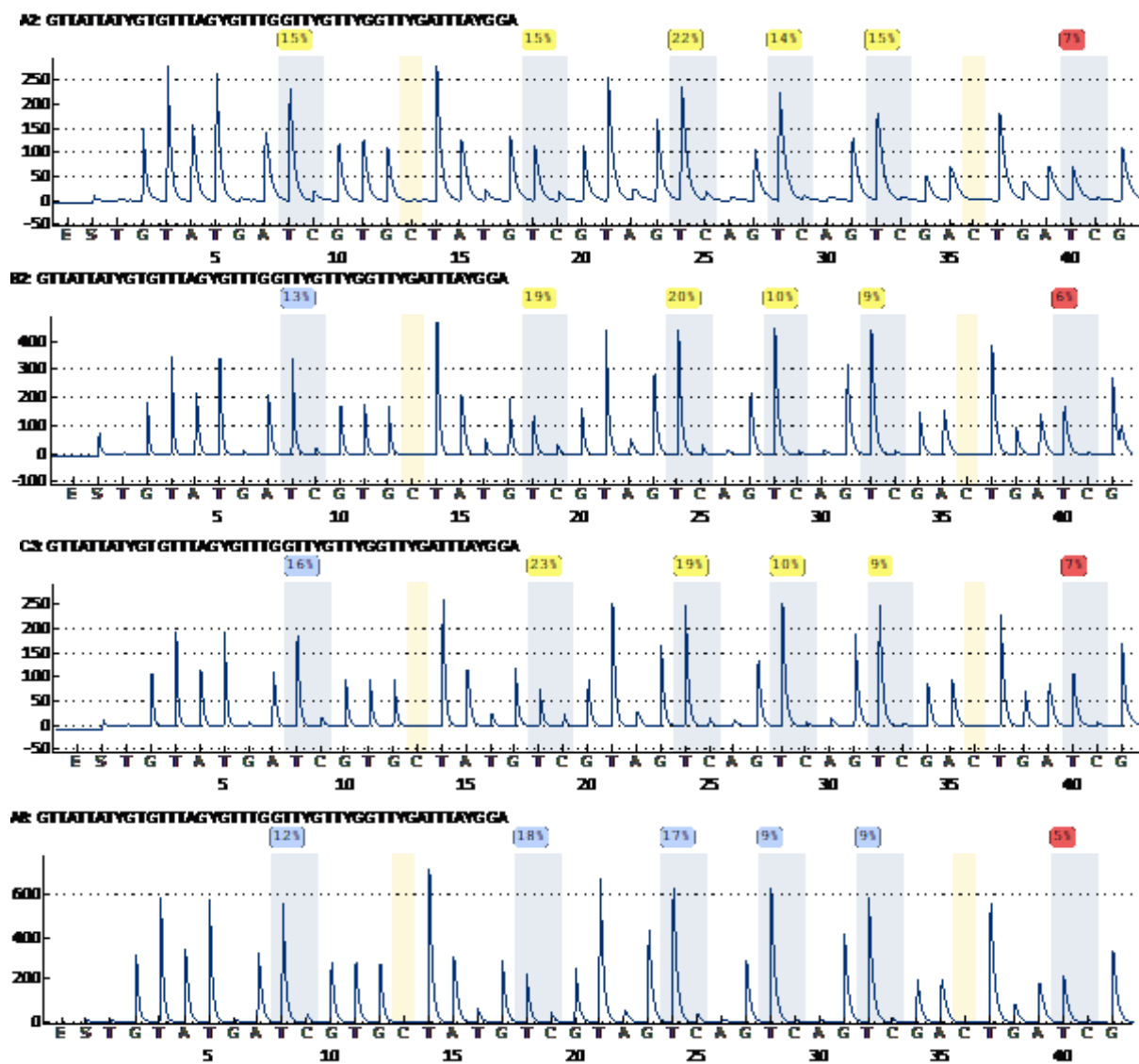
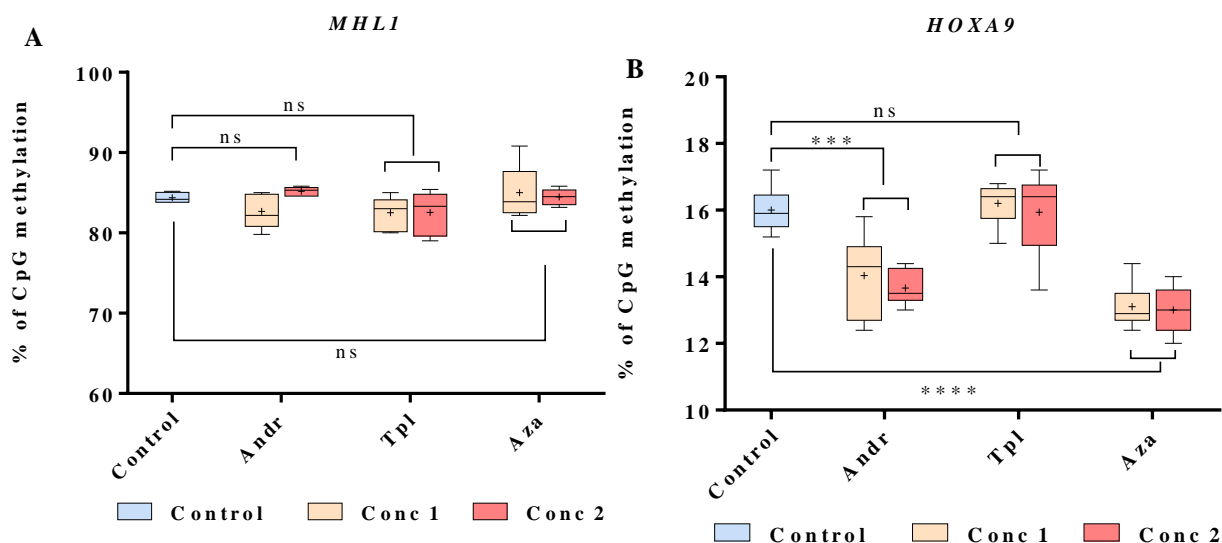


Figure 4. 18: CpG methylation pyrograms of *HOXA9* gene in CIS-A2780 cells. Control (A), and Andr (B), Tpl (C) and Aza (D) treated representative samples.



**Figure 4. 19: CpG methylation analysis of *MLH1* (A) and *HOXA9* (B) genes in CIS-A2780 cell line after treatment with Andr and Tpl. 5’azacytidine as positive control.** Conc 1 and 2 are 5 and 10 $\mu$ M for Andr and Aza, and 0.02 and 0.04  $\mu$ M for Tpl. The data represent the mean  $\pm$  SD (n=3). The percentage CpG methylation activity of each compound was compared with the control and the significant level is denoted with asterisk (\*), (\*\*\* $p$  < 0.001).

#### 4.2.13 Inhibition of DNMT enzymatic activities by Andr and Tpl

The role of diterpenoids (Andr and Tpl) in the inhibition of enzymatic activities of DNMTs which are enzymes that catalyse the addition of methyl group to the cytosine backbone of the DNA was evaluated in this study. Direct inhibition of the activities of these enzymes could be an important mechanism towards DNA demethylation. The DNMT enzyme inhibitory activities of Andr and Tpl were evaluated on the nuclear extracts of CIS-A2780 and OVCAR-4 containing the DNMTs. The results presented in Figure 4.20 show that Tpl and Aza inhibit the DNMT activity in the nuclear extract of CIS-A2780 cell line. No DNMT inhibitory activity was found in the nuclear extracts treated with Andr at both lower and higher concentrations. However, DNMT activity was slightly increased. The DNMT

inhibitory activity of Tpl was slightly higher than that of the positive control (Aza). Furthermore, for OVCAR-4, slight DNMT inhibitory activity was found in cell nuclear extracts treated with Tpl. Although, this does not show any significant different with the control (Figure 4.20). The DNMT inhibitory activity of the positive control (Aza) was more than that of Tpl. Contrastingly, no significant DNMT inhibitory activity was found in Andr.

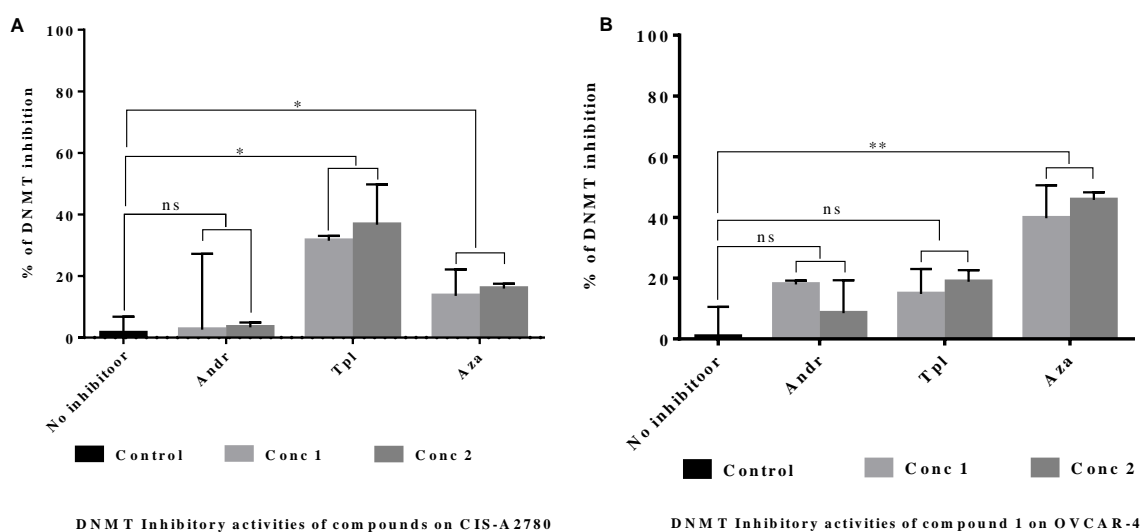


**Figure 4. 20: DNMT inhibitory activities of Andr and Tpl on the nuclear extracts of CIS-A2780 (A) and OVCAR-4 (B) cell lines.** 5’azacytidine was used as positive control and the mean  $\pm$  SD values were presented in histogram. Conc 1 and 2 are 10 and 20 $\mu$ M for Andr and Aza, and 0.02 and 0.04  $\mu$ M for Tpl respectively. The DNMT enzymatic activity of each compound was compared with the control using one-way ANOVA, and the significant difference is denoted with (\*). The significance level at  $p < 0.05$  and  $p < 0.01$  are represented as (\*) and (\*\*) respectively, while no significant different is denoted with (ns).

#### **4.2.14 Gene expression modulatory effects of Andr and Tpl using RT-qPCR**

The effects of Andr and Tpl on the expression of the different types of *DNMT* and tumour suppressor genes was further evaluated using quantifast<sup>®</sup> SYBR green quantitative RT-PCR (qPCR) kit to quantitatively measure the expression level of the various genes. In this procedure, mRNA isolated from the CIS-A2780 cell line treated with different concentrations of Andr and Tpl including Aza was used as starting material. Data were collected in triplicate, and the mRNA expression was calculated with the cycle threshold (Ct) values. *GAPDH* gene was used for normalizing variations in gene expression. The data collected were analysed using one-way ANOVA and graphically presented as mean  $\pm$ SD. The results show that Andr significantly downregulated the expression of *DNMT1* and *DNMT3B*. In a similar manner, Tpl downregulated the expression of *DNMT3A* and *DNMT3B*, while Aza significantly downregulated the expression of *DNMT1* (Figure 4.21). Additionally, Andr further significantly upregulated the expression of *BRCA1*, *MLH1*, *TP53* and *FOLR1*. Similarly, the expression of *TP53* and *FOLR1* was upregulated by Tpl (Figure 4.22). However, *TUSC3* was downregulated by Andr and Tpl. The positive control drug (Aza) significantly upregulated the expression of *MLH1*, *APC* and *FOLR1* and downregulated the expression of *TUSC3* in similar manner with the diterpenoids. Furthermore, Andr, Tpl and the positive control (Aza) up-regulated the expression of *RASSF1* gene, but the result was not significant when compared with the control.

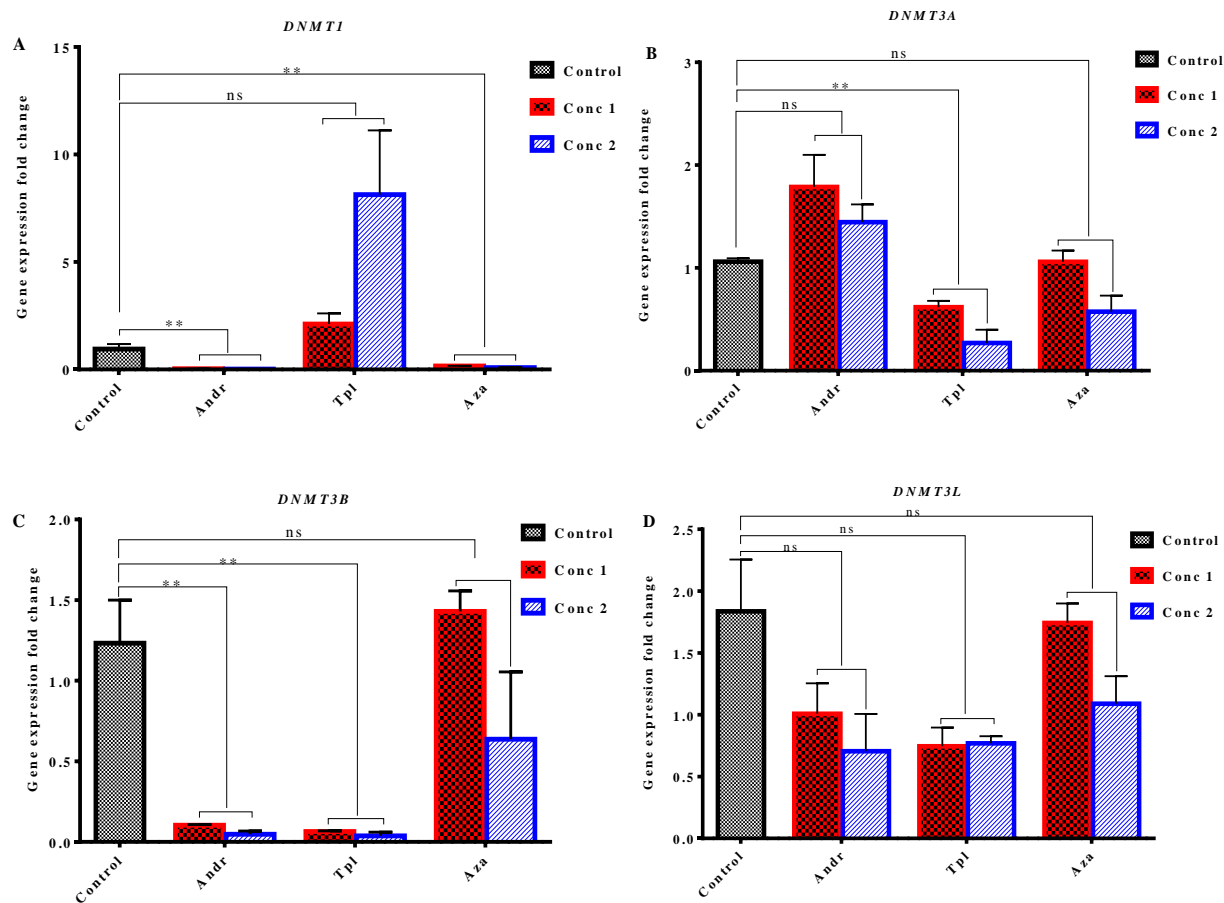


**Figure 4. 21: Modulation of *DNMTs* expression in response to treatment with Andr and Tpl using RT-qPCR. *DNMT1* (A), *DNMT3A* (B), *DNMT3B* (C) and *DNMT3L* (D).** Aza was used as positive control and the result was presented as the mean  $\pm$  SD values gene expression fold change. Conc 1 and 2 are 5 and 10 $\mu$ M for Andr and Aza, and 0.02 and 0.04  $\mu$ M for Tpl. The significance level at  $p < 0.05$ ,  $p < 0.01$ ,  $p < 0.001$  and  $p < 0.0001$  are represented as (\*), (\*\*), (\*\*\*) and (\*\*\*\*) respectively while no significant different is denoted with (ns).

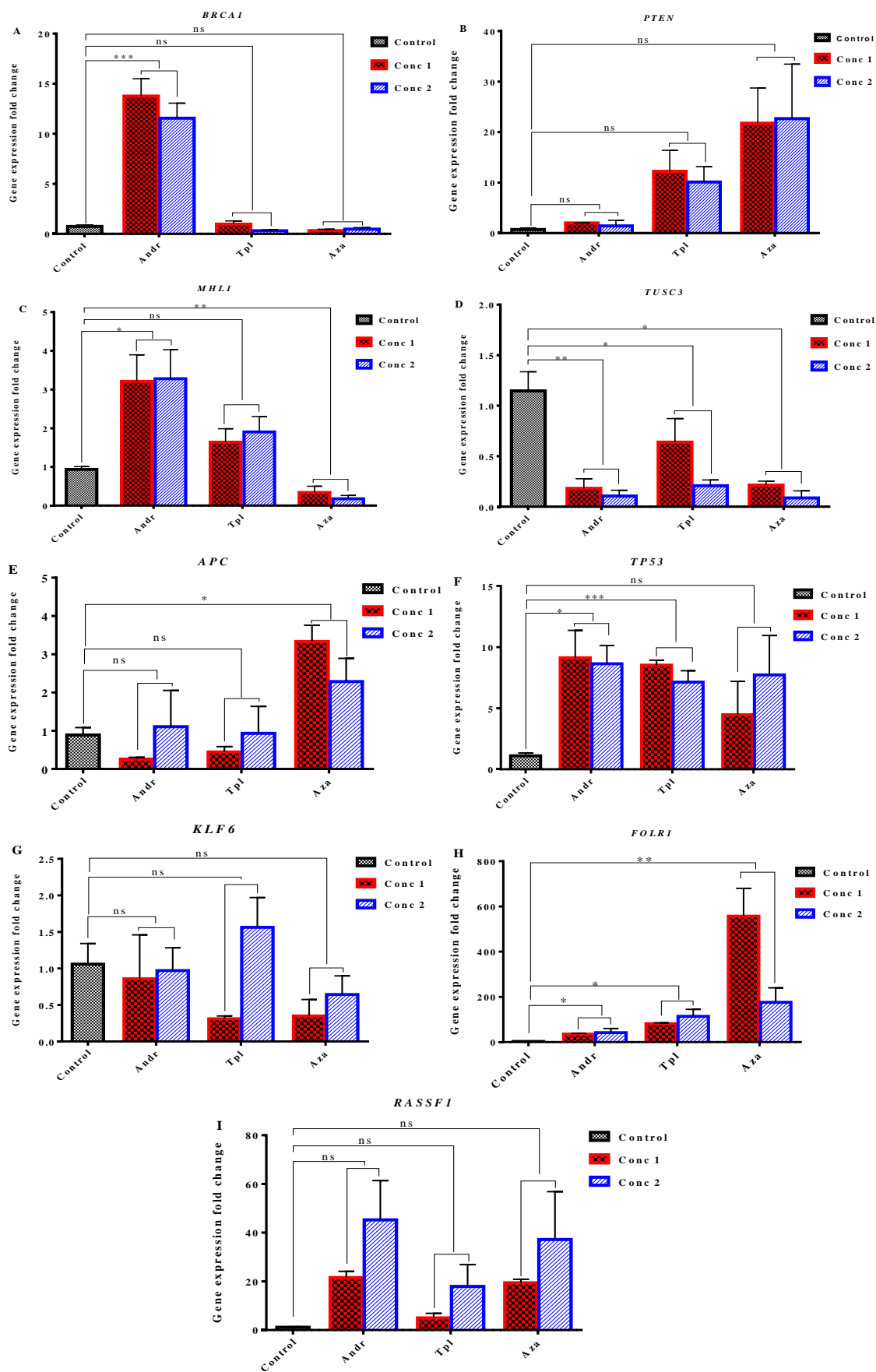


Figure 4.22: Modulation of the expression of different tumour suppressor genes in response to drug treatment. Fold of change of gene expression relative to control for

(BRCA1 (A), PTEN (B), MLH1 (C), TUSC3 (D), APC (E), TP53 (F), KLF6 (G), FOLR1 (H) and RASSF1 (I) genes. Aza was used as positive control and the result was presented as the mean  $\pm$  SD values gene expression fold change. Conc 1 and 2 are 5 and 10 $\mu$ M for Andr and Aza, and 0.02 and 0.04  $\mu$ M for Tpl. The significance level at  $p < 0.05$ ,  $p < 0.01$ ,  $p < 0.001$  and  $p < 0.0001$  are represented as (\*), (\*\*), (\*\*\*) and (\*\*\*\*) respectively while no significant different is denoted with (ns).

### **4.3 Discussion**

#### **4.3.1 Antiproliferative activity of andrographolide and triptolide**

The sustaining proliferative features of cancer cells is one of the multistep phenomenon that distinguished them from normal cells. The evaluation of the anti-proliferative activity of natural compounds is usually the initial method to discover their anti-cancer activity. Generally, most of the compounds that could possibly be a potential anti-cancer drug do show high anti-proliferative activity. Several studies have reported that andrographolide and triptolide which are diterpenoids that are usually isolated from of *Andrographis paniculata* and *Tripterygium wilfordii* respectively reduced the proliferation of different cancer types, such as colon, gastric, prostate, breast and pancreatic cancers (Dai *et al.*, 2017; Islam *et al.*, 2018; Khan *et al.*, 2018; Kim *et al.*, 2018; Varghese *et al.*, 2018; Forestier-Román *et al.*, 2019). The results of the growth inhibitory activity of Andr from the SRB assay in this study showed that its growth inhibitory activity was concentration dependent in CIS-A2780, OVCAR-8 and OVCAR-4. However, this compound showed higher growth inhibitory activity in CIS-A2780 and OVCAR-8, which suggested cell line dependent activity of this compound. Several other studies have reported slightly higher IC<sub>50</sub> values for Andr against different cancer types. Zhang *et al.* (2017) reported that Andr suppressed growth in colon cancer, the activity was also concentration dependent, with IC<sub>50</sub> value of 20  $\mu$ M over 24 h

treatment period. In a similar manner, Peng *et al.* (2018) reported breast cancer cell line dependent sensitivity to Andr with IC<sub>50</sub> values between 20 and 35 µM over 48 h treatment period were reported. Furthermore, Bao *et al.* (2013) demonstrated that Andr inhibited the proliferation of pancreatic cancer cells in time and concentration dependent manner, the cancer cells further showed different sensitivities to this compound. The lower IC<sub>50</sub> values reported for Andr in this study could be due to the longer treatment period used in this study or possibly that ovarian cancer cell lines are more sensitive to this compound than some of the other cancer types. Yunos *et al.* (2013) has also reported that Andr inhibited the growth of cisplatin resistant ovarian cancer cells (CIS-A2780) with an IC<sub>50</sub> value of 6.7 µM, this was slightly higher than the IC<sub>50</sub> value (2.1 µM) reported for Andr against CIS-A2780 cells in this study. The slight difference might be due to the different growth inhibitory assay (3-(4,5-dimethylthiazol-2-yl)-2,5-diphenyltetrazolium bromide) (MTT) used, or possible due to higher cell number seeded by Yunos *et al.* (2013).

In like manner, Tpl inhibited the growth of CIS-A2780, OVCAR-8 and OVCAR-4 in a dose dependent manner, and its growth inhibitory activity was higher in CIS-A2780 and OVCAR-4 with IC<sub>50</sub> of 2 nM than in OVCAR-8 with IC<sub>50</sub> of 30 nM. The result was similar to the report of Chan, Cheng and Sin (2001) who demonstrated that triptolide inhibited the growth of human promyelocytic leukemia, T cell lymphoma and liver cancer with an IC<sub>50</sub> between 7.5 – 32 nM in a dose dependent manner. This result was also similar to the growth inhibitory activity of Tpl reported by Kim *et al.* (2018) on pancreatic cancer with IC<sub>50</sub> between 9.6 – 20 nM in a dose dependent manner. Furthermore, Hu *et al.* (2016) has reported that Tpl inhibited ovarian cancer growth with an IC<sub>50</sub> of 30nM. This report was similar to the IC<sub>50</sub> reported for Tpl against OVCAR-8 in this study. However, the 100 nM dose of Tpl that inhibited almost 50% of the growth of osteosarcoma over a 48 h treatment as reported by Li *et al.* (2018) is slightly higher than the reports of this study. This suggested

that cancer types are more sensitive to Tpl than each other. In addition, Tpl showed higher growth inhibitory activity than Andr in CIS-A2780, OVCAR-8 and OVCAR-4. The growth inhibitory activity of the positive control (Ptx) was similar to that of Tpl but higher than the growth inhibitory activity of Andr. Andr further showed lesser growth inhibitory activity against immortalized human ovarian epithelial cells, which suggested that it is less cytotoxic to normal cells. However, Tpl and the positive control (Ptx) were more cytotoxic to the immortalized human ovarian epithelial cells. This shows that the activity of Andr was more cancer specific than Tpl and Ptx. Furthermore, the trypan blue exclusion assay result showed that Andr reduced the viability of CIS-A2780 cell by causing significant 40-65% cell death at the tested doses (5, 10 and 20  $\mu\text{M}$ ) over 48 h. This result agreed with the data of Khan *et al.* (2018) that showed that Andr caused approximately 35 – 50% cell death in colon cancer at 4, 8 and 16  $\mu\text{M}$  concentrations over 48 h treatment period. Zhang *et al.* (2017) had also reported that Andr caused significant cell death in colon cancer cell line. Still further, the percentage of cell death induced by Tpl was similar to that of Andr and Ptx, and also showed dose dependent activity, resulting in reduced cancer viability. This result was similar to the reports of other researchers on other cancer types such as breast and bone cancer (Gao *et al.*, 2018; Li *et al.*, 2018; Varghese *et al.*, 2018).

#### **4.3.2 Pro-apoptotic activity of andrographolide and triptolide**

Induction of cell death through programmed events within the cell is one of the major mechanisms often evaluated by several researchers to assess the anti-cancer activities of any potential drug (Menyhárt *et al.*, 2016). In this study, the ability of Andr and Tpl to induce apoptosis through different mechanisms were systematically investigated. At first, morphological changes in ovarian cancer cells in response to drug treatment was evaluated using direct observation with the light microscopy to demonstrate if the cytotoxic activity

of Andr and Tpl was due to induction of apoptosis. The result clearly showed that Andr and Tpl caused cell detachment and shrinkage, and reduced cell number which are features of apoptosis. The morphological changes induced by Tpl in this study was consistent with the reports from previous studies which showed that Tpl caused cell detachment and induced changes to breast cancer cell shape (Varghese *et al.*, 2018). Furthermore, fluorescence staining of the nucleus and actin filament with DAPI and Actin red showed that that Andr and Tpl caused nuclear changes such as small and fragmented nuclei condensed nuclei and reduced actin filament network. The findings above conforms with the reports from previous studies that demonstrated that Andr and Tpl caused nuclear fragmentation and condensation in other human cancer types (Zhao *et al.*, 2010; Gao *et al.*, 2018; Khan *et al.*, 2018). The apoptosis-inducing activity of Andr and Tpl was further quantified with flow cytometry after staining treated and untreated cells with annexin V-FITC and PI. The result showed that Andr induced significant apoptosis in both CIS-A2780 and OVCAR-8 ovarian cancer cell lines, but only showed dose dependent effect in CIS-A2780 cell lines. This result agrees with the report of Khan *et al.* (2018), which showed that Andr induced apoptosis in concentration dependent manner in colon cancer. In similar manner, Tpl also showed induced apoptosis in the two ovarian cancer cell lines. This result was consistent with previous report that Tpl induced apoptosis in liver cancer, breast cancer and osteosarcoma (Sun *et al.*, 2017; Gao *et al.*, 2018; Li *et al.*, 2018). Furthermore, the caspase 3/7 activity assay, showed that Andr activated caspase 3/7 in CIS-A2780 and OVCAR-8. This suggested that the apoptosis-inducing activity Andr was through activation of caspase 3/7 activity. Additionally, Andr activated caspase 8 and 9 activities in a concentration dependent manner. The caspase 3/7 and 9 activities of Andr reported in this study was consistent with the data from previous studies (Zhang *et al.*, 2017; Forestier-Román *et al.*, 2019). Likewise, Tpl activated caspase 3/7 activity in ovarian cancer cells through activation of both caspase 8

and 9. Also, Tpl further lead to greater loss of active mitochondrial membrane potential in CIS-A2780 cells. The loss of mitochondrial membrane potential activeness is a marker of early apoptosis through an intrinsic pathway (Ly *et al.*, 2003; Wu *et al.*, 2011). The results of the caspase 3/7, 9 and mitochondrial potential activity of Tpl was consistent with the data of Wu *et al.* (2011) who reported that Tpl increased the caspase 3 and 9 activities in human adrenal cancer and decreased the activeness of the mitochondrial potential of the cell. Cai, He and Yang, (2013) and Zhao *et al.* (2010) had further reported that Tpl reduced the mitochondrial membrane potential activity of ovarian cancer cell (OVAR-3 and SKOV-3) and increased caspase 3 activity in myeloma cancer. This suggested that Andr and Tpl induced apoptosis through both intrinsic and extrinsic pathways. The apoptosis-inducing activity of Andr and Tpl through both intrinsic and extrinsic pathways could further explain why they both showed high cytotoxic activity against ovarian cancer cell lines viability. Furthermore, the effects of Andr and Tpl on the ovarian cancer cell cycle was evaluated by using flow cytometry analysis to quantify the DNA contents of PI treated CIS-A2780 and OVCAR-8 cells. The results confirmed that Andr decreased cells in the G<sub>0</sub>-G<sub>1</sub> cycle and arrested cells in the S and G<sub>2</sub>-M phases in OVCAR-8 and at S phase in CIS-A2780. This result agrees with the previous reported cell cycle arrest activity of Andr at G<sub>2</sub>-M phase in colon cancer (Khan *et al.*, 2018). The result also agrees with the report of Bao *et al.* (2013) and Dai, Wang and Pan (2017). Tpl also arrested cells at the S and G<sub>2</sub>-M phases in CIS-A2780 cells. This result was similar to the reports of Zhao *et al.* (2010) and Wu *et al.* (2019) who showed that Tpl caused cell cycle arrest at G<sub>2</sub>-M and S phases in multiple myeloma and nasopharyngeal carcinoma cells respectively. Furthermore, Andr and Tpl increased the percentage of CIS-A2780 and OVCAR-8 cells in the subG<sub>1</sub> phase. The cell cycle arrest activity of Andr and Tpl at G<sub>2</sub>-M phase enhances the rate of apoptosis inducing activities

of Andr and Tpl, which suggested why these compounds showed high antiproliferative effects on ovarian cancer cells.

### **4.3.3 DNA methylation and gene expression modulatory activities of Andr and Tpl**

The global 5-methylcytosine DNA demethylating and gene specific DNA demethylating activities of Andr and Tpl were evaluated using ELISA based assay and pyrosequencing technique. The percentage of global 5-methylcytosine DNA methylation level in CIS-A2780 cell was reduced by Andr and the positive control (Aza), while Tpl showed no major demethylating activity. Furthermore, the result also showed that Andr and Tpl did not cause any significant changes to the CpG methylation profile of *MLH1* gene, even though that high CpG methylation was observed at the promoter region of this gene. Contrastingly, Andr and Aza significantly reduced the DNA methylation at the CpG site of *HOXA9*. While Tpl does not show any significant demethylation at the CpG site of this gene. DNA methylation is known to be catalysed by group of enzymes known as DNA methyltransferase which include *DNMT1*, *DNMT3A*, *DNMT3B* and *DNMT3L*. The *DNMT* enzymatic inhibitory activity of Andr and Tpl was investigated, and the result showed that Andr did not inhibit the enzymatic activity of DNMT, while Tpl showed high DNMT inhibitory activity. Furthermore, the expression level of the mRNA of each DNMT type in response to Andr and Tpl treatment was evaluated. The result revealed that Andr downregulated the expression of *DNMT1* and *DNMT3B* while Tpl showed high down-regulatory effect on *DNMT3A*, *DNMT3B* and slight down-regulatory effect on *DNMT3L*. This study seems to be the first to report the DNMT activity of Andr and Tpl. In addition, the expression level of different tumour genes in response to drug treatment was evaluated. The result asserts that Andr upregulated the expression of *BRCA1*, *MLH1*, *TP53* and *FOLR1* while Tpl up regulated the expression of *TP53* and *FOLR1*. The upregulation of the expression of *TP53*

gene that function in cell cycle arrest, DNA repair and apoptosis by Andr in gastric cancer had been previously reported (Lim *et al.*, 2017). Nateewattana *et al.* (2014) had also reported that Andr-analogue upregulated the expression of *TP53*. Zhang and Qiu (2015) has further reported upregulation of *TP53* in ovarian cancer. These reports agree with the result of this study. Also, the up-regulatory activity of Tpl on *TP53* gene reported in this study agrees with the data from previous studies that showed that Tpl increased the expression of *TP53* gene in lung and liver cancers (Sun *et al.*, 2017; Mao *et al.*, 2018). Even though Andr does not reduce the DNA methylation level at the CpG site of *MLH1*, it upregulated the expression of this gene. It could be suggested that gene expression is not only regulated by change in the DNA methylation at the promoter region of genes alone. *BRCA1* and *TP53* are both tumour suppressor genes that help to control the rate of cell division, regulate cell growth and prevent uncontrolled cell proliferation. While *MLH1* and *FOLR1* genes both help to make proteins that function in DNA repair. The expression of *PTEN* was further slightly upregulated by Tpl and this result agrees with the reports from previous studies (Wu *et al.*, 2019). The down-regulatory effects of Andr and Tpl on the *DNMT1* and *3A*, and *DNMT3A* and *3B* respectively could explain why an upregulation of the expression of some of the tumour suppressor genes was observed. These mechanistic changes induced by Andr and Tpl at the gene level may cause high anti-proliferative and apoptosis inducing activity and may be the reason why these agents are active to cisplatin-resistant ovarian cancer cell, which is a serious issue for ovarian cancer sensitivity to treatment.

#### **4.4 Conclusion**

In conclusion, the anti-proliferative and apoptotic activities of diterpenoids (Andr and Tpl) against three ovarian cancer cell lines was investigated in this chapter. Their role in *DNMT* inhibition, DNA demethylation and modulation of gene expression was also evaluated.

Andr and Tpl were found to show high anti-proliferative activities through induction of cell death that was mediated via the activation of caspase 3/7 through intrinsic and extrinsic pathways. However, Andr showed lesser cytotoxic activities than Tpl and the positive control (Ptx). Andr and Tpl were also found to show lesser cytotoxic activity against immortalised human ovarian epithelial cells (HOE) than Ptx. This made them a bit safer potential drug. Although, several studies have reported the anti-proliferative activities of these compounds on different cancer types, little knowledge is known about their roles in DNA methylation and inhibition of DNMTs activity. Therefore, this study further reported that Andr downregulated the expression of *DNMT1* and *DNMT3B* and that Tpl downregulated the expression of *DNMT3A* and *DNMT3B*. Furthermore, Andr upregulated the expression of notable anti-cancer genes such as *BRCA1*, *MLH1*, *TP53* and *FOLR1* while Tpl upregulated the expression of *TP53* and *FOLR1*. Furthermore, Andr showed significant global 5-methylcytosine DNA methylation activity, and gene specific demethylating activity at the CpG of the promoter region of *HOXA9* gene, but does not caused any change in the methylation level of the promoter region of *MLH1*. However, Tpl did not show any global and gene specific DNA demethylating activities in *MLH1* and *HOXA9* genes. This study seems to be the first to report the *DNMT* inhibitory and DNA demethylating activities of Andr and Tpl against ovarian cancer cells. These compounds are promising anti-cancer agents with epigenetic activity, and worth been taking ahead for further studies.

## **Chapter Five**

# **Antiproliferative, Apoptotic and DNMT Inhibitory Activities of Sesquiterpene Lactones (SLs) in Ovarian Cancer Treatment**

## 5.1 Introduction

Sesquiterpene lactones (SLs) are known natural compounds present in plants that are often used in traditional medicine for the treatment of diverse diseases. They formed the large group of plant secondary metabolites that are mainly present in the family Asteraceae and Magnoliaceae, and they are 15-carbon compounds comprising of three isoprene units and a lactone group with different sub types (Ghantous *et al.*, 2010; Yang *et al.*, 2011; Gao *et al.*, 2017). This group of compounds possess the ability to target specific signalling pathways, and this has made them a good candidate for drug discovery. Despite the potential relevance of these compounds in disease treatment, little is known about their roles in epigenetic regulation, especially in DNA methylation and inhibition of DNMTs. Study have shown that parthenolide which is a known sesquiterpene lactone inhibited the expression of *DNMT1* (Liu *et al.*, 2009). Therefore, this study investigated the anti-ovarian cancer activities of four SLs (dehydroleucodine, alantolactone, costunolide and parthenolide) along with the positive control 5'-azacytidine (a known demethylation agent) (Lübbert *et al.*, 2001; Kaminskis *et al.*, 2011), and further evaluated their roles in DNA methylation, DNMT inhibition and modulation of gene expression.

The growth inhibitory activity of SLs against three ovarian cancer cell lines (CIS-A2780, OVCAR-8, and OVCAR-4) and immortalised human ovarian epithelia (HOE) cell lines were studied using Sulforhodamine B (SRB) assay. The concentration that caused 50% inhibition in the cancer growth (IC<sub>50</sub>) and their selectivity index (SI) were determined. Their cytotoxic activity was also evaluated using trypan blue exclusion assay. Further evaluation of their apoptotic activities was done using caspase 3/7, 8, and 9 assays, and other apoptotic markers such as phosphatidylserine protein, mitochondrial membrane potential and change in cell morphology using light and fluorescence microscopy. Furthermore, their roles in

DNA methylation, *DNMT* inhibition and modulation of gene expression were evaluated using ELISA based colorimetric assays, pyrosequencing and RT-qPCR.

## 5.2 Results

### 5.2.1 Antiproliferative activity of sesquiterpene lactones (SLs) and 5'azacytidine

The antiproliferative activity of SLs and 5-azacytidine (Aza) was evaluated on the growth of ovarian cancer cell lines (CIS-A2780, OVCAR-8 and OVCAR-4) and immortalised human ovarian epithelial (HOE) cells using SRB assay, which is a cell growth assay that estimated the cell number based on the protein stained with the SRB dye. The concentration that caused 50% inhibition ( $IC_{50}$ ) in the cancer growth was determined. The selectivity index (SI) which is an indicator of safety of the drugs on normal cell lines was also determined.

The mean concentration response growth curves are shown in Figure 5.1 and the  $IC_{50}$  value for each compound is presented in Table 5.1. The results show that the four SLs significantly inhibited ovarian cancer growth with  $IC_{50}$  values of 2.0-12.2 $\mu$ M in CIS-A2780, OVCAR-8 and OVCAR-4 cell lines. Deh, and Ala show higher *in vitro* anti-ovarian cancer activity with the least  $IC_{50}$  values in the three ovarian cancer cell lines than Pat and Cos with slightly higher  $IC_{50}$  values (Table 5.1). The positive control (Aza) which is an FDA approved drug for the treatment of myelodysplastic syndrome shows a significance growth inhibitory activity against ovarian cancer cell lines (CIS-A2780, OVCAR-8 and OVCAR-4) with  $IC_{50}$  values of 3.5-6.4 $\mu$ M. Furthermore, the growth inhibitory activity of the four SLs was higher against CIS-A2780 and OVCAR-8 than in OVCAR-4 (Table 5.1).

In addition, the higher  $IC_{50}$  values of each of the SLs on HOE (Table 5.1) compared with ovarian cancer cell lines shows that SLs possess stronger antiproliferative activity against ovarian cancer cell lines than immortalised normal ovarian epithelial cells. Pat and Cos

showed higher SI of approximately 3, while Deh and Ala showed slightly lower SI of approximately 2. However, Aza showed relatively equal antiproliferative activity against ovarian cancer cell lines and HOE. The SI results suggest that the antiproliferative activity of Pat and Cos are more cancer specific than Deh and Ala, while Aza showed least cancer specific activity. Hence, the SLs would be promising agents in drug discovery. The antiproliferative effects of these compounds necessitated the need to investigate their mechanism of action in the ovarian cancer cell lines.

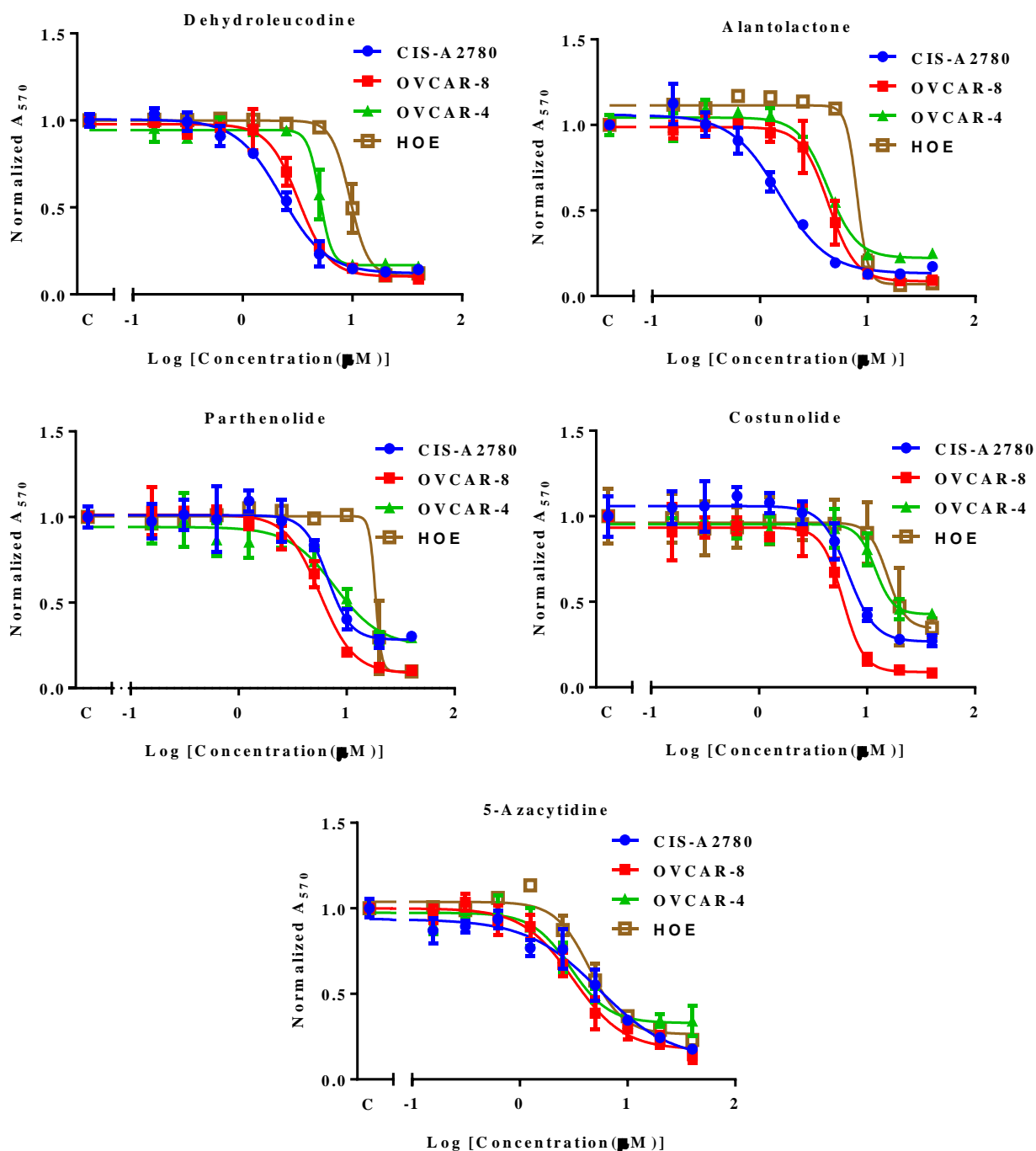


**Figure 5. 1: Mean concentration-response curve of antiproliferative activities of SLs and Aza on CIS-A2780, OVCAR-8 and OVCAR-4 cell lines.** The cancer cell lines were treated with different concentrations of each compound (0.16-40 µM) for 72h. The data generated were analysed as mean ± SEM of five repeated experiments. The negative control is denoted with C (cells without drug dose i.e. only medium with 0.2% DMSO).

**Table 5. 1 Results of the antiproliferative activities of SLs and Aza on ovarian cancer cell lines (CIS-A2780, OVCAR-8 and OVCAR-4) and HOE cell line using cell growth inhibitory assay. The number of cells was estimated by SRB staining after post-treatment period of 72hours. The IC<sub>50</sub> results are expressed as mean ±SEM of five independently repeated experiments in triplicate. Nine different concentration of each drug was used ranging from highest to lowest (0.16-40 μM) and the control contains 0.2% vehicle (DMSO). SI is the ratio of IC<sub>50</sub> of HOE to IC<sub>450</sub> on each cancer cell line. Mean SI is calculated based on three individual SIs.**

Natural Compounds	Abbrev.	CIS-A2780	OVCAR-8	OVCAR-4	HOE IC <sub>50</sub>	SI with	SI with	SI with	Mean SI (n=3)
		IC <sub>50</sub> (μM)	IC <sub>50</sub> (μM)	IC <sub>50</sub> (μM)	IC <sub>50</sub> (μM)	CIS-A2780	OVCAR-8	OVCAR-4	
Dehydroleucodine	Deh	2.4±0.2	4.1±1.5	7.4±1.9	8.7±0.4	3.6	2.1	1.2	2.3±1.0
Alantolactone	Ala	2.0±0.4	4.6±0.5	7.4±0.8	8.2±0.4	4.1	1.8	1.1	2.3±1.3
Parthenolide	Pat	5.7±0.5	7.2±2.4	10.7±2.0	24.3±3.9	4.3	3.4	2.3	3.3±0.8
Costunolide	Cos	8.1±1.4	7.8±1.9	12.2±0.7	25.2±0.3	3.1	3.2	2.1	2.8±0.5
5-Azacytidine	Aza	6.4±0.8	3.5±0.4	3.8±0.3	4.9±0.6	0.8	1.4	1.3	1.2±0.3

### **5.2.2 Cytotoxic activities of SLs and Aza using trypan blue exclusion assay**

Based on the antiproliferative activities of the SLs and Aza using SRB assay, which does not specifically show whether the mechanism of the compounds anti-cancer activity was through inhibition of cell division (cytostatic) or by induction of cell death (cytotoxic). Trypan blue exclusion assay was used to investigate further on the route of activity. Based on the IC<sub>50</sub> values of each compound, three different concentrations (5, 10 and 20 µM) at three different time points (24, 48 and 72h) were investigated for cell death assay. The results were analysed by calculating the percentage of cell death. The percentage of cell death induced by each compound in CIS-A2780, OVCAR-8 and OVCAR-4 is presented in Figure 5.2, 5.3 and 5.4 respectively.

In CIS-A2780 cell line, the result shows that the four SLs (Deh, Pat, Cos and Ala) and the positive control induced significant cell death when compared with the control. The percentage of cell death induced by each of these compounds was concentration and time dependent. Furthermore, the percentage of cell death induced by Deh (23-83%, 17-93% and 14-93%) and Ala (21-73%, 25-92% and 27-91%) at 24, 48 and 72 h time points respectively were higher than that of Pat (14-49%, 16-68% and 12-71%) and Cos (14-46%, 14-74% and 13-73%) which induced slightly lesser cell death than the positive control (Aza) (24-41%, 52-81% and 65-83%).

In OVCAR-8, Deh, Cos and Aza induced significant cell death at time and concentration dependent manner, while Pat and Ala induced only concentration dependent but no time dependent cell death. Deh (30-68%, 41-77% and 43-88%), and Ala (37-73%, 43-84% and 40-96%) induced slightly higher cell death at the different concentrations and time points respectively than the cell death induced by Pat (26-50%, 25-57% and 26-69%), Cos (28-44%, 27-69 and 30-66% at) and Aza (25-35%, 27- 63% and 60-68%). Also, in OVCAR-4

cells, Ala (51-89%, 22-73 and 42-91%) induced the highest cell death, while the cell death induced by Deh (34-58%, 33-54% and 29-83%) and Aza (18-47%, 26-51% and 37-81%) at 24, 48 and 72 h time point was slightly higher than the percentage of cell death induced by Pat (12-28%, 20-46% and 23-60%) and Cos (14-33%, 29-48% and 24-56%). Furthermore, only Pat induced time and concentration dependent cell death. Deh, Ala, Cos and Aza induced significant concentration dependent cell death. The cytotoxic activities of the compounds suggest that their antiproliferative activity was mainly through induction of cell death.

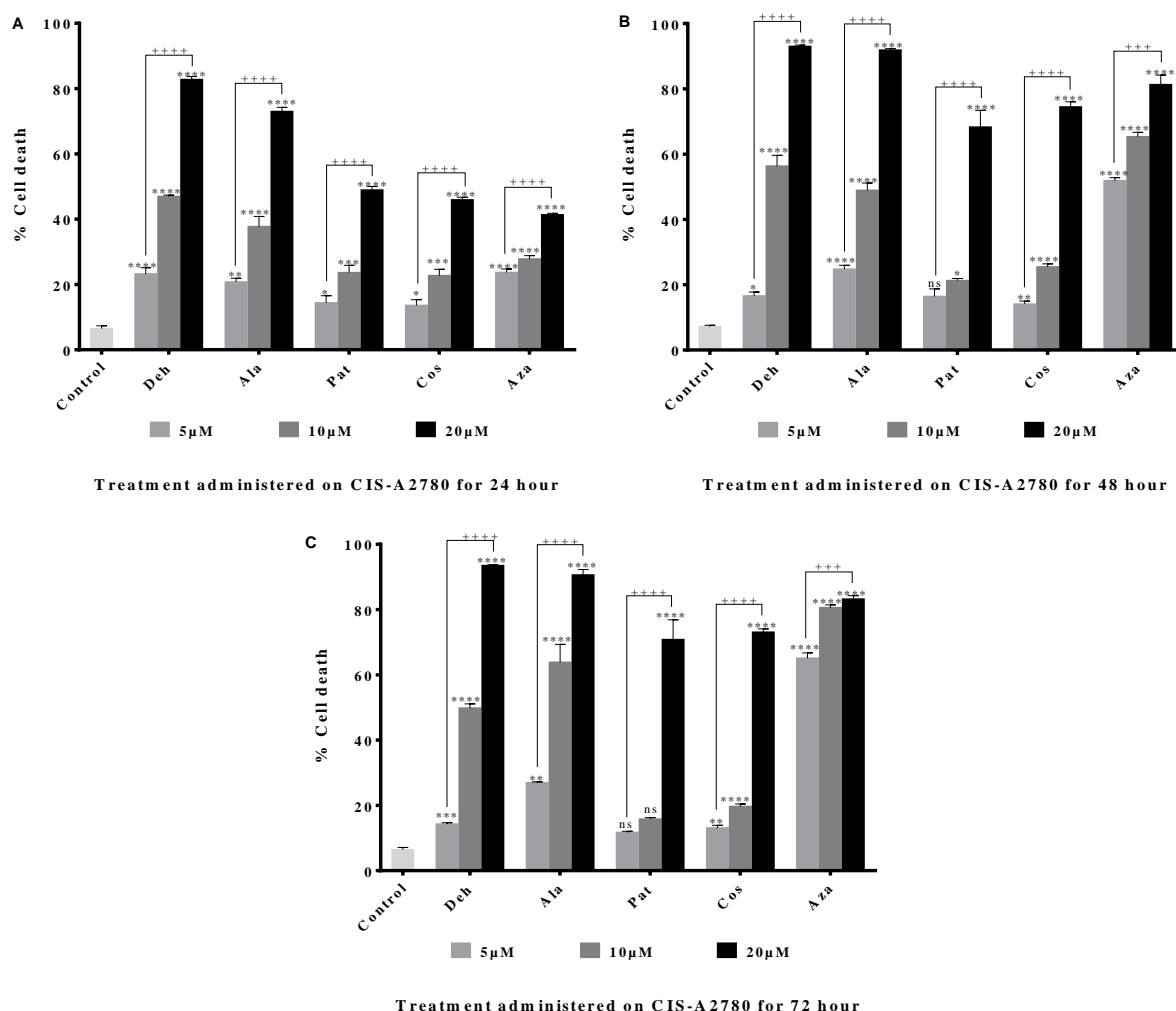


**Figure 5. 2: Trypan blue exclusion cytotoxic test for four SLs (Deh, Pat Cos and Ala) against CIS-A2780 ovarian cancer cell line at different concentrations (5, 10 and 20 μM) and time point 24 h (A), 48 h (B) and 72 hr (C). Aza was used as positive control**

and negative control group was treated with ordinary medium with 0.1% DMSO. The percentage cell deaths were estimated and recorded as means  $\pm$  SEM of three repeated experiments. The significant level of the Dunnett's multiple comparison test of each compound with the control is denoted with asterisk (\*), while the concentration dependent activity significant level using one-way ANOVA is represented as plus (+). The significance level at  $p < 0.05$ ,  $p < 0.01$ ,  $p < 0.001$  and  $p < 0.0001$  are represented as (\*), (\*\*), (\*\*\*) and (\*\*\*\*). Similar pattern was followed for significant difference within concentrations of the same compound.

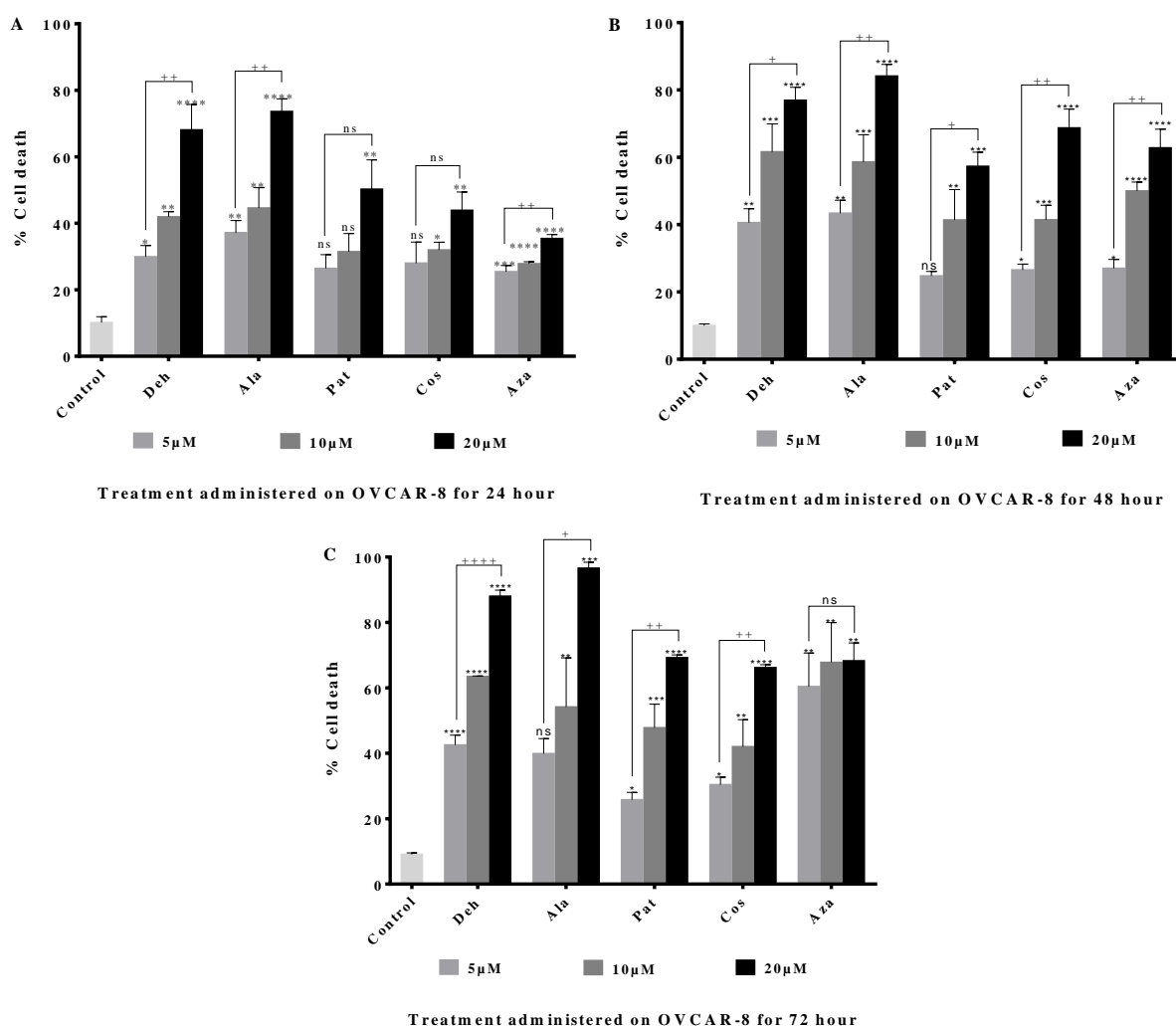


**Figure 5. 3: Trypan blue exclusion test for four SLs (Deh, Pat Cos and Ala) against OVCAR-8 ovarian cancer cell line at different concentrations (5, 10 and 20  $\mu$ M) and time point 24 h (A), 48 h (B) and 72 hr (C). Aza was used as positive control and negative**

control group was treated with ordinary medium with 0.1% DMSO. The data represent the means  $\pm$  SEM (n=3). One-way ANOVA with multiple comparison test was used to test for compound significant activity with control, and the multiple comparison significance level is denoted with asterisk (\*). Concentration dependent activity was tested with one-way ANOVA and the significant level represented as plus (+). The significance level at  $p < 0.05$ ,  $p < 0.01$ ,  $p < 0.001$  and  $p < 0.0001$  are represented as (\*), (\*\*), (\*\*\*) and (\*\*\*\*).

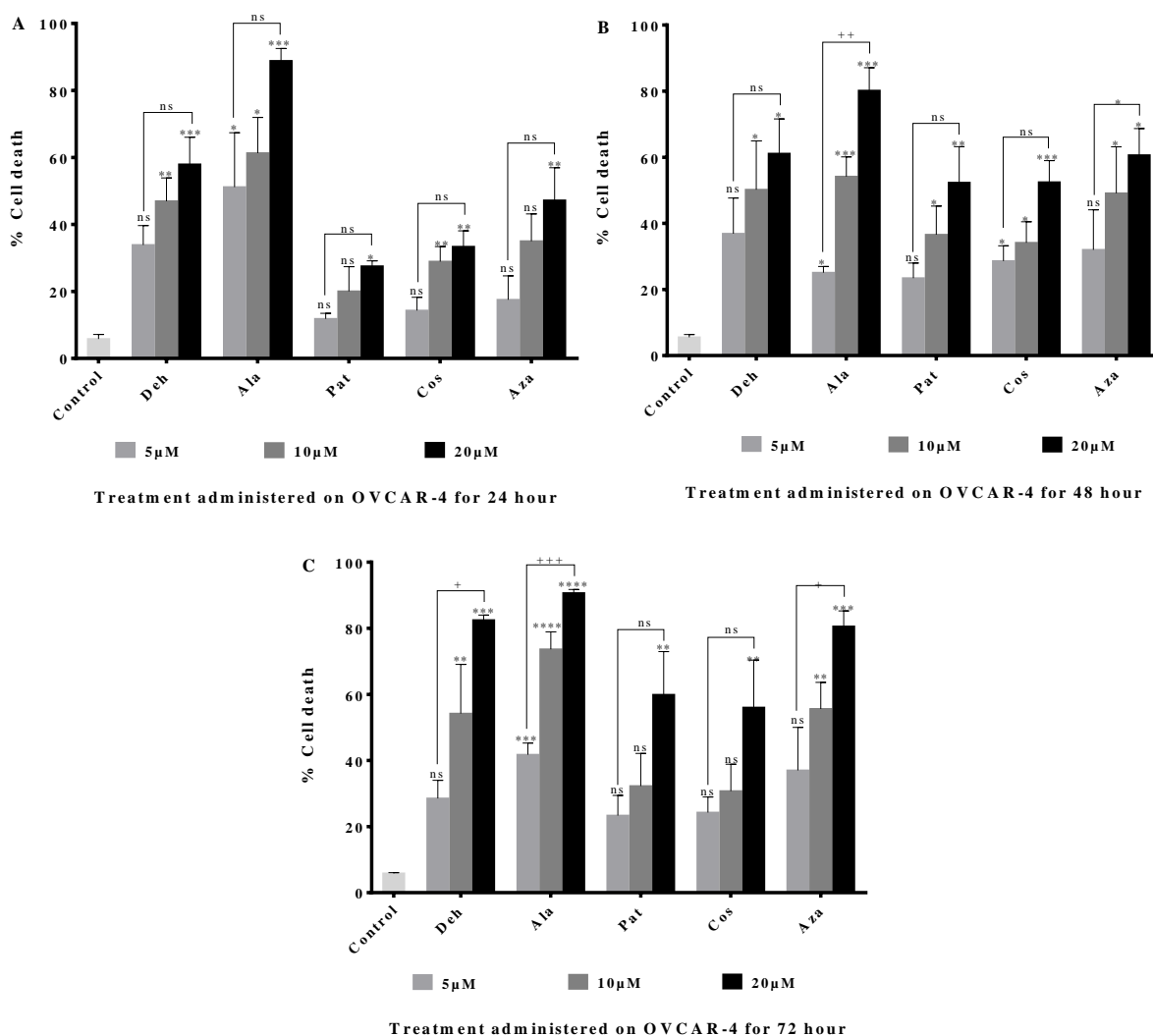


**Figure 5. 4: Trypan blue exclusion test for SLs (Deh, Pat Cos and Ala) against OVCAR-4 ovarian cancer cell line at different concentrations (5, 10 and 20  $\mu$ M) and time point 24 h (A), 48 h (B) and 72 hr (C). The negative control group contains ordinary medium with 0.1% DMSO, while Aza was used as positive control. The means  $\pm$  SEM**

(n=3) percentage cell deaths were estimated and analysed using one-way ANOVA with Dunnett's multiple comparison test to compare control with each compound, and the significance level is denoted with asterisk (\*). The concentration dependent activity of each compound was tested with one-way ANOVA and the significant level denoted with plus (+). The significance level at  $p < 0.05$ ,  $p < 0.01$ ,  $p < 0.001$  and  $p < 0.0001$  are represented as (\*), (\*\*), (\*\*\*) and (\*\*\*\*).

### **5.2.3 Morphological effects of SLs and Aza on ovarian cancer cell lines**

Evaluation of the morphological effects of SLs (Deh, Pat, Cos and Ala) and Aza on ovarian cancer cell lines (CIS-A2780 and OVCAR-4) were investigated using light microscopy. Briefly, cells treated with two different concentrations of each compound, at different time point (48 and 72h) were observed directly under the microscope and images captured with X10 objective lens. In CIS-A2780 cell line, the morphological alterations induced by Deh, Ala, Pat, Cos and Aza include cell detachment, cell shrinkage and membrane blebbing (Figure 5.5). The morphological alteration induced by the each of the SLs was similar to that of Aza. However, the morphological changes induced by Deh, Ala and Pat were slightly higher than that of Cos and the positive control (Aza). The morphological changes were prominent at the different concentrations but no major differences were observed at the different time points. Similar morphological changes such as cell shrinkage, cell detachment and membrane blebbing were also observed in OVCAR-4 (Figure 5.6). The changes were more prominent in Deh and Ala than Pat, Cos and Aza treated cells. The morphological changes induced by each compound and the positive control was also concentration dependent. However, no major morphological differences were observed at the two time points. The higher morphological changes induced by Deh and Ala suggest why they showed higher growth inhibitory and cytotoxic activities than Pat and Cos.

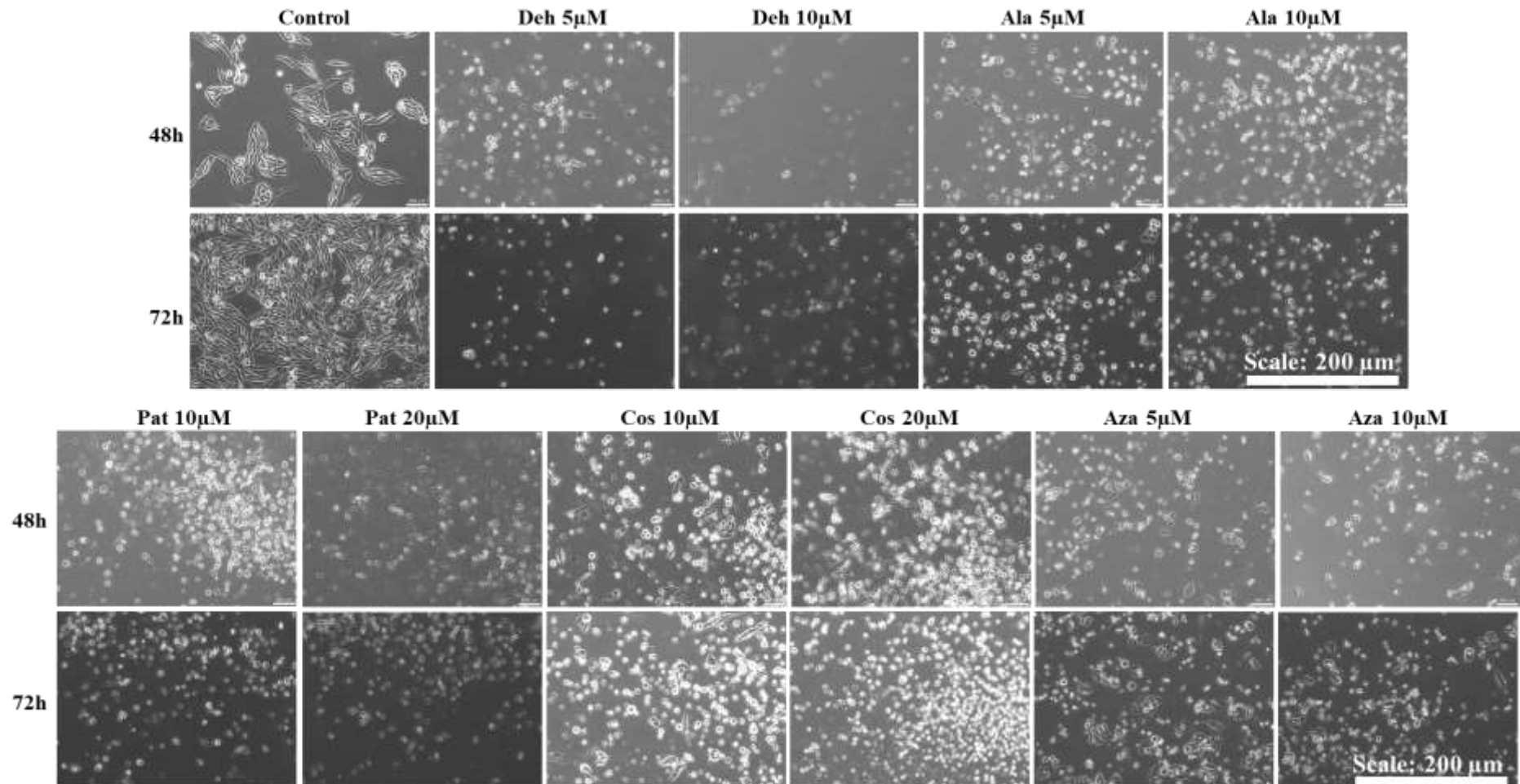


**Figure 5. 5:** Morphological effects of SLs (Deh, Pat, Cos and Ala) and Aza on CIS-A2780 cells at time (48 and 72h) and concentration dependent manner using light microscopy. Media containing 0.1% DMSO as negative control. Images were taken with X10 objective lens.

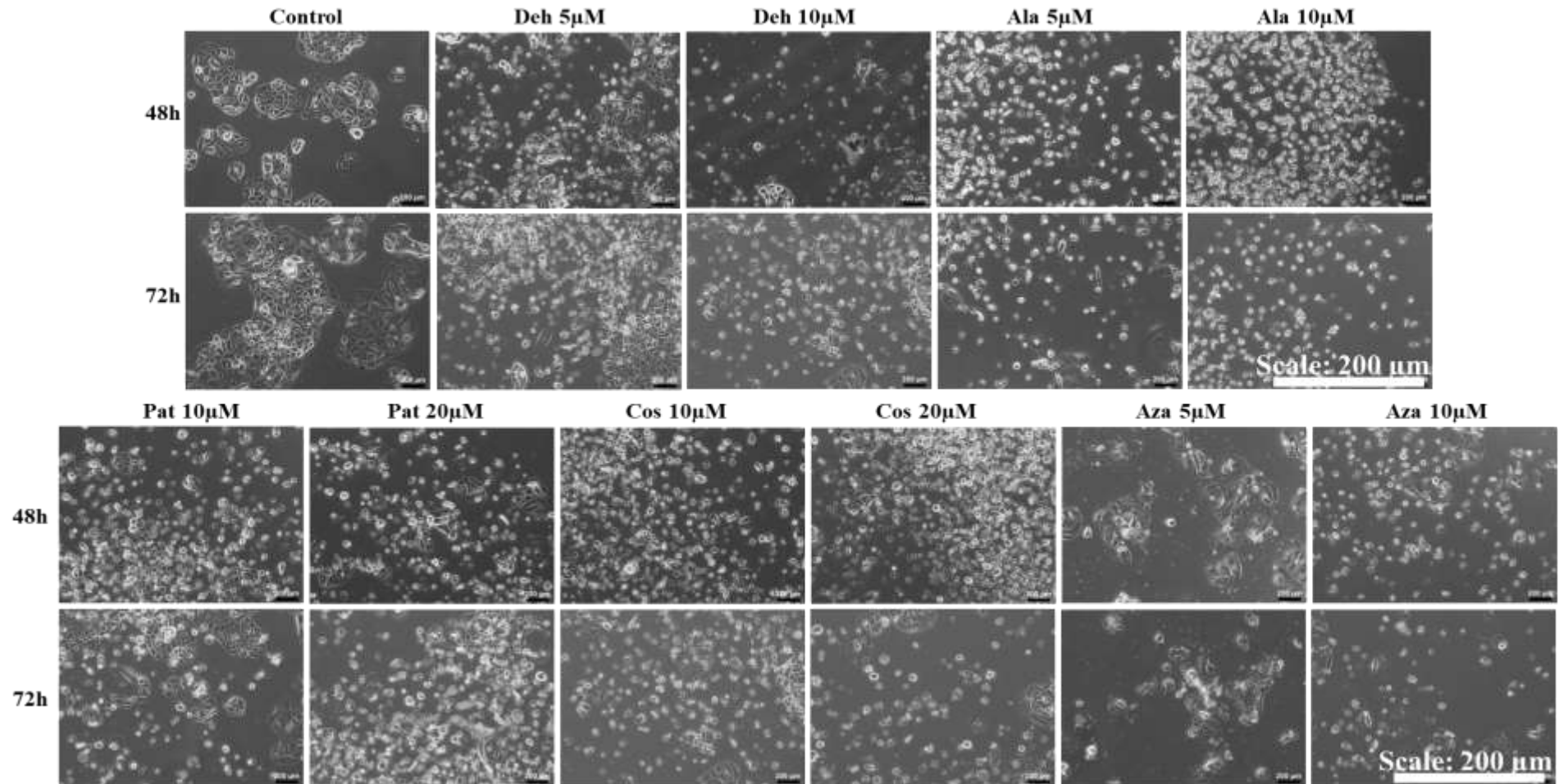


**Figure 5. 6: Morphological effects of SLs (Deh, Pat, Cos and Ala) and Aza on OVCAR-4 cells at time (48 and 72h) and concentration dependent manner using light microscopy.** Negative control contains media with 0.1% DMSO. Images taken with X10 objective lens.

#### **5.2.4 Evaluation of change in nuclear and actin structure of ovarian cancer cells**

Fluorescence microscopy was used in the evaluation of change in the nuclear and actin structure of ovarian cancer cell lines after treatment with SLs (Deh, Pat, Cos and Ala). Change in cellular structure and disruption to the actin filament networks are known features of cells undergoing apoptosis. CIS-A2780 and OVCAR-8 cells treated with compound SLs and Aza at two-time points (48 and 72 h) were imaged with fluorescence microscopy using 40x objective lens after staining with DAPI and actin red<sup>TM</sup> 555 ready probes. Apoptotic cells were identified when cells show features such as; smaller and fragmented nuclei, condensed chromatin and high fluorescence intensity.

The four SLs (Deh, Pat, Cos and Ala) caused morphological changes to the nuclei and actin structure of CIS-A2780 and OVCAR-8 cell lines (Figures 5.7 and 5.8). The morphological changes caused by SLs and Aza include: fragmented nuclei, shrunk nuclei, chromatin condensation. These compounds further reduced the capacity of the actin filament to form a network. The actin filaments aggregated rather than forming a network compared with the control. Similar results were also obtained for Aza used as positive control when compared with the untreated cells (negative control). Major nuclei and actin morphological changes were observed in cells treated with Deh, Ala and Cos compared with Pat that showed least morphological changes in CIS-A2780 and OVCAR-8 cells. The apoptotic features caused by these compounds increased with concentration but the difference was not time dependent.

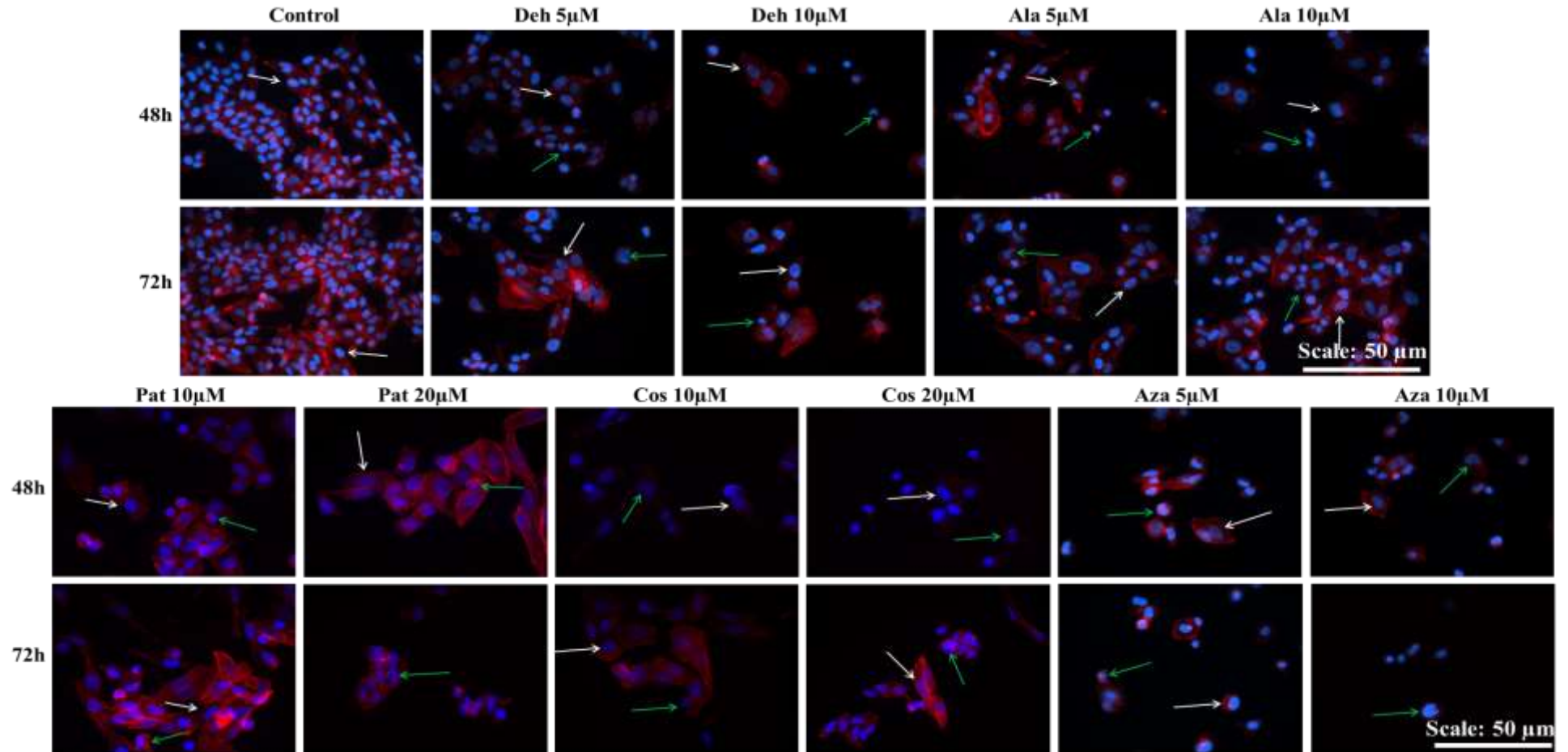


**Figure 5. 7:** Fluorescence microscopy images of CIS-A2780 cell line taking with 40x objective lens, showing morphological changes in the nucleus and actin filament in response to drug treatment. Nuclei and actin were stained with DAPI (blue) and actinRed<sup>TM</sup> 555 (red) respectively. White and green arrows are pointing to viable cell nuclei and apoptotic cell nuclei respectively.

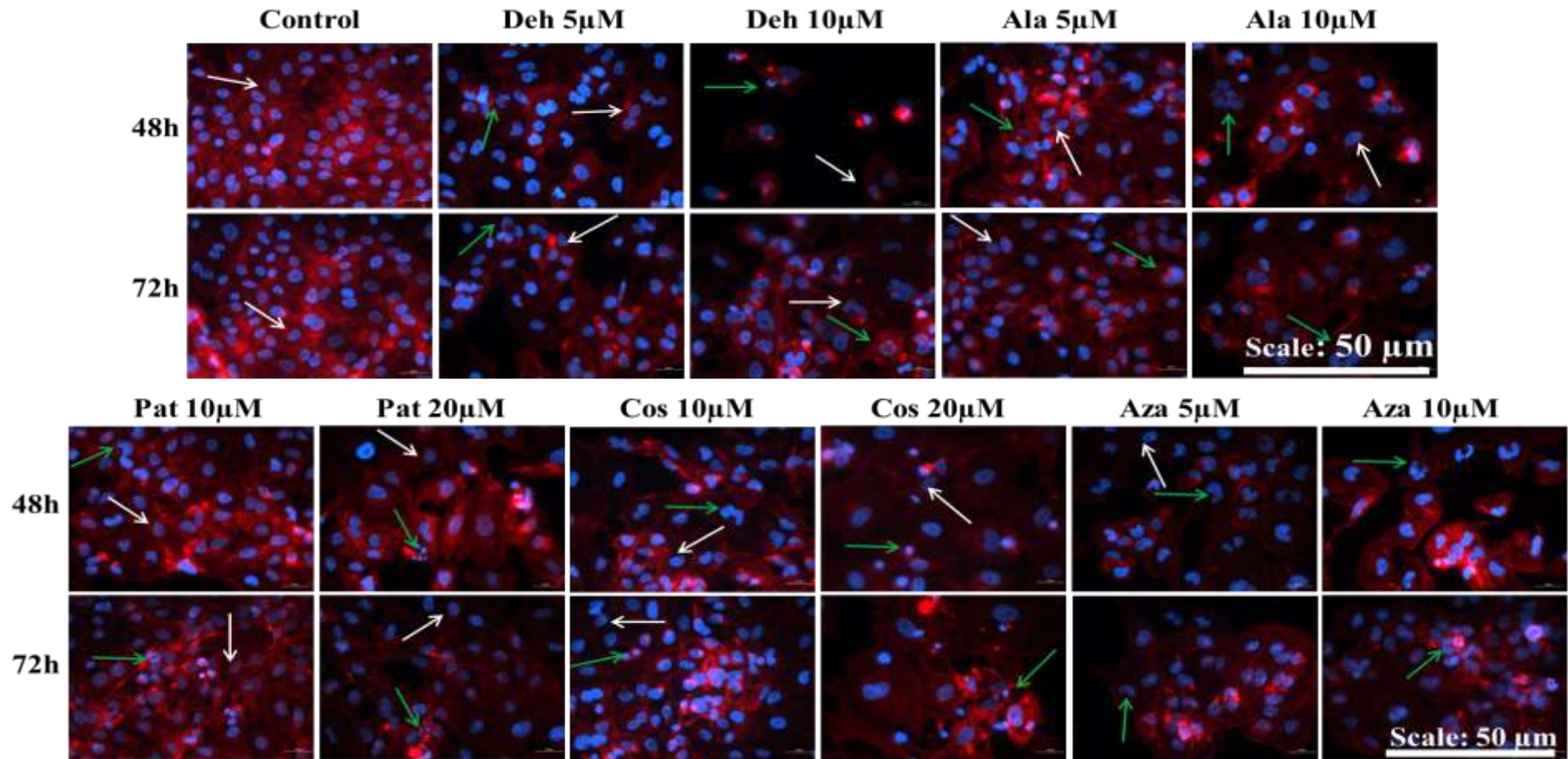
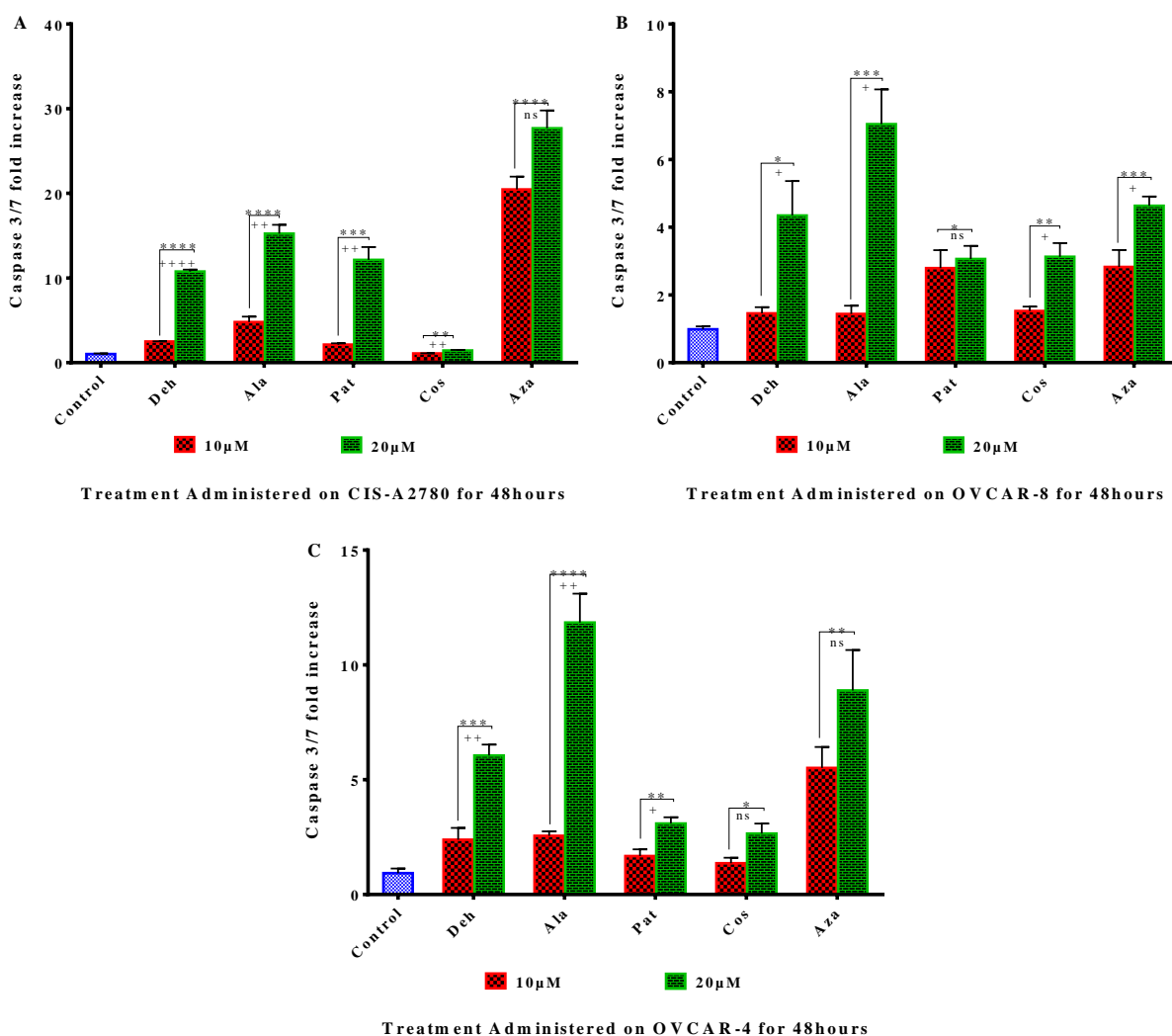


Figure 5. 8: Fluorescence microscopy images of OVCAR-8 cell line showing morphological changes in the nucleus and actin filament in response to drug treatment. Images were taking with 40x objective lens. DAPI (blue) and actinRed™ 555 (red) were used for Nuclei and actin staining respectively. White and green arrows are pointing to viable cell nuclei and apoptotic cell nuclei respectively.

### **5.2.5 Evaluation of apoptotic activities of SLs and Aza using caspase 3/7 assay**

The Caspase 3/7 activity marker was evaluated to give an indication whether the significant decrease in cell viability by four SLs (Deh, Pat, Cos and Ala) and Aza was due to induction of programmed cell death. Caspase 3/7 activity was measured in ovarian cancer cell lines (CIS-A2780, OVCAR-8, and OVCAR-4) after 48 h treatment with four SLs and Aza (positive control). The results revealed that the SLs increased the activity of caspase 3/7 in CIS-A2780 cells. The positive control (Aza) showed the highest caspase 3/7 activity with 28-fold increase than the SLs. Deh, Pat and Ala showed similar caspase 3/7 activity in CIS-A2780 cells with fold increase of 11, 12 and 15 respectively, while Cos caused the least increase in caspase 3/7 activity with 5-fold increase at the highest concentration. All the SLs induced concentration dependent change in caspase 3/7 activities. However, the caspase 3/7 activity effect of the positive control (Aza) was not concentration dependent. In OVCAR-8 cell line, the four SLs (Deh, Pat, Cos and Ala) and the positive control (Aza) increased caspase 3/7 activity (Figure 5.9). When compared with the control, Deh, Pat, Cos and Ala caused the caspase 3/7 activity to increase by 4, 3, 3 and 7 folds respectively at higher concentration, while Aza caused a fold increase of approximately 5. The caspase 3/7 activity by Deh and Ala was higher than that of Pat and Cos, but relatively closely similar to that of the positive control (Aza). Multiple comparison test analysis shows that the caspase 3/7 activity in the four SLs (Deh, Pat, Cos and Ala) and Aza were significant at higher concentration (20 $\mu$ M) when compared with control. The caspase 3/7 activity effect of Deh, Cos and Ala including the positive control (Aza) was concentration dependent. Furthermore, Deh, Pat, Cos and Ala, and the positive control (Aza) increased caspase 3/7 activity in OVCAR-4, with a fold increase of 6, 3, 3, 12 and 9 respectively at higher concentration (Figure 5.9). Deh and Ala increased caspase 3/7 activity in a similar manner with the positive control (Aza), their caspase 3/7 activity effect was higher than that of Pat and Cos

which showed moderate caspase 3/7 activity. The caspase 3/7 activity by the four SLs (Deh, Pat, Cos and Ala) and Aza in OVCAR-4 was also significant at higher concentration (20 $\mu$ M) when compared with the control using one-way ANOVA and Dunnett's multiple comparison test. The caspase 3/7 activity effect of Deh, Pat and Ala was also concentration dependent in OVCAR-4.



**Figure 5. 9: Effect of SLs (Deh, Pat, Cos and Ala) on caspase 3/7 activity in ovarian cancer cell lines; CIS-A2780 (A), OVCAR-8 (B) and OVCAR-4 (C).** Aza was used as positive control at the same concentrations with tested compounds. The fold increase in caspase 3/7 activity of each compound was compared with the control using one-way ANOVA with Dunnett's multiple comparisons test and student T test was used to test

caspase 3/7 concentration dependent activity. Significance difference between drug and control is denoted with asterisk (\*) (\*,  $p < 0.05$ , \*\*,  $p < 0.01$ , \*\*\*,  $p < 0.001$  and \*\*\*\*,  $p < 0.0001$ ), while significant concentration dependent activity was denoted with plus (+) in a similar manner.

### **5.2.6 Effect of SLs and Aza on caspase 8 activity**

The effect of SLs (Deh, Pat, Cos and Ala) and Aza was investigated on caspase 8 marker (initiator caspase) to determine their possible pathway of apoptosis induction. The increase of caspase 3/7 activities by SLs and Aza described above have suggested that the anti-ovarian cancer activity of these compounds was mainly through induction of cell death, hence the need to determine their apoptotic pathway of cell death induction. Caspase 8 activity in ovarian cancer cell lines (CIS-A2780, OVCAR-8 and OVCAR-4) was measured after 48 h treatment of SLs and Aza. In CIS-A2780 cells, the results show that SLs (Deh, Pat, Cos and Ala) and Aza increased caspase 8 activity (Figure 5.10). The caspase 8 activity of the positive control (Aza) was 13-fold higher when compared with the negative control and significantly higher than the caspase 8 activity of each of the SLs. Ala showed slightly higher caspase 8 activity with a fold increase of 5, than Deh, Pat and Cos that showed least caspase 8 activity with a fold increase of 2. Multiple comparison analysis further showed that the caspase 8 activity of the four SLs and Aza was significant with the control at both concentrations (10 and 20  $\mu\text{M}$ ).

In OVCAR-8 cell line, caspase 8 activity was significantly increased when compared with the control (Figure 5.10). Similar to the caspase 8 activity of the positive control (Aza) and SLs in CIS-A2780 cell line, Aza caused 4-fold increase in the caspase 8 activity in OVCAR-8 cells which was slightly higher than the caspase 8 activity of Deh, Pat and Ala that showed a 3-fold increase in caspase activity and Cos had the least caspase activity with 2-fold

increase. The caspase 8 activity caused by the four SLs (Deh, Pat, Cos and ala) was concentration dependent, while Aza does not show concentration dependent activity. Additionally, the caspase 8 activity effects of Deh, Cos, Ala and Aza was significant when compared with the control at both lower and higher concentrations (10 and 20  $\mu\text{M}$ ). while the activity by Pat was only significant at higher concentration (20  $\mu\text{M}$ ). The caspase 8 activity in OVCAR-4 cell line was also significantly increased by Deh, Pat, Cos and the positive control (Aza) (Figure 5.10). The caspase 8 activity by Deh was closely similar to the caspase activity of that of the positive control (Aza) with a fold increase of 3. The caspase activity caused by Deh was higher than that of Pat that showed a fold increase of approximately 2, while Cos and Ala does not show any significant change in caspase 8 activity in OVCAR-4.

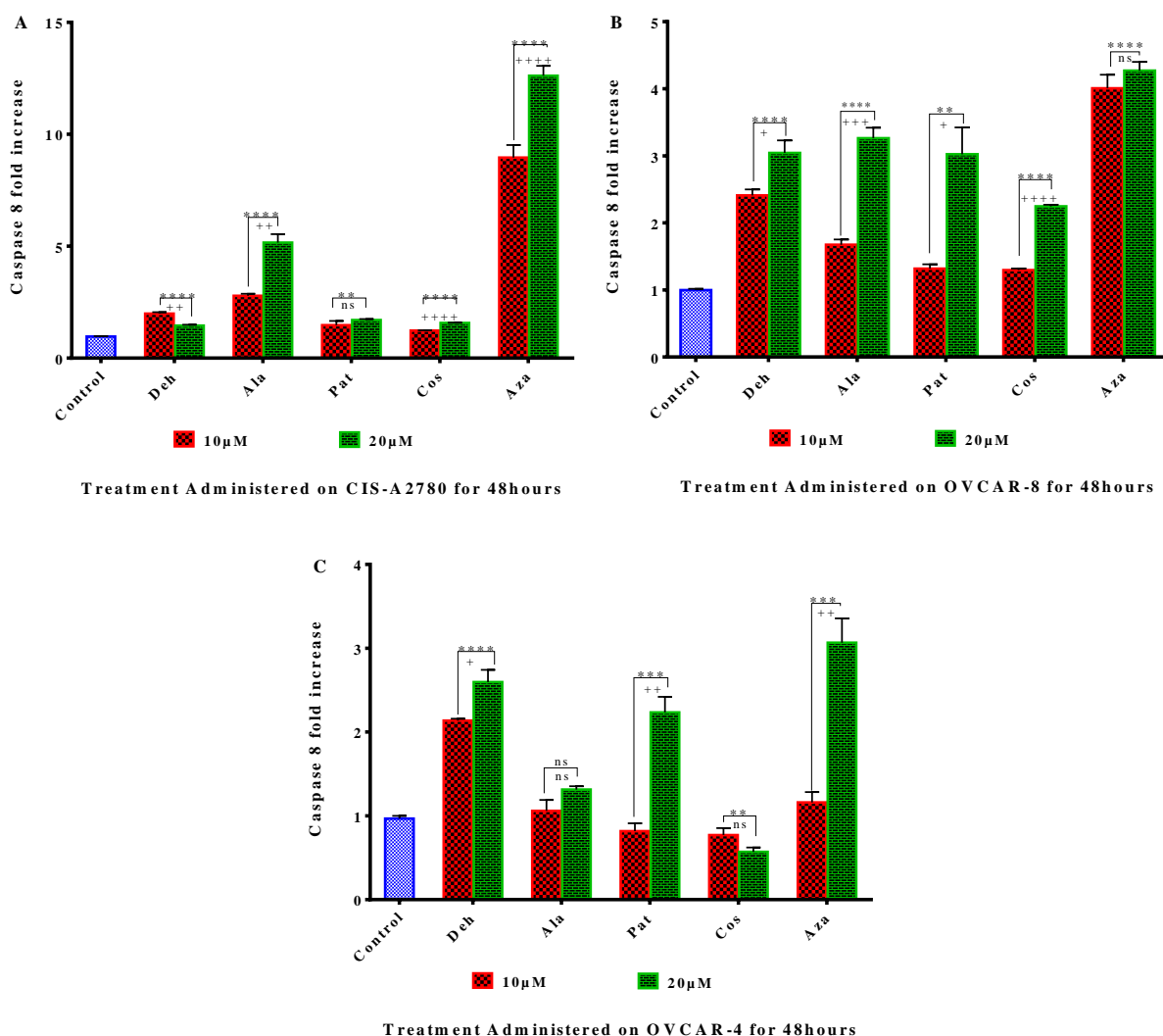


**Figure 5. 10: Caspase 8 activity caused by four SLs (Deh, Pat, Cos and Ala) on ovarian cancer cell lines CIS-A2780 (A), OVCAR-8 (B) and OVCAR-4 (C).** Aza was used as positive control. Data were analysed using one-way ANOVA with Dunnett’s multiple comparisons test to compare significance caspase 8 activity with the control, and student T test was used to test concentration dependent activity. Significance difference between drug and control is denoted with asterisk (\*), (\*,  $p < 0.05$ , \*\*,  $p < 0.01$ , \*\*\*,  $p < 0.001$  and \*\*\*\*,  $p < 0.0001$ ), while significant concentration dependent activity was denoted with plus (+) in a similar manner.

### **5.2.7 Evaluation of caspase 9 activity by SLs and Aza**

To further investigate the pathway of apoptotic induction by the four SLs (Deh, Pat, Cos and Ala) and Aza, the activity of caspase 9 marker was evaluated in ovarian cancer cell lines (CIS-A2780, OVCAR-8, and OVCAR-4) after 48 h post-treatment with different concentration of the tested compounds. This marker is known to be an initiator of an intrinsic pathway of apoptosis. Therefore, change in the level of this marker in response to drug treatment is an indication of the possible pathway of the drug activity. The caspase 9 activity result in CIS-A2780 cells shows that the four SLs (Deh, Pat, Cos and Ala) and the positive control (Aza) significantly increased caspase 9 activity when compared with the control, with Ala showing the highest fold increase of 10, while Deh and Pat showed a 3-fold increase, and Cos showed the least fold increase of approximately 2 at higher concentration. However, the positive control (Aza) showed higher 22-fold increase of caspase 9 than the SLs. Furthermore, the caspase 9 activity effect of Deh, Pat, Ala and the positive control were significant when compared with the control at both lower and higher concentration (10 and 20  $\mu$ M), while the caspase activity by Cos was only significant at higher concentration. Only, Pat and Ala including the positive control showed concentration dependent activity (Figure 5.11). Similarly, the four SLs (Deh, Pat, Cos and Ala) and the positive control (Aza) further increased caspase 9 activities in OVCAR-8, with only Deh, Cos and Ala showing significant effect on caspase 9 activity at both concentrations (10 and 20 $\mu$ M). The increase in caspase 9 activity due to Pat and the positive control (Aza) was only significant at higher concentration (20  $\mu$ M). Pat, Cos and Ala caused the highest caspase 9-fold increase of 5, 4 and 4 respectively, while Deh and Aza caused the lowest fold increase of 3. In OVCAR-4, Deh, Ala and the positive control were the only compounds that significantly increased caspase 9 activity, with Ala causing the highest caspase activity with 4-fold increase, while

Pat and Cos do not significantly increase caspase activity in OVCAR-4 cell line. The caspase 9 activity by Deh was comparably similar to that of the positive control (Aza).

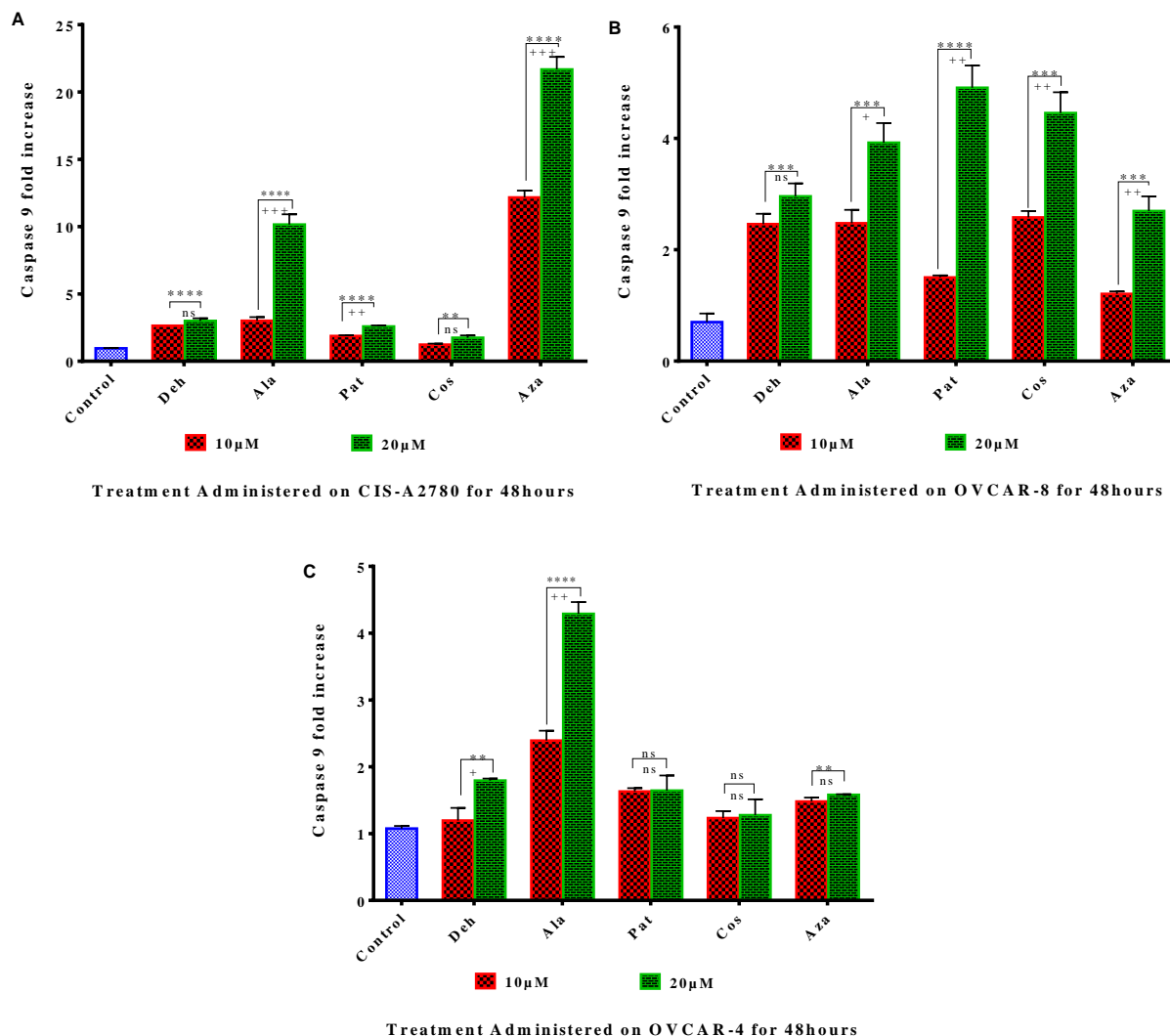


**Figure 5. 11: Effect of four SLs (Deh, Pat, Cos and Ala) on caspase 9 activity in ovarian cancer cell: CIS-A2780 (A), OVCAR-8 (B) and OVCAR-4 (C).** The standard drug (Aza) was used as positive control. Data were presented as mean  $\pm$  SEM (=3) and analysed using one-way ANOVA to compare the caspase activity of each compound with the control and the significance difference is denoted with asterisk (\*). Student T test was used to test for concentration dependent activity of each compound and the significant difference is denoted with plus (+). (\*,  $p < 0.05$ , \*\*,  $p < 0.01$ , \*\*\*,  $p < 0.001$  and \*\*\*\*,  $p < 0.0001$ ).

### **5.2.8 Flow cytometry analysis of apoptosis using annexin V and propidium iodide**

Further evaluation of the proapoptotic activity of SLs (Deh, Pat, Cos and Ala) and Aza was studied on CIS-A2780 and OVCAR-8 cell lines (Figures 5.12 and 5.13) using flow cytometry analysis with annexin V and propidium iodide (PI). In CIS-A2780 cells, the results show that the four SLs (Deh, Pat, Cos and Ala,) and Aza induced significant apoptosis when compared with the control (Figure 5.14). The percentage of early and late apoptosis induced by Ala at 5 $\mu$ M (25.4% and 36.7%) and 10  $\mu$ M (8.3% and 64.1%) respectively, were higher than that of Deh at 5 $\mu$ M (14.2% and 10.9%) and 10  $\mu$ M (16.3% and 27.5%), Pat at 10  $\mu$ M (11.0% and 10.4%) and 20  $\mu$ M (26.6% and 30.0%) and Cos at 10  $\mu$ M (13.7% and 9.0%) and 20  $\mu$ M (21.4% and 49.4%) respectively. Furthermore, the percentage of apoptosis induced by Ala and Cos was relative to that of the positive control (Aza) at 5 $\mu$ M (13.8% and 63.3%) and 10  $\mu$ M (13.1% and 68.7%) respectively. The result further shows that only Pat and Cos showed concentration dependent apoptotic activity in CIS-A2780. In a similar manner, the four SLs (Deh, Pat, Cos and Ala,) and the positive control (Aza) showed significant apoptotic activity when compared with the control (Figure 5.14). Ala induced the highest percentage of apoptosis (early and late apoptosis) at 5 $\mu$ M (39.8% and 38.8%) and at 10  $\mu$ M (18.2% and 73.2%) than that of other SLs (Pat at 10  $\mu$ M (30.6% and 25.6%) and 20  $\mu$ M (34.3% and 41.4%), and Cos at 10  $\mu$ M (35.8% and 21.5%) and 20  $\mu$ M (29.2% and 44.5%) respectively, and the positive control (Aza) at 5  $\mu$ M (40.8% and 37.7%) and 10  $\mu$ M (32.7% and 48.2%). While Deh induced the lowest percentage of apoptosis at 5  $\mu$ M (31.7% and 23.1%) and 10  $\mu$ M (30.6% and 28.4%) in OVCAR-8. Furthermore, the apoptotic activity of the four SLs (Deh, Pat, Cos and Ala) and Aza was not concentration dependent.

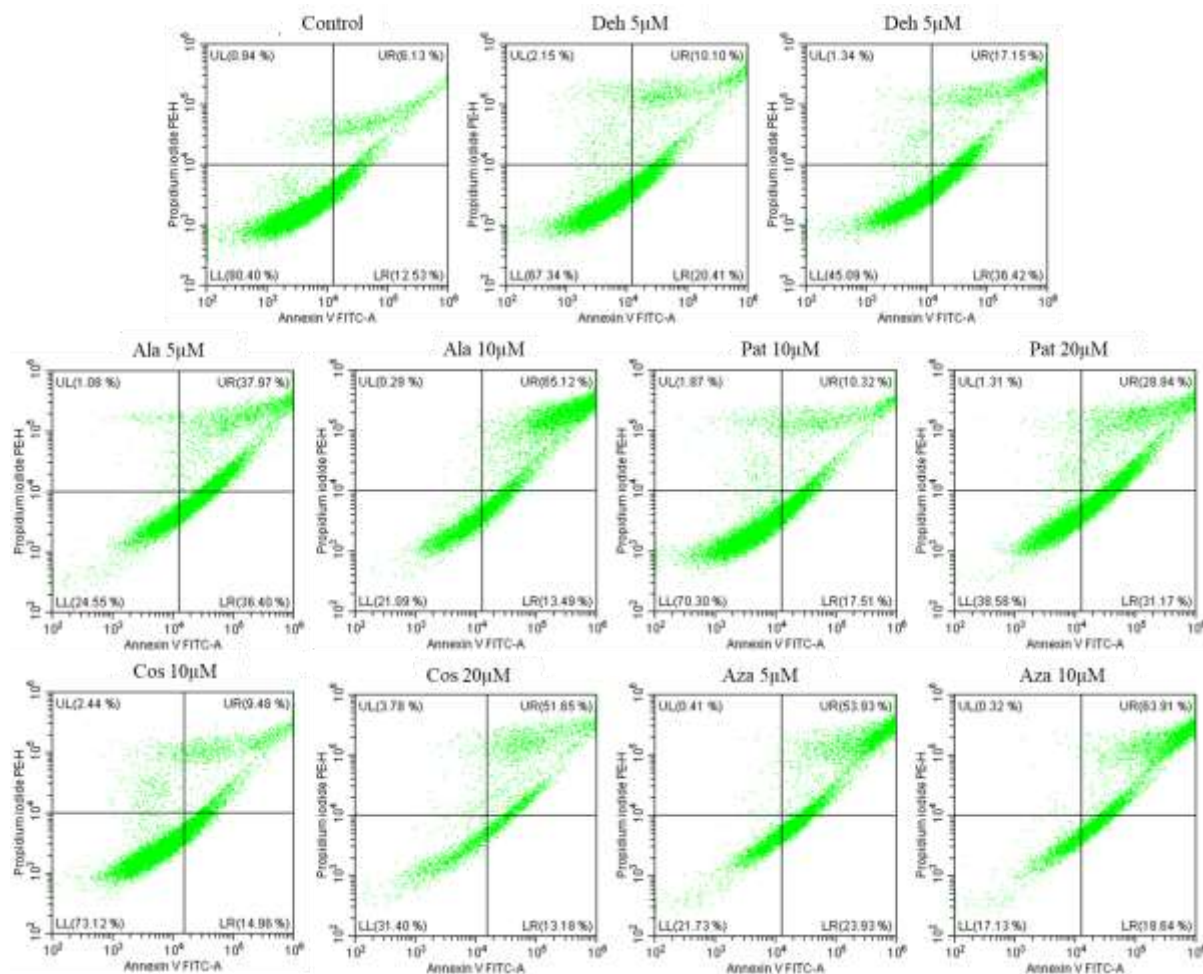


**Figure 5. 12: Representative samples of flow cytometry graph of CIS-A2780 cell line treated with four SLs (Deh, Pat, Cos and Ala) and Aza, and stained with annexin V and propidium iodide. Lower left (LL), upper left (UL), lower right (LR) and upper right (UR) represent live cells, necrotic cells, cells in early apoptosis and cells in late apoptosis respectively.**

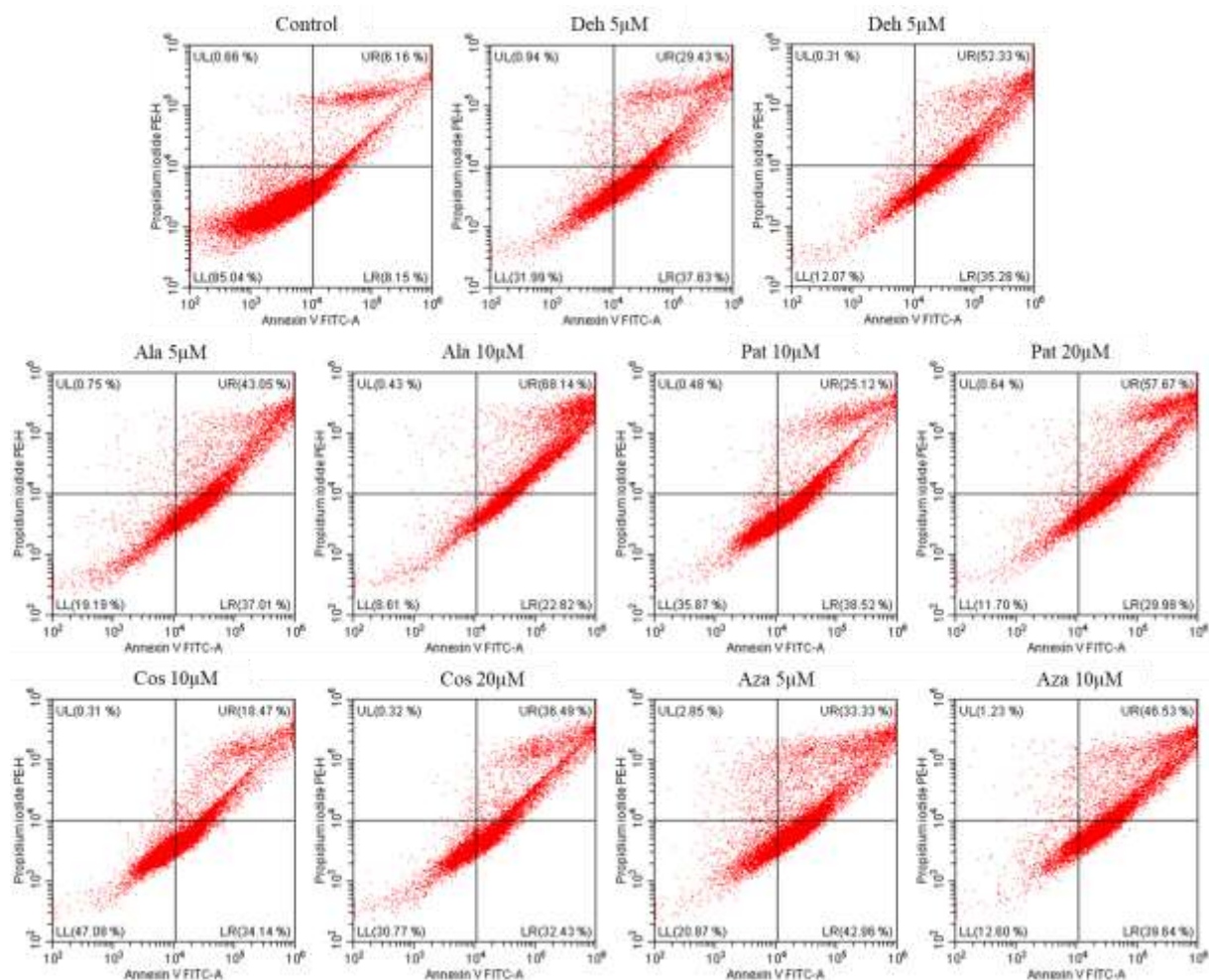
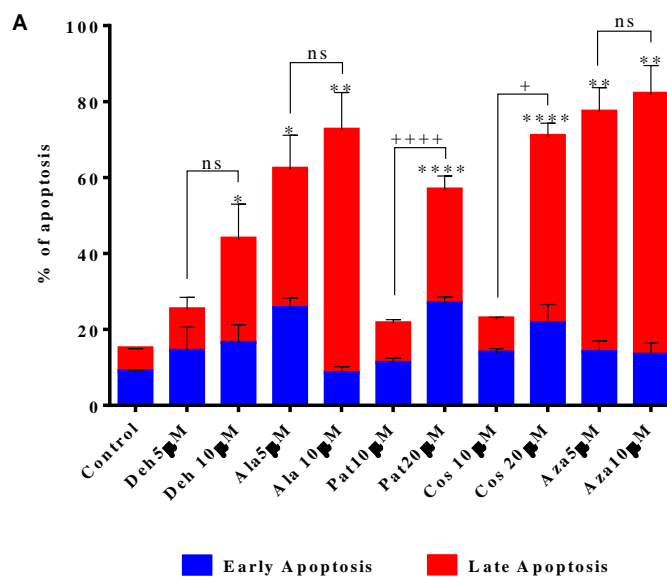
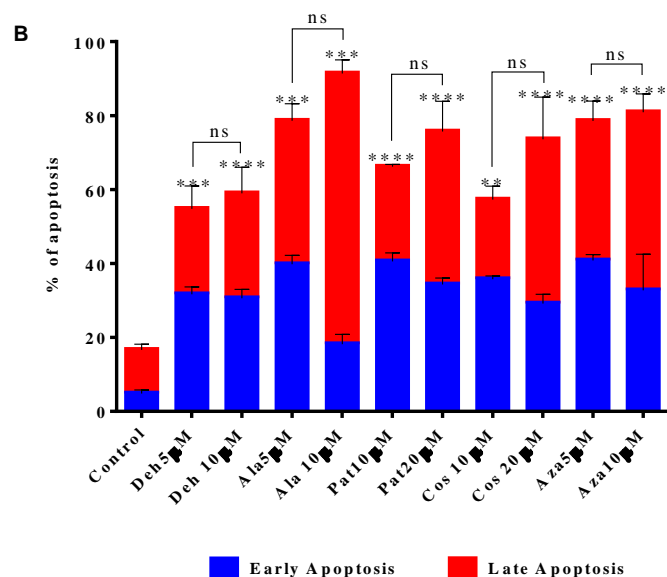


**Figure 5. 13: Representative samples of flow cytometry graph of OVCAR-8 cell line treated with SLs (Deh, Pat, Cos and Ala) and the positive control (Aza) using annexin V and propidium iodide staining. Lower left (LL), upper left (UL), lower right (LR) and upper right (UR) represent live cells, necrotic cells, cells in early apoptosis and cells in late apoptosis respectively.**



Analysis of apoptosis in CIS-A2780 cell line



Analysis of apoptosis in OVCAR-8 cell line

**Figure 5. 14: Flow cytometry analysis of the apoptotic activities of SLs (Deh, Pat, Cos and Ala) and Aza using annexin V and propidium iodide staining.** The data represent the mean  $\pm$  SD of three repeated experiments. The apoptotic activity of each compound was compared with the control using one-way ANOVA with Dunnett's multiple comparisons test denoted with asterisk (\*) and student T test was used to test for concentration dependent activity denoted with plus (+). (\*,  $p < 0.05$ , \*\*,  $p < 0.01$ , \*\*\*,  $p < 0.001$  and \*\*\*\*,  $p < 0.0001$ ).

### **5.2.9 Mitochondrial membrane potential activities of SLs and Aza**

Disruption of the mitochondrial potential is an important step towards the release of cytochrome *c* into the cell cytoplasm, which is capable of activating the downstream of intrinsic apoptotic pathway. The role of the four SLs (Deh, Pat, Cos and Ala) and Aza on the cell mitochondrial membrane potential activity was investigated using mitoprobe™ DiIC1(5) assay. This dye is capable of accumulating in the mitochondrial of cells with active membrane potential. The quantitative measure of the accumulated dye in the cell is relative to the activeness of the mitochondrial potential of the cell. The level of decrease in the accumulated dye in CIS-A2780 cell line in response to drug treatment was quantitatively measured using flow cytometry (Figure 5.15). The result shows that Ala, Cos and the positive control (Aza) significantly reduced the intensity of accumulated DiIC1 (5) stain in CIS-A2780 when compared with the control. The mitochondrial membrane potential activity of Ala and Cos was only significant at higher concentration while the mitochondrial potential activity of the positive control (Aza) was significant at both concentrations (Figure 5.16). The positive control showed higher mitochondrial membrane potential activity than the SLs, by reducing the accumulation of the DiIC1(5) dye to 25.74%. Ala and Cos reduced the accumulation of the dye to 65.3% and 81.5% respectively, while Deh and Pat reduced it to 79.2% and 83.4% respectively, but their mitochondrial membrane potential activity was not significant when compared with the control. This suggest that Ala and Cos has higher mitochondrial membrane potential activity than Deh and Pat. Furthermore, the mitochondrial membrane potential activity of the four SLs (Deh, Pat, Cos and Ala) and the positive control (Aza) was not concentration dependent.

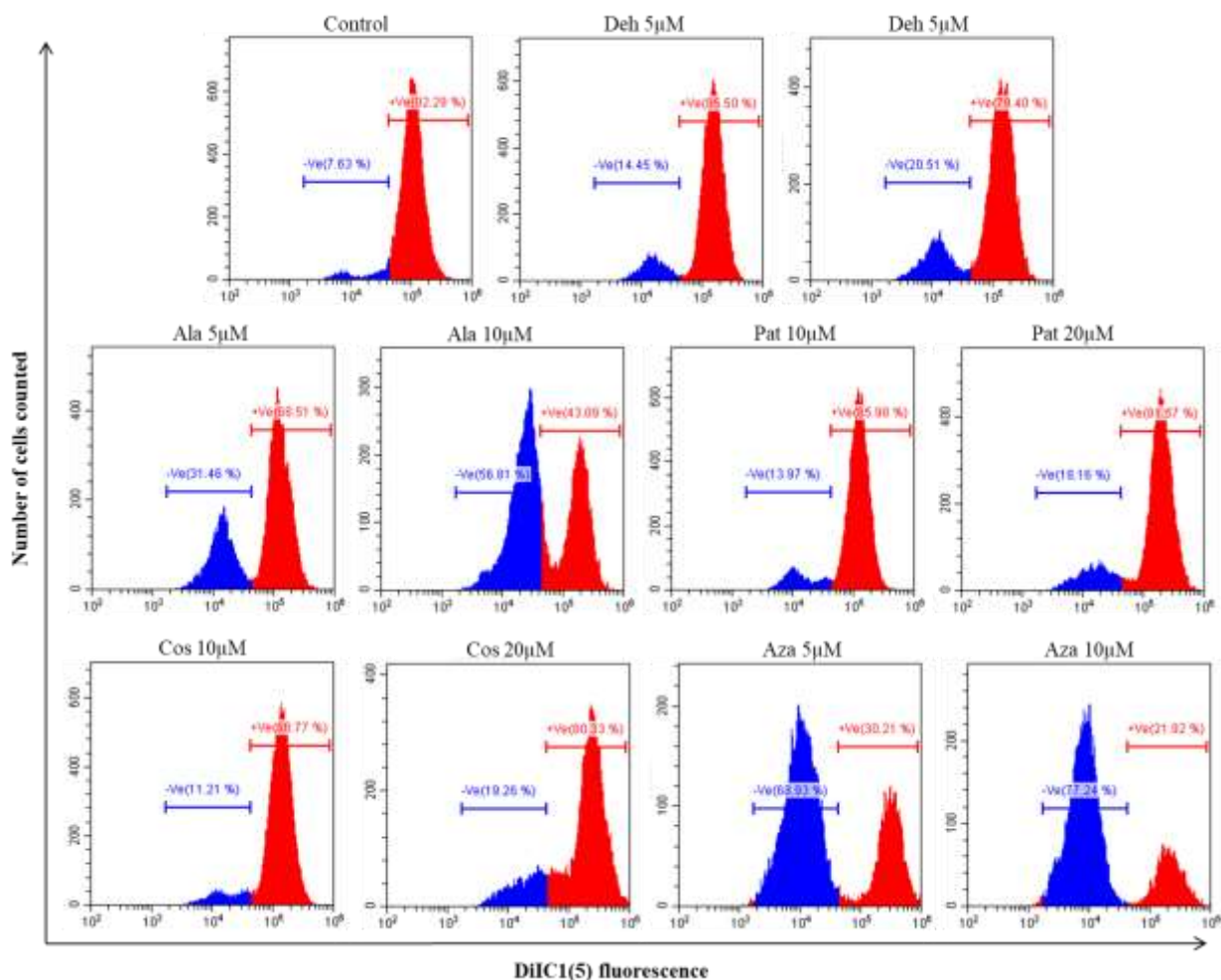
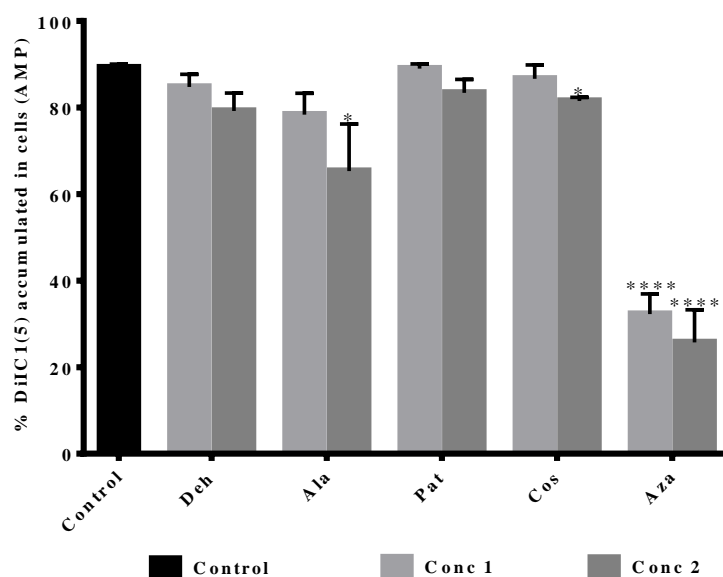


**Figure 5. 15:** Flow cytometry graph of representative samples of CIS-A2780 cell line treated with SLs (Deh, Pat, Cos and Ala) and Aza using DiIC1(5) staining. The red histogram (+Ve) represents intensity of accumulated DiIC1(5) stain in cells (intact/active mitochondrial membrane potential) while the blue histogram (-Ve) represents reduction in the DiIC1(5) accumulated within the cell (disrupted mitochondrial membrane potential).



Treatment Administered on CIS-A2780 for 48hours

**Figure 5. 16: Flow cytometry analysis of the mitochondrial membrane potential activity of the four SLs (Deh, Pat, Cos and Ala) and Aza in CIS-A2780 ovarian cancer cell line using DiIC1 (5) stain.** Conc 1 and 2 are 5 and 10  $\mu$ M respectively for Deh, Ala and Aza, and 10 and 20  $\mu$ M for Pat and Cos. The data represent the mean  $\pm$  SD (n=3). Further analysis was done using one-way ANOVA with Dunnett's multiple comparisons test, and the significant level is denoted with asterisk (\*). (\*,  $p < 0.05$ , \*\*,  $p < 0.01$ , \*\*\*,  $p < 0.001$  and \*\*\*\*,  $p < 0.0001$ ).

#### 5.2.10 Cell cycle analysis of ovarian cancer cell lines in response to SLs treatment

Basically, apoptosis and cell cycle are major mechanisms that regulate cell proliferation. The roles of the four SLs (Deh, Pat, Cos and Ala) and Aza have been well investigated in this study. Therefore, to further elucidate the mechanism of anti-cancer activities of these compounds, their roles in the cell cycle arrest was investigated on ovarian cancer cell lines (CIS-A2780 and OVCAR-8) after 48 hrs treatment using propidium iodide (PI) followed by flow cytometry analysis. In CIS-A2780 cell line, the results show that the four SLs (Deh, Pat, Cos and Ala) and the positive control (Aza) significantly reduced the percentage of cells

at the G<sub>0</sub>-G<sub>1</sub> phase when compared with the control. Additionally, Ala, Cos and Aza reduced the percentage of cells in the G<sub>0</sub>-G<sub>1</sub> phase at both lower and higher concentrations while Deh and Pat only reduced it at higher concentration (Figure 5.19). Deh, Pat, Cos and Ala arrested cells at both S and G<sub>2</sub>-M phase, while Aza strongly caused cell cycle arrest at S phase. Ala, Pat, Cos and the positive control (Aza) significantly increased the percentage of cells in the subG<sub>1</sub> phase, this result was consistent with the apoptosis assay results. In the same manner, further significant reduction in the percentage of cells at G<sub>0</sub>-G<sub>1</sub> was also observed in OVCAR-8. In this cell line, multiple comparison test further shows that the cell reduction at the G<sub>0</sub>-G<sub>1</sub> phase caused by Pat, Cos, Ala and the positive control (Aza) was significant at both lower and higher concentrations, while the activity of Deh was only significant at higher concentration. Pat, Cos and Ala further caused cell cycle arrest at both S and G<sub>2</sub>-M phases while Deh and Aza arrested cells at the G<sub>2</sub>-M phase (Figure 5.19). The effects of the four SLs (Deh, Pat, Cos and Ala) and the positive control (Aza) was consistent in both CIS-A2780 and OVCAR-8 cell lines. However, the cells in the subG<sub>1</sub> phase was only increased by Ala and Cos in OVCAR-8 cells.

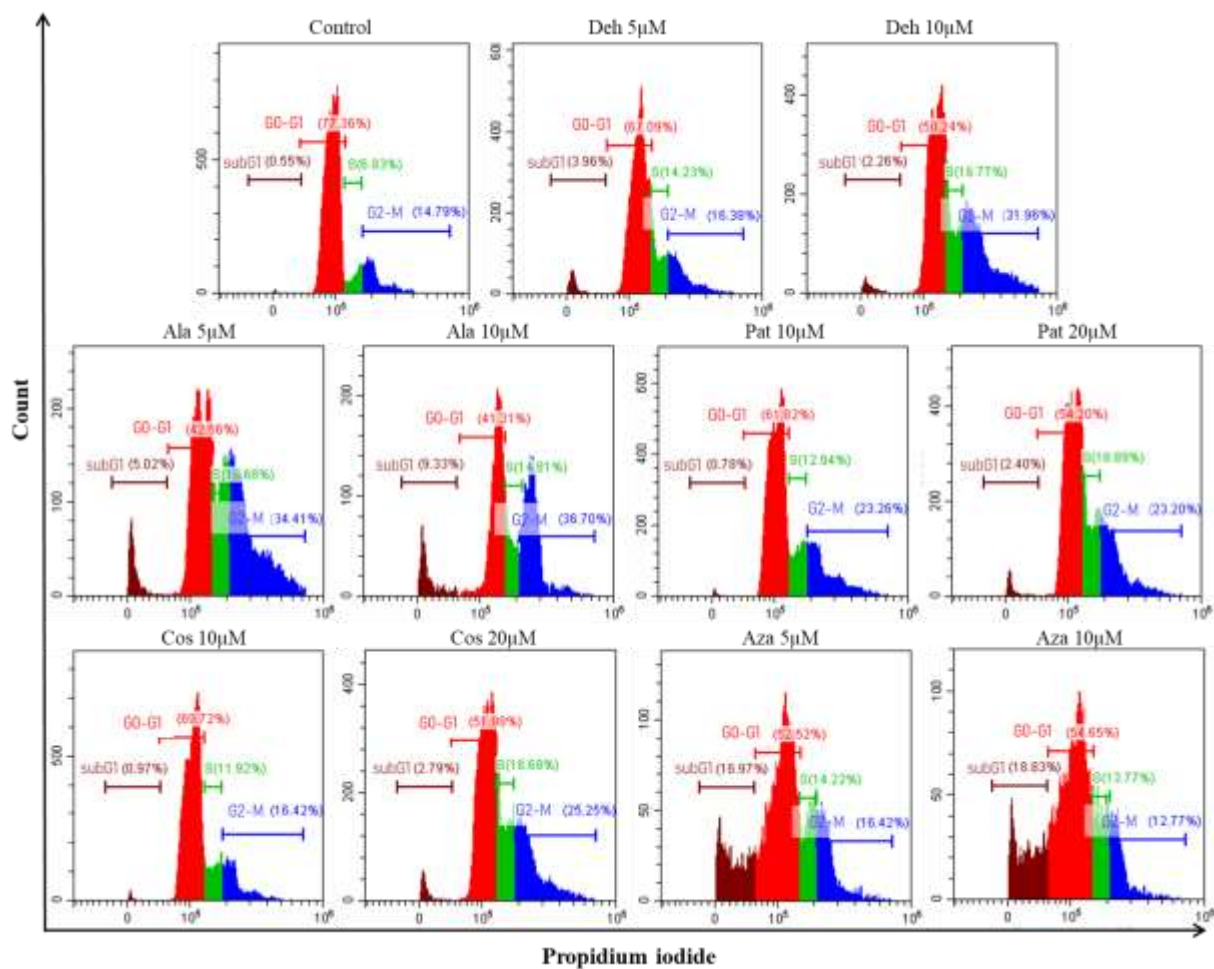


**Figure 5. 17: Representative samples of flow cytometry graph of the cell cycle effects of SLs (Deh, Pat, Cos and Ala) and Aza on CIS-A2780 cells using propidium iodide staining.**

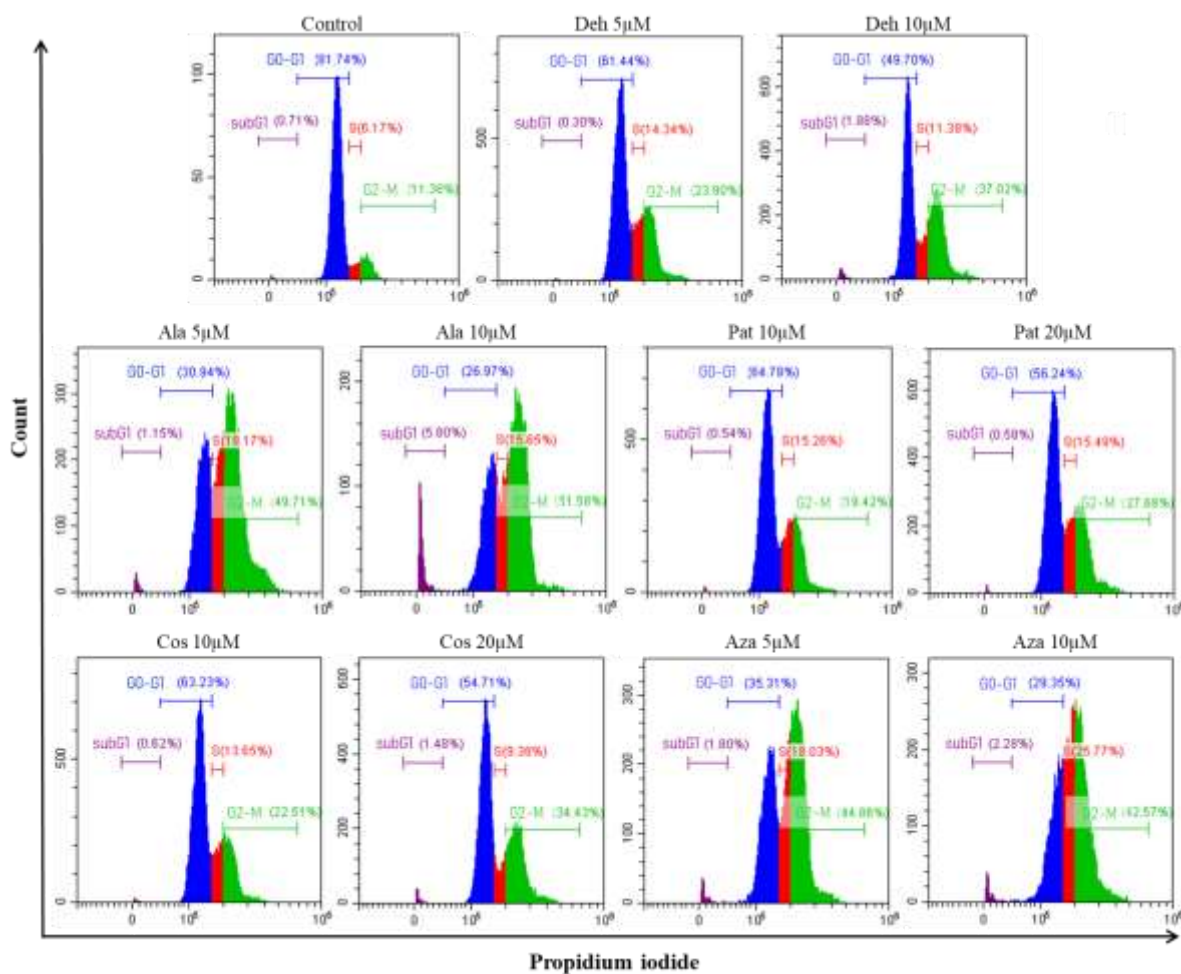
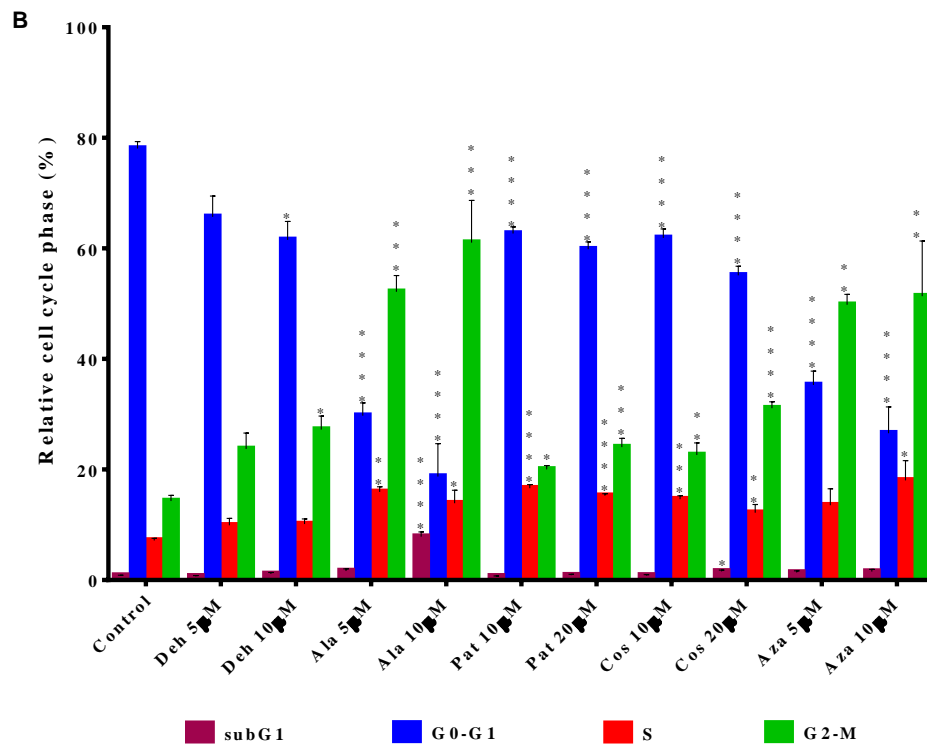
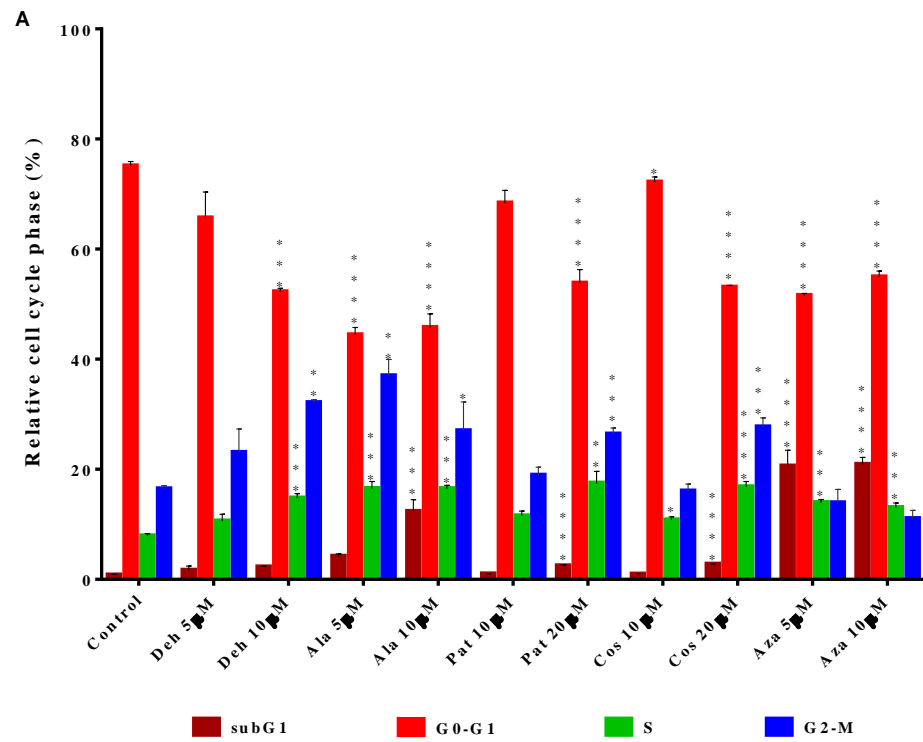


Figure 5. 18: Representative samples of flow cytometry graph of the cell cycle effects of SLs (Deh, Pat, Cos and Ala) and the positive control (Aza) on OVCAR-8 cells using propidium iodide staining.



**Figure 5. 19: Flow cytometry analysis of the cell cycle activity of SLs (Deh, Pat, Cos and Ala) and Aza on CIS-A2780 cell line (A) and OVCAR-8 cell line (B) using**

**propidium iodide staining.** The data represent the mean  $\pm$  SD of three repeated experiments. The cell cycle effects of each compound at the three individual phases were compared with the control using one-way ANOVA with Dunnett's multiple comparisons test, and the significant level is denoted with asterisk (\*). (\*,  $p < 0.05$ , \*\*,  $p < 0.01$ , \*\*\*,  $p < 0.001$  and \*\*\*\*,  $p < 0.0001$ ).

### **5.2.11 Quantification of Global 5-methylcytosine DNA Methylation**

The roles of four SLs (Deh, Pat, Cos and Ala) on global 5-methylcytosine DNA methylation were studied on CIS-A2780 and OVCAR-4 cell lines. Briefly, DNA extracted from cells treated with each of the compounds and the positive control was used as the starting material for the DNA methylation assay. Total DNA methylation in each sample was quantified using ELISA based kit. The optimal standard curve was generated with 5-mC standard control (Figure 3.27 presented in chapter 3), and the percentage of global DNA methylation was calculated according to the manufacturer's procedure. In CIS-A2780 cells, the result shows that Deh, Pat, Cos and Ala significantly reduced the level of 5-mC in the cell when compared with the control using one-way ANOVA (Figure 5.20). The positive control (Aza) also significantly reduced the level of 5-mC in CIS-A2780 cells. However, Deh and Pat induced higher DNA demethylation than Cos and Ala. Furthermore, Deh, Ala and Cos reduced the level of 5-mC in OVCAR-4 significantly when compared with the control. The positive control (Aza) and Pat also reduced 5-mC in the cells. However, the 5-mC activity of Pat and the positive control (Aza) was not significant when compared with the control.

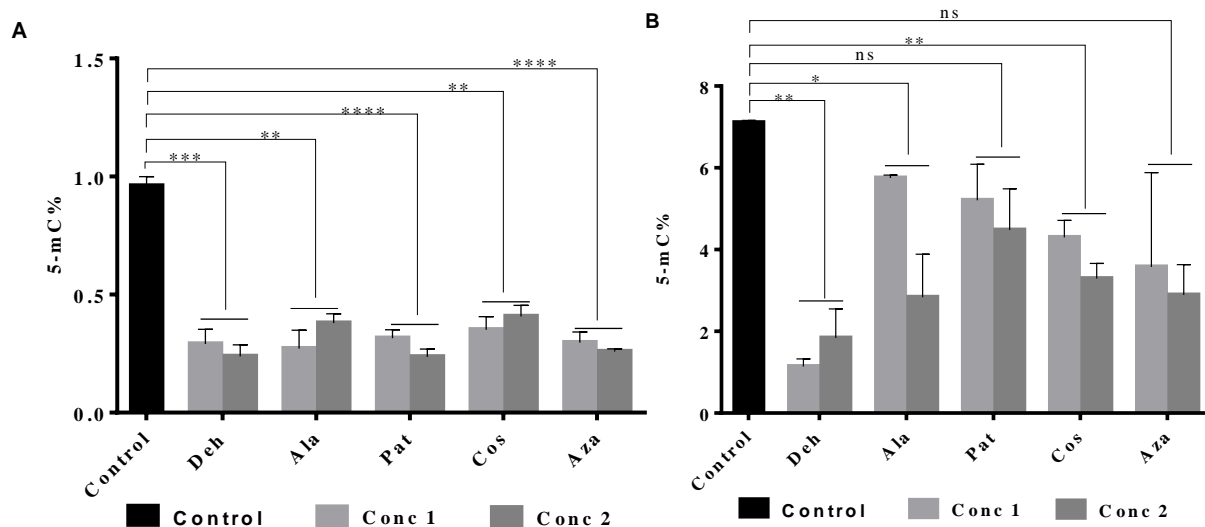


**Figure 5. 20: Quantification of 5-methylcytosine DNA methylation in ovarian cancer cells, CIS-A2780 (A) and OVCAR-4 (B) treated with the SLs (Deh, Pat, Cos and Ala). Aza was used as positive control and media was used as negative control (without drug). Conc 1 (low) and 2 (high) are 5 and 10 $\mu$ M respectively for Deh, Ala and Aza, and 10 and 20  $\mu$ M respectively for Pat and Cos. The percentage of 5-mC was presented as 5-mC/(5-mC+C). The percentage of 5-mC of the control was compared with each drug treated cells using one-way ANOVA, and the significant level was denoted with asterisk (\*). (\*,  $p < 0.05$ , \*\*,  $p < 0.01$ , \*\*\*,  $p < 0.001$  and \*\*\*\*,  $p < 0.0001$ ).**

### 5.2.12 Quantitative assessment of change in gene specific promoter methylation in response to treatment with SLs using pyrosequencing assay

Change in the methylation profile of different tumour genes (*MLH1*, *HOXA9* and *TP53*) at the CpG sites in response to SLs and Aza treatment was evaluated using pyrosequencing technique. Briefly, DNA was extracted from CIS-A2780 cell pellets collected from cells treated for 72 h with different concentrations of each tested compounds. The isolated DNA samples were bisulfite converted and amplified using PCR. The PCR amplified bisulfite converted DNA samples were used as template for the pyrosequencing assay. The data

generated were arranged and the percentage of methylation at the CpG sites was calculated for each gene. The level of significant change in gene specific CpG methylation in response to SLs treatment compared with the control was tested using one-way ANOVA. The results show that Deh and Ala reduced the CpG methylation at the promoter region of *MLH* (Figure 5.21). Furthermore, the CpG methylation level of the of the promoter region of *HOXA9* was significantly reduced by Pat and the positive control. Additionally, Pat and Cos significantly reduced the CpG methylation level of *TP53* gene. Deh and the positive control slightly reduced the CpG methylation level of *TP53*, but the result was not significant when compared with the control (Figure 5.21).

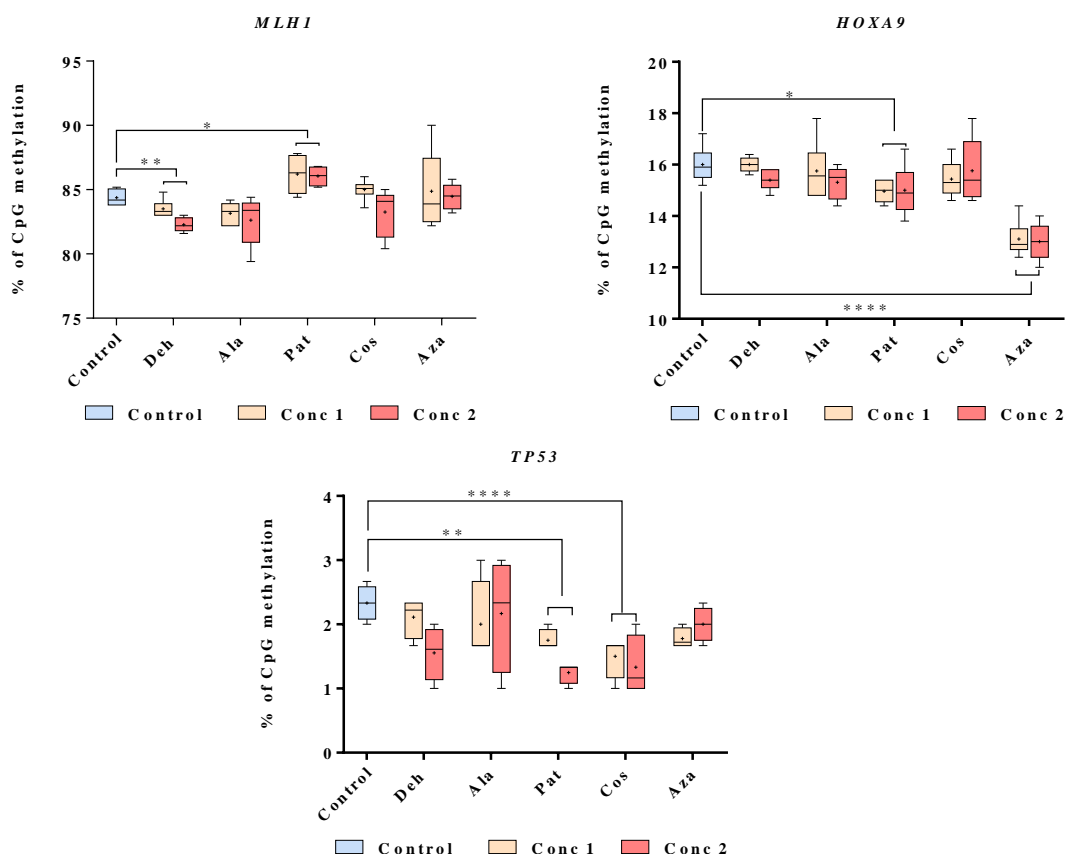


**Figure 5. 21: Percentage of gene specific promoter methylation of ovarian cancer cell line (Cis-A2780) in response to drug treatment, using 5’azacytidine as positive control.** Conc 1 and 2 are 5 and 10 $\mu$ M for Deh, Ala and Aza respectively, and 10 and 20 $\mu$ M for Pat and Cos. Results are presented as mean  $\pm$ SD of three repeats in duplicate. Significant

different between each compound activity compared with the control is denoted with asterisk (\*). P- Value < 0.05 (\*) and < 0.01 (\*\*).

**MLH1 Gene**

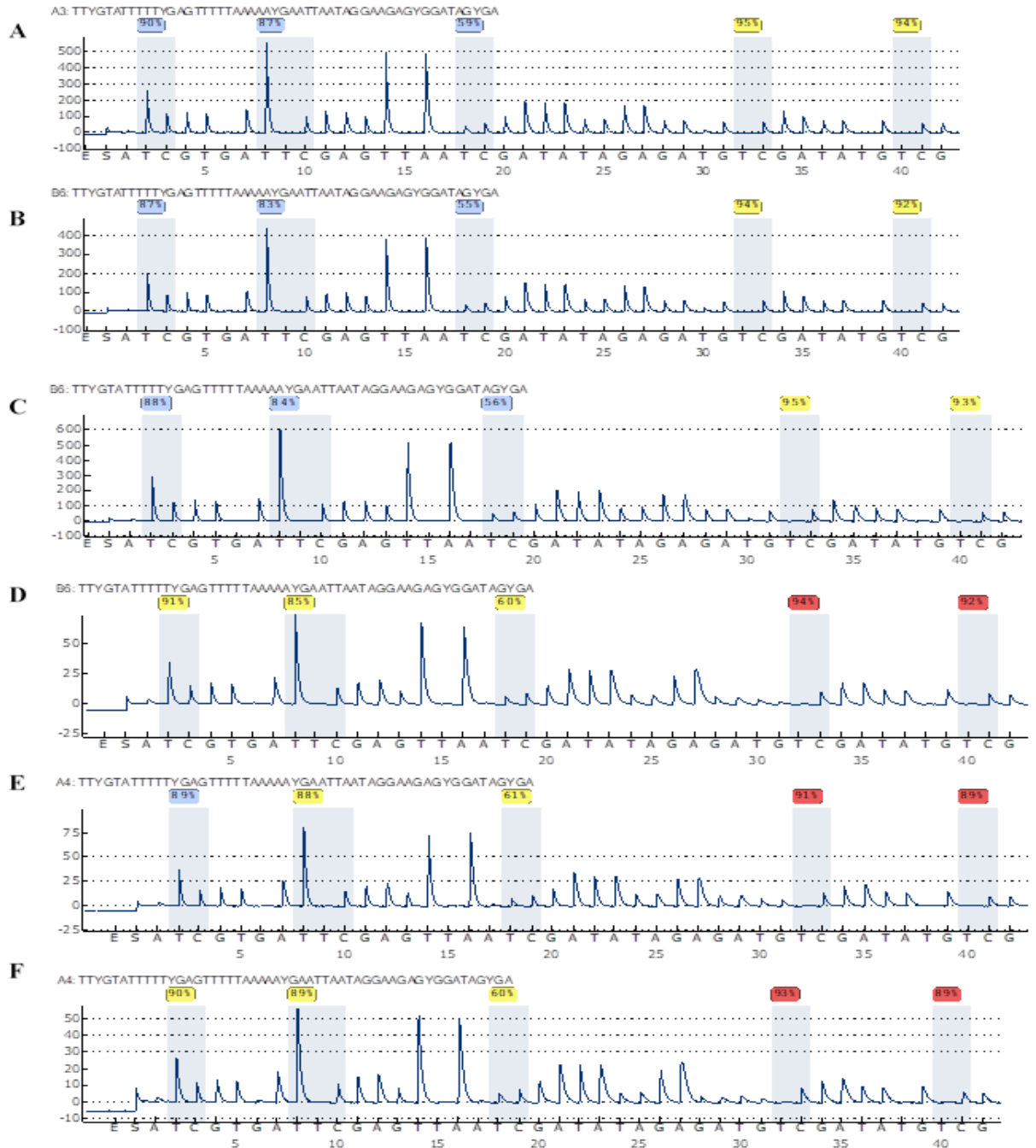


**Figure 5. 22: Representative samples of pyrosequencing CpG pyrogram report for MLH1 gene on CIS-A2780 cell line. Control (A), Deh (B), Ala (C), Pat (D), Cos (E) and Aza (F).**

**HOXA9 Gene**

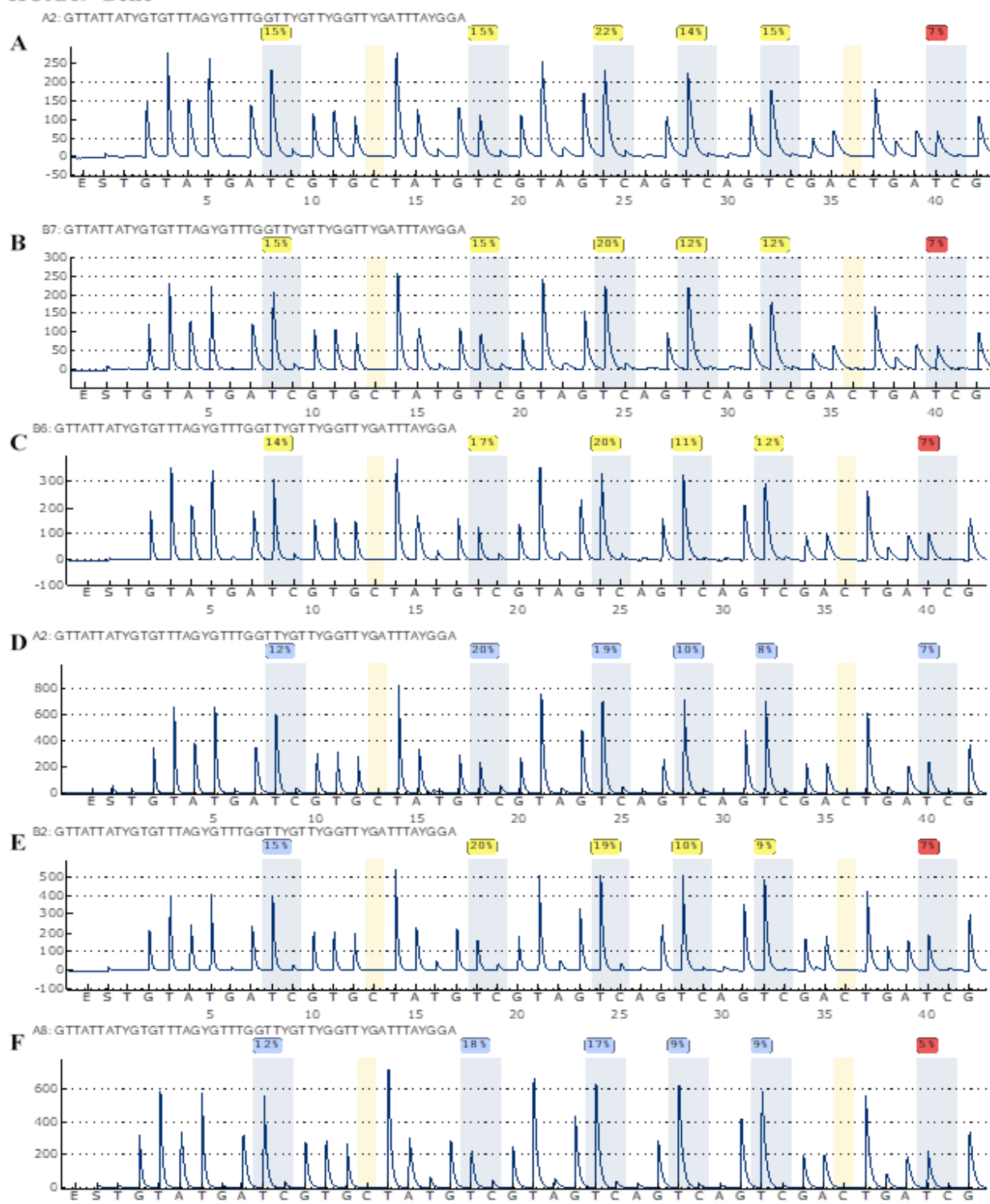


**Figure 5. 23: Representative samples of pyrosequencing CpG pyrogram report for HOXA9 gene on CIS-A2780 cell line. Control (A), Deh (B), Ala (C), Pat (D), Cos (E) and Aza (F).**

**TP53 Gene**

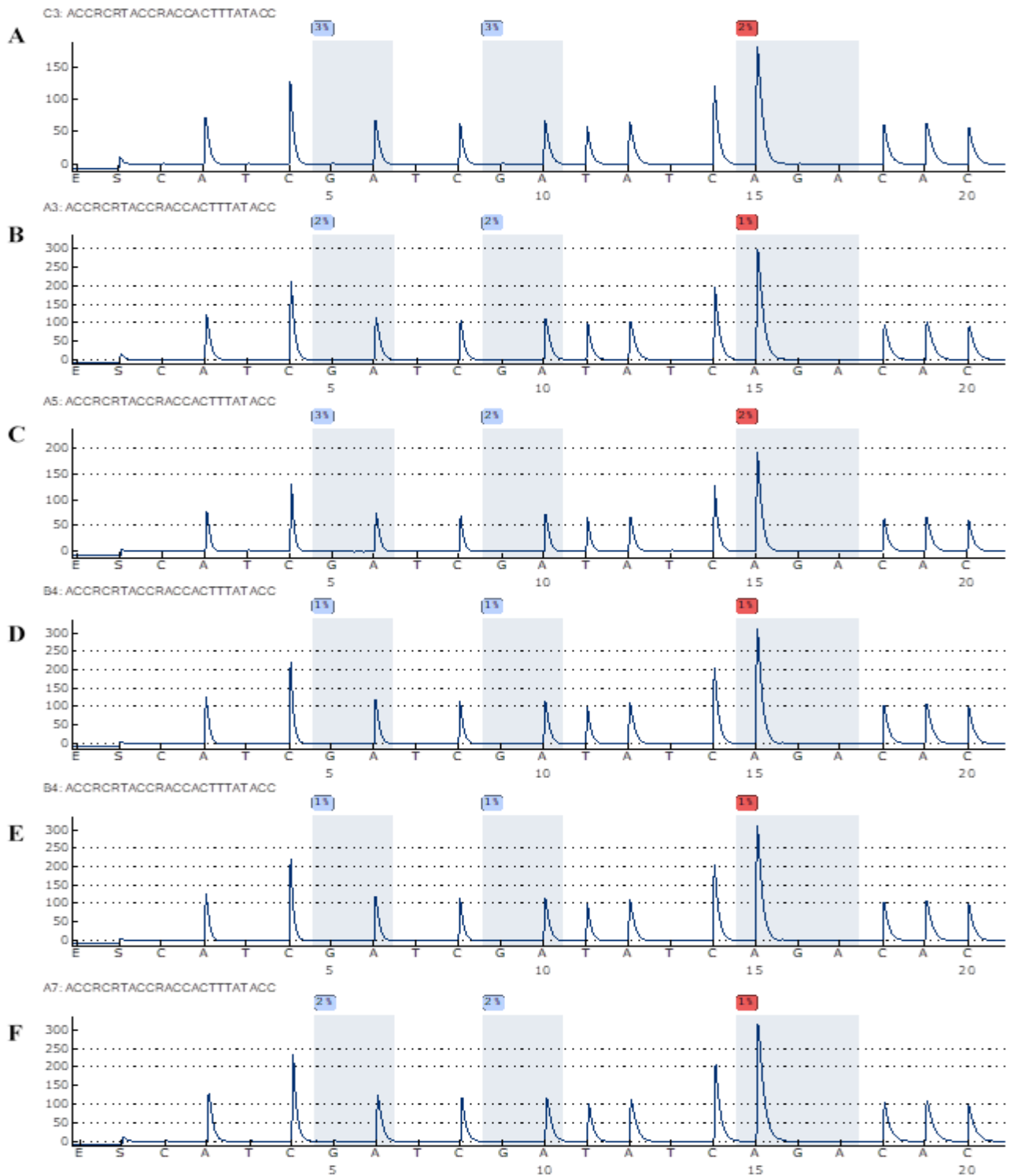


**Figure 5. 24: Representative samples of CpG pyrogram report for TP53 gene on CIS-A2780 cell line. Control (A), Deh (B), Ala (C), Pat (D), Cos (E) and Aza (F).**

### 5.2.13 DNMT inhibitory activities of SLs and Aza

DNMTs play key roles in DNA methylation, therefore down regulation of DNMTs is an important step towards DNA demethylation. The DNMT inhibitory activity of SLs was investigated on ovarian cancer cell lines (CIS-A2780 and OVCAR-4) using colorimetric assay. In brief, nuclear proteins were extracted from CIS-A2780 and OVCAR-4 cell pellets collected from cultured cells. The nuclear proteins were quantified using standard Bradford protein measurement assay (Figure 5.25). The DNMT inhibitory activities of the four SLs (Deh, Pat, Cos and ala) and Aza were quantified using ELISA based technique. The results presented in Figure 5.26 show that Pat and the positive control (Aza) significantly inhibited the enzymatic activity of DNMT in CIS-A2780 cell line, while a slight inhibitory activity was also found in Deh and Ala treated samples, but no significant difference was observed when compared with the control. Furthermore, Deh, Ala, Cos and Pat including the positive control (Aza) significantly inhibited the enzymatic activity of DNMT in OVCAR-4. Additionally, there was not major difference in the DNMT inhibitory enzymatic activity of Deh, Pat, Ala and the positive control (Aza), while Cos showed the least inhibitory activity.

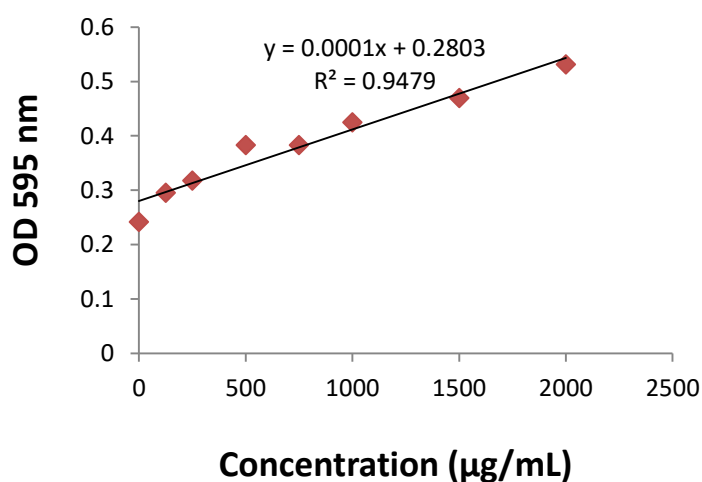


**Figure 5. 25: Bradford protein standard curve generated with bovine serum albumin (BSA).**

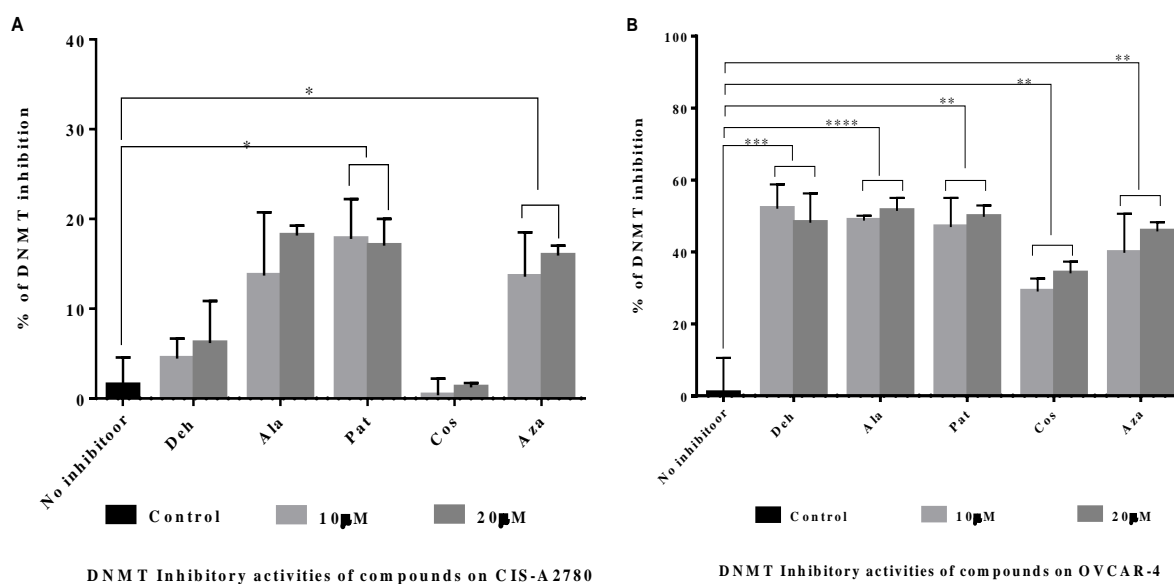


**Figure 5. 26: DNMT inhibitory activities of the SLs (Deh, Pat, Cos and Ala) on CIS-A2780 (A) and OVCAR-4 (B) cell lines. 5'azacytidine which is a known DNMT inhibitor was used as positive control. Results were presented as mean  $\pm$  SD (n=3). The DNMT inhibitory activity of each compound was compared with the control using one-way ANOVA, and the significant level is denoted with asterisk (\*).  $p$  value  $< 0.05$  (\*),  $< 0.01$  (\*\*),  $< 0.001$  (\*\*\*) and  $< 0.0001$  (\*\*\*\*).**

#### 5.2.14 Quantitative evaluation of change in gene expression using quantitative reverse transcription polymerase chain reaction ((RT-qPCR)

RT-qPCR was performed to quantitatively measure the down and up-regulatory effects of SLs (Deh, Pat, Cos and Ala) and Aza on *DNMTs* and other tumour genes (Tumour protein p53 (*TP53*), mutL homolog 1 (*MLH1*), phosphatase and tensin homolog (*PTEN*), breast cancer type 1 susceptibility gene (*BRCA1*), folate receptor 1 (*FOLR1*), tumour suppressor candidate 3 (*TUSC3*), kruppel like factor 6 (*KLF6*) and WNT signalling pathway regulator (*APC*) expression in ovarian cancer using CIS-A2780 as a model cell line. Briefly, RNA was isolated from cell pellets treated with different tested compounds. Experiments were performed in three repeats, and the mRNA expression was calculated with the cycle

threshold (Ct) values using *GAPDH* as an internal control gene (housekeeping gene) to normalize the variations in gene expression. Data generated were graphically presented and analysed using one-way ANOVA. The results show that Ala significantly downregulated the expression of *DNMT1*, *DNMT3B* and *DNMT3L* and slightly downregulated the expression of *DNMT3A* but this was not significant when compared with the control. Deh downregulated the expression of *DNMT3A* and *DNMT3B*. The expression of *DNMT3L* was downregulated by Cos, further downregulation in the expression of *DNMT1*, *DNMT3A* and *DNMT3B* was also observed in Cos treated cells but the results were not significant when compared with the control. Furthermore, Pat slightly downregulated the expression of *DNMT3A*, *DNMT3B* and *DNMT3B* but this was not significant when compared with the control. The positive control (Aza) significantly downregulated the expression of *DNMT1* and also showed slight *DNMT3A* activity (Figure 5.27). Deh significantly upregulated the expression of *PTEN* gene, and slightly increased the expression of *FOLR1* and *APC*. In a similar manner, Ala significantly upregulated the expression of *PTEN*, *APC*, *MLH1* and *KLF6*, and a slight upregulation of the expression of *BRCA1*, *TUSC3*, *TP53* and *FOLR1* was also observed (Figure 5.28). Furthermore, the expression of *BRCA1* and *PTEN* was upregulated by Pat, while a down regulation was also observed in *TUSC3*, *TP53* and *KLF6* expression. Aza caused a slight upregulation of *TP53* and *PTEN*, and significantly upregulated the expression of *APC* and *FOLR1*. Contrastingly, no significant up-regulatory activity was observed in Cos, but a slight increase in the expression of *BRCA1* is reported (Figure 5.28).

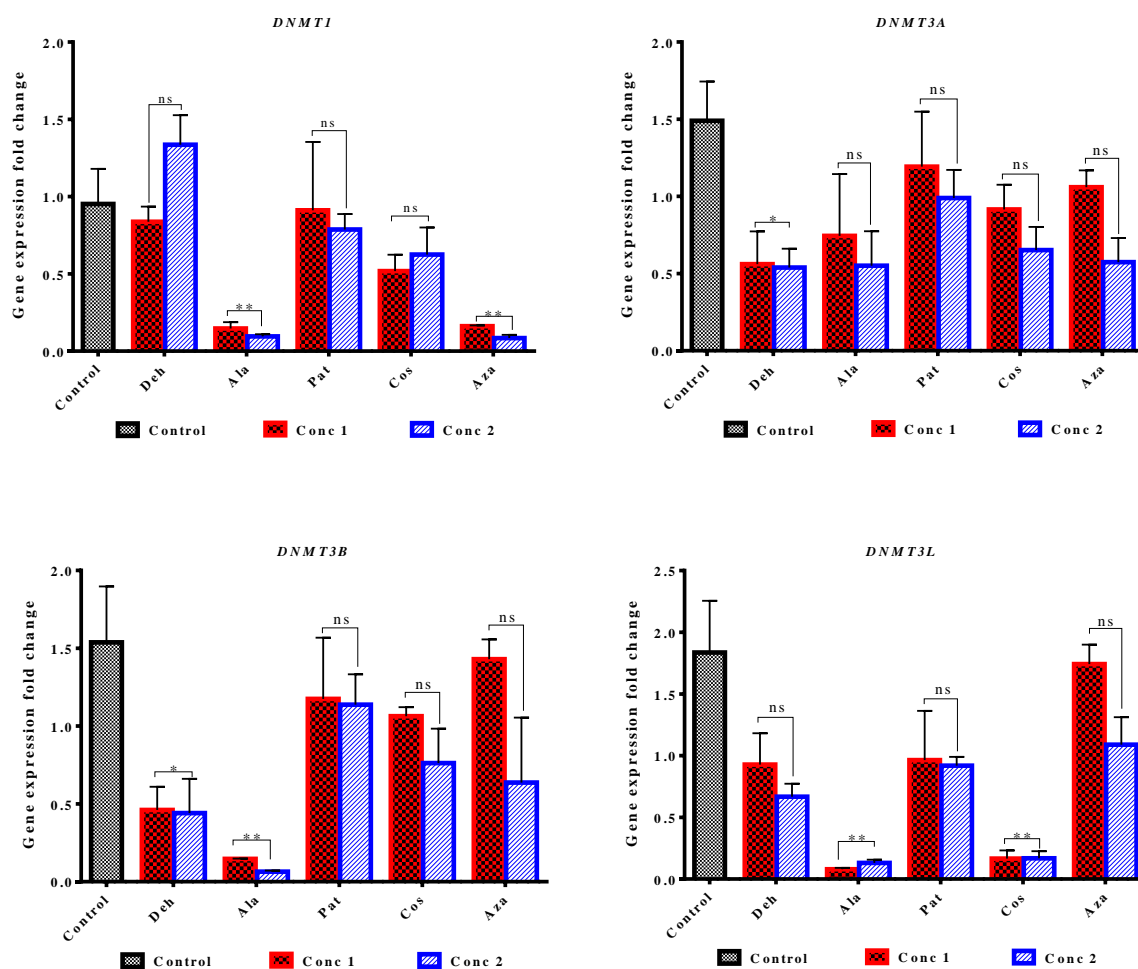


**Figure 5. 27: Modulation of DNMTs expression in response to treatment with SLs and Aza using RT-qPCR.** Results were presented as mean  $\pm$  SD (n=3). One-way ANOVA was used to test for significant difference in the expression level of each gene between control and drug treatment, and the significant difference is denoted with (\*). The significance level at  $p < 0.05$ ,  $p < 0.01$ ,  $p < 0.001$  and  $p < 0.0001$  are represented as (\*), (\*\*), (\*\*\*) and (\*\*\*\*) respectively.

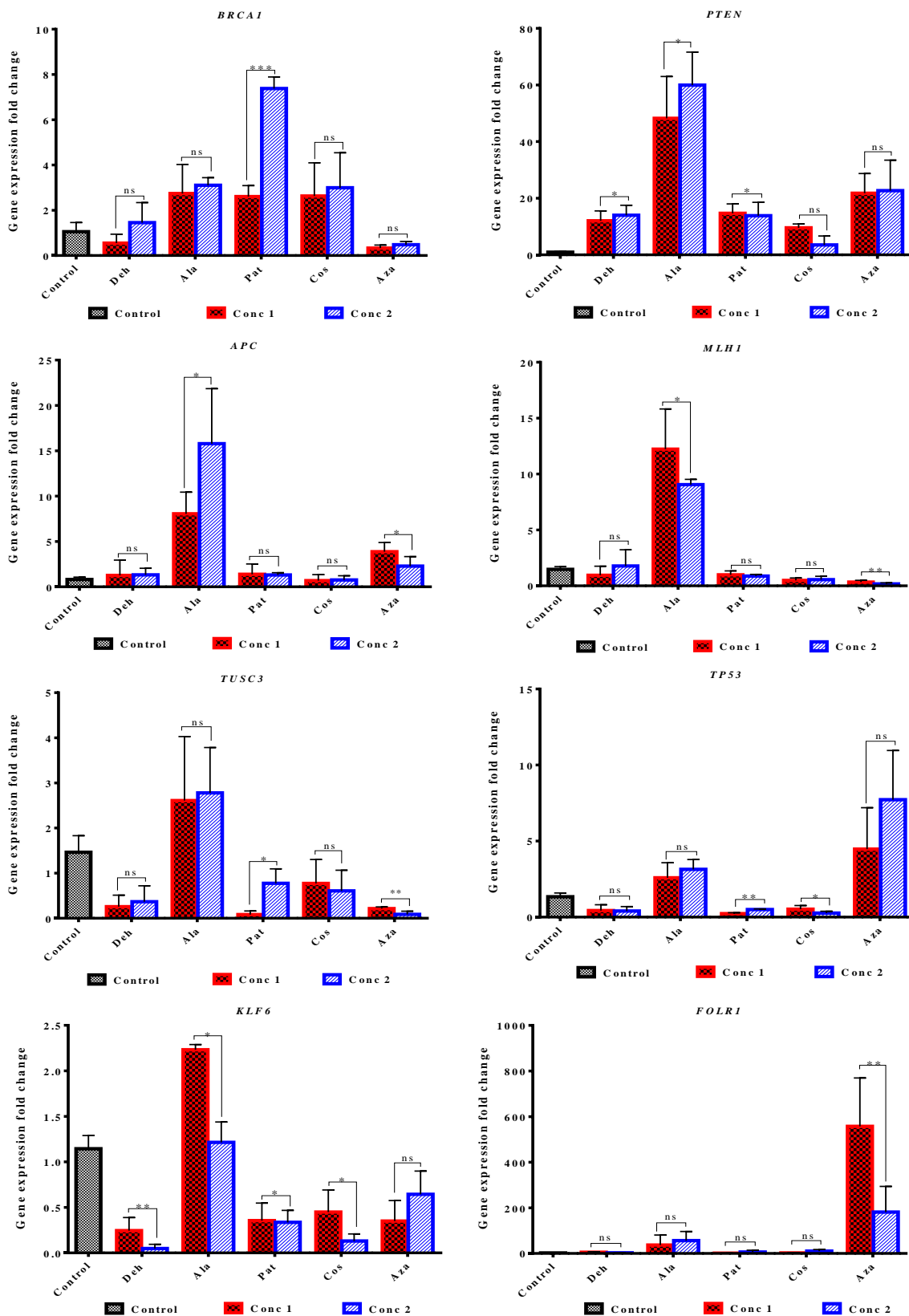


Figure 5. 28: Down and up-regulatory activities of SLs and Aza on the expression of tumour genes using RT-qPCR. Results were presented as mean  $\pm$  SD of three repeats.

Data were analysed using one-way ANOVA to test for significant difference in the expression level of each gene in the control and treated samples. The significant difference is denoted with (\*). The significance level at  $*p < 0.05$ ,  $**p < 0.01$ ,  $***p < 0.001$  and  $****p < 0.0001$ .

## **5.3 Discussion**

### **5.3.1 Effect of SLs on cell proliferation**

Resistance of ovarian cancer to standard treatment such as plant-derived chemotherapy is a big issue. Therefore, searching for novel drug candidate to overcome drug resistance is urgent. The anti-ovarian cancer activities of four SLs (Deh, Pat, Cos and Ala) were investigated in this study. The results from the SRB assay in this study clearly show that the four SLs and the positive control (Aza) have high growth inhibitory activity against ovarian cancer cell lines including cisplatin resistant cell line (CIS-A2780) with  $IC_{50}$  between 2.0-12.2 $\mu$ M. The four SLs inhibited the growth of CIS-A2780 and OVCAR-8 cells with lesser  $IC_{50}$  values (2.0-8.1 and 4.1-7.8  $\mu$ M respectively), but inhibited OVCAR-4 cells with slightly higher  $IC_{50}$  values (7.4-12.2  $\mu$ M), this suggests the possible cell line dependent activity of these compounds. Deh and Ala inhibited the growth of ovarian cancer cell lines at lower  $IC_{50}$  values (2.0-7.4 $\mu$ M) compared with Cos and Pat that inhibited growth at slightly higher  $IC_{50}$  values (5.7-12.2 $\mu$ M). The growth inhibitory activity of Deh on ovarian cancer cell lines reported in this study was similar to the reports of Ordóñez *et al.* (2016) on acute myeloid leukaemia and Costantino *et al.* (2013) on breast cancer. Similarly, the cytotoxic activity ( $IC_{50}$  value, 7.8-12.2 $\mu$ M) reported for Cos in this study was closely related to the report of Yang *et al.* (2011) (2.92-14.7 $\mu$ M), and the  $IC_{50}$  value of 11.8 $\mu$ M on human epidermoid carcinoma KB3-1 cells by Jeong *et al.* (2002). However, the result widely differs from the reported values (21.1- 27.6 $\mu$ M and 25  $\mu$ M) on A2780 and OAW42-A ovarian cell

lines by Barla *et al.* (2007) and Fang *et al.* (2019) respectively over a 48h treatment period. Also, Ala showed very high growth inhibitory activity with IC<sub>50</sub> values between 2.0-7.4µM against the ovarian cancer cell lines (CIS-A2780, OVCAR-8 and OVCAR-4). The IC<sub>50</sub> values reported for Ala against ovarian cancer cells in this study was similar to the IC<sub>50</sub> value (7µM) reported against human HepG2 cells by Kang *et al.* (2019). Its growth inhibitory activities have also been previously reported against lung squamous cancer (IC<sub>50</sub> value, 40µM) (Zhao *et al.*, 2015). Its cytotoxic activity against human glioblastoma and pancreatic cancer have also been reported (Wang *et al.*, 2017; He *et al.*, 2018). The result of the growth inhibitory activity of Pat reported in this study is similar to the report of Lin *et al.* (2017) that Pat inhibited the proliferation of non-small cell lung cancer cells with IC<sub>50</sub> value between 6.07 and 15.38µM. Liu *et al.* (2009) had reported that Pat inhibited growth in breast cancer cells with an IC<sub>50</sub> value of approximated 24µM. Li *et al.* (2018) had also reported that Pat inhibited the proliferation of drug resistance human gastric carcinoma cells and also sensitized it to cisplatin treatment. The anti-ovarian cancer activities of Aza reported in this study was lower when compared with its activity against lymphoid and colorectal cancers reported by Stresemann *et al.* (2006). Furthermore, the cytotoxic activities of the four SLs were found to be cancer specific, as they showed lesser cytotoxicity against immortalised human ovarian epithelial cells (HOE). Pat and Cos were shown to be less cytotoxic to HOE than Deh and Ala. Oka *et al.* (2007) had also demonstrated that Pat was more cytotoxic to tumour cell than normal cells, and this shows that its cytotoxic activity is more specific to cancer cells. In contrast, selectivity index of Aza was 1, which suggest that its cytotoxic activity was not cancer specific. The slight cancer specific activity of SLs might make them a better safer drug candidate than the positive control (Aza). Further evaluation of their cytotoxic activity using trypan blue exclusion cell viability testing revealed that the SLs (Deh, Pat, Cos and Ala) and the positive control reduced the

viability of CIS-A2780, OVCAR-8 and OVCAR-4 cells by causing significant cell death at concentration and time dependent manner. Ala and Deh induced higher cell death in the ovarian cancer (CIS-A2780, OVCAR-8 and OVCAR-4) cell lines than Pat and Cos, their cell death inducing activity was consistent with their SRB results which show that they had higher growth inhibitory activities against the ovarian cancer cells. The high cell death induced by Ala and Deh in concentration dependent manner is similar to the reports of Zhao *et al.* (2015) on lung cancer, Costantino *et al.* (2016) on melanoma and Bailon-Moscoco *et al.* (2015) against astrocytoma cells. Their chemical properties such as alkylating centre reactivity, side chain and lipophilicity and their molecular geometry have been suggested to be responsible for their high biological activities (Ghantous *et al.*, 2010).

### **5.3.2 Induction of apoptosis**

The anti-ovarian cancer activity of each of the four SLs (Deh, Pat, Cos and Ala) was investigated further, to establish their roles in the induction of cell death through programmed events (apoptosis). The apoptosis-inducing activity of the SLs and Aza was evaluated using flow cytometry analysis after cell staining with annexin V-FITC and PI. The result showed that the SLs (Deh, Pat, Cos and Ala) induced significant apoptosis in ovarian cancer (CIS-A2780 and OVCAR-8) cell lines. The apoptosis activity of the SLs was concentration dependent in CIS-A2780 cells. Ala showed higher apoptotic activity in both cell lines. The cytotoxic activities of the SLs and Aza are accompanied with significant morphological changes in the ovarian cancer cells, which clearly show apoptotic features. The morphological changes such as cell detachment, cell shrinkage, rounded and smaller and fragmented nuclei which are established features of apoptosis induced by each of the SLs have also been reported in other cancer types and parasites (Choi *et al.*, 2012; Costantino *et al.*, 2013; Jimenez *et al.*, 2014; Zhao *et al.*, 2015; Costantino *et al.*, 2016).

Kang *et al.* (2019) had also reported that Ala caused nuclear morphological changes such as fragmentation, condensed chromatin and intense fluorescence in human liver cancer. These compounds (Deh, Pat, Cos, and Ala) including Aza were further established to induce apoptosis through the activation of caspase 3/7, which is an apoptosis executioner marker. This suggested that the high percentage of cell death induced by these compounds at time and concentration dependent manner was mainly due to induction of apoptosis. In addition to that, the mechanism of apoptosis induction activities of SLs and Aza was by both intrinsic and extrinsic pathways through caspase dependent activity which was shown via activation of caspase 9 and 8 activities. Zhao *et al.* (2015), Costantino *et al.* (2016) had also reported that Ala and Deh induced apoptosis in lung cancer cells and breast cancer respectively. Liu *et al.* (2019) had also reported that Ala induced apoptosis in lung cancer cell lines. In like manner, Ala, Cos and Aza reduced the activeness of the mitochondrial membrane potential of the cell which is capable of causing the release of cytochrome *c* into the cytoplasm capable of activating the cascade of caspase 9 through an intrinsic pathway. Wang *et al.* (2017) had further established that Ala increased the expression of caspase 3 and 9 in glioblastoma cancer, and further induced the release of cytochrome *c* into the cytoplasm. Wei *et al.* (2013) and Khan *et al.* (2012; 2013) had also confirmed that Ala disrupted the mitochondrial membrane potential of chronic myelogenous leukaemia and glioblastoma and liver cancer respectively. Kang *et al.* (2019) had further reported that Ala induced significance apoptosis in human HepG2 cells by increasing caspase 3 activity and cleaved PARP. Furthermore, Yin *et al.* (2019) had also reported that Ala induced apoptosis in breast cancer cell lines and caused cell cycle arrest at G<sub>2</sub>-M phase.

The apoptotic activities of Cos through both intrinsic and extrinsic pathways agrees with the report of Lee *et al.* (2001) who demonstrated that Cos induced apoptosis in human leukaemia by activating caspase 3, 8 and 9, and further altered the mitochondria potential

of the cancer cells that further lead to the release of cytochrome *c* that caused down-stream activation. Yan *et al.* (2019) had also reported that Cos inhibited the growth of human gastric adenocarcinoma BGC-823 cells and induced apoptosis through lowering the mitochondrial membrane potential of the cells and increasing the expression of Bax, cleaved caspase 3, 7, 9 and lowering the expression of Bcl-2. Furthermore, this result agree with the reports that Cos induced apoptosis through the activation of caspase 3 and caspase 8 but differs from the report that Cos does not induce apoptosis through intrinsic pathway because it does not activate caspase 9 nor reduce the active potential membrane of the cell (Choi *et al.*, 2012). Mao *et al.* (2019) had also reported that Cos induced apoptosis in liver cancer HepG2 cell line by upregulation of the expression of caspase 3, 8, 9 and Bax and downregulation of Bcl-2. Still further, the results that showed that Pat induced apoptosis through both intrinsic and extrinsic pathways agrees with the report of Suvannasankha *et al.* (2008) on the apoptotic activities of Pat on multiple myeloma, that it induced apoptosis through both extrinsic and intrinsic pathways through the activation of caspase 3, 8 and 9, and cleavage PARP. Li *et al.* (2018) had also reported that Pat induced apoptosis and activated caspase 3 and 9 activities. Likewise, Talib and Al Kury (2018) had reported that Pat inhibited the growth of lung cancer and induce apoptosis by increasing caspase 3, 7, 8 and 9 activities. In addition to the apoptotic activity of SLs. SLs and Aza caused cell cycle arrest in ovarian cancer cell lines. Deh and Aza caused cell cycle arrest at G<sub>2</sub>-M phase, while Ala, Pat and Cos arrested the cells at S and G<sub>2</sub>-M phases and subsequently resulted in significant decrease in the number of cells in the G<sub>0</sub>-G<sub>1</sub> phase and increase in the percentage of cells in the subG<sub>1</sub> phase. The ability of SLs and Aza to cause cell cycle arrest and induce apoptosis through both intrinsic and extrinsic pathways explains why they showed very high anti-proliferative and cytotoxic activities against ovarian cancer cell lines. The cell cycle arrest induced by these compounds was similar to the reports of Bailon-Moscoso *et al.* (2015) and Costantino

*et al.* (2013) that Deh induced cell cycle arrest at G<sub>2</sub>-M phase in human cerebral astrocytoma cell line and breast cancer respectively. In a similar manner, the cell cycle arrest activity of Cos at the G<sub>2</sub>-M phase was similar to the report of Choi *et al.* (2012) and Liu *et al.* (2011) that Cos caused cell cycle arrest at G<sub>2</sub>-M phase in breast and hepatocellular carcinoma respectively. Likewise, Lei *et al.* (2012) and Kang *et al.* (2019) had demonstrated that Ala induced cell cycle arrest at G<sub>2</sub>-M phase in liver cancer.

### **5.3.3 Effects on global and gene specific DNA methylation, DNMTs and tumour suppressor gene expression and DNMT enzymatic activity.**

DNA methylation is known to be among the underlying mechanisms for the multistep processes involved the transformation of normal cells into tumour cells. DNA methylation especially at the promoter region of genes are known to modulate gene expression, and this is capable altering various cellular mechanisms involved in cancer formation (Gopisetty *et al.*, 2006). However, the fact that this process is reversible makes it a good target for cancer treatment. Interestingly, sesquiterpene lactones are group of compounds like flavonoids that have the capacity to cause DNA demethylation. In this study, SLs (Ala, Deh, Cos and Pat) strongly decreased the global DNA methylation level of ovarian cancer cells. Previous studies had also demonstrated that Pat decreased the level of global DNA methylation and gene specific promoter methylation (HIN-1 promoter methylation) in breast cancer (Liu *et al.*, 2009). In like manner, Aza also decreased the global DNA methylation. Similar global and gene specific promoter DNA demethylating activity of Aza had also been reported in different cancer types (Stresemann *et al.*, 2006; Braiteh *et al.*, 2008; Stresemann and Lyko, 2008). Additionally, the results from this study showed that each of the SLs investigated, and the positive control (Aza), inhibited the enzymatic activity of DNMTs in OVCAR-4, while only Pat and Aza showed strong DNMTs enzymatic inhibitory activity in CIS-A2780

cells. Furthermore, the SLs modulated the expression of specific *DNMT* genes. The expression of *DNMT1* was downregulated by Ala and Aza. *DNMT3A* was downregulated by Deh, while the expression of *DNMT3B* and *DNMT3L* was downregulated by Deh and Ala, and Cos and Ala respectively. These enzymes function as catalyst, for the maintenance and addition of methyl to cytosine on position 5 of the DNA. The DNMTs inhibitory activity of SLs and Aza reported in this study could be due to their strong affinity to inhibit the enzymatic activity of DNMTs. Furthermore, Deh slightly decreased the CpG methylation at the promoter region of tumour suppressor gene *MLH1*. However, this does not result in any significant changes in the expression of *MLH1*. This could be that the level of DNA demethylation at the promoter level of this gene was not sufficient enough to cause significant increase in its expression, or possibly because gene expression is not only regulated by level of DNA methylation at the promoter region alone. The CpG methylation of the promoter region of *HOXA9* was reduced by Pat and Aza, while Pat and Cos decreased the CpG methylation level of *TP53* gene.

Still further, Deh, Pat and Ala upregulated the expression of *PTEN*, which is a tumour suppressor gene that function in the regulation of cell division (National Institutes of Health, 2020). The expression of *APC*, *KLF6* and *MLH1* was further upregulated by Ala. *APC* and *KLF6* are tumour suppressor genes while the protein of *MLH1* functions in DNA repair (National Institutes of Health, 2020). Furthermore, Pat upregulated the expression of *BRCA1* and *TUSC3* which are tumour suppressor genes, while Aza upregulated the expression of *APC* and *FOLR1* genes. The *FOLR1* gene expresses folate receptor alpha protein that functions in the transportation of B-vitamin into the cell which helps in DNA repair. The DNMT inhibitory and down-regulatory activities of SLs including Aza are suggested to be the major reason for their DNA demethylating activity and modulation of gene expression. In spite of that, it was observed that Ala does not caused any significant

change in the CpG DNA methylation level of the promoter region of *MLH1*, *HOXA9* and *TP53* genes while Cos and Ala do not cause any significant change in the CpG methylation level of the promoter region of *MLH1* gene. Nevertheless, there was an upregulation and down regulation of the expression of some of these genes. It could therefore be suggested that *DNMT* could also be regulating gene expression through other mechanisms that does not involve DNA demethylation. This was similar to the view of Milutinovic *et al.* (2004) who demonstrated that the knock down of *DNMT1* caused the re-expression of genes involved in cell cycle regulation by acting either directly or indirectly on proteins that interact with these genes, without any significant change in the DNA methylation profile of the genes involved. It was therefore suggested that DNMT1 could also regulate gene expression through mechanism that does not involve DNA methylation and histone modification. Therefore, the high antiproliferative and apoptotic activities of SLs including Aza reported in this study was suggested to be mediated by their *DNMT* inhibitory activity and their capacity to modulate of gene expression.

#### **5.4 Conclusion**

In summary, the anti-ovarian cancer activities of sesquiterpene lactones and 5'azacytidine were investigated in this chapter, their DNMT inhibitory and DNA demethylating activities and modulation of gene expression were also evaluated. All the sesquiterpene lactones investigated, especially Ala and Deh were found to be potential candidate for ovarian cancer treatment. Additionally, sesquiterpene lactones showed similar anti-cancer potency with 5-azacytidine. Their cytotoxic activities were found to be cancer specific, because they showed lesser cytotoxicity against immortalised human ovarian epithelial cells (HOE). This made them a better drug candidate than 5-azacytidine that showed higher cytotoxicity against HOE. Even though, the anti-cancer activities of these compounds have been reported

in different other cancer types, this study had further extended their anti-cancer potency to ovarian cancer, and brought to light some of their mechanisms of activities which have not been reported in previous studies. Furthermore, the antiproliferative activity of sesquiterpene lactones was established to be through induction of apoptosis which is mediated by activation of caspase 3/7 via both intrinsic and extrinsic pathways. Still further, these compounds caused cell cycle arrest and most especially Ala and Cos reduced the activeness of the mitochondria potential membrane of the cells. In addition to that, sesquiterpene lactones modulated the expression of *DNMT1*, *DNMT3A*, and *DNMT3L*. In the same manner, 5-azacytidine which is a known DNMT1 inhibitor and an approved drug for the treatment of myelodysplastic syndrome inhibited *DNMT1*. These compounds further caused global and gene specific DNA demethylation and upregulation of the expression of some tumour suppressor genes. Notably, *PTEN* expression was upregulated by Deh, Pat and Ala. Pat further upregulated the expression of *BRCA1* while Ala upregulated the expression of *APC*, *MLH1* and *KLF6*. In spite of the promising anti-cancer activities of the sesquiterpene lactones investigated in this study, there is little knowledge about their mechanisms of activities especially in the area of apoptosis, while their epigenetic mechanisms of activity especially their DNMT inhibitory and DNA demethylating activities remains a grey area of research. Therefore, this study seems to be the first to report the DNMT inhibitory and DNA demethylating activities of Ala, Deh and Cos against ovarian cancer cells. However, further investigation on their efficacy and mechanisms of action in animal models and roles in histone modulation and regulation of miRNA expression and post-transcriptional activities should be carried out.

## **Chapter Six**

### **General Discussion, Conclusions and Future Study**

## **6.1 General discussion**

Cancer is a serious global health issue that is unavoidable in human race due to the complexity of the genetic mechanisms involved in its formation and the multiple risk factors associated with its development. The malignant and metastasis properties of the different cancer types such as ovarian cancer makes the treatment challenging. The poor prognosis of ovarian cancer and its resistance to chemotherapy drugs such as carboplatin and cisplatin in recent years had worsen the problem and made the treatment of ovarian cancer an uttermost concern. At present, the available treatment for ovarian cancer include: surgery, radiotherapy and chemotherapy. The most common chemotherapy drugs used for ovarian cancer treatment are carboplatin and paclitaxel. Others include: cisplatin, gemcitabine, etoposide, topotecan, liposomal doxorubicin and cyclophosphamide. Targeted drugs such as Olaparib (Lynparza), Niraparib (Zejula), bevacizumab (Avastin) and rucaparib (Rubraca) are used with or after other chemotherapy for advanced ovarian cancer treatment (Cancer Research UK, 2020; FDA, 2020). However, these drugs are very expensive and there are developments of drug resistance in cancer treatment. Furthermore, these treatments are often available in the developed countries, the low income developing nations such as Africa and Asia are often in difficult situation as most of the cancer patients could not afford the expensive drugs. Therefore, the search for new drugs that could overcome the resistant nature of cancer and comparably cheaper and affordable in the low income countries is highly essential. Plant-based or natural product-based therapies could provide alternative treatment option for cancer especially for people in the developing countries, because these therapies are often cheaper as they are derived from plant sources which are mostly present in the developing nations.

The traditional use of plants in the treatment of diseases such as cancer, malaria, pain and diabetes has been of pharmacological relevance over thousand years ago. Beyond their medicinal values, they are also essential towards human existence (Cragg and Newman, 1996, 2005). High percentage of the population worldwide especially developing nations depend mostly on traditional medicine for the treatment of diseases (Cragg and Newman, 2013). Majority of these plants are found in different continents such as Asia and Africa. Several families and species of plants have been reported to have anti-tumour activities (Cragg and Newman, 1996; Sultana and Asif, 2014) . However, their diverse biological activities as a result of numerous constituents have made the characterisation, isolation and identification of the bioactive natural products from these plants essential. This has been the general focus of research over years. Several compounds with anti-cancer activities have been derived from plants over the ages. However, there are still numerous plants with ethnopharmacological relevance that are yet to be investigated (Cragg and Newman, 2005). Natural products derived from plant and their derivatives have received attention for drug discovery in the treatment of many diseases (Krifa *et al.*, 2013; Harvey, Edrada-Ebel and Quinn, 2015). Several drugs such as artemisinin, quinine, tubocurarine, colchicine, nicotine and majority of the cancer drugs such as vinblastine, vincristine, topotecan and irinotecan, etoposide, teniposide and paclitaxel are derived from plants (Cragg and Newman, 2005; Mittal, Sharma and Batra, 2014; Krifa *et al.*, 2015; Newman and Cragg, 2016). However, majority of these anti-cancer agents function through different mechanisms involved in cancer formation and progression.

The ethnopharmacological use of *J. insularis* in the treatment of different diseases guided our choice for the investigation of its anti-ovarian cancer activities, characterised and identified its bioactive compounds and evaluated their roles in DNMT inhibition and DNA demethylation. The genus *Justicia* is the largest genus in the Acanthaceae family with many

species. The most investigated species are *J. pectoralis*, *J. procumbens*, *J. gendarussa* and *J. anselliana*, while majority of the other species such as *J. insularis* have not been investigated. *J. insularis* is an edible plant that is widely used for the treatment of different diseases in the tropical part of Africa (Telefo, Moundipa and Tchouanguép, 2004). Based on the medicinal values of *J. insularis*, its anti-ovarian cancer activity was investigated in this study. Furthermore, this study also evaluated the anti-ovarian cancer activities of sesquiterpene lactones and diterpenoids and determined their roles in DNA methylation and DNMT inhibition.

Two diterpenoids (compound **1** and **2**) in *J. insularis* were characterised and identified for the first time in this study. Their anti-ovarian cancer activities against ovarian cancer cell lines including cisplatin resistant cells, as well as their roles in DNMT inhibition and DNA demethylation were also reported for the first time. Furthermore, the data from this study showed for the first time that Deh, Ala and Andr downregulated the expression of specific DNMTs, Deh and Ala further inhibited the enzymatic activities of DNMTs and caused DNA demethylation. Tpl was further shown to inhibit DNMTs enzymatic activities and downregulated the expression of *DNMT1*, *DNMT3A* and *DNMT3B* in this study, even though previous study has reported the gene specific (*WIF-1*) DNA demethylating activities of Tpl (Mao *et al.*, 2018). This study does not observe any significant DNA demethylating activity for Tpl both at global 5-methylcytosine and CpG sites of *MLH1* and *HOXA9* genes.

Generally, chemical properties such as alkylating properties, side chain and lipophilic nature and molecular geometry of sesquiterpene lactones have been suggested to be responsible for their high biological activities (Ghantous *et al.*, 2010). The cytotoxic activity of sesquiterpene lactone has been associated with their  $\alpha$ -methylene- $\gamma$ -lactone structure that is capable of forming stable adducts with cysteine residue of proteins, thus inducing cellular

changes capable of causing apoptosis. The cytotoxic activity of sesquiterpene lactones is further suggested to be enhanced by the presence of  $\alpha,\beta$ -unsaturated carbonyl structure (Kupchan *et al.*, 1971; Scotti *et al.*, 2007). Chen *et al.* (2017) had further established the importance of the  $\alpha$ -methylene moiety in the biological activities of 1 $\beta$ -hydroxy alantolactone, five derivatives of this compound were prepared. The first three derivatives of 1 $\beta$ -hydroxy alantolactone were through oxidation and esterification of the hydroxyl group on position 1. While the remaining 2 other compounds were derived by reduction and 1,3-dipolar cycloaddition at the methylene on position 13. It was found that the first three derivatives retained their biological activities while the last 2 derivatives showed no biological activity. This demonstrated that the biological activity of this compound is associated with the  $\alpha$ -methylene moiety structure. The significant loss of cytotoxic activity in both 11,13-dihydroalantolactone and 11,13-dihydroisoalantolactone ( $IC_{50} >125 \mu\text{g/mL}$ ) derived from alantolactone and isoalantolactone ( $IC_{50}$  values 36.2 and 10.0  $\mu\text{g/mL}$  respectively) had further revealed the importance of the  $\alpha,\beta$ -unsaturated lactone moiety in their biological activities (Cantrell *et al.*, 2010). This shows that the anti-ovarian cancer activities of alantolactone reported in this study, could be associated with the  $\alpha$ -methylene- $\gamma$ -lactone group. Furthermore, dehydroleucodine is a guaianolide, this group of sesquiterpene lactone have been suggested to have higher biological activity than the other groups of sesquiterpene lactones. dehydroleucodine has double bond at position 3 and a methyl group at position 4. These features in addition to the  $\alpha$ -methylene- $\gamma$ -lactone structure have been suggested to be important in its biological activity (Scotti *et al.*, 2007). Polo *et al.* (2007) reported a loss in cytotoxic activity in dehydroleucodine derivative (11,13-dihydro-dehydroleucodine), while dehydroleucodine retained its cytotoxic activity. This suggested the importance of the  $\alpha$ -methylene- $\gamma$ -lactone structure in its biological activity. Therefore, the high anti-ovarian cancer activities reported for dehydroleucodine in this study

is therefore suggested to be associated with its structure. In addition, Robinson *et al.* (2008) demonstrated that the cytotoxicity of costunolide was associated with its  $\alpha,\beta$ -unsaturated carbonyl structure. He revealed that the substitution of the unsaturated double bond on position 13 with methoxy group lead to significant decrease in cytotoxicity. The cytotoxic activity of parthenolide was further linked with the lactone moiety, and the methyl group on position 14 have been suggested to possibly be playing an important role in its cytotoxic activity (Long *et al.*, 2016).

The cytotoxic activity of andrographolide was suggested to be associated with the  $\alpha$ -alkylidene- $\gamma$ -butyrolactone moiety in the andrographolide structure. This was showed through the loss of cytotoxic activity in analogues of andrographolide with lost double bond between carbon 12 and carbon 13 ( $\alpha$ -alkylidene) (Das *et al.*, 2010). The importance of the lactone moiety and the double bond at C12 and C13 in the cytotoxic activity of andrographolide had further been proved by Nanduri *et al.* (2004), who reported loss of cytotoxic activity in andrographolic acid and 12,13-dihydroandrographolide derived by modifying the lactone moiety and double bond at carbon 12 and carbon 13 respectively. Furthermore, the biological activity of triptolide have been associated with the unsaturated lactone ring (Xu *et al.*, 2014). Zhao *et al.* (1991) established the relevance of the hydroxyl group on position 16 of compound **1**, he observed a lesser cytotoxic activity in compound **1** derivatives with substituted hydroxyl group with acetyl.

Finally, this study warranted that sesquiterpene lactones (Deh, Ala, Pat and Cos) and diterpenoids (Andr, Tpl and compound **1**) are potential drug candidates for ovarian cancer treatment, in particular, for overcoming the drug-resistance problem in ovarian cancers. However, some of the potential drawback of sesquiterpene lactones and diterpenoids to be developed into drugs include their hydrophobicity, which could affect their

pharmacokinetics including: absorption, distribution, metabolism and excretion (ADME). Nevertheless, chemical modification of these compounds could help to improve their water solubility. Also, the use of novel delivery such as liposome could also help in their pharmacokinetics. There are studies that have investigated this goal on triptolide, using liposome delivery or conjugated triptolide with antibody (Cai *et al.*, 2019; Lin *et al.*, 2017; Xu and Liu, 2019).

## 6.2 Limitations of study

The anti-ovarian cancer activities of the investigated compounds reported in this study were only evaluated using *in vitro* cell based model, not 3D organoid model or *in vivo* animal xenograft, which have closer features of human ovarian tumour. Furthermore, only limited number of panels of tumour suppressor gene CpG promoter methylation have been studied using pyrosequencing technique rather than advanced methods such as targeted bisulfite next generation sequencing (tNGBS) or whole genome bisulfite sequencing which could evaluate multiple regions per gene on multiple panel of genes at a go. Also, the limited amount of *J. insularis* plant material and extracts would not allow the study of the minor components of *J. insularis* and identify their structures, which are potentially novel compounds. In addition, compound **2** identified and other minor components isolated were not studied further due to limited amounts.

## 6.3 Conclusions

In the search for natural compounds from plants with anti-cancer activities and the discovery of new DNMT inhibitors for ovarian cancer treatment, this study investigated the anti-ovarian cancer activities of a Nigerian plant, *J. insularis* T. Anderson, characterised and identified their bioactive compounds. In addition, this study further investigated the anti-

proliferative and apoptotic activities of sesquiterpene lactones (Deh, Ala, Pat and Cos) and diterpenoids (Andr, and Tpl from traditional Chinese medicine). Their roles in DNMT inhibition, DNA demethylation and modulation of gene expression were also evaluated. *J. insularis* plant was discovered to be a good and potential anti-ovarian cancer agent. The major bioactive compounds with anti-cancer activities in this plant were identified as diterpenoids: 16 $\alpha$ / $\beta$ -hydroxy-cleroda-3,13 (14) dien-15,16-olide (compound **1**) and 16-oxocleroda-3,13(14) dien-15-oic acid (compound **2**) by GC-MS, LC-MS and NMR spectroscopy. Compound **1** was discovered as the most promising anti-ovarian cancer compound in *J. insularis*. The results from this study also form the basis to come to the conclusion that all the sesquiterpene lactones tested especially Deh and Ala, and diterpenoids (Andr, Tpl and compound **1**) investigated are effective antiproliferative agents against ovarian cancer cells that exerted their anti-ovarian cancer activities through induction of apoptosis via both intrinsic and extrinsic pathways. Furthermore, based on the findings from this study, it could be deduced that the apoptotic activities of sesquiterpene lactones and diterpenoids that resulted in their high antiproliferative activities were mediated through their DNMT inhibitory/down-regulatory activities and modulation of gene expression. It was found that the four sesquiterpene lactones (Deh, Ala, Pat and Cos) caused global DNA demethylation, while Pat decreased the CpG promoter methylation of *HOXA9* and *TP53* genes, while Deh and Cos decreased promoter CpG methylation of *MLH1* and *TP53* genes respectively in ovarian cancer cells. However, no significant global DNA demethylation activity was found in Tpl. However, Andr and compound **1** caused global DNA demethylation, Andr further decreased the CpG methylation of the promoter region of *HOXA9* gene while compound **1** decreased CpG methylation at the promoter region of *PTEN* gene. Additionally, Deh down-regulated the expression of *DNMT3A* and *DNMT3B*, Ala down-regulated *DNMT1*, *DNMT3B* and *DNMT3L* expression while Pat down-regulated

the expression of *DNMT3L*. Andr decreased *DNMT1* and *DNMT3B* expression, while Tpl decreased the expression of *DNMT3A* and *DNMT3B*. Compound **1** down regulated the expression of *DNMT1*, *DNMT3B* and *DNMT3L*. The DNMT inhibitory/down-regulatory activity of these compounds was suggested to be associated with their chemical structure. In addition to that, each of the sesquiterpene lactones and diterpenoids upregulated the expression of different tumour suppressor genes. Finally, the sesquiterpene lactones (Deh, Ala, Pat and Cos) and diterpenoids (Andr, Tpl and compound **1**) investigated bear the potential to be developed as drug candidates for ovarian cancer treatment. Therefore, the four sesquiterpene lactones and the three diterpenoids investigated in this study could be investigated further using *in vivo* assays and even clinical trials to confirm their efficacy and safety profiles.

#### **6.4 Future study**

This study investigated the *in vitro* anti-ovarian cancer activities of sesquiterpene lactones and diterpenoids, and most importantly, evaluated their roles in epigenetic modulation. Current study is still on-going on the DNA demethylating activities of sesquiterpene lactones and diterpenoids on the CpG sites of other tumour genes that are yet to be reported in this study. However, the epigenetic mechanism of activities of the compounds investigated in this study was only limited to their roles in DNA demethylation and modulation of gene expression. Therefore, their epigenetic activities would be investigated further. Their roles in histone methylation and acetylation, regulation of miRNA expression and post-transcriptional activities in ovarian and other cancer types such as breast, prostate and lung cancers would be investigated. Furthermore, their protein most importantly DNMTs specific activities evaluated would be evaluated via *in vitro* studies. Additionally, their mechanism of apoptosis induction such as modulation of the expression of pro-

apoptotic (Bax) and anti-apoptotic (Bcl-2) genes and induction of PARP (Poly (ADP-Ribose) polymerase) cleavage would be investigated. Their effects on other cancer hallmarks like angiogenesis, cell invasion and metastasis, etc. would also be investigated in the future.

Further study would also focus on the characterisation and identification of other minor bioactive and potentially novel compounds from the other bioactive fractions of *J. insularis*. Their roles in apoptosis, DNA methylation and modulation of gene expression would also be investigated.

Finally, drug combinatory and/or synergic activities of sesquiterpene lactones and diterpenoids with the standard drug (carboplatin) to improve its anti-ovarian cancer activities would be carried out, and their *in vivo* anti-cancer activities would be investigated.

---

## References

- Abood, S., Eichelbaum, S., Mustafi, S., Veisaga, M. L., López, L. A. and Barbieri, M. (2017) 'Biomedical properties and origins of sesquiterpene lactones, with a focus on dehydroleucodine', *Natural Product Communications*, 12(6), pp. 995–1005.
- Abood, S., Veisaga, M. L., López, L. A. and Barbieri, M. A. (2018) 'Dehydroleucodine inhibits mitotic clonal expansion during adipogenesis through cell cycle arrest', *Phytotherapy Research*, 32(8), pp. 1583–1592.
- Abu-Ghefreh, A. A., Canatan, H. and Ezeamuzie, C. I. (2009) 'International immunopharmacology in vitro and in vivo anti-inflammatory effects of andrographolide', *International Immunopharmacology*, 9(3), pp. 313–318.
- Acunzo, M., Romano, G., Wernicke, D. and Croce, C. M. (2015) 'MicroRNA and cancer - A brief overview', *Advances in Biological Regulation*, 57, pp. 1–9.
- Adeyemi, O. T. and Babatunde, O. (2014) 'Chemical composition and antioxidant capacity of the leaf extract of *Justicia insularis*', *International Journal of Physical Sciences*, 9(20), pp. 454–458.
- Afolabi, S., Olorundare, O., Ninomiya, M., Babatunde, A., Mukhtar, H. and Koketsu, M. (2017) 'Comparative antileukemic activity of a tetranorditerpene isolated from *Polyalthia longifolia* leaves and the derivative against human leukemia HL-60 cells', *Journal of Oleo Science*, 66(10), pp. 1169–1174.
- Agirre, X., Novo, F. J., Clasan, M. J., Larrayoz, M. J., Lahortiga, I., Valganon, M., Garcia-Delgado, M. and Vizmanos, J. L. (2003) 'TP53 is frequently altered by methylation, mutation, and / or deletion in acute lymphoblastic leukaemia', *Molecular Carcinogenesis*, 38, pp. 201–208.
- Agirre, X., Vizmanos, J. L., Calasan, M. J., Garcia-Delgado, M., Larrayoz, M. J. and Novo, F. J. (2003) 'Methylation of CpG dinucleotides and / or CCWGG motifs at the promoter of TP53 correlates with decreased gene expression in a subset of acute lymphoblastic leukemia patients', *Oncogene*, 22, pp. 1070–1072.
- Ajibesin, K. K., Ekpo, B. A., Bala, D. N., Essien, E. E. and Adesanya, S. A. (2007) 'Ethnobotanical survey of Akwa Ibom State of Nigeria', *Journal of Ethnopharmacology*, 115(3), pp. 387–408.
- Ajiboye, T. O., Yakubu, M. T. and Oladiji, A. T. (2013) 'Cytotoxic, antimutagenic, and antioxidant activities of methanolic extract and chalcone dimers (lophirones B and C) derived from *Lophira alata* (Van Tiegh. Ex Keay) stem bark', *Journal of Evidence-Based Complementary and Alternative Medicine*, 19(1), pp. 20–30.
- Akone, S. H., Ntie-Kang, F., Stuhldreier, F., Ewonkem, M. B., Noah, A. M., Mouelle, S. E. M. and Müller, R. (2020) 'Natural products impacting DNA methyltransferases and histone deacetylases', *Frontiers in Pharmacology*, 11, pp. 1–26.

- Amatya, V. J., Naumann, U., Weller, M. and Ohgaki, H. (2005) 'TP53 promoter methylation in human gliomas', *Acta Neuropathologica*, 110, pp. 178–184.
- American Cancer Society (2016) *Ovarian cancer*. Available at: <https://www.cancer.org/cancer/ovarian-cancer/about/what-is-ovarian-cancer.html> (Accessed: 19 November 2016).
- American Cancer Society (2018) *Cancer facts & figures 2018*, Atlanta: American Cancer Society, pp. 1–71.
- Amin, A., Gali-Muhtasib, H., Ocker, M. and Schneider-Stock, R. (2009) 'Overview of major classes of plant-derived anticancer drugs', *International Journal of Biomedical Science*, 5(1), pp. 1–11.
- Bailon-Moscoso, N., González-Arévalo, G., Velásquez-Rojas, G., Malagon, O., Vidari, G., Zentella-Dehesa, A., Ratovitski, E. A. and Ostrosky-Wegman, P. (2015) 'Phytometabolite dehydroleucodine induces cell cycle arrest, apoptosis, and DNA damage in human astrocytoma cells through p73/p53 regulation', *Plos One*, 10(8), pp. 1–18.
- Balachandran, P. and Govindarajan, R. (2005) 'Cancer - An ayurvedic perspective', *Pharmacological Research*, 51(1), pp. 19–30.
- Banerjee, S. and Kaye, S. (2011) 'The role of targeted therapy in ovarian cancer', *European Journal of Cancer*, 47, pp. 116–130.
- Bao, G., Shen, B., Pan, C., Zhang, Y., Shi, M. and Peng, C. (2013) 'Andrographolide causes apoptosis via inactivation of STAT3 and Akt and potentiates antitumor activity of gemcitabine in pancreatic cancer', *Toxicology Letters*, 222(1), pp. 23–35.
- Bao, Z., Guan, S., Cheng, C., Wu, S. and Wong, S. H. (2009) 'A novel antiinflammatory role for andrographolide in asthma via inhibition of the nuclear factor- $\kappa$ B pathway', *American Journal of Respiratory and Critical Care Medicine*, 179, pp. 657–665.
- Barla, A., Topcu, G., Oksuz, S., Tumen, G. and Kingston, D. (2007) 'Identification of cytotoxic sesquiterpenes from *Laurus nobilis* L.', *Food Chemistry*, 104(4), pp. 1478–1484.
- Baylin, S. B. and Jones, P. A. (2012) 'A decade of exploring the cancer epigenome-biological and translational implications', *Nature Reviews Cancer*, 11(10), pp. 726–734.
- Beumer, J. H., Parise, R. A., Newman, E. M. and Doroshow, J. H. (2008) 'Concentrations of the DNA methyltransferase inhibitor 5-fluoro-2'-deoxycytidine (FdCyd) and its cytotoxic metabolites in plasma of patients treated with FdCyd and tetrahydrouridine (THU)', *Cancer Chemotherapy and Pharmacology*, 62(2), pp. 363–368.
- Bocca, C., Gabriel, L., Bozzo, F. and Miglietta, A. (2004) 'A sesquiterpene lactone, costunolide, interacts with microtubule protein and inhibits the growth of MCF-7 cells', *Chemico-Biological Interactions*, 147(1), pp. 79–86.
- Braitheh, F., Soriano, A. O., Garcia-Manero, G., Hong, D., Johnson, M. M., Silva, L. D. P., Yang, H., Alexander, S., Wolff, J. and Kurzrock, R. (2008) 'Phase I study of epigenetic

modulation with 5-azacytidine and valproic acid in patients with advanced cancers', *Clinical Cancer Research*, 14(19), pp. 6296–6301.

Bray, F., Ferlay, J., Soerjomataram, I., Siegel, R. L., Torre, L. A. and Jemal, A. (2018) 'Global cancer statistics 2018: GLOBOCAN estimates of incidence and mortality worldwide for 36 cancers in 185 countries', *A Cancer Journal for Clinicians*, 68(6), pp. 394–424.

Burghaus, S., Fasching, P. A., Häberle, L., Rübner, M., Büchner, K., Blum, S., Engel, A., Ekici, A. B., Hartmann, A., Hein, A., Beckmann, M. W. and Renner, S. P. (2017) 'Genetic risk factors for ovarian cancer and their role for endometriosis risk', *Gynecologic Oncology*, 145(1), pp. 142–147.

Busch, C., Burkard, M., Leischner, C., Lauer, U. M., Frank, J. and Venturelli, S. (2015) 'Epigenetic activities of flavonoids in the prevention and treatment of cancer', *Clinical Epigenetics*, 7(64), pp. 1-18.

Cai, H., He, X. and Yang, C. (2018) 'Costunolide promotes imatinib-induced apoptosis in chronic myeloid leukemia cells via the Bcr/Abl–Stat5 pathway', *Phytotherapy Research*, 32(9), pp. 1764–1769.

Cai, X., Fei, W., Xu, Y., Xu, H., Yang, G., Cao, J., Ni, J. and Wang, Z. (2019) 'Combination of metronomic administration and target delivery strategies to improve the anti-angiogenic and anti-tumor effects of triptolide', *Drug Delivery and Translational Research*, 10(1), pp. 93–107.

Cai, Y., Lin, W., Li, A. and Xu, J. (2013) 'Combined effects of curcumin and triptolide on an ovarian cancer cell line', *Asian Pacific Journal of Cancer Prevention*, 14(7), pp. 4267–4271.

Campos-Xolalpa, N., Alonso-Castro, Á. J., Sánchez-Mendoza, E., Zavala-Sánchez, M. Á. and Pérez-Gutiérrez, S. (2017) 'Cytotoxic activity of the chloroform extract and four diterpenes isolated from *Salvia ballotiflora*', *Brazilian Journal of Pharmacognosy*, 27(3), pp. 302–305.

Cancer Research UK (2018) *Cancer incidence statistics*. Available at: <https://www.cancerresearchuk.org/health-professional/cancer-statistics/incidence> (Accessed: 22 January 2020).

Cancer Research UK (2018) *Worldwide cancer statistics*. Available at: <https://www.cancerresearchuk.org/health-professional/cancer-statistics/worldwide-cancer> (Accessed: 23 December 2018).

Cancer Research UK (2019) *Ovarian cancer- stages and grades*. Available at: <https://about-cancer.cancerresearchuk.org/about-cancer/ovarian-cancer/stages-grades/about-stages-and-grades> (Accessed: 14 July 2019).

Cancer Research UK (2020) *Ovarian cancer statistics*. Available at: <https://www.cancerresearchuk.org/health-professional/cancer-statistics/statistics-by-cancer-type/ovarian-cancer> (Accessed: 17 June 2020).

- Cancer Research UK (2020) *Targeted cancer drugs*. Available at: <https://about-cancer.cancerresearchuk.org/about-cancer/ovarian-cancer/treatment/targeted-cancer-drugs/drugs> (Accessed: 17 June 2020).
- Cantrell, C. L., Abate, L., Fronczek, F. R., Franzblau, S. G., Quijano, L. and Fischer, N. H. (1999) 'Antimycobacterial eudesmanolides from *Inula helenium* and *Rudbeckia subtomentosa*', *Planta Medica*, 65, pp. 351–355.
- Cantrell, L., Pridgeon, J. W., Fronczek, F. R. and Becnel, J. J. (2010) 'Structure – activity relationship studies on derivatives of eudesmanolides from *Inula helenium* as toxicants against *Aedes aegypti* larvae and adults although there is a safe and effective vaccine for the yellow fever virus , epidemic transmission still occ', *Chemistry and Biodiversity*, 7, pp. 1681–1697.
- Chan, E. W., Cheng, S. C. and Sin, F. W. (2001) 'Triptolide induced cytotoxic effects on human promyelocytic leukemia, T cell lymphoma and human hepatocellular carcinoma cell lines', *Toxicology Letter*, 122, pp. 81–87.
- Chen, C. C., Wang, K. Y. and Shen, C. K. J. (2012) 'The Mammalian de Novo DNA methyltransferases DNMT3A and DNMT3B are also DNA 5-hydroxymethylcytosine dehydroxymethylases', *Journal of Biological Chemistry*, 287(40), pp. 33116–33121.
- Chen, L., Zhang, J. P., Liu, X., Tang, J. J., Xiang, P. and Ma, X. M. (2017) 'Semisynthesis, an anti-inflammatory effect of derivatives of 1 $\beta$ -hydroxy alantolactone from *Inula britannica*', *Molecules*, 22(11), pp. 1–8.
- Cheng, J. C., Matsen, C. B., Gonzales, F. A., Ye, W., Greer, S., Marquez, V. E., Jones, P. A. and Selker, E. U. (2003) 'Inhibition of DNA methylation and reactivation of silenced genes by zebularine', *Journal of the National Cancer Institute*, 95(5), pp. 399–409.
- Chmelarova, M., Krepinska, E., Spacek, J., Laco, J., Beranek, M. and Palicka, V. (2013) 'Methylation in the p53 promoter in epithelial ovarian cancer', *Clinical and Translational Oncology*, 15(2), pp. 160–163.
- Choi, Y. K., Seo, H. S., Choi, H. S., Choi, H. S., Kim, S. R., Shin, Y. C. and Ko, S. G. (2012) 'Induction of Fas-mediated extrinsic apoptosis, p21WAF1-related G2-M cell cycle arrest and ROS generation by costunolide in estrogen receptor-negative breast cancer cells, MDA-MB-231', *Molecular and Cellular Biochemistry*, 363(1–2), pp. 119–128.
- Christman, J. K. (2002) '5-Azacytidine and 5-aza-2'-deoxycytidine as inhibitors of DNA methylation: mechanistic studies and their implications for cancer therapy', *Oncogene*, 21(35), pp. 5483–5495.
- Chun, J., Li, R., Cheng, M. and Shik, Y. (2015) 'Alantolactone selectively suppresses STAT3 activation and exhibits potent anticancer activity in MDA-MB-231 cells', *Cancer Letters*, 357(1), pp. 393–403.
- Chung, S., Yao, H., Caito, S., Hwang, J., Arunachalam, G. and Rahman, I. (2010) 'Regulation of SIRT1 in cellular functions : role of polyphenols', *Archives of Biochemistry and Biophysics*, 501(1), pp. 79–90.

- Colombo, P., Fabbro, M., Theillet, C., Bibeau, F., Rouanet, P. and Ray-coquard, I. (2014) 'Sensitivity and resistance to treatment in the primary management of epithelial ovarian cancer', *Critical Reviews in Oncology / Hematology*, 89(2), pp. 207–216.
- Corrêa, G. M. and de Alcântara, A. F. C. (2011) 'Chemical constituents and biological activities of species of *Justicia* -a review', *Brazilian Journal of Pharmacognosy*, 22(1), pp. 220–238.
- Cortez, A. J., Tudrej, P., Kujawa, K. A. and Lisowska, K. M. (2017) 'Advances in ovarian cancer therapy', *Cancer Chemotherapy and Pharmacology*, pp. 1-23.
- Costantino, V. V., Mansilla, S. F., Speroni, J., Amaya, C., Cuello-Carrión, D., Ciocca, D. R., Priestap, H. A., Barbieri, M. A., Gottifredi, V. and Lopez, L. A. (2013) 'The sesquiterpene lactone dehydroleucodine triggers senescence and apoptosis in association with accumulation of DNA damage markers', *Plos One*, pp. 8(1), pp. 1-16.
- Costantino, V. V., Lobos-Gonzalez, L., Ibañez, J., Fernandez, D., Cuello-Carrión, F. D., Valenzuela, M. A., Barbieri, M. A., Semino, S. N., Jahn, G. A., Quest, A. F. G. and Lopez, L. A. (2016) 'Dehydroleucodine inhibits tumor growth in a preclinical melanoma model by inducing cell cycle arrest, senescence and apoptosis', *Cancer Letters*, 372(1), pp. 10–23.
- Cragg, G. M. and Newman, D. J. (1996) 'A report on plants evaluated from collections in Belize during 1987 – 1996', pp. 1-16
- Cragg, G. M. and Newman, D. J. (2005) 'Plants as a source of anti-cancer agents', *Journal of Ethnopharmacology*, 100(1–2), pp. 72–79.
- Cragg, G. M. and Newman, D. J. (2013) 'Natural products: A continuing source of novel drug leads', *Biochimica et Biophysica Acta*, 1830, pp. 3670–3695.
- Cui, D. and Xu, X. (2018) 'DNA methyltransferases, DNA methylation, and age-associated cognitive function', *International Journal of Molecular Sciences*, 19(5), pp.1-16.
- Cui, L., Bu, W., Song, J., Feng, L., Xu, T., Liu, D., Ding, W., Wang, J., Li, C., Ma, B., Luo, Y., Jiang, Z., Wang, C., Chen, J., Hou, J., Yan, H., Yang, L. and Jia, X. (2018) 'Apoptosis induction by alantolactone in breast cancer MDA-MB-231 cells through reactive oxygen species-mediated mitochondrion-dependent pathway', *Archives of Pharmacal Research*, 41(3), pp. 299–313.
- Dai, L., Wang, G. and Pan, W. (2017) 'Andrographolide inhibits proliferation and metastasis of SGC7901 gastric cancer cells', *BioMed Research International*, pp. 1-10.
- Dai, Y., Chen, S. R., Chai, L., Zhao, J., Wang, Y. and Wang, Y. (2019) 'Overview of pharmacological activities of andrographis paniculata and its major compound andrographolide', *Critical Reviews in Food Science and Nutrition*, 59(1), pp. 17–29.
- Das, B., Chowdhury, C., Kumar, D., Sen, R., Roy, R., Das, P. and Chatterjee, M. (2010) 'Synthesis, cytotoxicity, and structure-activity relationship (SAR) studies of andrographolide analogues as anti-cancer agent', *Bioorganic and Medicinal Chemistry Letters*, 20(23), pp. 6947–6950.

- Datta, J., Ghoshal, K., Denny, W. A., Gamage, S. A., Brooke, D. G., Phiasivongsa, P., Redkar, S. and Jacob, S. T. (2009) 'A new class of quinoline-based DNA hypomethylating agents reactivates tumor suppressor genes by blocking DNA methyltransferase 1 activity and inducing its degradation', *Cancer Research*, 69(10), pp. 4277–4285.
- Dawson, M. A. and Kouzarides, T. (2012) 'Cancer Epigenetics: From Mechanism to Therapy', *Cell*, 150(1), pp. 12–27.
- de Andrade, J. P., Pigni, N. B., Torras-Claveria, L., Berkov, S., Codina, C., Viladomat, F. and Bastida, J. (2012) 'Bioactive alkaloid extracts from *Narcissus broussonetii*: mass spectral studies', *Journal of Pharmaceutical and Biomedical Analysis*, 70, pp. 13–25.
- Desouza, M., Gunning, P. W. and Stehn, J. R. (2012) 'The actin cytoskeleton as a sensor and mediator of apoptosis', *BioArchitecture*, 2(3), pp. 75–87.
- Di Leva, G., Garofalo, M. and Croce, C. M. (2014) 'MicroRNAs in cancer', *Annual Review of Pathology: Mechanisms of Disease*, 9, pp. 287–314.
- Ding, Y., Wang, H., Niu, J., Luo, M., Gou, Y. and Miao, L. (2016) 'Induction of ROS overload by alantolactone prompts oxidative DNA damage and apoptosis in colorectal cancer cells', *International Journal of Molecular Sciences*, 17, pp. 1–14.
- Dong, A., Lu, Y. and Lu, B. (2016) 'Genomic/Epigenomic alterations in ovarian carcinoma: translational insight into clinical practice', *Journal of Cancer*, 7(11), pp. 1441–1451.
- Duru, N., Gernapudi, R., Eades, G., Eckert, R. and Zhou, Q. (2015) 'Epigenetic regulation of miRNAs and breast cancer stem cells', *Current Pharmacology Reports*, 1(3), pp. 161–169.
- Earp, M. A. and Cunningham, J. M. (2015) 'DNA methylation changes in epithelial ovarian cancer histotypes', *Genomics*, 106(6), pp. 311–321.
- Eliza, J., Daisy, P. and Ignacimuthu, S. (2010) 'Antioxidant activity of costunolide and eremanthin isolated from *Costus speciosus* (Koen ex. Retz) Sm.', *Chemico-Biological Interactions*, 188(3), pp. 467–472.
- Erdmann, A., Halby, L., Fahy, J. and Arimondo, P. B. (2015) 'Targeting DNA methylation with small molecules: What's next?', *Journal of Medicinal Chemistry*, 58(6), pp. 2569–2583.
- Esteller, M. (2008) 'Epigenetics in Cancer', *The new England Journal of Medicine*, 358(11), pp. 1148–1159.
- Fahy, J., Jeltsch, A. and Arimondo, P. B. (2012) 'DNA methyltransferase inhibitors in cancer: a chemical and therapeutic patent overview and selected clinical studies', *Expert Opinion*, 22(12), pp. 1427–1442.
- Fallahian, F., Ghanadian, M., Aghaei, M. and Zarei, S. M. (2017) 'Induction of G2-M phase arrest and apoptosis by a new tetrahydroingenol diterpenoid from *Euphorbia erythradenia* Bioss. in melanoma cancer cells', *Biomedicine and Pharmacotherapy*, 86, pp. 334–342.

- Fang, M., Chen, D. and Yang, C. S. (2007) 'Dietary polyphenols may affect DNA methylation', *The Journal of Nutrition*, 137, pp. 223–228.
- Fang, Y., Li, J., Wu, Y., Gui, J. and Shen, Y. (2019) 'Costunolide inhibits the growth of OAW42-a multidrug-resistant human ovarian cancer cells by activating apoptotic and autophagic pathways, production of reactive oxygen species (ROS), cleaved caspase-3 and cleaved caspase-9', *Medical Science Monitor*, 25, pp. 3231–3237.
- FDA (2020) 'FDA approves niraparib for first-line maintenance of advanced ovarian cancer.', Available at: <https://www.fda.gov/drugs/drug-approvals-and-databases/fda-approves-niraparib-first-line-maintenance-advanced-ovarian-cancer> (Accessed 1 October 2020).
- Ferlay, J., Colombet, M., Soerjomataram, I., Mathers, C., Parkin, D. M., Piñeros, M., Znaor, A. and Bray, F. (2019) 'Estimating the global cancer incidence and mortality in 2018: GLOBOCAN sources and methods', *International Journal of Cancer*, 144(8), pp. 1941–1953.
- Floean, C., Schnekenburger, M., Lee, J. Y., Kim, K. R., Mazumder, A., Song, S., Kim, J. M., Grandjenette, C., Kim, J. G., Yoon, A. Y., Dicato, M., Kim, K. W., Christov, C., Han, B. W., Proksch, P. and Diederich, M. (2016) 'Discovery and characterization of Isofistularin-3, a marine brominated alkaloid, as a new DNA demethylating agent inducing cell cycle arrest and sensitization to TRAIL in cancer cells', *Oncotarget*, 7(17), pp. 24027–24049.
- Forestier-Román, I. S., López-Rivas, A., Sánchez-Vázquez, M. M., Rohena-Rivera, K., Nieves-Burgos, G., Ortiz-Zuazaga, H., Torres-Ramos, C. A. and Martínez-Ferrer, M. (2019) 'Andrographolide induces DNA damage in prostate cancer cells', *Oncotarget*, 10(10), pp. 1085–1101.
- Fulda, S. and Debatin, K. (2006) 'Extrinsic versus intrinsic apoptosis pathways in anticancer chemotherapy', *Oncogene*, 25(34), pp. 4798–4811.
- Gao, H., Zhang, Y., Dong, L., Qu, X. Y., Tao, L. N., Zhang, Y. M., Zhai, J. H. and Song, Y. Q. (2018) 'Triptolide induces autophagy and apoptosis through ERK activation in human breast cancer MCF-7 cells', *Experimental and Therapeutic Medicine*, 15(4), pp. 3413–3419.
- Gao, S., Wang, Q., Tian, X., Li, H., Shen, Y. and Xu, X. (2017) 'Total sesquiterpene lactones prepared from *Inula helenium* L. has potentials in prevention and therapy of rheumatoid arthritis', *Journal of Ethnopharmacology*, 196, pp. 39–46.
- Garcia-Lafuente, A., Guillamon, E., Villares, A., Rostagno, M. A. and Martinez, A. J. (2009) 'Flavonoids as anti-inflammatory agents: implications in cancer and cardiovascular disease', *Inflammation Research*, 58, pp. 537–552.
- Geethangili, M., Rao, Y. K., Fang, S. and Tzeng, Y. (2008) 'Cytotoxic constituents from andrographis paniculata induce cell cycle arrest in jurkat cells', *Phytotherapy Research*, 22, pp. 1336–1341.
- Ghantous, A., Gali-muhtasib, H., Vuorela, H., Saliba, N. A. and Darwiche, N. (2010) 'What

- made sesquiterpene lactones reach cancer clinical trials?', *Drug Discovery Today*, 15(15–16), pp. 668–678.
- Ghantous, A., Sinjab, A., Herceg, Z. and Darwiche, N. (2013) 'Parthenolide : from plant shoots to cancer roots', *Drug Discovery Today*, 18(17–18), pp. 894–905.
- Ghobrial, I. M., Witzig, T. E. and Adjei, A. A. (2005) 'Targeting apoptosis pathways in cancer therapy', *A cancer Journal of Clinicians*, 55(3), pp. 178–194.
- Gloss, B. S. and Samimi, G. (2014) 'Epigenetic biomarkers in epithelial ovarian cancer', *Cancer Letters*, 342(2), pp. 257–263.
- Godwin, A. K., Meister, A., O'Dwyer, P. J., Huang, C. S., Hamilton, T. C. and Anderson, M. E. (1992) 'High resistance to cisplatin in human ovarian cancer cell lines is associated with marked increase of glutathione synthesis', *Proceedings of National Academy of Sciences*, 89, pp. 3070–3074.
- Gokbulut, A. and Sarer, E. (2013) 'Isolation and quantification of alantolactone/ isoalantolactone from the roots of *Inula helenium* subsp . *Turcoracemosa*', *Turkish Journal of Pharmaceutical Sciences*, 10(3), pp. 447–452.
- Gopisetty, G., Ramachandran, K. and Singal, R. (2006) 'DNA methylation and apoptosis', *Molecular Immunology*, 43, pp. 1729–1740.
- Guardia, T., Juarez, A. O., Guerreiro, E., Guzmán, J. A. and Pelzer, L. (2003) 'Anti-inflammatory activity and effect on gastric acid secretion of dehydroleucodine isolated from *Artemisia douglasiana*', *Journal of Ethno-Pharmacology*, 88, pp. 195–198.
- Guzman, M. L., Rossi, R. M., Karnischky, L., Li, X., Peterson, D. R., Howard, D. S. and Jordan, C. T. (2017) 'The sesquiterpene lactone parthenolide induces apoptosis of human acute myelogenous leukemia stem and progenitor cells', *Blood*, 105(11), pp. 4163–4170.
- Gyparakı, M. and Papavassiliou, A. G. (2015) 'Epigenetic pathways offer targets for ovarian cancer treatment', *Clinical Ovarian and other Gynecologic Cancer*, pp. 10–12.
- Ha, M. T., Tran, M. H., Phuong, T. T., Kim, J. A., Woo, M. H., Choi, J. S., Lee, S., Lee, J. H., Lee, H. K. and Min, B. S. (2017) 'Cytotoxic and apoptosis-inducing activities against human lung cancer cell lines of cassaine diterpenoids from the bark of *Erythrophleum fordii*', *Bioorganic and Medicinal Chemistry Letters*, 27(13), pp. 2946–2952.
- Haafteń, C., Van, Boot, A., Corver, W. E., Eendenburg, J. D. H. Van, Trimbos, B. J. M. Z. and Wezel, T. Van. (2015) 'Synergistic effects of the sesquiterpene lactone, EPD, with cisplatin and paclitaxel in ovarian cancer cells', *Journal of Experimental & Clinical Cancer Research*, 34(38), pp. 1–9.
- Hahn, M. A., Qiu, R., Wu, X., Li, A. X., Zhang, H., Wang, J., Jui, J., Jin, S., Jiang, Y., Pfeifer, G. P. and Lu, Q. (2013) 'Report dynamics of 5-hydroxymethylcytosine and chromatin marks in mammalian neurogenesis', *Cell Reports*, 3(2), pp. 291–300.
- Hanahan, D. and Weinberg, R. A. (2000) 'The hallmarks of cancer', *Cell*, 100, pp. 57–70.

- Hanahan, D. and Weinberg, R. A. (2011) 'Hallmarks of cancer : The next generation', *Cell*, 144(5), pp. 646–674.
- Hara, N., Asaki, H., Fujimoto, Y., Gupta, Y. K., Singh, A. K. and Sahai, M. (1995) 'Clerodane and ent-halimane diterpenes from *Polyalthia longifolia*', *Phytochemistry*, 38(1), pp. 189–194.
- Harvey, A. L. (2008) 'Natural products in drug discovery', *Drug Discovery Today*, 13(19–20), pp. 894–901.
- Harvey, A. L., Edrada-Ebel, R. and Quinn, R. J. (2015) 'The re-emergence of natural products for drug discovery in the genomics era', *Nature Reviews Drug Discovery*, 14(2), pp. 111–129.
- He, R., Shi, X., Zhou, M., Zhao, Y., Pan, S., Zhao, C., Guo, X., Wang, M., Li, X. and Qin, R. (2018) 'Alantolactone induces apoptosis and improves chemosensitivity of pancreatic cancer cells by impairment of autophagy-lysosome pathway via targeting TFEB', *Toxicology and Applied Pharmacology*, 356(1095), pp. 159–171.
- Hehner, S. P., Hofmann, T. G., Dröge, W., Hehner, S. P., Hofmann, T. G. and Dro, W. (2017) 'The antiinflammatory sesquiterpene lactone parthenolide inhibits NF- $\kappa$ B by targeting the I $\kappa$ B kinase complex', *The Journal of Immunology*, 163, pp. 5617–5623.
- Hervouet, E., Peixoto, P., Delage-Mourroux, R., Boyer-Guittaut, M. and Cartron, P. F. (2018) 'Specific or not specific recruitment of DNMTs for DNA methylation, an epigenetic dilemma', *Clinical Epigenetics*, 10(1), pp. 1–18.
- Hodek, P., Trefil, P. and Stiborova, M. (2002) 'Flavonoids-potent and versatile biologically active compounds interacting with cytochromes', *Chemico-Biological Interactions*, 139, pp. 1–21.
- Hu, H., Luo, L., Liu, F., Zou, D., Zhu, S., Tan, B. and Chen, T. (2016) 'Anti-cancer and sensibilisation effect of triptolide on human epithelial ovarian cancer', *Journal of Cancer*, 7(14), pp. 2093–2099.
- Hu, M., Liu, L. and Yao, W. (2018) 'Activation of p53 by costunolide blocks glutaminolysis and inhibits proliferation in human colorectal cancer cells', *Gene*, 678, pp. 261–269.
- Huang, J., Plass, C. and Gerhäuser, C. (2011) 'Cancer chemoprevention by targeting the epigenome', *Current Drug Targets*, 12(11), pp. 1–32.
- IARC (2019) *Cancer today- population fact sheets*. Available at: <https://gco.iarc.fr/today/data/factsheets/populations/566-nigeria-fact-sheets.pdf> (Accessed: 10 August 2019).
- IARC (2020) *Cance today- population fact sheets*. Available at: <https://gco.iarc.fr/today/data/factsheets/populations/903-africa-fact-sheets.pdf> (Accessed: 18 May 2020).
- Islam, M. T., Ali, E. S., Uddin, S. J., Islam, M. A., Shaw, S., Khan, I. N., Saravi, S. S. S.,

- Ahmad, S., Rehman, S., Gupta, V. K., Găman, M. A., Găman, A. M., Yele, S., Das, A. K., de Castro e Sousa, J. M., de Moura Dantas, S. M. M., Rolim, H. M. L., de Carvalho Melo-Cavalcante, A. A., Mubarak, M. S., ... Kamal, M. A. (2018) 'Andrographolide, a diterpene lactone from *Andrographis paniculata* and its therapeutic promises in cancer', *Cancer Letters*, 420, pp. 129–145.
- Jafari, N., Nazeri, S. and Enferadi, S. T. (2018) 'Parthenolide reduces metastasis by inhibition of vimentin expression and induces apoptosis by suppression elongation factor  $\alpha - 1$  expression', *Phytomedicine*, 41, pp. 67–73.
- Jarukamjorn, K. and Nemoto, N. (2008) 'Pharmacological aspects of andrographis paniculata on health and its major diterpenoid constituent', *Journal of Health Science*, 54(4), pp. 370–381.
- Jasek, K., Kubatka, P., Samec, M., Liskova, A., Smejkal, K., Vybohova, D., Bugos, O., Biskupska-Bodova, K., Bielik, T., Zubor, P., Danko, J., Adamkov, M., Kwon, T. K. and Büsselberg, D. (2019) 'DNA methylation status in cancer disease: Modulations by plant-derived natural compounds and dietary interventions', *Biomolecules*, 9(7), pp. 1–19.
- Jeong, S., Itokawa, T., Shibuya, M. and Kuwano, M. (2002) 'Costunolide, a sesquiterpene lactone from *Saussurea lappa*, inhibits the VEGFR KDR / Flk-1 signaling pathway', *Cancer letters*, 187, pp. 129–133.
- Jian, B., Zhang, H., Han, C. and Liu, J. (2018) 'Anti-cancer activities of diterpenoids derived from *Euphorbia fischeriana* steud', *Molecules*, 23(2), pp. 1–11.
- Jiang, Y., Xu, H. and Wang, J. (2016) 'Alantolactone induces apoptosis of human cervical cancer cells via reactive oxygen species generation, glutathione depletion and inhibition of the Bcl-2/Bax signaling pathway', *Oncology Letters*, (15), pp. 4203–4207.
- Jimenez, V., Kemmerling, U., Paredes, R., Maya, J. D., Sosa, M. A. and Galanti, N. (2014) 'Natural sesquiterpene lactones induce programmed cell death in *Trypanosoma cruzi*: A new therapeutic target?', *Phytomedicine*, 21(11), pp. 1411–1418.
- Johnson-Ajinwo, O. R. (2017) 'Identification, semi-synthesis and evaluation of anti-ovarian cancer compounds from plants used in traditional medicines'.
- Johnson-ajinwo, O. R., Richardson, A. and Li, W. (2015) 'Phytomedicine Cytotoxic effects of stem bark extracts and pure compounds from *Margaritaria discoidea* on human ovarian cancer cell lines', *Phytomedicine*, 22, pp. 1–4.
- Johnson-Ajinwo, O. R., Richardson, A. and Li, W. W. (2019) 'Palmatine from unexplored *Rutidea parviflora* showed cytotoxicity and induction of apoptosis in human ovarian cancer cells', *Toxins*, 11(237), pp. 1-11.
- Johnson, S. J., Sorg, R. A., Borker, R. D. and Duh, M. S. (2014) 'Patients initially diagnosed with advanced ovarian cancer', *Clinical Ovarian and other Gynecologic Cancer*, 5(2), pp. 67-77.
- Joseph, L., Aranjani, J. M., Pai, K. S. R. and Srinivasan, K. K. (2017) 'Promising anticancer

- activities of *Justicia simplex* D. Don. in cellular and animal models', *Journal of Ethnopharmacology*, 199, pp. 231–239.
- Kadayifci, F. Z., Zheng, S. and Pan, Y. X. (2018) 'Molecular mechanisms underlying the link between diet and DNA methylation', *International Journal of Molecular Sciences*, 19(12), pp. 1–20.
- Kaminskas, E., Farrell, A. T., Wang, Y. C., Sridhara, R., and Pazdur, R. (2011) 'FDA drug approval summary: azacitidine (5-azacytidine, Vidaza) for injectable suspension', *The Oncologist*, 16, pp. 176–182.
- Kang, J. H., Kim, S. J., Noh, D., Park, I. A., Choe, K. J., Yoo, O. J. and Kang, H. (2001) 'Methylation in the p53 promoter is a supplementary route to breast carcinogenesis: correlation between CpG methylation in the p53 promoter and the mutation of the p53 gene in the progression from ductal carcinoma in situ to invasive ductal carcinoma', *Laboratory Investigation*, 81(4), pp. 573–579.
- Kang, X., Wang, H., Li, Y., Xiao, Y., Zhao, L., Zhang, T., Zhou, S., Zhou, X., Li, Y., Shou, Z., Chen, C. and Li, B. (2019) 'Alantolactone induces apoptosis through ROS-mediated AKT pathway and inhibition of PINK1-mediated mitophagy in human HepG2 cells', *Artificial Cells, Nanomedicine and Biotechnology*, 47(1), pp. 1961–1970.
- Khan, I., Khan, F., Farooqui, A. and Ansari, I. A. (2018) 'Andrographolide exhibits anticancer potential against human colon cancer cells by inducing cell cycle arrest and programmed cell death via augmentation of intracellular reactive oxygen species level', *Nutrition and Cancer*, 70(5), pp. 787–803.
- Khan, M., Li, T., Ahmad Khan, M. K., Rasul, A., Nawaz, F., Sun, M., Zheng, Y. and Ma, T. (2013) 'Alantolactone induces apoptosis in HepG2 cells through GSH depletion, inhibition of STAT3 activation, and mitochondrial dysfunction', *BioMed Research International*, 2013, pp. 1–11.
- Khan, M., Yi, F., Rasul, A., Li, T., Wang, N., Gao, H., Gao, R. and Ma, T. (2012) 'Alantolactone induces apoptosis in glioblastoma cells via GSH depletion, ROS generation, and mitochondrial dysfunction', *Life*, 64(9), pp. 783–794.
- Kijjoa, A., Pinto, M. M. M., Pinho, P. M. M. and Herzt, W. (1993) 'Clerodanes from *Polyalthia viridis*', *phytochemistry*, 34(2), pp. 2–5.
- Kim, D. Y. and Choi, B. Y. (2019) 'Costunolide- A bioactive sesquiterpene lactone with diverse therapeutic potential', *International Journal of Molecular Sciences*, 20, pp. 1–21.
- Kim, S. T., Kim, S. Y., Lee, J., Kim, K., Park, S. H., Park, Y. S., Lim, H. Y., Kang, W. K. and Park, J. O. (2018) 'Triptolide as a novel agent in pancreatic cancer: The validation using patient derived pancreatic tumor cell line', *BMC Cancer*, 18(1), pp. 1–7.
- Kraus, T. F. J., Globisch, D., Wagner, M., Eigenbrod, S., Widmann, D., Münzel, M., Müller, M., Pfaffeneder, T., Hackner, B., Feiden, W., Schüller, U., Carell, T. and Kretschmar, H. A. (2012) 'Low values of 5-hydroxymethylcytosine (5hmC), the "sixth base," are associated with anaplasia in human brain tumors', *International Journal of Cancer*, 131(7), pp. 1577–

1590.

Kriaucionis, S. and Heintz, N. (2009) 'The nuclear DNA base, 5-hydroxymethylcytosine is present in brain and enriched in Purkinje neurons', *Science*, 324(5929), pp. 929–930.

Krifa, M., Alhosin, M., Muller, C. D., Gies, J., Chekir-Ghedira, L., Ghedira, K., Mély, Y., Bronner, C. and Mousli, M. (2013) 'Limoniastrum guyonianum aqueous gall extract induces apoptosis in human cervical cancer cells involving p16INK4A re-expression related to UHRF1 and DNMT1 down-regulation', *Journal of Experimental & Clinical Cancer Research.*, 32(1), pp. 1-10.

Kumar, A., Kumar, S., Kumar, D. and Agnihotri, V. K. (2014) 'UPLC / MS / MS method for quantification and cytotoxic activity of sesquiterpene lactones isolated from *Saussurea lappa*', *Journal of Ethnopharmacology*, 155(2), pp.

Kupchan, S. M., Eakin, M. A. and Thomas, A. M. (1971) 'Tumor inhibitors 69 structure-cytotoxicity relationships among the sesquiterpene lactones', *Journal of Medicinal Chemistry*, 14(12), pp. 1147–1152.

Kurdyukov, S. and Bullock, M. (2016) 'DNA methylation analysis: Choosing the right method', *Biology*, 5(1), pp. 3.

Lavanya, C., Rao, B. G. and Ramadevi, D. (2018) 'Phytochemical and pharmacological studies on *Polyalthia longifolia*', *Pharmaceutical Science and Research*, 3(4), pp. 1–7.

Lee, C. S., Kim, Y. J., Lee, S. A., Myung, S. C. and Kim, W. (2012) 'Combined effect of Hsp90 inhibitor geldanamycin and parthenolide via reactive oxygen species-mediated apoptotic process on epithelial ovarian cancer cells', *Basic and Clinical Pharmacology and Toxicology*, 111(3), pp. 173–181.

Lee, M. L., Lee, K., Chi, S. C. and Park, J. P. (2001) 'Costunolide induces apoptosis by ROS-mediated mitochondrial permeability transition and cytochrome c release', *Biological and Pharmaceutical Bulletin*, 24(3), pp. 303–306.

Lee, W. J., Shim, J. and Zhu, B. T. (2005) 'Mechanisms for the inhibition of DNA methyltransferases by tea catechins and bioflavonoids', *Molecular Pharmacology*, 68(4), pp. 1018–1030.

Lei, J., Yu, J., Yin, Y., Liu, Y. and Zou, G. (2012) 'Alantolactone induces activation of apoptosis in human hepatoma cells', *Food and Chemical Toxicology*, 50(9), pp. 3313–3319.

Li, H., Lu, H., Lv, M., Wang, Q. and Sun, Y. (2018) 'Parthenolide facilitates apoptosis and reverses drug-resistance of human gastric carcinoma cells by inhibiting the STAT3 signaling pathway', *Oncology Letters*, 15(3), pp. 3572–3579.

Li, R., Morris-Natschke, S. L. and Lee, K. (2016) 'Clerodane diterpenes: sources, structures, and biological activities', *Natural Product Reports*, 33(2), pp. 1166–1226.

Li, X., Lu, Q., Xie, W., Wang, Y. and Wang, G. (2018) 'Anti-tumor effects of triptolide on angiogenesis and cell apoptosis in osteosarcoma cells by inducing autophagy via repressing

- Wnt/ $\beta$ -Catenin signaling', *Biochemical and Biophysical Research Communications*, 496(2), pp. 443–449.
- Lim, S. C., Jeon, H. J., Kee, K. H., Lee, M. J., Hong, R. and Han, S. I. (2017) 'Andrographolide induces apoptotic and non-apoptotic death and enhances tumor necrosis factor-related apoptosis-inducing ligand-mediated apoptosis in gastric cancer cells', *Oncology Letters*, 13(5), pp. 3837–3844.
- Lin, C., Wong, B. C. K., Chen, H., Bian, Z., Zhang, G., Zhang, X., Kashif Riaz, M., Tyagi, D., Lin, G., Zhang, Y., Wang, J., Lu, A. and Yang, Z. (2017) 'Pulmonary delivery of triptolide-loaded liposomes decorated with anti-carbonic anhydrase IX antibody for lung cancer therapy', *Scientific Reports*, 7(1), pp. 1–12.
- Lin, M., Bi, H., Yan, Y., Huang, W., Zhang, G., Zhang, G., Tang, S., Liu, Y., Zhang, L., Ma, J. and Zhang, J. (2017) 'Parthenolide suppresses non-small cell lung cancer GLC-82 cells growth via B-Raf/MAPK/Erk pathway', *Oncotarget*, 8(14), pp. 23436–23447.
- Lisanti, S., Omar, W. A. W., Tomaszewski, B., De Prins, S., Jacobs, G., Koppen, G., Mathers, J. C. and Langie, S. A. S. (2013) 'Comparison of methods for quantification of global DNA methylation in human cells and tissues', *Plos One*, 8(11), pp. 1–11.
- Liu, C., Chang, H., Chen, I., Chen, C., Hsu, M. and Fu, S. (2011) 'Costunolide causes mitotic arrest and enhances radiosensitivity in human hepatocellular carcinoma cells', *Radiation Oncology*, 6(56), pp. 1-11.
- Liu, J., Yang, Z., Kong, Y., He, Y., Xu, Y. and Cao, X. (2019) 'Antitumor activity of alantolactone in lung cancer cell lines NCI-H1299 and Anip973', *Journal of Food Biochemistry*, 43(9), pp. 1–10.
- Liu, Y. C., Kim, S. L., Park, Y. R., Lee, S. T. and Kim, S. W. (2017) 'Parthenolide promotes apoptotic cell death and inhibits the migration and invasion of SW620 cells', *Intestinal Research*, 15(2), pp. 174–181.
- Liu, Z., Liu, S., Xie, Z., Pavlovicz, R. E., Wu, J., Chen, P., Aimiwu, J., Pang, J., Bhasin, D., Neviani, P., Fuchs, J. R., Plass, C., Li, P., Li, C., Huang, T. H., Wu, L., Rush, L., Wang, H., Perrotti, D., ... Chan, K. K. (2009) 'Modulation of DNA methylation by a sesquiterpene lactone parthenolide', *Journal of Pharmacology and Experimental Therapeutics*, 329(2), pp. 505–514.
- Liu, Z., Wu, J., Xie, Z., Liu, S., Fan-Havard, P., Huang, T. H.-M., Plass, C., Marcucci, G. and Chan, K. K. (2009) 'Quantification of regional DNA methylation by liquid chromatography/tandem mass spectrometry', *Analytical Biochemistry*, 391(2), pp. 106–113.
- Livak, K. J. and Schmittgen, T. D. (2001) 'Analysis of relative gene expression data using real-time quantitative PCR and the 2- $\Delta\Delta$ CT method', *Methods*, 25(4), pp. 402–408.
- Long, J., Ding, Y. H., Wang, P. P., Zhang, Q. and Chen, Y. (2016) 'Total syntheses and structure-activity relationship study of parthenolide analogues', *Tetrahedron Letters*, 57(8), pp. 874–877.

- Lopez-Serra, P. and Esteller, M. (2012) 'DNA methylation-associated silencing of tumor-suppressor microRNAs in cancer', *Oncogene*, 32, pp. 1609–1622. doi: 10.1038/onc.2011.354.
- Lübbert, M., Wijermans, P., Kunzmann, R., Verhoef, G., Bosly, A., Ravoet, C., Andre, M. and Ferrant, A. (2001) 'Cytogenetic responses in high-risk myelodysplastic syndrome following low-dose treatment with the DNA methylation inhibitor 5-aza-2'-deoxycytidine', *British Journal of Haematology*, 114(2), pp. 349–357.
- Luo, H., Jiang, B., King, S. M., Chen, Y. C., Luo, H., Jiang, B., King, S. M., Chen, Y. C., Luo, H., King, S. M. and Chen, Y. C. (2008) 'Inhibition of cell growth and VEGF expression in ovarian cancer cells by flavonoids', *Nutrition and Cancer*, 60(6), pp. 800–809.
- Ly, J. D., Grubb, D. R. and Lawen, A. (2003) 'The mitochondrial membrane potential ( $\Delta\psi_m$ ) in apoptosis; an update', *Apoptosis*, 8(2), pp. 115–128.
- Lyko, F. and Brown, R. (2005) 'DNA methyltransferase inhibitors and the development of epigenetic cancer therapies', *Journal of the National Cancer Institute*, 97(20), pp. 1498–1506.
- Ma, X., Lee, I. S., Chai, H. B., Zaw, K., Farnsworth, N. R., Soejarto, D. D., Cordell, G. A., Pezzuto, J. M. and Kinghorn, A. D. (1994) 'Cytotoxic clerodane diterpenes from *Polyalthia barnesii*', *Phytochemistry*, 37(6), pp. 37–40.
- Maldonado, L. and Hogue, M. O. (2010) 'Epigenomics and ovarian carcinoma', *Biomarkers in Medicine*, 4(4), pp. 543–570.
- Mao, J., Yi, M., Tao, Y., Huang, Y. and Chen, M. (2019) 'Costunolide isolated from *Vladimiria souliei* inhibits the proliferation and induces the apoptosis of HepG2 cells', *Molecular Medicine Reports*, 19(2), pp. 1372–1379.
- Mao, X., Tong, J., Wang, Y., Zhu, Z., Yin, Y. and Wang, Y. (2018) 'Triptolide exhibits antitumor effects by reversing hypermethylation of WIF - 1 in lung cancer cells', *Molecular Medicine Reports*, (2), pp. 3041–3049.
- Maria, A. O., Repetto, M., Llesuy, S., Giordano, O., Guzman, J., and Guerreiro, E. (2000) 'Antioxidant activity of artemisia douglasiana besser extract and dehydroleucodine', *Phytotherapy Research*, 14, pp. 558–560.
- Mccloud, T. G. (2010) 'High throughput extraction of plant, marine and fungal specimens for preservation of biologically active molecules', *Molecules*, 15, pp. 4526–4563.
- Menyhárt, O., Harami-Papp, H., Sukumar, S., Schäfer, R., Magnani, L., de Barrios, O. and Györfy, B. (2016) 'Guidelines for the selection of functional assays to evaluate the hallmarks of cancer', *Biochimica et Biophysica Acta - Reviews on Cancer*, 1866(2), pp. 300–319.
- Milutinovic, S., Brown, S. E., Zhuang, Q. and Szyf, M. (2004) 'DNA methyltransferase 1 knock down induces gene expression by a mechanism independent of DNA methylation and histone deacetylation', *Journal of Biological Chemistry*, 279(27), pp. 27915–27927.

- Mittal, J., Sharma, M. M. and Batra, A. (2014) 'Tinospora cordifolia: a multipurpose medicinal plant-A review', *Journal of Medicinal Plants Studies*, 2(2), pp. 32–47.
- Momparler, R. L., Momparler, L. F. and Samson, J. (1984) 'Comparison of the antileukemic activity of 5-aza-2'-deoxycytidine, 1- $\beta$ -d-arabinofuranosylcytosine and 5-azacytidine against L1210 leukemia', *Leukemia Research*, 8(6), pp. 1043–1049.
- Montgomery, M. and Srinivasan, A. (2019) 'Epigenetic gene regulation by dietary compounds in cancer prevention', *Advances in Nutrition*, 10(6), pp. 1012–1028.
- Monticelli, S. (2019) 'DNA (Hydroxy) methylation in T helper lymphocytes', *Trends in Biochemical Sciences*, 44(7), pp. 589–598.
- Morales, S., Monzo, M. and Navarro, A. (2017) 'Epigenetic regulation mechanisms of microRNA expression', *Biomolecular Concepts*, 8(5–6), pp. 203–212.
- Moundipa, F. P., Kamtchouing, P., Koueta, N. and Tantchou, J. (1999) 'Effects of aqueous extracts of *Hibiscus macranthus* and *Basella alba* in mature rat testis function', *Journal of Ethno-Pharmacology*, 65, pp. 133–139.
- Mpiana, P., Bokota, M. T., Ndjele, M. B. L., Mudogo, V., Tshibangu, D. S. T., Ngbolua, K. N., Atibu, E. K., Kwembe, J. T. . and Makelele, L. K. (2011) 'Antisickling activity of three species of *Justicia* from Kisangani (D.R. Congo): *J. tenella*, *J. gendarussa* and *J. insularis*', *International Journal of Biological and Chemical Sciences*, 4(6), pp. 1953–1961.
- Müller, D. S., Untiedt, N. L., Dieskau, A. P., Lackner, G. L. and Overman, L. E. (2015) 'Constructing quaternary stereogenic centers using tertiary organocuprates and tertiary radicals. Total synthesis of trans-clerodane natural products', *Journal of the American Chemical Society*, 137(2), pp. 660–663.
- Münzel, M., Globisch, D. and Carell, T. (2011) '5-Hydroxymethylcytosine, the sixth base of the genome', *Angewandte Chemie International Edition*, 50(29), pp. 6460–6468.
- Murai, M., Toyota, M., Satoh, A., Suzuki, H., Akino, K., Mita, H., Sasaki, Y., Ishida, T. and Shen, L. (2005) 'Aberrant DNA methylation associated with silencing BNIP3 gene expression in haematopoietic tumours', *British Journal of Cancer*, 92(6) pp. 1165–1172.
- Mustafi, S., Veisaga, M. L., López, L. A. and Barbieri, M. A. (2015) 'A novel insight into dehydroleucodine mediated attenuation of *Pseudomonas aeruginosa* virulence mechanism', *BioMed Research International*, pp. 1–13.
- Nanduri, S., Nyavanandi, V. K., Rao, S., Kasu, S., Pallerla, K., Ram, P. S., Rajagopal, S., Kumar, R. A., Ramanujam, R., Babu, J. M., Vyas, K., Devi, A. S., Om, G. and Akella, V. (2004) 'Synthesis and structure – activity relationships of andrographolide analogues as novel cytotoxic agents', *Bioorganic and Medicinal Chemistry Letters*, 14(18), pp. 4711–4717.
- Nardi, I., Reno, T., Yun, X., Sztain, T., Wang, J., Dai, H., Zheng, L., Shen, B., Kim, J. and Raz, D. (2018) 'Triptolide inhibits Wnt signaling in NSCLC through upregulation of multiple Wnt inhibitory factors via epigenetic modifications to histone H3', *International*

---

*Journal of Cancer*, 143(10), pp. 2470–2478.

Nateewattana, J., Dutta, S., Reabroi, S. and Saeeng, R. (2014) ‘Induction of apoptosis in cholangiocarcinoma by an andrographolide analogue is mediated through topoisomerase II alpha inhibition’, *European Journal of Pharmacology*, 723, pp. 148–155.

National Institutes of Health (2020) *Genetics home reference: MLH1 gene*. Available at: <https://ghr.nlm.nih.gov/gene/MLH1#conditions> (Accessed: 1 October 2020).

National Institutes of Health (2020) ‘*Genetics home reference: PTEN gene*. Available at: <https://ghr.nlm.nih.gov/gene/PTEN#conditions> (Accessed: 1 October 2020)

Newman, D. J. and Cragg, G. M. (2016) ‘Natural products as sources of new drugs from 1981 to 2014’, *Journal of Natural Products*, 79(3), pp. 629–661.

Notaro, S., Reimer, D., Fiegl, H., Schmid, G., Wiedemair, A., Rössler, J., Marth, C. and Zeimet, A. G. (2016) ‘Evaluation of folate receptor 1 ( FOLR1 ) mRNA expression, its specific promoter methylation and global DNA hypomethylation in type I and type II ovarian cancers’, *BMC Cancer*, 16(1). pp. 1-13.

Odukogbe, A. A., Adebamowo, C. A., Ola, B., Olayemi, O. and Oladokun, A. (2004) ‘Ovarian cancer in Ibadan : characteristics and management’, *Journal of Obstetrics and Gynaecology*, 24(3), pp. 294–297.

Oka, D., Nishimura, K., Shiba, M., Nakai, Y., Arai, Y. and Nakayama, M. (2007) ‘Sesquiterpene lactone parthenolide suppresses tumor growth in a xenograft model of renal cell carcinoma by inhibiting the activation of NF- j B’, *International Journal of Cancer*, 120(12), pp. 2576–2581.

Ordóñez, P. E., Sharma, K. K., Bystrom, L. M., Alas, M. A., Enriquez, R. G., Malagón, O., Jones, D. E., Guzman, M. L. and Compadre, C. M. (2016) ‘Dehydroleucodine, a sesquiterpene lactone from *Gynoxys verrucosa* , demonstrates cytotoxic activity against human leukemia cells’, *Journal of Natural Products*, 79(4), pp. 691–696.

Orellana, E. and Kasinski, A. (2016) ‘Sulforhodamine B (SRB) assay in cell culture to investigate cell proliferation’, *Bio-Protocol*, 6(21), pp. 1–7.

Pajak, B., Gajkowska, B. and Orzechowski, A. (2008) ‘Molecular basis of parthenolide-dependent proapoptotic activity in cancer cells.’, *Folia Histochemica et Cytobiologica*, 46(2), pp. 129–135.

Pandey, M., Shukla, S. and Gupta, S. (2010) ‘Promoter demethylation and chromatin remodeling by green tea polyphenols leads to re-expression of GSTP1 in human prostate cancer cells’, *International Journal of Cancer*, 126, pp. 2520–2533.

Pareek, A., Suthar, M., Rathore, G. S. and Bansal, V. (2011) ‘Feverfew (*Tanacetum parthenium* L.): A systematic review’, *Pharmacognosy Reviews*, 5(9), pp. 103–10.

Park, H., Jung, W.-T., Basnet, P., Kadota, S. and Namba, T. (1996) ‘Syringin 4-O-β-glucoside, a new phenylpropanoid glycoside, and costunolide, a nitric oxide synthase

- inhibitor, from the stem bark of *Magnolia sieboldii*', *Journal of Natural Product*, 59(12), pp. 1128–1130.
- Peng, Y., Wang, Y., Tang, N., Sun, D., Lan, Y., Yu, Z., Zhao, X., Feng, L., Zhang, B., Jin, L., Yu, F., Ma, X. and Lv, C. (2018) 'Andrographolide inhibits breast cancer through suppressing COX-2 expression and angiogenesis via inactivation of p300 signaling and VEGF pathway', *Journal of Experimental and Clinical Cancer Research*, 37(1), pp. 1–14.
- Phadnis, A. P., Patwardhan, S. A., Dhaneshwar, N. N., Tavale, S. S. and Row, T. N. G. (1988) 'Clerodane diterpenoids from *Polyalthia longifolia*', *Phytochemistry*, 27(9), pp. 2899–2901.
- Pils, D., Horak, P., Vanhara, P., Anees, M., Petz, M., Alfan, A., Gugerell, A., Wittinger, M., Gleiss, A., Auner, V., Tong, D., Zeillinger, R., Braicu, E., Sehouli, J. and Krainer, M. (2013) 'Methylation status of TUSC3 is a prognostic factor in ovarian cancer', *Cancer*, 119(5), pp. 946–954.
- Pogribny, I. P. and James, S. J. (2002) 'Reduction of p53 gene expression in human primary hepatocellular carcinoma is associated with promoter region methylation without coding region mutation', *Cancer Letter*, 176, pp. 169–174.
- Polo, L. M., Castro, C. M., Cruzado, M. C., Collino, C. J. G., Cuello-Carrión, F. D., Ciocca, D. R., Giordano, O. S., Ferrari, M. and López, L. A. (2007) '11,13-dihydro-dehydroleucodine, a derivative of dehydroleucodine with an inactivated alkylating function conserves the anti-proliferative activity in G2 but does not cause cytotoxicity', *European Journal of Pharmacology*, 556(1–3), pp. 19–26.
- Pop, S., Enciu, A. M., Tarcomnicu, I., Gille, E. and Tanase, C. (2019) 'Phytochemicals in cancer prevention: modulating epigenetic alterations of DNA methylation', *Phytochemistry Reviews*, 18(4), pp. 1005–1024.
- Pradhan, N., Kar, S., Parbin, S., Sengupta, D., Deb, M., Das, L., and Patra, S. K. (2019) 'Epigenetic Dietary Interventions for Prevention of Cancer', *Epigenetics of Cancer Prevention*, pp. 23-48.
- Rajavelu, A., Tulyasheva, Z., Jaiswal, R., Jeltsch, A. and Kuhnert, N. (2011) 'The inhibition of the mammalian DNA methyltransferase 3a (DNMT3A) by dietary black tea and coffee polyphenols', *BioMed Central Biochemistry*, 12(16), pp. 1-8.
- Rasmussen, K. D. and Helin, K. (2020) 'Role of TET enzymes in DNA methylation, development, and cancer', *Genes and Development*, 30(7), pp. 733–750.
- Rasul, A., Khan, M., Ali, M., Li, J. and Li, X. (2013) 'Targeting apoptosis pathways in cancer with alantolactone and isoalantolactone', *The Scientific World Journal*, pp. 1–9.
- Rasul, A., Parveen, S. and Ma, T. (2012) 'Costunolide: A novel anti-cancer sesquiterpene lactone', *Bangladesh Journal of Pharmacology*, 7(1), pp. 6–13.
- Reid, B. M., Permeth, J. B. and Sellers, T. A. (2017) 'Epidemiology of ovarian cancer : a review', *Cancer Biology and Medicine*, 14(1), pp. 9–32.

- Rhode, J., Fogoros, S., Zick, S., Wahl, H., Griffith, K. A., Huang, J. and Liu, J. R. (2007) 'Ginger inhibits cell growth and modulates angiogenic factors in ovarian cancer cells', *BMC Complementary and Alternative Medicine*, 7(44), pp. 1-9.
- Robinson, A., Kumar, T. V., Sreedhar, E., Naidu, V. G. M., Krishna, S. R., Babu, K. S., Srinivas, P. V. and Rao, J. M. (2008) 'A new sesquiterpene lactone from the roots of *Saussurea lappa*: Structure-anticancer activity study', *Bioorganic and Medicinal Chemistry Letters*, 18(14), pp. 4015-4017.
- Robinson, E., Nandi, M., Wilkinson, L. L., Arrowsmith, D. M., Curtis, A. D. M. and Richardson, A. (2013) 'Preclinical evaluation of statins as a treatment for ovarian cancer', *Gynecologic Oncology*, 129(2), pp. 417-424.
- Robison, K., Olson, C., Sakr, B. J., Rizack, T., Legare, R., Stuckey, A., Granai, C. O. and Dizon, D. S. (2013) 'Outcomes for women receiving bevacizumab for treatment of ovarian cancer versus other solid tumors at an academic oncology center', *Clinical Ovarian and Other Gynecologic Cancer*, 6(1-2), pp. 21-24.
- Rocha, M. A., Veronezi, G. M. B., Felisbino, M. B., Gatti, M. S. V., Tamashiro, W. M. S. C. and Mello, M. L. S. (2019) 'Sodium valproate and 5-aza-2'-deoxycytidine differentially modulate DNA demethylation in G1 phase-arrested and proliferative HeLa cells', *Scientific Reports*, 9(1), pp. 1-12.
- Rogan, A. M., Hamilton, T. C., Young, R. C., Klecker, R. W. and Ozols, R. F. (1984) 'Reversal of adriamycin resistance by verapamil in human ovarian cancer', *Science*, 224(4652), pp. 994-996.
- Rubinstein, L. V., Shoemaker, R. H., Paull, K. D., Simon, R. M., Tosini, S., Skehan, P., Scudiero, D. A., Monks, A. and Boyd, M. R. (1990) 'Comparison of in vitro anticancer-drug-screening data generated with a tetrazolium assay versus a protein assay against a diverse panel of human tumor cell lines', *Journal of the National Cancer Institute*, 82(13), pp. 1113-1117.
- Salehi, F., Dunfield, L., Phillips, K. P., Krewski, D., Salehi, F., Dunfield, L., Phillips, K. P. and Krewski, D. (2008) 'Risk factors for ovarian cancer: An overview with emphasis on hormonal factors', *Journal of Toxicology and Environmental Health*, 11(3-4), pp. 301-321.
- Saosathan, S., Khounvong, J., Rungrojsakul, M., Katekunlaphan, T., Tima, S., Chiampanichayakul, S., Berkland, C., and Anuchapreeda, S. (2019) 'Costunolide and parthenolide from *Champi sirindhorn* (*Magnolia sirindhorniae*) inhibit leukemic cell proliferation in K562 and molt-4 cell lines', *Natural Product Research*, pp. 1-5.
- Sari, D. P., Ninomiya, M., Efdi, M., Santoni, A., Ibrahim, S., Tanaka, K. and Koketsu, M. (2013) 'Clerodane diterpenes isolated from *Polyalthia longifolia* induce apoptosis in human leukemia HL-60 cells', *Journal of Oleo Science*, 62(10), pp. 843-848.
- Sashidhara, K. V., Singh, S. P., Sarkar, J. and Sinha, S. (2010) 'Cytotoxic clerodane diterpenoids from the leaves of *Polyalthia longifolia*', *Natural Product Research*, 24(18), pp. 1687-1694.

- Sashidhara, K. V., Singh, S. P., Srivastava, A., Puri, A., Chhonker, Y. S., Bhatta, R. S., Shah, P. and Imran, M. (2011) 'Discovery of a new class of HMG-CoA reductase inhibitor from *Polyalthia longifolia* as potential lipid lowering agent', *European Journal of Medicinal Chemistry*, 46(10), pp. 5206–5211.
- Schatz, P. (2004) 'Rapid analysis of CpG methylation patterns using RNase T1 cleavage and MALDI-TOF', *Nucleic Acids Research*, 32(21), pp. 167–167.
- Schefer, F. A., Ricardo, S., Blind, C. L. Z., Luis, P., Souza, B. L. O., Filippin, M. F. B., Weber, B. M. and Orofino, K. M. R. (2017) 'Antitumoral activity of sesquiterpene lactone diacetylptocarphol in mice', *Journal of Ethnopharmacology*, 198, pp. 262–267.
- Schmid, B. C. and Oehler, M. K. (2014) 'Maturitas New perspectives in ovarian cancer treatment', *Maturitas*, 77(2), pp. 128–136.
- Scotti, M. T., Fernandes, M. B., Ferreira, M. J. P. and Emerenciano, V. P. (2007) 'Quantitative structure-activity relationship of sesquiterpene lactones with cytotoxic activity', *Bioorganic and Medicinal Chemistry*, 15(8), pp. 2927–2934.
- Scottish Intercollegiate Guidelines Network (SIGN) (2013) *Management of epithelial ovarian cancer*. Edinburgh: SIGN publication.
- Shankar, E., Kanwal, R., Candamo, M. and Gupta, S. (2016) 'Dietary phytochemicals as epigenetic modifiers in cancer: Promise and challenges', *Seminars in Cancer Biology*, 40(41), pp. 82–99.
- Sharma, S., Kelly, T. K. and Jones, P. A. (2010) 'Epigenetics in cancer', *Carcinogenesis*, 31(1), pp. 27–36.
- Sharmila, K. and Padma, P. R. (2013) 'Anticancer activities of artemisia vulgaris on hepatocellular carcinoma (Hepg2) cells', *International Journal of Pharmacy and Pharmaceutical Sciences*, 5(595), pp. 479–483.
- Sheeja, K., Guruvayoorappan, C. and Kuttan, G. (2007) 'Antiangiogenic activity of *Andrographis paniculata* extract and andrographolide', 7, pp. 211–221.
- Shi, L., Zhang, G., Zheng, Z., Lu, B. and Ji, L. (2017) 'Andrographolide reduced VEGFA expression in hepatoma cancer cells by inactivating HIF-1 $\alpha$ : The involvement of JNK and MTA1/HDCA', *Chemico-Biological Interactions*, 273, pp. 228–236.
- Shi, Y., Bao, Y. L., Wu, Y., Yu, C. L., Huang, Y. X., Sun, Y., Zheng, L. H., and Li, Y. X. (2011) 'Alantolactone inhibits cell proliferation by interrupting the interaction between cripto-1 and activin receptor type II A in activin signaling pathway', *Journal of Biomolecular Screening*, 16(5), pp. 525–535.
- Siegel, R. L., Miller, K. D. and Jemal, A. (2020) 'Cancer statistics, 2020', *Cancer Journal for Clinicians*, 70(1), pp. 7–30.
- Skehan, P., Storeng, R., Scudiero, D., Monks, A., McMahon, J., Vistica, D., Warren, J. T., Bokesch, H. Kenney, S., and Boyd, M. R. (1990) 'New colorimetric cytotoxicity assay for

- anticancer-drug screening', *Journal of the National Cancer Institute*, 82(13), pp. 1107–1112.
- Smolinski, A. T. and Pestka, J. J. (2005) 'Comparative effects of the herbal constituent parthenolide (Feverfew) on lipopolysaccharide-induced inflammatory gene expression in murine spleen and liver', *Journal of Inflammation*, 2(6), pp. 1–8.
- Soegaard, M., Jensen, A., Høgdall, E., Christensen, L., Høgdall, C., Blaaekær, J. and Kjaer, S. K. (2007) 'Different risk factor profiles for mucinous and nonmucinous ovarian cancer : results from the danish malova study', 16, pp. 1160–1167.
- Stresemann, C., Brueckner, B., Musch, T., Stopper, H. and Lyko, F. (2006) 'Functional diversity of DNA methyltransferase inhibitors in human cancer cell lines', *Cancer Research*, 66(5), pp. 2794–2800.
- Stresemann, C. and Lyko, F. (2008) 'Modes of action of the DNA methyltransferase inhibitors azacytidine and decitabine', *International Journal of Cancer*, 123(1), pp. 8–13.
- Subramaniam, D., Thombre, R., Dhar, A. and Anant, S. (2014) 'DNA methyltransferases : a novel target for prevention and therapy', *Frontiers in Oncology*, 4, pp. 1–13.
- Suhaiman, L., Carlos, J., Sartor, T., Palmada, N., Giordano, O. S. and Lopez, L. A. (2010) 'Effect of dehydroleucodine on the reproductive tract of male mice', *Andrologia*, 43, pp. 297–302.
- Sultana, S. and Asif, H. M. (2014) 'Medicinal plants combating against hypertension: A green antihypertensive approach', *Pakistan Journal of Pharmaceutical Sciences*, 30(6), pp. 2311–2319.
- Sun, Y. Y., Xiao, L., Wang, D., Ji, Y. C., Yang, Y. P., Ma, R. and Chen, X. H. (2017) 'Triptolide inhibits viability and induces apoptosis in liver cancer cells through activation of the tumor suppressor gene p53', *International Journal of Oncology*, 50(3), pp. 847–852.
- Sung, H. K., Ma, S. H., Choi, J., Hwang, Y., Ahn, C., Kim, B., Kim, Y., Kim, J. W., Kang, S., Kim, J., Kim, T. J., Yoo, K., Kang, D. and Park, S. (2016) 'The Effect of breastfeeding duration and parity on the risk of epithelial ovarian cancer : A Systematic Review and Meta-analysis', *Journal of Preventive Medicine and Public Health*, pp. 349–366.
- Suvannasankha, A., Crean, C. D., Shanmugam, R., Farag, S. S., Abonour, R., Boswell, H. S. and Nakshatri, H. (2008) 'Cancer therapy: preclinical antimyeloma effects of a sesquiterpene lactone parthenolide', *Clinical Cancer Research*, 14(8), pp. 1814–1822.
- Tahiliani, M., Koh, K. P., Shen, Y., Pastor, W. A., Brudno, Y., Agarwal, S., Iyer, L. M., David, R., Aravind, L. and Rao, A. (2009) 'Conversion of 5-methylcytosine to 5-hydroxymethylcytosine in mammalian DNA by MLL partner TET1', *Science*, 324(5929), pp. 930–935.
- Talib, W. H. and Al Kury, L. T. (2018) 'Parthenolide inhibits tumor-promoting effects of nicotine in lung cancer by inducing P53 - dependent apoptosis and inhibiting VEGF expression', *Biomedicine and Pharmacotherapy*, 107, pp. 1488–1495.

- Tan, L. and Shi, Y. G. (2012) 'TET family proteins and 5-hydroxymethylcytosine in development and disease', *Development*, 139(11), pp. 1895–1902.
- Telefo, P. ., Moundipa, P. . and Tchouanguép, F. . (2004) 'Inductive effect of the leaf mixture extract of *Aloe buettneri*, *Justicia insularis*, *Dicliptera verticillata* and *Hibiscus macranthus* on in vitro production of estradiol', *Journal of Ethnopharmacology*, 91(2–3), pp. 225–230.
- Telefo, Phelix Bruno, Tagne, S. R., Koona, O. E. S., Yemele, D. M. and Tchouanguép, F. M. (2012) 'Effect of the aqueous extract of *Justicia insularis* T. Anders ( Acanthaceae ) on ovarian folliculogenesis and fertility of female rats', *African Journal of Traditional, Complementary and Alternative Medicines*, 9(2), pp. 197–203.
- Tellez-plaza, M., Tang, W., Shang, Y., Umans, J. G., Francesconi, K. A., Goessler, W., Ledesma, M., Laclaustra, M., Pollak, J., Guallar, E., Cole, S. A., Fallin, M. D. and Navasacien, A. (2014) 'Association of global DNA methylation and global DNA hydroxymethylation with metals and other exposures in human blood DNA samples', *Environmental Health Perspectives*, 946(9), pp. 946–954.
- Tengchaisri, T., Chawengkirttikul, R. and Rachaphaew, N. (1998) 'Antitumor activity of triptolide against cholangiocarcinoma growth in vitro and in hamsters', *Cancer Letters*, 133, pp. 165–175.
- Thakur, V. S., Deb, G., Babcook, M. A. and Gupta, S. (2014) 'Plant phytochemicals as epigenetic modulators: Role in cancer chemoprevention', *American Association of Pharmaceutical Scientists Journal*, 16(1), pp. 151–163.
- Theriault, B. L., Basavarajappa, H. D., Lim, H., Pajovic, S., Gallie, B. L. and Corson, T. W. (2014) 'Transcriptional and epigenetic regulation of KIF14 overexpression in ovarian cancer', *Plos One*, 9(3), pp. 1–13.
- Thun, M. J., DeLancey, J. O., Center, M. M., Jemal, A. and Ward, E. M. (2010) 'The global burden of cancer: priorities for prevention', *Carcinogenesis*, 31(1), pp. 100–110.
- Tomar, T., de Jong, S., Alkema, N. G., Hoekman, R. L., Meersma, G. J., Klip, H. G., van der Zee, A. G. and Wisman, G. B. A. (2016) 'Genome-wide methylation profiling of ovarian cancer patient-derived xenografts treated with the demethylating agent decitabine identifies novel epigenetically regulated genes and pathways', *Genome Medicine*, 8(1), pp. 1–15.
- Tomasetti, M., Gaetani, S., Monaco, F., Neuzil, J. and Santarelli, L. (2019) 'Epigenetic regulation of miRNA expression in malignant mesothelioma: mirnas as biomarkers of early diagnosis and therapy', *Frontiers in Oncology*, 9, pp. 1–14.
- Tona, L., Kambu, K., Ngimbi, N., Cimanga, K. and Vlietinck, A. J. (1998) 'Antiamoebic and phytochemical screening of some Congolese medicinal plants', *Journal of Ethnopharmacology*, 61(1), pp. 57–65.
- Torre, L. A., Trabert, B., DeSantis, C. E., Miller, K. D., Samimi, G., Runowicz, C. D., Gaudet, M. M., Jemal, A. and Siegel, R. L. (2018) 'Ovarian cancer statistics, 2018', *Cancer Journal for Clinicians*, 68(4), pp. 284–27

- Tost, J. and Gut, I. G. (2007) 'DNA methylation analysis by pyrosequencing', *Nature Protocols*, 2(9), pp. 2265–2275.
- Uche, F. I., Abed, M. N., Abdullah, M. I., Drijfhout, F. P., McCullagh, J. Claridge, T. W. D, Richardson, A. and Li, W. W. (2017) 'Isochondrodendrine and 2'-norcocosuline: Additional alkaloids from *Triclisia subcordata* induce cytotoxicity and apoptosis in ovarian cancer cell lines', *RSC Advances*, 7, pp. 44154–44161.
- Uche, F. I. (2017) 'Phytochemical Analysis and Evaluation of Anticancer and Antimalarial Properties of Four Medicinal Plants'.
- Uche, F. I., Drijfhout, F., Mccullagh, J. and Richardson, A. (2016) 'Cytotoxicity effects and apoptosis induction by bisbenzylisoquinoline alkaloids from *Triclisia subcordata*', 44, pp. 1–22.
- Varghese, E., Samuel, S. M., Varghese, S., Cheema, S., Mamtani, R. and Büsselberg, D. (2018) 'Triptolide decreases cell proliferation and induces cell death in triple negative MDA-MB-231 breast cancer cells', *Biomolecules*, 8(63). pp. 1-14.
- Vega, A. E., Wendel, G. H., Maria, A. O. M. and Pelzer, L. (2009) 'Antimicrobial activity of *Artemisia douglasiana* and dehydroleucodine against *Helicobacter pylori*', *Journal of Ethnopharmacology*, 124(3), pp. 653–655.
- Vera, M. E., Persia, F. A., Mariani, M. L., Rudolph, M. I., Fogal, T. H., Ceñal, J. P., Favier, L. S., Tonn, C. E. and Penissi, A. B. (2012) 'Activation of human leukemic mast cell line LAD2 is modulated by dehydroleucodine and xanthatin', *Leukemia & Lymphoma*, 53(9), pp. 1795–1803.
- Vichai, V. and Kirtikara, K. (2006) 'Sulforhodamine B colorimetric assay for cytotoxicity screening', *Nature Protocols*, 1(3), pp. 1112–1116.
- Villar-Garea, A., Fraga, M. F., Espada, J. and Esteller, M. (2003) 'Procaine is a DNA-demethylating agent with growth-inhibitory effects in human', *Cancer Research*, 63, pp. 4984–4989.
- Wang, S., Zhang, H., Cheng, L., Evans, C. and Pan, C. X. (2010) 'Analysis of the cytotoxic activity of the carboplatin and gemcitabine combination', *Anticancer Research*, 30(11), pp. 4573–4578.
- Wang, X., Yu, Z., Wang, C., Cheng, W., Tian, X., Huo, X., Wang, Y., Sun, C., Feng, L., Xing, J., Lan, Y., Sun, D., Hou, Q. and Zhang, B. (2017) 'Alantolactone, a natural sesquiterpene lactone, has potent antitumor activity against glioblastoma by targeting IKK  $\beta$  kinase activity and interrupting NF- $\kappa$ B / COX-2-mediated signaling cascades', *Journal of Experimental and Clinical Cancer Research*, 36(1), pp. 1–14.
- War, A. R., Paulraj, M. G., Ahmad, T., Buhroo, A. A., Hussain, B., Ignacimuthu, S. and Sharma, H. C. (2012) 'Mechanisms of plant defense against insect herbivores', *Plant Signaling and Behaviour*, 7(10), pp. 1306–1320.
- Wei, W., Huang, H., Zhao, S., Liu, W., Liu, C., Chen, L., Li, J., Wu, Y. and Yan, H. (2013)

‘Alantolactone induces apoptosis in chronic myelogenous leukemia sensitive or resistant to imatinib through NF- $\kappa$ B inhibition and Bcr/Abl protein deletion’, *Apoptosis*, 18(9), pp. 1060–1070.

Wendel, G. H., María, A. O. M., Guzmán, J. A., Giordano, O. and Pelzer, L. E. (2008) ‘Antidiarrheal activity of dehydroleucodine isolated from *Artemisia douglasiana*’, *Fitoterapia*, 79(1), pp. 1–5.

Wentzensen, N., Poole, E. M., Trabert, B., White, E., Arslan, A. A., Patel, A. V, Setiawan, V. W., Visvanathan, K., Weiderpass, E., Adami, H., Black, A., Bernstein, L., Brinton, L. A., Buring, J., Butler, L. M., Chamosa, S., Clendenen, T. V, Dossus, L., Fortner, R., ... Tworoger, S. S. (2016) ‘Ovarian cancer risk factors by histologic subtype : an analysis from the ovarian cancer cohort consortium’, *Journal of Clinical Oncology*, 34(24), pp. 4–7.

White, H. E. (2006) ‘Quantitative analysis of SRNPN gene methylation by pyrosequencing as a diagnostic test for prader-willi syndrome and angelman syndrome’, *Clinical Chemistry*, 52(6), pp. 1005–1013.

White, S. R., Williams, P., Wojcik, K. R., Sun, S., Hiemstra, P. S., Rabe, K. F. and Dorscheid, D. R. (2001) ‘Initiation of apoptosis by actin cytoskeletal derangement in human airway epithelial cells’, *American Journal of Respiratory Cell and Molecular Biology*, 24, pp. 282–294.

Witham, J., Valenti, M. R., De-Haven-Brandon, A. K., Vidot, S., Eccles, S. A., Kaye, S. B. and Richardson, A. (2007) ‘The Bcl-2/Bcl-XL family inhibitor ABT-737 sensitizes ovarian cancer cells to carboplatin’, *Clinical Cancer Research*, 13(23), pp. 7191–7198.

Wong, R. S. Y. (2011) ‘Apoptosis in cancer : from pathogenesis to treatment’, *Journal of Experimental and Clinical Cancer Research*, 30(1), pp. 1–14.

Wu, C. W., Wang, S. G., Lin, M. L. and Chen, S. S. (2019) ‘Downregulation of miR-144 by triptolide enhanced p85 $\alpha$ -PTEN complex formation S phase arrest of human nasopharyngeal carcinoma cells’, *European Journal of Pharmacology*, 855, pp. 137–148.

Wu, H. and Zhang, Y. (2011) ‘Mechanisms and functions of Tet protein- mediated 5-methylcytosine oxidation’, *Genes and Development*, 25, pp. 2436–2452.

Wu, P., Liu, K., Huang, W., Ma, C., Lin, H., Yang, J. and Chung, J. (2011) ‘Triptolide induces apoptosis in human adrenal cancer NCI-H295 cells through a mitochondrial-dependent pathway’, *Oncology Reports*, 25(2), pp. 551–557.

Xu, H. and Liu, B. (2019) ‘Triptolide-targeted delivery methods’, *European Journal of Medicinal Chemistry*, 164, pp. 342–351.

Xu, H., Tang, H., Feng, H. and Li, Y. (2014) ‘Design, synthesis and structure-activity relationships studies on the d ring of the natural product triptolide’, *ChemMedChem*, 9(2), pp. 290–295.

Yan, Z., Xu, T., An, Z., Hu, Y., Chen, W., Ma, J., Shao, C. and Zhu, F. (2019) ‘Costunolide induces mitochondria-mediated apoptosis in human gastric adenocarcinoma BGC-823

- cells', *BMC Complementary and Alternative Medicine*, 19(1), pp. 1–10.
- Yang, A. S. (2006) 'DNA methylation changes after 5-aza-2'-deoxycytidine therapy in patients with leukemia', *Cancer Research*, 66(10), pp. 5495–5503.
- Yang, H. P., Trabert, B., Murphy, M. A., Sherman, M. E., Sampson, J. N., Brinton, L. A., Hartge, P., Hollenbeck, A., Park, Y. and Wentzensen, N. (2012) 'Ovarian cancer risk factors by histologic subtypes in the NIH-AARP diet and health study', *International Journal of Cancer*, 948, pp. 938–948.
- Yang, Y., Kim, J., Lee, K. and Choi, J. (2011) 'Gynecologic oncology costunolide induces apoptosis in platinum-resistant human ovarian cancer cells by generating reactive oxygen species', *Gynecologic Oncology*, 123(3), pp. 588–596.
- Yao, Q., Chen, Y. and Zhou, X. (2019) 'The roles of microRNAs in epigenetic regulation', *Current Opinion in Chemical Biology*, 51, pp. 11–17.
- Yao, Y., Xia, D., Bian, Y., Sun, Y. and Zhu, F. (2015) 'Alantolactone induces G1 phase arrest and apoptosis of multiple myeloma cells and overcomes bortezomib resistance', *Apoptosis*, 20(8), pp. 1122–1133.
- Yin, C., Dai, X., Huang, X., Zhu, W., Chen, X., Zhou, Q., Wang, C., Zhao, C., Zou, P., Liang, G., Rajamanickam, V., Wang, O., Zhang, X. and Cui, R. (2019) 'Alantolactone promotes ER stress-mediated apoptosis by inhibition of TrxR1 in triple-negative breast cancer cell lines and in a mouse model', *Journal of Cellular and Molecular Medicine*, 23(3), pp. 2194–2206.
- Yuan, W., Yang, G., Zhang, J., Zhang, Y., Chen, D., Li, S., Di, Y. and Hao, X. (2016) 'Three new diterpenes with cytotoxic activity from the roots of *Euphorbia ebracteolata* Hayata', *Phytochemistry Letters*, 18, pp. 176–179.
- Yunos, N. M., Mutalip, S. S. M., Jauri, M. H., Yu, J. Q. and Huq, F. (2013) 'Anti-proliferative and pro-apoptotic effects from sequenced combinations of andrographolide and cisplatin on ovarian cancer cell lines', *Anticancer Research*, 33(10), pp. 4365–4372.
- Zhan, Z., Fan, C., Ding, J. and Yue, J. (2005) 'Novel diterpenoids with potent inhibitory activity against endothelium cell HMEC and cytotoxic activities from a well-known TCM plant *Daphne genkwa*', *Bioorganic and Medicinal Chemistry*, 13(3), pp. 645–655.
- Zhang, C., He, X. J., Li, L., Lu, C. and Lu, A. P. (2017) 'Effect of the natural product triptolide on pancreatic cancer: a systematic review of preclinical studies', *Frontiers in Pharmacology*, 8, pp. 1–9.
- Zhang, C. and Qiu, X. (2015) 'Andrographolide radiosensitizes human ovarian cancer SKOV3 xenografts due to an enhanced apoptosis and autophagy', *Tumor Biology*, 36(11), pp. 8359–8365.
- Zhang, C. Y., Zhang, L. J., Lu, Z. C., Ma, C. Y., Ye, Y., Rahman, K., Zhang, H., and Zhu, J. Y. (2018) 'Antitumor activity of diterpenoids from *Jatropha gossypifolia*: cell cycle arrest and apoptosis-inducing activity in RKO colon cancer cells', *Journal of Natural*

*Products*, 81(8), pp. 1701–1710.

Zhang, J., Li, Y., Duan, D., Yao, J., Gao, K. and Fang, J. (2016) ‘Inhibition of thioredoxin reductase by alantolactone prompts oxidative stress-mediated apoptosis of HeLa cells’, *Biochemical Pharmacology*, 102, pp. 34–44.

Zhang, L., Li, P., Wang, T. and Zhang, X. (2015) ‘Prognostic values of 5-hmC, 5-mC and TET2 in epithelial ovarian cancer’, *Archives of Gynecology and Obstetrics*, 292(4), pp. 891–897.

Zhang, M., Binns, C. W. and Lee, A. H. (2002) ‘Tea consumption and ovarian cancer risk in a population-based cohort’, *Achieves of Internal Medicine*, 11, pp. 713–718.

Zhang, R., Zhao, J., Xu, J., Jiao, D. X., Wang, J., Gong, Z. Q. and Jia, J. H. (2017) ‘Andrographolide suppresses proliferation of human colon cancer SW620 cells through the TLR4/NF- $\kappa$ B/MMP-9 signaling pathway’, *Oncology Letters*, 14(4), pp. 4305–4310.

Zhang, W. and Xu, J. (2017) ‘DNA methyltransferases and their roles in tumorigenesis’, *Biomarker Research*, 5(1), pp. 1–8.

Zhang, X., Li, F., Zhao, Z., Liu, X., Tang, Y. and Wang, M. (2012) ‘Diterpenoids from the root bark of *Jatropha curcas* and their cytotoxic activities’, *Phytochemistry Letters*, 5(9), pp. 721–724.

Zhang, Yong, Weng, Q., Han, J. and Chen, J. (2020) ‘Alantolactone suppresses human osteosarcoma through the PI3K/AKT signaling pathway’, *Molecular Medicine Reports*, 21(2), pp. 675–684.

Zhang, Y. and Chen, H. (2011) ‘Genistein, an epigenome modifier during cancer prevention’, *Epigenetics*, 6 (7), pp. 888–891.

Zhang, X. and Zhang, H. M. (2019) ‘Alantolactone induces gastric cancer BGC-823 cell apoptosis by regulating reactive oxygen species generation and the AKT signaling pathway’, *Oncology Letters*, 17(6), pp. 4795–4802.

Zhao, F., Chen, Y., Li, R., Liu, Y., Wen, L. and Zhang, C. (2010) ‘Triptolide alters histone H3K9 and H3K27 methylation state and induces G0-G1 arrest and caspase-dependent apoptosis in multiple myeloma in vitro’, *Toxicology*, 267, pp. 70–79.

Zhao, F., Chen, Y., Zeng, L., Li, R., Zeng, R., Wen, L., Liu, Y. and Zhang, C. (2010) ‘Role of triptolide in cell proliferation, cell cycle arrest, apoptosis and histone methylation in multiple myeloma U266 cells’, *European Journal of Pharmacology*, 646(1–3), pp. 1–11.

Zhao, G., Jung, J. H., Smith, D. L., Wood, K. V. and Mclaughlin, J. L. (1991) ‘Cytotoxic clerodane diterpenes from *Polyalthia ion gfoiia*’, *Planta Medica*, 57, pp. 380–383.

Zhao, P., Pan, Z., Luo, Y., Zhang, L., Li, X., Zhang, G., Zhang, Y., Cui, R., Sun, M. and Zhang, X. (2015) ‘Alantolactone induces apoptosis and cell cycle arrest on lung squamous cancer SK-MES-1 cells’, *Journal of Biochemical and Moleuclar Toxicology*, 29(5), pp. 199–206.

- Zheng, H., Yang, L., Kang, Y., Chen, M., Lin, S., Xiang, Y., Li, C., Dai, X., Huang, X., Liang, G., and Zhao, C. (2019) 'Alantolactone sensitizes human pancreatic cancer cells to EGFR inhibitors through the inhibition of STAT3 signaling', *Molecular Carcinogenesis*, 58(4), pp. 565–576.
- Zheng, S., Löw, K., Wagner, S., Yang, X., Briesen, H. V. and Zou, S. (2011) 'Cytotoxicity of Triptolide and Triptolide loaded polymeric micelles in vitro', *Toxicology in Vitro*, 25(8), pp. 1557–1567.
- Zhou, F., Shen, C., Xu, J., Gao, J., Zheng, X., Ko, R., Dou, J., Cheng, Y., Zhu, C., Xu, S., Tang, X., Zuo, X., Yin, X., Cui, Y., Sun, L., Tsoi, L. C., Hsu, Y.-H., Yang, S. and Zhang, X. (2016) 'Epigenome-wide association data implicates DNA methylation-mediated genetic risk in psoriasis', *Clinical Epigenetics*, 8(1), pp. 131.
- Zhou, G., Hu, Z., Fang, H., Zhang, F., Pan, X., Chen, X., Hu, A., Xu, L. and Zhou, G. (2011) 'Biologic activity of triptolide in t(8; 21) acute myeloid leukemia cells', *Leukemia Research*, 35(2), pp. 214–218.
- Zhu, T., Wang, D., Zhang, W., Liao, X., Guan, X., Bo, H. and Sun, J. (2013) 'Andrographolide protects against LPS-induced acute lung injury by inactivation of NF- $\kappa$ B', *Plos One*, 8(2), pp. 1-12.
- Zhu, X., Li, H., Long, L., Hui, L., Chen, H., Wang, X., Shen, H. and Xu, W. (2012) 'MiR-126 enhances the sensitivity of non-small cell lung cancer cells to anticancer agents by targeting vascular endothelial growth factor A', *Acta Biochimica et Biophysica Sinica*, 44(6), pp. 519–526.
- Zhuge, W., Chen, R., Vladimir, K., Dong, X., Zia, K., Sun, X., Dai, X., Bao, M., Shen, X. and Liang, G. (2018) 'Costunolide specifically binds and inhibits thioredoxin reductase 1 to induce apoptosis in colon cancer', *Cancer Letters*, 412, pp. 46–58.
- Zuberi, M., Mir, R., Dholariya, S., Najjar, I., Yadav, P., Javid, J., Guru, S., Mirza, M., Gandhi, G., Khurana, N., Ray, P. C. and Saxena, A. (2015) 'RASSF1 and PTEN promoter hypermethylation influences the outcome in epithelial ovarian cancer', *Clinical Ovarian and Other Gynecologic Cancer*, 7(1–2), pp. 33–39.

## Appendices

### Appendix I: DNA sequences and primers for genes evaluated for mRNA expression

Parameter Set: General PCR (Primers only) *TP53*

Sequence Name: Sequence 1

Amplicon Length: 383

	Start	Stop	Length	Tm	GC%
Forward					
<u><b>GTTTCCGTCTGGGCTTCTT (Sense)</b></u>	323	342	19	62(51.1)	52.6
Reverse					
<u><b>GTTGTAGTGGATGGTGGTACAG (AntiSense)</b></u>	684	706	22	62(54.8)	50

ATGGAGGAGCCGCAGTCAGATCCTAGCGTCGAGCCCCCTCTGAGTCAGGAAA  
 CATTTCAGACCTATGGAAACTACTTCCTGAAAACAACGTTCTGTCCCCCTTGC  
 CGTCCCAAGCAATGGATGATTTGATGCTGTCCCCGGACGATATTGAACAATGG  
 TTCACTGAAGACCCAGGTCCAGATGAAGCTCCAGAATGCCAGAGGCTGCTCC  
 CCCC**GTG**GCCCCCTGCACCAGCAGCTCCTACACCGGCGGCCCTGCACCAGCCC  
 CCTCCTGGCCCCCTGTCATCTTCTGTCCCTTCCCAGAAAACCTACCAGGGCAGCT  
 ACGGTTTCCGTCTGGGCTTCTTGCATTCTGGGACAGCCAAGTCTGTGACTTGCA  
 CGTACTCCCCTGCCCTCAACAAGATGTTTTGCCAACTGGCCAAGACCTGCCCT  
 GTGCAGCTGTGGGTTGATTCCACACCCCCGCCCGCACCCGCGTCCGCGCCAT  
 GGCCATCTACAAGCAGTCACAGCACATGACGGAGGTTGTGAGGCGCTGCCCC  
 CACCATGAGCGCTGCTCAGATAGCGATGGTCTGGCCCCCTCCTCAGCATCTTAT  
 CCGAGTGGAAGGAAATTTGCGTGTGGAGTATTTGGATGACAGAAACACTTTTC  
 GACATAGTGTGGTGGTGCCTATGAGCCGCCTGAGGTTGGCTCTGACTGTACC  
 ACCATCCACTACAACACTACATGTGTAACAGTTCCTGCATGGGCGGCATGAACCG  
 GAGGCCCATCCTCACCATCATCACACTGGAAGACTCCAGTGGTAATCTACTGG  
 GACGGAACAGCTTTGAGGTGCGTGTGTTGTGCCTGTCTGGGAGAGACCGGCGC  
 ACAGAGGAAGAGAATCTCCGCAAGAAAGGGGAGCCTCACCACGAGCTGCCCC  
 CAGGGAGCACTAAGCGAGCACTGCCCAACAACACCAGCTCCTCTCCCCAGCC

AAAGAAGAAACCACTGGATGGAGAATATTTACCCCTTCAGGACCAGACCAGC  
TTTCAAAAAGAAAATTGTAA

**Parameter Set: General PCR (Primers only) *BRCA1***

**Sequence Name: Sequence 1**

**Amplicon length 301**

	Start	Stop	Length	Tm	GC%
Forward					
<u>CTCAGTGTCCAACCTCTTAACC</u> (Sense)	4540	476	22	62 (54.8)	50
Reverse					
<u>GCTTCTCAGTGGTGTCAAATC</u> (AntiSense)	733	755	22	62(53)	45.5

ATGGATTTATCTGCTCTTCGCGTTGAAGAAGTACAAAATGTCATTAATGCTAT  
GCAGAAAATCTTAGAGTGTCCCATCTGTCTGGAGTTGATCAAGGAACCTGTCT  
CCACAAAGTGTGACCACATATTTTGCAAATTTTGCATGCTGAAACTTCTCAAC  
CAGAAGAAAGGGCCTTCACAGTGTCTTTATGTAAGAATGATATAACCAAAA  
GGAGCCTACAAGAAAGTACGAGATTTAGTCAACTTGTTGAAGAGCTATTGAA  
AATCATTTGTGCTTTTCAGCTTGACACAGGTTTGGAGTATGCAAACAGCTATA  
ATTTTGCAAAAAGGAAAATAACTCTCCTGAACATCTAAAAGATGAAGTTTCT  
ATCATCCAAAGTATGGGCTACAGAAACCGTGCCAAAAGACTTCTACAGAGTG  
AACCCGAAAATCCTTCCTTGCAGGAAACCAGTCTCAGTGTCCAACCTCTTAAC  
CTTGGAACCTGTGAGAACTCTGAGGACAAAGCAGCGGATACAACCTCAAAGA  
CGTCTGTCTACATTGAATTGGGATCTGATTCTTCTGAAGATACCGTTAATAAGG  
CAACTTATTGCAGTGTGGGAGATCAAGAATTGTTACAAATCACCCCTCAAGGA  
ACCAGGGATGAAATCAGTTTGGATTCTGCAAAAAGGCTGCTTGTGAATTTTC  
TGAGACGGATGTAACAAATACTGAACATCATCAACCCAGTAATAATGATTTGA  
ACACCACTGAGAAGCGTGCAGCTGAGAGGCATCCAGAAAAGTATCAGGGTAG  
TTCTGTTTCAAACCTTGCATGTGGAGCCATGTGGCACAAATACTCATGCCAGCT  
CATTACAGCATGAGAACAGCAGTTTATTACTCACTAAAGACAGAATGAATGTA  
GAAAAGGCTGAATTCTGTAATAAAAGCAAACAGCCTGGCTTAGCAAGGAGCC  
AACATAACAGATGGGCTGGAAGTAAGGAAACATGTAATGATAGGCGGACTCC

CAGCACAGAAAAAAGGTAGATCTGAATGCTGATCCCCTGTGTGAGAGAAAA  
GAATGGAATAAGCAGAACTGCCATGCTCAGAGAATCCTAGAGATACTGAAG  
ATGTTCTTGGATAAACTAAATAGCAGCATTAGAGAAAGTTAATGAGTGGTTT  
TCCAGAAGTGATGAACTGTTAGGTTCTGATGACTCACATGATGGGGAGTCTGA  
ATCAAATGCCAAAGTAGCTGATGTATTGGACGTTCTAAATGAGGTAGATGAAT  
ATTCTGGTTCTTCAGAGAAAATAGACTTACTGGCCAGTGATCCTCATGAGGCT  
TTAATATGTAAAAGTGAAAGAGTTCCTCCAAATCAGTAGAGAGTAATATTGA  
AGACAAAATATTTGGGAAAACCTATCGGAAGAAGGCAAGCCTCCCCAACTTA  
AGCCATGTAAGTAAAATCTAATTATAGGAGCATTGTTACTGAGCCACAGAT  
AATACAAGAGCGTCCCCTCACAAATAAATTAAGCGTAAAAGGAGACCTACA  
TCAGGCCTTCATCCTGAGGATTTTATCAAGAAAGCAGATTTGGCAGTTCAAAA  
GACTCCTGAAATGATAAATCAGGGAACCTAACCAAACGGAGCAGAATGGTCAA  
GTGATGAATATTAATAAGTGGTCATGAGAATAAAACAAAAGGTGATTCTAT  
TCAGAATGAGAAAAATCCTAACCCAATAGAATCACTCGAAAAAGAATCTGCT  
TTCAAACGAAAGCTGAACCTATAAGCAGCAGTATAAGCAATATGGAACCTCG  
AATTAATATCCACAATTCAAAGCACCTAAAAAGAATAGGCTGAGGAGGAA  
GTCTTCTACCAGGCATATTCATGCGCTTGAAGTACTAGTAGCAGTAGAAATCTAA  
GCCCACCTAATTGTACTGAATTGCAAATTGATAGTTGTTCTAGCAGTGAAGAG  
ATAAAGAAAAAAAAGTACAACCAAATGCCAGTCAGGCACAGCAGAAACCTAC  
AACTCATGGAAGGTAAAGAACCTGCAACTGGAGCCAAGAAGAGTAACAAGCC  
AAATGAACAGACAAGTAAAAGACATGACAGCGATACTTTCCAGAGCTGAAG  
TTAACAAATGCACCTGGTTCTTTTACTAAGTGTTCAAATACCAGTGAACCTAA  
AGAATTTGTCAATCCTAGCCTTCCAAGAGAAGAAAAAGAAGAGAAACTAGAA  
ACAGTTAAAGTGTCTAATAATGCTGAAGACCCCAAAGATCTCATGTTAAGTGG  
AGAAAGGGTTTTGCAAACCTGAAAGATCTGTAGAGAGTAGCAGTATTTATTGG  
TACCTGGTACTGATTATGGCACTCAGGAAAGTATCTCGTTACTGGAAGTTAGC  
ACTCTAGGGAAGGCAAAAACAGAACCAAATAAATGTGTGAGTCAGTGTGCAG  
CATTTGAAAACCCCAAGGGACTAATTCATGGTTGTTCCAAAGATAATAGAAAT  
GACACAGAAGGCTTTAAGTATCCATTGGGACATGAAGTTAACCACAGTCGGG  
AAACAAGCATAGAAATGGAAGAAAGTGAACCTGATGCTCAGTATTTGCAGAA  
TACATTCAAGGTTTCAAAGCGCCAGTCATTTGCTCCGTTTTCAAATCCAGGAA  
ATGCAGAAGAGGAATGTGCAACATTCTCTGCCACTCTGGGTCTTAAAGAAA  
CAAAGTCCAAAAGTCACTTTTGAATGTGAACAAAAGGAAGAAAATCAAGGAA  
AGAATGAGTCTAATATCAAGCCTGTACAGACAGTTAATATCACTGCAGGCTTT

CCTGTGGTTGGTCAGAAAGATAAGCCAGTTGATAATGCCAAATGTAGTATCAA  
AGGAGGCTCTAGGTTTTGTCTATCATCTCAGTTCAGAGGCAACGAACTGGAC  
TCATTACTCCAAATAAACATGGACTTTTACAAAACCCATATCGTATAACCACCA  
CTTTTTCCCATCAAGTCATTTGTTAAACTAAATGTAAGAAAAATCTGCTAGA  
GGAAAACTTTGAGGAACATTCAATGTCACCTGAAAGAGAAATGGGAAATGAG  
AACATTCCAAGTACAGTGAGCACAATTAGCCGTAATAACATTAGAGAAAATG  
TTTTTAAAGAAGCCAGCTCAAGCAATATTAATGAAGTAGGTTCCAGTACTAAT  
GAAGTGGGCTCCAGTATTAATGAAATAGGTTCCAGTGATGAAAACATTCAAGC  
AGAACTAGGTAGAAACAGAGGGCCAAAATTGAATGCTATGCTTAGATTAGGG  
GTTTTGCAACCTGAGGTCTATAAACAAAGTCTTCCTGGAAGTAATTGTAAGCA  
TCCTGAAATAAAAAAGCAAGAATATGAAGAAGTAGTTCAGACTGTTAATACA  
GATTTCTCTCCATATCTGATTTCAAGATAACTTAGAACAGCCTATGGGAAGTAG  
TCATGCATCTCAGGTTTGTCTGAGACACCTGATGACCTGTTAGATGATGGTG  
AAATAAAGGAAGATACTAGTTTTGCTGAAAATGACATTAAGGAAAGTTCTGCT  
GTTTTAGCAAAAGCGTCCAGAAAGGAGAGCTTAGCAGGAGTCCTAGCCCTTT  
CACCCATACACATTTGGCTCAGGGTTACCGAAGAGGGGCCAAGAAATTAGAG  
TCCTCAGAAGAGAACTTATCTAGTGAGGATGAAGAGCTTCCCTGCTTCCAACA  
CTTGTTATTTGGTAAAGTAAACAATATACCTTCTCAGTCTACTAGGCATAGCAC  
CGTTGCTACCGAGTGTCTGTCTAAGAACACAGAGGAGAATTTATTATCATTGA  
AGAATAGCTTAAATGACTGCAGTAACCAGGTAATATTGGCAAAGGCATCTCA  
GGAACATCACCTTAGTGAGGAAACAAAATGTTCTGCTAGCTTGTTTTCTTCAC  
AGTGCAGTGAATTGGAAGACTTGACTGCAAATACAAACACCCAGGATCCTTTC  
TTGATTGGTTCTTCCAAACAAATGAGGCATCAGTCTGAAAGCCAGGGAGTTGG  
TCTGAGTGACAAGGAATTGGTTTCAGATGATGAAGAAAGAGGAACGGGCTTG  
GAAGAAAATAATCAAGAAGAGCAAAGCATGGATTCAAACCTTAGGTGAAGCAG  
CATCTGGGTGTGAGAGTGAAACAAGCGTCTCTGAAGACTGCTCAGGGCTATCC  
TCTCAGAGTGACATTTTAACCACTCAGCAGAGGGATACCATGCAACATAACCT  
GATAAAGCTCCAGCAGGAAATGGCTGAACTAGAAGCTGTGTTAGAACAGCAT  
GGGAGCCAGCCTTCTAACAGCTACCCTTCCATCATAAGTGACTCTTCTGCCCTT  
GAGGACCTGCGAAATCCAGAACAAAGCACATCAGAAAAAGATTCGCATATAC  
ATGGCCAAAGGAACAACCTCCATGTTTTCTAAAAGGCCTAGAGAACATATATCA  
GTATTAACCTCACAGAAAAGTAGTGAATACCCTATAAGCCAGAATCCAGAAG  
GCCTTTCTGCTGACAAGTTTGAGGTGTCTGCAGATAGTTCTACCAGTAAAAAT  
AAAGAACCAGGAGTGGAAAGGTCATCCCCTTCTAAATGCCCATCATTAGATGA

TAGGTGGTACATGCACAGTTGCTCTGGGAGTCTTCAGAATAGAACTACCCAT  
 CTCAAGAGGAGCTCATTAAGGTTGTTGATGTGGAGGAGCAACAGCTGGAAGA  
 GTCTGGGCCACACGATTTGACGGAAACATCTTACTTGCCAAGGCAAGATCTAG  
 AGGGAACCCCTTACCTGGAATCTGGAATCAGCCTCTTCTCTGATGACCCTGAA  
 TCTGATCCTTCTGAAGACAGAGCCCCAGAGTCAGCTCGTGTTGGCAACATAACC  
 ATCTTCAACCTCTGCATTGAAAGTTCCCCAATTGAAAGTTGCAGAATCTGCCC  
 AGAGTCCAGCTGCTGCTCATACTACTGATACTGCTGGGTATAATGCAATGGAA  
 GAAAGTGTGAGCAGGGAGAAGCCAGAATTGACAGCTTCAACAGAAAGGGTCA  
 ACAAAGAATGTCCATGGTGGTGTCTGGCCTGACCCCAGAAGAATTTATGCTC  
 GTGTACAAGTTTGCCAGAAAACACCACATCACTTTAACTAATCTAATTACTGA  
 AGAGACTACTCATGTTGTTATGAAAACAGATGCTGAGTTTGTGTGTGAACGGA  
 CACTGAAATATTTTCTAGGAATTGCGGGAGGAAAATGGGTAGTTAGCTATTTC  
 TGGGTGACCCAGTCTATTAAGAAAGAAAATGCTGAATGAGCATGATTTTGA  
 AGTCAGAGGAGATGTGGTCAATGGAAGAAACCACCAAGGTCCAAAGCGAGCA  
 AGAGAATCCCAGGACAGAAAGATCTTCAGGGGGCTAGAAATCTGTTGCTATG  
 GGCCCTTCACCAACATGCCACAGATCAACTGGAATGGATGGTACAGCTGTGT  
 GGTGCTTCTGTGGAAGGAGCTTTCATCATTACCCCTTGGCACAGGTGTCCA  
 CCCAATTGTGGTTGTGCAGCCAGATGCCTGGACAGAGGACAATGGCTTCCATG  
 CAATTGGGCAGATGTGTGAGGCACCTGTGGTGACCCGAGAGTGGGTGTTGGA  
 CAGTGTAGCACTCTACCAGTGCCAGGAGCTGGACACCTACCTGATACCCCAGA  
 TCCCCACAGCCACTACTGA

**Parameter Set: General PCR (Primers only) *RASSF1***

**Sequence Name: Sequence 1**

**Amplicon Length: 295**

	Start	Stop	Length	Tm	GC%
Forward					
<u><b>GGAGTACAATGCCAGATCAA</b></u>	420	441	21	62 (52.4)	47.6
<u><b>(Sense)</b></u>					
Reverse	695	715	20	62(51.8)	50

**GTCATCCACCACCAAGAACT****(AntiSense)**

ATGTCGGGGGAGCCTGAGCTCATTGAGCTGCGGGAGCTGGCACCCGCTGGGC  
 GCGCTGGGAAGGGCCGCACCCGGCTGGAGCGTGCCAACGCGCTGCGCATCGC  
 GCGGGGCACCGCGTGCAACCCACACGGCAGCTGGTCCCTGGCCGTGGCCAC  
 CGCTTCCAGCCCGCGGGGCCCGCCACGCACACGTGGTGCGACCTCTGTGGCGA  
 CTTTCATCTGGGGCGTCGTGCGCAAAGGCCTGCAGTGCGCGCATTGCAAGTTCA  
 CCTGCCACTACCGCTGCCGCGCGCTCGTCTGCCTGGACTGTTGCGGGCCCCGG  
 GACCTGGGCTGGGAACCCGCGGTGGAGCGGGACACGAACGTGGACGAGCCTG  
 TGGAGTGGGAGACACCTGACCTTTCTCAAGCTGAGATTGAGCAGAAGATCAA  
 GGAGTACAATGCCAGATCAACAGCAACCTCTTCATGAGCTTGAACAAGGAC  
 GGTTCCTTACACAGGCTTCATCAAGGTTTCAGCTGAAGCTGGTGCGCCCTGTCTCT  
 GTGCCCTCCAGCAAGAAGCCACCCTCCTTGCAGGATGCCCGGCGGGGCCAG  
 GACGGGGCACAAGTGTCAGGCGCCGCACTTCTTTTACCTGCCCAAGGATGCT  
 GTCAAGCACCTGCATGTGCTGTCACGCACAAGGGCACGTGAAGTCATTGAGGC  
 CCTGCTGCGAAAGTTCTTGGTGGTGGATGACCCCCGCAAGTTTGCACCTTTG  
 AGCGCGCTGAGCGTCACGGCCAAGTGTACTTGCGGAAGCTGTTGGATGATGA  
 GCAGCCCCTGCGGCTGCGGCTCCTGGCAGGGCCCAGTGACAAGGCCCTGAGCT  
 TTGTCCTGAAGGAAAATGACTCTGGGGAGGTGAACTGGGACGCCTTCAGCATG  
 CCTGAACTACATAACTTCTACGTATCCTGCAGCGGGAGGAGGAGGAGCACCT  
 CCGCCAGATCCTGCAGAAGTACTCCTATTGCCGCCAGAAGATCCAAGAGGCC  
 TGCACGCCTGCCCCCTTGGGTGA

Parameter Set: General PCR (Primers only) *TUSC3*

Sequence Name: Sequence 1

Amplicon Length: 455

	Start	Stop	Length	Tm	GC%
Forward					
<b><u>AACTCCTGGCGCTATTCATC</u></b> <b><u>(Sense)</u></b>	340	360	20	62 (51.8)	50
Reverse					
<b><u>TGTCCATTGTGTGGGTTCTT</u></b> <b><u>(AntiSense)</u></b>	775	795	20	62(49.7)	45

ATGGGGGCCCCGGGGCGCTCCTTCACGCCGTAGGCAAGCGGGGCGGCGGCTGC  
 GGTACCTGCCACCGGGAGCTTTCCTTCCTTCTCCTGCTGCTGCTGCTCTGCA  
 TCCAGCTCGGGGGAGGACAGAAGAAAAAGGAGAATCTTTTAGCTGAAAAAGT  
 AGAGCAGCTGATGGAATGGAGTTCAGACGCTCAATCTTCCGAATGAATGGTG  
 ATAAATTCCGAAAATTTATAAAGGCACCACCTCGAACTATTCCATGATTGTT  
 ATGTTCACTGCTCTTCAGCCTCAGCGGCAGTGTTCTGTGTGCAGGCAAGCTAA  
 TGAAGAATATCAAATACTGGCGAACTCCTGGCGCTATTCATCTGCTTTTTGTAA  
 CAAGCTCTTCTTCAGTATGGTGGACTATGATGAGGGGACAGACGTTTTTCAGC  
 AGCTCAACATGAACTCTGCTCCTACATTCATGCATTTTCCTCCAAAAGGCAGA  
 CCTAAGAGAGCTGATACTTTTGACCTCCAAAGAATTGGATTTGCAGCTGAGCA  
 ACTAGCAAAGTGGATTGCTGACAGAACGGATGTTTCATATTCGGGTTTTTCAGAC  
 CACCCAACACTCTGGTACCATTGCTTTGGCCCTGTTAGTGTCGCTTGTGGAG  
 GTTTGCTTTATTTGAGAAGGAACAACACTTGGAGTTCATCTATAACAAGACTGGT  
 TGGGCCATGGTGTCTCTGTGTATAGTCTTTGCTATGACTTCTGGCCAGATGTGG  
 AACCATATCCGTGGACCTCCATATGCTCATAAGAACCCACACAATGGACAAGT  
 GAGCTACATTCATGGGAGCAGCCAGGCTCAGTTTGTGGCAGAATCACACATTA  
 TTCTGGTACTGAATGCCGCTATCACCATGGGGATGGTTCTTCTAAATGAAGCA  
 GCAACTTCGAAAGGCGATGTTGGAAAAAGACGGATAATTTGCCTAGTGGGAT  
 TGGGCCTGGTGGTCTTCTTCTTCAGTTTTCTACTTTCAATATTTTCGTTCCAAGTA  
 CCACGGCTATCCTTATAGCTTTTTAATTAATGA

**Parameter Set: General PCR (Primers only) *MLH1***

**Sequence Name: Sequence 1**

**Amplicon Length: 368**

	Start	Stop	Length	Tm	GC%
Forward					
<u><b>GCCATTGTCACAGAGGATAAGA</b></u>	1228	1250	22	62(53)	45.5
<u><b>(Sense)</b></u>					
Reverse					
<u><b>CCCACGAAGGAGTGGTTATG</b></u>	1576	1596	20	62 (53.8)	55
<u><b>(AntiSense)</b></u>					

ATGTCGTTTCGTGGCAGGGGTTATTCGGCGGCTGGACGAGACAGTGGTGAACCG  
CATCGCGGCGGGGGAAGTTATCCAGCGGCCAGCTAATGCTATCAAAGAGATG  
ATTGAGAACTGTTTAGATGCAAAATCCACAAGTATTCAAGTGATTGTAAAGA  
GGGAGGCCTGAAGTTGATTCAGATCCAAGACAATGGCACCGGGATCAGGAAA  
GAAGATCTGGATATTGTATGTGAAAGGTTCACTACTAGTAAACTGCAGTCCTT  
TGAGGATTTAGCCAGTATTTCTACCTATGGCTTTCGAGGTGAGGCTTTGGCCA  
GCATAAGCCATGTGGCTCATGTTACTATTACAACGAAAACAGCTGATGGAAAG  
TGTGCATACAGAGCAAGTTACTCAGATGGAAAAGTAAAGCCCCTCCTAAACC  
ATGTGCTGGCAATCAAGGGACCCAGATCACGGTGGAGGACCTTTTTTACAACA  
TAGCCACGAGGAGAAAAGCTTTAAAAAATCCAAGTGAAGAATATGGGAAAAT  
TTTGAAGTTGTTGGCAGGTATTCAGTACACAATGCAGGCATTAGTTTCTCAG  
TTAAAAACAAGGAGAGACAGTAGCTGATGTTAGGACACTACCCAATGCCTC  
AACCGTGGACAATATTCGCTCCATCTTTGGAAATGCTGTTAGTCGAGAAGTGA  
TAGAAATTGGATGTGAGGATAAAACCCTAGCCTTCAAATGAATGGTTACATA  
TCCAATGCAAACACTACTCAGTGAAGAAGTGCATCTTCTTACTCTTCATCAACCAT  
CGTCTGGTAGAATCAACTTCCTTGAGAAAAGCCATAGAAACAGTGTATGCAGC  
CTATTTGCCCAAAAACACACACCCATTTCCTGTACCTCAGTTTAGAAATCAGTC  
CCCAGAATGTGGATGTTAATGTGCACCCACAAAGCATGAAGTTCACCTTCCTG  
CACGAGGAGAGCATCCTGGAGCGGGTGCAGCAGCACATCGAGAGCAAGCTCC  
TGGGCTCCAATTCCTCCAGGATGTACTTCACCCAGACTTTGCTACCAGGACTTG  
CTGGCCCCTCTGGGGAGATGGTTAAATCCACAACAAGTCTGACCTCGTCTTCT  
ACTTCTGGAAGTAGTGATAAGGTCTATGCCACCAGATGGTTCGTACAGATTC  
CCGGGAACAGAAGCTTGATGCATTTCTGCAGCCTCTGAGCAAACCCCTGTCCA  
GTCAGCCCCAGGCCATTGTCACAGAGGATAAGACAGATATTTCTAGTGGCAGG  
GCTAGGCAGCAAGATGAGGAGATGCTTGAAGTCCCAGCCCCTGCTGAAGTGG  
CTGCCAAAATCAGAGCTTGGAGGGGGATAACAACAAGGGGACTTCAGAAAT  
GTCAGAGAAGAGAGGACCTACTTCCAGCAACCCAGAAAGAGACATCGGGAA  
GATTCTGATGTGGAAATGGTGGAAAGATGATTCGAAAGGAAATGACTGCAG  
CTTGTACCCCCGAGAAAGGATCATTAACTCACTAGTGTGTTTGTAGTCTCCAG  
GAAGAAATTAATGAGCAGGGACATGAGGTTCTCCGGGAGATGTTGCATAACC  
ACTCCTTCGTGGGCTGTGTGAATCCTCAGTGGGCCTTGGCACAGCATCAAACC  
AAGTTATACCTTCTCAACACCACCAAGCTTAGTGAAGAACTGTTCTACCAGAT  
ACTCATTTATGATTTTGCCAATTTTGGTGTCTCAGGTTATCGGAGCCAGCACC  
GCTCTTTGACCTTGCCATGCTTGCCTTAGATAGTCCAGAGAGTGGCTGGACAG

AGGAAGATGGTCCCAAAGAAGGACTTGCTGAATACATTGTTGAGTTTCTGAAG  
 AAGAAGGCTGAGATGCTTGCAGACTATTTCTCTTTGGAAATTGATGAGGAAGG  
 GAACCTGATTGGATTACCCCTTCTGATTGACAACATATGTGCCCCCTTTGGAGG  
 GACTGCCTATCTTCATTCTTCGACTAGCCACTGAGGTGAATTGGGACGAAGAA  
 AAGGAATGTTTTGAAAGCCTCAGTAAAGAATGCGCTATGTTCTATTCCATCCG  
 GAAGCAGTACATATCTGAGGAGTCGACCCTCTCAGGCCAGCAGAGTGAAGTG  
 CCTGGCTCCATTCCAAACTCCTGGAAGTGGACTGTGGAACACATTGTCTATAA  
 AGCCTTGCGCTCACACATTCTGCCTCCTAAACATTTACAGAAGATGGAAATA  
 TCCTGCAGCTTGCTAACCTGCCTGATCTATACAAAGTCTTTGAGAGGTGTTAA

**Parameter Set: General PCR (Primers only) *HOXA9***

**Sequence Name: Sequence 1**

**Amplicon Length: 461**

	Start	Stop	Length	Tm	GC%
Forward					
<u>TACTACGTGGACTCGTTCCT (Sense)</u>	28	48	20	62(51.8 )	50
Reverse					
<u>GGAGGAGAACCACAAGCATAG</u> <u>(AntiSense)</u>	468	489	21	62 (54.4)	52.4

ATGGCCACCACTGGGGCCCTGGGCAACTACTACGTGGACTCGTTCCTGCTGGG  
 CGCCGACGCCGCGGATGAGCTGAGCGTTGGCCGCTATGCGCCGGGGACCCTG  
 GGCCAGCCTCCCCGGCAGGCGGCGACGCTGGCCGAGCACCCCGACTTCAGCC  
 CGTGCAGCTTCCAGTCCAAGGCGACGGTGTGTTGGCGCCTCGTGGAACCCAGTG  
 CACGCGGCGGGCGCCAACGCTGTACCCGCTGCGGTGTACCACCACCATCACCA  
 CCACCCCTACGTGCACCCCCAGGCGCCCGTGGCGGGCGGCGGCCG **GAC**GGC  
 AGGTACATGCGCTCCTGGCTGGAGCCACGCCCGGTGCGCTCTCCTTCGCGGG  
 CTTGCCCTCCAGCCGGCCTTATGGCATTAAACCTGAACCGCTGTCGGCCAGAA  
 GGGGTGACTGTCCCACGCTTGACACTCACACTTTGTCCCTGACTGACTATGCTT  
 GTGGTTCTCCTCCAGTTGATAGAGAAAAACAACCCAGCGAAGGCGCCTTCTCT  
 GAAAACAATGCTGAGAATGAGAGCGGCGGAGACAAGCCCCCATCGATCCCA  
 ATAACCCAGCAGCCAACCTGGCTTCATGCGCGCTCCACTCGGAAAAAGCGGTGC  
 CCCTATACAAACACCAGACCCTGGAACCTGGAGAAAGAGTTTCTGTTCAACAT

GTACCTCACCAGGGACCGCAGGTACGAGGTGGCTCGACTGCTCAACCTCACCG  
 AGAGGCAGGTCAAGATCTGGTTCCAGAACCGCAGGATGAAAATGAAGAAAAT  
 CAACAAAGACCGAGCAAAAGACGAGTGA

**Parameter Set: General PCR (Primers only) *KLF6***

**Sequence Name: Sequence 1**

**Amplicon Length: 413**

	Start	Stop	Length	Tm	GC%
Forward					
<u><b>CTTAGAGACCAACAGCCTGAAC</b></u> <b>(Sense)</b>	294	316	22	62(54.8)	50
Reverse					
<u><b>CTTCCATGAGCATCTGTAAGG</b></u> <b>(AntiSense)</b>	685	707	22	62(54.8)	50

ATGGACGTGCTCCCATGTGCAGCATCTTCCAGGAGCTCCAGATCGTGCACGA  
 GACCGGCTACTTCTCGGCGCTGCCGTCTCTGGAGGAGTACTGGCAACAGACCT  
 GCCTAGAGCTGGAACGTTACCTCCAGAGCGAGCCCTGCTATGTTTCAGCCTCA  
 GAAATCAAATTTGACAGCCAGGAAGATCTGTGGACCAAAATCATTCTGGCTCG  
 GGAGAAAAGGAGGAATCCGAACTG**AAG**ATATCTTCCAGTCCTCCAGAGGAC  
 ACTCTCATCAGCCCGAGCTTTTGTTACAACCTTAGAGACCAACAGCCTGAACTC  
 AGATGTCAGCAGCGAATCCTCTGACAGCTCCGAGGAACTTTCTCCACGGCCA  
 AGTTTACCTCCGACCCATTGGCGAAGTTTTGGTCAGCTCGGGAAAATTGAGC  
 TCCTCTGTACCTCCACGCCTCCATCTTCTCCGAACTGAGCAGGGAACCTTCT  
 CAACTGTGGGGTTGCGTGCCCGGGGAGCTGCCCTCGCCAGGGAAGGTGCGCA  
 GCGGGACTTCGGGGAAGCCAGGTGACAAGGGAAATGGCGATGCCTCCCCCGA  
 CGGCAGGAGGAGGGTGCACCGGTGCCACTTTAACGGCTGCAGGAAAGTTTAC  
 ACCAAAAGCTCCCACTTGAAAGCACACCAGCGGACGCACACAGGAGAAAAGC  
 CTTACAGATGCTCATGGGAAGGGTGTGAGTGGCGTTTTTGCAAGAAGTGATGAG  
 TTAACCAGGCACTTCCGAAAGCACACCGGGGCCAAGCCTTTTAAATGCTCCCA  
 CTGTGACAGGTGTTTTTCCAGGTCTGACCACCTGGCCCTGCACATGAAGAGGC  
 ACCTCTGA

**Parameter Set: General PCR (Primers only) *PTEN*****Sequence Name: Sequence 1****Amplicon Length: 475**

	Start	Stop	Length	Tm	GC%
Forward					
<u><b>CCCACCACAGCTAGAACTTATC</b></u> <b>(Sense)</b>	282	304	22	62 (54.8)	50
Reverse					
<u><b>ATCACACACACAGGTAACG</b></u> <b>(AntiSense)</b>	737	757	20	62(51.8)	50

ATGACAGCCATCATCAAAGAGATCGTTAGCAGAAACAAAAGGAGATATCAAG  
 AGGATGGATTCGACTTAGACTTGACCTATATTTATCCAAACATTATTGCTATGG  
 GATTTCTGCAGAAAGACTTGAAGGCGTATACAGGAACAATATTGATGATGTA  
 GTAAGGTTTTTGGATTCAAAGCATAAAAACCATTACAAGATATAACAATCTTTG  
 TGCTGAAAGACATTATGACACCGCCAAATTTAATTGCAGAGTTGCACAATATC  
 CTTTTGAAGACCATAACCCACCACAGCTAGAACTTATCAAACCCTTTTGTGAA  
 GATCTTGACCAATGGCTAAGTGAAGATGACAATCATGTTGCAGCAATTCCTG  
 TAAAGCTGGAAAGGGACGAACTGGTGTAAATGATATGTGCATATTTATTACATC  
 GGGGCAAATTTTTAAAGGCACAAGAGGCCCTAGATTTCTATGGGGAAAGTAAG  
 GACCAGAGACAAAAGGGAGTAACTATTCCCAGTCAGAGGGCGCTATGTGTAT  
 TATTATAGCTACCTGTAAAGAATCATCTGGATTATAGACCAGTGGCACTGTT  
 GTTTCACAAGATGATGTTTGAAGTATTCCAATGTTTCAGTGGCGGAACTTGCA  
 ATCCTCAGTTTGTGGTCTGCCAGCTAAAGGTGAAGATATATTCCTCCAATTCA  
 GGACCCACACGACGGGAAGACAAGTTCATGTACTTTGAGTTCCTCAGCCGTT  
 ACCTGTGTGTGGTGTATCAAAGTAGAGTTCTTCCACAAACAGAACAAGATGC  
 TAAAAAAGGACAAAATGTTTCACTTTTGGGTAAATACATTCTTCATACCAGGA  
 CCAGAGGAAACCTCAGAAAAAGTAGAAAATGGAAGTCTATGTGATCAAGAAA  
 TCGATAGCATTTCAGTATAGAGCGTGCAGATAATGACAAGGAATATCTAGTA  
 CTTACTTTAACAAAAAATGATCTTGACAAAGCAAATAAAGACAAAGCCAACC  
 GATACTTTTCTCAAATTTTAAGGTGAAGCTGTACTTCACAAAAACAGTAGAG  
 GAGCCGTCAAATCCAGAGGCTAGCAGTTCAACTTCTGTAACACCAGATGTTAG

TGACAATGAACCTGATCATTATAGATATTCTGACACCACTGACTCTGATCCAG  
AGAATGAACCTTTTGGATGAAGATCAGCATAACAAATTACAAAAGTCTGA

**Parameter Set: General PCR (Primers only) APC (WNT SIGNALING PATHWAY  
REGULATOR (APC))**

**Sequence Name: Sequence 1**

**Amplicon Length: 418**

	<b>Start</b>	<b>Stop</b>	<b>Length</b>	<b>Tm</b>	<b>GC%</b>
Forward					
<u><b>AGCCTCGATGAGCCATTATAC</b></u> <b>(Sense)</b>	4528	4550	22	62(53)	45.5
Reverse					
<u><b>TAGGTGTCCTTCAACAATAC</b></u> <b>(AntiSense)</b>	4923	4946	23	62(53.5)	43.5

ATGGCTGCAGCTTCATATGATCAGTTGTTAAAGCAAGTTGAGGCACTGAAGAT  
GGAGAACTCAAATCTTCGACAAGAGCTAGAAGATAATTCCAATCATCTTACAA  
AACTGGAACTGAGGCATCTAATATGAAGGAAGTACTTAAACAACACTACAAGG  
AAGTATTGAAGATGAAGCTATGGCTTCTTCTGGACAGATTGATTTATTAGAGC  
GTCTTAAAGAGCTTAACTTAGATAGCAGTAATTTCCCTGGAGTAAAAGTGGCG  
TCAAAAATGTCCCTCCGTTCTTATGGAAGCCGGGAAGGATCTGTATCAAGCCG  
TTCTGGAGAGTGCAGTCCTGTTCTTATGGGTTTCAATTTCCAAGAAGAGGGTTTGT  
AAATGGAAGCAGAGAAAGTACTGGATATTTAGAAGAAGTGGAGAAAGAGAGG  
TCATTGCTTCTTGCTGATCTTGACAAAGAAGAAAAGGAAAAGACTGGTATTA  
CGCTCAACTTCAGAATCTCACTAAAAGAATAGATAGTCTTCTTTAACTGAAA  
ATTTTCTTACAAACAGATATGACCAGAAGGCAATTGGAATATGAAGCAAGG  
CAAATCAGAGTTGCGATGGAAGAACAACACTAGGTACCTGCCAGGATATGGAAA  
AACGAGCACAGCGAAGAATAGCCAGAATTCAGCAAATCGAAAAGGACATACT  
TCGTATACGACAGCTTTTACAGTCCCAAGCAACAGAAGCAGAGAGGTCATCTC  
AGAACAAGCATGAAACCGGCTCACATGATGCTGAGCGGCAGAATGAAGGTCA  
AGGAGTGGGAGAAATCAACATGGCAACTTCTGGTAATGGTCAGGGTTCAACT  
ACACGAATGGACCATGAAACAGCCAGTGTTTTGAGTTCTAGTAGCACACACTC  
TGCACCTCGAAGGCTGACAAGTCATCTGGGAACCAAGGTGGAAATGGTGTATT

CATTGTTGTCAATGCTTGGTACTCATGATAAGGATGATATGTCGCGAACTTTGC  
TAGCTATGTCTAGCTCCCAAGACAGCTGTATATCCATGCGACAGTCTGGATGT  
CTTCCTCTCCTCATCCAGCTTTTACATGGCAATGACAAAGACTCTGTATTGTTG  
GGAAATTCCCGGGGCGAGTAAAGAGGCTCGGGCCAGGGCCAGTGCAGCACTCC  
ACAACATCATTCACTCACAGCCTGATGACAAGAGAGGCAGGCGTGAAATCCG  
AGTCCTTCATCTTTTGGAACAGATACGCGCTTACTGTGAAACCTGTTGGGAGT  
GGCAGGAAGCTCATGAACCAGGCATGGACCAGGACAAAAATCCAATGCCAGC  
TCCTGTTGAACATCAGATCTGTCTGCTGTGTGTGTTCTAATGAAACTTTCATT  
TGATGAAGAGCATAGACATGCAATGAATGAACTAGGGGGACTACAGGCCATT  
GCAGAATTATTGCAAGTGGACTGTGAAATGTATGGGCTTACTAATGACCACTA  
CAGTATTACACTAAGACGATATGCTGGAATGGCTTTGACAAACTTGACTTTTG  
GAGATGTAGCCAACAAGGCTACGCTATGCTCTATGAAAGGCTGCATGAGAGC  
ACTTGTGGCCCAACTAAAATCTGAAAGTGAAGACTTACAGCAGGTTATTGCGA  
GTGTTTTGAGGAATTTGTCTTGGCGAGCAGATGTAAATAGTAAAAAGACGTTG  
CGAGAAGTTGGAAGTGTGAAAGCATTGATGGAATGTGCTTTAGAAGTTAAAA  
AGGAATCAACCCTCAAAGCGTATTGAGTGCCTTATGGAATTTGTCAGCACAT  
TGCACTGAGAATAAAGCTGATATATGTGCTGTAGATGGTGCCTTGCATTTTT  
GGTTGGCACTCTTACTTACCGGAGCCAGACAAACACTTTAGCCATTATTGAAA  
GTGGAGGTGGGATATTACGGAATGTGTCCAGCTTGATAGCTACAAATGAGGA  
CCACAGGCAAATCCTAAGAGAGAACAACCTGTCTACAACTTTATTACAACACT  
TAAAATCTCATAGTTTGACAATAGTCAGTAATGCATGTGGAACCTTTGTGGAAT  
CTCTCAGCAAGAAATCCTAAAGACCAGGAAGCATTATGGGACATGGGGGCAG  
TTAGCATGCTCAAGAACCTCATTCAATTCAAAGCACAAAATGATTGCTATGGGA  
AGTGCTGCAGCTTTAAGGAATCTCATGGCAAATAGGCCTGCGAAGTACAAGG  
ATGCCAATATTATGTCTCCTGGCTCAAGCTTGCCATCTCTTCATGTTAGGAAAC  
AAAAAGCCCTAGAAGCAGAATTAGATGCTCAGCACTTATCAGAACTTTTGAC  
AATATAGACAATTTAAGTCCCAAGGCATCTCATCGTAGTAAGCAGAGACACA  
AGCAAAGTCTCTATGGTGATTATGTTTTTTGACACCAATCGACATGATGATAAT  
AGGTCAGACAATTTTAATACTGGCAACATGACTGTCCTTTCACCATATTTGAAT  
ACTACAGTGTTACCCAGCTCCTCTTCATCAAGAGGAAGCTTAGATAGTTCTCG  
TTCTGAAAAAGATAGAAGTTTGGAGAGAGAACGCGGAATTGGTCTAGGCAAC  
TACCATCCAGCAACAGAAAATCCAGGAACTTCTTCAAAGCGAGGTTTGCAGAT  
CTCCACCACTGCAGCCCAGATTGCCAAAGTCATGGAAGAAGTGTGAGCCATTC  
ATACCTCTCAGGAAGACAGAAGTTCTGGGTCTACCACTGAATTACATTGTGTG

ACAGATGAGAGAAATGCACTTAGAAGAAGCTCTGCTGCCCATACACATTCAA  
ACACTTACAATTTCACTAAGTCGGAAAATTCAAATAGGACATGTTCTATGCCT  
TATGCCAAATTAGAATACAAGAGATCTTCAAATGATAGTTTAAATAGTGTGAG  
TAGTAGTGATGGTTATGGTAAAAGAGAGTCAAATGAAACCCTCGATTGAATCCT  
ATTCTGAAGATGATGAAAGTAAGTTTTGCAGTTATGGTCAATACCCAGCCGAC  
CTAGCCCATAAAATACATAGTGCAAATCATATGGATGATAATGATGGAGAACT  
AGATACACCAATAAATTATAGTCTTAAATATTCAGATGAGCAGTTGAACTCTG  
GAAGGCAAAGTCCTTCACAGAATGAAAGATGGGCAAGACCCAAACACATAAT  
AGAAGATGAAATAAAACAAAGTGAGCAAAGACAATCAAGGAATCAAAGTAC  
AACTTATCCTGTTTATACTGAGAGCACTGATGATAAACACCTCAAGTTCCAAC  
CACATTTTGGACAGCAGGAATGTGTTTCTCCATACAGGTCACGGGGAGCCAAT  
GGTTCAGAAACAAATCGAGTGGGTCTAATCATGGAATTAATCAAAATGTAAG  
CCAGTCTTTGTGTCAAGAAGATGACTATGAAGATGATAAGCCTACCAATTATA  
GTGAACGTTACTCTGAAGAAGAACAGCATGAAGAAGAAGAGAGACCAACAA  
ATTATAGCATAAAATATAATGAAGAGAAACGTCATGTGGATCAGCCTATTGAT  
TATAGTTTAAATATGCCACAGATATTCCTTCATCACAGAAACAGTCATTTTCA  
TTCTCAAAGAGTTCATCTGGACAAAGCAGTAAAACCGAACATATGTCTTCAAG  
CAGTGAGAATACGTCCACACCTTCATCTAATGCCAAGAGGCAGAATCAGCTCC  
ATCCAAGTTCTGCACAGAGTAGAAGTGGTCAGCCTCAAAGGCTGCCACTTGC  
AAAGTTTCTTCTATTAACCAAGAAACAATACAGACTTATTGTGTAGAAGATAC  
TCCAATATGTTTTTCAAGATGTAGTTCATTATCATCTTTGTCATCAGCTGAAGA  
TGAAATAGGATGTAATCAGACGACACAGGAAGCAGATTCTGCTAATACCCTG  
CAAATAGCAGAAATAAAAGAAAAGATTGGAAGTGGTTCAGCTGAAGATCCTG  
TGAGCGAAGTTCCAGCAGTGTACAGCACCCCTAGAACCAAATCCAGCAGACT  
GCAGGGTTCTAGTTTATCTTCAGAATCAGCCAGGCACAAAGCTGTTGAATTTT  
CTTCAGGAGCGAAATCTCCCTCCAAAAGTGGTGCTCAGACACCCAAAAGTCCA  
CCTGAACACTATGTTTCAGGAGACCCCACTCATGTTTAGCAGATGTACTTCTGTC  
AGTTCACTTGATAGTTTTGAGAGTCGTTTCGATTGCCAGCTCCGTTTCAGAGTGA  
ACCATGCAGTGAATGGTAAGTGGCATTATAAGCCCCAGTGATCTTCCAGATA  
GCCCTGGACAAACCATGCCACCAAGCAGAAGTAAAACACCTCCACCACCTCCT  
CAAACAGCTCAAACCAAGCGAGAAGTACCTAAAATAAAGCACCTACTGCTG  
AAAAGAGAGAGAGTGGACCTAAGCAAGCTGCAGTAAATGCTGCAGTTCAGAG  
GGTCCAGGTTCTTCCAGATGCTGATACTTTATTACATTTTGGCACGGAAAGTAC  
TCCAGATGGATTTTCTTGTTTCATCCAGCCTGAGTGCTCTGAGCCTCGATGAGCC

ATTTATACAGAAAGATGTGGAATTAAGAATAATGCCTCCAGTTCAGGAAAATG  
ACAATGGGAATGAAACAGAATCAGAGCAGCCTAAAGAATCAAATGAAAACCA  
AGAGAAAGAGGCAGAAAAAACTATTGATTCTGAAAAGGACCTATTAGATGAT  
TCAGATGATGATGATATTGAAATACTAGAAGAATGTATTATTTCTGCCATGCC  
AACAAAGTCATCACGTAAAGCAAAAAAGCCAGCCCAGACTGCTTCAAATTA  
CCTCCACCTGTGGCAAGGAAACCAAGTCAGCTGCCTGTGTACAACTTCTACC  
ATCACAAAACAGGTTGCAACCCCAAAGCATGTTAGTTTTACACCGGGGGATG  
ATATGCCACGGGTGTATTGTGTTGAAGGGACACCTATAAACTTTTCCACAGCT  
ACATCTCTAAGTGATCTAACAATCGAATCCCCTCAAATGAGTTAGCTGCTGG  
AGAAGGAGTTAGAGGAGGGGCACAGTCAGGTGAATTTGAAAAACGAGATACC  
ATTCCTACAGAAGGCAGAAGTACAGATGAGGCTCAAGGAGGAAAAACCTCAT  
CTGTAACCATACTGAATTGGATGACAATAAAGCAGAGGAAGGTGATATTCTT  
GCAGAATGCATTAATTCTGCTATGCCCAAAGGGAAAAGTCACAAGCCTTTCCG  
TGTGAAAAAGATAATGGACCAGGTCCAGCAAGCATCTGCGTCTTCTTCTGCAC  
CCAACAAAATCAGTTAGATGGTAAGAAAAAGAAACCAACTTCACCAGTAAA  
ACCTATACCACAAAATACTGAATATAGGACACGTGTAAGAAAAAATGCAGAC  
TCAAAAATAATTTAAATGCTGAGAGAGTTTTCTCAGACAACAAAGATTCAAA  
GAAACAGAATTTGAAAAATAATTCCAAGGTCTTCAATGATAAGCTCCCAAATA  
ATGAAGATAGAGTCAGAGGAAGTTTTGCTTTTGATTACCTCATCATTACACG  
CCTATTGAAGGAACCTTACTGTTTTTCACGAAATGATTCTTTGAGTTCTCTA  
GATTTTGATGATGATGATGTTGACCTTTCCAGGGAAAAGGCTGAATTAAGAAA  
GGCAAAGAAAATAAGGAATCAGAGGCTAAAGTTACCAGCCACACAGAACTA  
ACCTCCAACCAACAATCAGCTAATAAGACACAAGCTATTGCAAAGCAGCCAA  
TAAATCGAGGTCAGCCTAAACCCATACTTCAGAAACAATCCACTTTTCCCCAG  
TCATCCAAAGACATAACCAGACAGAGGGGCAGCAACTGATGAAAAGTTACAGA  
ATTTTGCTATTGAAAATACTCCGGTTTGCTTTTCTCATAATTCCTCTCTGAGTTC  
TCTCAGTGACATTGACCAAGAAAACAACAATAAAGAAAATGAACCTATCAAA  
GAGACTGAGCCCCCTGACTCACAGGGGAGAACCAAGTAAACCTCAAGCATCAG  
GCTATGCTCCTAAATCATTTCATGTTGAAGATACCCAGTTTGTTTCTCAAGAA  
ACAGTTCTCTCAGTTCTCTTAGTATTGACTCTGAAGATGACCTGTTGCAGGAAT  
GTATAAGCTCCGCAATGCCAAAAAAGAAAAAGCCTTCAAGACTCAAGGGTGA  
TAATGAAAAACATAGTCCCAGAAATATGGGTGGCATATTAGGTGAAGATCTG  
ACACTTGATTTGAAAGATATACAGAGACCAGATTCAGAACATGGTCTATCCCC  
TGATTCAGAAAATTTTGATTGGAAAGCTATTCAGGAAGGTGCAAATTCCATAG

TAAGTAGTTTACATCAAGCTGCTGCTGCTGCATGTTTATCTAGACAAGCTTCGT  
CTGATTCAGATTCCATCCTTTCCCTGAAATCAGGAATCTCTCTGGGATCACCAT  
TTCATCTTACACCTGATCAAGAAGAAAAACCCTTTACAAGTAATAAAGGCCCA  
CGAATTCTAAAACCAGGGGAGAAAAGTACATTGGAAACTAAAAGATAGAAT  
CTGAAAGTAAAGGAATCAAAGGAGGAAAAAAGTTTATAAAAAGTTTGATTAC  
TGGAAAAGTTTCGATCTAATTCAGAAATTTTCAGGCCAAATGAAACAGCCCCTTC  
AAGCAAACATGCCTTCAATCTCTCGAGGCAGGACAATGATTCATATTCCAGGA  
GTTTCGAAATAGCTCCTCAAGTACAAGTCCTGTTTCTAAAAAAGGCCACCCCT  
TAAGACTCCAGCCTCCAAAAGCCCTAGTGAAGGTCAAACAGCCACCACTTCTC  
CTAGAGGAGCCAAGCCATCTGTGAAATCAGAATTAAGCCCTGTTGCCAGGCA  
GACATCCCAAATAGGTGGGTCAAGTAAAGCACCTTCTAGATCAGGATCTAGA  
GATTCGACCCCTTCAAGACCTGCCCAGCAACCATTAAGTAGACCTATACAGTC  
TCCTGGCCGAAACTCAATTTCCCTGGTAGAAATGGAATAAGTCCTCCTAACA  
AATTATCTCAACTTCCAAGGACATCATCCCCTAGTACTGCTTCAACTAAGTCCT  
CAGGTTCTGGAAAAATGTCATATACATCTCCAGGTAGACAGATGAGCCAACA  
GAACCTTACCAAACAAACAGGTTTATCCAAGAATGCCAGTAGTATTCCAAGAA  
GTGAGTCTGCCTCCAAAGGACTAAATCAGATGAATAATGGTAATGGAGCCAA  
TAAAAAGGTAGAACTTTCTAGAATGTCTTCAACTAAATCAAGTGGAAAGTGAAT  
CTGATAGATCAGAAAGACCTGTATTAGTACGCCAGTCAACTTTCATCAAAGAA  
GCTCCAAGCCCAACCTTAAGAAGAAAATTGGAGGAATCTGCTTCATTTGAATC  
TCTTTCTCCATCATCTAGACCAGCTTCTCCCACTAGGTCCCAGGCACAAACTCC  
AGTTTTAAGTCCTTCCCTTCCCTGATATGTCTCTATCCACACATTCGTCTGTTTCAG  
GCTGGTGGATGGCGAAAACCTCCACCTAATCTCAGTCCCCTATAGAGTATAA  
TGATGGAAGACCAGCAAAGCGCCATGATATTGCACGGTCTCATTCTGAAAGTC  
CTTCTAGACTTCCAATCAATAGGTGAGAACCTGGAAACGTGAGCACAGCAA  
ACATTCATCATCCCTTCCCTCGAGTAAGCACTTGGAGAAGAAGTGGAAAGTTCAT  
CTTCAATTCTTCTGCTTCATCAGAATCCAGTGAAAAAGCAAAAAGTGAGGAT  
GAAAAACATGTGAACTCTATTTTCAGGAACCAAACAAAGTAAAGAAAACCAAG  
TATCCGCAAAGGAACATGGAGAAAAATAAAAAGAAAATGAATTTTCTCCCAC  
AAATAGTACTTCTCAGACCGTTTCCCTCAGGTGCTACAAATGGTGCTGAATCAA  
AGACTCTAATTTATCAAATGGCACCTGCTGTTTCTAAAACAGAGGATGTTTGG  
GTGAGAATTGAGGACTGTCCCATTAACAATCCTAGATCTGGAAGATCTCCCAC  
AGGTAATACTCCCCGGTGATTGACAGTGTTTCAGAAAAGGCCAAATCCAAACA  
TTAAAGATTCAAAGATAATCAGGCAAAAACAAAATGTGGGTAAATGGCAGTGT

TCCCATGCGTACCGTGGGTTTGGAAAATCGCCTGAACTCCTTTATTCAGGTGG  
 ATGCCCTGACCAAAAAGGAACTGAGATAAAACCAGGACAAAATAATCCTGT  
 CCCTGTATCAGAGACTAATGAAAGTTCTATAGTGGAACGTACCCCATTCAGTT  
 CTAGCAGCTCAAGCAAACACAGTTCACCTAGTGGGACTGTTGCTGCCAGAGTG  
 ACTCCTTTTAATTACAACCAAGCCCTAGGAAAAGCAGCGCAGATAGCACTTC  
 AGCTCGGCCATCTCAGATCCCAACTCCAGTGAATAACAACACAAAGAAGCGA  
 GATTCAAAACACTGACAGCACAGAATCCAGTGGAACCCAAAGTCCTAAGCGCC  
 ATTCTGGGTCTTACCTTGTGACATCTGTTTAA

**Parameter Set: General PCR (Primers only) *FOLR1***

**Sequence Name: Sequence 1**

**Amplicon Length: 413**

	Start	Stop	Length	Tm	GC%
Forward					
<u><b>GGAAGAATGCCTGCTGTTCTA</b></u> <u><b>(Sense)</b></u>	182	203	21	62(52.4)	47.6
Reverse					
<u><b>CTGTAGGAGTGAGTCCAGATTTC</b></u> <u><b>(AntiSense)</b></u>	571	595	24	62 (55.7)	45.8

**ATG**GCTCAGCGGATGACAACACAGCTGCTGCTCCTTCTAGTGTGGGTGGCTGT  
 AGTAGGGGAGGCTCAGACAAGGATTGCATGGGCCAGGACTGAGCTTCTCAAT  
 GTCTGCATGAACGCCAAGCACCACAAGGAAAAGCCAGGCCCGAGGACAAGT  
 TGCATGAGCAGTGTGACCCCTGGAGGAAGAATGCCTGCTGTTCTACCAACACC  
 AGCCAGGAAGCCCATAAGGATGTTTCCCTACCTATATAGATTCAACTGGAACCA  
 CTGTGGAGAGATGGCACCTGCCTGCAAACGGCATTTCATCCAGGACACCTGCC  
 TCTACGAGTGCTCCCCCAACTTGGGGCCCTGGATCCAGCAGGTGGATCAGAGC  
 TGGCGCAAAGAGCGGGTACTGAACGTGCCCTGTGCAAAGAGGACTGTGAGC  
 AATGGTGGGAAGATTGTCGCACCTCCTACACCTGCAAGAGCAACTGGCACAA  
 GGGCTGGAACCTGGACTTCAGGGTTTAAACAAGTGCGCAGTGGGAGCTGCCTGCC  
 AACCTTTCCATTTCTACTTCCCCACACCCACTGTTCTGTGCAATGAAATCTGGA  
 CTCACTCCTACAAGGTCAGCAACTACAGCCGAGGGAGTGGCCGCTGCATCCAG  
 ATGTGG**TTC**GACCCAGCCCAGGGCAACCCCAATGAGGAGGTGGCGAGGTTCT

ATGCTGCAGCCATGAGTGGGGCTGGGCCCTGGGCAGCCTGGCCTTTCCTGCTT  
AGCCTGGCCCTAATGCTGCTGTGGCTGCTCAGCTGA

**Appendix II: DNA sequences and primers of all the genes used for PCR and pyrosequencing**

***APC* Gene**

**DNA sequence**

GGGGCTGGGACAGAATTTTATTCATCTTTCTATCATCAGCGTCTAGTACGGGG  
AGTAGCAAATAGTGAGCACTCGATAGATGTTTGC GGAATAATGGACTAGTGTG  
TGCAGAAGGATCTATTA ACTGGGCTGCAGCACAATTCAGAGAAGGCCAGTAA  
GTGCTGCAACTGAGACTCGGCTGCCTAGGCAGCAATGGCTCACGGGACAGAA  
CAGCGAAGCAGTGCCCGGCAAGCGGAGCGCAGCACCCATTGCGCCTGCGCAT  
AACAGGCTCTAGTCTCCGGGCTGTGGGAAGCCAGCAACACCTCTCACGCATGC  
GCATTGTAGTCTTCCCACCTCCCACAAGATGGCGGAGGGCAAGTAGCAAGGG  
GGCGGGGTGTGGCCGCCGGAAGCCTAGCCGCTGCTCGGGGGGGACCTGCGGG  
CTCAGGCCCGGGAGCTGCGGACCGAGGTTGGCTCGATGCTGTTCCCAGGTACT  
GTTGTTGGCTGTTGGTGAGGAAGGTGAAGCACTCAGTTGCCTTCTCGGGCCTC  
GGCGCCCCCTATGTACGCCTCCCTGGGCTCGGGTCCGGTCCGCCCTTTGCCCGC  
TTCTGTACCACCCTCAGTTCTCGGGTCCCTGGAGCACCGGCGGCAGCAGGAGCT  
GCGTCCGGCAGGAGACGAAGAGCCCGGGCGGCGCTCGTACTTCTGGCCACTG  
GGCGAGCGTCTGGCAGGTGAGTGAGGCTGCAGGCATTGACGTCTCCTCCCGGC  
AAAGCTTCCTCGGCTTTGCCCGCCGCTGCTCGGGACCCTACGGTGCTCGGCC  
CGACTCTGTGGCTCTCTTCTCTCCATGTCTCACCTCTCCCCTCCCCGCACTCCC  
CATTAGGCCTCCAGTTGGCCCCTGGCTTTGCAGGTCCTCCATTCTCACGCAGT  
GGATGGGGGTGCGGACGCCCGCCGTCCTCCACCTTTCCTGGCTGCTGCTGGAG  
CTTCGCCCTGCAAGTGGTGCCCCATTCGCGTTAGGTGGG

**BSC sequence**

GGGGTTGGGATAGAATTTTATTTATTTTTTTATTATTAGCGTTTAGTACGGGGA  
GTAGTAAATAGTGAGTATTCGATAGATGTTTGC GGAATAATGGATTAGTGTG  
GTAGAAGGATTTATTAATTGGGTTGTAGTATAATTTAGAGAAGGTTAGTAAGT  
GTTGTAATTGAGATTCGGTTGTTTAGGTAGTAATGGTTTACGGGATAGAATAG

CGAAGTAGTGTTCGGTAAGCGGAGCGTAGTATTTATTGCGTTTTCGCTATAATA  
 GGTTTTAGTTTTTCGGGTTGTGGGAAGTTAGTAATATTTTTTACGTATGCGTATT  
 GTAGTTTTTTTTATTTTTTATAAGATGGCGGAGGGTAAGTAGTAAGGGGGCGGG  
 GTGTGGTCGTCGGAAGTTTAGTCGTTGTTTCGGGGGGGATTGCGGGTTTAGGT  
 TCGGGAGTTGCGGATCGAGGTTGGTTCGATGTTGTTTTTAGGTATTGTTGTTGG  
 TTGTTGGTGAGGAAGGTGAAGTATTTAGTTGTTTTTTTCGGGTTTCGGCGTTTTT  
 TATGTACGTTTTTTTTGGGTTTCGGGTTTCGGTCGTTTTTTTTGTTTCGTTTTTTGTATTA  
 TTTTAGTTTTTCGGGTTTTGGAGTATCGGCGGTAGTAGGAGTTGCGTTCGGTAG  
 GAGACGAAGAGTTCGGGCGGCGTTCGTATTTTTGGTTATTGGGCGAGCGTTTG  
 GTAGGTGAGTGAGGTTGTAGGTATTGACGTTTTTTTTTCGGTAAAGTTTTTTTCGG  
 TTTTGTTTCGTCGTTGTTTCGGGATTTTACGGTGTTTCGGTTCGATTTTGTGGTTTT  
 TTTTTTTTTATGTTTTATTTTTTTTTTTTTTCGTATTTTTTATTTAGGTTTTTAGTT  
 GGTTTTTGGTTTTGTAGGTTTTTATTTTTACGTAGTGGATGGGGGTTCGCGACG  
 TTCGTCGTTTTTTATTTTTTTTTGGTTGTTGTTGGAGTTTCGTTTTTGTAAAGTGGT  
 GTTTTATTCGCGTTAGGTGGG

Primer Set 1			Score: 79 Quality: Medium		
Primer	Id	Sequence	Nt	T <sub>m</sub> , °C	%GC
└─ PCR	F1	AGAGAAGGTTAGTAAGTGTTGTAAT	25	59.0	32.0
┌─ PCR	R1	CCCCCCCCCTTACTACTTACCCT	23	61.5	60.9
→ Sequencing	S1	GTTGTTTAGGTAGTAATGGTTTA	23	45.0	30.4
Target Polymorphisms	Position6				
Sequence to Analyze	YGGGATAGAA TAG				

**BRCA1 Gene****DNA Sequence**

TCTCACGGAAATCCAGTGGATAGATTGGAGACCTGTGCGCGCTTGTACTTGTC  
AACAGTTATGGACTGGAGTGTTATGTTTTTCGTATTTTGAAAGCAGAACTAGG  
CCTTAAAAAGATACGTACAACCTTTAGGGAGACTACAATTCCCATCCAGCCC  
CAGGAGTCTGGGGCAAGTAGTCTTGTAAGGTCAGTGGCCTGCGGGGACGCAG  
TGAGCGCCGAATTTGCCTGGGGCAGGGGAAATGCGCTCTGGCCCATGTCTGCG  
CACTCGTAGTTCACCCCTCAGCCCCAGTGTTTGTATTTTTTCGGGTTTCAGCTT  
GCTTTTGCCTCGTCTCCGTCGACGCAATCGCCACCAGTCAATGGGGTGGTCGT  
TTTGAGGGACAAGTGGTAAGAGCCAATCTTCTTGGCGAAAACGCGGAGAAAC  
GGGACTAGTTACTGTCTTTGTCCGCCATGTTAGATTCACCCACAGAGATAGC  
GGCAGAGCTGGCAGCGGACGGTCTTTGCATTGCCGCCTCCCCAGGGGGCGGG  
AAGCTGGTAAGGAAGCAGCCTGGGTTAGCTAGGGGTGGGGTACGTCACACT  
AAGAGGGTTTGGAGAAGTTCAAGGGAGGAATCCTGCAAAGAAGAGGGGCGA  
CTTTTTCCGTGTCTCCGGACAGCTAATCGTTTTAGTGACAGGATGAGAGAGCC  
CTTCGTGTTCTGAGGGACCGAGTGGGCGAAAAGCGCCGGAGA

**BSC sequence**

TTTTACGGAAATTTAGTGGATAGATTGGAGATTTGTGCGCGTTTGTATTTGTTA  
ATAGTTATGGATTGGAGTGTTATGTTTTTCGTATTTTGAAAGTAGAAATTAGGTT  
TAAAAAGATACGTATAATTTTTTAGGGAGATTATAATTTTTATTTAGTTTTAG  
GAGTTTGGGGTAAGTAGTTTTGTAAGGTTAGTGGTTTGCGGGGACGTAGTGAG  
CGTCGAATTTGTTTGGGGTAGGGGAAATGCGTTTTGGTTTATGTTTGCGTATTC  
GTAGTTTTATTTTTAGTTTTAGTGTGTTATTTTTTCGGGTTTAGTTTGTTTTTG  
TTTCGTTTTTCGTCGACGTAATCGTTATTAGTTAATGGGGTGGTCGTTTTGAGGG  
ATAAGTGGTAAGAGTTAATTTTTTTGGCGAAAACGCGGAGAAACGGGATTAGT  
TATTGTTTTTGTTCGTTATGTTAGATTTATTTTATAGAGATAGCGGTAGAGTTG  
GTAGCGGACGGTTTTTGTATTGTCGTTTTTTTTAGGGGGCGGGAAGTTGGTAAG  
GAAGTAGTTTGGGTTAGTTAGGGGTGGGGTTACGTTATATTAAGAGGGTTTGG  
AGAAGTTTAAGGGAGGAATTTTGTAAGAAGAGGGGCGATTTTTTTTCGTGTTT  
TCGGATAGTTAATCGTTTTAGTGATAGGATGAGAGAGTTTTTTCGTGTTTTGAGG  
GATCGAGTGGGCGAAAAGCGTCGGGA

Primer Set 1			Score: 83 Quality: Medium		
Primer	Id	Sequence	Nt	Tm, °C	%GC
→ PCR	F1	AGTTTGGGGTAAGTAGTTTTGTAAG	25	60.2	36.0
← PCR	R1	TCCCTCAAACCACCACCCCATTA	24	59.3	50.0
→ Sequencing	S1	GGTAAGTAGTTTTGTAAGGT	20	46.5	35.0
Target Polymorphisms	Position6				
Sequence to Analyze	TAGTGGTTTG YGGGGAYGTA GTGAG				

### ***KLF6* Gene**

#### **DNA sequence**

ACAAATCCGTTAAAAAAAAACAACAAAAACAAACAAACAAAAAAAAAAC  
 ACCTTGGCAGGCAGAGCAAGTTGGTCCCCATGACAAGCTCCAGCTGTGGCGTC  
 TGGAGCGGGGACAGGCTCCGAACCTCGTGCCAGGGGCTCGGCCGGGCTGTGCC  
 GGGAGTTGGGGCTTCCCTGGGCGGACGCTGATCGCAGCCTGGAGGATCGATC  
 GGCGGGGGCGCTGCGCCCGCTCCCCCGGTGACAGCGCGGGGCCAGGCCAG  
 CGGACCGCAGAGAGCACCGGGTCTGAACCCCAAACAGCCGACCCGGCCCGCG  
 CCCC GGCGCCCGCAGGGAACCGCGGCCGGCTGCGTTTACCTGTTGCCAGTACT  
 CCTCCAGAGACGGCAGCGCCGAGAAGTAGCCGGTCTCGTGCACGATCTGGAG  
 CTCCTGGAAGATGCTGCACATGGGGAGCACGTCCATGTCCGGGCCGGGTTGGAC  
 GGAGCCCGCGGTTCGCGAGGGGCGGCGAGGCGCGCGGTGGGAGCCGGAGCCGA  
 AAGTCTCCCCGGAGCGCAGGTGAAAGTTTCATGCAAACCTCCAGGCTCGCAGA  
 GACGCCCGGCCGGACCCTCCCGCAGCCCGCAGCGCGCGGAGCCACACAATA  
 TTTGCAAACACCGGACTGACTGCAAACGTAACCCCTGCAAACTTCCCTATTC  
 AAAGTCCGCTGCCAGCCTCCCCCTCCGCCCCCGCCTGGCTCCCCCACTCCCC  
 CTCCCCCACGTGACTCGCCCCGCGCCCGCCCCGTGCGCGGCCCAATCCCGTG

GCTCCCGGCCCGGGGGCTGCGCGCCGATGATGTCAGCTCCGGCCAATCGCAGG  
CGGCGACACACAGCGGCCCGCCTGGCGTGACCGAGACTCTCCATCACGGCCC  
GCACCATTTGGCTCAATTCGAACTCTGCTCGTTCTGATTGGAAAGTGGCCTCGC  
AGGCTATTTTTAGCAGGGTATATAAGGCGCGGGCGGCCGCGCGCCGGAGGAG  
TCCGCGCTGTGAGGTGCGCGGCCGAGCCCTGCACTGCGCCCGCGGCCGGAGCT  
AAGGGAGCCGGGGCTGGGAGAGCCGGGGCGGGCCGCGTCGCCTGTCCCCAGT  
CCCGGTCTCTTCCCCGCTGCCCGGTCCCGCCACCCACGCCCGTCCCGGTCA  
CCAAGCCGGGCCCTGTGCGCCGCGGAGCCCCGGTTCCGGCAGCTCACCTGCG  
GGCGGCCGTCCGGTCCCGGGGCCCGCCGGTCCCCCGTCCCCTTCTATGCC  
CGAGGCCGCCCGTCCCAACTGTCCCCTTCTACGCCGGGGGCTTCCCGGTGCG  
CCAAGTGTCCCCTTCTATGCCCGGGGCCCGCCCGTCCCAACTGTCTCTTCTG  
CGCCGCTCTGTTCCCTACATCCCCCTAGTCATCCTCTGTTCTTAACCTTGGG  
GTACCCCTCTCTGTCTCTCCACCTCCGGGTCCCTCTCTGTCCCCCTCCA

**BSC sequence**

ATAAAATTCGTTAAAAAAAATAATAAAAAATAAATAAATAAAAAAAAATA  
TTTTGGTAGGTAGAGTAAGTTGGTTTTTATGATAAGTTTTAGTTGTGGCGTTTG  
GAGCGGGGATAGGTTTCGAATTCGTGTTAGGGGTTCCGGTCGGGTTGTGTCGGG  
AGTTGGGGTTTTTTTTGGGCGGACGTTGATCGTAGTTTGGAGGATCGATCGGCG  
GGGGCGTTGCGTTCGTTTTTTCGGTGATAGCGCGGGGTTTAGGTTTAGCGGAT  
CGTAGAGAGTATCGGGTTTGAATTTTAAATAGTCGATTCGGTTCGCGTTTCGG  
CGTTCGTAGGGAATCGCGGTCGGTTGCGTTTATTTGTTGTTAGTATTTTTTTAG  
AGACGGTAGCGTCGAGAAGTAGTCGGTTTCGTGTACGATTTGGAGTTTTTGGGA  
AGATGTTGTATATGGGGAGTACGTTTATGTCCGGTCCGGTTCGGACGGAGTTTCG  
CGGTCGCGAGGGCGGCGAGGCGCGCGGTGGGAGTCGGAGTCGAAAGTTTTTTT  
CGGAGCGTAGGTGAAAGTTTTATGTAAATTTTAGGTTTCGTAGAGACGTTCCGGT  
CGGATTTTTTCGTAGTTCGTAGCGCGCGGAGTTTATATAATATTTGTAAATATC  
GGATTGATTGTAAACGTAATTTTTGTAAATTTTTTTATTTAAAGTTTCGTTGTT  
AGTTTTTTTTTTTCGTTTTCGTTTGGTTTTTTTTATTTTTTTTTTTTTTACGTGATTC  
GTTTCGCGTTCGTTTCGTGCGCGGTTTAAATTCGTGGTTTTTCGGTTCGGGGGTT  
GCGCGTCGATGATGTTAGTTTCGGTTAATCGTAGGCGGCATATATAGCGGTT  
TCGTTTGGCGTGATCGAGATTTTTTATTACGGTTCGTATTATTGGTTTAAATTCG  
AATTTTGTTCGTTTTGATTGGAAAGTGGTTTCGTAGGTTATTTTTAGTAGGGTA  
TATAAGGCGCGGGCGGTCGCGCGTCGGAGGAGTTCGCGTTGTGAGGTGCGCG

GTCGAGTTTTGTATTGCGTTCGCGGTCGGAGTTAAGGGAGTCGGGGTTGGGAG  
 AGTCGGGGCGGGTCGCGTCGTTTGTTTTTAGTTTCGGTTTTTTTTTCGTTGTT  
 CGGTTTCGTTATTTTACGTTTCGTTTCGGTTATTAAGTCGGGTTTTGTCGTCGCGC  
 GAGTTTCGGTTTCGGTAGTTTATTTTTCGGGGCGGTCGTTTCGGTTTCGGGGTCGT  
 TCGGTTTTTTTTTCGTTTTTTTTTATGTTTCGAGGTCGTTTCGTTTTTAATTGTTTTT  
 TTTTACGTCGGGGGTTTTTCGGTCGTTAATTGTTTTTTTTTATGTTTCGGGGTCGT  
 TTCGTTTTTAATTGTTTTTTTTTTCGTCGTTTTGTTTTTTTTATATTTTTTTAGTTA  
 TTTTTGTTTTTTAATTTTGGGGTATTTTTTTTTGTTTTTTTTATTTTCGGGTTTT  
 TTTTTGTTTTTTTTTA

Primer Set 2			Score: 72 Quality: Medium		
Primer	Id	Sequence	Nt	Tm, °C	%GC
↳ PCR	F2	GGAGTTTTTGGAAAGATGTTGTATAT	25	58.4	32.0
↶ PCR	R1	CTCTACCAACCTAAAATTTACATAAAACT	29	54.6	27.6
→ Sequencing	S2	AGATGTTGTATATGGGG	17	45.4	41.2
Target Polymorphisms	Position41				
Sequence to Analyze	GTAYGTTTA TGTYGGGT				

**MLH1 Gene**

**DNA Sequence**

GTCCAAGGCAAGAGAATAGGCTTTAAAGTCCCTGGCTCGGTTAAAAAGCTGGT  
 TCGGTAGATTCCGTGCAATGCTCAGGATCCTCTGCCTTGTGATATCTGGAGATA  
 AGTCAACGCCTTGCAGGACGCTTACATGCTCGGGCAGTACCTCTCTCAGCAAC  
 ACCTCCATGCACTGGTATACAAAGTCCCCCTCACCCAGCCGCGACCCTTCAA  
 GGCCAAGAGGCGGCAGAGCCCAGGCCTGCACGAGCAGCTCTCTCTTCAGGA

GTGAAGGAGGCCACGGGCAAGTCGCCCTGACGCAGACGCTCCACCAGGGCCG  
CGCGCTCGCCGTCCGCCACATAACCGCTCGTAGTATTCGTGCTCAGCCTCGTAGT  
GGCGCTGACGTCGCGTTCGCGGGTAGCTACGATGAGGGCGGCGACAGACCAG  
GCACAGGGCCCCATCGCCCTCCGGAGGCTCCACCACCAAATAACGCTGGGTCC  
ACTCGGGCCGGAAAACACTAGAGCCTCGTCGACTTCCATCTTGCTTCTTTTGGGC  
GTCATCCACATTCTGCGGGAGGCCACAAGAGCAGGGCCAACGTTAGAAAGGC  
CGCAAGGGGAGAGGAGGAGCCTGAGAAGCGCCAAGCACCTCCTCCGCTCTGC  
GCCAGATCACCTCAGCAGAGGCACACAAGCCCGGTTCCGGCATCTCTGCTCCT  
ATTGGCTGGATATTTTCGTATTCCCCGAGCTCCTAAAAACGAACCAATAGGAAG  
AGCGGACAGCGATCTCTAACGCGCAAGCGCATATCCTTCTAGGTAGCGGGCA  
GTAGCCGCTTCAGGGAGGGACGAAGAGACCCAGCAACCCACAGAGTTGAGAA  
ATTTGACTGGCATTCAAGCTGTCCAATCAATAGCTGCCGCTGAAGGGTGGGGC  
TGGATGGCGTAAGCTACAGCTGAAGGAAGAACGTGAGCACGAGGCACTGAGG  
TGATTGGCTGAAGGCACTTCCGTTGAGCATCTAGACGTTTCCTTGGCTCTTCTG  
GCGCCAAAATGTCGTTTCGTGGCAGGGGTTATTCGGCGGCTGGACGAGACAGT  
GGTGAACCGCATCGCGGCGGGGGAAGTTATCCAGCGGCCAGCTAATGCTATC  
AAAGAGATGATTGAGA ACTGGTACGGAGGGAGTCGAGCCGGGCTCACTTAAG  
GGCTACGACTTAACGGGCCGCGTCACTCAATGGCGCGGACACGCTCTTTGCC  
CGGGCAGAGGCATGTACAGCGCATGCCACAACGGCGGAGGCCGCCGGGTTC  
CCTGACGTGCCAGTCAGGCCTTCTCCTTTTCCGCAGACCGTGTGTTTCTTTACC  
GCTCTCCCCCGAGACCTTTTAAAGGGTTGTTTGGAGTGTAAGTGGAGGAATATA  
CGTAGTGTTGTCTTAATGGTACCGTTAACTAAGTAAGGAAGCCACTTAATTTA  
AAATTATGTATGCAGAACATGCGAAGTTAAAAGATGTATAAAAGCTTAAGAT  
GGGGAGAAAACCTTTTTTCAGAGGGTACTGTGTTACTGTTTTCTTGCTTTTC

**BSC sequence**

GTTTAAGGTAAGAGAATAGGTTTTAAAGTTTTTGGTTCGGTTAAAAAGTTGGT  
TGCGTAGATTTTTGTTAATGTTTAGGATTTTTTGTGTTTGTGATATTTGGAGATA  
AGTTAACGTTTTGTAGGACGTTTATATGTTCCGGTAGTATTTTTTTTAGTAATA  
TTTTTATGTATTGGTATATAAAGTTTTTTTTATTTTAGTCGCGATTTTTTAAGGT  
TAAGAGGCGGTAGAGTTCGAGGTTTGTACGAGTAGTTTTTTTTTTAGGAGTGA  
AGGAGGTTACGGGTAAGTCGTTTTGACGTAGACGTTTTATTAGGGTTCGCGCGT  
TCGTCGTTTCGTTATATATCGTTTCGTAGTATTCGTGTTTAGTTTTCGTAGTGGCGTT  
TGACGTCGCGTTCGCGGGTAGTTACGATGAGGGCGGCGATAGATTAGGTATAGG

GTTTTATCGTTTTTCGGAGGTTTTATTATTAATAACGTTGGGTTTATTCGGGT  
 CGGAAAATTAGAGTTTCGTCGATTTTTATTTTGTTTTTTTTGGGCGTTATTTATA  
 TTTTGCGGGAGGTTATAAGAGTAGGGTTAACGTTAGAAAGGTCGTAAGGGGA  
 GAGGAGGAGTTTGAGAAGCGTTAAGTATTTTTTTTCGTTTTGCGTTAGATTATTT  
 TAGTAGAGGTATATAAGTTCGGTTTCGGTATTTTTGTTTTTATTGGTTGGATAT  
 TTCGTATTTTTTCGAGTTTTTAAAAACGAATTAATAGGAAGAGCGGATAGCGAT  
 TTTAACGCGTAAGCGTATATTTTTTTAGGTAGCGGGTAGTAGTCGTTTTAGGG  
 AGGGACGAAGAGATTTAGTAATTTATAGAGTTGAGAAATTTGATTGGTATTTA  
 AGTTGTTTAATTAATAGTTGTCGTTGAAGGGTGGGGTTGGATGGCGTAAGTTA  
 TAGTTGAAGGAAGAACGTGAGTACGAGGTATTGAGGTGATTGGTTGAAGGTA  
 TTTTCGTTGAGTATTTAGACGTTTTTTTTGGTTTTTTTTGGCGTTAAAATGTCGTTT  
 GTGGTAGGGGTTATTCGGCGGTTGGACGAGATAGTGGTGAATCGTATCGCGGC  
 GGGGAAGTTATTTAGCGGTTAGTTAATGTTATTAAGAGATGATTGAGAATT  
 GGTACGGAGGGAGTCGAGTCGGGTTTATTTAAGGGTTACGATTTAACGGGTCG  
 CGTTATTTAATGGCGCGGATACGTTTTTTTTGTTTCGGGTAGAGGTATGTATAGCG  
 TATGTTTATAACGGCGGAGGTCGTCGGGTTTTTTGACGTGTTAGTTAGGTTTTT  
 TTTTTTTTCGTAGATCGTGTGTTTTTTTATCGTTTTTTTTTCGAGATTTTTTAAGG  
 GTTGTTTGGAGTGTAAGTGGAGGAATATACGTAGTGTTGTTTAATGGTATCG  
 TTAATTAAGTAAGGAAGTTATTTAATTTAAAATTATGTATGTAGAATATGCGA  
 AGTTAAAAGATGTATAAAAGTTTAAGATGGGGAGAAAAATTTTTTTTTAGAGG  
 GTATTGTGTTATTGTTTTTTTTGTTTTTT

Primer Set 2			Score: 73 Quality: Medium		
Primer	Id	Sequence	Nt	T <sub>m</sub> , °C	%GC
└ PCR	F2	TAAGGGGAGAGGAGGAGT	18	60.3	55.6
↶ PCR	R1	AATACCAATCAAATTTCTCAACTCTAT	27	58.0	25.9
→ Sequencing	S1	TTGTTTTTATTGGTTGGATAT	21	44.3	23.8
Target Polymorphisms	Position50				

Sequence to Analyze	TTYGTATTTT TYGAGTTTT AAAAA
---------------------	----------------------------

### ***TP53 Gene***

#### **DNA sequence**

ATGGTTATGGAGATCAAAATAAAGGTGGGGTCGGGAATCGACTGGGAAGAGA  
 CGTGATGAAACGTTTCTGGGACGATGAAAAGGGTCTGTGACTTGGTAGGCATC  
 ACGGAGCGGTTAGGGGCCAAAACATCTTCTGTGCACTTGCTGTGTGCACT  
 GGCCTGTGTGTAATGCCACCTCGATTTAGGAAAAGATGACGTAAGTACG  
 GCACAAAGTGGCCGGTACGCGGCAGGTGCATGGGAAGAACTGCGGAATGAA  
 ACAACCGCGAGCTAAGAGATGGGGCAGCGGGAGAAATGAATTCGAGTTCGCG  
 CTCCTACCAGGAAGAACCGGCTCGGGCCGGAGGGCTGCACGGAGGACCACAC  
 GGACGCCTGCGGGCCCGCCCTTCCGCTTCACGACGTTACGCCTGCGTCTGGA  
 ACTGGAATGGCCTAGCCCAAAGCTAGATAACAGGTAGATTGTTTTTCCGACAA  
 ATTATCAAACGACCCATCATTGCACTCTTTCAAATTTGATTCTCAGACGTACC  
 CATTCTTTTTTTTTTCTCCGGGAAGATGAGATATACTCATTCTTGAAAATAC  
 CTCCGGGCTTGCCTTCTGCACACTTCTTTCCCT

#### **BSC sequence**

ATGGTTATGGAGATTA AAAATAAAGGTGGGGTCGGGAATCGATTGGGAAGAGA  
 CGTGATGAAACGTTTTTTGGGACGATGAAAAGGGTTTGTGATTTGGTAGGTATT  
 ACGGAGCGGTTAGGGGTTAAAATTTATTTTTTTGTGTATTTGTTGTGTGTATTG  
 GCGTTGTGTGTAATGTTATTTTCGATTTAGGAAAAGATGACGTAAGTACGGT  
 AATAAGTGGTCGGTACGCGGTAGGTGTATGGGAAGAAATTGCGGAATGAAAT  
 AATCGCGAGTTAAGAGATGGGGTAGCGGGAGAAATGAATTCGAGTTTCGTTTT  
 TTATTAGGAAGAATCGGTTCCGGTCCGGAGGGTTGTACGGAGGATTATACGGAC  
 GTTTGCGGGTTCGTTTTTTTCGTTTTACGACGTTTAGTTTGCGTTTGAATTGGA  
 ATGGTTTAGTTTAAAGTTAGATAATAGGTAGATTGTTTTTTTCGATAAATTATTA  
 AACGATTTATTATTGTATTTTTTTAAAATTTGATTTTTTAGACGTATTTATTTTT  
 TTTTTTTTTTTTCGGGAAGATGAGATATATTTATTTTTGAAAATATTTTCGGGTT  
 TGTTTTTTGTATATTTTTTTTTTT

Primer Set 1			Score: 78 Quality: Medium		
Primer	Id	Sequence	Nt	Tm, °C	%GC
→ PCR	F1	GGGTTTGTGATTTGGTAGGTATT	23	59.0	39.1
← PCR	R1	TCTCCCCCTACCCCATCTCTTAACT	25	61.0	52.0
← Sequencing	S1	TCTTCCCATACACCT	15	44.3	46.7
Target Polymorphisms	Position14				
Sequence to Analyze	ACRCRTACC RACCACTTTA TACC				

### ***PTEN* Gene**

#### **DNA Sequence**

GAACCAAAGGGTTCACCCTAAGCGGCAGGGCATCAGCGATGGAGAGGCCCG  
AGAGCCCTAGCGCCCAGCTCCTTTTCCCACGTTTGGGAAGGCGCAGAATAGGT  
CGATGTAGAGCAAGGAGTGAGTCTCAGGTCTCAGTCCTTTGGCTTGCTCTTAG  
GGTAGCAGGCGAGGAGTGGCACCAGTTTGGGGACTCTCTCCCCGCGTTCTGTA  
AGAATCGGCGGCAGCCAGCAGGCGGGGAGGCGGGGGCACGTGTTTGGATGTG  
GGTGCTTGTGTAACCAGTTCCCAAGCGCCAGCCCCGACAGCGCTCCTTCGGG  
AGGCTGGTCCGAGCCCCTGTTTCCGCCGCGGCGCAGGAAGGGTTGGGGTTCCG  
CTGCCTGCACCAGGCAAGAGCACCCCGAGCAAAGGAAGAAGACGACTTGCCT  
CCGGAGCTATCACTGGGGAGTGGGAATTTGGAAAGTTCCCAACTAGGGACA  
CACGTGACCTCCTTCGGAAAGTAGTTCGACTGTGGCCCGTGTATCCTTCCACC  
TCCTTTTGAACCCTCCTAGGTCTCCTCGCCCCGCCACTCGCTGGGCTGCAGCT  
TCCTACCGTTCCGTA CTTTCCACTCAACCCGGTAACCCCAAACGTGCACGGTCC  
GGCCGGGGCGCGCGGAGCCTGGCCCCGGGCGATCCATCCTGCCGGGTTTTAC  
GGCGGCCAAGGGGGGGCGGGGCTAGGTGGTCTCTGAGAACCGAGCTTGACTC  
CGACGCCGCGAACCACCTGGAGCCCCGAGGGGAAAGATGCTCGACTCTCTTG

---

GGGGCACCGGAGCGGGCGCAGGAGAGGCCTGCGGGGTGCGTCCCCTCACAG  
GGATCCTCTTTCAGTTCATTTAGATAGGTGCCCTTTGGGCCCTTGAAATTCAAC  
GGCTATGTGTTACGTTACGCACGCTCGGCTGAGAGCTTTCATTTTTAGGGCA  
AACGAGCCGAGTTACCGGGGAAGCGAGAGGTGGGGCGCTGCAAGGGAGCCG  
GATGAGGTGATACACGCTGGCGACACAATAGCAGGTTGCTCTTTGTGCTAAGA  
CTGACACCATGAGGACACAGATTTGGGGGAAGGGGAATCTCTAGGCAAAGG  
CTGTTACAGTCAAATCTCTGCGAACGATTGTGATCCGACAGCGGTGCAAAGG  
AAAGAGCGAATGCAGTCCACGCCGCGGAAATCTAGGGGTAGAGGCAAGGGG  
GGAGGGTATTCCC

**BSC sequence**

GAATTAAGGGTTTATTTAAGCGGTAGGGTATTAGCGATGGAGAGGTTCGA  
GAGTTTTAGCGTTTAGTTTTTTTTTTTACGTTTGGGAAGGCGTAGAATAGGTCG  
ATGTAGAGTAAGGAGTGAGTTTTAGGTTTTAGTTTTTTGGTTTGTTTTTAGGGT  
AGTAGGCGAGGAGTGGTATTAGTTTGGGGATTTTTTTTTTCGCGTTTTGTAAGAA  
TCGGCGGTAGTTAGTAGGCGGGGAGGCGGGGGTACGTGTTTGGATGTGGGTG  
TTTGTGTAATTAGTTTTTTAAGCGTTAGTTTCGATAGCGTTTTTTTCGGGAGGTT  
GGTTCGAGTTTTTGTTCGTCGCGGCGTAGGAAGGGTTGGGGTTTCGTTGTTT  
GTATTAGGTAAGAGTATTTTCGAGTAAAGGAAGAAGACGATTTGTTTTCGGAGT  
TATTATTGGGGAGTGGGAATTTGGAAAGTTTTTTAATTAGGGATATACGTGAT  
TTTTTTTCGGAAAGTAGTTTCGATTGTGGTTCGTGTATTTTTTTATTTTTTTTTGA  
ATTTTTTTAGGTTTTTTTCGTTTCGTTTATTCGTTGGGTTGTAGTTTTTTATCGTTT  
CGTATTTTTTTATTTAATTCGGTAATTTTAAACGTGTACGGTTCGGTCGGGGCGC  
GCGGAGTTTGGTTTCGGGCGATTTATTTTGTCTGGGTTTTTACGGCGGTTAAGGG  
GGGGCGGGGTTAGGTGGTTTTTGTGAGAATCGAGTTTGATTTTCGACGTCGCGAAT  
CGATTTGGAGTTCGAGGGGAAAGATGTTTCGATTTTTTTGGGGGTATCGGAGCG  
GGCGTAGGAGAGGTTTTCGGGGTGCCTTTTATTTATAGGGATTTTTTTTTTAGTT  
TATTTAGATAGGTGTTTTTTGGGTTTTTGTGAAATTTAACGGTTATGTGTTTACGTT  
TAGTACGTTTCGGTTGAGAGTTTTTATTTTTAGGGTAAACGAGTCGAGTTATCGG  
GGAAGCGAGAGGTGGGGCGTTGTAAGGGAGTCGGATGAGGTGATATACGTTG  
GCGATATAATAGTAGGTTGTTTTTTGTGTTAAGATTGATATTATGAGGATATAG  
ATTTGGGGGAAGGGGGAATTTTTAGGTAAAGGTTGTTATAGTTAAATTTTTGC  
GAACGATTGTGATTCGATAGCGGTGTAAAAGGAAAGAGCGAATGTAGTTTAC  
GTCGCGGAAATTTAGGGGTAGAGGTAAGGGGGGAGGGTATTTTT

Primer Set 1			Score: 85 Quality: Medium		
Primer	Id	Sequence	Nt	Tm, °C	%GC
↳ PCR	F1	GGTGTTTTTTGGGTTTTTCAAAT	23	58.1	30.4
↶ PCR	R1	TCCCCCAAATCTATATCCTCATAATATC	28	60.1	35.7
→ Sequencing	S1	GAGAGTTTTTATTTTTAGGGTAA	23	44.9	26.1
Target Polymorphisms	Position 69				
Sequence to Analyze	AYGAGTYGAG TTAT				

### ***RASSF1* sequence**

#### **DNA Sequence**

CTTCCACATTCCAGCAGCTGGTGACAGGCCAGAACAGGGAAGAGGTGAGGGC  
TCAGCTGGCTCCATACAGGAGTGCAGATGGAGGAGCAGGATCTCTCTCTGCCT  
CTCAAGTTTTCTAAACATACTTCTCAATTCCTGGCGAGGACTCTTCCCTCTCC  
ACATCCTCCCCTAGTCTCCCCAAGGAGGGAGCAGGAGCATTTCGAACGCGGAA  
ATCGAGGTGCTAGTCCAAACTGCTCGGTCGGCTTTAGTCATAGCTGGATAATG  
CCCGGCTCAGGTCTACCACAAGCCATACAGCTGCTTTTTCCGTGTTCAACCTGT  
CTGTGACAGAAACCAAGGGGGCCCCGGCACCCAGCATCTAGGCGGTGGAATC  
GGGGTCTTACGCACGGTTCCGCGGGCAGGTCCCCGGCCAGGACCCGCGGGGA  
GCCACGTAGCCAGGAGGGTGGGGCTGCCACCCAGCCAGGACGCGGCAACGG  
ACCGGGGAGGGCGGAGCTCCAGCGACCGCTTCCCCTCCCGCCCGCCGGCACCC  
CCTGGCTCCCACCTGGTCCCAGGCGCGGCCTGCGAGCTAGCGAGGTTTCGCGCGG  
TGAAGTACTGCTCGAGCTCCGAGTCCGAGTCCTCTTGGCTGCAGTAGCCACTG  
CTCGTTCGTGCTGCTCCAGGTCATTTCGAAAGAAGGCGCCTCCGCCTCGCCAT  
AGCCGTACCCGCCCGTCCCCAGTCCTGCGCGTCCGTAGCCGCCAACCACCGC  
CCCGGTCGCGTGCGTGCGTGTACGCGTGTGAGTGTGCGCGTGCGCCCGGGCCA  
GAGCCGCGCCGCAACCGTTAAGACTGAAACGTAGATCGCCGGGATCTAGCTCT

TGTCTCATTGGGGCAGGAACGCCGGGGCGGGGACACGCACGCTTCGCCCCCA  
GGAATGACCTCATCGCTCCGGAGCTCCACTCACAGACCCACCTACCACAGGG  
AACGGGGGGCGGGTGCCAGCGTCCGGGCAAGCGCACAAGAGTGGCCTCTGGCC  
GGAGGCGAGGGCGGGAAGGTGCGGGAAGTGC GCGTGC GCGGAGCCTGGGTC  
AGCCTGGGCCCCGGGTCCGCTTGCAGCGGGTGGAGTACTTGC GGAGCCGGCAA  
TCCAGGCTCCCCCTCCAGCCCCCGCGCAGAATTAGCCTCTCTGTGCCGCCGGG  
AAATCGGCAATTAGAACGCTCCTTGC GCGCGGCACCCAGGCAGCCCTCGAGA  
ATGCCTGCACTGTGGCCTGCCCATCCTCGCCCTTCCCATA CGCCCTCGGCCCCG  
CGCTACCACGTTTCGTGTCCCGCTCCACCGCGGGTTC CAGCCCAGGTCCCGG  
GGCCCGCAACAGTCCAGGCAGACGAGCGCGCGGCAGCGGTAGTGGCAGGTGA  
ACTTGCAATCTGCAGAGAGGCCTGGCGGTGAGGCGGAGGAGCTCCAGGTCCG  
GGAAATGTCCCGGAGATTGAAGGGAAGCCCCAGGGAGAGGGCCGCTGCTCGC  
CAGGCTCCGCAGGCCCGACCTATCTCAGTGGGTACCTCACACTGCTACGCGG  
ACTCTAATGTTGGCCACCTGGGCGTCTGGAAACCGGCCGGAAGGCCACAGGC  
AGAGAGGCCTGCTCAACAGTTGGATCTCTATCGCCTAGCACAGAACTTCCCCT  
TTCCTCATTGGCAATTA AAAAAACAACA AAAAAACTGCGTCTTGCTTTTGT  
CACCCAGGCTGGAGTGCAATGGCGCGATTTCCGGCTACC GCAACCTCCGCCTC  
CTGGGTTCAAGCGATTCTTCTGCCTCAG

**BSC sequence**

TTTTTATATTTTAGTAGTTGGTGATAGGTTAGAATAGGGAAGAGGTGAGGGTT  
TAGTTGGTTTTATATAGGAGTGTAGATGGAGGAGTAGGATTTTTTTTTGTTTTT  
TAAGTTTTTTTAAATATATTTTTTAATTTTTGGCGAGGATTTTTTTTTTTTTATAT  
TTTTTTTTAGTTTTTTAAGGAGGGAGTAGGAGTATTCGAACGCGGAAATCGA  
GGTGTTAGTTTTAAATTGTTCCGGTCCGGTTTTAGTTATAGTTGGATAATGTTCCGGT  
TTAGGTTTATTATAAGTTATATAGTTGTTTTTTTTCGTGTTAATTTGTTTGTGAT  
AGAAATTAAGGGGGTTTCGGTATTTAGTATTTAGGCGGTGGAATCGGGGTTTT  
ACGTACGGTTTTCGCGGGTAGGTTTTCCGGTTAGGATTCGCGGGGAGTTACGTAG  
TTAGGAGGGTGGGGTTGTTTATCGATTTAGGACGCGGTAACGGATCGGGGAG  
GGCGGAGTTTTAGCGATCGTTTTTTTTTTTCGTTTCGTCGGTATTTTTTGGTTTTTA  
TTTGGTTTCGGCGCGGTTTGCGAGTTAGCGAGGTTTCGCGCGGTGAAGTATTGT  
TCGAGTTTCGAGTTCGAGTTTTTTTTGGTTGTAGTAGTTATTGTTTCGTCGTGTTGT  
TTTAGGTTATTTCGAAAGAAGGCGTTTTTCGTTTCGTTTATAGTCGTATTCGTTT  
GTTTTTTAGTTTTGCGCGTTCGTAGTCGTTAATTATCGTTTCGGTCGCGTGCGT

GCGTGACGCGTGTTAGTGTGCGCGTGCGTTCGGGTTAGAGTCGCGTCGTAAT  
 CGTTAAGATTGAAACGTAGATCGTCGGGATTTAGTTTTTGTATTATTGGGGTAG  
 GAACGTCGGGGCGGGGATACGTACGTTTCGTTTTTAGGAATGATTTTATCGTTT  
 CGGAGTTTTATTTATAGATTTTATTTATTATAGGGAACGGGGGCGGGTGTAG  
 CGTTCGGGTAAGCGTATAAGAGTGGTTTTTGGTCGGAGGCGAGGGCGGGAAG  
 GTGCGGGAAGTGC GCGTGCGCGGAGTTTGGGTTAGTTTGGGTTTCGGGTTTCGTT  
 TG TAGCGGGTGGAGTATTTGCGGAGTCGGTAATTTAGGTTTTTTTTTTAGTTTT  
 CGCGTAGAATTAGTTTTTTTTGTGTCGTCGGGAAATCGGTAATTAGAACGTTTTT  
 TGC GCGCGGTATTTAGGTAGTTTTCGAGAATGTTTGTATTGTGGTTTTGTTTATT  
 TTCGTTTTTTTTTATACGTTTTTCGGTTTTCGCGTTTATTACGTTTCGTGTTTCGTTTTA  
 TCGCGGGTTTTTAGTTTTAGTTTTCGGGTTCGTAATAGTTTAGGTAGACGAGC  
 GCGCGGTAGCGGTAGTGGTAGGTGAATTTGTAATTTGTAGAGAGGTTTGGCGG  
 TGAGGCGGAGGAGTTTTAGGTTCGGGGAAATGTTTCGGAGATTGAAGGGAAGT  
 TTTAGGGAGAGGGTCGTTGTTTCGTTAGGTTTCGTAGGTTTCGATTTATTTAGTG  
 GGTTATTTTATATTGTTACGCGGATTTTAATGTTGGTTATTTGGGCGTTTGGAA  
 ATCGGTCGGAAGGTTATAGGTAGAGAGGTTTGTTTAATAGTTGGATTTTTATC  
 GTTTAGTATAGAATTTTTTTTTTTTTTTTATTGGTAATTAATAATAATAATAAAA  
 AAATTGCGTTTTTGTTTTTGTTATTTAGGTTGGAGTGTAATGGCGCGATTTTCGGT  
 TTATCGTAATTTTCGTTTTTTGGGTTTAAGCGATTTTTTTTGTTTTAG

Primer Set 1			Score: 76 Quality: Medium		
Primer	Id	Sequence	Nt	Tm, °C	%GC
└─ PCR	F1	AGTTTTTGTTTTATTGGGGTAGGAA	25	58.1	32.0
← PCR	R1	CCTCCCACCAAAAACCACTCTTATAC	26	57.8	46.2
→ Sequencing	S1	TTATAGATTTTATTTATTATAGGGA	25	40.3	16.0
Target Polymorphisms	Position83				
Sequence to Analyze	AYGGGGGYGG GTGTTAG				

**TUSC3 Gene**

TAGGCCCCAGGTAAAGTGCTGGACTACCCAGTAATTGGGTTTCAGTAGCAGGAT  
 GGCCTCAGATTGAGGTCCCAGGGCCAAAGGACCACTCCTCTCCTCAGCGCTGG  
 TCCGGGAAAGGCAAGCTCCGGGCGGGAGCGCACGCCGCGCCCCGAAGCCTG  
 GCTCCCTCGCCACGCCCACTTCCTGCCCCCATCCCGCGCCTTTCCAGGTCTTCT  
 CCCGGTGAACCGGATGCTCTGTCAGTCTCCTCCTCTGCGTCCTCGGCCGCGGCC  
 CGGGTCCCTCGCAAAGCCGCTGCCATCCCGGAGGGCCCAGCCAGCGGGCTCCC  
 GGAGGCTGGCCGGGCAGGCGTGGTGC GCGGTAGGAGCTGGGCGCGCACGGCT  
 ACCGCGCGTGGAGGAGACACTGCCCTGCCGCGATGGGGGCCCCGGGGCGCTCC  
 TTCACGCCGTAGGCAAGCGGGGCGGCGGCTGCGGTACCTGCCACCGGGAGC  
 TTTCCCTTCCTTCTCCTGCTGCTGCTGCTCTGCATCCAGCTCGGGGGAGGACAG  
 AAGAAAAGGAGGTAGAATGGATCCCCTTGGCCTTCCCCTGTGGGCGGGGGC  
 GGGCCAGGGTGGGCCGCGTTGCCAGGCAGCCCTGCCGTGTTGCTAGGCAGCCT  
 GGTCGCCGGCGTGGGCGATGCCGGCGCTGGGGCGGGAGCCGCGAGGGTGGGA  
 GGCCCTGGGGCGTTTCCGGGACGTGGAGTTAGCAGGGTTCTGACTTGAAAAC  
 GACGGCAAAGCGTGTCTTGACTGCTTCTGAGCACCTCACACCTTTCAGACCC  
 AGGGCGCCTTTATTCCCAGCTGGAAGCCAGCTTAGAGCAATGGTGCCACTAA  
 AAGGGG

**BSC sequences**

TAGTTTTAGGTAAAGTGTTGGATTATTTAGTAATTGGGTTTAGTAGTAGGAT  
 GGTTTTAGATTGAGGTTTTAGGGTTAAAGGATTATTTTTTTTTTTAGCGTTGGT  
 TCGGAAAGGTAAGTTTCGGGCGGGAGCGTACGTCGCGTTTTTCGAAGTTTGGT  
 TTTTCGTTACGTTTATTTTTGTTTTTATTTTCGCGTTTTTTTAGGTTTTTTTCG  
 GTGAATCGGATGTTTTGTTAGTTTTTTTTTTTTGCGTTTTTCGGTTCGCGGTTCCGGT  
 TTTTCGTAAAGTCGTTGTTATTTTCGGAGGGTTTAGTTAGCGGGTTTTTCGGAGGT  
 TGGTCGGGTAGGCGTGGTGC GCGGTAGGAGTTGGGCGCGTACGGTTATCGCGC  
 GTGGAGGAGATATTGTTTTGTGCGGATGGGGGTTCCGGGGCGTTTTTTTACGTC  
 GTAGGTAAGCGGGGCGGCGGTTGCGGTATTTGTTTATCGGGAGTTTTTTTTTTTT  
 TTTTTTTGTTGTTGTTGTTTTGTATTTAGTTTCGGGGGAGGATAGAAGAAAAGG  
 AGGTAGAATGGATTTTTTTGGTTTTTTTTTTGTGGGCGGGGGCGGGTTAGGGTG  
 GGTCGCGTTGTTAGGTAGTTTTGTGCGTGTGTTAGGTAGTTTGGTTCGTCGGCGT  
 GGGCGATGTCGGCGTTGGGGCGGGAGTCGCGAGGGTGGGAGGTTTTGGGGCG  
 TTTTCGGGACGTGGAGTTAGTAGGGTTTTGATTTGAAAACGACGGTAAAGCG  
 TGTTTTTGATTGTTTTGAGTATTTTATTTTTTTAGATTTAGGGCGTTTTTATTT  
 TTAGTTGGAAGTTTAGTTTAGAGTAATGGTGTATTAAAAGGGG

Primer Set 1			Score: 73 Quality: Medium		
Primer	Id	Sequence	Nt	T <sub>m</sub> , °C	%GC
└PCR	F1	GGATAGAAGAAAAGGAGGTAGAA	24	58.2	37.5

↖ PCR	R1	CCCCTTTTAATAACACCATTACTC	24	57.8	37.5
→ Sequencing	S1	GTGTTGTTAGGTAGTTTG	18	44.1	38.9

### **HOXA9 Gene**

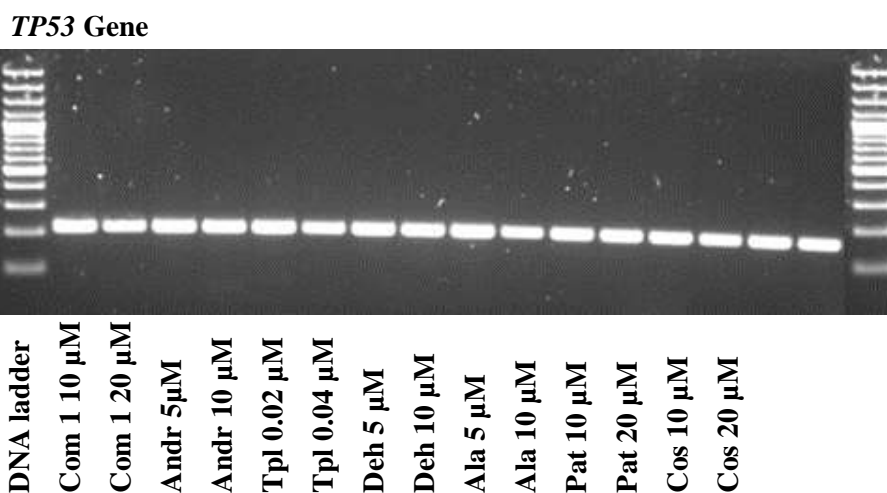
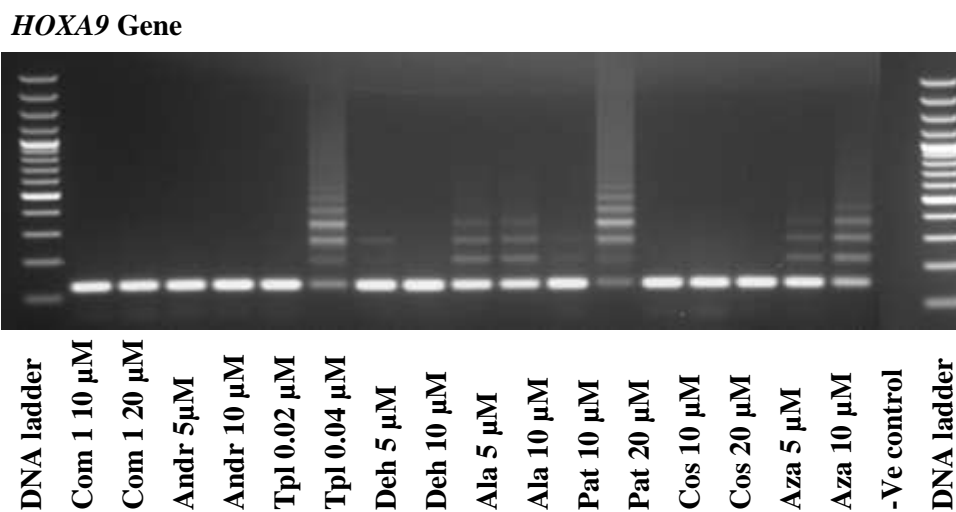
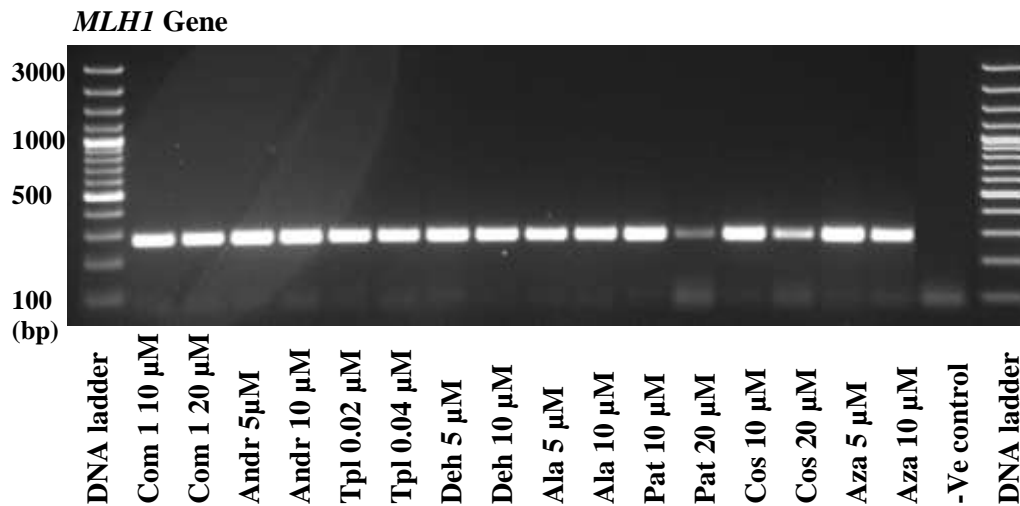
CTGCCGGGGAGGCTGGCCCAGGGTCCCCGGCGCATAGCGGCCAACGCTCAGC  
 TCATCCGCGGCGTCGGCGCCCAGCAGGAACGAGTCCACGTAGTAGTTGCCAG  
 GGCCCCAGTGGTGGCCATCACCGTGCCCAGCGCCTGGCCCCGCCCGGCCGACC  
 CACGGAAATTATGAAACTGCAGATTTTCATGTAACAACCTTGGTGGCACCGGGGG  
 GGAAGTACAGTCACCTAATAAGTTGCCGGCGCCCCGCGCCCCCATTGGCCGTGC  
 GCGTCACGTGCCCGTCCAGCAGAACAATAACGCGTAAATCACTCCGCACGCTA  
 TTAAT

BCS sequence:

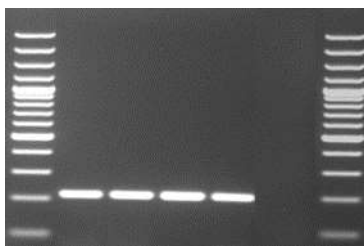
TTGTCGGGGAGGTTGGTTTAGGGTTTTCGGCGTATAGCGGTTAACGTTTAGTTT  
 ATTCGCGGCGTCGGCGTTTAGTAGGAACGAGTTTACGTAGTAGTTGTTTAGGG  
 TTTTAGTGGTGGTTATTATCGTGTTTAGCGTTTGGTTCGTTTCGGTTCGATTTACG  
 GAAATTATGAAATTGTAGATTTTATGTAATAATTTGGTGGTATCGGGGGGGAA  
 GTATAGTTATTTAATAAGTTGTCGGCGTTCGCGTTTTTATTGGTCGTGCGCGTT  
 ACGTGTTTCGTTTAGTAGAATAATAACGCGTAAATTATTTTCGTACGTTATTAAT

Primer Set 1			Score: 73 Quality: Medium		
Primer	Id	Sequence	Nt	T <sub>m</sub> , °C	%GC
↗ PCR	F1	GGATAGAAGAAAAGGAGGTAGAA	24	58.2	37.5
↖ PCR	R1	CCCCTTTTAATAACACCATTACTC	24	57.8	37.5
→ Sequencing	S1	AATTGTAGATTTTATGTAATAATT	18	44.1	38.9

**Appendix III: Gel electrophoresis of PCR products of panel of genes evaluated for CpG methylation**

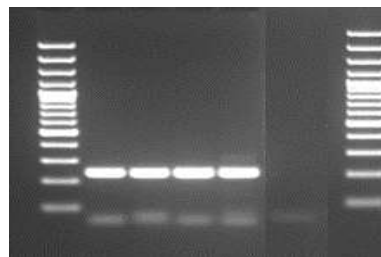


***PTEN* Gene**



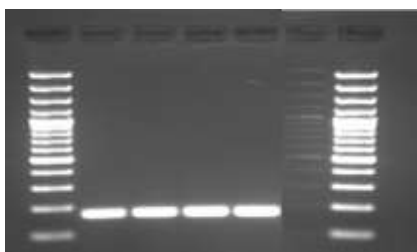
DNA ladder  
Com 1 10  $\mu$ M  
Com 1 20  $\mu$ M  
Aza 5  $\mu$ M  
Aza 10  $\mu$ M  
-Ve control  
DNA ladder

***APC* Gene**



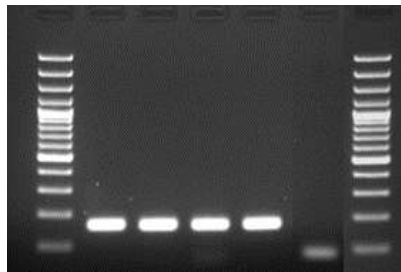
DNA ladder  
Com 1 10  $\mu$ M  
Com 1 20  $\mu$ M  
Aza 5  $\mu$ M  
Aza 10  $\mu$ M  
-Ve control  
DNA ladder

***RASSF1* Gene**

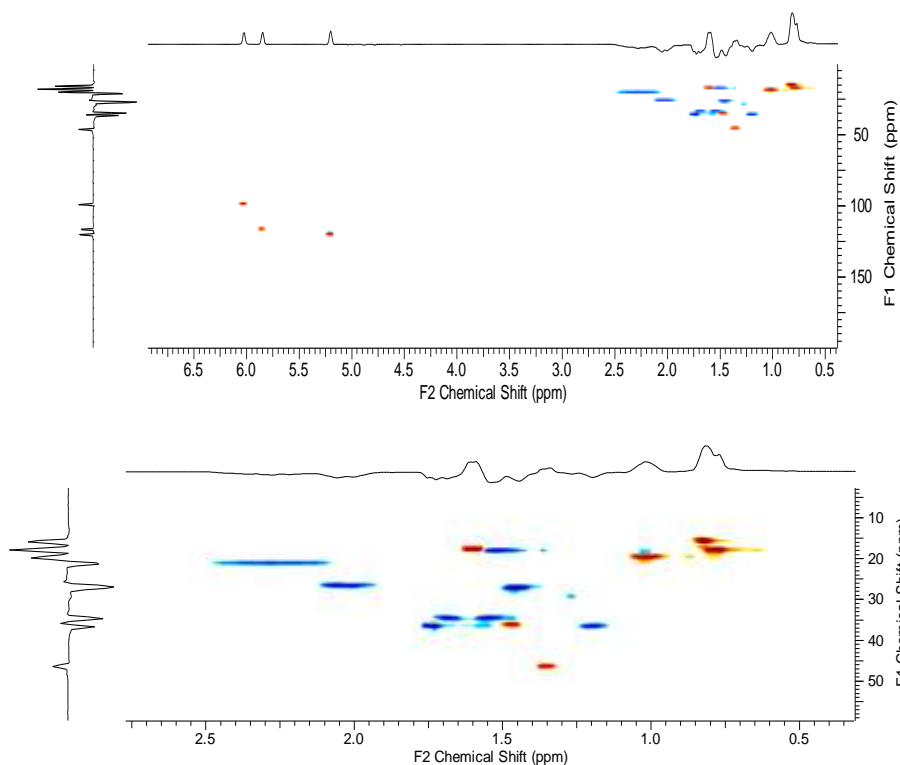
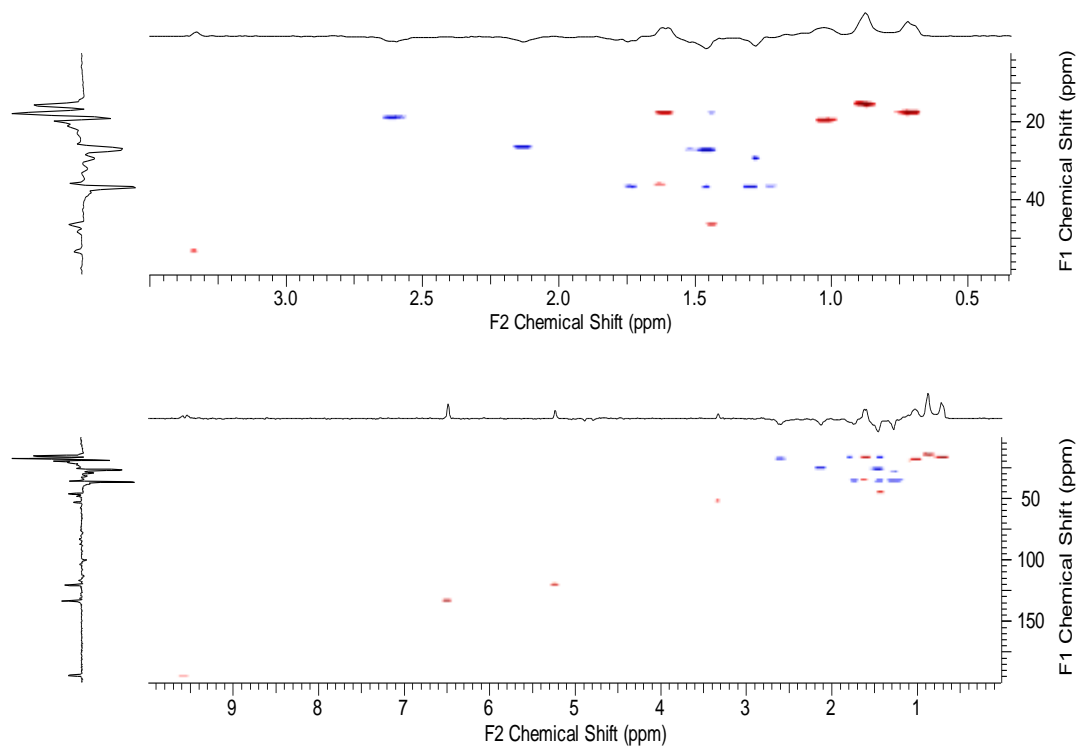


DNA ladder  
Com 1 10  $\mu$ M  
Com 1 20  $\mu$ M  
Aza 5  $\mu$ M  
Aza 10  $\mu$ M  
-Ve control  
DNA ladder

***KLF6* Gene**



DNA ladder  
Com 1 10  $\mu$ M  
Com 1 20  $\mu$ M  
Aza 5  $\mu$ M  
Aza 10  $\mu$ M  
-Ve control  
DNA ladder

**Appendix IV: Heteronuclear single quantum coherence (HSQC) spectroscopy****HSQC spectrum of 16 $\alpha$ / $\beta$ -hydroxy-cleroda-3,13(14) dien-15,16-olide (Compound 1)****HSQC spectrum of 16-oxocleroda-3,13(14) dien-15-oic acid (Compound 2)**